Foundations of Engineering Mechanics

Series Editors: V. I. Babitsky, J. Wittenburg

V. I. Feodosiev

Advanced Stress and Stability Analysis

Worked Examples

Translated by S. A. Voronov and S. V. Yaresko

With 487 Figures

Springer

Series Editors:
Vladimir I. Babitsky
Mechanical and Manufacturing Engineering
Loughborough University
Loughborough LE11 3TU, Leicestershire
United Kingdom

Jens Wittenburg
Institut für Technische Mechanik
Universität Karlsruhe (TH)
Kaiserstraße 12
76128 Karlsruhe
Germany

Translators:
S.A. Voronov
Baikalskaya Str. 25-3-99
107207 Moscow,
Russian Federation
voronov@rk5.bmstu.ru

S. V. Yaresko
Ismailovky bul. 71/25-2-42
105077 Moscow,
Russian Federation

Library of Congress Controll Number: 2005922878

ISBN 3-540-23935-9 Springer Berlin Heidelberg New York
ISBN 978-3-540-2395-2 Springer Berlin Heidelberg New York

Springer-Verlag is a part of Springer Science+Business Media
springeronline.com

Printed in The Netherlands

Typesetting: data delivered by author
Cover design: deblik Berlin
Printed on acid free paper 62/3141/M 5 4 3 2 1 0

Vsevolod I. Feodosiev

Advanced Stress and Stability Analysis
Worked Examples

Translated by Sergey A. Voronov and Sergey V. Yaresko

With 487 Figures

February 28, 2005

Springer-Verlag
Berlin Heidelberg NewYork
London Paris Tokyo
HongKong Barcelona
Budapest

Summary.

The problems and exercises in Strength and Stability that exceed the bounds of the ordinary university course in complexity and their statement are considered. The advanced problems liberalizing the readers and allowing to see the connection of the Strength of Materials with some adjacent courses are collected in this book. All the problems and exercises are accompained with the detailed solutions. The set of new problems connected with the development of computer methods and with the application of composite materials in engineering are introduced in this publication.

Author:
Vsevolod I. Feodosiev
Bauman Moscow State
Technical University
2-nd Baumanskaya st.5
105005 Moscow
Russian Federation
Translators:
Sergey A.Voronov
Sergey V.Yaresko
Department of Applied Mechanics
Bauman Moscow State
Technical University
2-nd Baumanskaya st.5
105005 Moscow
Russian Federation
E-mail: voronov@rk5.bmstu.ru

Contents

Preface

This is a book, written by the famous late Russian engineer and educator Vsevolod I.Feodosiev, who formed the tradition of stress and stability analysis for generations of engineers and researchers working in those fields, where the Soviet Union accomplished the greatest technological breakthrough of the 20th century – a race into space.

Prof. Feodosiev continued the best tradition of the Russian engineering school with his innovative and unique concepts based on deep penetration into the mechanical and practical nature of problems. Four times revised and republished in Russia and translated into some languages, the book became a classical desk text for training of top mechanical specialists. Written with a great pedagogical skill, it gives to the reader a fresh and original outlook on analysis of some advanced engineering problems.

The research and educational work of Prof. V.I. Feodosiev was carried out in the Bauman Moscow State Technical University (BMSTU), where he studied and worked for over 50 years. For a long time Prof. V.I. Feodosiev was head of the Space Missile Engineering Department.

His outstanding ability, extraordinary memory and diligence revealed itself quite early. Feodosiev's final student project was qualified as a PhD thesis. He was awarded his DSc degree for research in application of flexible shells in machines when he was 27 years old.

For 50 years Prof. Feodosiev delivered in BMSTU his course of lectures on strength of materials. His textbook of the course, republished more than ten times, became the basic book on the subject for top Russian technical universities and was awarded the State Prize. V.I. Feodosiev was awarded also the Lenin Prize (the main scientific award in the Soviet Union) for his contribution into fundamental tree-volume monograph "Strength Analysis in Mechanical Engineering".

The fundamentals of strength and reliability in aero-space engineering were published in his monographs: "Elastic Elements of Precision Engineering", "Strength Analysis of High-Loaded Parts of Jet Engines", "Introduction into Missile Engineering".

Deep insight into engineering problems, clearness of concepts and elegance of solutions enhanced by undoubted pedagogical talent are the main features of Feodosiev's style.

I hope that the English-speaking readers will enjoy this brilliant and instructive book.

Valery A. Svetlitsky
Moscow Bauman State Technical University

From the Author's Preface to the Russian Edition.

This book is not a collection of problems in the ordinary sense. The exercises are not intended for beginning students in a "Strength of Materials" course but for those who have completed the course. Neither does the book intend to interpret a full coursev, but it draws the reader's attention either to some specific problems that are not at all included in the course, or to such problems that often escape the student's attention not only in the process of training but also in their further engineering activity.

The problem complexity is also different. Some are ordinary problems and others are rather complicated. Some of them require only common knowledge and quickness of wit and others require application of primary aspects of the theory of elasticity. Many of them are complicated at first glance, but their solution may be found to be unexpectedly simple. In other cases the at first glance obvious solution may be incorrect. Even experienced readers may find themselves making mistakes. That is why all problems are provided with detailed solutions for those who are interested in the principles of the problem-solving process, or to provide the possibility for testing the obtained results in case the readers intend to solve the problems in their own manner.

Experience shows that students are often dissatisfied with the solutions of typical problems presented in ordinary textbooks. Many students have questions that are beyond the training course and require more fundamental understanding. They naturally want to test themselves in solving more complex and more interesting problems where alertness, knowledge, and intuition are required. The book is aimed at the demands of those students, most of all.

New problems appear not at a writing-table. They arise as a result of new developments and sometimes simply by friendly conversations, as a result of opinion exchange and creative search of suitable statements. The author was fortunate for encountering such kind discussions with colleagues and specialists and extremely thanks his lucky stars and friends for that.

Vsevolod I. Feodosiev

Part I

Problems and Questions

1. Tension, Compression and Torsion

1. System consisting of two rods is loaded simultaneously by forces P_1 and P_2, directed along rods (Fig. 1a). Strain potential energy is obviously equal to

$$U = \frac{P_1^2 l_1}{2E_1 A_1} + \frac{P_2^2 l_2}{2E_2 A_2} \quad .$$

If we take partial derivatives of potential energy with respect to forces P_1 and P_2, we shall obtain displacements of point A in directions 1 and 2 (u_1 and u_2, Fig. 1b):

$$u_1 = \frac{P_1 l_1}{E_1 A_1} \ , \quad u_2 = \frac{P_2 l_2}{2E_2 A_2} \quad .$$

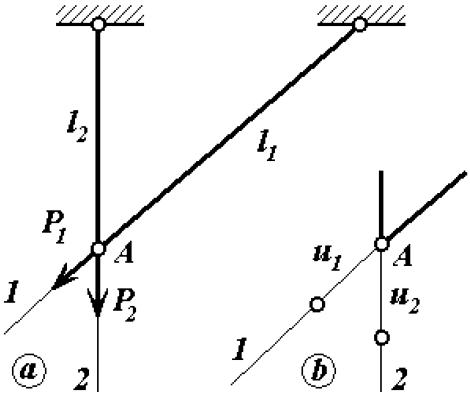

Fig. 1

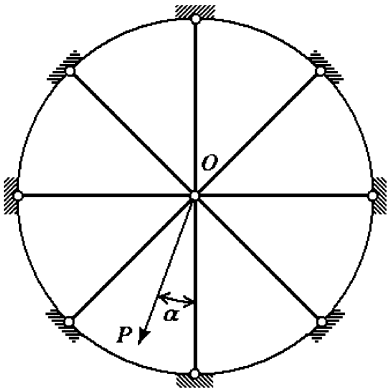

Fig. 2

Show graphically the full displacement of point A.

2. Plane truss (Fig. 2) consists of $n > 2$ equal and equally spaced rods connected in common node. The force P acts in the plane of the truss. Show that the displacement of the node O is always directed along the force P and that the value of this displacement does not depend on the angle α.

3. An absolutely rigid slab has a hole. An elastic bolt is inserted into this hole and is tightened with the force of preliminary tension N_t. The force P

is applied to the nut after the tightening (Fig. 3). What change in the force accounting for the bolt will occur under this condition?

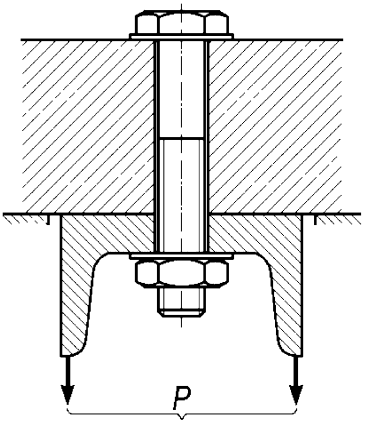

Fig. 3

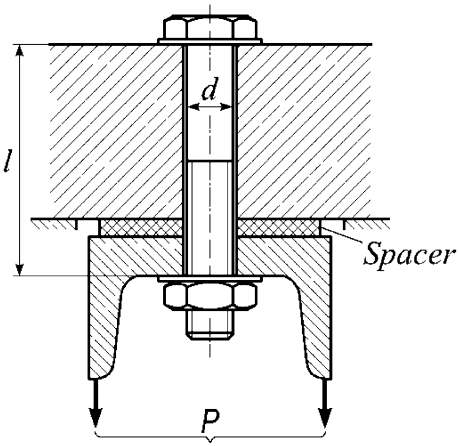

Fig. 4

4. Predicative of the previous problem is complicated by the fact that an elastic spacer is installed between the lower nut and the slab (Fig. 4). What change in the force acting on the bolt will occur in this case after applying the force P to the lower nut if it is known that the spacer's thickness decreases under compression with the force P by the value $\Delta = \dfrac{P}{c}$ where c is the stiffness of the spacer?

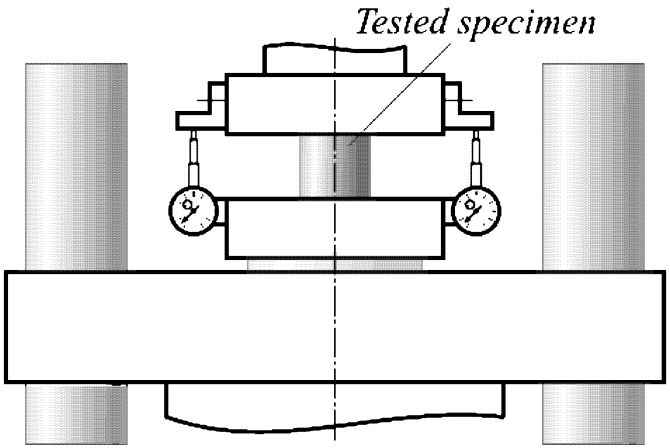

Fig. 5

5. The following experiment was carried out to determine the elasticity modulus of some material under compression. The cylindrical specimen was compressed between two massive steel slabs (Fig. 5).

Two indicators were installed for measuring of the specimen's strain with the consideration to exclude the error caused by misalignment of slabs. The measurements showed that the elasticity modulus of tested metal under compression is $E = 80\ GPa$.

Can we be rely on this result?

And in case not 80 but, say only 5 GPa... What then?

6. A straight rod of constant cross-section is rigidly clamped at its ends (Fig. 6). Show without calculation that no axial displacements occur under homogeneous heating.

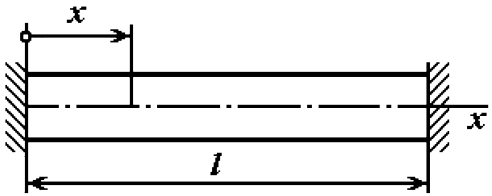

Fig. 6

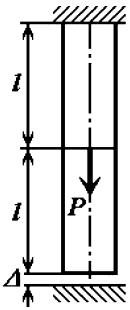

Fig. 7

7. Let us set the previous problem in another way. Determine the law of the rod's cross-section area change $A(x)$ which is necessary to obtain a specified law of axial displacements' change $u(x)$ in the homogeneously heated rod.

8. A rod clamped at its upper end is loaded with axial force P (Fig. 7). There is a clearance Δ between the rod's lower end and rigid lower support. The lower clearance vanishes under $P \geq EA\Delta\ /\ l$. Then the lower supporting force N is determined from the condition

$$\frac{(P-N)\,l}{EA} - \frac{Nl}{EA} = \Delta\ ;$$

therefore the force in the rod's lower part will be

$$N = \frac{P}{2} - \frac{\Delta}{l}\,\frac{EA}{2}\ .$$

The upper part is strained with the force

$$P - N = \frac{P}{2} + \frac{\Delta}{l}\,\frac{EA}{2}\ .$$

So the displacement of force P application point will be

$$\delta = \frac{Pl}{2EA} + \frac{\Delta}{2}\ .$$

Let us determine the elastic energy, stored by the rod. On the one hand this energy can be determined as the sum of energies contained in the upper and lower parts of the rod, that is

$$U = \frac{(P-N)^2 l}{2EA} - \frac{N^2 l}{2EA}\ , \quad \text{or} \quad U = \frac{P^2 l}{4EA} + \frac{EA\Delta^2}{4l}\ . \tag{1}$$

On the other hand this energy is equal to the work produced by the force P at displacement δ , that is

$$U = \frac{P\Delta}{2} = \frac{P^2 l}{4EA} + \frac{P\Delta}{4}\ . \tag{2}$$

As one can see, the expressions we have obtained are different. Which of these expressions is correct and which is not?

9. Straight uniform rod (Fig. 8a) sits on rigid foundation. Let us find the displacement of the rod's centre of gravity under action of its dead weight. There are two ways to do it.

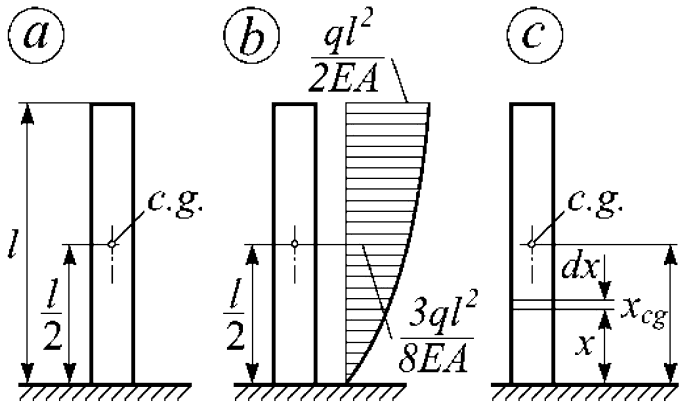

Fig. 8

First method. We find with the usual technique the displacement of the point (centre of gravity), situated at a distance of $l\ /\ 2$ from the foundation {see the epure of displacements, Fig. 8b). This displacement, as one can easily check, will be equal to

$$\Delta = \frac{3}{8}\frac{ql^2}{EA}\ , \tag{1}$$

where q is the rod's dead weight per unit length (linear weight), EA is the compression rigidity.

Second method. We find the distance from the foundation to the deformed rod's centre of gravity (Fig. 8c). This distance will be the following:

$$x_{cg} = \frac{\int_0^l (x-u)\ dm}{m}\ . \tag{2}$$

Here dm is the mass of element having length dx :

$$dm = \frac{q}{g}dx\ , \qquad m = \frac{q}{g}l\ ,$$

u is current displacement which is determined according to epure (Fig. 8b) by the formula

$$u = \frac{qx}{EA}\left(l - \frac{x}{2}\right) .$$

Substituting u, m and dm into Eq. (2) and integrating we find

$$x_{cg} = \frac{l}{2} - \frac{1}{3}\frac{ql^2}{EA}$$

Therefore the sought displacement will be

$$\Delta = \frac{l}{2} - x_{cg} = \frac{1}{3}\frac{ql^2}{EA} , \tag{3}$$

that does not converge Eq. (1) obtained previously.

What is the reason of the discrepancy?

10. Flexible filament laying on horizontal plane is strained with force T_0 between two fixed supports (Fig. 9).

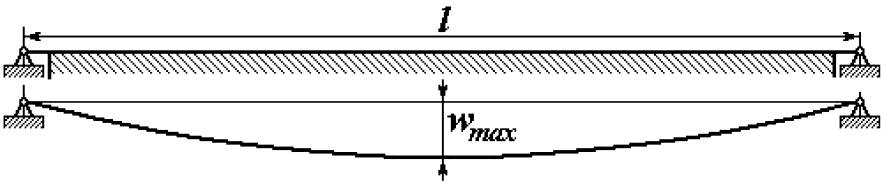

Fig. 9

As the supporting plane is taken away the filament will weigh down.

Clear up, how the sag $w_{\max}$ depends on initial tension force T_0 and the filament's linear weight q, considering that the filament's tension rigidity EA and filament's length l are given.

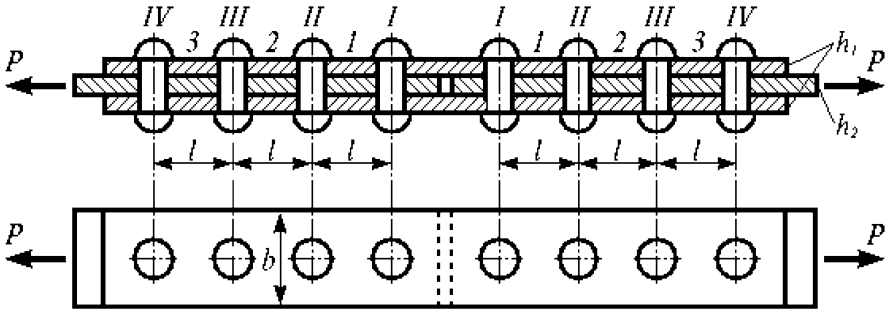

Fig. 10

11. How can we find the force distribution between rivets I, II, III, IV of the rivet joint, shown in Fig. 10, if the results of the following preliminary experiment are known?

Three sheets having thicknesses h_1, h_2 and h_1 and width b joined with one rivet are tested for tension (Fig. 11).

Depending on force T the change of distance between points A (at upper sheet) and B (at middle sheet) shown in Fig. 11 is established by precise measurements. This dependence has the following appearance: $\Delta a = T \,/\, k$, where k - constant. The measurements' base a was chosen sufficiently large to consider stresses distribution in cross-sections A and B to be uniform.

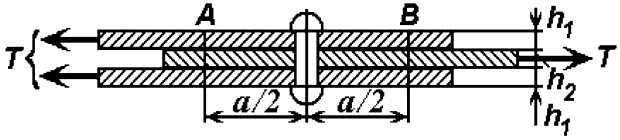

Fig. 11

12. Generalize the solution of the previous problem to the case of an arbitrary number of rivets n.

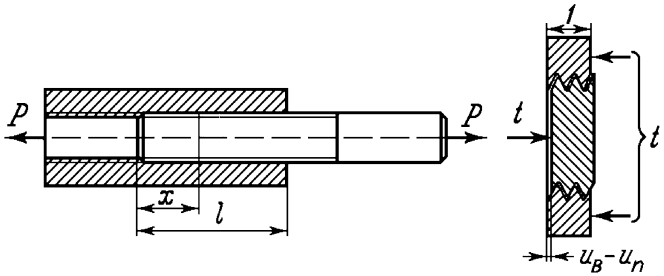

Fig. 12

13. Bolt and nut (Fig. 12) are stretched by force P.

Reveal the law of normal force distribution along the length of bolt and nut (as a function of x) if the force occurring at each thread turn is known to be proportional to the mutual displacement of bolt and nut $t = k\,(u_b - u_n)$; t is force occurring at unit length, k is an experimentally determined coefficient, $u_b - u_n$ is mutual displacement of bolt and nut due to thread deformation (Fig. 12).

14. Bolt with nut screwed on it (Fig. 13).is strained with forces P.

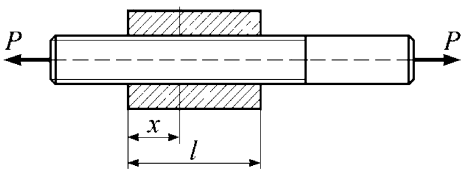

Fig. 13

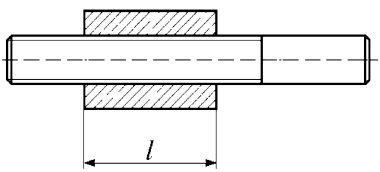

Fig. 14

Under the conditions of the previous problem reveal the law of normal force distribution and force at thread along the length of screw and nut.

15. Nut is screwed on bolt (Fig. 14). The nut's pitch of thread is smaller than the screw's pitch of thread s by the value Δ. What is the law of distribution of forces occurring under this condition in bolt and nut and what is the force at thread if, as in the two previous problems, $t = k\ (u_b - u_n)$?

16. What constructive design of nut (the first or the second type, Fig. 15) provides more favorable working conditions for thread turns?

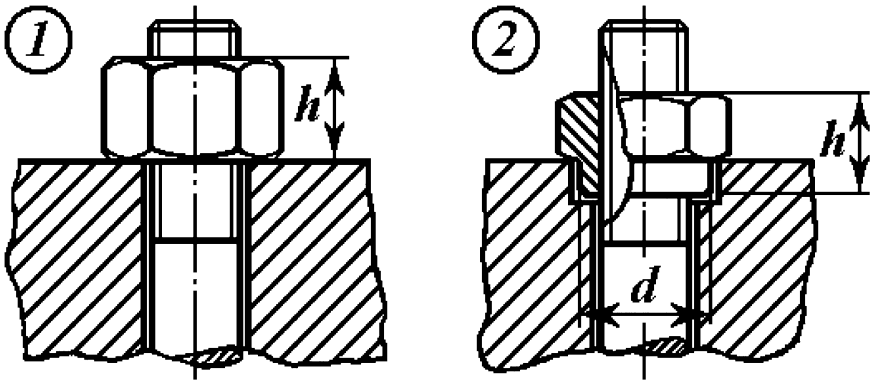

Fig. 15

17. In connection with the problems considered above one similar additional problem can be set.

An elastic homogeneous continuum contains sufficiently rare and uniformly distributed in volume inclusions having the form of finite length parallel fibers. It is necessary to determine the nature of force interactions between continuum (filler) and fibers under axial tension (Fig. 16).

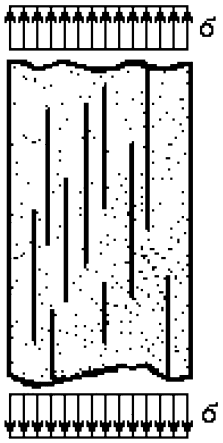

Fig. 16

18. What does the elongation test diagram (σ, ε) look like and what is the breaking point for a filament bundle composed of elastic brittle filaments?

19. Three identical rubber rods (Fig. 17) are loaded by the force P.

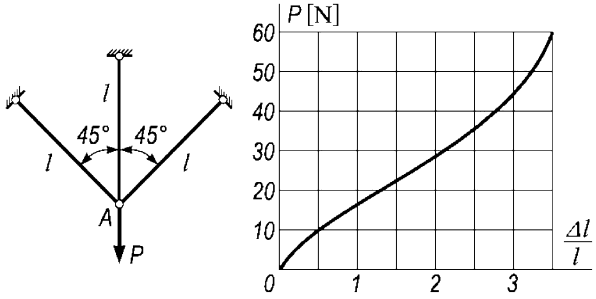

Fig. 17

Determine the displacement of the nodal point A in its dependence on force P, if the elongation diagram is given in the form of the curve shown in Fig. 17.

20. A circular two-ply rubber-cord cylinder is under action of internal pressure (Fig. 18)

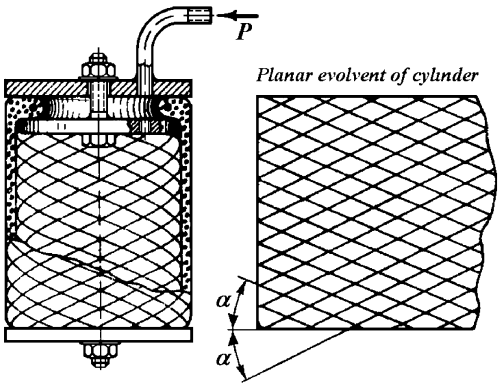

Fig. 18

There was observed that depending on the threads' arrangement angle α the cylinder, being deformed under action of internal pressure, may take one of the forms shown in Fig. 19.

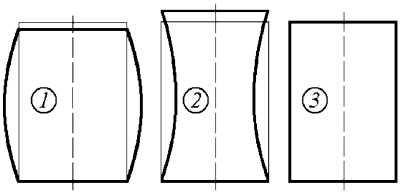

Fig. 19

In case 1 the deflected cylinder generatrix convexity is directed outwards, in case 2 - inwards. In case 3 no perceptible deformations are observed and the cylinder preserves its form to the extent in which the threads may be considered inextensible. What values of angle α does each of the observed deformation types correspond to?

21. A thin-walled sphere is reinforced with a multitude of rigid filaments arranged along the meridian (Fig. 20).

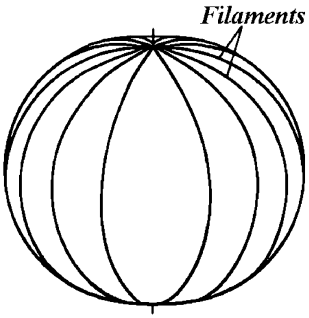

Fig. 20

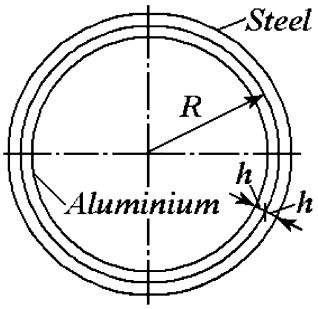

Fig. 21

Experiment shows that if the air is pumped inside the sphere under pressure then the sphere will enlarge at its equator, shorten along the axis of revolution and taking the form of a pumpkin. Determine the extent of flattening for this form neglecting rigidity of the rubber shell.

22. A steel ring is fitted with specified tightness on aluminium one (Fig. 21). Experiment shows that in some cases after heating and follow-on cooling internal ring slips out of the external one.

Determine what conditions this phenomenon is possible under.

What data are necessary to obtain numerical evaluation of the above-mentioned phenomenon?

23. A thin ring is freely fitted on a massive rigid cone (Fig. 22).

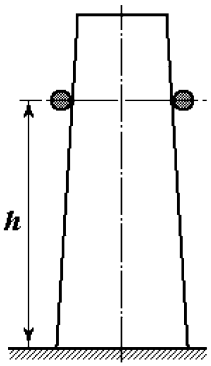

Fig. 22

Cone and ring are simultaneously subjected to influence of periodically changing temperature. How may this influence have an effect on the ring's location along the cone axis? In other words, will the value h be changing in time?

24. There is an absolutely rigid rod and a thin elastic tube having an internal diameter less than the diameter of the rod by a value of 2Δ. The tube is heated and fitted on the rod (Fig. 23).

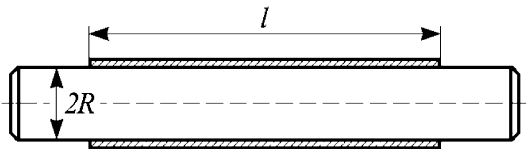

Fig. 23

Hoop stresses and (in the presence of friction) also axial ones arise in the tube while cooling.

Determine the character of distribution of stresses arising within .

25. Let us complicate the previous problem situation. Determine the force P which one needs to apply to the tube in order to take it off the rod (Fig. 24). Consider two variants: a) the force P is compressive; b) the force P is tensile.

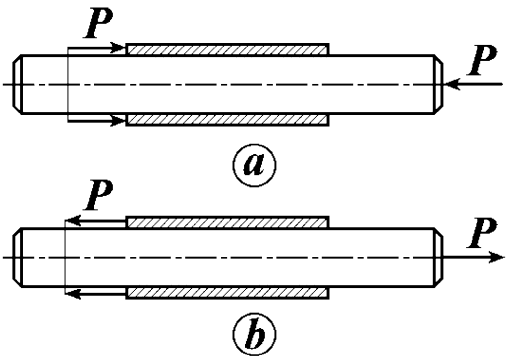

Fig. 24

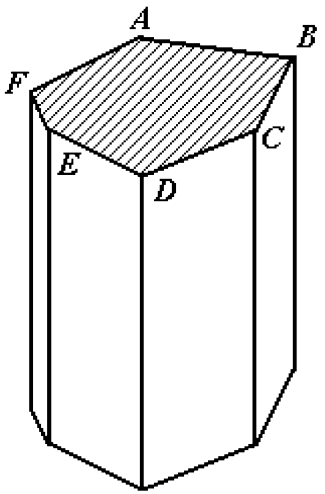

Fig. 25

26. Show that under torsion of a prismatic rod, with a cross-section in the form of a polygon, tangential stresses in any external angle $A, B, C, \ldots$ (Fig. 25) are equal to zero.

27. Tangential stresses τ proportional to the distance r from the rod's axis arise in a straight circular rod under torsion (Fig. 26).

According to the twoness law the same tangential stresses τ' arise in the plane of the rod's axial section. Stresses τ' produce the resulting moment relative to the z axis. The cut off part of the rod must be in equilibrium state. What does counterbalance the mentioned moment?

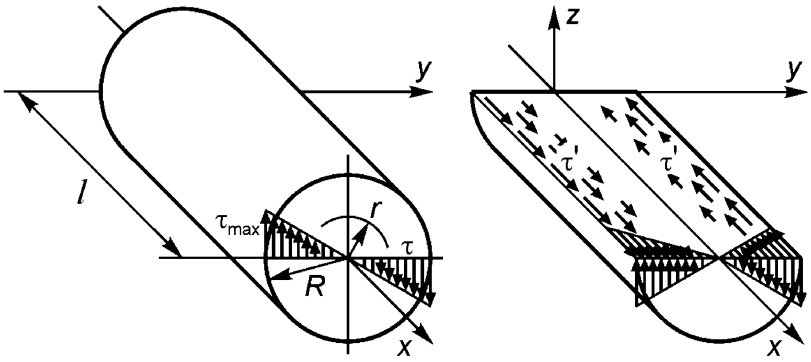

Fig. 26

28. How does torsional rigidity of a thin strip depend on axial tensile force P (Fig. 27), acting simultaneously with torque M ?

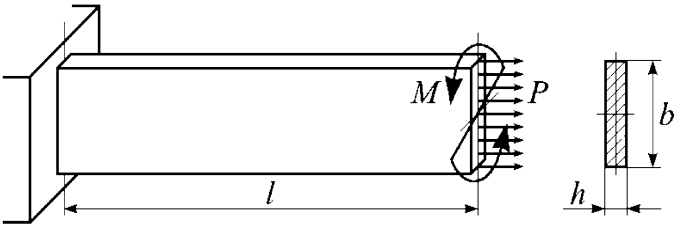

Fig. 27

29. A circular shaft (Fig. 28) inserted into a tube is kept in it by friction forces. The value of tightness contact pressure which produces these friction forces as well as the value of the friction coefficient may be considered constant for the whole contact zone with sufficient degree of accuracy. Equal and opposite moments M are applied to shaft and tube. Under $M > M_0$ shaft and tube are turning relative to each other. It is necessary to sketch the torque epure for shaft and tube under $M < M_0$.

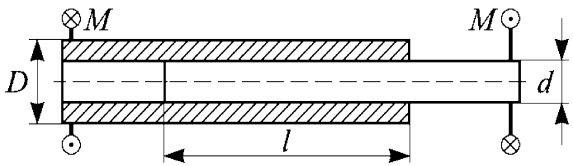

Fig. 28

30. How can the strength of a glued joint between a rigid gusset plate and rigid foundation be estimated under arbitrary shape of the glued spot (Fig. 29).

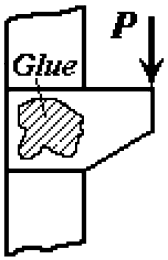

Fig. 29

The shape of the glued spot is known. Tangential stress arising in the glue layer is proportional to the local mutual displacement of the glued members. Breaking stress for the glue is given.

31. Let us draw an arbitrarily closed curve in the cross-section of a twisted rod (Fig. 30).

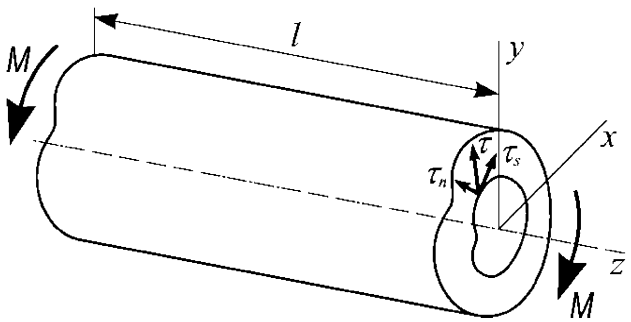

Fig. 30

Tangential stresses in each point of the curve are decomposed to normal τ_n and tangent τ_s components relative to the drawn contour. Normal stresses in the cross-section are absent (torsion is unconstrained).

Prove that regardless of the rod's cross-section shape and drawn curve shape the following formulas are valid:

$$\oint_S \tau_n ds = 0 \tag{1}$$

$$\oint_S \tau_s ds = 2GA_0\vartheta \ , \tag{2}$$

where ds is contour arc element, G is shear modulus, A_0 is area enclosed within the curve, ϑ is twist angle per unit length of the rod. (Integration applies to the whole contour of the closed curve).

32. As known, secondary (indirect) normal stresses arise in cross-sections of narrow rectangular strips under torsion. Tensile stresses arise near the edges of the strip and compressive ones – in its middle (Fig. 31).

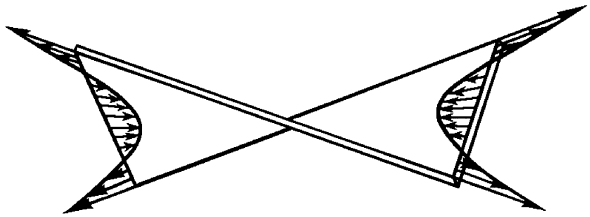

Fig. 31

What parameters and do these stresses depend on in the case of arbitrary shapes of a thin-walled profile?

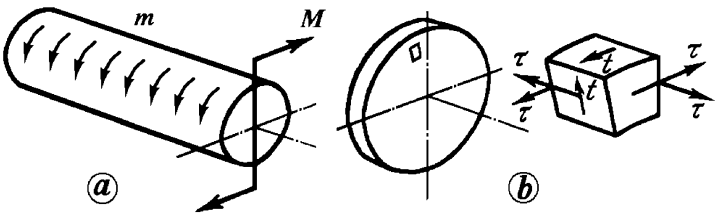

Fig. 32

33. A cylindrical rod is twisted by moments m uniformly distributed over its surface which are counterbalanced with moment M at the flank (Fig. 32a).

Tangential stresses t in cylindrical and axial sections arise under such loading in addition to usual tangential stresses τ acting in the cross-sections (Fig. 32b).

Determine the distribution of these stresses throughout the rod's volume. Make a comparative τ and t values estimation.

34. Shear stresses τ in a rod's cross-sections under pure torsion can be decomposed to two components τ_x and τ_y (Fig. 33).

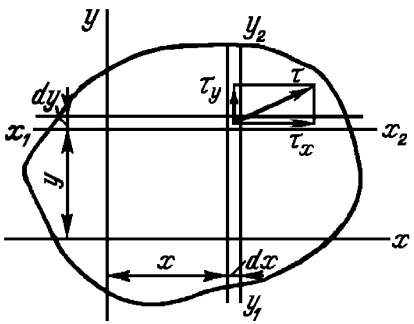

Fig. 33

Torque in the cross-section is obviously determined by the following expression:

$$T = \int\limits_x \int\limits_y \tau_x \, y \, dx \, dy - \int\limits_x \int\limits_y \tau_y \, x \, dx \, dy \; .$$

Show that regardless of the rod's cross-section shape the following formulas are valid:

$$\int\limits_x \int\limits_y \tau_x \, y \, dx \, dy = \frac{T}{2} \; , \quad - \int\limits_x \int\limits_y \tau_y \, x \, dx \, dy = \frac{T}{2} \; .$$

2. Cross-Section Geometry Characteristics: Bending

35. Derive without integration the product of inertia J_{xy} of a right triangle with respect to the centroidal axes parallel to its legs (Fig. 34).

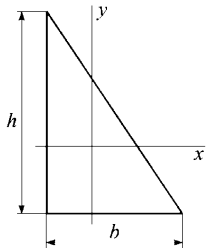

Fig. 34

36. Find the geometric locus where polar moments of inertia for a plane figure are constant.

37. Prove the following statement:

If it is possible to indicate more than one pair of noncoincident principal axes for the set of axes intersecting some point then we may assert that in general every axis passing through this point is principal.

38. For an arbitrary plane figure find the point possessing the property that every axis, passing through it, is principal.

39. Let us consider a beam loaded by two moments M (Fig. 35). No stresses occur in the neutral plane OO under pure bending as is well known. Accordingly, force interactions between upper and lower parts of the beam in this plane are absent. Then one can divide the beam by the cross-section OO into two thinner beams and this will have absolutely no effect on system operation.

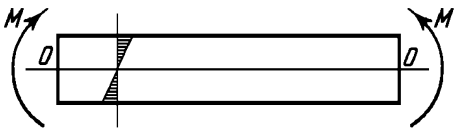

Fig. 35

Fig. 36

From another point of view doubts arise if such action is legal. As you see, these two beams set together and loaded by moments M will bend in such a manner that longitudinal sliding will occur at the contact surface (Fig. 36) and the stress diagram at a normal cross-section of both beams will be quite not the same as it was in the whole beam.

So how is that? May the beam be divided into two parts so that this will not influence its operation or not?

40. How to square a round log in order to obtain a beam of rectangular cross-section having maximal strength under bending (Fig. 37)?

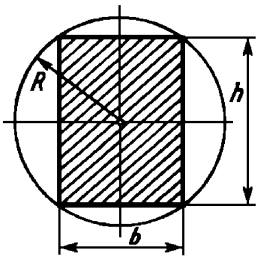

Fig. 37

41. As is well-known the neutral axis of a high curvature rod under bending does not coincide with the cross-section centroid and is slightly displaced towards the curvature center of the rod's axial line.

If the rod is not only bent but is also tensed, then the resultant stress diagram neutral axis may be displaced, generally speaking, at any value depending on the magnitude of tensile or compressive load.

What distance x from the curvature center O should the load P be applied to the high curvature rod (Fig. 38) in order to obtain coincidence of the resultant stress diagram's neutral axis with the centroid of the cross-section $I - I$?

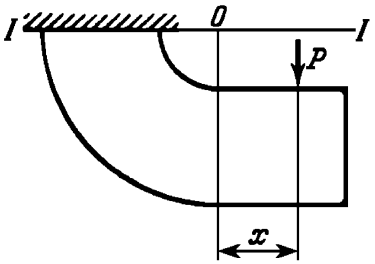

Fig. 38

42. It is known that a straight beam of constant rigidity effected by an external moment M (Fig. 39) is bent taking the form of a quadratic parabola

$$y = \frac{M}{EJ}\frac{x^2}{2} . \tag{1}$$

On the other hand, we know the following expression

$$\frac{1}{\rho} = \frac{M_b}{EJ} . \tag{2}$$

Fig. 39

If M_b and EJ are constant as we supposed for our case, then $\frac{1}{\rho}$ is constant, too. But only an arc of a circle has a constant curvature and not a parabola. So how will the beam bend: by arc of parabola or of circle?

43. What distance x from the beam end should the load P be applied to in order to obtain a deflection of point A equal to zero (Fig. 40)?

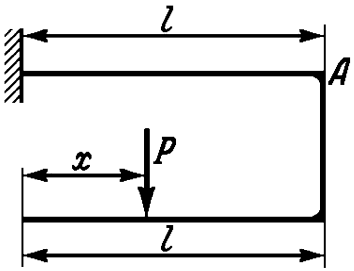

Fig. 40

44. A rectangular polyline beam (Fig. 41) clamped at its lower end is loaded by force P at the other end. Select the force inclination angle α in order to obtain displacement of point A in the line of force P action.

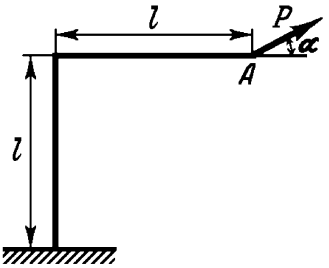

Fig. 41

45. Draw configuration of deflection curves for the systems shown in Fig. 42.

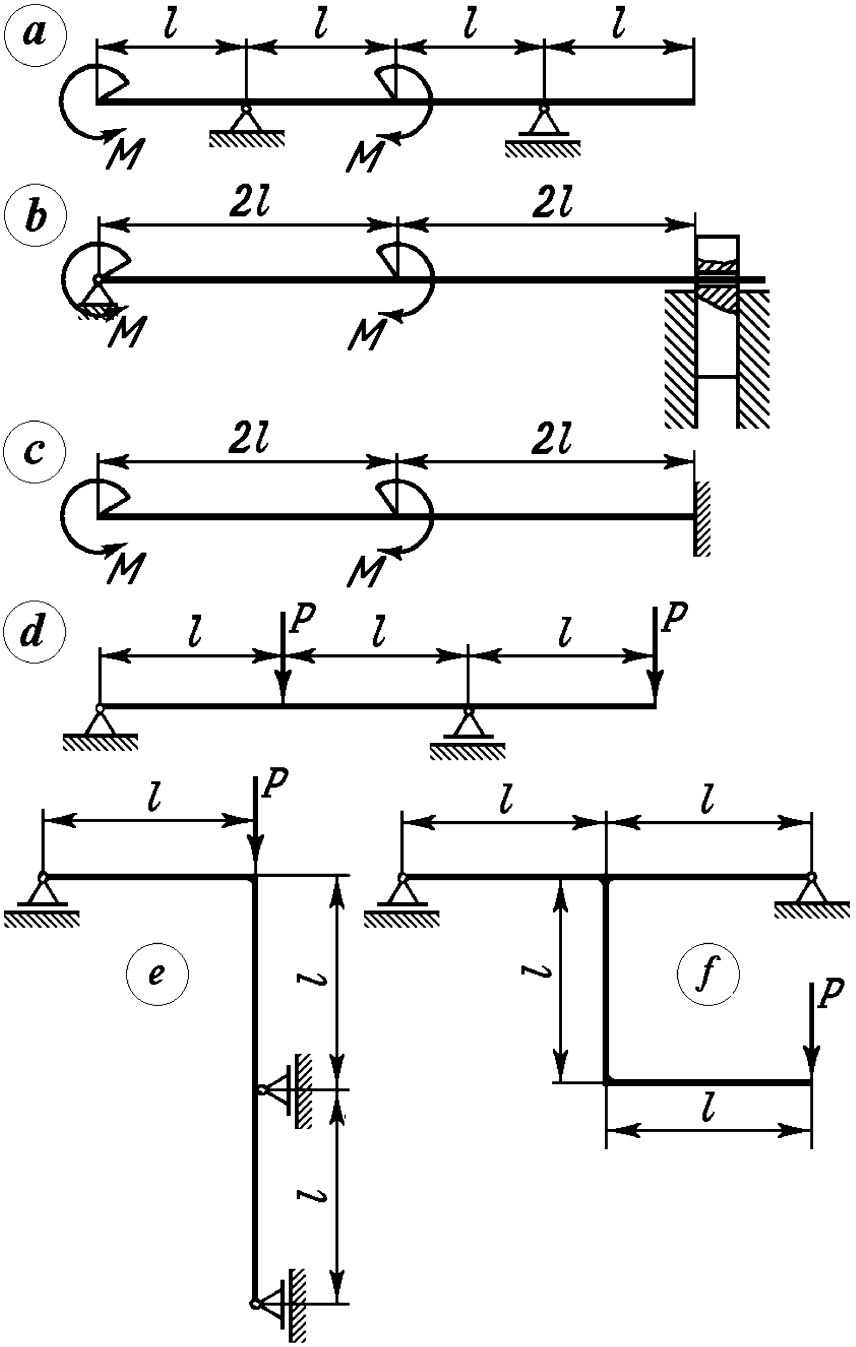

Fig. 42

46. In which direction will point A displace (Fig. 43)?

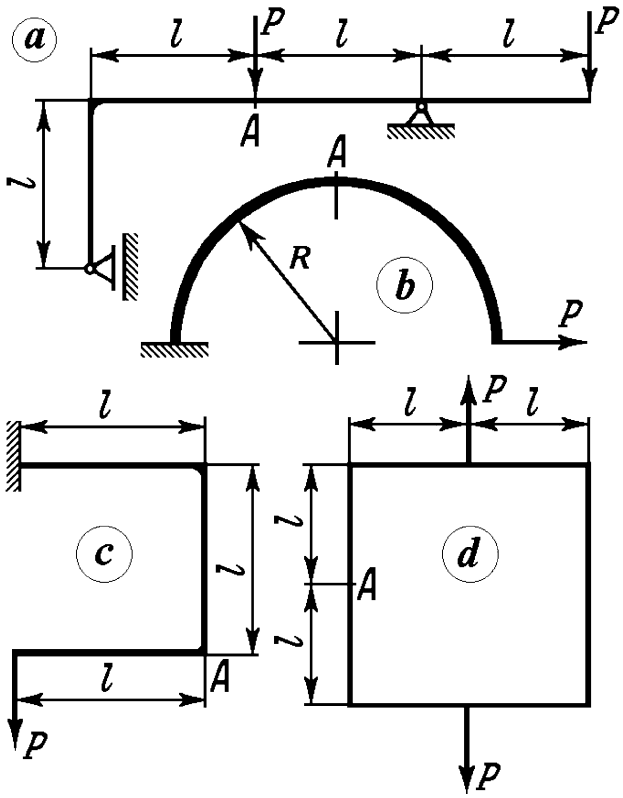

Fig. 43

Upwards, downwards, left or right?

47. The frame shown in Fig. 44 is loaded by force P. Is the rod AB tensed or compressed?

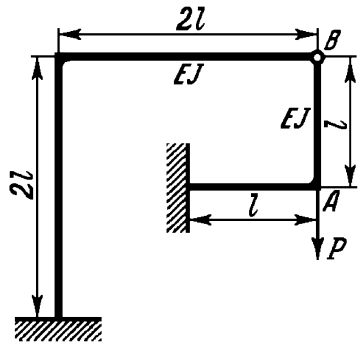

Fig. 44

48. The deflection curve configuration of a strongly bent flexible rod (Fig. 45) under specified value of load P is obtained experimentally.

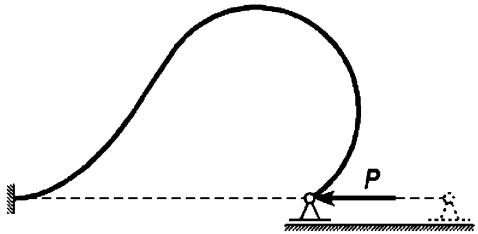

Fig. 45

What is the simplest way to calculate the possible reactions of supports?

49. A massive device of weight 2P is installed in a ring frame (Fig. 46).

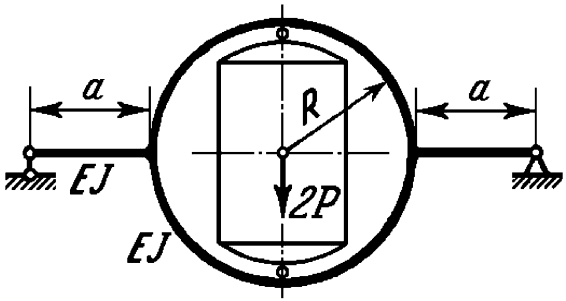

Fig. 46

Select dimension a in order to provide the maximal suspension member stiffness value. Flexural rigidities of ring and beams are equal.

50. Which of the three frames shown in Fig. 47 is the most rigid, i.e. provides minimal displacement δ_A under action of load P? Dimensions of cross-sections are the same.

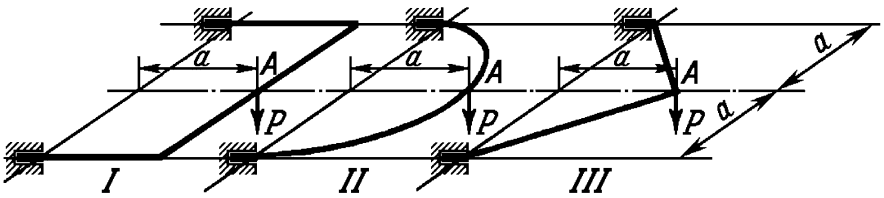

Fig. 47

51. Suppose that you take a piston ring (Fig. 48a) in your hand. If you compress it by its diameter you will notice that compliance of the ring changes depending on the direction of compression. Let us simplify this problem by presenting the ring coupling at point A as a pin.

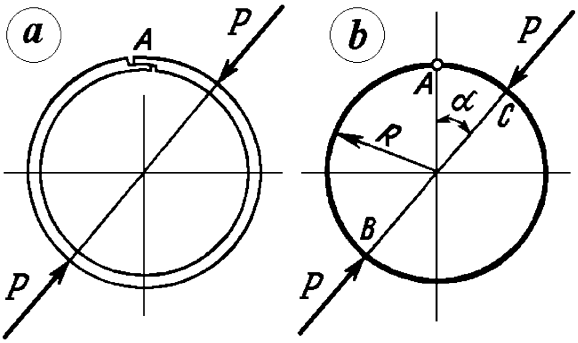

Fig. 48

Calculate the angle α (Fig. 48b) under which mutual displacement of points B and C will be minimal if the magnitude of load does not vary.

52. A square frame is produced by welding of the profile shown in Fig. 49 and is loaded by four forces P.

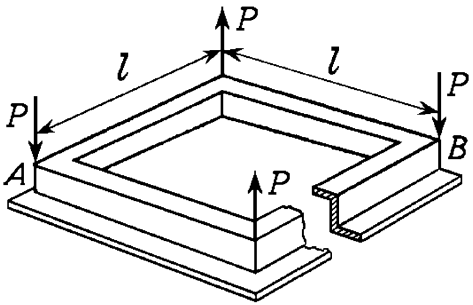

Fig. 49

Will the diagonal AB of the frame increase, decrease or remain unchanged under action of this system of loads?

53. A coiled cylindrical spring fixed at its left end is loaded by lateral force P at its right end (Fig. 50). Determine vertical displacement at the load's application point. The helix angle should be considered as small.

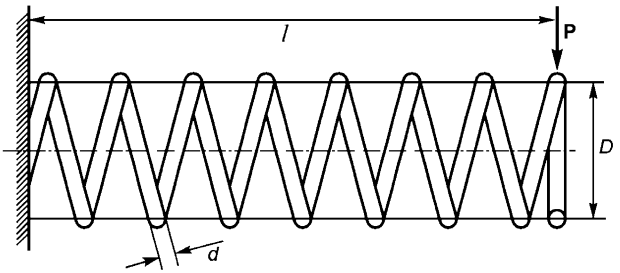

Fig. 50

54. The balance spring of a hand or pocket watch is a plane spiral band (Fig.51). The outer end of the band is clamped and the inner end is rigidly attached to the barrel fitted at the balance axle. The barrel rotates during balance oscillation and the spring band is bent. Such a case of loading is in general not pure bending, as shear forces and longitudinal ones may occur in spring cross-sections. The presence of such forces is undesirable for watch mechanism operation as they increase friction in supports, cause the distortion of balance axle and decrease precision of watch running.

Clarify the geometric conditions required for spring configuration to provide its pure bending under small rotation of the barrel.

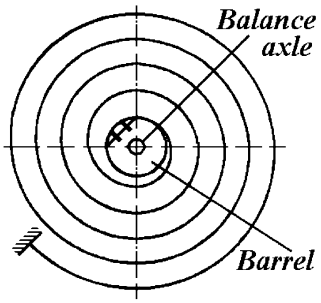

Fig. 51

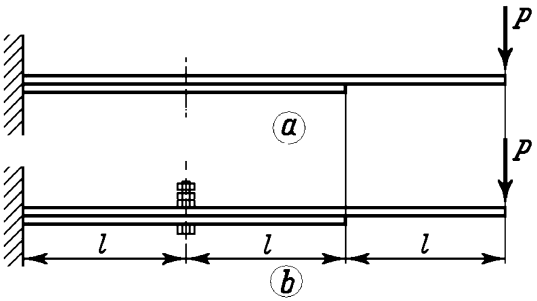

Fig. 52

55. A plane spring consisting of two sheets with lengths $2l$ and $3l$, correspondingly, is subjected to load P at its right end (Fig. 52a).

Determine how the spring deflection and stresses change if the sheets are fastened together at distance l from the clamped end (Fig. 52b). The constraint is assumed to be close but allowing free longitudinal displacement of sheets.

56. The spring consisting of three sheets with lengths $6l$, $4l$ and $2l$ (Fig. 53) is loaded by the forces P.

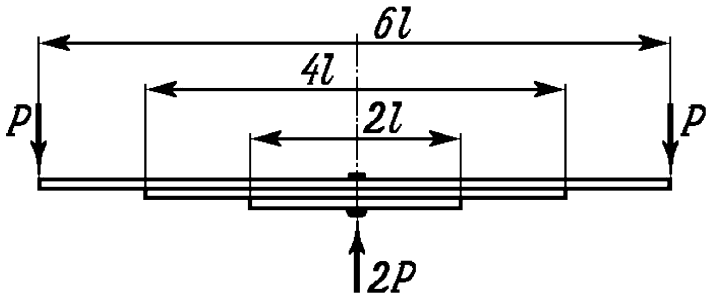

Fig. 53

Determine deflection of the spring and find stresses in the sheets under action of a specified load. Friction should be neglected.

57. A beam of length $5l$ (Fig. 54) is under action of load P. The dependence of load application point deflection f on load P has apiece-wise linear character. Its form is defined by restraints on beam deflection due to four equally spaced supports placed under the beam with the same clearance.

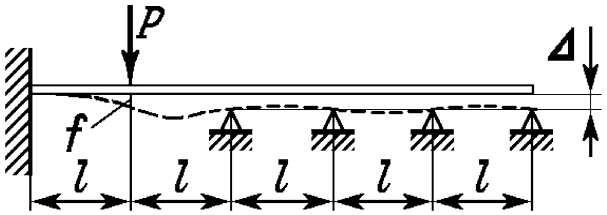

Fig. 54

Analyze how will the stiffness $c = \dfrac{dP}{df}$ change as the force P increases.

58. A flat spring of constant cross-section (Fig. 55) under bending is laying on a rigid mould having a profile specified by the function $y = y(x)$. The question about adjacency of the spring to the mould arises first of all while considering spring sags. Two principal cases are possible here:

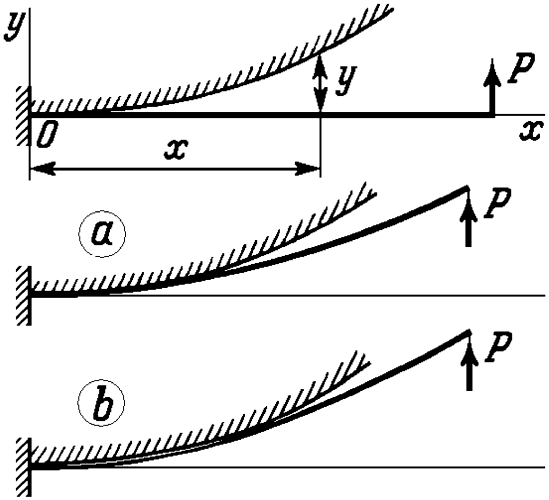

Fig. 55

1) The spring is closely adjacent to the mould at the segment from the clamped end to some point (Fig. 55a);

2) The spring touches the mould at one point only (Fig. 55b).

Establish the conditions when one or another mentioned type of adjacency will take place considering that function $y(x)$ is monotonic as well as its lower derivatives and that y is significantly less than x.

59. A homogeneous straight beam of length l and weight P lies on a solid plane (Fig. 56). Derive stresses arising in the beam under application of load $P/3$ at its end.

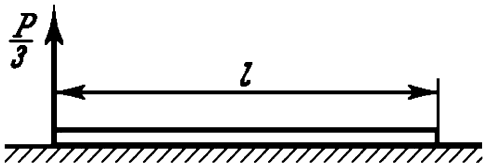

Fig. 56

60. A flexible sloping spring having the form of a radius R circle arc is pressed down to a rigid plane by two forces (Fig. 57). What magnitude of forces P is necessary to put points A in contact with the plane?

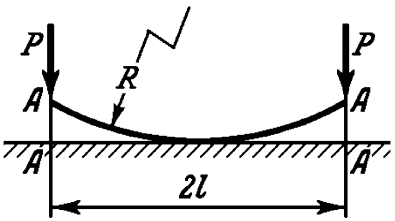

Fig. 57

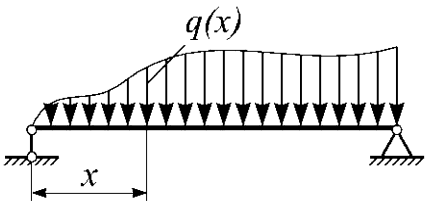

Fig. 58

61. Is it possible to select such a law of load distribution $q(x)$ being not identically equal to zero (Fig. 58) and that the beam's axis would remain straight?

62. An elastic ring is fitted with interference but without friction on a rigid bush (Fig. 59). Which limit value the force P should not exceed so that the contact between ring and bush would not open? The inner diameter of the ring in its natural state is less than the diameter of the bush by value Δ.

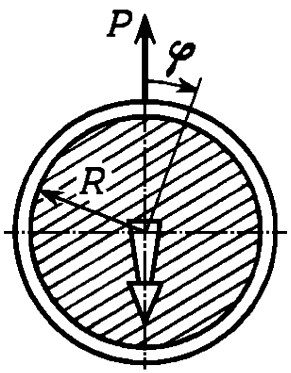

Fig. 59

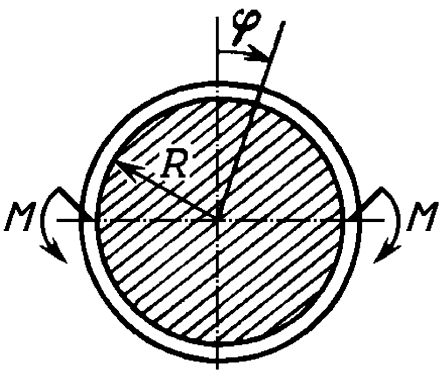

Fig. 60

63. Let us change the predicative of the previous problem so that two equal and oppositely directed moments are applied instead of force P (Fig. 60).

64. A split elastic ring of inner diameter $D - \Delta$ is fit over a rigid axle of diameter D (Fig. 61), i.e. the diameter of the ring is less by Δ than the axle diameter. Evidently the ring is slightly bent off under fitting.

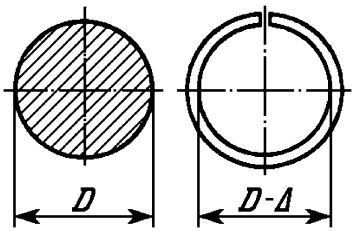

Fig. 61

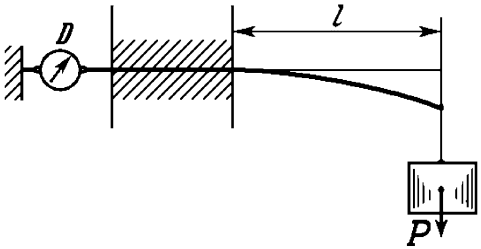

Fig. 62

Determine the law of bending moment variation along the ring's contour and reveal the character of force interaction between ring and axle.

65. An elastic beam is fitted without clearance and friction in the hole of a solid base (Fig. 62). It seems evident that under loading by lateral force P the beam will slide out from the clamped support. But... it is not clear what forces will be responsible? What will dynamometer D show if friction forces are absent?

66. Two beams of channel cross-section are tied by narrow lateral strips of high stiffness welded at upward and downward shelves. The compound beam constructed in such a manner is clamped at one end and loaded by forces P at another end (Fig. 63). What forces will the lateral strips take up?

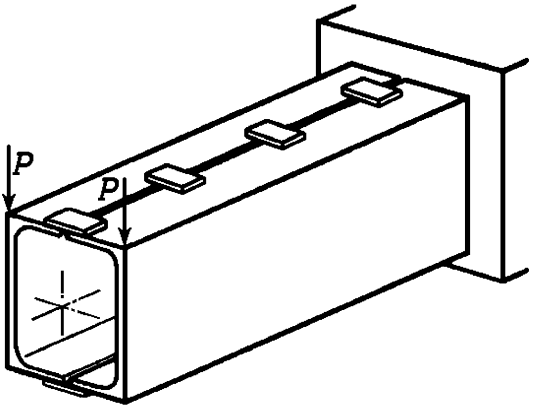

Fig. 63

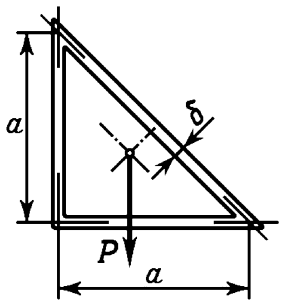

Fig. 64

67. Analyze the shear stress distribution in a closed thin-walled triangle profile under lateral bending (Fig. 64).

68. Determine the shear stress distribution law in a beam cross-section of varying thickness h (Fig. 65).

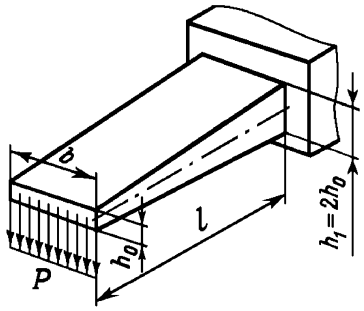

Fig. 65

69. A very long whole beam consisting of a great number of equal spans is loaded by moment M at the left end (at first support) as shown in Fig. 66. Derive bending moment and slope of the beam at the i-th support.

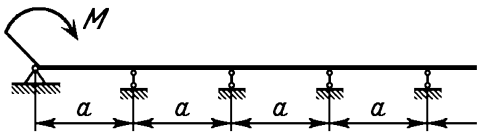

Fig. 66

70. Solve the previous problem in case of a finite number n of supports (Fig. 67).

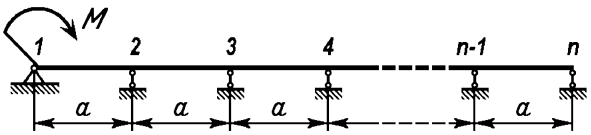

Fig. 67

71. Disclose static indeterminacy of the system shown in Fig. 68 applying displacement equations. Under loading of the frame by force P, point A slides with friction along the rigid horizontal plane. The friction factor is f. The flexural rigidity of each frame segment is equal to EJ.

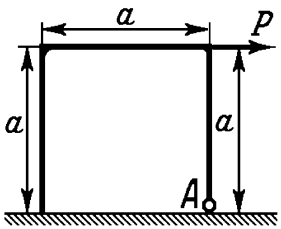

Fig. 68

72. A geometrically unchanged system consisting of rods joined by pins is called a truss. Truss rods are only tensed or compressed under loads applied to truss nodes.

In real structures truss rods are joined rigidly (not pinned) by welding or by riveting. Is it admissible in this case to analyze truss considering that rods are tensed or compressed only and neglect the rods' bending? If rods are joined rigidly then in fact the truss ceases to be a truss and transforms into a frame, isn't it?

73. Determine the axial displacement of a slotted spring (Fig. 69) compressed by load P. Assume that cross connections between rings have stiffness considerably higher than other parts of the spring.

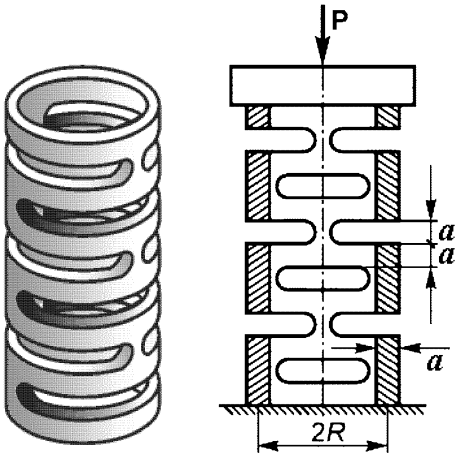

Fig. 69

The spring dimensions are shown in Fig. 69.

74. Show that the internal moment M_x diagram area is equal to zero for any closed contour of constant rigidity plane frame, i.e.

$$\int_S M_x ds = 0.$$

75. Show that area the restricted by the contour of a non-stretched plane ring frame under bending by a system of plane loads in case of small displacements remains unchanged that is equal to πR^2 (Fig. 70).

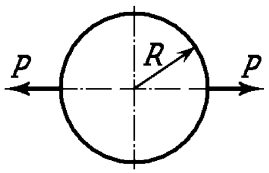

Fig. 70

76. Two sheets of the same thickness h and width b are glued together so they overlap (Fig. 71). The sheets are bent in the plane of drawing. Determine the law of load transfer from sheet to sheet considering that the glue layer is elastic. The thickness of the glue layer is δ, the modulus of elasticity and shear modulus are E_g and G_g.

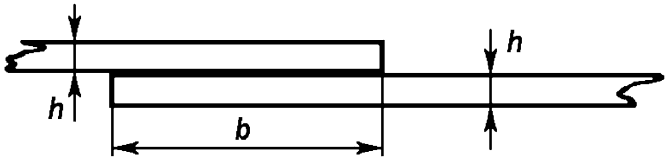

Fig. 71

77. So-called bimetallic elements are often used in various temperature regulators. The bimetallic element consists of two rigidly adjoined metallic strips of different temperature expansion factors α_1 and α_2 (Fig. 72). The bimetallic plate under heating is bent due to different elongations of its constituent parts. If one end of the strip is clamped, then the other - free - end deflects by some value. The displacements obtained in such a manner are used as a source of motion and of required mechanic load. Study the influence of the strip's geometric dimensions and of heating temperature on the strip curvature.

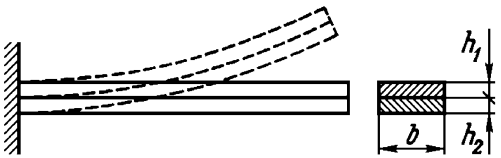

Fig. 72

78. A bimetallic ring having the dimensions shown in Fig. 73 is heated up by temperature t. Determine the ring cross-section rotation angle φ assuming the cross-section shape to be unchanged. The thermal expansion factors of ring constituent parts are $\alpha_1$and α_2.

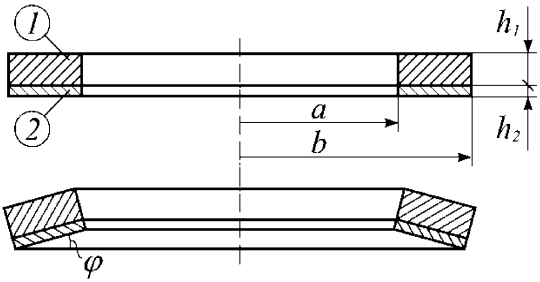

Fig. 73

79. The temperature regulator of a thermostat is designed as to have the bimetallic plate installed as shown in Fig. 74 as the sensitive element.

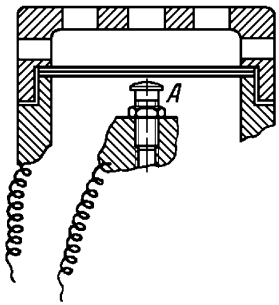

Fig. 74

According to the designer's concept the plate begins to bend under the rise of temperature. When the temperature rises up to a specified value the contact A will close and relay controlling thermostat heating will operate. Can such a system actually operate?

80. Prove that the closed plane bimetallic frame of a constant cross-section does not change its curvature under uniform heating independently on frame contour configuration (Fig. 75).

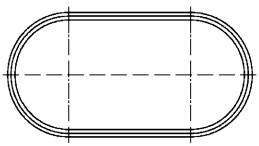

Fig. 75

81. A cantilever beam of rectangular cross-section (Fig. 76a) is loaded by force P directed along the diagonal of the beam's cross-section. Let us assume that the material is ideally elasto-plastic (Fig. 76b). Calculate the limit value of the bending moment in the beam.

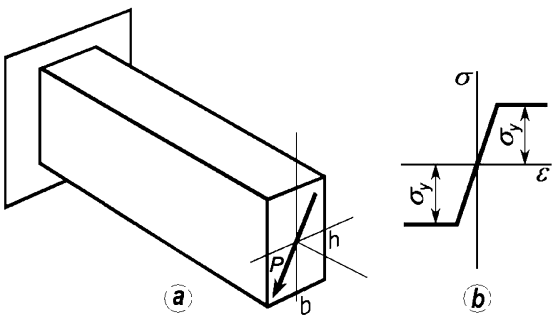

Fig. 76

82. A simply supported concrete beam has a rectangular cross section $b \times h_0$ (Fig. 77).

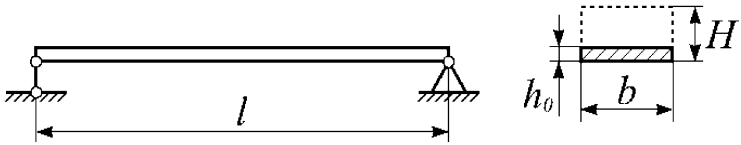

Fig. 77

Bending moments and corresponding stresses arise in the beam under action of its own weight forces. In order to strengthen the beam its thickness was increased directly at the exploitation place by putting thin layers of concrete on the beam. Thus the thickness was brought to the value H. Each layer of concrete was put on only after complete solidification of the previous layer. Derive the law of stress distribution along the cross-section height under own weight forces action, neglecting the effect of concrete shrinkage. How will the solution of the problem change in case of concrete solidification with a relative shrinkage factor α?

3. Complex Stress State, Strength Criteria, Anisotropy

83. A hollow cylinder of internal diameter d_1 and external diameter d_2 is loaded by the pressure uniformly distributed: a) over top and bottom faces; b) over internal and external cylindrical surfaces; c) over the entire surface (Fig. 78).

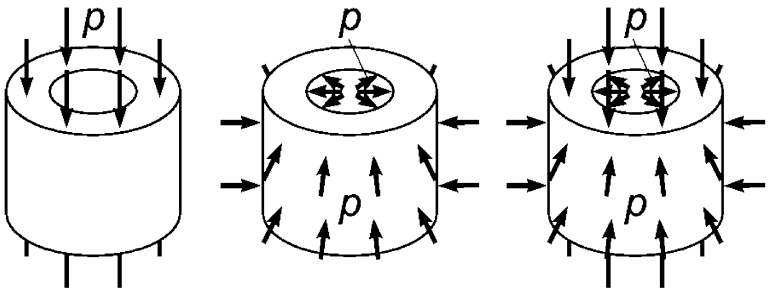

Fig. 78

Determine the internal diameter variation and the internal cavity volume variation for each of the given cases.

84. Determine the principal stresses for the stress state shown in Fig. 79.

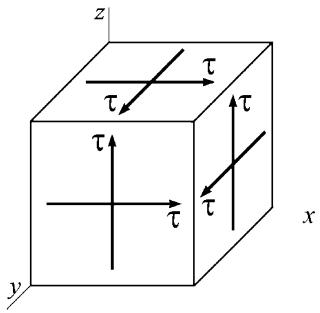

Fig. 79

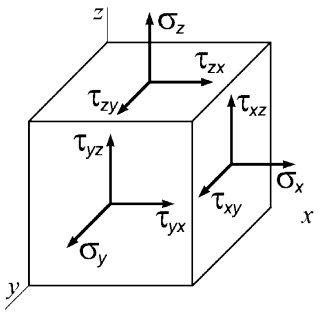

Fig. 80

85. For the general case of the stress state (Fig. 80) show:
1) whether the conditions

$$\tau_{yx} = k\sigma_x, \quad \tau_{yz} = k\tau_{xz}, \quad \sigma_y = k\tau_{xy}, \tag{1}$$

where k is some constant, are valid for two mutually perpendicular planes (for example, for planes, perpendicular to the x and y axes), the stress state can't be triaxial (it is biaxial or uniaxial).

2) whether besides the relations (1) the following conditions

$$\tau_{zx} = n\sigma_x, \quad \sigma_z = n\tau_{xz}, \quad \tau_{zy} = n\tau_{xy} \tag{2}$$

are valid and whether then the stress state is also uniaxial.

86. Determine which of the two stress states (Fig. 81) is more dangerous according to energetic criteria of strength without determining principal stresses and without calculating σ_{eq}.

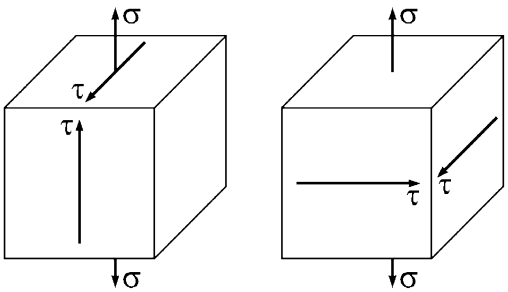

Fig. 81

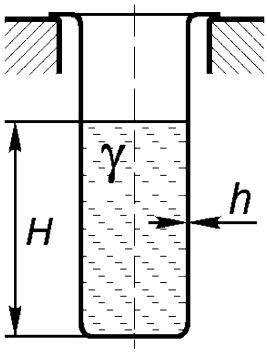

Fig. 82

87. Plot the σ_{eq} diagram along the generatrix of the cylinder (Fig. 82) filled with liquid of specific weight γ up to the height H according to the criterion of maximum shear stresses. Assume during solution that the cylinder is thin-walled and bending stresses arising in its walls have no essential significance.

88. A thin-walled tube (Fig. 83) is loaded with internal pressure p and with bending moment M.

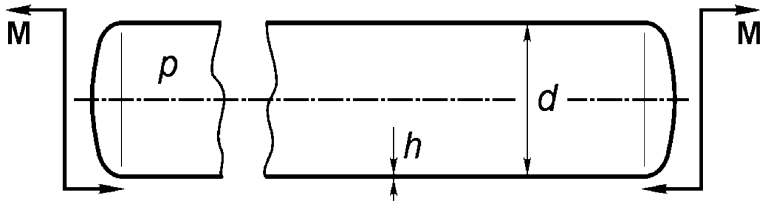

Fig. 83

Using the maximum shear stresses strength criterion analyze the calculated σ_{eq} stress dependence on moment M under given pressure p.

89. A thin-walled spherical vessel of radius $R = 0.5\ m$ and of thickness $h = 1\ cm$ is loaded with internal pressure $p_1 = 32\ MPa$ and external pressure $p_2 = 30\ MPa$ (Fig. 84).

It is necessary to determine a vessel wall's safety factor s_y if the yield limit stress of its material is known to be $\sigma_y = 300\ MPa$.

Let's consider an element taken from the wall near the internal surface of the vessel (Fig. 85). Main stresses σ_1 and σ_2 are calculated by the known formula for the spherical vessel: $\sigma_1 = \sigma_2 = \dfrac{(p_1 - p_2)}{2h} R$, $\sigma_3 = -p_1$.

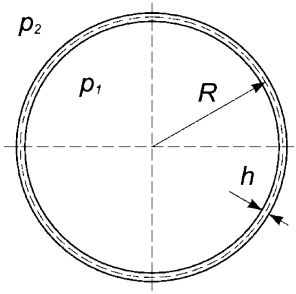

Fig. 84

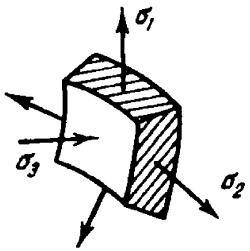

Fig. 85

According to the theory of maximum shear stresses

$$\sigma_{eq} = \sigma_1 - \sigma_3 = \frac{(p_1 - p_2)\, R}{2h} + p_1 ,$$

$$\sigma_{eq} = \frac{2 \cdot 50}{2 \cdot 1} + 32 = 82\ MPa ,$$

$$s_y = \frac{\sigma_y}{\sigma_{eq}} = \frac{300}{82} = 3.66 .$$

Will the above solution be correct?

90. A thin-walled tube of thickness h is tightly fitted over a solid cylinder but without interference (Fig. 86). The system is plunged in liquid and effected by uniform pressure p. Starting from maximum shear stress strength theory conceptions ascertain conditions under which the loss of the tube's elastic properties is possible. Elastic constants of the cylinder and tube are given.

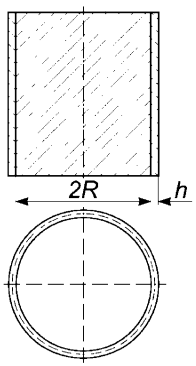

Fig. 86

91. An absolutely flexible thin wire is placed into the vessel (Fig. 87). The ends of the wire are taken out through the holes in the vessel bottom. Gaskets are ideal made, and there is no friction between them and the wire.

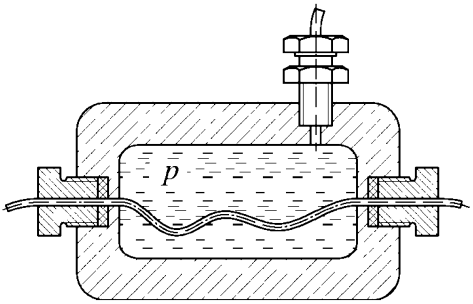

Fig. 87

How will the wire behave, if the pressure p is pumped inside the vessel? What stress state will be in the wire?

92. In one of the books on hydraulics we discovered a description of an experimental assembly for liquid compressibility coefficient determination.

"While determining compressibility of a liquid it is necessary to eliminate the influence of the vessel's extension under pressure action. For this purpose vessel A, filled with tested liquid C and mercury D, is placed in a Reknagel's apparatus filled with water (Fig. 88). Pressure produced on the plunger will according to Pascal law act on mercury and through it on the tested liquid in vessel A, thus compressing it. Vessel A experiences the same internal and external pressure which is why it is not able to change its volume capacity".

Will this arrangement of the experiment eliminate the influence of vessel volume changing under pressure action?

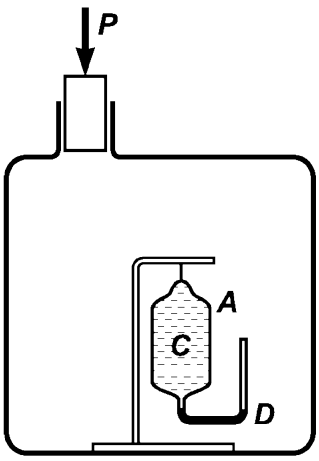

Fig. 88

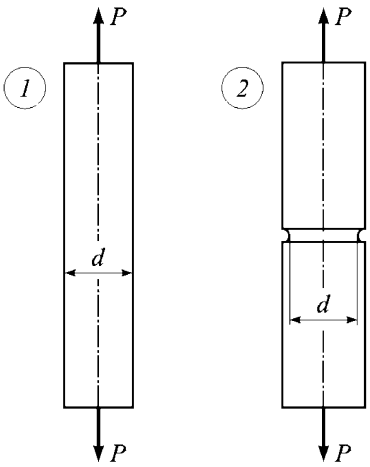

Fig. 89

93. Two rods of soft steel are tested for tension (Fig. 89). The first rod of diameter d is smooth. The second rod has a narrow ring recess. The diameter of the weakened cross-section is also d.

Which rod will withstand greater static load under otherwise equal conditions?

94. What methods can you suggest for embodiment of pure shear?

95. By what method can the all-round uniform tension stress state

$$(\sigma_1 = \sigma_2 = \sigma_3 = \sigma > 0)$$

be put into practice?

96. It was found that while studying material properties under high pressures the straight cylindrical rod loaded by pressure along the cylinder surface and free from faces can be torn under sufficiently high pressure with forming of a neck as shown in Fig. 90. So-called "cross-cutting" will take place.

Explain the reasons of this type of breakdown.

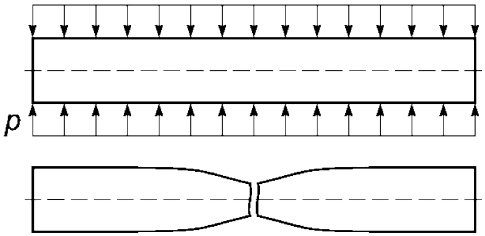

Fig. 90

97. A specimen with annular recess was made from material having the tension diagram shown in Fig. 91a. The normal stress diagram along the cross-section in the recess zone according to the theoretical investigation of G.V. Ugik [20] has the form of the curve shown in Fig. 91b.

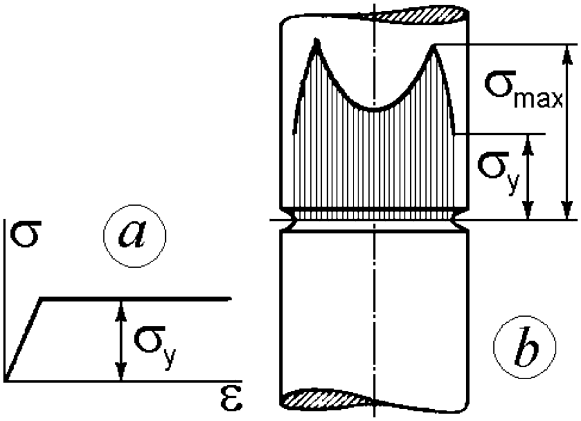

Fig. 91

However, from the tension diagram one can see that $\sigma_{\max}$ cannot be greater than σ_y. Thus the stresses diagram, shown above, gives reason for doubts in its validity and in the correctness of calculations by which it was obtained.

Are these doubts justified?

98. There is a long stretched strip with a hole (Fig. 92). Can you show a point where the stress state will be uniaxial compression with the same stress σ as when the strip is stretched?

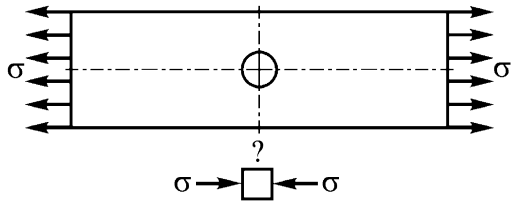

Fig. 92

99. A thin-walled circular cylinder with a small hole in the wall is twisted by moments M and simultaneously stretched by forces P (Fig. 93).

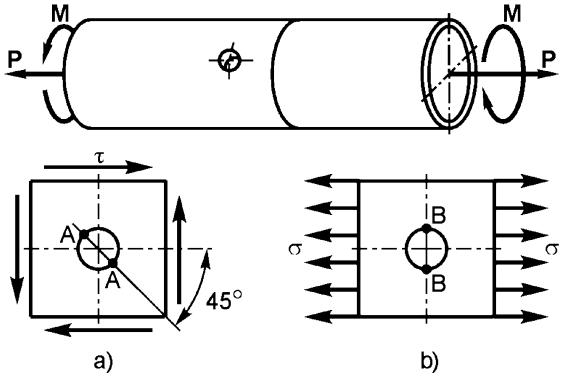

Fig. 93

If the cylinder was only twisted, then maximum stress $\sigma_{\max}$ would take place in points A (Fig. 93a) and would be equal to 2τ. If the cylinder were tensed only, then stress $\sigma_{\max}$ would take place in points B (Fig. 93b) and would be equal to 3σ.

What is $\sigma_{\max}$ when torques M and forces P act simultaneously? What point will this stress occur in? Only local stress reference data should be used for solution.

100. A straight beam of circular cross-section is twisted by two moments M. Plastic deformations occur in the beam under this loading. How can the relationship between torque moment M and twist angle θ be determined if the tension diagram of the material $\sigma = f(\varepsilon)$ is given?

101. What number of elastic constants does one have to introduce in order to characterize the elastic properties of wood completely?

102. Elastic constants of a composite material were obtained after testing of its sheet. It was determined that $E_1/E_2 = 16$ and $\mu_{21} = 0.32$. The result was shown to a specialist who categorically said that there had to be a mistake.

What was his confidence based on?

103. A sheet of plywood is an example of an anisotropic plate. If we cut from it two differently directed strips (Fig. 94) then during tensile testing they will obtain different elongations under equal force.

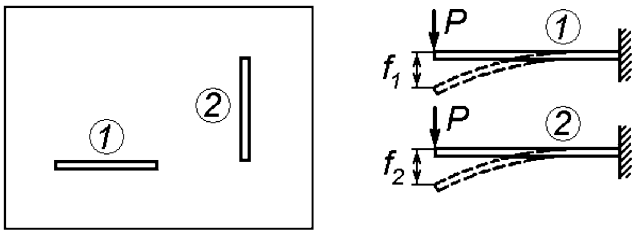

Fig. 94

Let tensile elasticity modulus of the first strip be E_{1t} and of the second - E_{2t}.

Can we say that deflections f_1 and f_2 of the strips under bending will relate as E_{2t}/E_{1t}?

104. The wire netting of a "halffang" braiding (Fig. 95) is loaded in its plane. If the number of cells is large then the netting can be treated as a solid medium with anisotropic properties. The reduced moduli of elasticity along axis 1 and 2, Poisson's ratios and shear modulus are to be determined. Parameters of cells a, b, α and bending rigidity of the wire are given.

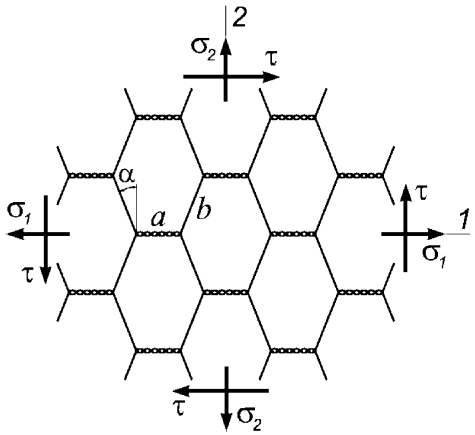

Fig. 95

105. For the determination of "filament-matrix"-type composite materials' reduced (averaged) stiffness characteristics the following model is often used (Fig. 96). Constituent elements of the composite are represented as interlacing strips attached to each other. Elasticity moduli of the strips for filament and matrix will be E_f and E_m, respectively.

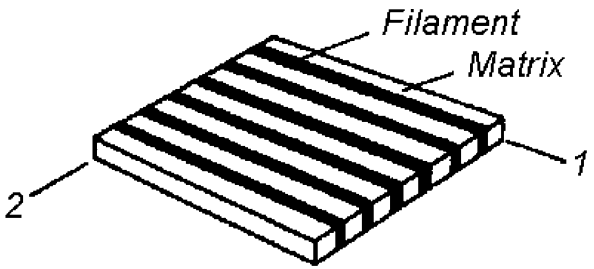

Fig. 96

Determine the elasticity moduli of the composite along axis 1 and 2, respectively.

106. The elasticity modulus of a crosshatch reinforced ($\pm\varphi$) material (Fig. 97a) was found by testing one-directional reinforced specimens that were cut off by the angle φ to the axis of tension (Fig. 97b) for simplicity.

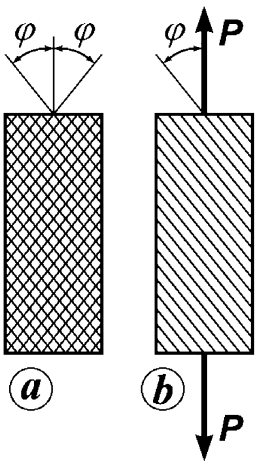

Fig. 97

Is it permissible to use such a method?

107. A tensile test was carried out for two specimens cut from sheet material in two orthogonal directions. Moduli of elasticity occurred to be equal. Does it prove that the sheet is isotropic in its plane?

4. Stability

108. A slender elastic rod is installed in a vertical guide (Fig. 98). The low end of the rod is fixed in a moving plug supported by a spiral spring having stiffness c $(\lambda = P/c)$. As compressive force P grows the length of the rod's prominent free part $l - \lambda$ decreases and the length of the rod's lower part λ increases. What value of stiffness c is necessary to prevent buckling of the rod's upper part as well as of the lower one while the rod moves down to value l ?

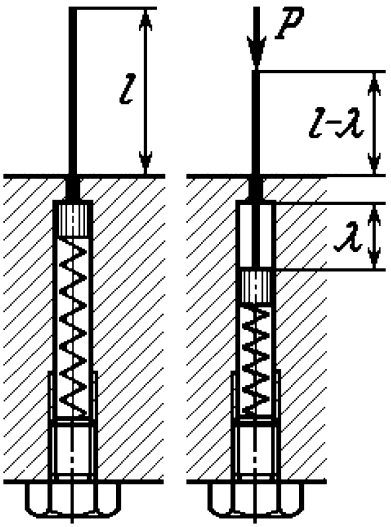

Fig. 98

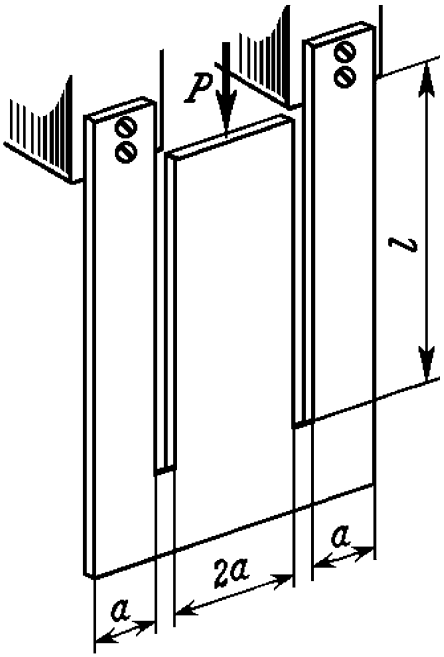

Fig. 99

109. A shaped plate is fastened and loaded as shown in Fig. 99. Determine the critical force for the plate in two cases:

1) force is directed downward; 2) force is directed upward.

The bending rigidity of the middle part is equal to the sum of the outer parts' rigidities.

110. A long bolt is inserted with clearance into a tube (Fig. 100).

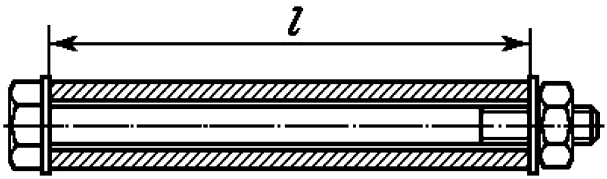

Fig. 100

Determine the bolt tightening force P under which the system will loose its stability. The tube has such dimensions that it must be analyzed as a long rod, but not as a shell. Bending rigidity of the tube is E_1J_1, of the bolt - E_2J_2.

111. Find the critical buckling value of force P for the column shown in Fig. 101. The ends of the column are pinned and have neither horizontal nor vertical displacements.

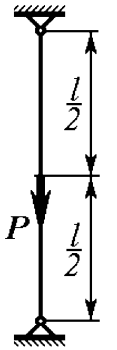

Fig. 101

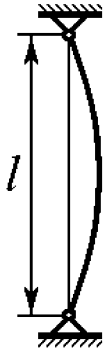

Fig. 102

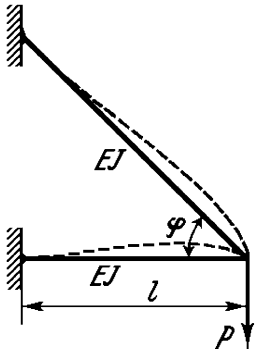

Fig. 103

112. The pin-ended column (Fig. 102) is heated uniformly. Let's find the normal compressive force supposing that the supports are absolutely incompliant. It evidently has the value $N = \alpha t EF$. Under force $N = \pi^2 EJ/l^2$ the straight-line mode of the column's equilibrium becomes unstable and the column will buckle under further heating. Then the critical temperature will be $t_{cr} = \dfrac{\pi^2 J}{\alpha F l^2}$.

However, there is the following doubt concerning this result. While we consider the problem of buckling for a column compressed by load P we suppose that force P does not change during buckling and is independent on column bending. And in the given case force N must decrease even under the smallest bending of the column, so there is no reason to apply formally the solution of Euler's basic problem to this case. That is why the critical force N here may be something different than $\pi^2 EJ/l^2$.

How can we clear this doubt?

113. The energy method is the main approximate method of critical force calculation. The sought buckling mode is taken approximately. This function must satisfy boundary conditions and be as close as possible to true equilibrium mode which is unknown to us but intuitively proposed in accordance with problem physical essence.

The question is whether the danger of obtaining an inexact value of the critical load exists here even when the approximate function is infinitely close to the exact shape of the rod deflection curve?

114. Find the critical force for the outrigger shown in Fig. 103.

The rods are clamped at left ends and rigidly connected with each other at right ends. Assume that buckling occurs in the plane of the rod system.

115. A plane square articulated frame consisting of rigid rods is stiffened by two elastic diagonal rods of length $2l$ connected with each other (Fig. 104).

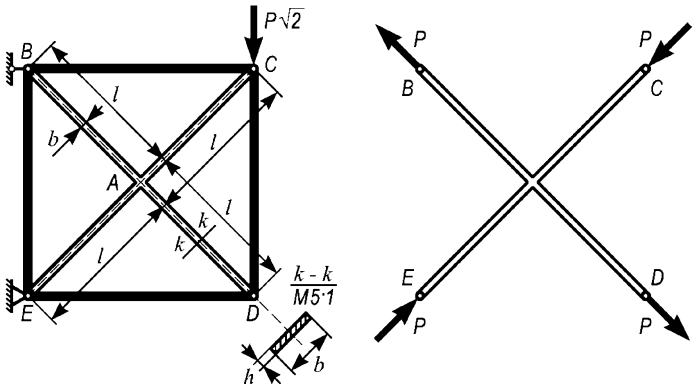

Fig. 104

Diagonal rods have a rectangular cross-section with measures b and h $(b >> h)$. If the frame is loaded by force $P\sqrt{2}$ as shown in Fig. 104 then one diagonal is stretched and another is compressed by forces P.

What value of force P will cause the rods' buckling out of the frame plane?

116. It is well known that a long straight rod twisted by two moments can loose its stability under certain conditions. Such type of buckling is observed in the most visual form in case of thread and cable torsion.

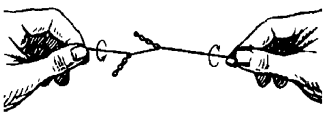

Fig. 105

If the thread is twisted, it quickly obtains a curvilinear shape approximately like the one presented in Fig. 105. It is absolutely evident that if the thread is stretched under torsion then we obtain a visible increase in torque

under which the thread looses stability. It is always necessary to stretch a cable during winding processes.

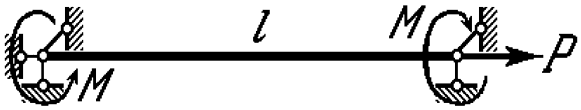

Fig. 106

Taking a simply supported rod (Fig. 106) as an example, determine the critical value of torque and ascertain its dependence on tensile force.

117. A rod with constant cross-section area A is subjected to uniform pressure p (Fig. 107). It is obvious that under these conditions axial compressive force $P = pA$ acts on the rod. Can this force cause the rod' buckling under sufficient pressure value?

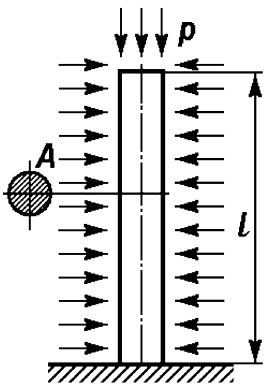

Fig. 107

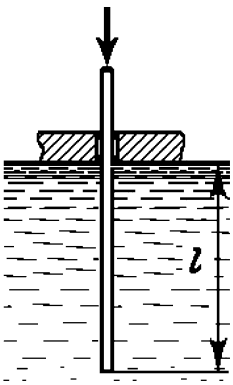

Fig. 108

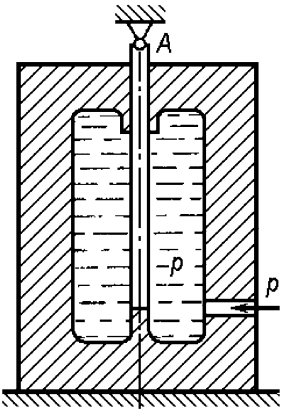

Fig. 109

118. A straight wooden rod of constant cross-section is immersed by its lower end into water. The rod is clamped at the water level (Fig. 108). Can this rod buckle under action of Archimede's buoyant force in case of sufficiently large length l?

119. A rod is effected by lateral pressure (Fig. 109). The upper end of the rod is taken out of the vessel through the gasket. If the pressure grows, the rod must elongate (Poisson's ratio is not equal to zero). But elongation is restricted by the rigid support A, and compressive force occurs in the rod.

Can the rod loose its stability under action of this force ?

120. A tube clamped at its base (Fig. 110) is filled by a liquid of specific weight γ through the upper hole. Can this tube loose its stability like a Euler column during filling?

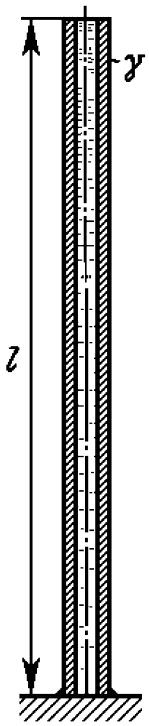

Fig. 110

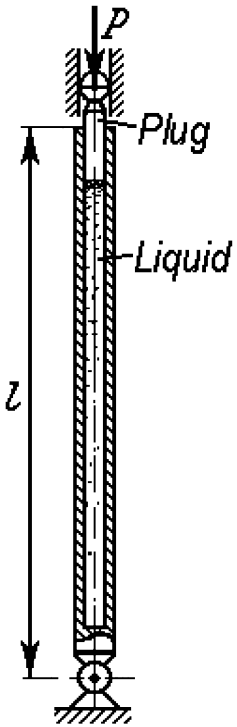

Fig. 111

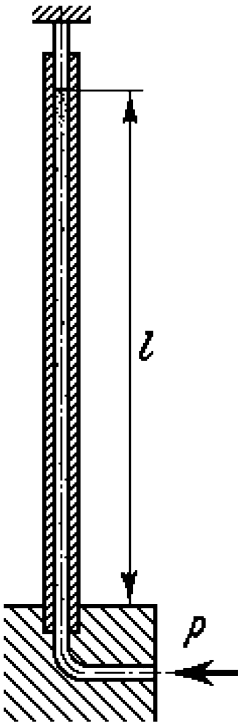

Fig. 112

121. A thick-walled straight tube is filled by an incompressible liquid (Fig. 111). A plug is inserted without friction into the upper hole of the tube. The tube and plug are pinned as shown in Fig. 111. When the load P is applied to the plug, the liquid is compressed but compressive force in the tube is absent.

Can this tube loose its stability in Euler's sense under these conditions?

122. The upper hole of a thin long tube is slipped over a solid stationary plug without friction. The lower end of the tube is clamped in a solid foundation. Pressure p is fed into the tube (Fig. 112). Can this tube buckle under sufficiently high pressure?

123. A liquid of specific weight γ runs through the tube pinned at both ends (Fig. 113).

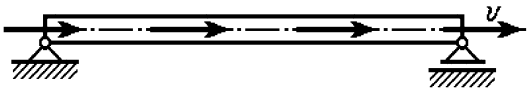

Fig. 113

Show that under some value of liquid velocity v the tube looses its stability like Euler's column.

124. Let us consider the following problem. A rod having roundings of radius R at its ends (Fig. 114) is compressed without friction between two solid slabs. It is necessary to determine the critical load.

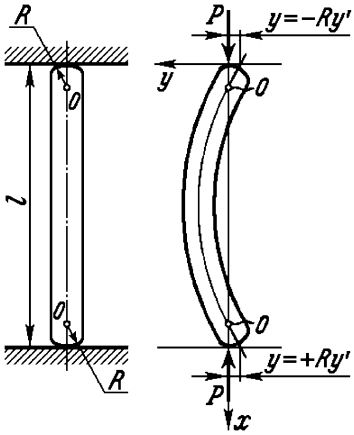

Fig. 114

Taking the line of compressive forces action as the x axis and designating the lateral deflection of the beam axis as y we obtain as usual:

$$EJy'' + Py = 0, \quad y'' + \alpha^2 y = 0,$$

$$y = A\sin\alpha x + B\cos\alpha x \quad \left(\alpha^2 = \frac{P}{EJ}\right)$$

The deflection y at the rod ends is proportional to the angle of rotation y', i.e. $y = -Ry'$ under $x = 0$. As the negative deflection y corresponds to the positive angle of rotation y' the sign before Ry' is negative. Thus we get

$$B = -\alpha RA\,, \quad y = A\,(\sin\alpha x - \alpha R\cos\alpha x)\,.$$

In addition, $y = +Ry'$ under $x = l$; here y is positive for positive y'. Hence

$$A\,(\sin\alpha l - \alpha R\cos\alpha l) = A\,(\alpha R\cos\alpha l + \alpha^2 R^2\sin\alpha l)$$

As $A \neq 0$ we obtain

$$\tan\alpha l = \frac{2\alpha\dfrac{R}{l}}{1 - (\alpha l)^2\dfrac{R^2}{l^2}}\,. \tag{1}$$

Solving this transcendental equation we determine the least non-zero value of αl dependent on the relation R/l and then find the critical load.

As $\alpha^2 = P/(EJ)$ the critical load is equal to

$$P_{cr} = \frac{(\alpha l)^2\,EJ}{l^2} \tag{2}$$

The first (the least) root of equation (1) must be substituted here instead of αl.

Now let us find the least root αl of equation (1) as a function of R/l. The most convenient way to ascertain this relationship is specifying values of αl and then determining R/l from equation (1).

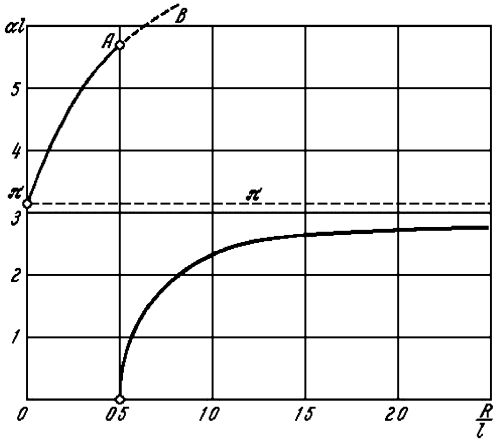

Fig. 115

The calculation results are shown as a curve (Fig. 115). We reveal that $\alpha l = \pi$ in case of $R/l = 0$, and therefore according to (2) :

$$P_{cr} = \frac{\pi^2 EJ}{l^2}$$

The critical load is equal to the ordinary Euler force as one would expect.

As R/l increases the value of αl grows too. Hence the critical load also increases. It also seems to be sufficiently obvious. But when $R/l = 0.5$ the critical load vanishes (falls to zero value) as it follows from the curve and then while further ascending of radius R the critical load begins to grow again tending under $R/l = \infty$ to a limit equal once more to Euler's force.

Interpret the result obtained above.

125. A long elastic rod with pinned ends is inserted with clearance Δ into a rigid channel (Fig. 116). What stresses will arise in the rod and what will the deflection curve be if the rod is compressed by a force greater than the first critical load, i.e. greater than $\pi^2 EJ/l^2$?

Assume that only in-plane bending is possible. Bending rigidity is EJ.

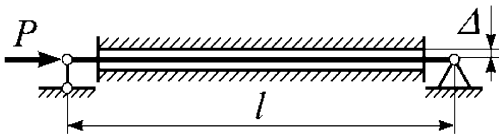

Fig. 116

126. The set of the previous task is slightly changed. Now let us consider the behavior of a rod with circular cross-section installed in a tube. Clearance remains the same: Δ.

The question is what stresses will arise in the rod if it is compressed by the force greater than the first critical load that is greater than $\pi^2 EJ/l^2$? Bending rigidity is EJ.

127. Determine the critical force for a column with two ends clamped.

The column has different bending rigidities (EJ_1 and EJ_2) depending on the sign of the bending moment. For example, such properties take place if a beam has cutouts with tightly inserted plates at one side (Fig. 117).

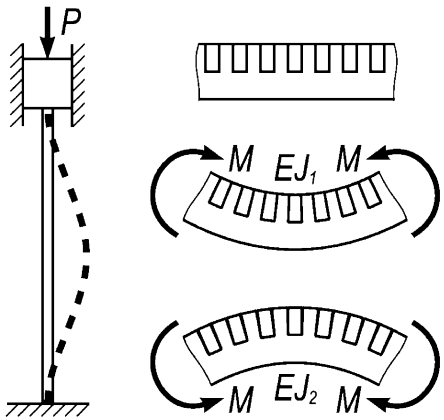

Fig. 117

Different bending rigidity depending on the sign of the bending moment occurs also in the case of a compressed rod with nonsymmetrical cross-section under plastic deformation (see problem 158).

128. A clamped at its base column has an axial through hole (Fig. 118). A flexible rope is inserted without clearance and friction into the hole. The rope is attached to the free end of the rod. Can this rod loose its stability if we suspend a sufficiently large weight P to the rope?

129. The scheme considered in the previous problem is changed. The rope is inserted with clearance of value Δ to each side of the hole (Fig. 119). Determine the lateral deflection f of the rod's free end in dependence of load P.

130. A cantilever column is loaded at its free end by a vertical compressive force transmitted by a rope (Fig. 120). Transfer of force through the rope occurs in two variants. In the first case the rope falls down freely. In the second case the rope is thrown over two rigid blocks without friction. What case yields a greater critical load P_{cr} for the column?

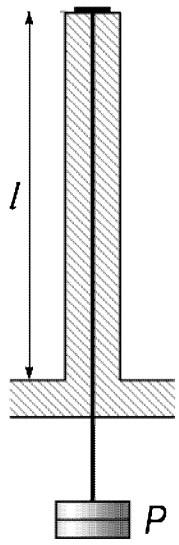

Fig. 118

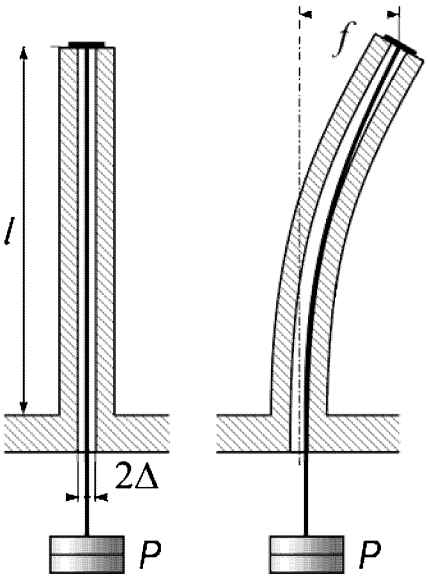

Fig. 119

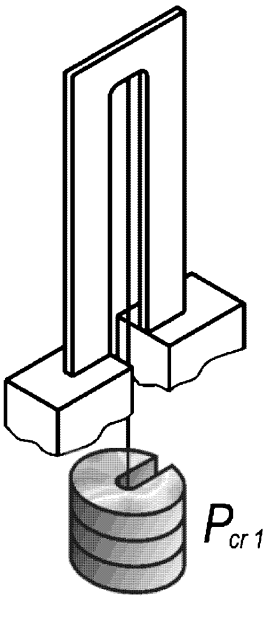

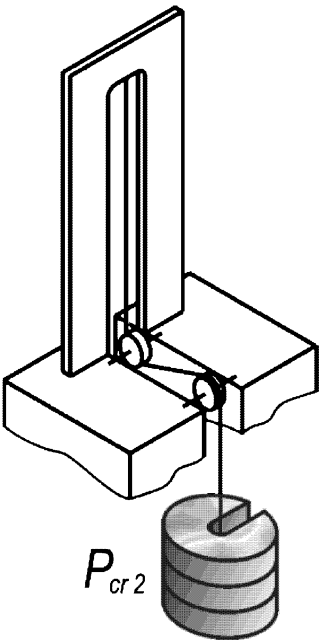

Fig. 120

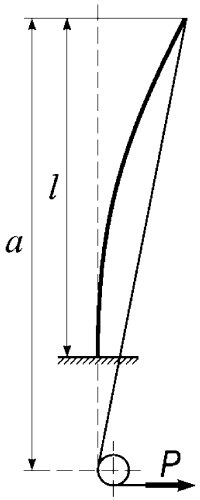

Fig. 121

131. The following problem can be set in conjunction with the previous question. Determine the critical load for a column of length l in dependence on distance a from the column's free end to the block (Fig. 121).

132. Two rods of equal rigidity but of different length are compressed by longitudinal force P (Fig. 122).

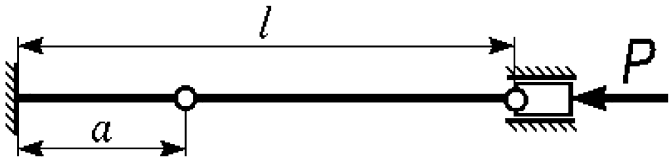

Fig. 122

What distance from the clamp point does one have to place a pin in order to get equal buckling safety factors for both rods?

133. A rope is thrown without friction over the block at the rod's end and the load $P/2$ is applied to the rope's free end, so the rod is compressed by force P. The left end of the rope is steady fixed (Fig. 123).

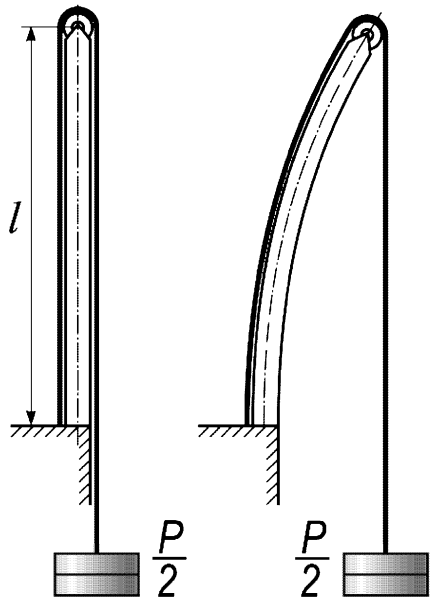

Fig. 123

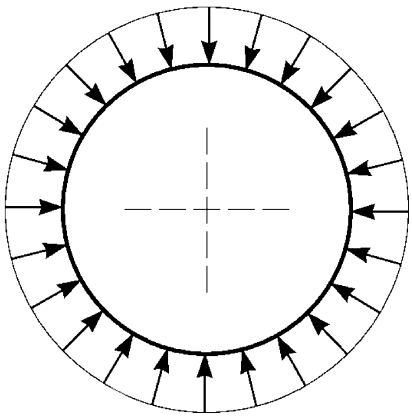

Fig. 124

Under deflection of rod from its vertical position the left half of the rope lays tightly upon the lateral surface of the rod and causes contact pressure. The rope at the right side of the rod freely takes a vertical position.

Calculate the critical load.

134. A ring is subjected to an external uniformly distributed load (Fig. 124). Will any difference be observed in values of the critical load: a) if it is caused by pressure which is permanently normal to the arc of the ring; b) if it is caused by radial forces directed permanently to the center?

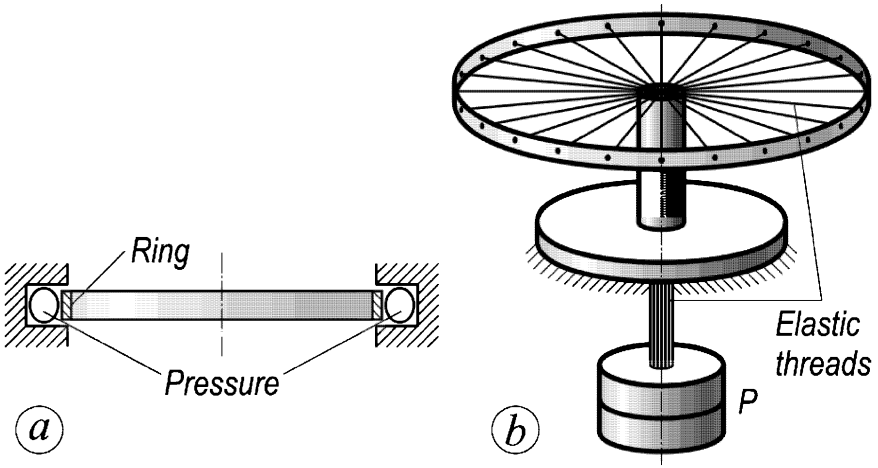

Fig. 125

The first case of loading may be implemented, for example by pressure of air injected into a plastic ring bag (Fig. 125a), and the second one – by set of a large number of elastic threads passing through a centrally arranged stationary bush (Fig. 125b).

135. Pressure p is supplied in the volume between a cylinder and two pistons (Fig. 126). Arising forces are transmitted to a strip of length l through the piston rod and two connecting rods. Thus we obtain that the strip is loaded by two equal opposite forces P subjected to its end.

Is this state of equilibrium stable?

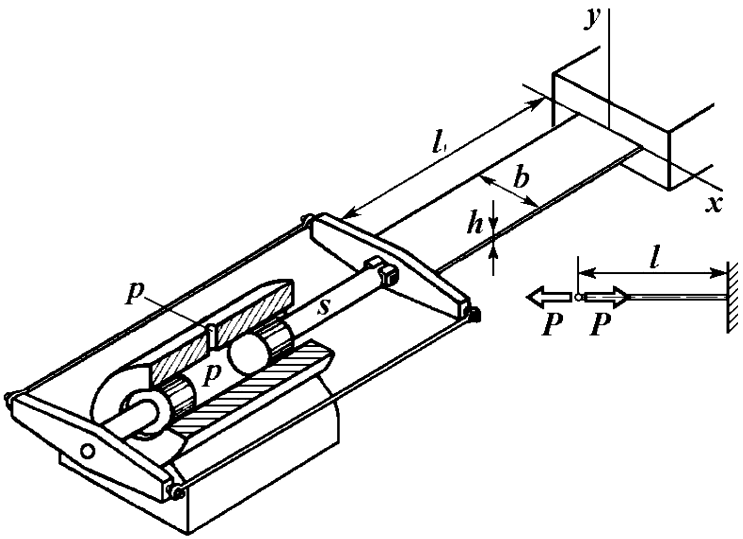

Fig. 126

136. A column clamped at its lower end is loaded on the upper end by two equal and opposite moments created by four weights P (Fig. 127).

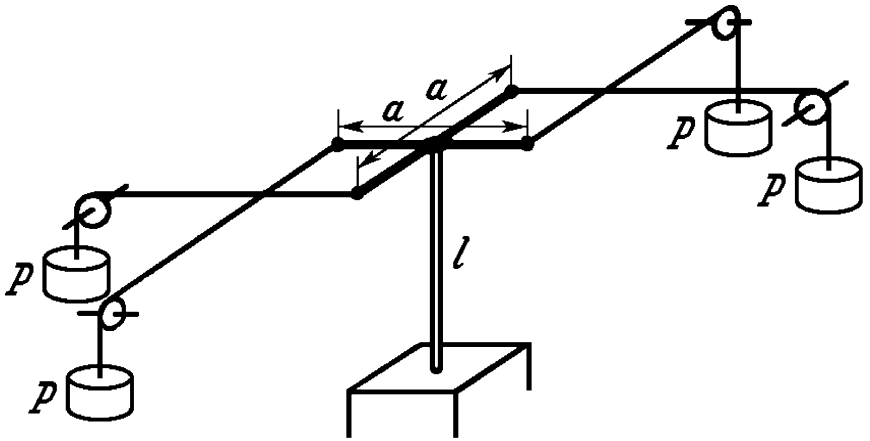

Fig. 127

Investigate the system's stability.

137. The following question arises in connection with the previous problem: Would the critical moment value depend on the forces arms orientation with respect to the principal axes of the column cross-section?

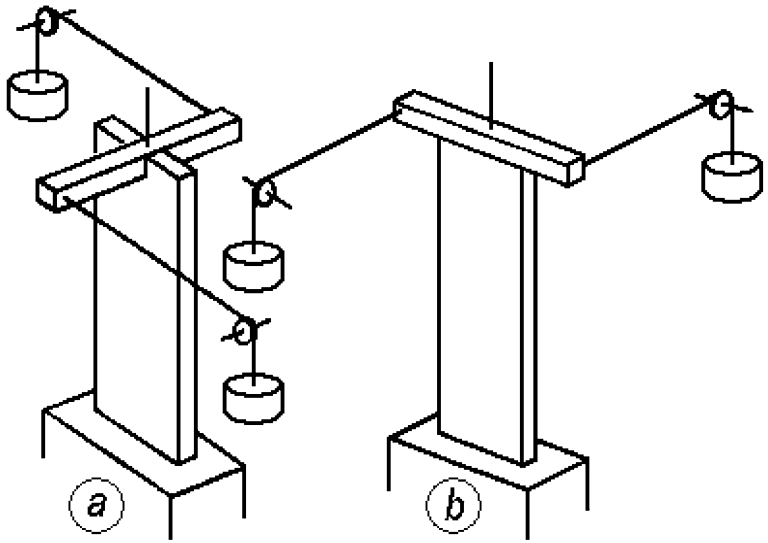

Fig. 128

In case a (Fig. 128) the plane of the moment M rotates together with the end cross-section of the column under bending in the plane of minimum rigidity and in case b— under bending in the plane of maximum rigidity.

138. How does the critical load P depend on the bowl radius R (Fig. 129)?

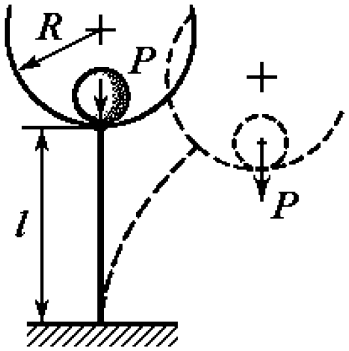

Fig. 129

139. A question about stability of the structure shown in Fig. 130 arises during water-tower design. What tank filling liquid level h will cause loss of the supporting mast's stability?

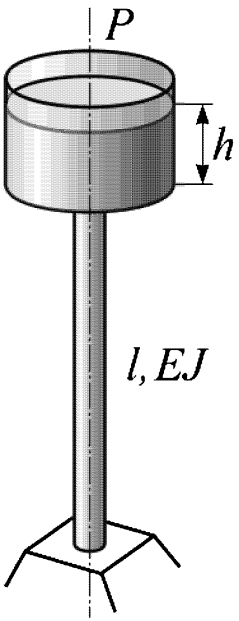

Fig. 130

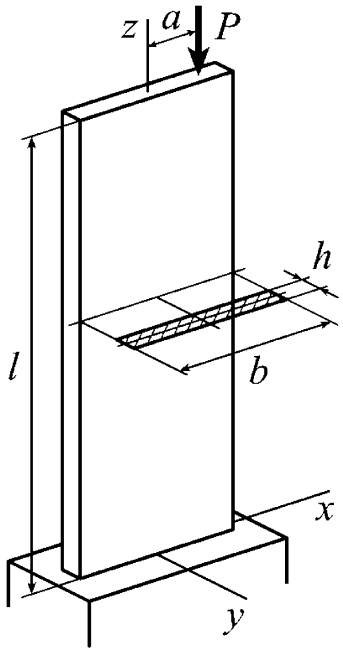

Fig. 131

140. Let us imagine a rod with narrow rectangular cross-section clamped at its lower end (Fig. 131). If load P is central then its critical value is known to be equal to $\pi^2 EJ/(4l^2)$. What will be the change in this result if the point of load application is displaced along axis z by the value a from the cross-section centroid?

141. A column with plane ends is compressed between two slabs (Fig. 132a). Two main equilibrium deflection curves are possible under buckling: the first one shown in Fig. 132b occurs under critical load

$$P_{cr} = \frac{4\pi^2 EJ}{(2l)^2} ,$$

and the second one shown in Fig. 132c occurs in case when the column leans on slabs by its corners only. It is evident that if column ends are not very wide then the second mode buckling will take place under load lower than for the first case. In particular, if the width of the column ends vanishes, the critical load will be $P_{cr} = \frac{\pi^2 EJ}{(2l)^2}$ .Determine the minimal critical load for the case when each end width is equal to $2e$.

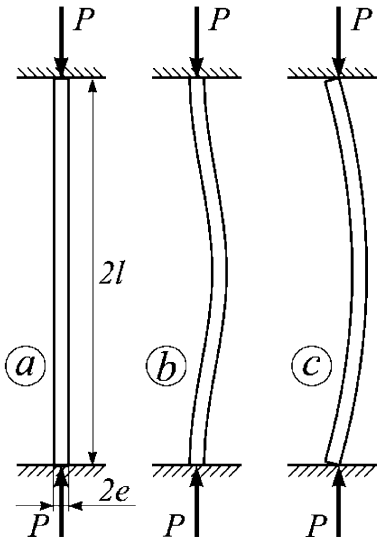

Fig. 132

142. A weightless beam clamped at its right end (Fig. 133) lies freely on a rigid base. The beam is loaded by force P applied at the free-end cross-section centroid and directed at angle δ to the rigid base.

What value of load P will cause the loss of the beam's stability? Angle δ value is given.

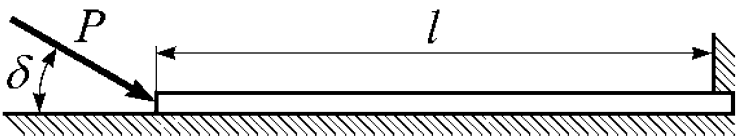

Fig. 133

143. An absolutely flexible non-stretched slender thread is fit over a thin-walled ring. Then the thread is tightened by force P (Fig. 134). Determine under what value of force P the ring will loose its stability. Friction between thread and ring surface may be neglected.

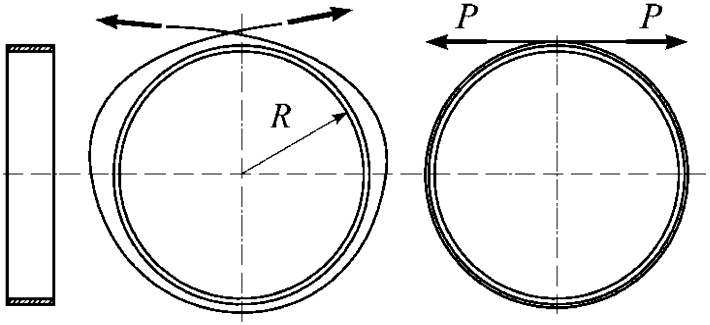

Fig. 134

144. A slender elastic rod simply supported at its ends is compressed by longitudinal force

$$P = \frac{10\pi^2 EJ}{l^2} .$$

Additional constraints placed between supports (Fig. 135) prevent the rod from buckling. The straight equilibrium mode of the rod without constraints would become unstable just under the load equal to $P/10$. It is known that at the force variation interval between $\pi^2 EJ/l^2$ and $10\pi^2 EJ/l^2$ there are two more values of critical load: $4\pi^2 EJ/l^2$ and $9\pi^2 EJ/l^2$. They correspond to the rod buckling modes with two and three half-waves.

Suppose that intermediate constraints supporting the rod are suddenly removed. Then the rod will undoubtedly buckle. But how will it buckle? By one, two or three half–waves?

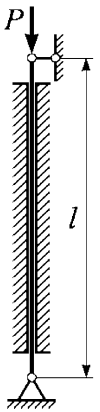

Fig. 135

145. A column (Fig. 136a) is clamped at its base. A force P directed permanently along the tangent to the rod's deflection curve is applied at the free end. Such load can be put into practice, for example by installation of a powder jet engine at the free end of the column (Fig. 136b). Analyze system stability.

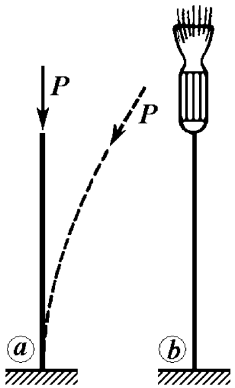

Fig. 136

146. A column clamped at its base has a rigid disk at its free end. The force P is applied to the disk at the point constantly disposed on the x axis (Fig. 137).

Analyze system stability for two cases:

a) The force P is generated by the flow of inelastic particles impacting the disk. In this case the direction of vector P remains unchanged under disk rotation.

b) The force P is applied to the disk through the roller connected by a plunger with the weight. In this case force P follows the perpendicular to the disk.

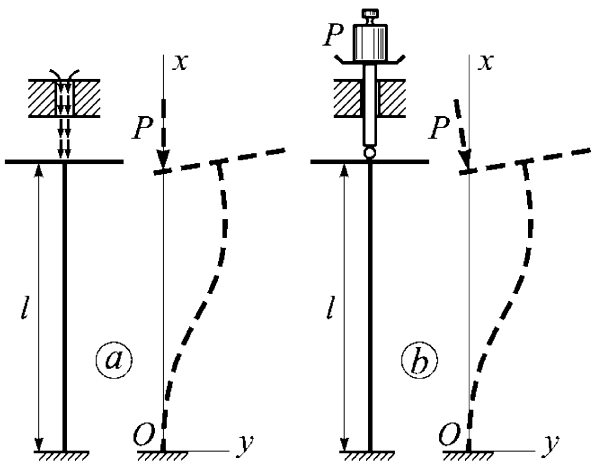

Fig. 137

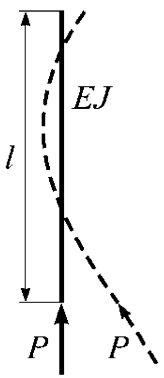

Fig. 138

147. A slender elastic homogeneous rod moves with constant acceleration under action of follower force applied at one of its ends (Fig. 138). Analyze the rod's straight configuration stability.

148. A homogeneous bar is compressed by two follower forces (Fig. 139). Analyze the system stability.

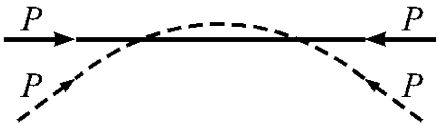

Fig. 139

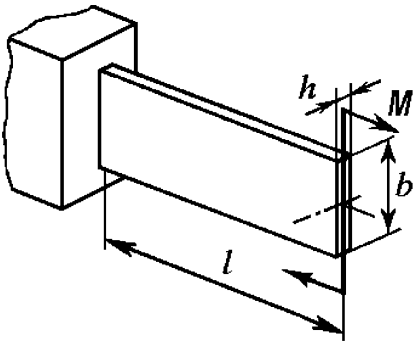

Fig. 140

149. Derive the value of moment M under which the cantilever beam (Fig. 140) will buckle out of its plane. Moment M acts permanently in the vertical plane during bending.

150. Analyze the stability of the cantilever column loaded at its free end by the torque M and the force P which remains vertical under buckling (Fig. 141).

Fig. 141

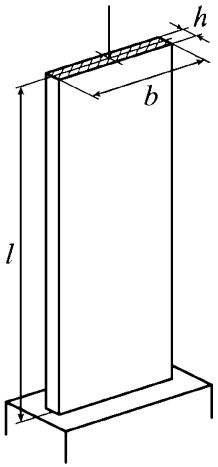

Fig. 142

151. A thin long strip (Fig. 142) is heated uniformly along length l and thickness h but irregularly along width b.

Derive the conditions when the strip looses its stability under twisting.

152. Study the stability of a cantilever pipe conveying fluid (Fig. 143). Assume that the parameters of the pipe and of liquid flow are specified.

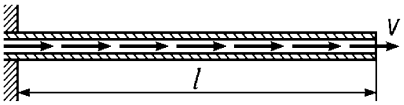

Fig. 143

153. Problems connected with plane bending mode stability are formulated in most monographs and manuals on stability of elastic systems with implicit assumption that the bending moment is applied in the plane of maximal rigidity (Fig. 144).

Can the plane bending mode of stability loss take place if the bending moment is applied in the plane of minimal rigidity and not in the plane of maximal rigidity?

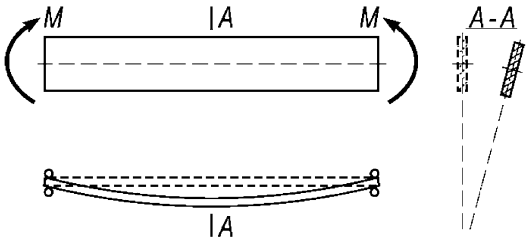

Fig. 144

154. The ring of radius R and rectangular cross-section (Fig. 145) is turned inside out in such a way that its internal surface becomes an external one and the external surface turns out to be inside. Under what ratios of b and h will this equilibrium configuration be stable? The strain state is considered to be elastic.

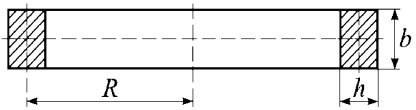

Fig. 145

155. A ring of rectangular cross-section (Fig. 146) is heated at the inner or external side. Thus the temperature varies along the ring thickness h . Derive the conditions of initial equilibrium mode stability supposing that $h << R$. Assume the linear law of temperature variation.

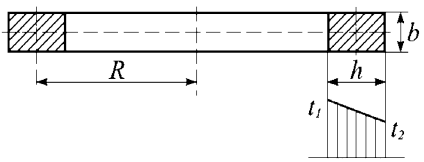

Fig. 146

156. An elastic ring of radius R and rectangular cross-section is cut through and then unrolled by two moments until its axis becomes straight (Fig. 147). The rod which is obtained in such a manner is clamped at its ends. Under what conditions will this equilibrium configuration be stable?

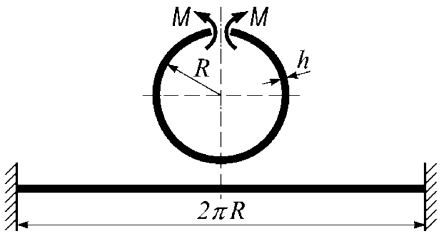

Fig. 147

157. Following schematically set problem that has obvious applied significance is considered.

The structure which represents a large plane ring is assembled in outer space. It consists of sections that are transported to orbit and attached there to each other. When the time has come to attach the last section to the first it was discovered that there were disparities of dimensions in the plane of the ring: along the tangent to the arc of the ring's axis Δ_1, along radius Δ_2 and also angular disparity ϑ (Fig. 148).

These disparities were forcedly eliminated and the ring was assembled. Internal normal and transverse forces and a bending moment also occur in the plane of the ring.

The question arises: Is the plane equilibrium mode stable or unstable? Under large values of disparities Δ_1, Δ_2 and ϑ the ring's buckling out of plane is apparently possible. And if torsional stiffness is insufficient then ring axis transformation into some similarity of the spatial figure eight cannot be excluded. Buckling in the plane of the ring may be possible too, when the ring, remaining plane, significantly deflects from a circular shape.

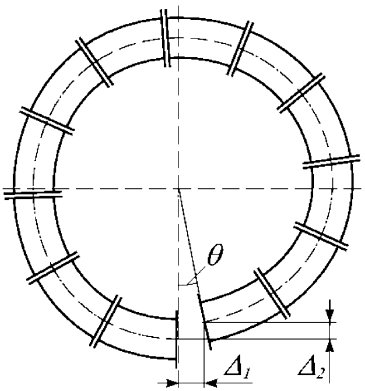

Fig. 148

158. A column of channel cross-section (Fig. 149) is compressed by central axial force P causing plastic strains in it. The question is to which side will the column most probably deflect under buckling: to the left or to the right?

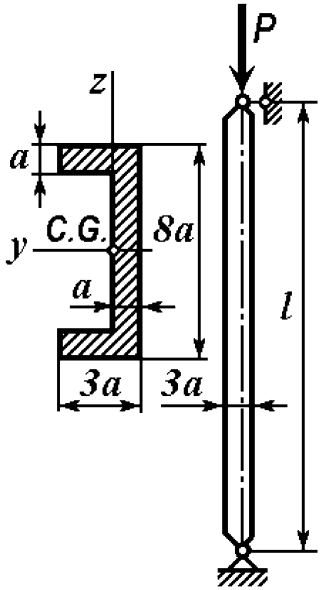

Fig. 149

159. Is buckling of a helical cylindrical spring under tension possible?

160. Two rods are loaded at a common node by force P (Fig. 150). Each rod is a telescopic device allowing large variations of length.

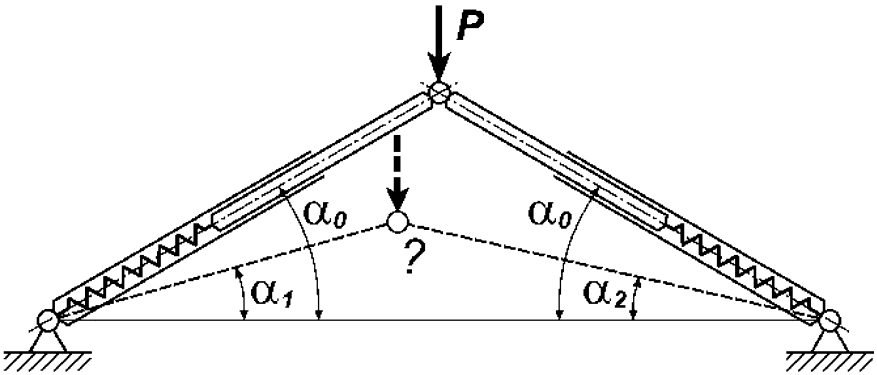

Fig. 150

Could conditions exist under which the transfer from symmetric to non-symmetric equilibrium mode is possible?

161. A straight homogeneous rod is in a state of full weightlessness (in interstellar space). But it has nonzero mass and all its particles gravitate to each other in accordance with Newton's law.

Can this rod loose its stability in Euler's sense due to mutual gravity forces and under what conditions may it happen?

162. The set of the previous problem is preserved. But now the matter concerns a circular homogeneous ring and not the rod.

163. Four identical balls of mass m are attached at rods as shown in Fig. 151.

The system is rotating about axis CC fixed in rigid bearings. If there were no bearings (the system, for example, would be hung from a thread) then as it is well known from physics the balls would rotate about axis AA and take up a position in a horizontal plane. In the given case the rigid bearings and elastic rods AA of circular cross-section oppose such rotation. Is it possible to select such angular velocity ω under which the balls will nevertheless rotate for some angle about the AA axis?

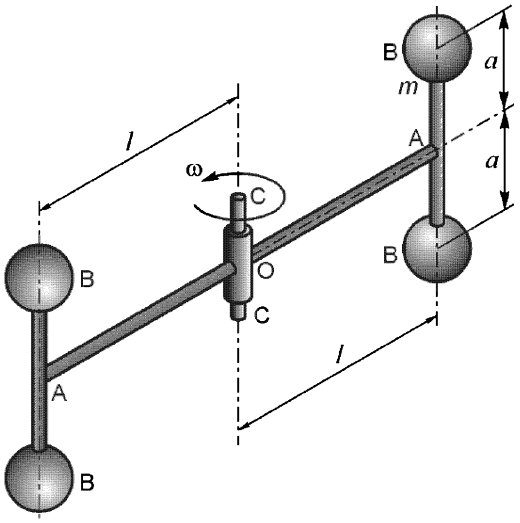

Fig. 151

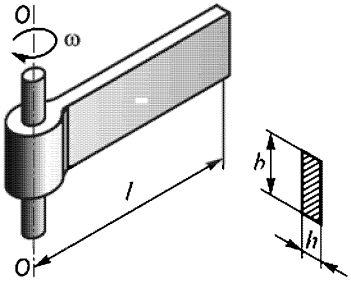

Fig. 152

164. A homogeneous rod of narrow rectangular cross-section is rotating about the axis OO (Fig. 152) which is parallel to the larger side of the cross-section. Determine the angular velocity ω under which the rod will be twisted like the rods AA of the system considered in the previous problem.

165. A thin homogeneous disk (Fig. 153) is rotating about the stationary axis normal to its plane. Can this disk loose the stability of its plane equilibrium mode?

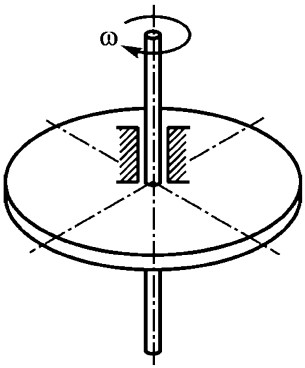

Fig. 153

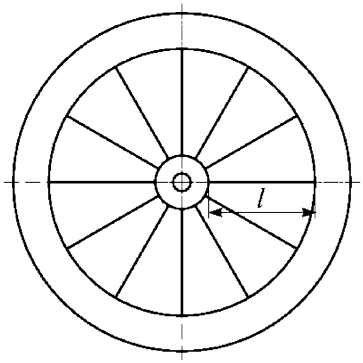

Fig. 154

166. Calculate the critical angular velocity value for a ring of mass m (Fig. 154) connected with its stationary axis by n equally distributed spokes. Tension rigidity of the spoke is EA.

167. A thin closed rubber spherical vessel is under action of internal pressure. Is the spherical shape always stable?

168. Explain from an equilibrium modes stability point of view the formation of a neck under a specimen's tension test.

169. Failure with formation of an inclined wave intersecting annual growth layers (Fig. 155) is often observed under longitudinal compression tests of wooden specimens.

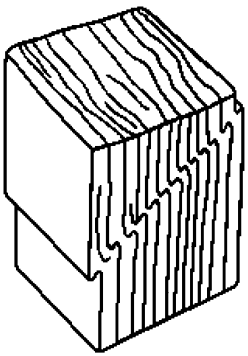

Fig. 155

May this phenomenon be interpreted as a specific example of stability loss?

5. Various Questions and Problems

170. What material has the highest ultimate stress?

171. What material bears a greater load in tension than in compression?

172. What material has the largest elasticity modulus?

173. What material has the smallest elasticity modulus?

174. Does rubber obey Hook's law?

175. Why do thin glass fibres have greater strength than pane glass?

176. Why is the reduced elasticity modulus of rope lower than elasticity modulus of its component threads?

177. It was necessary to make a measurement of the deflection curve that is to establish experimentally the dependence of vertical displacements upon coordinate x for some beam (Fig. 156) loaded by concentrated force P at point A. The shape of the beam was so intricate that calculation of the deflection curve would have been too difficult. The experimenter had only one indicator for deflections measurement as shown in Fig. 156.

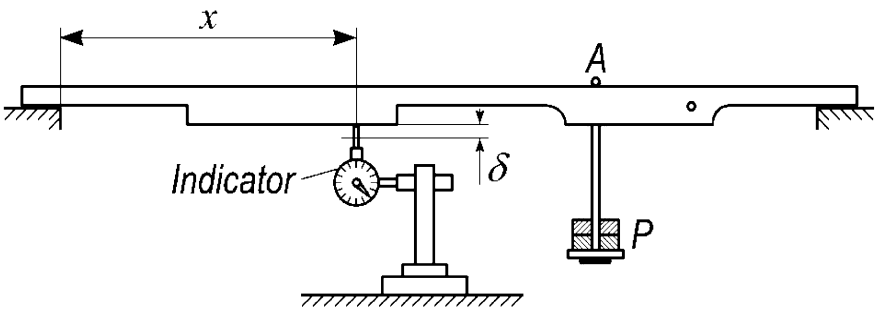

Fig. 156

What is the easiest way to measure the deflection curve under these conditions if it is a priori known that deflections are proportional to the acting force P?

178. Why does twisted thread have a greater strength than an untwisted?

179. A teacher in a student's design project pointed out that the shaft of the designed machine was too long so its rigidity would not be sufficient.

"It can be easily corrected without changing the structure", the student said, "I shall take a higher quality material and make the shaft of alloyed steel."

Was the student right?

180. A solid elastic cylinder of height H and radius R leaning on a rigid plane (Fig. 157) is loaded with gravity forces (weight of cylinder is P). How will its volume change if the cylinder is laid on its side?

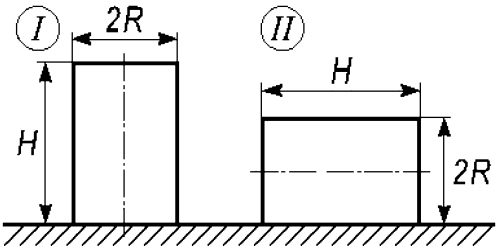

Fig. 157

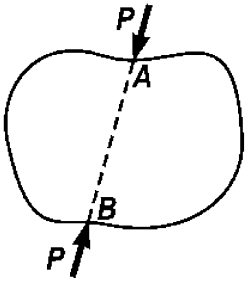

Fig. 158

181. An arbitrary elastic body is compressed by two opposite loads P (Fig. 158). Determine the change of the elastic body volume.

182. The main detail of pressure measuring devices is the so-called Bourdon's spring. It represents a thin-walled tube of a circular axis and oval or some other oblong cross-section (Fig. 159). The tube (1) slightly unbends under action of internal pressure and the tube's ends deflection is transmitted to a manometer pointer by an amplifying mechanism (2) (Fig. 160). The measured pressure value is defined by the pointer's deflection.

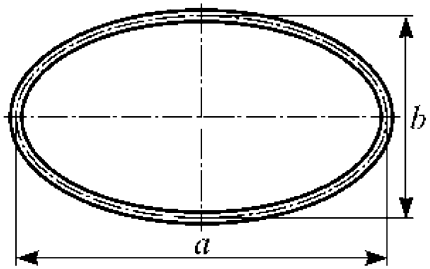

Fig. 159

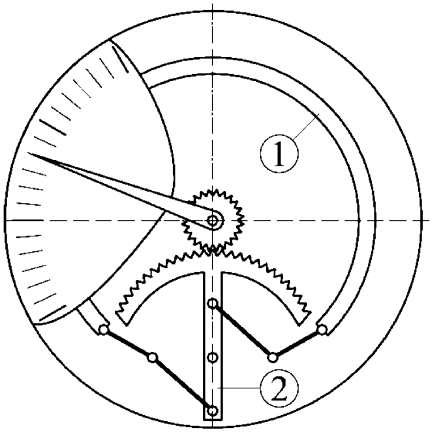

Fig. 160

In one of the books devoted to measuring devices we happened to see the following explanation of Bourdon's tube principle of operation:

"Bourdon's spring operation is based on the fact that pressure inside the tube is greater at the outer surface of the spring than at its internal surface. In fact, if we denote external and internal radii of tube as R_1 and R_2, then areas of the tube's external (S_1) and internal (S_2) surfaces will be equal to

$$S_1 = \frac{2\pi\varphi}{360} R_1 a \quad \text{and} \quad S_2 = \frac{2\pi\varphi}{360} R_2 a\,,$$

where φ is central angle of spring, a is horizontal dimension of tube cross-section, and R_1 and R_2 are radii.

Under the pressure p kN/cm^2 the resultant pressure force on the external surface is

$$P_1 = p\,S_1 \text{ kN}$$

and on the internal one

$$P_2 = p\,S_2 \text{ kN}\,.$$

As the force P_1 is greater than P_2 then it tends to unbend the spring."

Is this explanation correct?

183. Let us consider the closed toroidal shell of a car wheel tire inner tube type (Fig. 161) loaded by internal pressure p and derive stresses arising in this shell.

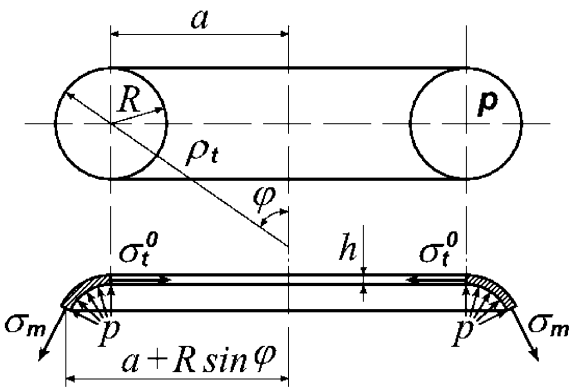

Fig. 161

From the equilibrium condition of the shell part cut off by cone section (Fig. 161) we obtain

$$p\pi[(a + R\sin\varphi)^2 - a^2] = \sigma_m 2\pi(a + R\sin\varphi)h\sin\varphi\,,$$

$$\sigma_m = \frac{pR}{2h}\frac{2a + R\sin\varphi}{a + R\sin\varphi}\,. \tag{1}$$

The circumferential stress σ_t will be found from the Laplace equation

$$\frac{\sigma_m}{\rho_m} + \frac{\sigma_t}{\rho_t} = \frac{p}{h} .$$

In our case

$$\rho_m = R , \quad \rho_t = \frac{a}{\sin\varphi} + R .$$

After substitution of ρ_m, ρ_t and σ_m we obtain

$$\sigma_t = \frac{pR}{2h} . \tag{2}$$

Now we move on to determining the displacements. Let us denote the displacement of the median surface points in the direction perpendicular to the rotation axis as u and displacement parallel to the rotation axis as v (Fig. 162).

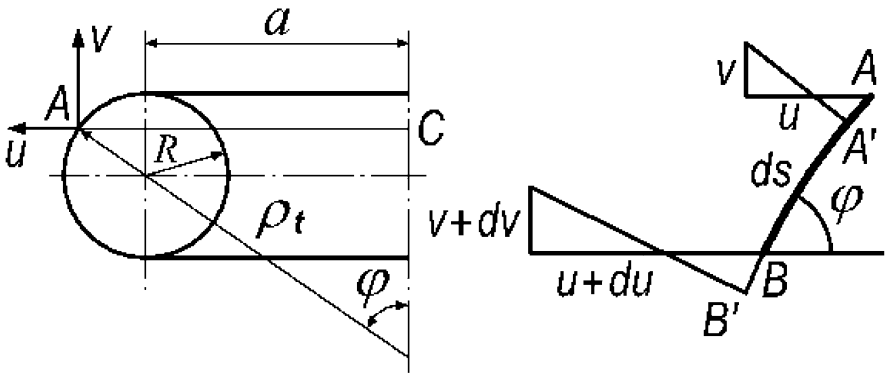

Fig. 162

The relative elongation in the circumferential direction is

$$\varepsilon_t = \frac{u}{AC} = \frac{u}{a + R\sin\varphi} . \tag{3}$$

The relative meridional elongation is

$$\varepsilon_m = \frac{A'B' - AB}{AB} = \frac{BB' - AA'}{AB} .$$

$$BB' = (u + du)\cos\varphi - (v + dv)\sin\varphi ,$$

$$AA' = u\cos\varphi - v\sin\varphi , \quad AB = Rd\varphi .$$

That is why the relative elongation along the meridian is equal to

$$\varepsilon_m = \frac{1}{R}\left(\frac{du}{d\varphi}\cos\varphi - \frac{dv}{d\varphi}\sin\varphi\right) . \tag{4}$$

On the other side

$$\varepsilon_t = \frac{1}{E}(\sigma_t - \mu\sigma_m) , \quad \varepsilon_m = \frac{1}{E}(\sigma_m - \mu\sigma_t).$$

Considering the relations (1), (2) and (3) we find

$$u = \frac{pR}{2Eh}\left[a(1+2\mu) + R(1-\mu)\sin\varphi\right].$$

Then from (4) we obtain

$$\frac{dv}{d\varphi} = \frac{pR^2}{2Eh}(1-\mu)\frac{\cos^2\varphi}{\sin\varphi} - \frac{\varepsilon_m R}{\sin\varphi} =$$

$$= \frac{pR^2}{2Eh}\left[-(1-\mu)\sin\varphi - \frac{a}{\sin\varphi(a+R\sin\varphi)}\right],$$

and integrating we arrive at

$$v = \frac{pR^2}{2Eh}\left[(1-\mu)\cos\varphi - \ln\tan\frac{\varphi}{2} + \frac{2R}{\sqrt{a^2-R^2}}\arctan\left(\frac{a\tan\frac{\varphi}{2}+R}{\sqrt{a^2-R^2}}\right)\right] + C.$$

Constant C defines the displacement of the whole tore as a rigid body along the axis of symmetry and can be set arbitrarily; $\ln\tan(\varphi/2)$ converges to infinity under $\varphi = 0$ and $\varphi = \pi$. Hence at these points the displacement v tends to infinity too. But it is obvious that this displacement can not be infinite. This means that the obtained expression for v does not give a correct solution of the problem.

What is the matter? Where is the mistake?

184. Pressure vessels are used in aircraft and space engineering among other constructive elements. As usual they have cylindrical or spherical shape. The application field makes it extremely important for them to meet the requirement of minimal weight.

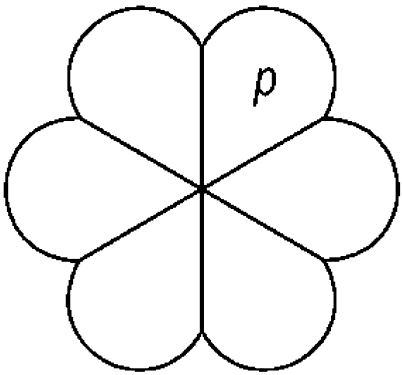

Fig. 163

The profiled cylinder structure shown in Fig. 163 is proposed. The vessel consists of several cylindrical sections connected by radial walls. As the radius of the cylindrical sections is less than the radius of the ordinary cylinder with the same volume then stresses in them will be less too. So one can hope that in spite of weight increase due to the radial walls the whole weight of the structure will be lower. To what extent are these expectations valid?

185. Weight P is put on a spring (Fig. 164). If the spring stiffness is c then the weight displaces down by value $\lambda = P/c$.

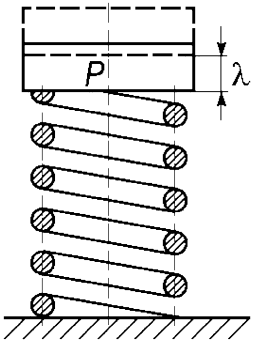

Fig. 164

Therefore the potential energy of the weight (position energy) decreases by

$$P\lambda = \frac{P^2}{c}. \tag{1}$$

The potential energy of the spring in the deformed state will be equal to

$$U_{spr} = \frac{P\lambda}{2} = \frac{P^2}{2c}, \tag{2}$$

i.e. it will be two times less than the energy lost by the weight.

What's the matter? Where did energy disappear?

186. Determine the spring coils rotation angle ψ in the axial plane (draft plane in Fig. 165) under compression of the spring.

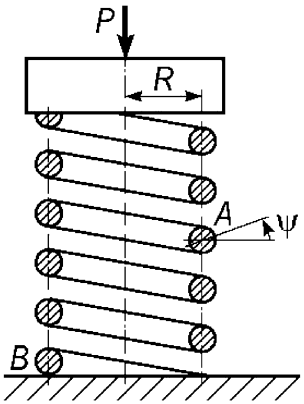

Fig. 165

187. A coil spring of helix angle α and radius of coils R is tensed by forces P. Determine spring height and diameter change as well as coils number change.

188. Shaped springs with coils landing are used in some devices to obtain nonlinear force dependence upon displacement (Fig. 166).

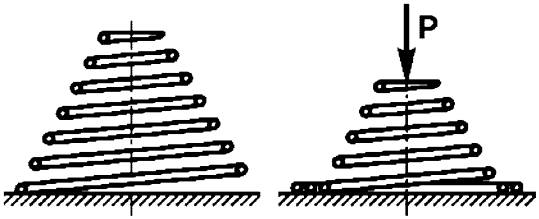

Fig. 166

If such a spring is compressed, its lower (bigger) coils are deformed greater than the upper ones, land on the base and almost completely come out of work. Thus as compressive force increases the spring's working coils number decreases, so the spring characteristics turn out to be nonlinear with increasing stiffness (Fig. 167a). The force derivative with respect to displacement $dP/d\lambda$ grows.

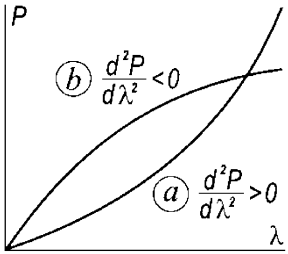

Fig. 167

Think, how can spring characteristics with decreasing stiffness like the one shown in Fig. 167b be obtained with the same spring?

189. A rectangular frame (Fig. 168) is pinned at its upper end. A roller leaning on a rigid base is at the lower end of the frame.

Determine the lower support reaction supposing that force P and frame rigidity have such values that deflections arising in the frame are small enough in comparison with its initial dimensions.

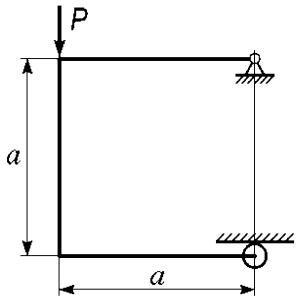

Fig. 168

190. A thin flexible cantilever rod is loaded by vertical concentrated force at its end (Fig. 169). The rod has constraints allowing it to bend only in the load action plane (draft plane). What equilibrium modes besides the shown one are possible for the rod?

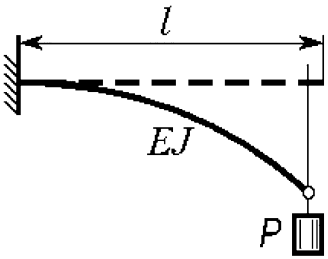

Fig. 169

191. A force P is applied at a point A of some elastic body (Fig. 170). What surface will be circumscribed by an arbitrarily taken point B if the force P will rotate in space about point A?

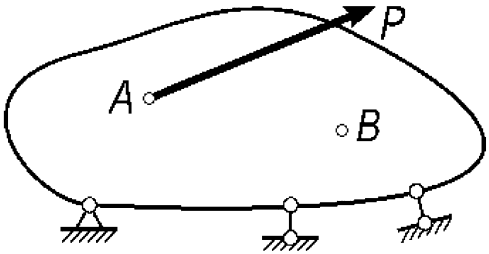

Fig. 170

192. A ring of circular cross-section (Fig. 171) is loaded by uniformly distributed moments of intensity m [N cm/cm].

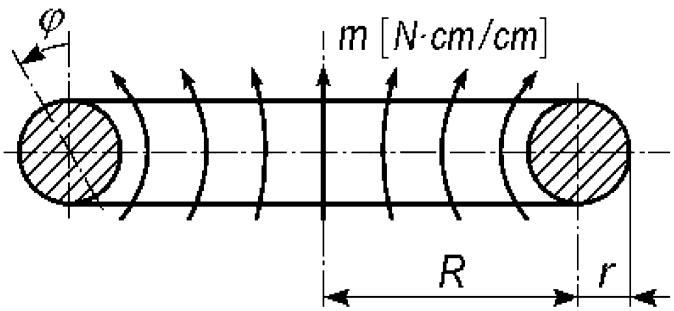

Fig. 171

Supposing r to be small in comparison to R determine the angle φ of the ring cross-section rotation in the axial plane depending on m if the material of the ring obeys Hook's law.

193. How does the solution of the previous problem change if the considered ring was produced by bending of a straight bar (Fig. 172) and preserves the stresses obtained under bending?

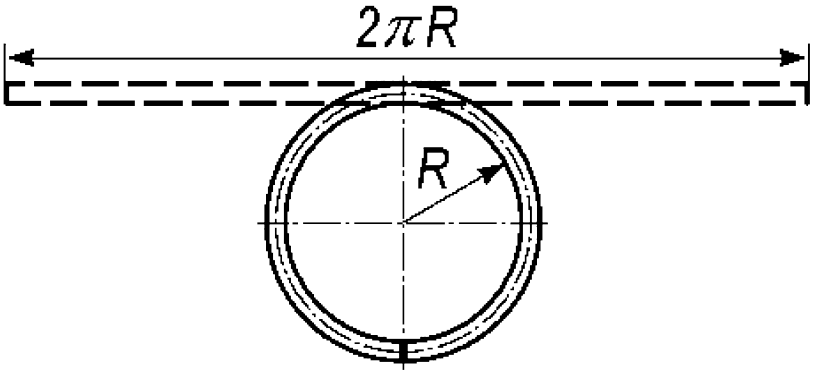

Fig. 172

Assume that bending stresses are completely elastic.

194. A flexible shaft representing a thin wire freely rotating in an immobile braid (Fig. 173) is used to transmit torque in many devices such as speedometers, for example. If one end of the wire is rotating uniformly then its second end is rotating uniformly too.

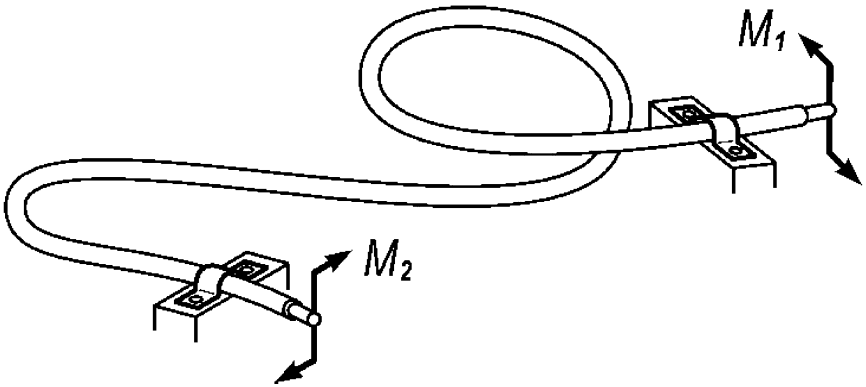

Fig. 173

In a defective wire this rotation evenness is however broken. The output cross-section is rotating at first with deceleration and then with acceleration in such a way that its angular velocity remains unchanged on average but includes a component varying with the period of wire rotation. It was found that this defect is connected to the initial curvature the wire had before its conversion into a braid.

Analyze this phenomenon and determine the conditions for elimination of motion irregularity. Friction forces between cable and braid can be neglected.

195. A thin-walled rod of circular cross-section intended for space structure is manufactured by stacking of composite cylindrical monolayers under angles $\pm\varphi$ (Fig. 174). It was noted during bench-tests that the rod begins to twist under tension (or under uniform heating).

Explain this phenomenon and suggest methods for its elimination.

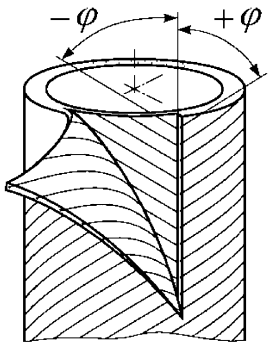

Fig. 174

196. Mass M fixed at the end of a rectangular frame contacts an immobile plane Π (Fig. 175). Friction between the mass and the plane is supposed to be dry. If the frame is bent and after this is released then mass M begins to oscillate. Determine the motion path of mass M neglecting frame mass.

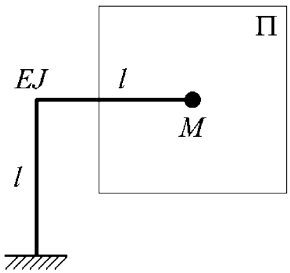

Fig. 175

197. Compressed air is fed into a closed thin-walled tube (Fig. 176).

How will tube vibration eigenfrequency change under air pressure growth?

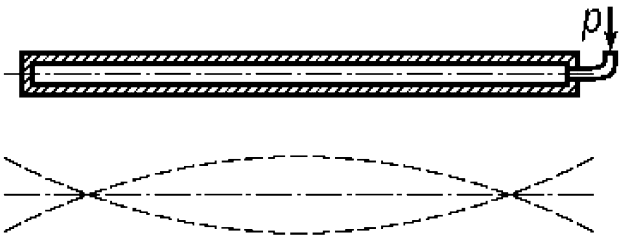

Fig. 176

198. A long cantilever beam under action of gravity forces q lays on a rigid horizontal plane disposed at a distance h below the support (Fig. 177a). A segment of length l remains free. Then the right end of the free segment is clamped and the supporting plane is removed (Fig. 177b).

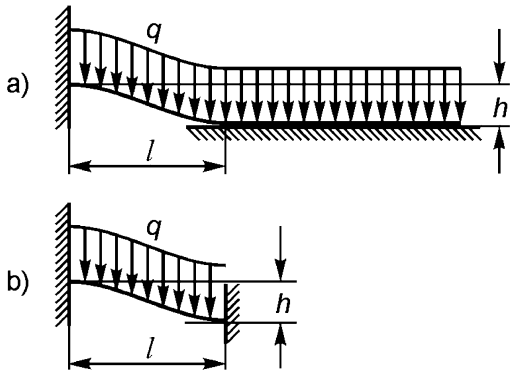

Fig. 177

Derive the lowest eigenfrequency of the beam obtained in such a way.

199. Let us imagine the following paradoxical situation. An elastic body is loaded with a system of forces and is in stable equilibrium state. We additionally load the body putting weight on it. And contrary to expectations the weight does not move down but moves up. The system performs work. We take the weight off - and the system returns to its initial state. Is this possible?

200. A thinwalled rubber cylinder open at both ends is turned inside-out (Fig. 178).

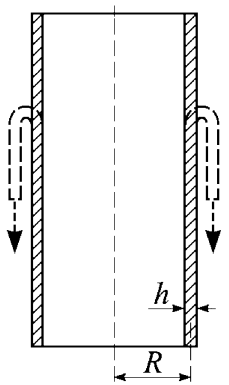

Fig. 178

Analyze its shape after a specified operation if the cylinder deformations are known to be pure elastic? We suppose rubber to obey Hook's law (see the answer to question 174).

201. The solution of the axisymmetric deformation problem for a thin-walled cylinder under internal pressure action (Fig. 179) is reduced as known to solving of the differential equation

$$w^{(IV)} + 4k^4 w = \frac{p}{D},$$

where w is radial displacement of the shell median surface points, $D = \dfrac{Eh^3}{12(1-\mu^2)}$ and $4k^4 = \dfrac{Eh}{R^2 D}$.

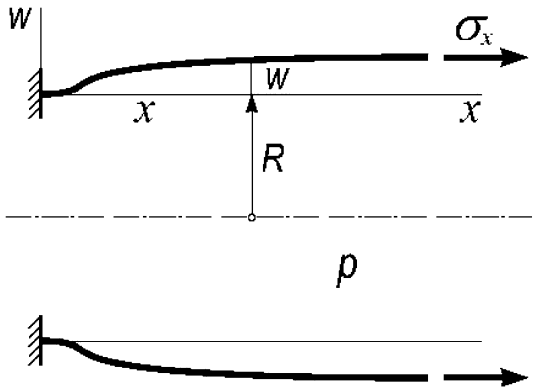

Fig. 179

If besides pressure p the shell is effected by axial tensile force producing axial stress σ_x then the summand $-\dfrac{\mu h \sigma_x}{RD}$, which reflects the presence of cylinder transverse narrowing due to Poisson's effect, is added to the right part of the equation and the question is usually considered to be settled. Meanwhile due to meridian curvature w'' longitudinal stress σ_x gives the force radial component acting conjointly with pressure p. As a result the summand $-\dfrac{h\sigma_x}{D} w''$ must be included into the left part of the equation which takes the form

$$w^{(IV)} - \frac{h\sigma_x}{D} w'' + 4k^4 w = \frac{p}{D} - \frac{\mu h \sigma_x}{RD} \ . \qquad (1)$$

What are the validity limits for standard neglect of the equation's left part second term?

202. Everybody knows well, how the cord of a telephone twists (Fig. 180). We shall term such a formation as a twine (look also Fig. 105) and consider it to be elastic. The twine can be untwined and residual deformations in the cord are not observed. Visible uniformity of coils gives reason to suppose force interaction uniformity along length l of the twine. One may assume that deviations from this uniformity depending on the nature of the forces applied out of length L borders occur at segments l_1 and l_2.

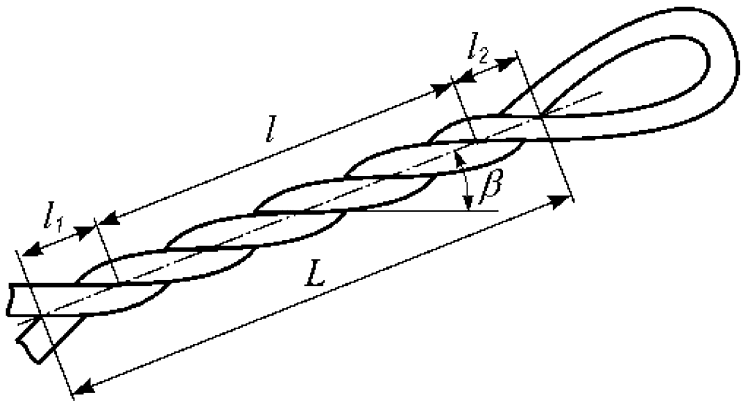

Fig. 180

Analyze branch (strand) force and contact interaction conditions of the l segment. List the parameters and how the twine angle β depend on them.

203. A ball of mass m is placed in a tube rotating with constant angular velocity ω. The ball is attached to a rubber string (Fig. 181).

The string tension diagram is specified by the curve shown in Fig. 181 (force and displacement are plotted in relative units). Derive the dependence of ball displacement u on angular velocity ω.

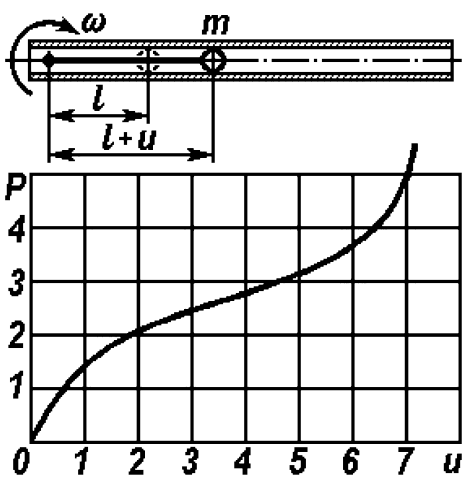

Fig. 181

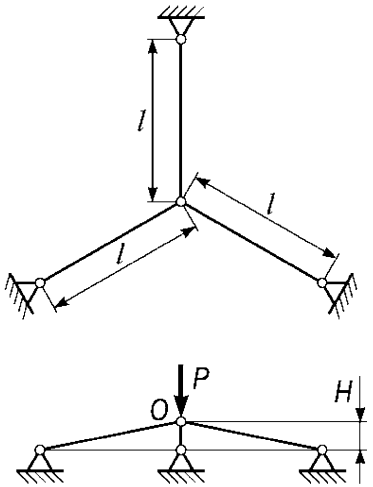

Fig. 182

204. A spatial rod system (Fig. 182) consisting of three articulated equal bars is loaded in a common node O by force P normal to the supports' plane.

Determine point O displacement w in relation to force P considering H to be small in comparison to l and supposing that the rods' material obeys Hook's law. Interpret the obtained result.

205. Determine disk spring (Fig. 183) deflection in relation to force P.

Treat the spring as a circular beam of rectangular cross-section $[h\times(b-a)]$. Assume that the spring cross-section inclination angle α is small. As thickness h and angle α are small then consider forces P applied at the circumferences of a and b radii.

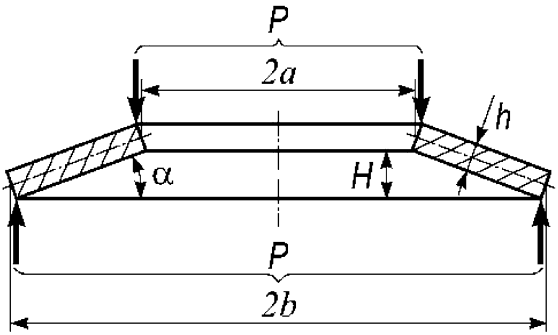

Fig. 183

206. Analyze the stability question and problem of large displacements for the system shown in Fig. 184.

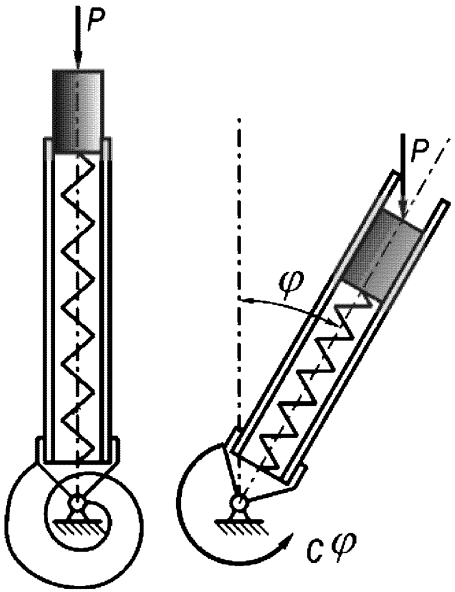

Fig. 184

A tube at its lower end is pinned and is connected with a spiral spring giving moment $c\varphi$ under tube rotation at angle φ. A spring and a piston capable of moving without friction are inserted into the tube. The inserted spring has stiffness c_1, i.e. under force P its shortening is P/c_1.

207. Preliminarily bent elastic rods are hooked by nips to a flexible thread. Each of the rods produces tensile force S in the thread (Fig. 185a).

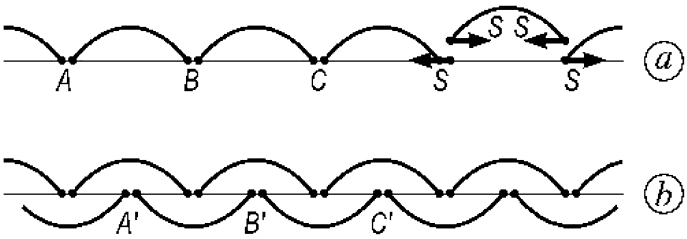

Fig. 185

At points $A, B, C...$ the rods are not joined to each other and so the system possesses kinematic variability and represents some kind of multilink mechanism. In order to eliminate this variability the second set of exactly the same prestressed rods is fastened to the thread at points $A', B', C', ...$ (Fig. 185b).

Though bent rods can freely rotate about the longitudinal axis of the thread, the thread itself, being tensed at all points, has characteristics of an elastic bar and in some necessary cases can be used as a carrying element of the structure.

Determine the flexural rigidity of the "beam" created in such a way.

208. Determine the forces acting in bicycle wheel spokes and stresses occurring in the wheel rim under force P applied to the wheel axis. The ground supporting the wheel can be treated as rigid. The spokes number n is sufficiently high to make it possible to consider the spokes not as separate rods but as a continuous medium.

The following data should be used under numerical calculations:

$P = 400$ N; wheel radius $R = 31$ cm; rim inertia moment $J = 0.3$ cm^4; spokes number $n = 36$; spokes diameter $d = 2$ mm. Rim and spokes are of steel, $E = 200$ GPa.

209. Determine the bow speed dependence arrow flying off on bow-string pull aside its initial state value w. If the bow-string is untied then the bow is a straight beam of length $2l$ and flexural rigidity EJ. Bow sag after bow-string tying is h.

Perform numerical calculations for the case:

$$l = 60 \text{ cm}, \quad h = 0.3\, l, \quad E = 10 \text{ GPa (wood)},$$

$$J = \frac{\pi d^4}{64} \quad (d = 2.0 \text{ cm}), \quad w = 0.6\, l, \quad \text{arrow weight is } 0.4 \text{ N}.$$

Suppose that the energy of the strained bow completely transfers to kinetic energy of the arrow. Assume that the bow-string is unstretched.

Part II

Answers and Solutions

1. Tension, Compression and Torsion

1. Full displacement will be, naturally, determined not by the diagonal of the parallelogram plotted on segments u_1 and u_2 (as often happens to be the answer for the formulated question) but by the length of the segment measured from point A to the point of intersection of the perpendiculars erected from the ends of segments $u_1$and u_2 (point B in Fig. 186).

The solution is based on the fact that displacement in a specified direction is the projection of full displacement onto a specified direction.

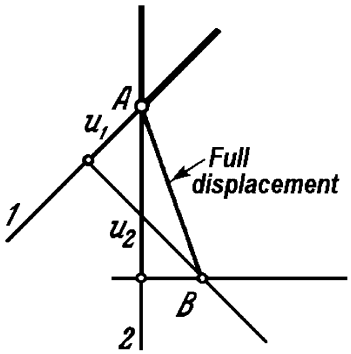

Fig. 186

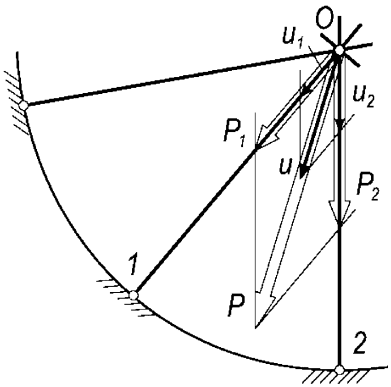

Fig. 187

2. Let us decompose force P to components P_1 and P_2 along the directions of two neighbouring rods *1* and *2* (Fig. 187). As each of these rods is situated in a symmetry plane, full displacements u_1 and u_2 caused by forces P_1 and P_2 will be directed along the lines of action of the corresponding forces, that is along rods *1* and *2*.

Stiffness coefficients for directions *1* and *2* are identical, therefore

$$u_1 = \frac{P_1}{c}\ , \quad u_2 = \frac{P_2}{c}\ .$$

And so the summary displacement u, obtained by composition of displacements u_1 and u_2 according to the rule of the parallelogram, will be directed along the line of action of force P and will have value $u = \dfrac{P}{c}$ regardless of angle α.

Comparing the solution of this problem with the solution of the previous one, it is important to remark that displacements u_1 and u_2 in the present problem represent full displacements caused by forces P_1 and P_2, correspondingly. So under simultaneous action of these forces displacements $u_1$and u_2 are composed according to the rule of the parallelogram. As to the previous problem, there u_1 and u_2 represented projections on directions *1* and *2* of full displacement caused by simultaneous action of forces P_1 and P_2. And so they were composed in another way.

3. As the slab is rigid, the length AB of the strained bolt remains unchanged up to opening of contacts. And so the internal tensile force remains unchanged also. In the case, where force P is greater than the force of preliminary tension, the contact between the slab and lower bracket will be opened. Then internal tensile force in the bolt will be equal to P.

Consequently, under $P \leq N_t$ the internal tensile force in the bolt is equal to $N = N_t$ and under $P > N_t$ it will be $N = P$.

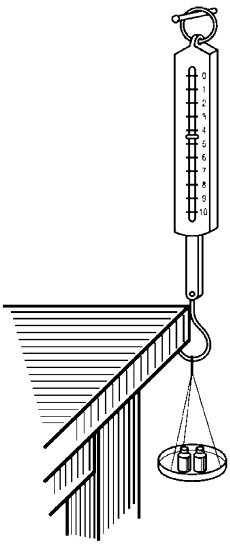

Fig. 188

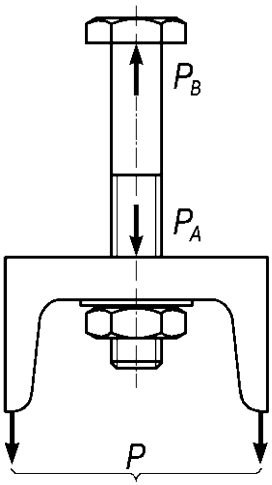

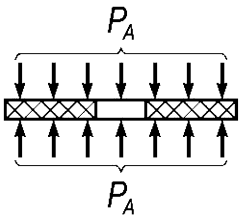

Fig. 189

The validity of the obtained result is well illustrated with the following simple example. Imagine a spring balance of a steelyard, the upper ring of which we put on a nail and the lower hook after tension hitch up by some rigid ledge, for example, up a table edge as shown in Fig. 188. The balance after this will indicate some value, for example, 4 Kg-wt. Let us liken this balance to the strained bolt. Now let us hang weights to the lower hook of the strained balance. Until the weight of the load remains less than the specified tension force, balance will permanently indicate four kilograms. And only when a load hanged on the hook will be greater than four kilograms then the indicator will move from its place and indicate the corresponding weight.

4. For solution of this problem let us consider bolt and spacer separately. Let us denote the force compressing the spacer as P_s and the force acting on the bolt's head from the side of the slab as P_b (Fig. 189).

As long as the lower contact is not opened the sum of the bolt's elongation and of the spacer's elongation

$$\frac{P_b}{EA} + \frac{P_s}{c}$$

remains invariable and equal to the sum of the same quantities under tightening (that is under $P = 0$); the latter is obviously equal to

$$\frac{N_t}{EA} + \frac{N_t}{c},$$

where A is the area of the bolt's cross-section. Consequently,

$$\frac{P_b}{EA} + \frac{P_s}{c} = \frac{N_t}{EA} + \frac{N_t}{c}.$$

Besides it we have equality

$$P_b - P_s = P.$$

From these two equations we find

$$P_s = N_t - \frac{P}{1 + \dfrac{EA}{cl}}, \qquad P_b = N_t + \frac{P\dfrac{EA}{cl}}{1 + \dfrac{EA}{cl}}.$$

The internal force N stretching the bolt will be equal to P_b and as long as the lower contact is not opened N remains invariable and equal to the tightening force N_t (see solution of the previous problem).

The opening condition for the lower contact will be $P_s = 0$ that leads to

$$P = N_t \left(1 + \frac{EA}{cl}\right).$$

Then $N = P$. Under $c = \infty$, that is when the spacer is absolutely rigid, we obtain the solution of the previous problem.

The graph of internal force N stretching the bolt depending on load P under different values of c ($c_2 < c_1 < \infty$) is plotted in Fig. 190.

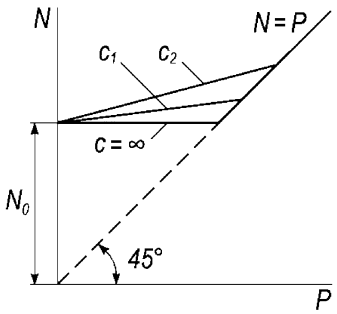

Fig. 190

5. In the mentioned scheme, indicators measure not the shortening of the specimen but the sum of this shortening and mutual displacement of the edges of the slabs (Fig.191), that is the quantity $\Delta l + \delta_1 + \delta_2$. In consequence of this fact the obtained elasticity modulus must be found to be less than actual one. The greater the elasticity modulus of tested specimen will be the greater will be the relative error.

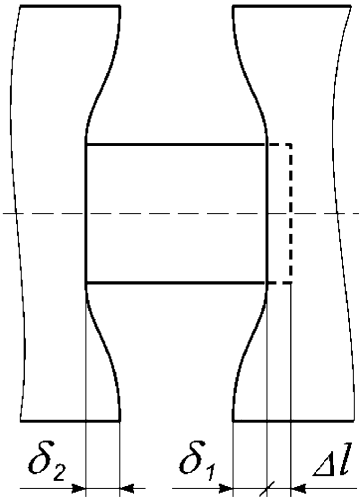

Fig. 191

The described procedure is suitable only for determining the elastic properties of rubber, wood or plastic, that is of those materials that have elasticity modulus essentially less than steel has. As the value of the elasticity modulus of the tested material (80 GPa) specified in the problem is commensurable to steel's elasticity modulus (200 GPa) we cannot be sure of the obtained result. And if the value of the elasticity modulus equal to 5 GPa was obtained then we could hope for sufficient accuracy.

6. In the middle cross-section of the rod due to the symmetry conditions no axial displacements occur. Now let us consider the left or the right part of the rod. Axial displacements at the ends of this part are absent, the rod is uniform and heating is homogeneous. Consequently, due to the symmetry conditions axial displacements in the middle cross-section of the rod's half are absent also. Reasoning in such a way we can divide the rod into arbitrarily small segments having axial displacements equal to zero at their ends. Hence we can make the deduction that axial displacements are absent for all cross-sections of the rod in general.

7. Let us denote compressive force arising as a result of homogeneous heating of the rod as N. Then displacement in some arbitrary cross-section can be described as

$$u(x) = \alpha t\, x - \frac{N}{E} \int\limits_0^x \frac{dx}{A(x)} \ ,$$

where αt is thermal elongation, and $A(x)$ is the sought law of a cross-sectional area A variation.

Differentiating we obtain

$$\frac{du}{dx} = \alpha t - \frac{N}{E} \frac{1}{A(x)}.$$

Hence

$$A(x) = \frac{N \ / \ E}{\alpha t - \dfrac{du}{dx}}. \tag{1}$$

There is a necessity for interpreting the found expression.

First of all area $A(x)$ is determined as accurate by a constant multiplier. The greater the value of A is, the greater the value of the corresponding compressive force N will be. If the area near the left fixing is denoted as A_0, then we obtain

$$A(x) = A_0 \frac{\alpha t - \left.\dfrac{du}{dx}\right|_{x=0}}{\alpha t - \dfrac{du}{dx}}.$$

It means that specifying an arbitrary value of A_0 we can define a law of a cross-sectional area $A(x)$ variation satisfying given condition of displacements' function $u(x)$ variation.

And one more peculiarity. The specified function $u(x)$ must not only be equal to zero at the ends of the rod but at the same time be such that the denominator of the expression (1) would be greater than zero, otherwise the function $A(x)$ would be negative which contradicts physical sense.

Let us postulate, for example, that displacements u were varying along the rod's axis according to the quadratic law

$$u(x) = K\alpha t \frac{x}{l} \left(1 - \frac{x}{l}\right),$$

where K is an undetermined multiplier.

As

$$\frac{du}{dx} = K\alpha t \left(1 - 2\frac{x}{l}\right),$$

then the denominator of the expression (1) takes the form

$$\alpha t - K\alpha t \left(1 - 2\frac{x}{l}\right),$$

from which we see that the coefficient K of a specified function $u(x)$ must be not greater than 1.

8. The first expression of U is correct. As to the second one, it is erroneous. In the specified case the work produced by force P

$$U \neq \frac{P\delta}{2},$$

as displacement δ is proportional to force P not at the entire interval of its change. This can easily be seen from the plot in Fig. 192 where the dependence of δ upon P for the considered system is represented by the diagram. The work produced by the force P is determined as the crosshatched area that is

$$U = \frac{\delta^2 EA}{2l} + \left(\frac{Pl}{2EA} - \frac{\Delta}{2}\right)\frac{\delta EA}{l} + \frac{1}{2}\left(P - \frac{\delta EA}{l}\right)\left(\frac{Pl}{2EA} - \frac{\Delta}{2}\right).$$

After reduction we obtain

$$U = \frac{P^2 l}{4EA} + \frac{EA\Delta^2}{4l}.$$

This expression coincides with the one obtained previously (see expression (1) in the set of the problem).

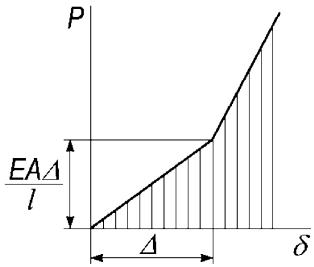

Fig. 192

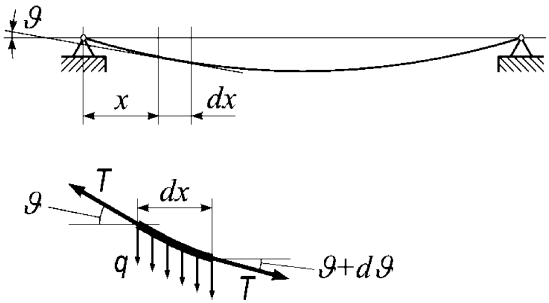

Fig. 193

9. In the first case we determine the displacement of the point where the rod's centre of gravity was before deformation. In the second case we determine the distance from the point of the new position of the centre of gravity to the point of its old position, and this is not the same.

Thus there is indeterminacy in the set of the question itself. It is necessary to stipulate neatly what should be understood by "displacement of the centre of gravity" because the centre of gravity is not rigidly connected with some point of the deformed body.

10. Let us consider the filament's element of length dx (Fig. 193) and denote an inclination angle of the weighed-down filament as ϑ and tensile force of the weighed-down filament as T. It is greater than the initial tensile force T_0, $(T > T_0)$.

Assuming angle ϑ to be small we shall obtain from the conditions of the equilibrium

$$T\vartheta - q\,dx - T\,(\vartheta + d\vartheta) = 0\,,$$

from which

$$\frac{q}{T} = -\frac{d\vartheta}{dx}\,. \tag{1}$$

After integration we find

$$\vartheta = \frac{q}{T}\,(C - x)\,;$$

under $x = l/2$ we have $\vartheta = 0$, so that $C = l/2$; therefore

$$\vartheta = \frac{q}{T}\left(\frac{l}{2} - x\right) \text{ and } w_{\max} = \int\limits_0^{l/2} \vartheta\,dx = \frac{ql^2}{8T}\,. \tag{2}$$

Now let us find T. As a result of inequality of forces $T > T_0$, the filament elongates by the value of the length's difference between the curved and the straight filament, that is

$$\frac{(T - T_0)\,l}{EA} = \int\limits_0^l \left(\frac{1}{\cos\vartheta} - 1\right) dx = \int\limits_0^l \frac{\vartheta^2}{2}\,dx\,,$$

from which

$$\frac{T - T_0}{EA} = \frac{q^2 l^2}{24\,T^2}.$$

Let us substitute here T from expression (2). Then we obtain

$$64\left(\frac{w_{\max}}{l}\right)^2 + 24\,\frac{w_{\max}}{l}\,\frac{T_0}{EA} = 3\,\frac{ql}{EA}. \tag{3}$$

That is the sought dependence of $w_{\max}$ upon T_0 and q. The obtained result is represented in Fig. 194 in the form of curves

$$\frac{w_{\max}}{l} = f\left(\frac{T_0}{EA}, \frac{ql}{EA}\right).$$

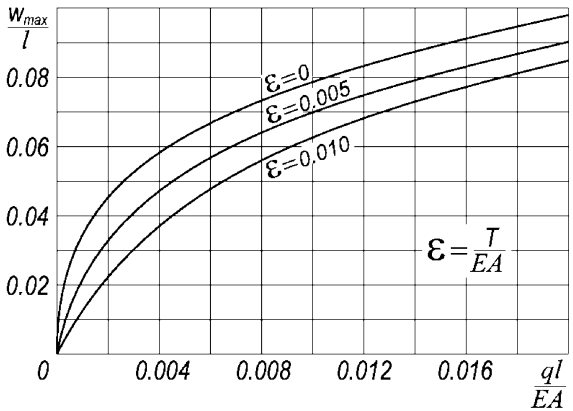

Fig. 194

11. If the sheets in the place of riveting were conjunct through the whole width b and this conjunction was absolutely rigid then for the sheets tested for tension we should have according to Hook's law

$$\Delta a_0 = \frac{T\frac{a}{2}}{E\,2\,b\,h_1} + \frac{T\frac{a}{2}}{E\,b\,h_2}, \tag{1}$$

where E is the elasticity modulus of the sheets. The obtained value Δa_0 would be less than the measured one, Δa.

The difference between the measured value Δa and the calculated one, Δa_0 (1) represents the result of deformation of rivet and sheets in the conjunction zone. Let us denote the obtained difference of elongations as Δ:

$$\Delta = T\left(\frac{1}{k} - \frac{a}{4\,E\,b\,h_1} - \frac{a}{2\,E\,b\,h_2}\right).$$

Let us denote also

$$\frac{1}{k} - \frac{a}{4\,E\,b\,h_1} - \frac{a}{2\,E\,b\,h_2} = \frac{1}{k_0}. \tag{2}$$

Then the difference of elongations will be $\Delta = \dfrac{T}{k_0}$.

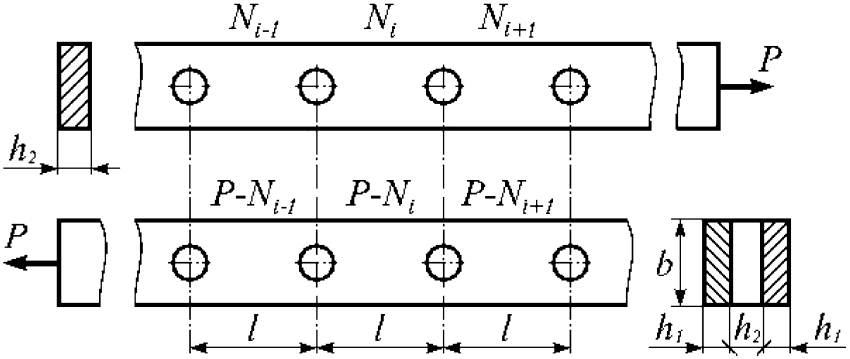

Fig. 195

Now let us consider the deformation of the sheets (Fig. 195). Let us denote normal tensile force in the span number i of the internal sheet as N_i. In two external sheets the summary force will be evidently equal to the difference $P - N_i$ (see Fig. 195). The difference of elongations of the internal sheet and of the external sheets in the span number i

$$\frac{N_i\,l}{E\,b\,h_2} - \frac{(P - N_i)}{2\,E\,b\,h_1}$$

is equal to the difference of displacements of the span ends due to deformation of the rivets, that is

$$\frac{N_{i+1} - N_i}{k_0} - \frac{N_i - N_{i-1}}{k_0},$$

where $N_i - N_{i-1}$ and $N_{i+1} - N_i$ are forces falling at the left and the right rivet of the span number i, correspondingly. Equating the above differences of displacements we obtain

$$N_{i-1}\alpha - N_i\beta + N_{i+1}\alpha = -P, \tag{3}$$

where

$$\alpha = \frac{2\,E\,b\,h_1}{l\,k_0}\ , \quad \beta = 2\alpha + 1 + \frac{2\,h_1}{h_2}\ . \tag{4}$$

The obtained equation (3) analogous to the known equation of the three moments is written down sequentially for the first, the second and the third span (Fig. 10):

$$\begin{aligned} 0\,\alpha - N_1\,\beta + N_2\,\alpha &= -P,\\ N_1\,\alpha - N_2\,\beta + N_3\,\alpha &= -P,\\ N_2\,\alpha - N_3\,\beta + \ P\,\alpha &= -P. \end{aligned}$$

From this we obtain formulas for normal forces

$$N_1 = P\frac{\beta^2 + \alpha^3 + \alpha\beta}{\beta\left(\beta^2 - 2\alpha^2\right)},$$

$$N_2 = P\frac{\beta\left(\beta + 2\alpha + \alpha^2\right)}{\beta\left(\beta^2 - 2\alpha^2\right)},$$

$$N_3 = P\frac{\beta^2\left(1+\alpha\right) - \alpha^3 + \alpha\beta}{\beta\left(\beta^2 - 2\alpha^2\right)}.$$

Forces falling at rivets will be the following

$$P_I = N_1 = P\frac{\beta^2 + \alpha^3 + \alpha\beta}{\beta\left(\beta^2 - 2\alpha^2\right)},$$

$$P_{II} = N_2 - N_1 = P\frac{\alpha\left(\beta + \alpha\beta - \alpha^2\right)}{\beta\left(\beta^2 - 2\alpha^2\right)},$$

$$P_{III} = N_3 - N_2 = P\frac{\alpha\left(\beta^2 - \alpha\beta - \alpha^2 - \beta\right)}{\beta\left(\beta^2 - 2\alpha^2\right)},$$

$$P_{IV} = P - N_3 = P\left[1 - \frac{\beta^2\left(1+\alpha\right) - \alpha^3 + \alpha\beta}{\beta\left(\beta^2 - 2\alpha^2\right)}\right].$$

In the case when $h_2 = 2\ h_1$ we have

$$\beta = 2(\alpha + 1)$$

and then forces will be

$$P_I = P_{IV} = \frac{P}{4}\,\frac{\alpha^3 + 6\alpha^2 + 10\alpha + 4}{(\alpha+1)\left(\alpha^2 + 4 + 2\right)},$$

$$P_{II} = P_{III} = \frac{P}{4}\,\frac{\alpha}{\alpha+1}.$$

If fastening is absolutely rigid ($k_0 = \infty$) then the coefficient $\alpha = 0$, and we shall obtain

$$P_I = P_{IV} = \frac{P}{2} \quad \text{and} \quad P_{II} = P_{III} = 0.$$

Therefore in such a case only two rivets (at the ends of the rivet joint) work.

Under highly compliant rivets the value k_0 will be small and α will be large. As a limit under $\alpha \to \infty$ we have

$$P_I = P_{II} = P_{III} = P_{IV} = \frac{P}{4}.$$

In the set of the problem it was said that coefficient k is determined by testing of riveted sheets with the measurements' base a being sufficiently large to consider the stresses distribution in cross-sections A and B to be uniform (Fig. 11). The obtained solution will be sufficiently accurate in this sense if the distance between rivets is greater than a. However even with less distance between rivets when the stresses along the sheet's width are not equalized from rivet to rivet, the solution of the problem remains valid. Only expression (2) for k_0 will be changed. There we must change the sheet's width b with some equivalent to its reduced value.

12. Assume that there are n rivets in the longitudinal joint. According to expression (3) for $n-1$ spans we have the following $n-1$ equations

$$\begin{aligned}
-N_1\,\beta + N_2\,\alpha &= -P,\\
N_1\,\alpha - N_2\,\beta + N_3\,\alpha &= -P,\\
N_2\,\alpha - N_3\,\beta + N_4\,\alpha &= -P,\\
&\cdots\\
N_{i-1}\,\alpha - N_i\,\beta + N_{i+1}\,\alpha &= -P,\\
&\cdots\\
N_{n-2}\,\alpha - N_{n-1}\,\beta &= -P\,(1+\alpha).
\end{aligned}$$

From these equations we must determine the unknowns

$$N_1,\ N_2,\ N_3,\ \ldots\ ,\ N_{n-1}.$$

Let us note that if we assume

$$N_1 = N_2 = N_3 = \cdots = N_{n-1} = -\frac{P}{2\alpha - \beta},$$

then all equations except the first and the last will be satisfied.

Assume further that

$$N_1 = Ax - \frac{P}{2\alpha - \beta}, \quad N_2 = Ax^2 - \frac{P}{2\alpha - \beta}, \ \cdots,$$

$$N_i = Ax^i - \frac{P}{2\alpha - \beta}, \ \cdots,$$

where A and x are some arbitrary constants.

Let us select x so that once more all equations except the first and the last are satisfied. After substitution of N_{i-1}, N_i and N_{i+1} into the equation

$$N_{i-1}\,\alpha - N_i\,\beta + N_{i+1}\,\alpha = -P,$$

we obtain

$$A\,x^{i-1}\alpha - \frac{P\alpha}{2\alpha-\beta} - A\,x^i\beta + \frac{P\beta}{2\alpha-\beta} + A\,x^{i+1}\alpha - \frac{P\alpha}{2\alpha-\beta} = -P,$$

or

$$\alpha - \beta\,x + \alpha\,x^2 = 0,$$

from which we find

$$x_1 = \frac{\beta + \sqrt{\beta^2 - 4\alpha^2}}{2\alpha}\,, \quad x_2 = \frac{\beta - \sqrt{\beta^2 - 4\alpha^2}}{2\alpha}.$$

Now evidently all equations except the first and the last will be satisfied by the following expressions

$$\begin{aligned} N_1 &= A\,x_1 + B\,x_2 - \frac{P}{2\alpha-\beta}\,,\\ N_2 &= A\,x_1^2 + B\,x_2^2 - \frac{P}{2\alpha-\beta}\,,\\ &\cdots\\ N_i &= A\,x_1^i + B\,x_2^i - \frac{P}{2\alpha-\beta}\,, \end{aligned}$$

under any values of arbitrary constants A and B. And we shall select these constants so that the first and the last equations of the system are satisfied

$$-\beta\left[Ax_1 + Bx_2 - \frac{P}{2\alpha-\beta}\right] + \alpha\left[Ax_1^2 + Bx_2^2 - \frac{P}{2\alpha-\beta}\right] = -P,$$

$$\alpha\left[Ax_1^{n-2} + Bx_2^{n-2} - \frac{P}{2\alpha-\beta}\right] - \beta\left[Ax_1^{n-1} + Bx_2^{n-1} - \frac{P}{2\alpha-\beta}\right] = -P\,(\alpha+1)$$

Hence we determine A and B and, taking into account that $x_1\,x_2 = 1$ and $x_1 + x_2 = \dfrac{\beta}{\alpha}$, after a simple reduction we obtain

$$N_i = \frac{P}{2\alpha-\beta}\left[\frac{(\beta-1-2\alpha)\left(x_1^i - x_2^i\right) + x_2^{n-i} - x_1^{n-i}}{x_2^n - x_1^n} - 1\right].$$

Forces in rivets are equal to

$$\begin{aligned} P_I &= N_1,\\ P_{II} &= N_2 - N_1,\\ P_{III} &= N_3 - N_2,\\ &\cdots\\ P_n &= P - N_{n-1}. \end{aligned}$$

13. Let us consider equilibrium conditions for element of bolt (Fig. 196).

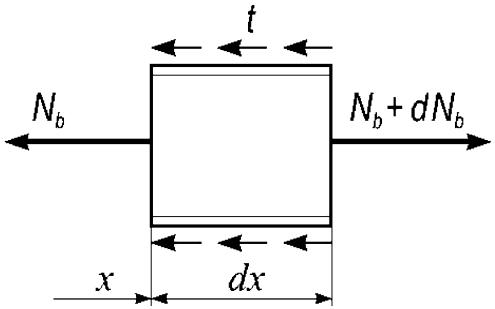

Fig. 196

Evidently

$$\frac{dN_b}{dx} = t. \tag{1}$$

Further, according to the set of the problem

$$t = k\ (u_b - u_n)\ ; \tag{2}$$

but

$$\frac{du_b}{dx} = \varepsilon_b\,, \quad \frac{du_n}{dx} = \varepsilon_n\,, \quad \text{and} \quad \varepsilon_b = \frac{N_b}{E_b A_b}\,, \quad \varepsilon_n = \frac{N_n}{E_n A_n}\,.$$

Therefore as a result of differentiating expression (2) we obtain

$$\frac{dt}{dx} = k\left(\frac{N_b}{E_b A_b} - \frac{N_n}{E_n A_n}\right).$$

Substituting here t from equilibrium equation (1) we have

$$\frac{d^2 N_b}{dx^2} = k\left(\frac{N_b}{E_b A_b} - \frac{N_n}{E_n A_n}\right).$$

Using condition $N_n = P - N_b$ we find

$$\frac{d^2 N_b}{dx^2} - \alpha^2 N_b = -\frac{kP}{E_n A_n}\,, \tag{3}$$

where

$$\alpha^2 = k\left(\frac{1}{E_b A_b} + \frac{1}{E_n A_n}\right)\,.$$

The general solution of the homogeneous equation

$$\frac{d^2 N_b}{dx^2} - \alpha^2 N_b = 0$$

will be

$$N_b = A \sinh \alpha x + B \cosh \alpha x\,.$$

Adding here a particular solution of equation (3) we obtain

$$N_b = A \sinh \alpha x + B \cosh \alpha x + \frac{k P}{\alpha^2 E_n A_n} .$$

Constants A and B can be found from boundary conditions

$$\text{at} \quad x = 0 \qquad N_b = 0 ,$$
$$\text{at} \quad x = l \qquad N_b = P .$$

Solving these conditions we obtain

$$A = - \frac{kP}{\alpha^2 E_n A_n} \frac{1 - \cosh \alpha l}{\sinh \alpha l} + \frac{P}{\sinh \alpha l} , \quad B = - \frac{k P}{\alpha^2 E_n A_n} .$$

Normal force in the bolt is equal to

$$N_b = \frac{P}{\dfrac{1}{E_b A_b} + \dfrac{1}{E_n A_n}} \frac{1}{\sinh \alpha l} \left[\frac{\sinh \alpha l - \sinh\big(\alpha (l - x)\big)}{E_n A_n} + \frac{\sinh \alpha x}{E_b A_b} \right] .$$

Normal force in the nut

$$N_n = P - N_b .$$

Force at thread's turns is equal to

$$t = \frac{dN_b}{dx} = \frac{P}{\dfrac{1}{E_b A_b} + \dfrac{1}{E_n A_n}} \frac{\alpha}{\sinh \alpha l} \left[\frac{\cosh\big(\alpha (l - x)\big)}{E_n A_n} + \frac{\cosh \alpha x}{E_b A_b} \right] .$$

The character of these quantities' distribution along the length of the bolt and the nut is shown in Fig. 197.

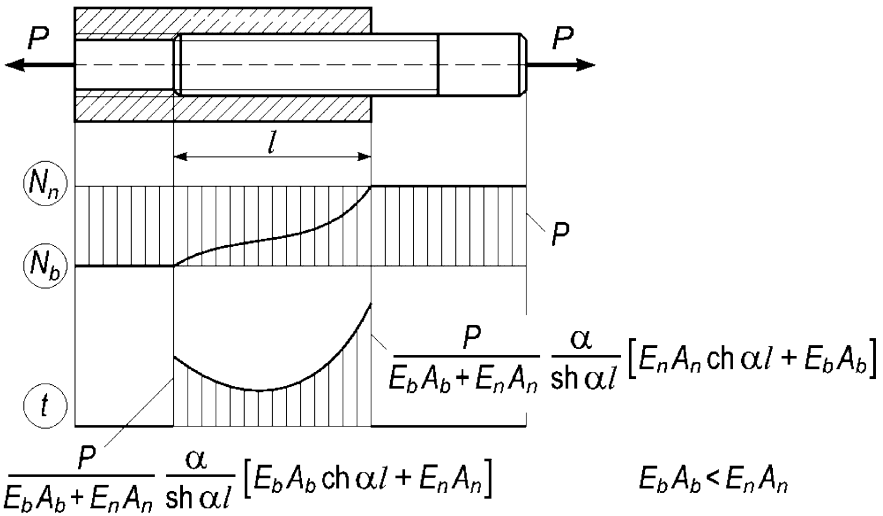

Fig. 197

14. The problem is solved just the same as the previous one. The difference is introduced only with boundary conditions that now will be the following

$$\text{at} \quad x = 0 \qquad N_b = P \,,$$
$$\text{at} \quad x = l \qquad N_b = P \,.$$

These conditions are satisfied with the following values of constants A and B

$$A = \frac{1 - \cosh \alpha l}{\sinh \alpha l} \left(P - \frac{k\,P}{\alpha^2 E_n\, A_n} \right), \quad B = P - \frac{k\,P}{\alpha^2 E_n\, A_n} \,.$$

Normal force in the screw will be

$$N_b = \frac{P}{\dfrac{1}{E_b\, A_b} + \dfrac{1}{E_n\, A_n}} \frac{1}{\sinh \alpha l} \left[\frac{\sinh \alpha x - \sinh\big(\alpha\,(l - x)\big)}{E_n\, A_n} + \frac{\sinh \alpha l}{E_b\, A_b} \right].$$

Normal force in the nut is equal to

$$N_n = P - N_b \,.$$

Force at thread's turns is equal to

$$t = \frac{dN_b}{dx} = \frac{P\alpha}{\dfrac{1}{E_b\, A_b} + \dfrac{1}{E_n\, A_n}} \frac{\cosh \alpha x - \cosh\big(\alpha\,(l - x)\big)}{E_b\, A_b \sinh \alpha l} \,.$$

The character of N_b, N_n and t quantities' distribution along the length of the screw and the nut is shown in Fig. 198.

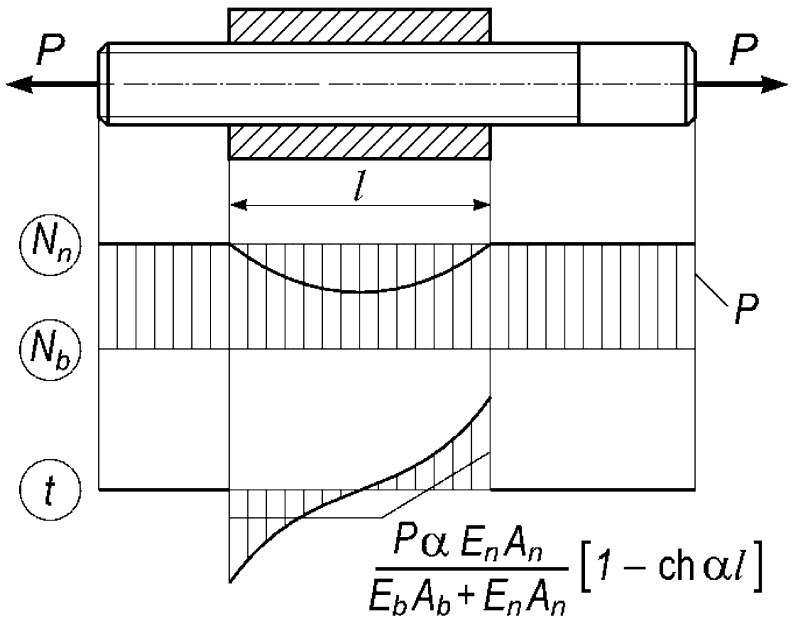

Fig. 198

15. If we apply the compressive force P to the screw on the assumption that its pitch of thread s decreases by the value Δ and after this screw the nut, then no forces in the thread will occur. If now we unload the screw then the forces arising in the system will be the same as in the system considered in the previous problem. So the solution obtained previously is suitable also for the present case assuming that the force P in the freely strained screw provides elongation Δ per one pitch of the thread. According to Hook's law

$$\Delta = \frac{Ps}{E_b A_b},$$

where s is a pitch of thread. Thus, to obtain the solution we are interested in, there is enough to replace P in the expressions of the previous problem with

$$\frac{\Delta}{s} E_b A_b .$$

16. Working conditions can be considered the most favorable when the forces on thread turns are distributed more uniformly.

In the first case the first turn is strongly overloaded.

In the second case the tightening force is applied to the nut beyond the first turn. The nut's diameter in its lower part is diminished. So the forces on the first turn in this case will be smaller. Thereby (under the same tightening force) the remaining turns are additionally loaded. Working conditions for thread turns in the second case will be more favorable.

However, the conclusion that generally in all cases the usage of type 2 (Fig. 13) nuts is preferable should not be drawn from the aforesaid. It is clear that complication of every construction especially of such widespread standard units as nuts will be appropriate only in the case when this complication gives really perceptible results. As the overload of some thread turns in comparison with the remaining turns is limiting the strength of the thread joint only in exclusive cases then correspondingly the usage of the mentioned type of nuts may be recommended as an exclusion.

17. This is a standard model for one of the possible composite material makeups. In common with a thread joints, interaction between the continuum of filler and the fibers can be considered as an elastic one. The only difference is that mutual elastic displacements in a thread joints are caused by deformation of the thread turns, and here – caused by local deformation of the filler continuum and the surface layer of the fiber.

Similarly to a thread joints

$$t = k\ (u_b - u_c)\,,$$

where $u_b - u_c$ is the displacement of the fiber's centre in relation to distant points of the filler continuum. Coefficient k can be approximately estimated by methods of elasticity theory. This depends on elasticity modules of fiber

and filler as well as on the percentage of volume occupied by them in the composite.

Simplifying the problem let us liken the part of the filler falling at one fiber to some isolated tube bearing the same functions as a nut in the previous problems.

Then without changes we obtain equation (3) of problem 13, where N_b must be understood now as normal force in the fiber. For this case let us replace A_n with A_c - cross-section area of the filler tube. Force P will be expressed through the specified mean stress σ, that is

$$P = \sigma\,(A_b + A_c)\,.$$

Ratios $\dfrac{A_b}{A_b + A_c}$ and $\dfrac{A_c}{A_b + A_c}$ represent the volume percentage of fibers and filler in the composite, that is V_b and V_c . And now instead of equation (3) (problem 13) we obtain

$$\frac{d^2 N_b}{dx^2} - \alpha^2 N_b = -\frac{k\sigma}{E_c V_c},$$

where

$$\alpha^2 = \frac{k}{A_b}\left(\frac{1}{E_b} + \frac{V_b}{E_c V_c}\right).$$

As a fiber is long, it is more suitable to express the solution of this equation not through hyperbolic functions as it was done for bolt and nut, but in the form of a damped exponent:

$$N_b = \frac{k\sigma}{\alpha^2 E_c V_c} + A\exp(-\alpha x)\,.$$

As at the end of the fiber (at $x = 0$) normal force N_b becomes zero, we obtain

$$N_b = \frac{\sigma\, E_b\, A_b}{E_b V_b + E_c V_c}\left[1 - \exp(-\alpha x)\right],$$

$$t = \frac{dN_b}{dx} = \frac{\sigma\, E_b\, A_b}{E_b V_b + E_c V_c}\,\alpha \exp(-\alpha x)\,.$$

Thus, maximal tangential stress occurs at the ends of fibers and then rapidly decreases. And normal force rapidly increases from zero to the constant value which is determined from the conditions of equality of extension strains for fiber and filler (Fig. 199).

The pattern described above clears up many things in spite of its simplicity. For example, if fiber elongation at rupture is less than filler elongation then destruction of composite under tension will begin from rupture of fibers in the middle part of their length. The disrupt fiber turns into two shorter ones, and a crack arises in filler at location of rupture. Evolution of crack in the beginning will be blocked by neighboring fibers. Under further tension of specimen already "half-length" fibers will be ruptured somewhere in their

middle part. Such dividing into fragments will stop evidently when fiber becomes so short that longitudinal tangential stresses at its ends will not be able to produce sufficient normal tensile force in its middle part. Such fiber length is called inefficient and is determined from simple considerations.

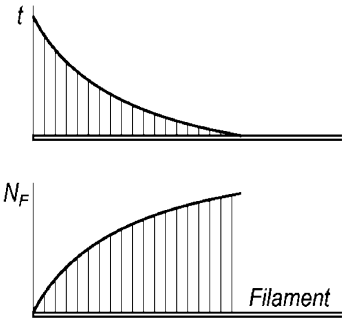

Fig. 199

Let us address the initial differential equation once more. But now, because we are talking about fibers with short length we need to express the function N_b through hyperbolic sine and cosine, that is

$$N_b = \frac{k\sigma}{\alpha^2 E_c V_c} + A \sinh \alpha x + B \cosh \alpha x .$$

Constants A and B are determined from such obvious conditions that at $x = 0$ and $x = l$ normal force N_b becomes zero. Then

$$N_b = \frac{\sigma E_b A_b}{E_b V_b + E_c V_c} \left[1 + \frac{\cosh \alpha l - 1}{\sinh \alpha l} \sinh \alpha x - \cosh \alpha x \right] .$$

Fiber length is considered inefficient if the stress in the fiber's middle point amounts to 90 percent of its possible maximum. So at $x = l/2$ the contents of the brackets must be equal to 0.9. From here without difficulties we find $\alpha l_{ie} \approx 6$ and if α is known then inefficient length l_{ie} is found also.

18. At first sight the breaking point for the filament bundle seems to be equal to the arithmetic average of the breaking points of the component filaments. In reality this is not the case, and the breaking point for the filament bundle depends also on scattering of the filaments' strength within the lot.

Suppose we have two bundles. Each of them consisting of ten filaments with breaking points that are written as conventional values in Fig. 200.

The mean breaking point for both bundles is the same at 5.5 but the dispersions are different. In the first bundle breaking point alternates from 1 to 10 while in the second one from 5 to 6. We consider, naturally, that the elasticity modules of all filaments are equal. Let us give step-by-step elongation to the first bundle. Linear dependence reflected in Fig. 200 is established between stress and strain. In the end of the first stage the same stress equal to 1 occurs in all filaments, and the first one, which is the weakest, is ruptured.

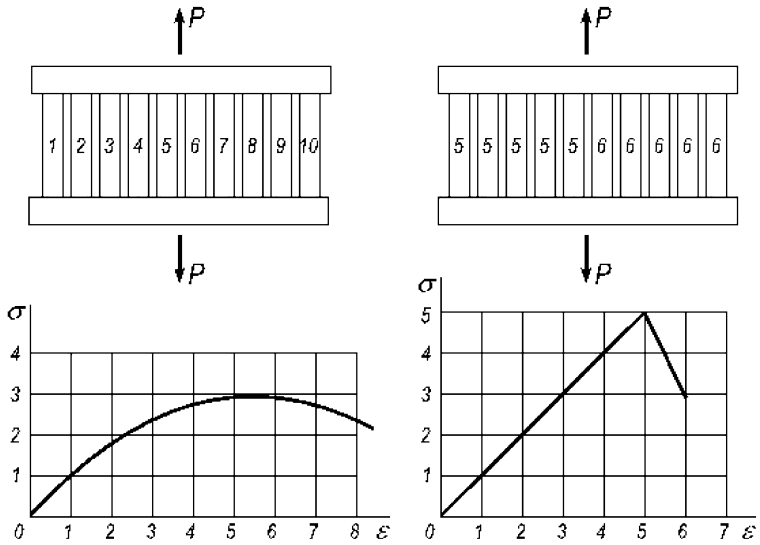

Fig. 200

Let us continue loading so that the strain is doubled. Then we mark the new point at the abscissa axis. Actual stress in all filaments is doubled correspondingly. The second filament is ruptured. And at the axis of the ordinates we must point not 2 but conventional stress in relation to the initial area of the bundle's cross-section, that is $2 \times 9/10 = 1.8$.

Let us apply additional strain to the specimen, the third "portion". Then in the remaining eight filaments actual stress equal to three conventional units occurs but... it must be recalculated in relation to the initial area that is multiplied by 8/10. As a result the ordinate of the third point of the test diagram will be equal to 2.4. In such a way, from point to point the whole test diagram is plotted for the first bundle and then for the second one (Fig. 200). The breaking point for the first bundle is equal to 3, and then for the second one equal to 5. Both values are less than mean. And this is the general rule: the breaking point decreases under dispersion. If dispersion is absent the breaking point of the bundle is equal to the breaking point of the filaments.

19. Let us consider the system of rods in the deformed state (Fig. 201) and under given displacement of nodal point A search for force P. In the drawing we measure angle α, $\Delta l_1 / l$ and u_A / l. Through the curve of Fig. 17 we find forces P_1 and P_2 corresponding to strains $\Delta l_1 / l$ and u_A / l. Force P is determined from the equilibrium condition

$$P = 2 P_1 \cos\alpha + P_2 .$$

Taking some given values of u_A we can plot the dependence of u_A on P. The curve $\dfrac{u_A}{l} = f(P)$ for the given rod elongation diagram is shown in Fig. 201.

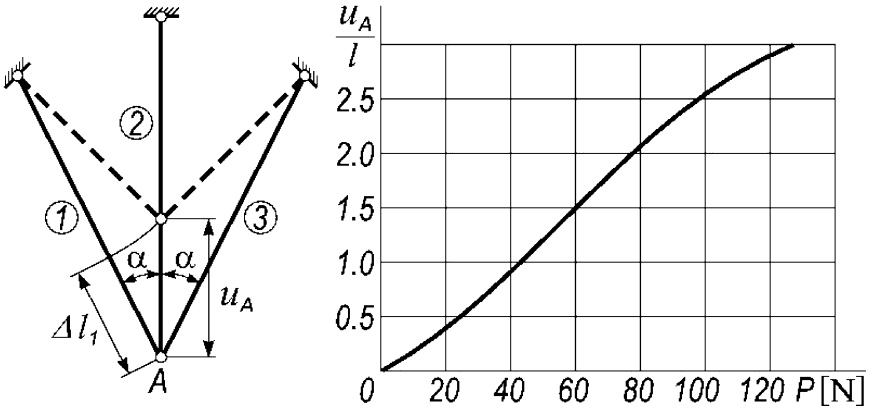

Fig. 201

20. Case *1* takes place under the large values of angle α, and case *2* under the small ones. Case 3 represents the boundary between the two first cases. The value of angle α, corresponding to case 3 can be found approximately supposing that the rigidity of filaments is significantly greater than the rigidity of rubber and therefore the loads are entirely reacted by the filaments.

Let us select the rubber-cord cylinder's element with the dimensions a and $a \times \tan\alpha$ (Fig. 202).

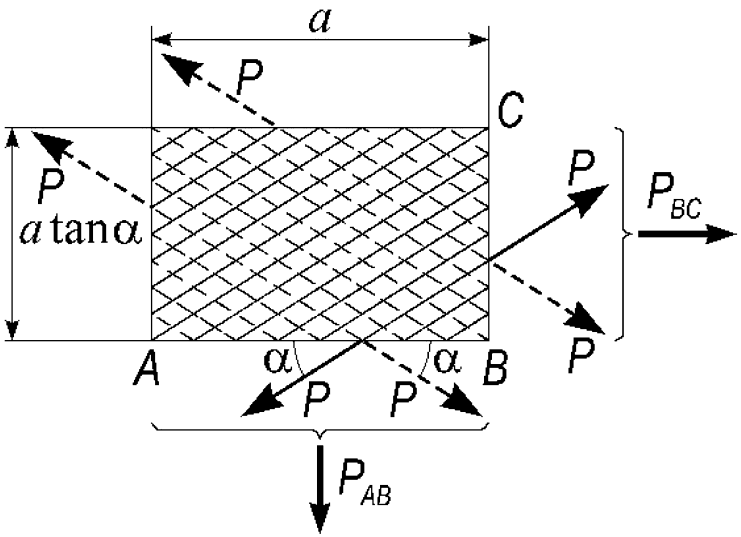

Fig. 202

Under such selection of element dimensions an equal number of filaments fall into both element sections AB and BC. Let us denote internal force in the filament as P, then the resultant of forces in section AB will be

$$P_{AB} = P\,n\,\sin\alpha\,,$$

where n is the number of filaments falling into section AB. In section BC the resultant of forces will be

$$P_{BC} = P\, n\, \cos\alpha\ .$$

But we know that under loading of the cylinder with internal pressure the mean hoopential stress is twice as much as the axial one. Consequently

$$\frac{P_{BC}}{a\ \tan\alpha} = 2\,\frac{P_{AB}}{a}\ .$$

Substituting P_{AB} and P_{BC} we find

$$\tan^2\alpha = \frac{1}{2}\,, \quad \alpha = 35^o16'\,.$$

Under this value of angle α the cylindrical shape of the shell is maintained. Under $\alpha > 35^o16'$ the cylinder becomes convex as in case 1 shown in Fig. 19, and under $\alpha < 35^o16'$, concave as in case 2 of Fig. 19.

Let us note among other things that the problems of investigating similar rubber-cord constructions arise under design calculations of automobile tires. The question of the filaments' arrangement angle selection (Fig. 203) has great significance for lifetime of the tire. Changing of angle to one or another side away from the value optimal for the given type of tire results in decreasing tire service life.

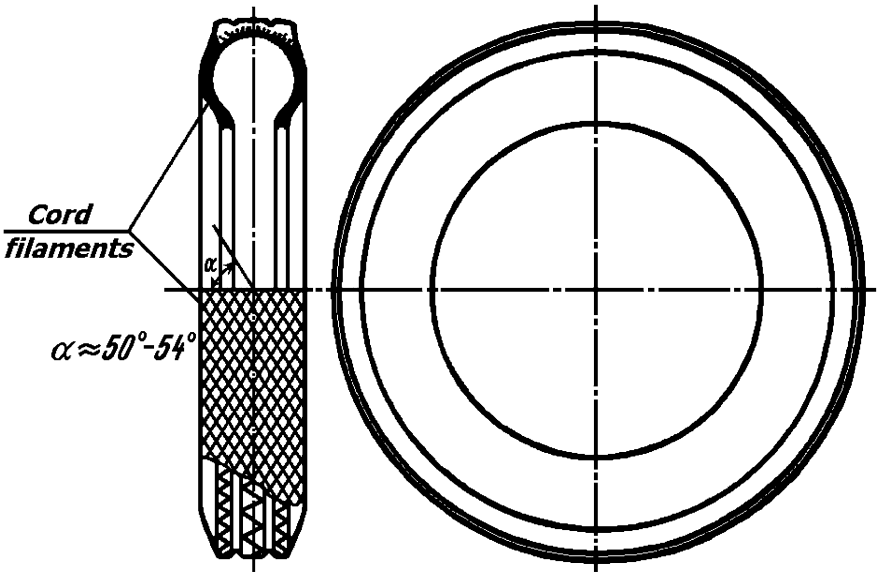

Fig. 203

However, it is necessary to say that the optimal angle for the tire is determined not from equilibrium conditions as in the example considered above, but from optimal conditions of filaments fatigue strength under alternating stresses arising during wheel rolling.

21. Let us consider equilibrium of the distinguished filament (Fig. 204).

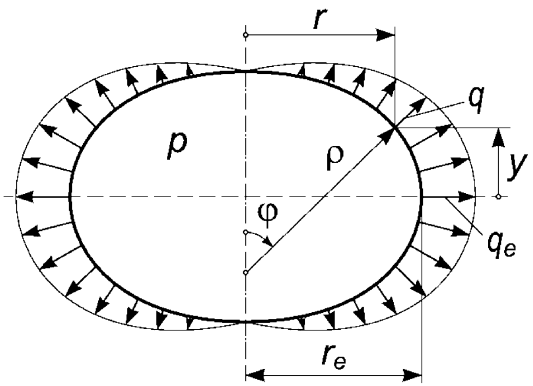

Fig. 204

The filament is affected by the distributed load q [N/m] from the side of the rubber shell. It is a variable load because the distance between filaments at different points is different. The distance is maximal at the equator where

$$q_e = p\,\frac{2\pi\, r_e}{n}\,,$$

p is the pressure and n is the number of filaments. At the point situated at the distance r from the axis

$$q = q_e\,\frac{r}{r_e}\,.$$

Tensile force T does not vary along the arc of the meridian. It is $T = q\,\rho$, where ρ is the local radius of the meridian's curvature.

Excluding q and then q_e from here we find

$$T = \frac{2\pi}{n}\,p\,\rho\,r\,.$$

On the other hand the half-sphere equilibrium condition gives

$$T = p\,\frac{\pi\, r_e^2}{n}\,. \tag{1}$$

Excluding we obtain

$$\rho = \frac{r_e^2}{2r}.$$

Let φ be the angle between the normal to the deformed surface and the axis of revolution. Then $dr = \rho\,\cos\varphi\,d\varphi$ or

$$dr = \frac{r_e^2}{2r}\,\cos\varphi\,d\varphi\,.$$

Integrating we obtain

$$r = r_e^2 \sin\varphi + C_1 .$$

As φ becomes zero under $r = 0$ then $C_1 = 0$ and

$$\sin\varphi = \frac{r^2}{r_e^2} . \tag{2}$$

Let us denote the distance of some point from the equator plane as y. It is obvious that $\dfrac{dy}{dr} = -\tan\varphi$ or

$$dy = \frac{\dfrac{r^2}{r_e^2}\,dr}{\sqrt{1 - \dfrac{r^4}{r_e^4}}} .$$

Let us substitute $r = r_e \cos\psi$ for integration of this expression.

Then

$$dy = r_e \frac{\cos^2\psi\, d\psi}{\sqrt{1 + \cos^2\psi}}$$

or

$$y = r_e \frac{\sqrt{2}}{2}\left[2\int_0^{\psi}\sqrt{1 - \frac{\sin^2\psi}{2}}\,d\psi - \int_0^{\psi}\frac{d\psi}{\sqrt{1 - \dfrac{\sin^2\psi}{2}}}\right] + C_2 .$$

The value of C_2 is equal to zero because at the equator $\psi = 0$ and y becomes zero also.

Relative flattening of the equilibrium figure is determined by the relation y_0/r_e where y_0 is the vertical semi-axis of the body of revolution:

$$\frac{y_0}{r_e} = \frac{\sqrt{2}}{2}\left[2\int_0^{\pi/2}\sqrt{1 - k^2\sin^2\psi}\,d\psi - \int_0^{\pi/2}\frac{d\psi}{\sqrt{1 - k^2\sin^2\psi}}\right]$$

or

$$\frac{y_0}{r_e} = \frac{\sqrt{2}}{2}(2E - F) .$$

Here E and F are full elliptic integrals of the first and second kind correspondingly, having modulus $k = \sqrt{1/2}$. These integrals are tabulated; from the tables we find

$$F = 1.85407 \quad \text{and} \quad E = 1.35064 .$$

As a result

$$\frac{y_0}{r_e} = 0.599 .$$

There is one interesting detail: the found shape of the shell has the greatest volume among the other bodies of revolution having a specified length of the meridian's arc. If the length of the filaments is given and therefore remains unchanged then the energy of the system is determined by the potential of the pressure forces only. The pressure produces work equal to pV. This work will be maximal under maximal volume V and the potential of the external forces $(-pV)$ correspondingly has a minimum in comparison to all neighboring shapes.

And one more question. If the filaments are compliant then how will the shape of the found body of revolution be changed due to the increase of internal pressure? The answer is sufficiently obvious. The extent of flattening will be the same but all dimensions of the "pumpkin" will be multiplied by $(1+\varepsilon)$ where ε is the relative elongation of the filaments. And ε depends on the form of the elongation diagram of the filaments.

Quantitative estimation follows from computations already carried out.

The length of the meridian's arc that is the new length of the filaments is determined by integration of the expression $ds = \sqrt{dz^2 + dy^2}$.

Omitting simple intermediary computations let us deduce the final result. The length of the arc from pole to equator will be

$$l = \frac{\sqrt{2}}{2}\, r_e\, F = 1.3110\, r_e\ .$$

Specifying r_e we compare l with the initial half-length of the filament and find ε. If the elongation diagram of the filaments is given, and this is necessary, we find from the graph the tensile force T, and the pressure p is determined from expression (1). In such a way from point to point one can construct the dependency of r_e upon p.

And finally one more instructive circumstance. The deduced solution undoubtedly contains some rudiments of the precomputer age. When a researcher had no computing engines in his hands, reducing of any problem to tabulated functions would be considered as an undoubted success. And the deduced example is the best proof of this fact. But this situation remains in the past. In fact, since expression (1) was derived, one should be able to write

$$dy = -\sin\varphi\, ds\ , \quad dr = \cos\varphi\, ds\ ,$$

where ds is the element of the filament's arc. Further, it is possible to make these expressions dimensionless assigning, for example

$$\frac{y}{r_e} = Y\ , \quad \frac{r}{r_e} = X\ , \quad \frac{s}{r_e} = S\ .$$

And then

$$Y = -\int_0^s X^2 dS\ , \quad X = \int_0^s \sqrt{1 - X^4}\, dS\ .$$

And, further, one can fulfil computer integration with respect to S taking zero initial values for Y and X and stop this calculation when X will reach its maximum. The value of Y found at the same time and taken with "plus" sign will give us exactly the extent of the spheroid's flattening we are looking for. The expected value of argument S, as one can easily understand, will be close to 1.5.

22. The mentioned phenomenon may take place only in the case when sufficiently large plastic deformations occur in the aluminium ring under heating.

Let us denote the difference between the external radius of the internal ring and the internal radius of the external ring before the fitting as Δ.

It is obvious, that

$$\varepsilon_A + \varepsilon_S = \frac{\Delta}{R}\,, \tag{1}$$

where ε_A is the relative shortening of the aluminium ring's arc and ε_S is the relative elongation of the steel ring's arc.

Within the limits of elastic deformations in the presence of additional heating

$$\varepsilon_A = \frac{\sigma_A}{E_A} - \alpha_A\, t\,, \quad \varepsilon_S = \frac{\sigma_S}{E_S} + \alpha_S\, t\,,$$

where σ_A and σ_S are the stresses in aluminium and steel rings, and α_A and α_S are the corresponding coefficients of temperature linear broadening. On the other hand, $\sigma_A = \sigma_S = \sigma$, as follows from the equilibrium conditions (Fig. 205) under equal thicknesses of the rings.

Then from equation (1) we have

$$\sigma = \frac{\dfrac{\Delta}{R} + t\,(\sigma_A - \sigma_S)}{\dfrac{1}{E_A} + \dfrac{1}{E_S}}\,. \tag{2}$$

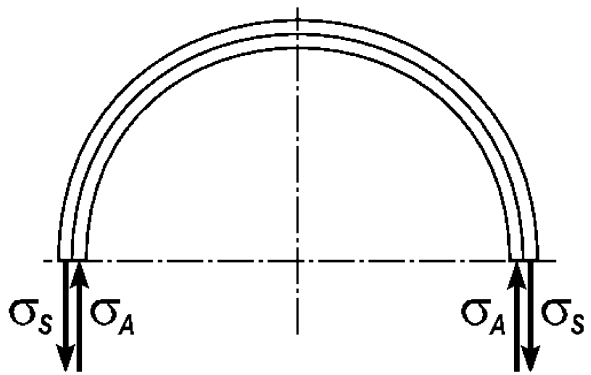

Fig. 205

Suppose that the tension or the compression diagram of aluminium can be schematized in such a way as shown in Fig. 206.

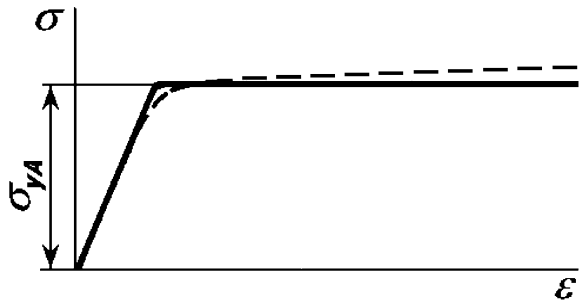

Fig. 206

The yield stress of aluminium is lower than the yield stress of steel. As the stresses in both rings are equal, the steel ring will work elastically in all the cases.

The stress of initial tightness of the rings which we denote as σ_0 will be

$$\sigma_0 = \frac{\frac{\Delta}{R}}{\frac{1}{E_A} + \frac{1}{E_S}} .$$

Then expression (2) will take the form

$$\sigma = \sigma_0 + \frac{t\ (\sigma_A - \sigma_S)}{\frac{1}{E_A} + \frac{1}{E_S}} . \tag{3}$$

Let us note that σ cannot be greater than σ_{yA}. If the temperature of heating is

$$t > (\sigma_{yA} - \sigma_0) \left(\frac{1}{E_A} + \frac{1}{E_S} \right) \frac{1}{(\alpha_A - \alpha_S)} ,$$

then plastic deformations will occur in the aluminium ring and $\sigma = \sigma_{yA}$.

Under cooling the rings will be deformed elastically. Then the residual stresses can be found as the algebraic sum of σ_{yA} and the stress of cooling, obtained from expression (3) by replacing the sign before t with the reverse one, that is

$$\sigma_{res} = \sigma_{yA} - \frac{t\ (\sigma_A - \sigma_S)}{\frac{1}{E_A} + \frac{1}{E_S}} . \tag{4}$$

Under $\sigma_{res} < 0$ the aluminium ring will be falling out of the steel one. Therefore the condition of falling out will be

$$t\ (\alpha_A - \alpha_S) > \sigma_{yA} \left(\frac{1}{E_A} + \frac{1}{E_S} \right) . \tag{5}$$

It is possible that plastic deformations in the aluminium ring arise already under the fitting that is before heating. The expressions (4) and therefore (5) also remain valid under these conditions, in no dependency upon the influences resulting from reaching the yield stress σ_{yA}.

23. If the temperature elongations of the ring and the cone are equal, the height h evidently is not changed. Let us suppose that temperature elongation of the conical rod is greater than temperature elongation of the ring:

$$\varepsilon_{tc} > \varepsilon_{tr}$$

In this case tensile stress σ having a value depending on the difference of the temperature deformations $\varepsilon_{tc} - \varepsilon_{tr}$ (Fig.207) will arise in the ring under heating.

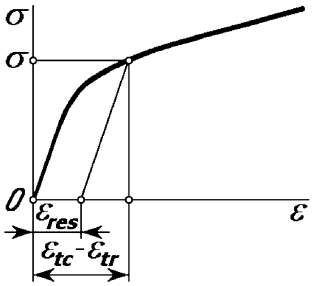

Fig. 207

If the stress σ remains lower than the limit of elasticity then under cooling the dimensions of the ring are reestablished and the height of its disposition h is not changed. If the difference $\varepsilon_{tc} - \varepsilon_{tr}$ is sufficiently large then the ring will receive residual deformation and under cooling the ring will descend. Under repeated heating it will elongate once more and henceforward will descend once more. This descending will continue until the elastic deformation ε_E will not become equal to the value of $\varepsilon_{tc} - \varepsilon_{tr}$ (Fig. 208). The new height of the ring's location is easily determined by the value of cumulative residual deformation $\sum \varepsilon_{res}$.

The analogous behavior takes place also under $\varepsilon_{tc} < \varepsilon_{tr}$. In this case the descending of the ring occurs under heating, while its elongation occurs under cooling.

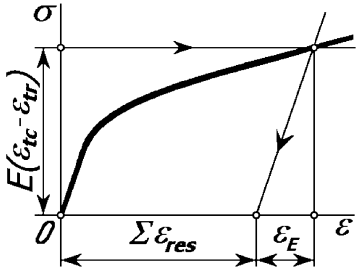

Fig. 208

24. The tube's deformation in the circumferential direction is specified by

$$\varepsilon_t = \frac{\Delta}{R} = \frac{1}{E}\left(\sigma_t - \mu\,\sigma_x\right).$$

Let us denote the contact pressure as p and the axial force arising in the tube as N. Then

$$\sigma_t = \frac{pR}{h}, \quad \sigma_x = \frac{N}{2\pi R h},$$

where h is the tube's thickness. Consequently

$$\frac{\Delta}{R} = \frac{1}{Eh}\left(pR - \mu\frac{N}{2\pi R}\right). \tag{1}$$

But the axial force in the section x is determined by the integral of frictional forces at interval $(0 \div x)$ that is

$$N = \int_0^x f p 2\pi R dx \tag{2}$$

where f is the friction coefficient. Now expression (1) will take the form

$$\frac{\Delta}{R} = \frac{1}{Eh}\left(pR - \mu f \int_0^x p dx\right).$$

Differentiating this expression with respect to x we obtain

$$\frac{dp}{dx} - \frac{\mu f}{R}p = 0,$$

from which

$$p = p_0 \exp\left(\frac{\mu f}{R}x\right).$$

The constant p_0 represents the contact pressure at the end of the tube. It can be found from expression (1) by assigning $N = 0$. So we have

$$p_0 = \frac{Eh}{R^2}\Delta.$$

Therefore

$$p = \frac{Eh\Delta}{R^2}\exp\left(\frac{\mu f}{R}x\right).$$

From expression (2) we find the axial force

$$N = \frac{2\pi Eh\Delta}{\mu}\left[\exp\left(\frac{\mu f}{R}x\right) - 1\right].$$

Consequently, the contact pressure and the axial force are increasing as the distance from the end of the tube is growing. This increment will evidently

cease at the section where axial elongation due to the forces N and p will become equal to the initial axial elongation of the tube. But as the heated tube is uniformly broadening in all directions, axial elongation at the moment of fitting was equal to the hoopential one, that is Δ/R. Let us express axial elongation through N and p :

$$\varepsilon_x = \frac{1}{E}\left(\sigma_x - \mu\sigma_t\right), \quad \varepsilon_x = \frac{\Delta}{\mu R}\left[\left(1-\mu^2\right)\exp\left(\frac{\mu f}{R}x\right) - 1\right].$$

Let us denote as a the length of the interval where the slippage takes place and frictional forces exist. Assigning $\varepsilon_x = \Delta/R$ and $x = a$ we find from the last expression

$$a = \frac{R}{\mu f}\ln\frac{1}{1-\mu}.$$

Under $x > a \quad \varepsilon_x = \varepsilon_t = \Delta/R = const$ and we have

$$N = \frac{2\pi Eh\Delta}{1-\mu}, \quad p = \frac{Eh\Delta}{R^2}\frac{1}{1-\mu}.$$

At the other end of the tube the distribution of the forces will be analogous.

Figure 209 shows the laws of distribution along the tube's axis for the normal force N, the frictional forces dN/dx and the contact pressure p.

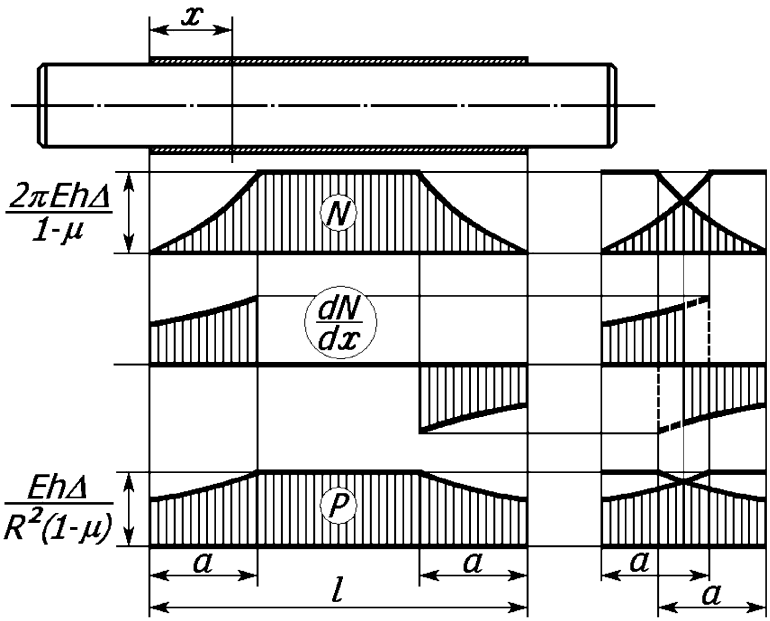

Fig. 209

The same graphs for the case of the shorter tube ($l < 2a$) are shown aside for the comparison.

25. Let us consider the case (a).

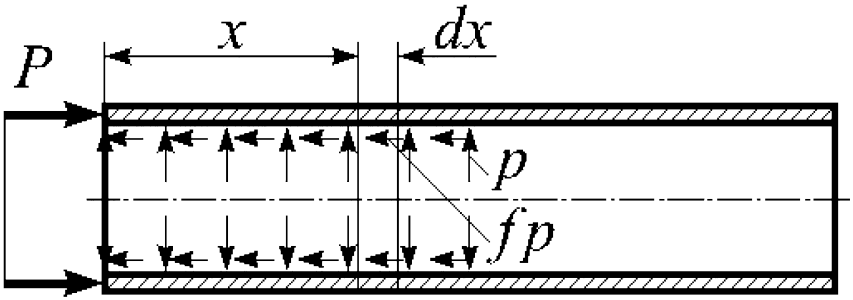

Fig. 210

The axial force in the section x of the tube (Fig. 210) will be

$$N = \int_0^x fp2\pi R dx - P\,. \tag{1}$$

Instead of expression (1) obtained in solving the previous problem we have

$$\frac{\Delta}{R} = \frac{1}{Eh}\left[pR - \frac{\mu}{2\pi R}\left(-P + 2\pi R f \int_0^x p dx\right)\right]. \tag{2}$$

As well as in the previous problem

$$p = p_0 \exp\left(\frac{\mu f}{R}x\right).$$

The value of p_0 is determined from equation (2) if we assign there $x = 0$:

$$\frac{\Delta}{R} = \frac{1}{Eh}\left(p_0 R + \frac{\mu}{2\pi R}P\right),$$

from which

$$p_0 = \frac{Eh}{R^2}\Delta - \frac{\mu P}{2\pi R^2}\,.$$

Consequently, we obtain

$$p = \left(\frac{Eh}{R^2}\Delta - \frac{\mu P}{2\pi R^2}\right)\exp\left(\frac{\mu f}{R}x\right),$$

and then from equation (1)

$$N = -\frac{2\pi Eh\Delta}{\mu} + \left(\frac{2\pi Eh\Delta}{\mu} - P\right)\exp\left(\frac{\mu f}{R}x\right).$$

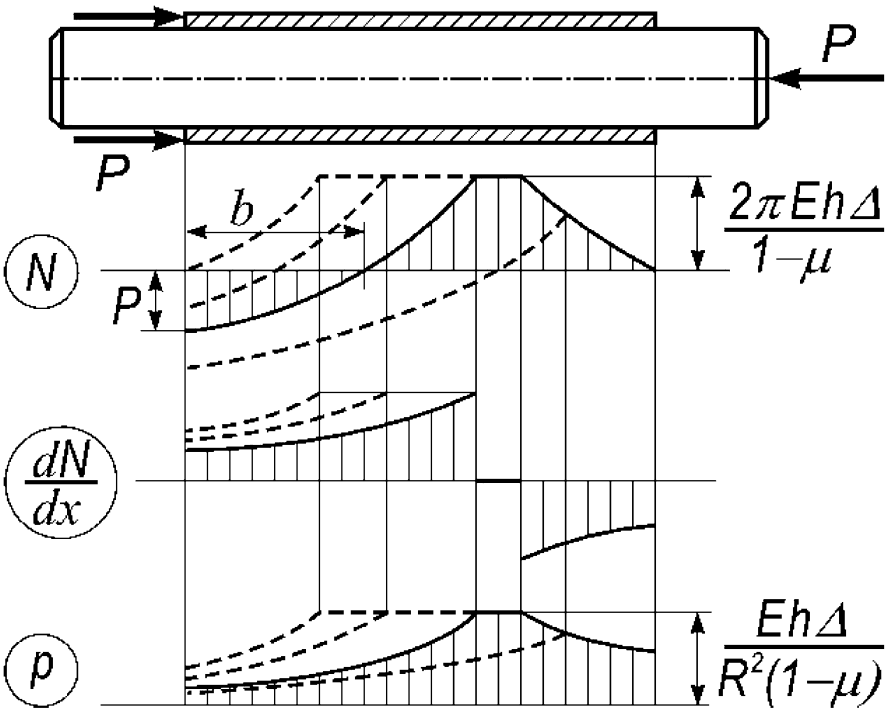

Fig. 211

Figure 211 shows the laws of distribution along the tube's axis for the normal force N, the frictional forces dN/dx and the contact pressure p.

The behavior of the curves under $P = 0$ and under some other values of P is shown by dashed line.

The tube will be taken off the rod under such value P^* of the force P when the segment b (Fig. 211) becomes equal to the tube's length l. Assigning $N = 0$ and $x = l$ in the last expression we find

$$P^* = \frac{2\pi Eh\Delta}{\mu}\left[1 - \exp\left(-\frac{\mu f}{R}l\right)\right].$$

Now let us consider the case (b). Here the force P as well as the frictional forces near the left end of the tube change their direction. Therefore

$$N = P - \int_0^x fp2\pi R dx$$

and instead of equation (2) we obtain

$$\frac{\Delta}{R} = \frac{1}{Eh}\left[pR - \frac{\mu}{2\pi R}\left(P - 2\pi Rf\int_0^x p dx\right)\right].$$

Then $p = p_0 \exp\left(-\frac{\mu f}{R} x\right)$, where $p_0 = \frac{Eh}{R^2}\Delta + \frac{\mu P}{2\pi R^2}$.

Further

$$N = -\frac{2\pi Eh\Delta}{\mu} + \left(\frac{2\pi Eh\Delta}{\mu} + P\right) \exp\left(-\frac{\mu f}{R} x\right).$$

The corresponding laws of distribution along the tube's axis for the normal force N, the frictional forces dN/dx and the contact pressure p are shown in Fig. 212. Under $x = b$ the frictional forces change their direction stepwise.

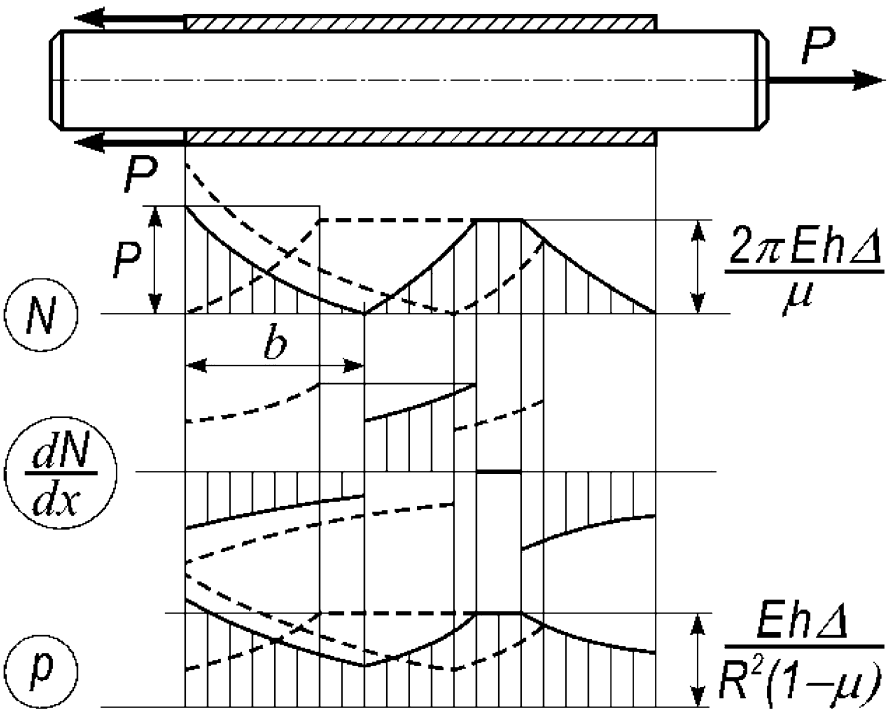

Fig. 212

Assigning $N = 0$ and $x = l$ in the last expression we find the sought value of the force P^* under which the tube will be taken off the rod.

$$P^* = \frac{2\pi Eh\Delta}{\mu}\left[\exp\left(\frac{\mu f}{R} l\right) - 1\right].$$

This value of the force proves to be greater than in case (a). This fact is sufficiently obvious because tensile force causes the narrowing of the tube and the augmentation of the frictional forces.

26. Let us suppose that some tangential stress τ occurs in any corner point of the rod's cross-section (Fig. 213).

Let us decompose this stress to components τ_1 and τ_2 perpendicular to the sides of the polygon. According to the twoness condition, the conjugate tangential stresses τ_1 and τ_2 must occur in the lateral faces of the rod. But the lateral surface is free of stresses. Therefore $\tau_1 = \tau_2 = 0$. Consequently, $\tau = 0$ too.

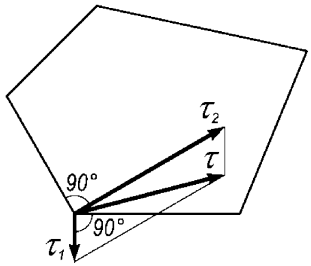

Fig. 213

It is clear that the proved thesis remains valid under any value of angle less than 180^o.

27. The resulting moment of the stresses τ' is counterbalanced with the moment of the resultant force Q occurring in the plane of the normal section (Fig. 214). The value of this force will evidently be the following

$$Q = \int_0^R \int_0^\alpha \tau\, r \sin\varphi \, dr\, d\varphi.$$

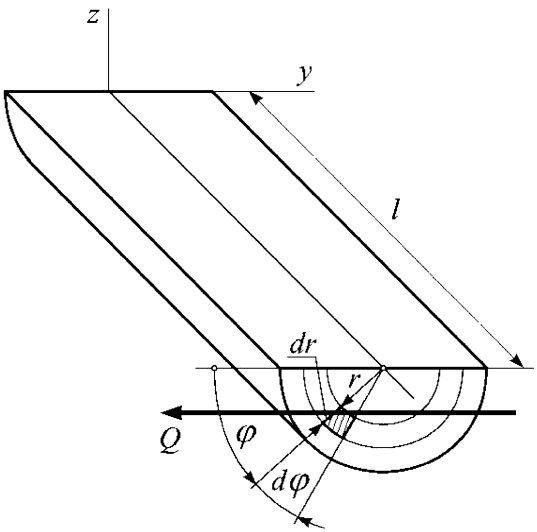

Fig. 214

But we have $\tau = \tau_{\max}\dfrac{r}{R}$, therefore

$$Q = \int_0^R \int_0^\pi \tau_{\max}\frac{r^2}{R}\sin\varphi\, dr d\varphi = \frac{2}{3}\tau_{\max}R^2.$$

The moment of the force Q relative to z axis is equal to

$$M = \frac{2}{3}\tau_{\max}R^2 l.$$

And the stresses τ' produce just the same moment

$$M = 2l\int_0^R \tau' r\, dr = \frac{2\tau_{\max}l}{R}\int_0^R r^2 dr = \frac{2}{3}\tau_{\max}R^2 l.$$

28. If the rod is twisted without tension then the dependency of the specific torsion angle θ upon the torque M would exist within the limits of small displacements

$$\theta = \frac{3M}{Gbh^3},$$

that is, the torsional rigidity would be equal to

$$C_0 = \frac{1}{3}Gbh^3.$$

Now let us consider the case of the rod's torsion in the presence of the axial tensile force P . The normal stresses $P/(bh)$ preserve the direction of the strip's longitudinal fibers during rotation of the end cross-section (Fig. 215).

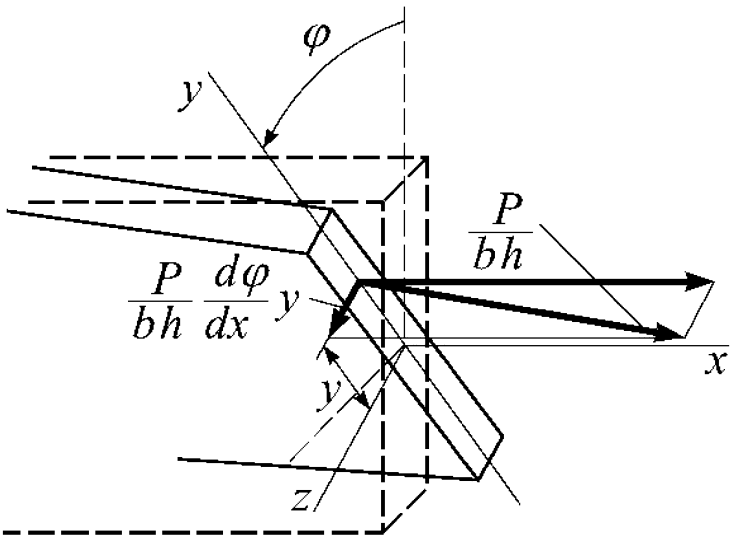

Fig. 215

The projections of these stresses onto the plane perpendicular to the strip's axis are equal to

$$\frac{P}{bh}\frac{d\varphi}{dx}y = \frac{P}{bh}\theta y$$

(Fig. 215). These stresses produce the additional twisting moment

$$M_P = \int\limits_{-h/2}^{+h/2} \frac{P}{bh}\theta y^2 h dy = P\theta\frac{b^2}{12}.$$

Adding this moment to the moment produced by tangential stresses we find

$$M = C_0\theta + P\theta\frac{b^2}{12} = \theta\left(C_0 + \frac{Pb^2}{12}\right).$$

Consequently, the torsional rigidity of the strip being stretched is equal to the rigidity of the unstretched one plus the value $Pb^2/12$.

29. As the tube and the shaft are not absolutely rigid, the local slippage begins earlier than the value of the moment will reach the quantity M_0. In the beginning, the slippage occurs in the marginal zones of the contact segment. Under $M = M_0$ the slippage embraces the whole surface of the contact. The moment of the frictional forces at the same time will reach its limiting value M_0 and the turning of the shaft relative to the tube is beginning at the whole length of the contact.

Let us divide the contact segment l into three zones a, b and c (Fig. 216).

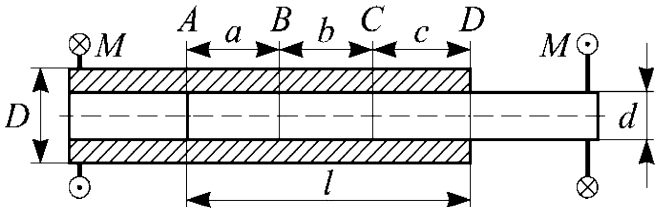

Fig. 216

At the segment a the twisting moment in the tube is greater than in the shaft and correspondingly the angle of torsion is greater, too. While transition from the cross-section A to the cross-section B the transfer of the twisting moment from the tube to the shaft takes place and in the cross-section B the twist angles of the tube and the shaft become equal.

There is no slippage at the segment b. At the segment c the slippage takes place again. Here the twisting moment in the shaft is already greater than in the tube. The angle of torsion in the shaft is greater correspondingly. While transition from the cross-section C to the cross-section D the moment in the tube descends to zero and in the shaft increases to M.

The intensity of the moments of the frictional forces is equal to

$$m = \frac{M_0}{l}. \tag{1}$$

The value of m is independent of the moment M. It is determined only by the value of the friction coefficient and the value of tightness.

Now let us determine the lengths of the segments a, b and c . For this purpose let us consider the tube and the shaft separately (Fig. 217). From the equilibrium condition we evidently have

$$m\,(a + c) = M, \tag{2}$$

and from the equality condition for the angles of torsion at the segment b we obtain

$$\frac{m\,c}{(GJ_p)_T} = \frac{m\,a}{(GJ_p)_S}. \tag{3}$$

From equations (2) and (3) we find

$$a = \frac{\dfrac{M}{M_0}\,l}{1 + \dfrac{(GJ_p)_T}{(GJ_p)_S}}, \quad c = \frac{\dfrac{M}{M_0}\,l}{1 + \dfrac{(GJ_p)_S}{(GJ_p)_T}}. \tag{4}$$

If the rigidities of the tube and the shaft are equal then from (4) we obtain

$$a = c = \frac{M}{2M_0}\,l.$$

Under the known a and c we are sketching torque epures (Fig. 217).

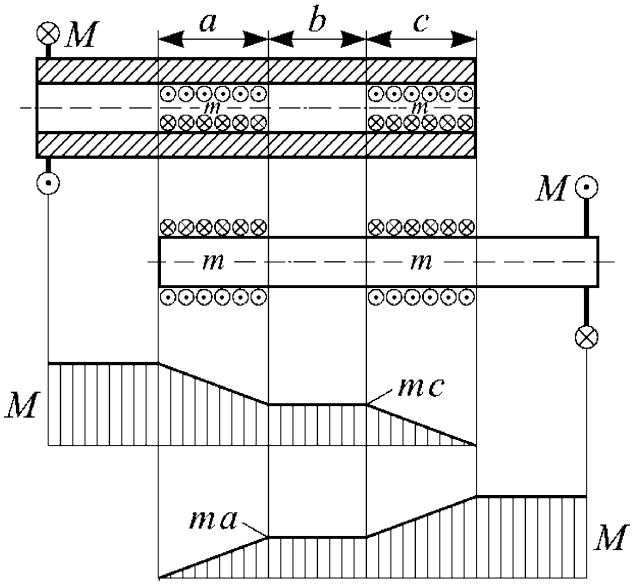

Fig. 217

As the moment M increases the segments a and c become longer and the segment b shortens. Under $M = M_0$ the sum $a + c$ is equal to l and $b = 0$. After that the moment of the frictional forces, which grew due to the increase of the segments a and c, cannot grow any further and the mutual slippage along the whole contact surface begins.

30. Let us locate the origin of coordinates x, y in the glued spot's center of gravity (Fig. 218). Let us assign that under loading the glued gusset plate has moved left by Δ_x and down by Δ_y and in addition has rotated clockwise by a small angle φ.

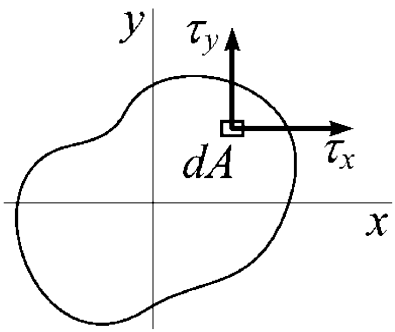

Fig. 218

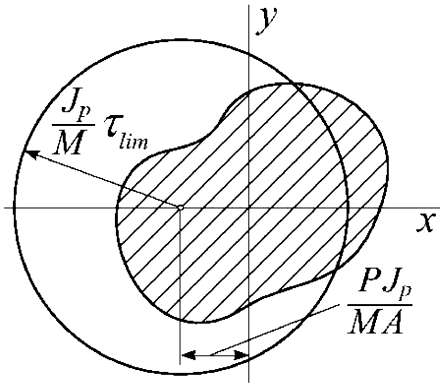

Fig. 219

Let us determine the stresses τ_x and τ_y effecting the gusset plate. They are proportional to the local displacement, that is, to the displacement of the point with coordinates x, y:

$$\tau_x = k\,(\Delta_x - \varphi\, y)\,, \quad \tau_y = k\,(\Delta_y + \varphi\, x)\,,$$

where k is some coefficient of proportionality between the stress and the displacement.

Let us write the equilibrium equations

$$\int\limits_A \tau_x\, dA = 0\,, \quad \int\limits_A \tau_y\, dA = P\,, \quad \int\limits_A (\tau_y\, x - \tau_x\, y)\, dA = M,$$

where M is the moment of the force P about the origin of coordinates. The integration applies to the area of the whole spot or to the total area of the spots if there are several of them.

Taking into account that the axes x and y are central ones we obtain

$$\Delta_x = 0\,, \quad k\,\Delta_y\, A = P\,, \quad k\varphi J_p = M,$$

where J_p is the polar moment of inertia of the glued spot about its center of gravity. Substituting Δ_x, Δ_y and φ into the expressions for the stresses τ_x and τ_y we obtain

$$\tau_x = -\frac{M}{J_p}\,y\,, \quad \tau_y = \frac{P}{A} + \frac{M}{J_p}\,x\,.$$

The full stress is equal to $\tau = \sqrt{\tau_x^2 + \tau_y^2}$. Substituting here the expressions for τ_x and τ_y let us determine the geometrical locus of points where the full stress reaches its limiting value $\tau_{\lim}$:

$$\left(x + \frac{P}{M}\,\frac{J_p}{A}\right)^2 + y^2 = \left(\frac{J_p\,\tau_{\lim}}{M}\right)^2.$$

As we see this is the circle of radius $\frac{J_p \tau_{\lim}}{M}$. The center of the circle is located at the x axis to the left from the origin of the coordinates by the value $\frac{P}{M}\,\frac{J_p}{A}$ (Fig. 219). If the circle intersects the contour of the glued spot then the stresses in the outer region of the spot are greater than the limiting (breaking) stress. If the whole spot is inscribed into the circle then the strength condition is fulfilled.

31. 1. Let us isolate the inner part of the rod by the cylindrical surface through-passing the specified contour (Fig. 220).

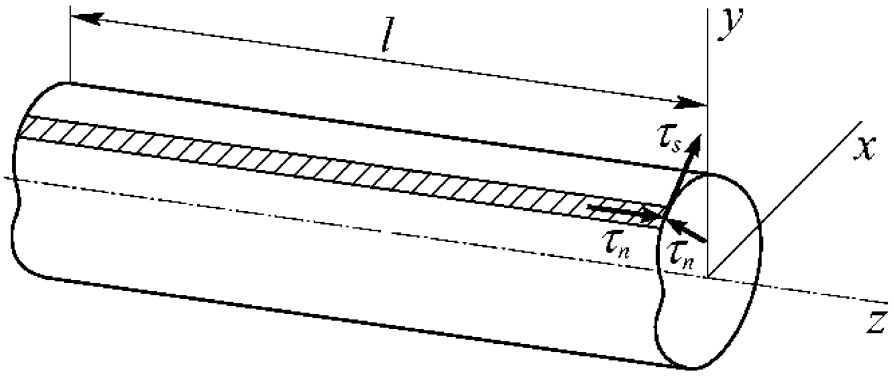

Fig. 220

Tangential stresses conjugate to τ_n occur at the traced cylindrical surface. Projecting on the axis z all the forces effecting at the isolated part of the rod we obtain

$$\oint_S \tau_n\, l\, ds = 0,$$

or otherwise

$$\oint_S \tau_n\, ds = 0.$$

2. Let us consider the element $ds\,dz$ of the cylindrical surface traced through the drawn contour (Fig. 221). After loading of the rod this element

will be disfigured and will take the form of a parallelogram represented in Fig. 221. The angle of shear γ will be determined by the sum of the angles α and β, that is

$$\gamma = \alpha + \beta.$$

Now let us find the expressions for every summand of the above-mentioned. The angle α is determined by the angle of torsion θ and by the distance from the center of twist; indeed from Fig. 221 we have

$$\alpha = \frac{AA'}{dz};$$

but $AA' = n\,d\varphi$, where $d\varphi$ is the relative rotation angle of the cross-sections lying in the distance dz from each other, and n is the distance from the center of twist O (Fig. 222) to the tangent to the contour in point A. As $d\varphi/dz = 0$, then $\alpha = \theta\, n$.

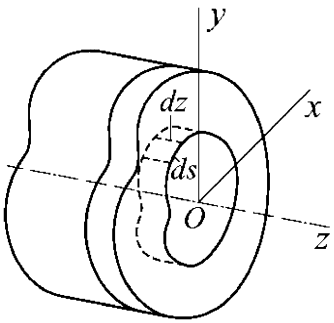

Fig. 221

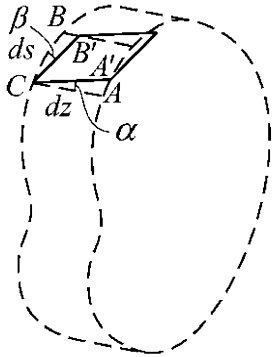

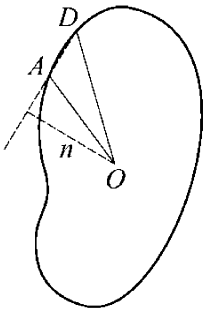

Fig. 222

The cross-section of the rod under torsion will not remain plane. It will receive some displacement $w(x, y)$ in the direction of the z axis. It is obvious (Fig. 221) that

$$\beta = \frac{dw}{ds}.$$

As $\gamma = \dfrac{\tau_s}{G}$ then

$$\frac{\tau_s}{G} = \theta n + \frac{dw}{ds},$$

from which we obtain

$$dw = \left(\frac{\tau_s}{G} - \theta n\right) ds.$$

The integral of dw applied to a closed contour is equal to zero. So

$$\frac{1}{G} \oint\limits_S \tau_s\, ds - \theta \oint\limits_S n\, ds = 0.$$

But nds is the doubled area of the OAB triangle (Fig. 222), therefore

$$\oint_S n\,ds = 2A_s, \qquad \oint_S \tau_s\,ds = 2GA_s\,\theta.$$

32. A thin-walled profile with the principal central axes of inertia is shown in Fig. 223. Let us suppose that under torsion the cross-section rotates by the angle φ about some point C having the coordinates x_C, y_C.

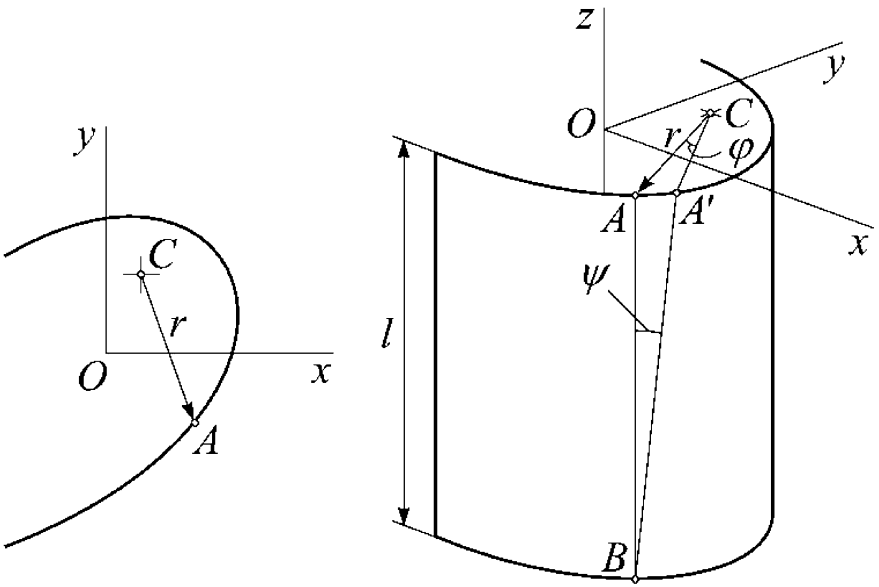

Fig. 223

The generatrix AB (Fig. 223) under this will rotate by the angle

$$\psi = \frac{r\,\varphi}{l} = r\,\theta.$$

As a result there will arise the longitudinal elongation

$$\varepsilon = \frac{A'B - AB}{AB} = \frac{1}{\cos\psi} - 1\,, \quad \varepsilon \approx \frac{1}{2}\,\psi^2$$

or

$$\varepsilon = \frac{1}{2}\,r^2\,\theta^2.$$

The mutual rotational displacement about the x and y axes and the mutual axial displacement of the cross-sections are possible simultaneously with the mutual rotational displacement about the longitudinal axis. Therefore the additional component, depending linearly upon x and y, will appear in the expression for ε, i.e. we have

$$\varepsilon = \frac{1}{2}\, r^2\, \theta^2 + a + b\, x + c\, y$$

and correspondingly the stress

$$\sigma = E\left(\frac{1}{2}\, r^2\, \theta^2 + a + b\, x + c\, y\right). \tag{1}$$

The warping of the cross-section will not have an influence on the elongation ε because we consider the unconstrained torsion (θ does not change along the rod's axis).

The constants a, b and c must be selected in such a way that the normal force in the cross-section as well as bending moments about x and y axes would become zero:

$$N = \int\limits_A \sigma\, dA = 0\,, \quad M_x = \int\limits_A \sigma\, y\, dA = 0\,, \quad M_y = \int\limits_A \sigma\, x\, dA = 0\,,$$

from which we obtain

$$a = -\frac{\theta^2 J_p}{2A}, \quad b = -\frac{\theta^2 H_y}{2J_y}, \quad c = -\frac{\theta^2 H_x}{2J_x},$$

where J_x, J_y and J_p are correspondingly axial and polar moments of inertia of the cross-section, and H_x and H_y are the new geometrical adjectives

$$H_x = \int\limits_A r^2\, y\, dA = 0, \quad H_y = \int\limits_A r^2 x\, dA = 0.$$

The expression (1) takes the form

$$\sigma = \frac{E\theta^2}{2}\left(r^2 - \frac{J_p}{A} - \frac{H_y}{J_y}\, x - \frac{H_x}{J_x}\, y\right). \tag{2}$$

The stresses σ create in the cross-section the additional twisting moment

$$M_z = \int\limits_A \sigma\, r\, \psi\, dA,$$

or

$$M_z = \frac{E\theta^3}{2} \int\limits_A \left(r^2 - \frac{J_p}{A} - \frac{H_y}{J_y} x - \frac{H_x}{J_x} y\right) r^2\, dA\,, \quad M_z = \frac{E\theta^3}{2} K.$$

where the quantity K represents the new geometrical adjective

$$K = \int\limits_A r^4\, dA - \frac{J_p^2}{A} - \frac{H_y^2}{J_y} - \frac{H_x^2}{J_x}. \tag{3}$$

The twisting moment in the cross-section consists of the "usual" moment produced by the tangential stresses and of the additional one

$$M_T = \frac{1}{3}\, s\,\delta^3 G\,\theta + \frac{E\,\theta^3}{2} K = \frac{1}{3}\, s\,\delta^3 G\,\theta \left(1 + \frac{E}{G}\,\frac{3}{2\delta^3 s}\,\theta^2 K\right), \tag{4}$$

where s is the length of the contour's arc.

Executing the replacement of r^2 with $(x - x_{C'})^2 + (y - y_{C'})^2$ in expressions (2) and (3) we shall notice that the coordinates $x_{C'}$ and $y_{C'}$ in the expressions for σ and K are excluded. It means that the selection of the pole C can be made arbitrarily and one may be guided here by the considerations of convenience only.

Let us consider the particular cases:

a) The strip of the rectangular cross-section with the sides b and h (Fig. 224a). In this case we have

$$A = b\delta\,, \quad J_p = \frac{b^3\delta}{12}\,, \quad H_x = H_y = 0\,, \quad K = \delta \int_{-b/2}^{+b/2} y^4\, dy - \frac{b^5\delta}{144} = \frac{b^5\delta}{180}.$$

Then

$$\sigma = \frac{E\theta^2}{2}\left(y^2 - \frac{b^2}{12}\right), \quad M_T = \frac{1}{3}\, b\,\delta^3 G\,\theta \left(1 + \frac{E}{G}\,\frac{b^4}{120\delta^2}\theta^2\right).$$

The last summand in the expression for M_T gives us the quantitative evaluation of the nonlinear effect.

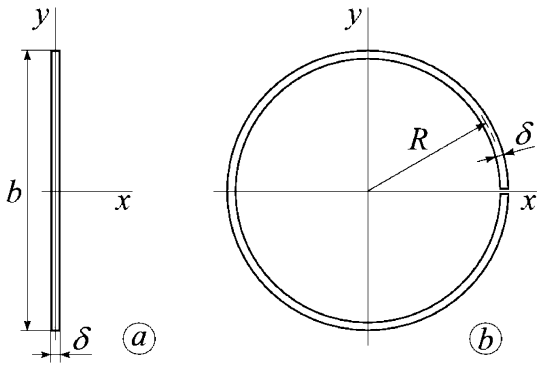

Fig. 224

b) The unclosed circular profile (Fig. 224b) is

$$A = 2\pi R\,\delta\,, \quad J_p = 2\pi R^3\,\delta\,, \quad H_x = H_y = 0\,, \quad K = 0\,,$$

therefore $\sigma = 0$,

$$M_T = \frac{1}{3}\, 2\pi R\,\delta^3 G\,\theta.$$

The nonlinear effect in this case is absent.

33. Let us isolate from the rod the elementary ring with the thickness dz by two cylindrical surfaces having radii r and $r+dr$ and by two cross-sections (Fig. 225).

Equating the sum of the moments about the z axis to zero we obtain

$$\left[\tau + \frac{\partial \tau}{\partial z} dz\right] 2\pi r^2 dr - \tau 2\pi r^2 dr = \left[t + \frac{\partial t}{\partial r} dr\right] 2\pi (r + dr)^2 dz - t\, 2\pi r^2 dz$$

from which

$$r^2 \frac{\partial \tau}{\partial z} = \frac{\partial}{\partial r}\left(t\, r^2\right). \tag{1}$$

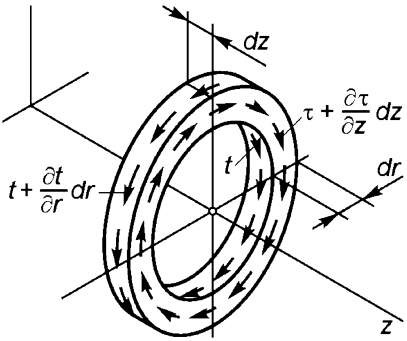

Fig. 225

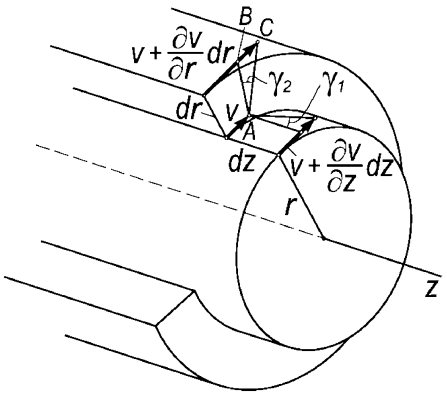

Fig. 226

Let us denote the displacement in the direction of the tangent to the circle's arc as v (Fig. 226). The angle of shear in the cylindrical surface is as usual

$$\gamma_1 = \frac{\partial v}{\partial z},$$

and the stress

$$\tau = G \frac{\partial v}{\partial z}. \tag{2}$$

The angle of shear in the plane of the cross-section γ_2 is equal to the segment's ratio BC/AB (Fig. 226). But

$$BC = v + \frac{\partial v}{\partial r} dr - v \frac{r + dr}{r}, \quad AB = dr,$$

therefore

$$\gamma_2 = \frac{\partial v}{\partial r} - \frac{v}{r},$$

and corresponding stress

$$t = -G\left(\frac{\partial v}{\partial r} - \frac{v}{r}\right). \tag{3}$$

Substituting τ and t into the equilibrium equation (1) we obtain

$$\frac{\partial^2 v}{\partial z^2} + \frac{\partial}{\partial r}\left[\frac{1}{r}\frac{\partial}{\partial r}(vr)\right] = 0\,. \tag{4}$$

It is natural to suppose that the displacement v depending on z is changing as under usual torsion in accordance with the quadratic law, that is

$$v = v_0 + v_1\, z + v_2\, z^2,$$

where v_0, v_1, v_2 depend on r only. Equation (4) after substitution of v is decomposed into the three following

$$\left[\frac{1}{r}\,(v_0\, r)'\right]' = -2v_2\,, \quad \left[\frac{1}{r}\,(v_1 r)'\right]' = 0\,, \quad \left[\frac{1}{r}\,(v_2 r)'\right]' = 0\,, \tag{5}$$

from which

$$v_1 = A_1\, r + \frac{B_1}{r}, \quad v_2 = A_2\, r + \frac{B_2}{r}.$$

Finally, substituting v_2 into the right side of the first of the equations (5) we obtain

$$v_0 = A_0\, r + \frac{B_0}{r} - \frac{A_2}{4}\, r^3 - B_2\, r\, \ln r.$$

As the displacements at the rod's axis are equal to zero it is necessary to assign $B_0 = B_1 = B_2 = 0$. Then

$$v = A_0\, r - \frac{A_2}{4}\, r^3 + A_1\, r\, z + A_2\, r\, z^2,$$

and according to expressions (2) and (3)

$$\tau = G\,(A_1 + 2A_2\, z)\, r, \quad t = G\,\frac{1}{2}\, A_2\, r^2.$$

At the left flank, that is under $z = 0$, tangential stresses are equal to zero. Consequently, $A_1 = 0$. At the surface of the cylinder (under $r = \frac{d}{2}$) $t = \frac{m}{\pi d}$, therefore $A_2 = \frac{8m}{\pi d^3 G}$ and as a result we obtain

$$\tau = \frac{16m}{\pi d^3}\, r\, z\,, \quad t = \frac{4m}{\pi d^3}\, r^2$$

Thus, the stresses τ are distributed linearly with regard to r and z as follows from the usual theory of torsion. The stresses t are distributed along the radius in accordance with the quadratic law. The ratio of τ and t maximal values will be

$$\frac{\tau_{\max}}{t_{\max}} = \left(\frac{16m}{\pi d^3}\,\frac{d}{2}\, l\right) : \left(\frac{4m}{\pi d^3}\,\frac{d^2}{4}\right) = 8\,\frac{l}{d}.$$

Consequently, for a long cylinder the stress $t_{\max}$ is significantly less than $\tau_{\max}$.

34. Let us consider the equilibrium conditions for the element $dxdydz$ (Fig. 227a) [12].

The equality of the sum of all forces projections onto the z axis to zero gives us

$$\frac{\partial \tau_x}{\partial x} + \frac{\partial \tau_y}{\partial y} = 0\,. \tag{1}$$

At the contour (Fig. 227b) we have the boundary condition

$$\tau_y \cos\alpha + \tau_x \sin\alpha = 0\,,$$

or

$$\tau_y \frac{dx}{ds} + \tau_x \frac{dy}{ds} = 0\,, \quad \tau_y\, dx = -\tau_x\, dy\,. \tag{2}$$

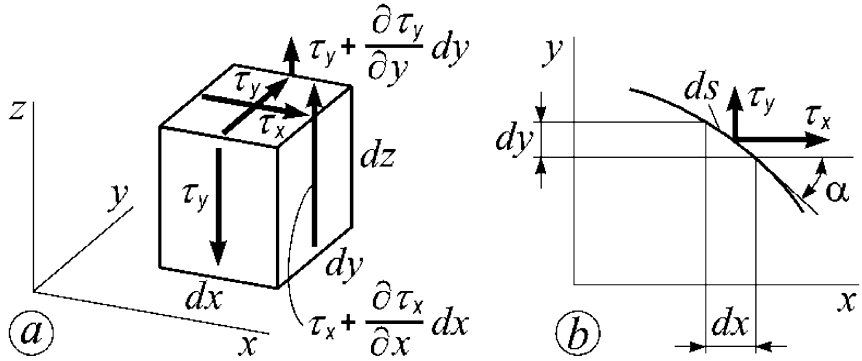

Fig. 227

Now let us consider the integrals specified in the set of the problem

$$\int_x \int_y \tau_x\, y\, dx\, dy\,, \quad \int_x \int_y \tau_y\, x\, dx\, dy\,.$$

Integrating by parts of the first expression with respect to x and of the second one with respect to y we obtain

$$\int_x \int_y \tau_x\, y\, dx\, dy = \int_y \left[|\, \tau_x\, x\, |_{x_1}^{x_2} - \int_x \frac{\partial \tau_x}{\partial x}\, x\, dx \right] y\, dy\,,$$

$$\int_x \int_y \tau_y\, x\, dy\, dx = \int_x |\, \tau_y\, y\, |_{y_1}^{y_2} - \int_x \frac{\partial \tau_y}{\partial y}\, y\, dy\, x\, dx\,,$$

that results in the expressions

$$\int_x \int_y \tau_x\, y\, dx\, dy = \int_y |\, \tau_x\, x\, |_{x_1}^{x_2}\, y\, dy - \int_y \int_x \frac{\partial \tau_x}{\partial x}\, x\, y\, dx\, dy\,,$$

$$\int_x \int_y \tau_y\, x\, dx\, dy = \int_x |\, \tau_y\, y\, |_{y_1}^{y_2}\, x\, dx - \int_x \int_x \frac{\partial \tau_y}{\partial y}\, x\, y\, dx\, dy\,.$$

According to the boundary condition (2) we obtain

$$\int_y \mid \tau_x x \mid_{x_1}^{x_2} y\,dy = -\int_x \mid \tau_y y \mid_{y_1}^{y_2} x\,dx\,,$$

and according to the equilibrium condition (1) we have

$$\int_y \int_x \frac{\partial \tau_x}{\partial x}\, x\, y\, dx\, dy = -\int_x \int_x \frac{\partial \tau_y}{\partial y}\, x\, y\, dx\, dy\,.$$

Consequently, we arrive at the equation

$$\int_x \int_y \tau_x\, y\, dx\, dy = -\int_x \int_y \tau_y\, x\, dx\, dy\,.$$

But as

$$\int_x \int_y \tau_x\, y\, dx\, dy - \int_x \int_y \tau_y\, x\, dx\, dy = T\,,$$

then finally we obtain

$$\int_x \int_y \tau_x\, y\, dx\, dy = \frac{T}{2}\,, \quad -\int_x \int_y \tau_y\, x\, dx\, dy = \frac{T}{2}\,.$$

The obtained relationships contain some element of didacticism. For example, under torsion of a thin rectangular strip (Fig. 228) we are always neglecting the stresses τ_x in comparison with τ_y. And that is correct.

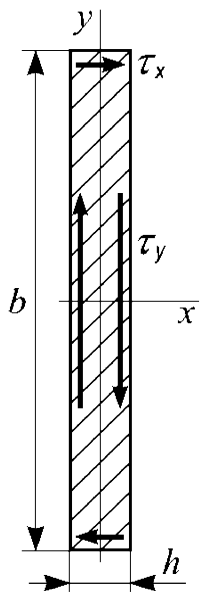

Fig. 228

But if we neglect the small stresses τ_x while determining the torque then we should make an error of exactly twofold amount because the small stresses τ_x at the large arm y produce the same moment as the large stresses τ_y at the small arm x.

2. Cross-Section Geometry Characteristics. Bending

35. The right triangle product of inertia with respect to the axes x_0, y_0 parallel to the legs and crossing their middle points is equal to zero (Fig. 229) because these axes are symmetry axes for two constituent triangles.

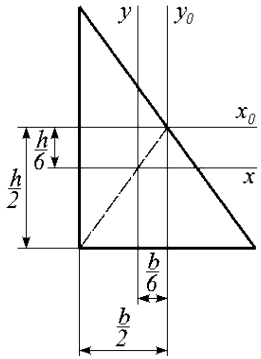

Fig. 229

Applying parallel-axis theorem we obtain

$$J_{xy} = J_{x_0y_0} - \frac{b}{6}\,\frac{h}{6}\,\frac{bh}{2},$$

where $J_{x_0y_0} = 0$, therefore $J_{xy} = -\dfrac{b^2h^2}{72}$.

36. Let us denote the figure's polar moment of inertia with respect to its centroid O as J_{p0} and with respect to some arbitrary point of coordinates a, b as J_p (Fig. 230).

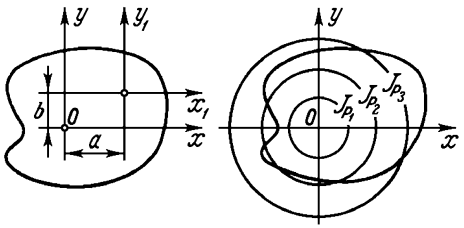

Fig. 230

It is obvious that

$$J_p = J_{x_1} + J_{y_1} = J_x + J_y + (a^2 + b^2)A \, .$$

where A is figure's area. As $J_x + J_y = J_{p_0}$ then

$$a^2 + b^2 = \frac{J_p - J_{p_0}}{A} \, .$$

Consequently, the plane figure's constant polar moments of inertia geometric locus represents the set of circumferences concentric about point O (see Fig. 230). Each circumference radius R is determined by J_p value:

$$R = \sqrt{\frac{J_p - J_{p_0}}{A}} \, .$$

37. Let the x and y axes of some plane area be principal (Fig. 231).

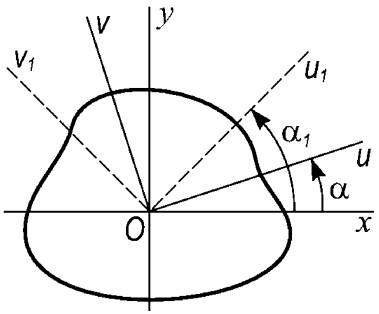

Fig. 231

Suppose that there is one more pair of principal axes u, v noncoincident with x, y (angle α is not a multiple of $\pi/2$). If axes u, v are principal then $J_{uv} = 0$. But it is known that

$$J_{uv} = J_{xy} \cos 2\alpha + \frac{J_x - J_y}{2} \sin 2\alpha \, .$$

As the x, y axes are also principal then $J_{xy} = 0$. Therefore

$$\frac{J_x - J_y}{2} \sin 2\alpha = 0 \, ,$$

but as $\sin 2\alpha \neq 0$ then

$$J_x = J_y \tag{1}$$

Considering an arbitrary taken pair of axes u_1, v_1 we can write

$$J_{u_1 v_1} = J_{xy} \cos 2\alpha_1 + \frac{J_x - J_y}{2} \sin 2\alpha_1 \, .$$

Obviously we have $J_{u_1 v_1} = 0$ independently of angle α_1, i.e. any pair of axes is principal.

It is evident from the above proof that for every cross-section of three or more axes of symmetry any central axis is principal and axial moment of inertia with respect to any central axis will be just the same. This follows from relation (1).

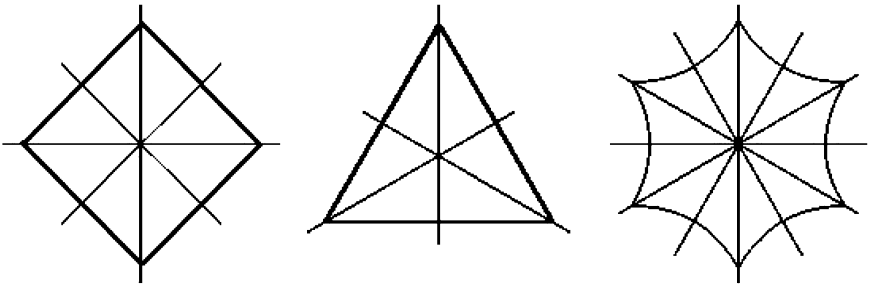

Fig. 232

The cross-sections presented, for example, in Fig. 232 (square, equilateral triangle, curved hexagon, etc..) have such property.

38. Assume that x, y are principal centroidal axes of the plane area (Fig. 233) and that the sought point A has the coordinates a, b. Now let us select a and b so that J_{uv} vanishes for any α.

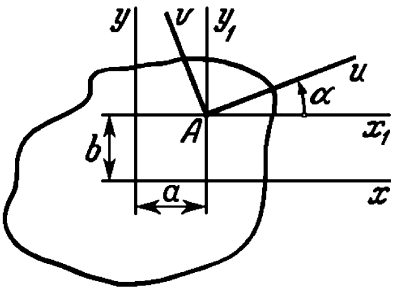

Fig. 233

At first we apply parallel-axis theorem (A – cross-section area)

$$J_{x_1} = J_x + b^2 A\,, \quad J_{y_1} = J_y + a^2 A\,, \quad J_{x_1 y_1} = a\,b\,A\,.$$

Then according to the axes rotation formulas for products of inertia

$$J_{uv} = J_{x_1 y_1} \cos 2\alpha + \frac{J_{x_1} - J_{y_1}}{2} \sin 2\alpha\,.$$

To obtain J_{uv} equal to zero under any α angle we obviously need that

$$J_{x_1 y_1} = 0\,, \quad J_{x_1} - J_{y_1} = 0\,,$$

or

$$a\,b\,A = 0\,, \quad J_x - J_y = (a^2 - b^2)\,A\,.$$

Either a or b or both a and b must be zero as follows from the first relation, i.e. the desired point in any case is on one of the principal centroidal axes.

Assume that $J_y \geq J_x$ and at first let $b = 0$. Then

$$a = \pm\sqrt{\frac{J_x - J_y}{A}}.$$

In $J_y > J_x$ case a is an imaginary value. If $J_y = J_x$ then $a = 0$.

Now suppose that $a = 0$. Then

$$b = \pm\sqrt{\frac{J_y - J_x}{A}}\ .$$

If $J_y > J_x$ then b is a real value. If $J_y = J_x$ then $b = 0$.

Thus we obtain four sought points with the coordinates:

1) $a = +\sqrt{\dfrac{J_x - J_y}{A}}$, $b = 0$;

2) $a = -\sqrt{\dfrac{J_x - J_y}{A}}$, $b = 0$;

3) $a = 0$, $b = +\sqrt{\dfrac{J_y - J_x}{A}}$;

4) $a = 0$, $b = -\sqrt{\dfrac{J_y - J_x}{A}}$.

The points lying on the axis of minimal moment of inertia are imaginary. The points lying on the axis of maximal moment of inertia are real.

In the case of equal principal moments of inertia ($J_y = J_x$) all four points are real and coincide with the area centroid. For such figures (circle, square, equilateral triangle, etc.) every axis intersecting area centroid will be principal.

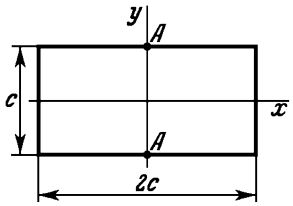

Fig. 234

For example, let us consider a rectangle of measures $c \times 2c$ (Fig. 234) where $J_x = \dfrac{2c\,c^3}{12}$, $J_y = \dfrac{c\,(2c)^3}{12}$, $A = 2c^2$. The coordinates of the sought real points are

$$a = 0, \qquad b = \pm\sqrt{\frac{\dfrac{c(2c)^3}{12} - \dfrac{2c\,c^3}{12}}{2c^2}} = \pm\frac{c}{2}.$$

These points are marked in Fig. 234 as A. Each axis intersecting these points will be principal.

39. If stresses at the neutral plane OO are absent, then the beam, of course, can be divided into two parts and stresses and strains in the beam will not be changed after this. But for this it is necessary to preserve the same conditions of loads application at the beam ends. When we draw the moment at the beam ends (for example as in the case of Fig. 35) it means only that the resultant moment of stresses effecting the beam end is equal to M. Thus we are usually neglecting the distribution law of the stresses at the very end which are reduced to M. But it is not significant indeed. Independent of the character of loads application, stresses are flattening rather quickly as the distance from the beam end grows, and the stress diagram takes the well-known linear form.

Step-by-step modification of the normal stress diagram form from the beam end to its middle is shown in Fig. 235. An arbitrary lattice diagram of the stresses at the beam end is considered as an example. The stress flattening falls in a very short beam segment but considerably large shear stresses arise at this segment in the neutral plane OO.

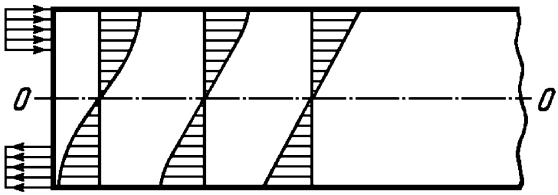

Fig. 235

If we consider the specified set of the problem then stress distribution at the beam ends in the one and in the other case is not indifferent. In the first variant of the beam (Fig. 35) stresses are supposed to be distributed at its end by one law (Fig. 236a and 236c), as in the second case (Fig. 36), by another law (Fig. 236b and 236d).

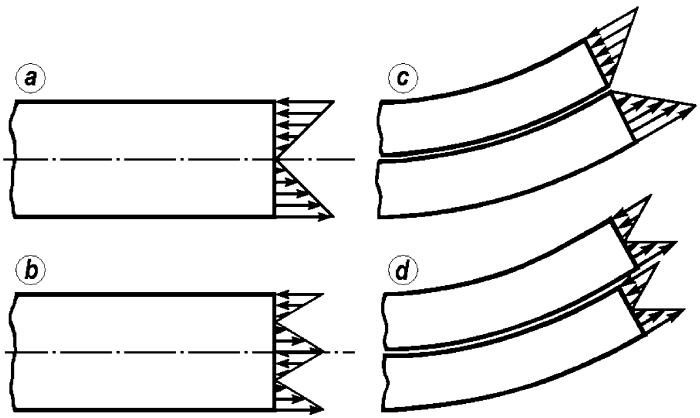

Fig. 236

The beam can be divided into two parts without disturbance of its operation if we manage to provide the same linear law of stress distribution at the ends of the slit beam as for the entire beam (Fig.236c).

Fig. 237

It is not difficult to fulfil this constructively. For example, rigid holds at the slit beam ends for both of its parts (Fig. 237) will be quite enough.

40. The problem is known as Parent's[1] problem. As $b^2 + h^2 = 4R^2$, then the section modulus W_x of the rectangle with respect to the x axis (Fig. 238) will be $W_x = \dfrac{bh^2}{6} = \dfrac{b}{6}(4R^2 - b^2)$. This function has a maximum under $b = 2R\sqrt{3}$ and correspondingly under $h = b\sqrt{2}$.

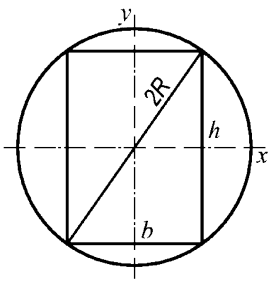

Fig. 238

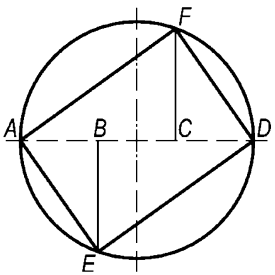

Fig. 239

Parent himself gave the answer in the form suitable for a carpenter. The circle diameter AD has to be divided into three equal parts $AB = BC = CD$ (Fig. 239). Then the perpendiculars BE and CF are erected up to the intersection with the circle. The rectangle $AEDF$ is the bar sought cross-section.

41. In order to provide that the neutral axis of the collective stress diagram σ passes through the cross-section $I-I$ centroid, the line of force action must intersect the center of the curvature, i.e. $x = 0$.

Bending stress in the point situated at the distance y from the neutral axis of a high curvature rod cross-section is calculated by the formula

$$\sigma_b = -\frac{M_b\, y}{A\, e\,(r + y)}\,,$$

[1] Antoine Parent (1666-1716) – French scientist.

where M_b is the bending moment, A is the cross-sectional area, r is the distance from the centre of curvature to the neutral axis and e is the distance from the neutral axis to the cross-section centroid. In our case $M_b = P(r + e + x)$. At the centroid (i.e. $y = e$) we have

$$\sigma_b = -\frac{P\,(r+e+x)\,e}{A\,e\,(r+e)}\,.$$

According to the problem predicative the algebraic sum of this stress and tensile stress must be equal to zero:

$$-\frac{P\,(r+e+x)\,e}{A\,e\,(r+e)} + \frac{P}{A} = 0\,,$$

whence we arrive at $x = 0\,.$

42. The relation (1) in the set of the problem results from the differential equation

$$y'' = \frac{M_b}{EJ}\,,$$

which was obtained from relation (2) under the assumption that deflections of the beam are so small that

$$\frac{1}{\rho} = \frac{y''}{(1+y'^{\,2})^{3/2}} \approx y''.$$

Therefore, strictly speaking, under pure bending a beam is bent by the arc of circle which in the case of small deflections can be approximated by a quadratic parabola with very high precision.

43. Figure 240 shows the upper part of the moments diagram caused by given force P and the moments diagram caused by unit force applied at point A. We find displacement δ_A calculating Mohr's integral of these moments' product by the graphico-analytic technique described in [7]. Coincidence of the unit force diagram's centroid (C.G.) with the zero point of the given force diagram (Fig. 240) is necessary to get zero value of δ_A. It is obvious that $x = l/3$.

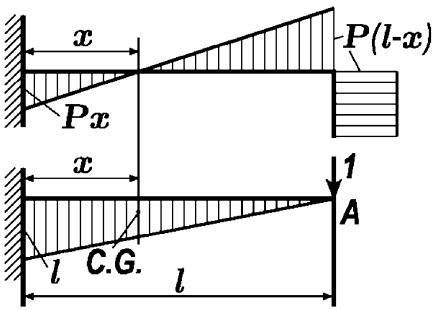

Fig. 240

44. The displacement of point A in direction perpendicular to the line of force action should vanish according to the set of the problem. So this is the condition the angle α is derived from.

Let us apply unit force at point A in direction normal to P and then draw diagrams of bending moments (Fig. 241).

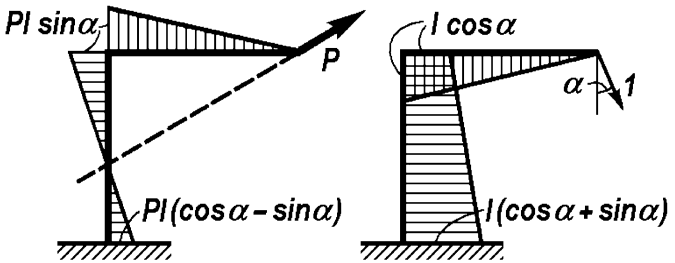

Fig. 241

Let us set to zero the displacement of point A, obtained by multiplying these diagrams [7]. Then we get

$$tg\ 2\alpha = 1, \quad \alpha = \frac{\pi n}{2} + \frac{\pi}{8},$$

where n is any integer.

45. See Fig. 243.

46. a) Point A (Fig. 42a) deflects upward by $\dfrac{Pl^3}{6EJ}$;

b) Point A (Fig. 42b) deflects to the right by $\dfrac{PR^3}{2EJ}$ and upward by $\dfrac{PR^3}{EJ}(1 - \dfrac{\pi}{4})$;

c) Point A (Fig. 42c) deflects upward by $\dfrac{Pl^3}{6EJ}$ and to the right by $\dfrac{Pl^3}{EJ}$;

d) For the case shown in Fig. 42d the question cannot be answered until the constraints, forbidding displacement of the frame as a solid body, are given. Point A deflection will be different depending on the constraint character (Fig. 242).

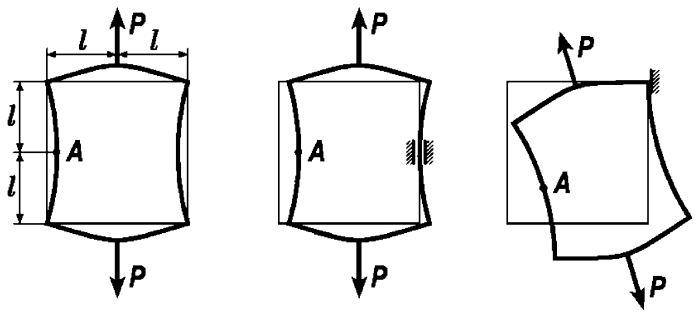

Fig. 242

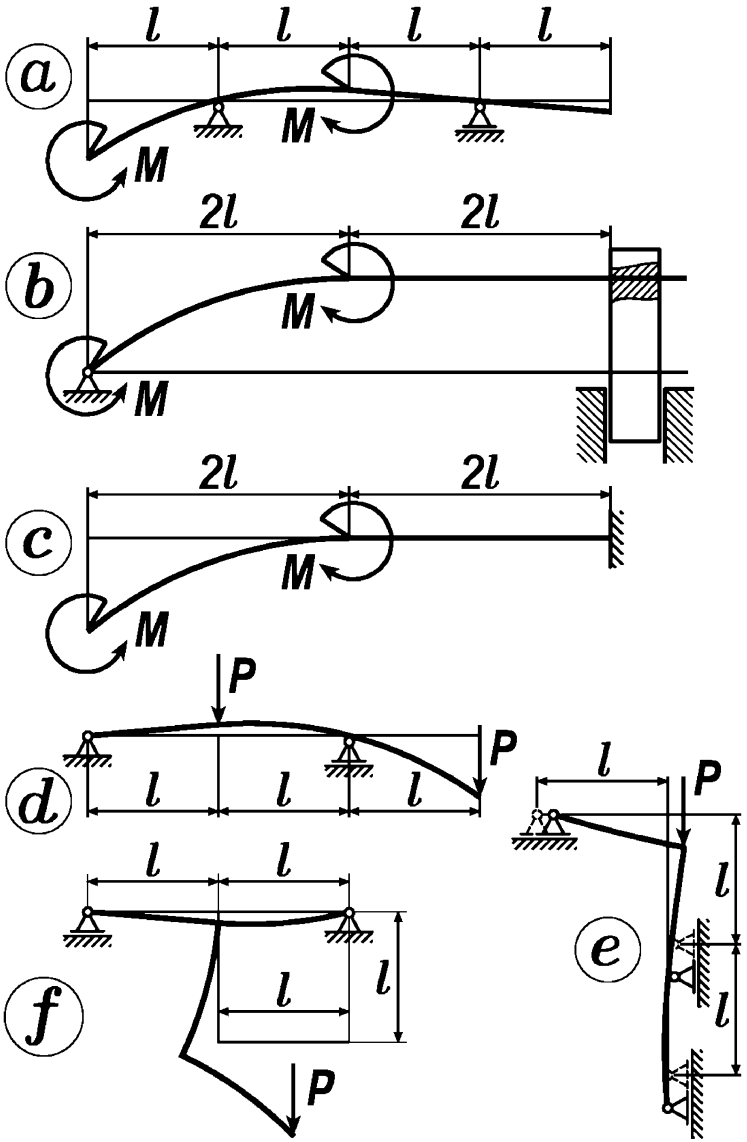

Fig. 243

For example, under indicated constraints (Fig. 242) point A deflects:

in the first case – to the right by $\dfrac{Pl^3}{16EJ}$;

in the second case – to the right by $\dfrac{Pl^3}{8EJ}$;

in the third case – to the right by $\dfrac{3Pl^3}{16EJ}$ and downwards by $\dfrac{Pl^3}{4EJ}$.

47. Bar AB is compressed. It is necessary to reveal statical indeterminacy of the frame to become convinced of it.

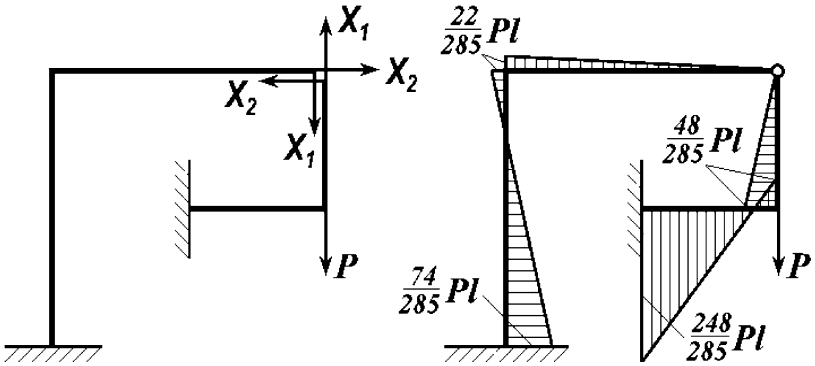

Fig. 244

The reaction forces in the pin (Fig. 244) will be as follows:

$$X_1 = -\frac{11}{285}P\,, \quad X_2 = \frac{48}{285}P\,.$$

48. The resultant of load P and of the right support reaction passes through the inflection point of the rod deflection curve (Fig. 245).

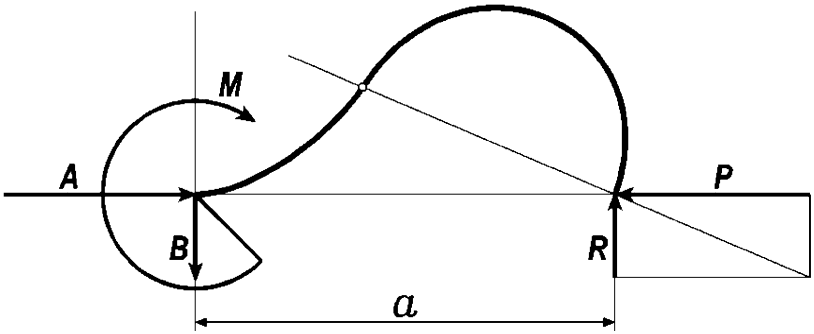

Fig. 245

Reaction R is derived from this condition. Remaining reactions are derived from equilibrium equations:

$$A = P\,, \quad B = R\,, \quad M = Ra\,.$$

49. The displacement of each load application point (Fig. 246) is derived by the usual method as follows:

$$\delta = \frac{PR^3}{\pi EJ}\left\{\left[\frac{3\pi^2}{8} - \pi - \frac{1}{2}\right] + \alpha\left[\frac{\pi^2}{2} - \pi - 2\right] + \alpha^2\left[\frac{\pi^2}{4} - 2\right] + \alpha^3\frac{\pi}{3}\right\},$$

where $\alpha = a/R$.

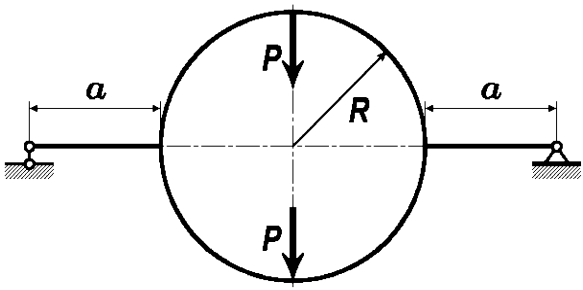

Fig. 246

The displacement δ takes its least value if $\alpha = 0.148$.

50. Deflections of point A for three frames will be as follows:

$$\delta_I = \frac{Pa^3}{3EJ},$$

$$\delta_{II} = \frac{Pa^3}{2}\left(\frac{\pi - 3}{GJ_p} + \frac{\pi/2 - 1}{EJ}\right),$$

$$\delta_{III} = \frac{Pa^3\sqrt{2}}{4}\left(\frac{1}{GJ_p} + \frac{1}{3EJ}\right).$$

For a beam of circular cross-section we have $\dfrac{EJ}{GJ_p} = 1.3$ and therefore we get

$$\delta_{II} = 1.13\,\delta_I, \quad \delta_{III} = 1.72\,\delta_I.$$

Hence the first frame is the most rigid one.

51. The ring stiffness may only decrease if a pin is cut in it. At least ring stiffness remains equal to its value for the closed ring. The last case will occur only if the pin is placed at a point where the bending moment in a closed ring vanishes (Fig. 247). The sought angle is $\alpha = \arcsin\dfrac{2}{\pi}$.

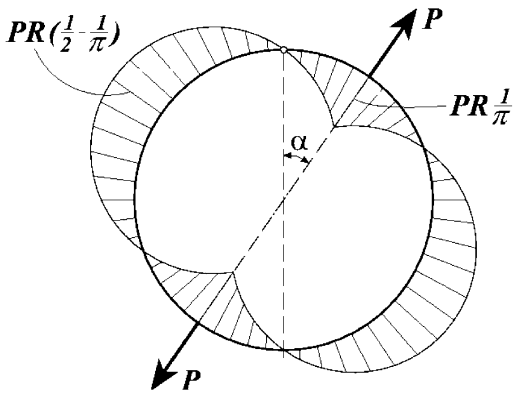

Fig. 247

52. If one of the principal axes lied in a frame plane we could give an instant answer: both diagonals of the frame do not change their length as the bending of the frame occurs only out of plane.

The other case takes place for a Z-shaped section. The cross sectional principal axis ζ does not lie in the frame plane. It is inclined by angle $\alpha \neq 0$ (Fig. 248). Thus a bending moment arising in planes perpendicular to the frame plane causes variation of curvature and correspondingly deflection of the frame in its plane.

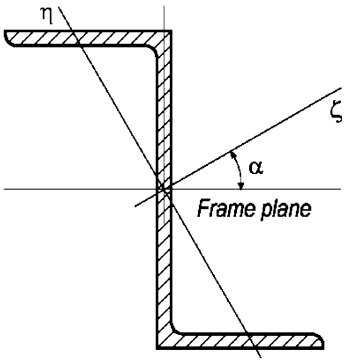

Fig. 248

Bending moments in cross-sections of the frame are derived from equilibrium conditions though the closed frame is statically indeterminable. This follows from system properties. The frame is symmetric with respect to its diagonals and load is antisymmetric with respect to the axes passing through the middle of the frame sides. If we cut a corner with sides $\frac{l}{2}$ out of the frame (Fig. 249a) it is easy to find the values of transverse forces $\frac{P}{2}$ and torsional moments $\frac{Pl}{4}$ from equilibrium conditions. Then diagrams of bending and torsional moments are constructed as presented in Fig. 249b.

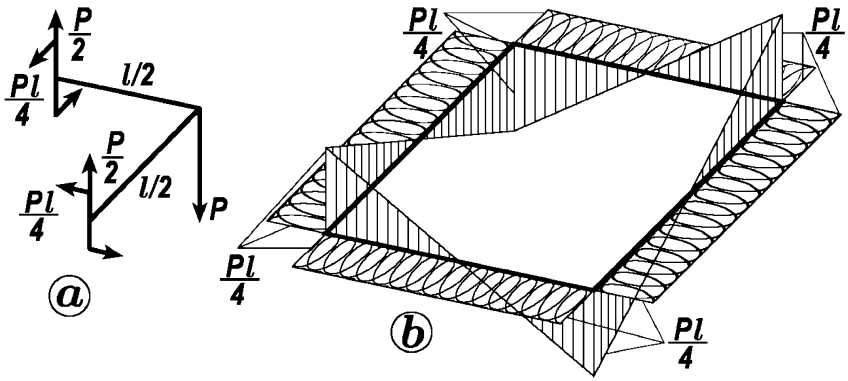

Fig. 249

Let us cut the frame at an arbitrary cross-section and apply unit forces at points A and B. The corresponding diagram of bending moments is shown in Fig. 250. Torsional moments are absent.

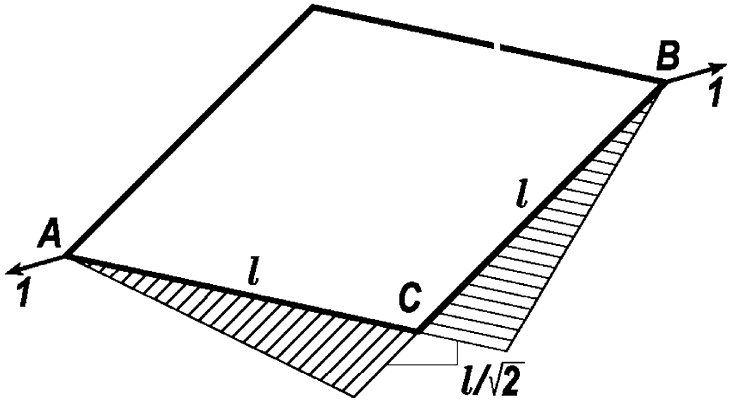

Fig. 250

In order to multiply unit diagram and diagram of moments corresponding to the given load (Fig.249b) both of them should be decomposed along section principal axes ζ and η (Fig.248). Decomposition of moments along new axes does not change diagram shape. Only ordinate scales are multiplied by $\sin\alpha$ and $\cos\alpha$ correspondingly. The product's signs should also be watched closely.

Diagram multiplication at segment CB yields:

$$\frac{1}{EJ_{\max}}\,\frac{1}{2}\,l\frac{\sqrt{2}}{2}\,l\sin\alpha\,\frac{1}{3}\,\frac{Pl}{4}\cos\alpha-\frac{1}{EJ_{\min}}\,\frac{1}{2}\,l\frac{\sqrt{2}}{2}\,l\cos\alpha\,\frac{1}{3}\,\frac{Pl}{4}\sin\alpha,$$

where $J_{\max}$ and $J_{\min}$ are cross-section principal moments of inertia about axes ζ and η correspondingly. Multiplication at segment AC gives the same result.

In the upshot elongation of diagonal AB will be

$$\Delta(AB)=Pl^3\frac{\sqrt{2}}{48}\left(\frac{1}{EJ_{\max}}-\frac{1}{EJ_{\min}}\right)\sin 2\alpha\,.$$

As $J_{\min}<J_{\max}$, it means that $\Delta(AB)$ will be negative. Therefore the diagonal AB shortens under action of load P. Correspondingly, the second diagonal elongates.

53. The posed problem can be solved by two methods.

The first way is suitable for springs of large helix angle also and lies in considering the spring as a spatial rod. Its displacements can be derived by Mohr's method. The complexity of geometric relations represents the main difficulty in applying this method.

The second simplified way, which we shall use below, lies in replacing the spring by some equivalent straight beam. Its bending rigidity is derived

depending on mutual rotation of coils (Fig. 251a). The distinct shear displacements in the vertical plane (Fig. 251b) are inherent for such beams besides bending deflections.

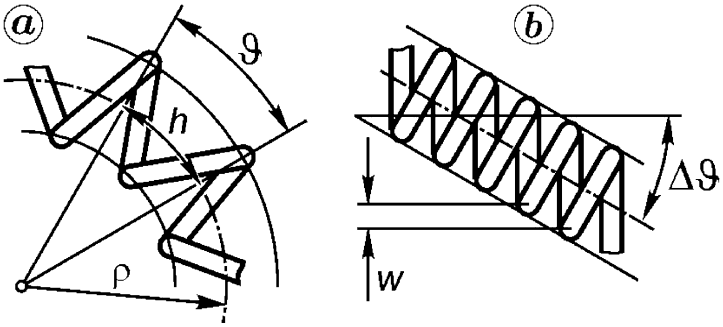

Fig. 251

In order to determine bending and shear stiffness of the according beam let us consider a single spring coil assuming that the helix angle is equal to zero. The coil is isolated by sections placed in a vertical plane (Fig. 252a). The moments M and forces Q arise at the coil ends. Their magnitudes are easily obtained from equilibrium conditions for the discarded part of the spring.

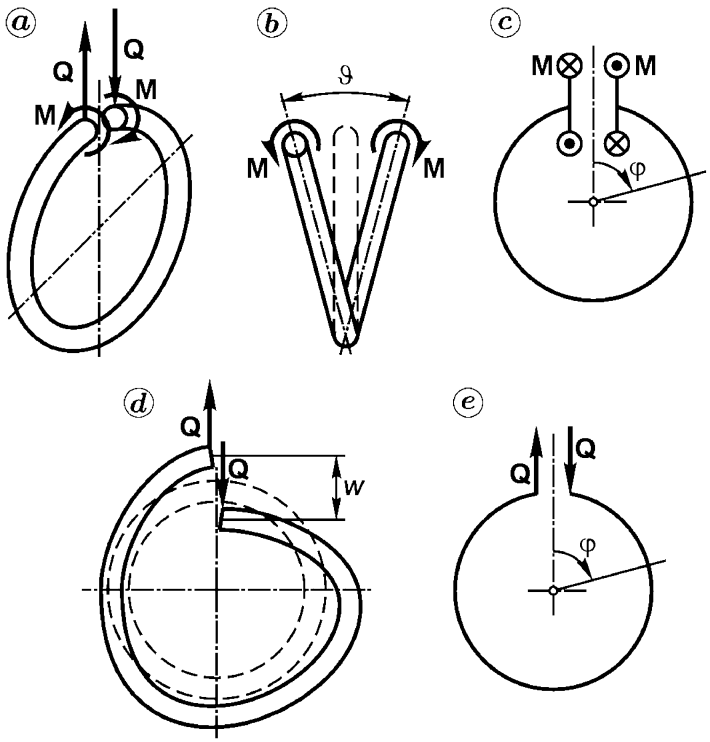

Fig. 252

Moment M causes a mutual cross-section rotation angle ϑ (Fig. 252b). The magnitude of ϑ is calculated applying Mohr's integral as follows:

$$\vartheta = \int_0^{2\pi} \frac{M_t\, M_{t1}\, R\, d\varphi}{GJ_p} + \int_0^{2\pi} \frac{M_b\, M_{b1}\, R\, d\varphi}{EJ},$$

where M_t and M_b are torsional and bending moments. We can see from Fig. 252c that

$$M_t = M\cos\varphi \quad \text{and} \quad M_b = M\sin\varphi\,.$$

Moments by unit load have the corresponding values:

$$M_{t1} = \cos\varphi \quad \text{and} \quad M_{b1} = \sin\varphi\,.$$

After integration we get

$$\vartheta = \frac{M\pi D}{2}\left(\frac{1}{GJ_p} + \frac{1}{EJ}\right)$$

or

$$\vartheta = \frac{32MD}{Ed^4}(2+\mu).$$

It we denote the lead of the helix as h then $1/\rho = \vartheta/h$, as follows from Fig. 251a. If n is the number of coils and l is the length of the spring, we have $h = l/n$. Then

$$\frac{1}{\rho} = \frac{\vartheta\, n}{l}$$

or

$$\frac{1}{\rho} = \frac{M}{\dfrac{Ed^4 l}{32Dn(2+\mu)}}\,.$$

The value

$$\frac{Ed^4 l}{32Dn(2+\mu)}$$

can be considered as bending stiffness of the equivalent beam. Let us denote it as C_b

$$C_b = \frac{Ed^4 l}{32Dn(2+\mu)} \tag{1}$$

then

$$\frac{1}{\rho} = \frac{M}{C_b}\,. \tag{2}$$

Shear displacements are caused by bending of the coil in its plane (Fig. 252d). Obviously we have

$$w = \int_0^{2\pi} \frac{M_b\, M_{b1}\, R\, d\varphi}{EJ} ,$$

where (see Fig. 252e)

$$M_b = QR\sin\varphi \quad \text{and} \quad M_{b1} = R\sin\varphi .$$

After integration we arrive at

$$w = \frac{QD^3\pi}{8EJ} .$$

An additional angular deflection will be

$$\Delta\vartheta = \frac{w}{h} = \frac{Q}{\dfrac{Ed^4l}{8D^3n}} .$$

This relation can be rewritten as

$$\Delta\vartheta = \frac{Q}{C_s} , \tag{3}$$

where

$$C_s = \frac{Ed^4l}{8D^3n} . \tag{4}$$

Deflection of the spring under action of transverse forces will be

$$f = f_b + f_s .$$

For the considered specific case of the beam clamped by its left end the bending displacement is equal to

$$f_b = \frac{Pl^3}{3EJ} ,$$

where flexural rigidity EJ should be replaced by C_b.

The shear deflection is

$$f_s = \Delta\vartheta\, l = \frac{Pl}{C_s} .$$

Thus we arrive at

$$f = \frac{Pl^3}{3C_b} + \frac{Pl}{C_s} .$$

Magnitudes of C_b and C_s are defined by relations (1) and (4). In other cases of loading the problem is analyzed in a similar way.

54. Let us release the balance axle from its bearing and introduce reactions as unknown forces X and Y. Let's also designate the moment acting on the spring from the oscillating balance mass as M (Fig. 253a).

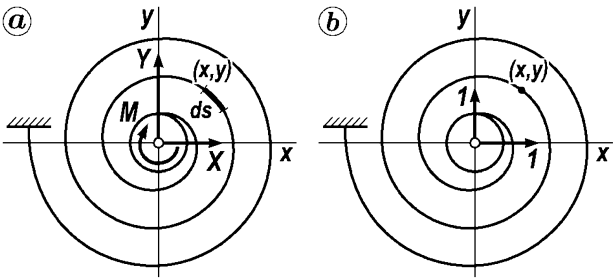

Fig. 253

Further let us write the conditions of the balance axle zero displacements in x and y directions. For that we apply the corresponding unit forces producing bending moments x and y in the section of (x, y) coordinates (Fig. 253b). Then we arrive at

$$\int_s X y\, y\, ds - \int_s Y x\, y\, ds - \int_s M\, y\, ds = 0\,,$$

$$-\int_s X y\, x\, ds + \int_s Y x\, x\, ds - \int_s M \cdot x\, ds = 0\,,$$

or

$$X\, I_x - Y\, I_{xy} = M\, S_x\,,$$
$$-X\, I_{xy} + Y\, I_y = -M\, S_y\,,$$

where

$$I_x = \int_s y^2 ds\,, \quad I_y = \int_s x^2 ds\,, \quad I_{xy} = \int_s x\, y\, ds\,,$$

$$S_x = \int_s y\, ds\,, \quad S_y = \int_s x\, ds\,.$$

In order to get zero X and Y forces it is necessary that $S_x = S_y = 0$.

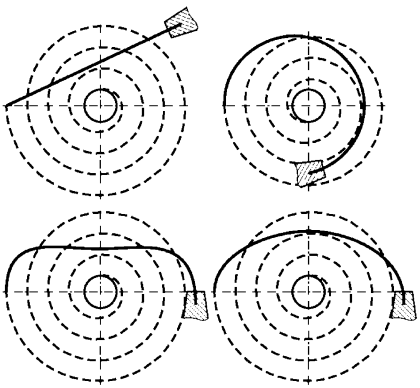

Fig. 254

It means that the required condition is valid if the spring coil's centre of gravity coincides with the balance axle. But the axial line of the spring is Archimedes spiral and its centroid does not coincide with the center of barrel rotation. That is why special spring designs created to satisfy the above-mentioned condition are common practice in watch manufacturing. Such balance springs have a deflected outer coil. Typical examples are shown in Fig. 254.

55. The main question arising in this problem solution is revealing the character of spring sheet contact. Let us suppose that fastened sheets osculate in the point at the shorter sheet's right end and also in the link point where vertical displacement and slope of both sheets are the same. The corresponding scheme of forces is presented in Fig. 255a. If sheets are not fastened, then $X_2 = X_3 = 0$.

Multiplying the unit diagrams of the moments (Fig. 255b) we obtain

$$EJ\,\delta_{11} = \frac{16}{3}\,l^3, \qquad EJ\,\delta_{12} = \frac{5}{3}\,l^3, \qquad EJ\,\delta_{13} = 3l^2,$$

$$EJ\,\delta_{22} = \frac{2}{3}\,l^3, \qquad EJ\,\delta_{23} = l^2, \qquad EJ\,\delta_{33} = 2l,$$

$$EJ\,\delta_{1P} = -\frac{14}{3}\,Pl^3, \quad EJ\,\delta_{2P} = -\frac{4}{3}\,Pl^3, \quad EJ\,\delta_{3P} = -\frac{5}{2}Pl^2.$$

Substituting these relations in the equations of the force method we have

$$\begin{aligned}
\frac{16}{3}\,X_1\,l + \frac{5}{3}\,X_2\,l + 3X_3 &= \frac{14}{3}\,Pl\,,\\
\frac{5}{3}\,X_1\,l + \frac{2}{3}\,X_2\,l + X_3 &= \frac{4}{3}\,Pl\,,\\
3X_1\,l + X_2\,l + 2X_3 &= \frac{5}{2}\,Pl\,.
\end{aligned}$$

Solving these equations we find

$$X_1 = \frac{5}{4}P\,, \qquad X_2 = -\frac{3}{4}P\,, \qquad X_3 = -\frac{1}{4}Pl.$$

In case of non-fastened sheets we have $X_1 = \dfrac{7}{8}P\,, \quad X_2 = 0\,, \quad X_3 = 0.$

The resultant diagrams for fastened sheets is plotted in Fig. 255c by solid line and for free sheets by dashed line.

Now it is necessary to validate the assumption made about the character of sheet contact. At first let us consider the dashed diagrams (Fig. 255c). The bending moment in a lower sheet and consequently its curvature at the point of sheet contact is greater than curvature of the upper sheet. This means that deflection curve of the lower sheet will be lower than the deflection curve of the upper sheet that corresponds to the above specified assumption.

Diagrams for fastened sheets at the first segment are absolutely identical. Hence full contact without force interaction takes place here and does not contradict the previous assumption.

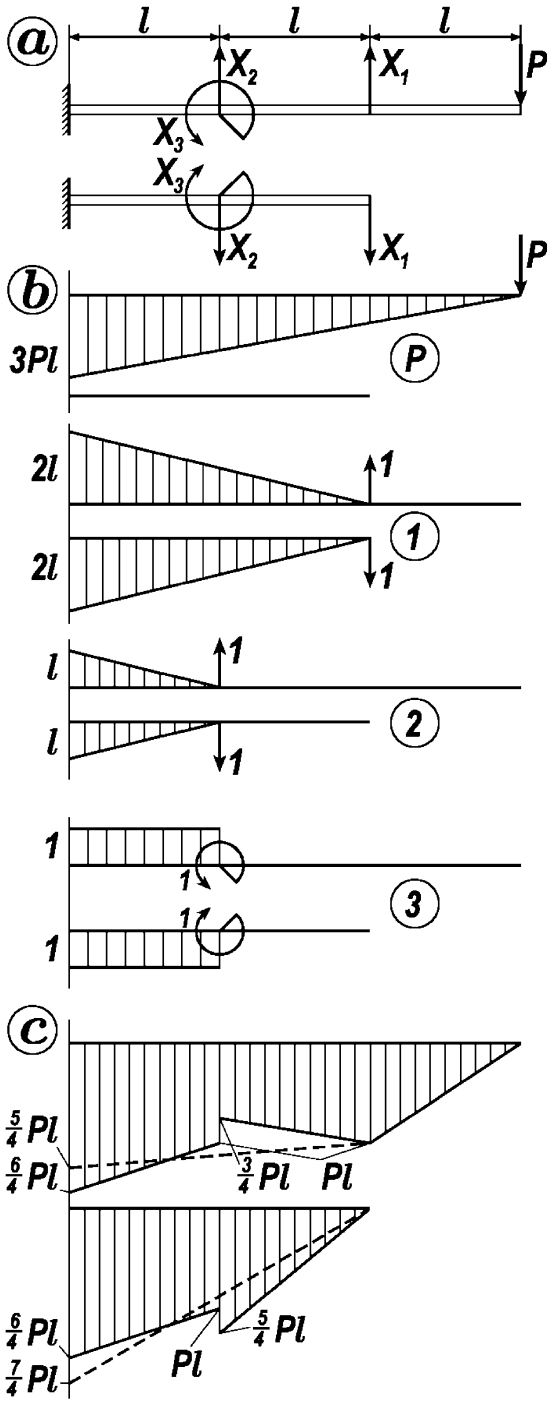
a
l
l
l
X2
X1
P
X3
X3
X2
X1
P
b
3Pl
P
2l
1
2l
1
1
l
1
2
l
1
1
1
1
3
1
c
5/4 Pl
6/4 Pl
3/4 Pl
Pl
6/4 Pl
7/4 Pl
Pl
5/4 Pl

Fig. 255

At the second segment of the diagram the deflection curve of the lower sheet is lower than the deflection curve of the upper sheet. Thus, the obtained solution confirms the assumption about the character of sheet contact.

The displacement of the load P application point is derived by the multiplication resultant diagram of the upper sheet and unit diagram. Finally we obtain the displacement for non-fastened sheets $\frac{118}{24}\frac{Pl^3}{EJ}$ and for fastened sheets $\frac{115}{24}\frac{Pl^3}{EJ}$.

Fastening of sheets reduces the maximal bending moment from $7Pl/4$ to $6Pl/4$.

56. Let us consider the right-hand half of the spring assuming that sheets contact at points A and B (Fig. 256a).

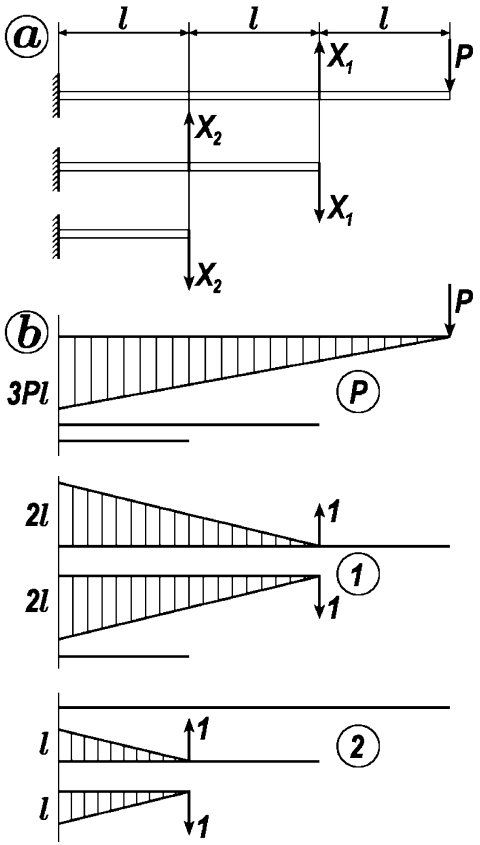

Fig. 256

Redundant forces X_1 and X_2 are derived from compatibility equations of the force method [7]

$$\delta_{11}X_1 + \delta_{12}X_2 = -\delta_{1P}\,, \quad \delta_{21}X_1 + \delta_{22}X_2 = -\delta_{2P}\,. \tag{1}$$

The coefficients δ_{11},δ_{12},δ_{22},δ_{1P} and δ_{2P} are determined by multiplication of the diagrams (Fig. 256b) [7]:

$$EJ\delta_{11} = \frac{16}{3}l^3, \quad EJ\delta_{12} = -\frac{5}{6}l^3, \quad EJ\delta_{22} = \frac{2}{3}l^3,$$
$$EJ\delta_{1P} = -\frac{14}{3}Pl^3, \ \delta_{2P} = 0.$$

Thus, from equations (1) we find X_1 and X_2 :

$$X_1 = \frac{112}{103}P, \quad X_2 = \frac{140}{103}P.$$

The resultant diagrams of bending moments are plotted in Fig. 257. It follows from these diagrams that at a clamped end the bending moment and consequently the curvature of the first sheet is greater than the curvature of the second sheet.

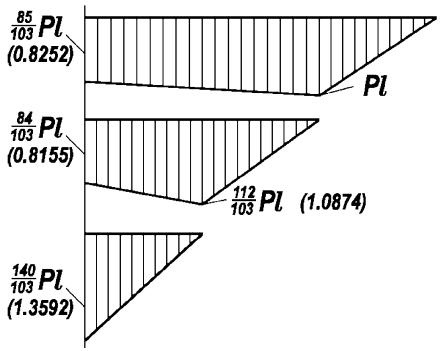

Fig. 257

This means that under these conditions the deflection curve of the second sheet must be higher than the deflection curve of the first sheet. Such a case is physically impossible. Hence the specified assumption about sheet contact character is not correct and the considered scheme must be changed.

Now let us suppose that the first and second sheets contact at two points: as previously at point A and also at a point C at some unknown distance a from the clamped end (Fig. 258).

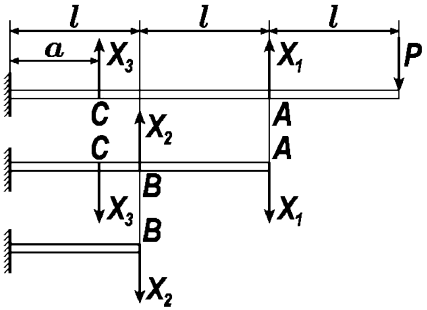

Fig. 258

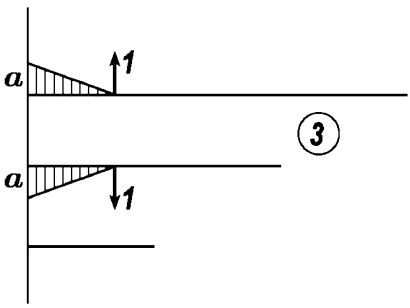

Fig. 259

If the unit diagram corresponding to the redundant force X_3 (Fig. 259) is added to the diagrams of Fig. 256b, then the coefficients of the force method equations (assuming that $a \leqslant l$) are derived as follows:

$$EJ\,\delta_{11} = \frac{16}{3}\,l^3, \qquad EJ\,\delta_{12} = -\frac{5}{6}\,l^3, \qquad EJ\,\delta_{13} = a^2(2l - \frac{a}{3}),$$

$$EJ\,\delta_{22} = \frac{2}{3}\,l^3, \qquad EJ\,\delta_{23} = -\frac{a^2}{2}(l - \frac{a}{3}), \quad EJ\,\delta_{33} = \frac{2}{3}\,a^3,$$

$$EJ\,\delta_{1P} = -\frac{14}{3}\,Pl^3, \quad EJ\,\delta_{2P} = 0, \qquad EJ\,\delta_{3P} = -\frac{a^2}{2}(3l - \frac{a}{3})P\,.$$

In this case the force method equations system looks like

$$\begin{aligned} 32X_1 - 5X_2 + 2\alpha^2\,(6-\alpha)\,X_3 &= 28P, \\ -5X_1 + 4X_2 - \alpha^2\,(3-\alpha)\,X_3 &= 0, \\ 2\,(6-\alpha)\,X_1 + (3-\alpha)\,X_2 + 4\alpha X_3 &= (9-\alpha)\,P, \end{aligned}$$

where $\alpha = a/l$. Solving these equations for the redundants, we obtain

$$\begin{aligned} X_1 &= \frac{P}{\Delta}(448 - 549\alpha + 228\alpha^2 - 31\alpha^3), \\ X_2 &= \frac{P}{\Delta}(560 - 684\alpha + 270\alpha^2 - 34\alpha^3), \\ X_3 &= \frac{P}{\Delta}\frac{1}{\alpha}(3 - 19\alpha), \\ \Delta &= 412 - 504\alpha + 204\alpha^2 - 28\alpha^3. \end{aligned}$$

The magnitude of a (or α) is derived from the condition that slopes of the first and the second sheets at a point C must be equal.

Applying unit moments to these sheets at this point (Fig. 260)leads to:

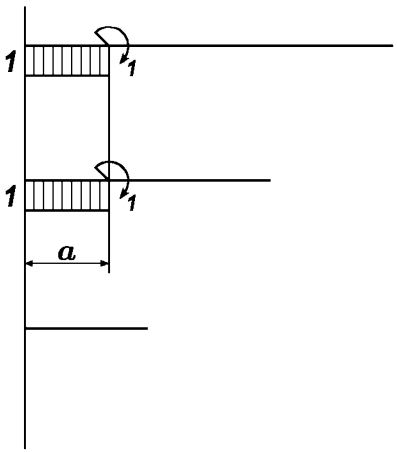

Fig. 260

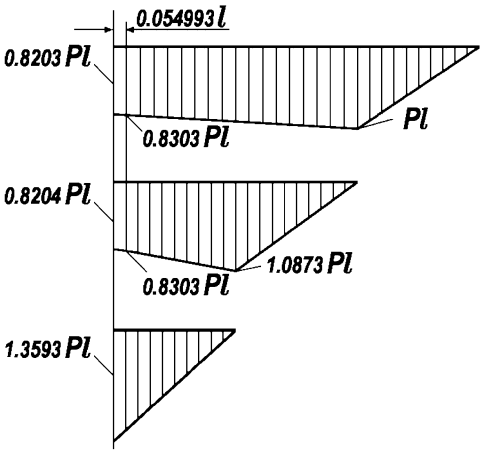

Fig. 261

and multiplying the corresponding diagrams we arrive at

$$a\left(3l-\frac{a}{2}\right)P-a\left(2l-\frac{a}{2}\right)X_1-\frac{a^2}{2}X_3$$
$$=a\left(2l-\frac{a}{2}\right)X_1-a\left(l-\frac{a}{2}\right)X_2+\frac{a^2}{2}X_3,$$
$$\text{or}\qquad 2(4-\alpha)X_1-(2-\alpha)X_2+2\alpha X_3=(6-\alpha)P.$$

Substituting the obtained values of X_1, X_2 and X_3 into this expression we get

$$3\alpha^3-15\alpha^2+19\alpha-1=0,$$

whence $\alpha=0.054993<1$. If the obtained value of α were be greater than 1, then the solution would have to be repeated considering that $a>l$.

For sought α we calculate the redundants X_1, X_2 and X_3 :

$$X_1=1.0873P,\quad X_2=1.3593P,\quad X_3=0.09237P.$$

Notice that forces X_1 and X_2 under the given sheet length ratio are almost the same as for the previous case. Let us draw up diagrams of bending moments again (Fig. 261). Examination of these diagrams shows that the curvature of the second sheet at the clamped end is greater than the curvature of first one, and that the curvature of the third sheet is greater than the curvature of the second one. Hence the deflection curve of each next sheet will be disposed below the deflection curve of the previous one. Thus, the assumption about the character of sheet contact is confirmed. The bending moment design value is equal to $M_b^{\max}=1,36Pl$ occurring at the clamped cross-section of the lower sheet.

The spring camber δ is determined by the first sheet end displacement, that is

$$EJ\,\delta=9Pl^3-\frac{14}{3}X_1\,l^3-\frac{1}{6}X_3\,a^2(9l-a).$$

Substituting X_1, X_3 and a, we obtain

$$\delta=3.926\frac{Pl^3}{EJ}.$$

57. If the reactions of redundant supports are not equal to zero they must be directed upwards only (Fig. 262). So the convexity of the beam deflection curve to the right of the load P application point is always directed downwards. Therefore the beam may have contact with one or two neighbouring supports only. Numbers of reactions X_2, X_3, X_4, X_5 (Fig. 262) correspond to the number of spans from the clamped end.

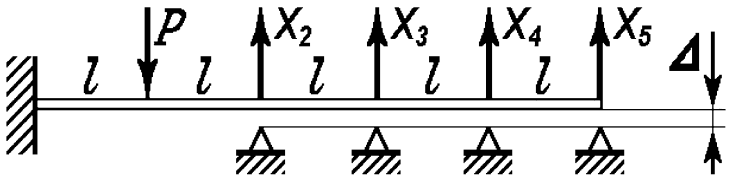

Fig. 262

Let us suppose that the beam deflection curve has the force interaction with two neighbouring supports: i-th and $(i+1)$-th. The reactions X_i and X_{i+1} can be found by the force method from the equations:

$$\delta_{11}\,X_i + \delta_{12}\,X_{i+1} + \delta_{1P} = -\Delta,$$
$$\delta_{21}\,X_i + \delta_{22}\,X_{i+1} + \delta_{2P} = -\Delta.$$

Coefficients of these equations are determined by multiplying the diagrams shown in Fig. 263:

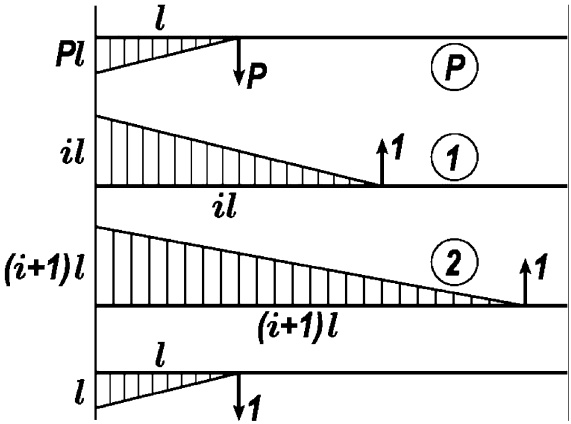

Fig. 263

$$\delta_{11} = \frac{i^3 l^3}{3\,EJ}, \quad \delta_{22} = \frac{(i+1)^3 l^3}{3\,EJ}, \quad \delta_{12} = \delta_{21} = \frac{i^2 l^3}{3\,EJ}\left(i + \frac{3}{2}\right),$$

$$\delta_{1P} = -\frac{Pl^3}{2\,EJ}\left(i - \frac{1}{3}\right), \quad \delta_{2P} = -\frac{Pl^3}{2\,EJ}\left(i + \frac{2}{3}\right).$$

After substituting coefficients and transformations, the equations arrive at

$$i^3 X_i + i^2\left(i + \frac{3}{2}\right) X_{i+1} = \frac{3P}{2}\left(i - \frac{1}{3}\right) - \frac{3\,EJ\,\Delta}{l^3},$$
$$i^2\left(i + \frac{3}{2}\right) X_i + (i+1)^3 X_{i+1} = \frac{3P}{2}\left(i + \frac{2}{3}\right) - \frac{3\,EJ\,\Delta}{l^3}, \qquad (1)$$

from which we have

$$X_i = \frac{1}{l^3}\,\frac{3}{3i+4}\left[P\left(i^3 + 2i^2 - \frac{2}{3}\right) - \frac{2\,EJ\,\Delta}{l^3}\left(3i^2 + 6i + 2\right)\right], \qquad (2)$$

$$X_{i+1} = \frac{1}{l^3}\,\frac{3}{3i+4}\left[-P\,i^2\,(i-1) + \frac{6\,EJ\,\Delta}{l^3}\,i^2\right]. \qquad (3)$$

Now we can determine deflection f. Applying unit force at point A and multiplying the obtained diagram (Fig. 263) with the diagram of the specified load P and also with two other unit diagrams enlarged by X_i and X_{i+1} and adding these products together we get

$$f = \frac{l^3}{2EJ}\left[\frac{2}{3}P - X_i\left(i-\frac{1}{3}\right) - X_{i+1}\left(i+\frac{2}{3}\right)\right] \tag{4}$$

or

$$f = \frac{Pl^3}{3EJ}\left[1 - \frac{1}{i^3}\frac{1}{3i+4}\left(9i^3 - 3i + 1\right)\right] + \Delta\frac{1}{i^3}\frac{1}{3i+4}\left(9i^2 - 2\right).$$

The sought stiffness is

$$c = \frac{3EJ}{l^3}\frac{1}{1 - \frac{1}{i^3}\frac{1}{3i+4}\left(9i^3 - 3i + 1\right)}. \tag{5}$$

While the load P increases, the reaction X_{i+1} decreases and in case of $P = \dfrac{6EJ}{l^3}\dfrac{\Delta}{i-1}$ vanishes. It means that the beam is already in contact only with the i-th support.

Let us suppose $X_{i+1} = 0$. Then from relation (1) we find

$$X_i = \frac{3P}{2\,i^3}(i - \frac{1}{3}) - \frac{3\,EJ\,\Delta}{i^3 l^3}, \tag{6}$$

and then from equation (4) we derive

$$f = \frac{Pl^3}{3\,EJ}\left[1 - \frac{9}{4i^3}\left(i-\frac{1}{3}\right)^2\right] + \frac{3\Delta}{2\,i^3}\left(i-\frac{1}{3}\right),$$

and stiffness

$$c = \frac{3\,EJ}{l^3}\frac{1}{1 - \frac{9}{4\,i^3}\left(i-\frac{1}{3}\right)^2}. \tag{7}$$

Now let us consider again relations (2) and (3). They allow us to obtain the magnitude of redundants in the case when the beam leans on two neighbouring supports – X_2 and X_3 (if $i = 2$), X_3 and X_4 (if $i = 3$), X_4 and X_5 (if $i = 4$).

Setting the first redundant of the listed pairs equal to zero we find the magnitude of the load P under which the contact with two neighbouring supports takes place. If we equate to zero not the first reaction but the second one, then we find the magnitude of the load under which the beam looses contact with the right support of the considered pair and begins to lean only on the left one. Corresponding values of the sought stiffness c can be derived by substitution of index i into relation (4) in accordance with the above listed contact pairs (Fig. 264).

If load is small enough, the beam deflects freely as clearances are not closed yet and the stiffness is $c = 3EJ/l^3$. The contact with the right end support is defined by the condition $X_5 = 0$ using relation (6), and the stiffnesses in case of contact with supports 5, 4, 3 and 2 are obtained from relation (7).

There is no wonder that the stiffness varies in jump-like manner. It is interesting that under increasing of the load P the stiffness sometimes may decrease.

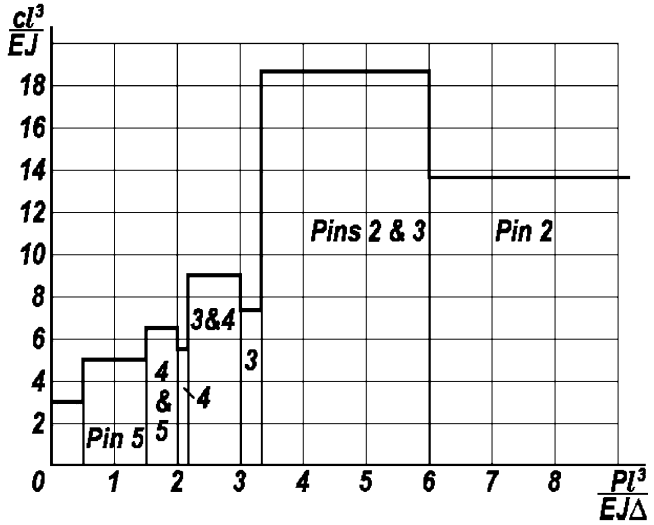

Fig. 264

58. Let us suppose that some segment of the spring was forced to take the shape of the profile gage. To reach it we obviously have to apply some forces and moments at the ends of this segment and also distributed load of intensity q in its intermediate points.

The deflection curve under bending is determined by the equation

$$q(x) = EJv^{(IV)},$$

where v is bending deflection. If the distributed load here acts upwards then it is considered to be positive: $q(x) > 0$.

Now it is quite clear that the spring will be away from the profile if $v^{IV} > 0$ and will be adjacent to it if $v^{IV} < 0$. If the contour of the profile gage is a power function curve of an order not higher than three then $v^{IV} = 0$. In this case the spring will be tightly adjacent to the profile without pressing it. Some concentrated force P_1 will arise at the end of the adjacent segment (Fig. 265).

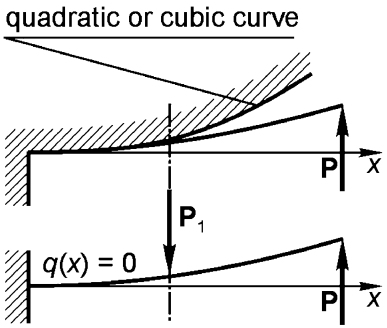

Fig. 265

59. After application of the force P_1 the left part of the beam (Fig. 266) raises at some length a. The right part lies on a plane and remains straight.

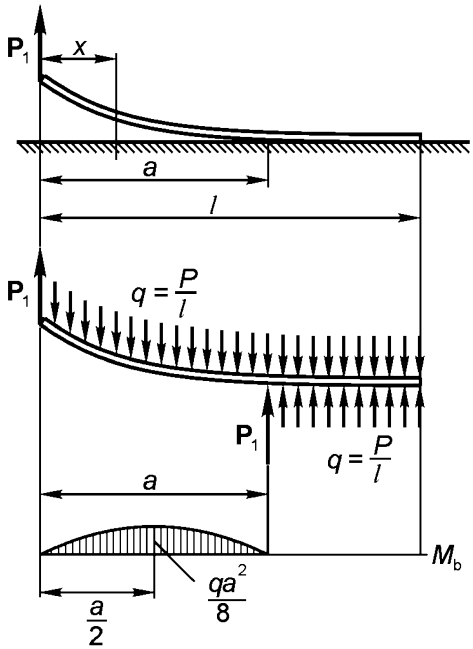

Fig. 266

Consequently, bending moment is equal to zero at every cross-section of the beam's right segment. Particularly the moment is also equal to zero at cross-section $x = a$.

The segment a length is derived from this condition, i.e. (see Fig. 266)

$$P_1\, a = \frac{P}{l}\,\frac{a^2}{2}\,, \quad a = \frac{2P_1}{P}\,l\,.$$

The resultant of all forces' vertical projections must be equal to zero. It is readily apparent from this equilibrium condition that the solid base reaction P_1 arises at the point $x = a$ (Fig. 266).

Under this set of forces we can consider the suspended left part of the beam as a simply supported beam of length a loaded by uniformly distributed force of intensity $\dfrac{P}{l}$. At the middle of the suspended segment a of the beam the bending moment takes its maximal value that is equal

$$\frac{qa^2}{8} = \frac{P_1^2\, l}{2P}\,.$$

In case of $P_1 = P/3$ we get

$$M_{\max} = \frac{Pl}{18}\,, \quad \sigma_{\max} = \frac{Pl}{18W}\,, \quad a = \frac{2}{3}\,l\,.$$

The concentrated force P_1 appearance at the adjacency segment boundary is the most interesting and instructive fact of the considered problem as well as of all problems where a contact of an elastic beam with a solid surface takes place.

At first sight the appearance of this force seems somewhat unexpected though its existence is formally in complete agreement with the equilibrium equations and deforming conditions. Nevertheless this question is worth considering in detail.

The technical theory of bending that we have used above is based on the hypothesis offered by D. Bernoulli, that considers plane cross-sections of a beam to remain normal to its deflection curve. Below we shall refer to such an approach as a Bernoulli beam. Certainly this theory takes into account the essential thing, i.e. perceives the origin of a beam axis deflection in a bending moment arising in a beam cross-section. But at the same time it is imperfect (incomplete) because it leaves aside the shear compliance of a beam. In reality cross-sections of a beam do not remain normal to its deflection curve but have some distortion. This distortion is connected with transverse shear force in a beam cross-sections and causes the additional deflection.

We realistically neglect this feature of bending in most cases of applied problems analysis. And it is correct. But in some cases this feature reveals itself in one or another form. The matter stands in a particular relation to the concentrated force arising at the boundary of a contact region.

The beam bending theory that takes into account shear displacements besides of bending ones is usually identified by the name of S.P. Timoshenko. So if the reader encounters the term "Timoshenko's beam" it must be kept in mind that just such a case is observed. As soon as we want not to exclude the concentrated contact force (by the way this is not necessary) and to understand the causes of its appearance we should address to the scheme of a Timoshenko beam.

Let us consider a beam element of length dx (Fig. 267a). Moments M and $M + dM$ and shear forces Q and $Q + dQ$ are applied at its ends. The increment of force dQ is balanced by the resultant of the distributed load $q dx$.

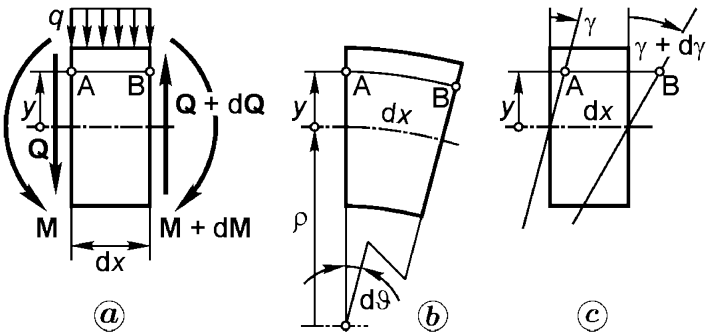

Fig. 267

Usually we consider that end sections remain plane and normal to the beam deflection curve. If we denote the angle of their mutual rotation as $d\theta$ (Fig. 267b) then the line AB disposed at distance y from the neutral layer elongates by $y d\theta$. Dividing this elongation by dx we obtain the longitudinal strain $\varepsilon = y/\rho$.

This is the usual scheme (Bernoulli beam). But in the given case we must not restrict ourselves to such an approach. The distortion caused by transverse shear forces also ought to be taken into account.

As the shear stresses are distributed along a section inhomogeneously then the shear strain varies correspondingly but we shall use only its average value. To obtain it we divide the average value of shear stress Q/A by shear modulus G, taking into account the influence of cross-section shape as usual by the coefficient k, i.e.

$$\gamma = \frac{kQ}{GA}\,.$$

For a rectangular cross-section $k = 6/5$, for a circular one $k = 10/9$, etc.

If the angle γ (Fig. 267c) remained constant along a beam length then it would not effect the elongation of line AB. But since the force Q varies from one section to another, the line AB obtains additional relative elongation $y\, d\gamma/dx$ (Fig. 267c).

After summation of the strains caused by the mutual rotation angles $d\theta$ and $d\gamma$ we arrive at

$$\epsilon = \frac{y}{\rho} + \frac{k\,y}{GA}\,\frac{dQ}{dx}\,.$$

The corresponding stress is

$$\sigma = E\,y\left(\frac{1}{\rho} + \frac{k\,Q'}{GA}\right),$$

and the bending moment will be found by integrating along the cross-section area as follows

$$M = \int\limits_A \sigma\, y\, dA \quad \text{or} \quad M = EJ\left(\frac{1}{\rho} + \frac{k\,Q'}{GA}\right).$$

Since $Q = M'$, and $\dfrac{1}{\rho} = v''$, finally we get the following deflection curve differential equation of the Timoshenko beam that will be used later:

$$v'' = \frac{M}{EJ} - \frac{k\,M''}{GA}\,. \tag{1}$$

And some notes in conclusion: Distinct differentiation between the cross-section rotation angle and the inclination angle $v'$of the deflection curve tangent is necessary for the Timoshenko beam. In usual technical theory of bending they are treated as identical. And here the section rotation angle θ differs from v' by the shear angle γ, i.e.

$$\theta = v' + \frac{k\,Q}{G\,A}\,. \tag{2}$$

If we are applying equation (1) for analysis of a beam having some segments where M or EJ or GA are described by different expressions, then in the joining sections of these segments the values of v and θ must be the same (the functions $v(z)$ and $\theta(z)$ must be uninterrupted or in other words continuous). Analyzing expression (2) we see that at the points where the functions $Q(z)$ or $GA(z)$ are interrupted (vary stepwise), the function $v'(z)$ varies stepwise as well. If $GA = const$, then the steps in the function $v'(z)$ occur at the same points as the steps in the function $Q(z)$, i.e. at the points where concentrated forces are applied. The concentrated force acting upwards leads to a negative step in the function $Q(z)$ and consequently to a positive step in the function $v'(z)$.

Now let us return to the considered problem.

If $x \le a$ (Fig. 266) we have

$$M = P_1\,x - \frac{P\,x^2}{2\,l}, \quad M'' = -\frac{P}{l}\,. \tag{3}$$

Substituting (3) into equation (1) we get

$$v'' = \frac{1}{EJ}\left[P_1\,x - \frac{P\,x^2}{2l}\right] + \frac{k\,P}{lGA}\,,$$

from which

$$v = \frac{1}{EJ}\left[P_1\,\frac{x^3}{6} - \frac{P\,x^4}{24\,l}\right] + \frac{k\,P}{lGA}\,\frac{x^2}{2} + C_1\,x + C_2\,. \tag{4}$$

The constant C_2 is not interesting for analysis. It can be easily fitted so that the deflection v is zero under $x = a$. This gives $C_2 = 0$. As for the calculation of the constant C_1, it is necessary to satisfy the specific condition of attachment to the second segment of the beam where the curvature is equal to zero. So from equation (1) we get

$$M'' - \alpha^2 M = 0, \quad \text{where } \alpha^2 = \frac{GA}{k\,E\,J}\,, \tag{5}$$

from which

$$M = C_3\,\sinh\alpha x + C_4\,\cosh\alpha x\,. \tag{6}$$

If $x = a$, then $M = P_1\,a - \dfrac{P\,a^2}{2\,l}$, and at $x = l$ we have $M = 0$. From these conditions we derive the arbitrary constants C_3 and C_4 and arrive at

$$M = \left(P_1\,a - \frac{P\,a^2}{2\,l}\right)\frac{\sinh\alpha(l-x)}{\sinh\alpha(l-a)}\,. \tag{7}$$

Further we need to require that the section rotation angle is the same for both beam segments at their joining point. At first we determine angle θ at

$x = a$ for the left part of the beam using relations (2) and (4). Then we arrive at

$$\theta = \frac{1}{EJ}\left(P_1\frac{a^2}{2} - \frac{P\,a^3}{6\,l}\right) + \frac{k\,P}{lGA}a + C_1 + \frac{k}{GA}\left(P_1 - \frac{Pa}{l}\right).$$

For the right part of the beam we have $v' \equiv 0$. Therefore, angle θ contains here the shear component only. Differentiating relation (7) to obtain Q we get

$$\theta = -\frac{k}{GA}\alpha\left(P_1\,a - \frac{P\,a^2}{2l}\right)\coth\alpha(l-a).$$

Equating these expressions for angles θ we find

$$C_1 = -\frac{1}{EJ}\left[P_1\,\frac{a^2}{2} - \frac{P\,a^3}{6\,l}\right] - \frac{k\,P_1}{GA} - \frac{k\,\alpha}{GA}\left[P_1\,a - \frac{P\,a^2}{2l}\right]\coth\alpha(l-a).$$

Now we must check whether the left segment deflection curve satisfies the condition of noncrossing the support plane. The matter is that if the shear exists then the function $v'(x)$ has breaks at the points where concentrated forces are applied. We don't know yet whether the concentrated force P_1 would arise at the end of the contact region or not. But if it does then the only option is that it acts upwards, i.e. will be positive. In this case the value of v' to the left of the P_1 application point will also be positive according to relation (2). It means that the left segment deflection curve will intersect the support plane.

So it is necessary to satisfy the condition $v' \leqslant 0$ at $x = a$.

Substituting the value of C_1 found above into relation (4) we obtain

$$v'_{x=a} = \frac{k}{GA}\left[P\,\frac{a}{l} - P_1 - \alpha l\,\frac{a}{l}\left(P_1 - \frac{1}{2}P\,\frac{a}{l}\right)\coth\alpha l\left(1 - \frac{a}{l}\right)\right].$$

Substituting the previously found value of $a = 2l/3$ and the given value of $P_1 = P/3$ we reveal that the derivative of v at $x = a$ turns out to be positive for the left segment and its deflection curve intersects the support plane. It is possible to obtain here the negative magnitude of v' by decreasing the value of a. Then the function $v'(z)$ will have the positive step at the joining point. But it means that at $x = a$ the set of the support reactions will contain a concentrated component acting downwards. This is inadmissible because of the unilateral nature of the constraints. Only one option remains: to assume that $v' = 0$ at $x = a$ and to derive a from this condition. Therefore we have

$$\frac{P_1}{P} - \frac{a}{l} = -\alpha l\,\frac{a}{l}\,\frac{\dfrac{P_1}{P} - \dfrac{1}{2}\dfrac{a}{l}}{\tanh\alpha l\left(1 - \dfrac{a}{l}\right)}.$$

As the specified value of $\dfrac{P_1}{P} = \dfrac{1}{3}$ we arrive at

$$\frac{1}{3} - \frac{a}{l} = -\alpha l \frac{a}{l} \frac{\frac{1}{3} - \frac{1}{2}\frac{a}{l}}{\tanh \alpha l \left(1 - \frac{a}{l}\right)} . \tag{8}$$

Now we can get $\frac{a}{l}$ by solving this transcendental equation under specified quantity

$$\alpha l = l \sqrt{\frac{GA}{EJk}} .$$

If $\alpha l = \infty$, i.e. if a beam has no shear strains, then from equation (7) we find $\frac{a}{l} = \frac{2}{3}$ that was obtained previously. If $\alpha l = 50$ we get $\frac{a}{l} = 0.646$, and under $\alpha l = 10$ we have $\frac{a}{l} = 0.58$.

Now let us derive the load q distributed along the second beam segment (q is the difference between the support plane distributed reaction and the beam's own weight forces P/l). From relation (6) we have

$$q = M'' = \frac{P}{l}\frac{a}{l}\alpha^2 l^2 \left(\frac{P_1}{P} - \frac{1}{2}\frac{a}{l}\right) \frac{sh\ \alpha(l-x)}{sh\ \alpha(l-a)} .$$

If $x = l$ then $q = 0$, i.e. the support plane distributed reaction is equal here to the beam weight per unit length. At $x = a$ we have

$$q_a = \frac{P}{l}\frac{a}{l}\alpha^2 l^2 \left(\frac{P_1}{P} - \frac{1}{2}\frac{a}{l}\right) .$$

If αl, i.e. shear stiffness increases then q_a tends to infinity and as a limit under $\alpha l = \infty$ we obtain the concentrated force at the point $x = a$.

The variation of the distribution law for the support plane reaction in its dependence on the αl value is shown in Fig. 268.

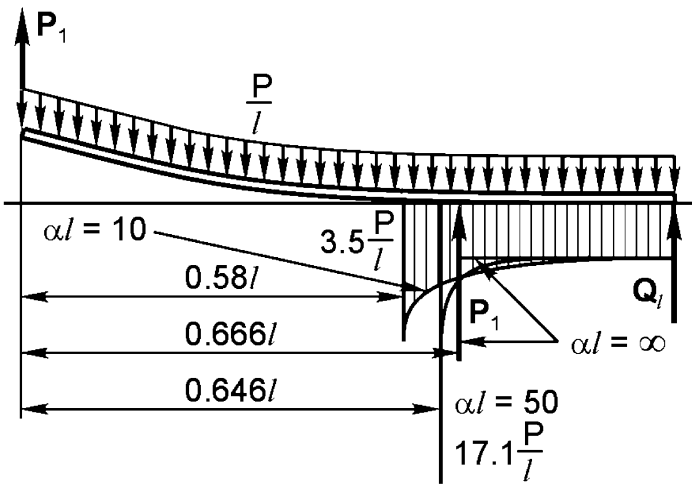

Fig. 268

It is curious to note that shear deflections in the beam changed the contact force distribution not only at the transient region but outside its limits, too. Now the concentrated reaction force arises at the right end of the beam. Differentiating the relation (7) and substituting $x = l$ we get the shear force as follows:

$$Q_1 = -\frac{a}{l}\left(P_1 - \frac{1}{2}P\frac{a}{l}\right)\frac{\alpha l}{sh\ \alpha l(1-a/l)}.$$

This expression allows us to analyze the role of shear deflections as the agent of deformation propagation along the straight beam. The force Q_1 quickly decreases as the shear stiffness increases.

60. In order to solve the flexible spring deformation problem (Fig. 57) we need to take into account the influence of shear on the shape of the spring deflection curve.

If we proceed from the usual relation between bending moment and curvature change, i.e.

$$\frac{1}{R} = \frac{M}{EJ},$$

then we shall inevitably come to the conclusion that points A will touch the base only under $P = \infty$. Actually, the bending moment at the spring ends is equal to zero under any finite value of forces P. As for the complete straightening of the spring it is necessary that the moment be equal to $M = \frac{EJ}{R}$ at each of its points. And in real practice the sought force is naturally finite.

The obtained contradiction is explained by the fact that under bending by forces P the curvature change near the spring ends, where the bending moments are small, is mainly the result of shear strains which must be taken into account while solving the problem.

Let us address the relation (1) of problem 59. The curvature change of the spring pressed to a solid base plane is $v'' = -\frac{1}{R}$. In this case we get

$$M'' - \alpha^2 M = \frac{1}{R}\frac{GA}{k}, \quad \alpha^2 = \frac{GA}{kEJ}.$$

Solving this equation we arrive at

$$M = A\sinh\alpha x + B\cosh\alpha x - \frac{EJ}{R}.$$

Constants are derived from the following boundary conditions

$$\text{at } x = 0, \quad Q = M' = 0, \qquad \text{at } x = l, \quad M = 0,$$

from which

$$A = 0, \quad B = \frac{EJ}{R}\frac{1}{\cosh\alpha l}, \qquad M = \frac{EJ}{R}\left(\frac{\cosh\alpha x}{\cosh\alpha l} - 1\right).$$

The sought force is

$$P = Q_{x=l} = M'_{x=l} = \frac{EJ}{R}\,\alpha \tanh \alpha l\,.$$

If $GA = \infty$ (shear is absent) then α turns out to infinity also. In this case $\tanh \alpha l = 1$ and $P = \infty$ as would be expected. The contact pressure along the surface of the spring contact with the solid base is determined as follows

$$q = M'' = \frac{EJ}{R}\,\alpha^2 \frac{\cosh \alpha x}{\cosh \alpha l} = \frac{GA}{k\,R}\,\frac{\cosh \alpha x}{\cosh \alpha l}\,.$$

The diagram of the load q distribution along the spring length is plotted in Fig. 269.

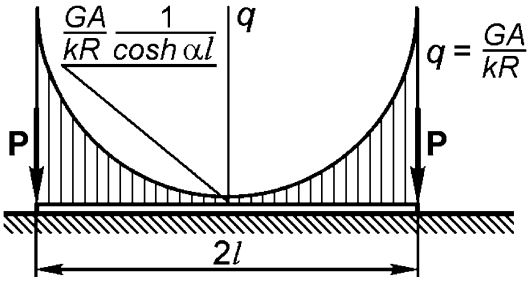

Fig. 269

61. It is possible to derive such distributed load under which the beam remains straight. But in this case the transverse shear forces are so large that it is necessary to calculate the beam deflection curve taking into account the shear strains. The following simple example shows us that determination of the proper distribution law for $q(x)$ is possible. Let us consider a beam tightly fixed in rigid guides (Fig. 270) and loaded by the moment applied at one of its ends.

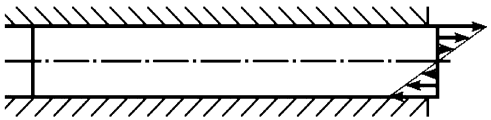

Fig. 270

Such a beam remains straight under bending and we can assert that the distributed load acting on the beam from the guides is of the sought type. The solution of problem 59 expresses the same. There the right part of the beam remains straight though the distributed load acting on it is not equal to zero.

Let us again consider equation (1) of problem 59

$$v'' = \frac{M}{EJ} - \frac{k\,M''}{GA}\,.$$

If we require that $v'' = 0$ then we get

$$M'' - \alpha^2 M = 0, \quad \alpha^2 = \frac{GA}{k\,EJ}.$$

The solution of this differential equation is

$$M = C_1 \sinh \alpha x + C_2 \cosh \alpha x; \tag{1}$$

differentiating step by step we obtain

$$Q = M' = C_1\,\alpha \sinh \alpha x + C_2\,\alpha \cosh \alpha x, \tag{2}$$

$$q = Q' = C_1\,\alpha^2 \sinh \alpha x + C_2\,\alpha^2 \cosh \alpha x, \tag{3}$$

where constants C_1 and C_2 should be specified in accordance with the boundary conditions. If the beam is simply supported at its ends we have

$$M = 0 \text{ at } x = 0 \text{ and at } x = l, \quad \text{then } C_1 = C_2 = 0 \quad \text{and} \quad q = 0.$$

It means that the beam remains straight only if the distributed load q vanishes.

However, there is the possibility to apply not only the distributed load but the concentrated forces and moments at the beam ends as well. For example, let us consider that the moment at the left support is equal to zero as it was previously and for the right support let us allow to apply any concentrated moment. Then supposing that $M = 0$ at $x = 0$ we have

$$C_2 = 0, \quad M = C_1 \sinh \alpha x,$$

where C_1 is an arbitrary constant. From relation (2) we have

$$Q = C_1\,\alpha \cosh \alpha x,$$

and the sought load from relation (3)

$$q(x) = C_1\,\alpha^2 \sinh \alpha x.$$

The reaction at the left support is

$$Q_{x=0} = C_1\,\alpha,$$

and at the right support

$$Q_{x=l} = C_1\,\alpha \cosh \alpha l, \quad M = C_1 \sinh \alpha l.$$

The system of required loads is presented in Fig. 271.

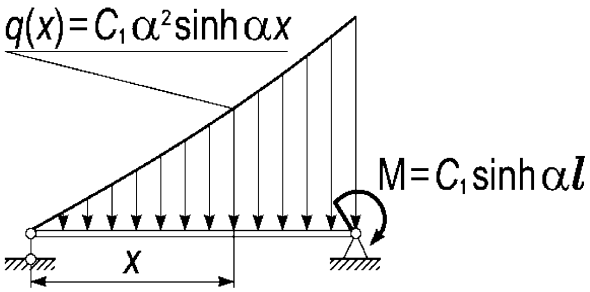

Fig. 271

62. This problem must be solved taking into account the shear strains of the ring, i.e. in accordance with the scheme of Timoshenko. The equations for a straight beam were already derived. And for a ring we need to derive the equations again.

Let us consider equilibrium equations for an element of a ring having length ds (Fig. 272). They will be as follows

$$\frac{dM}{ds} = Q\,, \quad \frac{dQ}{ds} + \frac{N}{R} = q\,, \quad \frac{dN}{ds} = \frac{Q}{R}\,. \tag{1}$$

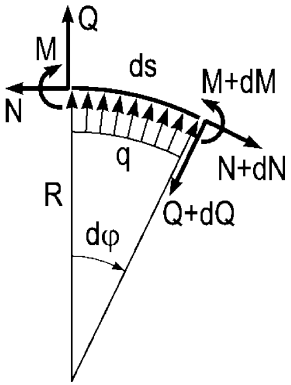

Fig. 272

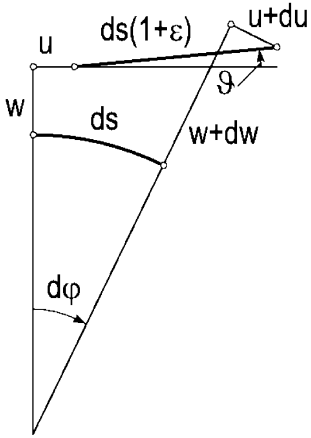

Fig. 273

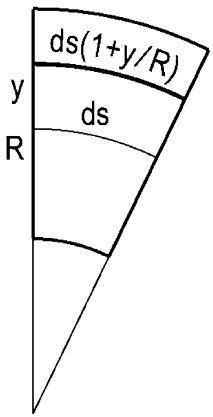

Fig. 274

Let us denote normal and tangent components of displacement as w and u, and the rotation angle of the tangent to a ring deflection curve as ϑ (Fig. 273).

Setting the sums of the closed polygon side projections on the axes u and w equal to zero we arrive at

$$\varepsilon = \frac{du}{ds} + \frac{w}{R}\,, \quad \vartheta = \frac{dw}{ds} - \frac{u}{R}\,. \tag{2}$$

Now we need to derive the relative elongation ε_y of the longitudinal fiber located at the distance y from the middle layer. The sought ε_y consists of two components. The first one is caused by the displacements of the points of this line and can be found from relation (2) by replacing R with $R+y$ and ds with $ds(1+y/R)$ (Fig.274). The second one is caused by mutual rotation of deflection curve tangents and mutual distortion of end cross-sections. The scheme of its determination was explained in detail during the solution of problem 59.

Thus we have

$$\varepsilon_y = \frac{du}{ds\left(1+\dfrac{y}{R}\right)} + \frac{w}{R+y} - y\left(\frac{d\vartheta}{ds} + \frac{d\gamma}{ds}\right).$$

As $\dfrac{1}{1+\dfrac{y}{R}} \approx 1 - \dfrac{y}{R}$ then

$$\varepsilon_y = \varepsilon - y\left(\frac{d\vartheta}{ds} + \frac{d\gamma}{ds} + \frac{1}{R}\frac{du}{ds} + \frac{w}{R^2}\right),$$

where ε is the relative elongation of the middle layer defined by relation (2).

Eliminating ϑ by means of the second expression of relation (2) and then substituting the known relation for γ defined in problem 59 we arrive at

$$\varepsilon_y = \varepsilon - y\left(\frac{d^2w}{ds^2} + \frac{w}{R^2} + \frac{k}{GA}\frac{dQ}{ds}\right).$$

Normal force and bending moment in a ring cross-section are derived by integration as follows

$$N = \int_A E\,\varepsilon_y\,dA = EA\,\varepsilon\,,$$

$$M = \int_A E\,\varepsilon_y\,y\,dA = EJ\left(\frac{d^2w}{ds^2} + \frac{w}{R^2} + \frac{k}{GA}\frac{dQ}{ds}\right).$$

Eliminating Q by means of the first expression of relations (1) we obtain

$$\frac{M}{EJ} = \frac{d^2w}{ds^2} + \frac{w}{R^2} + \frac{k}{GA}\frac{d^2M}{ds^2}.$$

Introducing the new independent variable $\varphi = \dfrac{s}{R}$ and denoting parameter β as

$$\beta = R\sqrt{\frac{GA}{k\,EJ}}\,,$$

we arrive at

$$\frac{d^2M}{d\varphi^2} - \beta^2 M = -\frac{1}{R^2}\left(\frac{d^2w}{d\varphi^2} + w\right).$$

The solution of this equation with respect to M under assumption that w is constant and equal to $\Delta/2$ is

$$M = B_1 \sinh\beta\varphi + B_2\cosh\beta\varphi + EJ\frac{\Delta}{2R^2}\,,$$

from which

$$Q = \frac{1}{R}\frac{dM}{d\varphi} = \frac{\beta}{R}\left(B_1\cosh\beta\varphi + B_2\sinh\beta\varphi\right). \tag{3}$$

Using the symmetry of loads with respect to vertical diameter we obtain the following boundary conditions for transverse shear force

$$Q = \frac{P}{2} \quad \text{at} \quad \varphi = 0 \quad \text{and} \quad Q = 0 \quad \text{at} \quad \varphi = \pi$$

Therefore

$$B_1 = \frac{PR}{2\beta} \quad \text{and} \quad B_2 = -PR\frac{\coth\beta\pi}{2\beta},$$

thus

$$Q = \frac{P}{2}\left(\cosh\beta\varphi - \coth\beta\pi\,\sinh\beta\varphi\right).$$

From the last of the relations (1) we obtain

$$N = \int Q d\varphi = \frac{P}{2\beta}\left(\sinh\beta\varphi - \coth\beta\pi\,\cosh\beta\varphi\right) + C_1,$$

where C_1 is a constant of integration. Before its determination we ought to obtain the displacement u from relation (2)

$$\frac{du}{d\varphi} = \varepsilon R - w \quad \text{or} \quad \frac{du}{d\varphi} = \frac{NR}{EA} - \frac{\Delta}{2}.$$

After integrating we obtain

$$u = \frac{PR}{2EA\beta^2}\left(\cosh\beta\varphi - \coth\beta\pi\sinh\beta\varphi\right) + \frac{C_1 R}{EA}\varphi + C_2.$$

As from the symmetry condition u is equal to zero at $\varphi = 0$ and at $\varphi = \pi$ it is easy to get

$$C_1 = \frac{\Delta}{2R}EA + \frac{P}{2\beta^2\pi}.$$

Now returning to the second of the equilibrium equations (1) we get

$$qR = \frac{dQ}{d\varphi} + N = \frac{P}{2}\frac{1+\beta^2}{\beta}\left(\sinh\beta\varphi - \coth\beta\pi\,\cosh\beta\varphi\right) + \frac{\Delta}{2R}EA + \frac{P}{2\beta^2\pi}.$$

The contact between the ring and the shaft opens obviously at the point of the force application. Therefore substituting $\varphi = 0$ and $q = 0$ in the above relation we shall find the sought force value

$$P = EA\frac{\Delta}{R}\frac{\pi\beta^2}{\left(1+\beta^2\right)\beta\pi\coth\beta\pi - 1}.$$

If the shear deformations in the ring are not taken into account in the solution we arrive at an incompetent conclusion because if $\beta \to \infty$ then the force P tends to infinity also.

63. Here due to the symmetry of loads with respect to the vertical diameter the transverse shear force vanishes under $\varphi = 0$. Therefore, from relation (3) of the previous problem we obtain $B_1 = 0$ and

$$Q = \frac{\beta}{R}B_2\sinh\beta\varphi.$$

The bending moment is

$$M_b = B_2\cosh\beta\varphi + EJ\frac{\Delta}{2R^2},$$

and at $\varphi = \pi/2$ takes the value $-M/2$ due to the antisymmetry of loads with respect to the horizontal diameter. Thus

$$B_2 = -\frac{M + EJ\dfrac{\Delta}{R^2}}{2\cosh\beta\dfrac{\pi}{2}}.$$

The normal force is

$$N = \int Q d\varphi = \frac{1}{R} B_2 \cosh\beta\varphi + C.$$

Due to the antisymmetry condition the normal force at $\varphi = \pi/2$ does not change after the moment M application. Therefore

$$\frac{1}{R} B_2 \cosh\beta\frac{\pi}{2} + C = N_{M=0} = \frac{\Delta}{2R} EA$$

Now we find q as follows:

$$qR = \frac{dQ}{d\varphi} + N = \frac{1+\beta^2}{R} B_2 \cosh\beta\varphi + C$$

or

$$qR = \frac{\Delta}{2R} EA - \frac{M + EJ\dfrac{\Delta}{R^2}}{2R\cosh\beta\dfrac{\pi}{2}} \left[\left(1+\beta^2\right)\cosh\beta\varphi - \cosh\beta\frac{\pi}{2}\right].$$

Due to the antisymmetry condition the load q must vanish at $\varphi = \pi/2$. Substituting $\varphi = \pi/2$ and $q = 0$ into the preceding expression we can find the value of the moment under which the contact opens:

$$M = \frac{\Delta}{\beta^2} EA - EJ\frac{\Delta}{R^2} = \frac{\Delta}{R^2} EJ\left(\frac{R^2 A}{\beta^2 J} - 1\right),$$

or

$$M = \frac{\Delta}{R^2} EJ\left(k\frac{E}{G} - 1\right) = \frac{\Delta}{R^2} EJ\left[2k(1+\mu) - 1\right].$$

64. The ring fitted on the axle will not contact it along the whole outline length. At the segments AB the ring is distant from the axle and the full contact takes place along the arc BCB only (Fig. 275).

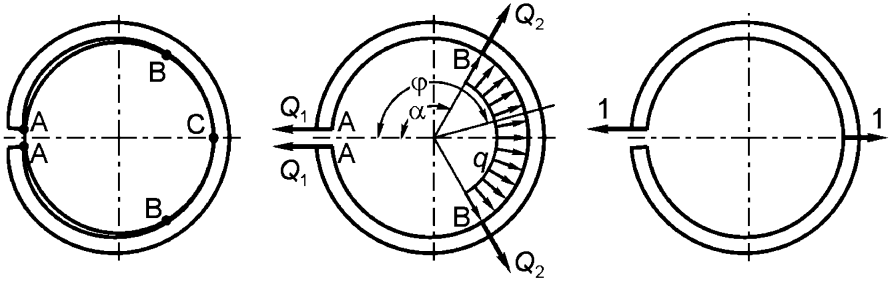

Fig. 275

The forces of interaction between the ring and the axle are shown in the central part of Fig. 275. The forces Q_1 act at the ring ends A and the forces Q_2 act at the points B. The nature of these forces is the same as in problem 59. The distributed load of intensity q occurs at the region of the full contact BB. If we manage to determine the forces Q_1, Q_2, q and the angle α satisfying all boundary conditions of the ring deformation, then we shall prove that the chosen scheme of the forces is valid.

As we assume that the segment BB is in full contact with the rigid axle it is obvious that the curvature of the ring along this segment is constant and equal to $2/D$. The curvature variation here

$$\frac{2}{D-\Delta}-\frac{2}{D}\approx\frac{2\Delta}{D^2}$$

is constant also. The bending moment along the same segment BB will be

$$M_{BB}=EJ\frac{2\Delta}{D^2},$$

where EJ is the bending rigidity of the ring. Therefore we must choose the forces Q_1, Q_2, q so that the moment along the segment BB is constant and would have the specified quantity.

In an arbitrary cross-section of the ring segment BB (Fig. 275) we have

$$M_{BB}=Q_1\frac{D}{2}\sin\varphi+Q_2\frac{D}{2}\sin(\varphi-\alpha)$$
$$+\frac{1}{2}\,q\frac{D^2}{4}\sin^2(\varphi-\alpha)+\frac{1}{2}\,q\frac{D^2}{4}\left[1-\cos(\varphi-\alpha)\right]^2,$$

or

$$M_{BB}=\sin\varphi\left[Q_1\frac{D}{2}+Q_2\frac{D}{2}\cos\alpha-q\frac{D^2}{4}\sin\alpha\right]$$
$$-\cos\varphi\left[Q_2\frac{D}{2}\sin\alpha+q\frac{D^2}{4}\cos\alpha\right]+q\frac{D^2}{4}.$$

The moment remains constant if we require that each of the expressions in square brackets vanishes

$$Q_1+Q_2\cos\alpha-q\frac{D}{2}\sin\alpha=0,$$
$$Q_2\sin\alpha+q\frac{D}{2}\cos\alpha=0, \tag{1}$$

then we obtain

$$q\frac{D^2}{4}=EJ\frac{2\Delta}{D^2},\quad\text{or}\quad q=EJ\frac{8\Delta}{D^4}.$$

Thus, q is found. These two equations (1) are not enough to evaluate the three unknowns Q_1, Q_2 and α.

Let us require now that the distance between points A and C of the ring increase by Δ. This condition can be written as follows

$$\Delta = \int_0^{\alpha} \frac{M_{AB}\, M_1\, D\, d\varphi}{2EJ} + \int_{\alpha}^{\pi} \frac{M_{BB}\, M_1\, D\, d\varphi}{2EJ},$$

where M_{AB} and M_{BB} are the bending moments in the ring segments AB and BB, and M_1 is the bending moment due to unit forces applied along the direction AC (see right part of Fig. 275). These moments are equal to

$$M_{AB} = Q_1 \frac{D}{2} \sin\varphi, \quad M_{BB} = EJ \frac{2\Delta}{D^2}, \quad M_1 = \frac{D}{2} \sin\varphi.$$

Substituting these relations and integrating we arrive at

$$\Delta = Q_1 \frac{D^3}{16EJ} \left(\alpha - \frac{1}{2} \sin 2\alpha \right) + \frac{\Delta}{2} (1 + \cos\alpha).$$

Solving this equation jointly with equations (1) we evaluate Q_1 and Q_2

$$Q_1 = \frac{4EJ\Delta}{D^3 \sin\alpha}, \quad Q_2 = -\frac{4EJ\Delta}{D^3} \cot\alpha.$$

The value of α is determined from the transcendent equation

$$2 = \frac{\alpha}{\sin\alpha} + \cos\alpha,$$

that has the solution $\alpha = 122°35'$. Therefore we have

$$Q_1 = 4.75 \frac{EJ\Delta}{D^3}, \quad Q_2 = 2.56 \frac{EJ\Delta}{D^3}.$$

Thus satisfying all the geometric boundary conditions we confirm that the specified scheme of the forces is valid.

The diagram of the bending moment is plotted in Fig. 276.

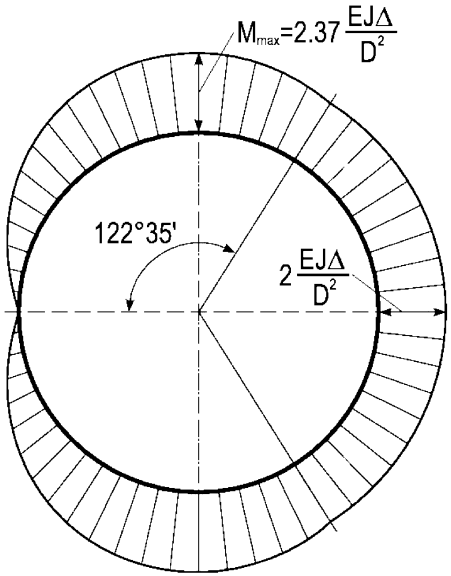

Fig. 276

65. At first let us consider the contact of the beam and the rigid guides when a small clearance space exists. The clearance magnitude is denoted as Δ (Fig. 277).

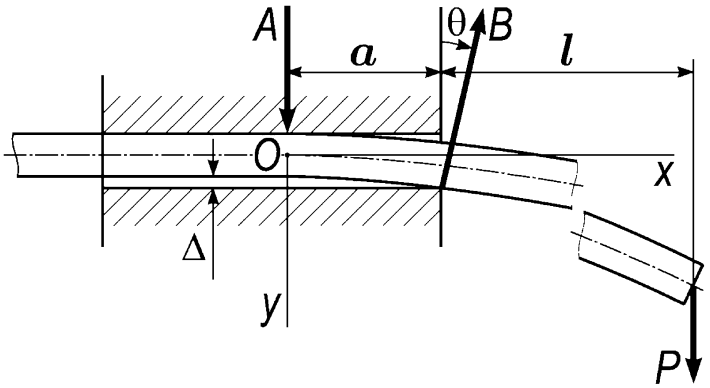

Fig. 277

At the left part the beam remains straight and tightly adjoins to the upper surface of the hole. The reaction $A = P\,l/a$ arises at the point of separation of the beam from this surface. The value of a remains indeterminate for the time being. The reaction B occurs at the point where the beam exits the hole. If friction forces are absent then this reaction is directed normally to the beam surface. As the angle θ of this force declination from the vertical is small then

$$B = P + A = P\left(1 + \frac{l}{a}\right).$$

If we put the coordinate origin into the point O then at $x = a$ the vertical deflection of the beam is equal to Δ:

$$\Delta = \frac{Aa^3}{6EJ} = \frac{Pla^2}{6EJ},$$

from which

$$a = \sqrt{\frac{6EJ\Delta}{Pl}}.$$

The slope angle θ at $x = a$ is

$$\theta = \frac{Aa^2}{2EJ} = \frac{1}{2}\sqrt{\frac{Pl}{EJ}6\Delta},$$

As the clearance Δ decreases, the angle θ and the value of a tend to zero and the forces A and B infinitely increase. Let us look how the horizontal component of the force B changes:

$$B\theta = P\left(1 + \frac{l}{a}\right)\frac{1}{2}\sqrt{\frac{Pl}{EJ}\,6\Delta},$$

or

$$B\theta = \frac{P}{2}\left(\frac{Pl^2}{EJ} + \sqrt{\frac{Pl}{EJ}\,6\Delta}\right).$$

As we see, at $\Delta \to 0$ the horizontal component of the force B converges to a certain limit

$$B\theta = \frac{P^2 l^2}{2EJ}.$$

This value of force will be shown by the dynamometer (see also in [4]).

66. Let us consider one half of the symmetric system shown in Fig. 68 as a separate beam (Fig. 278).

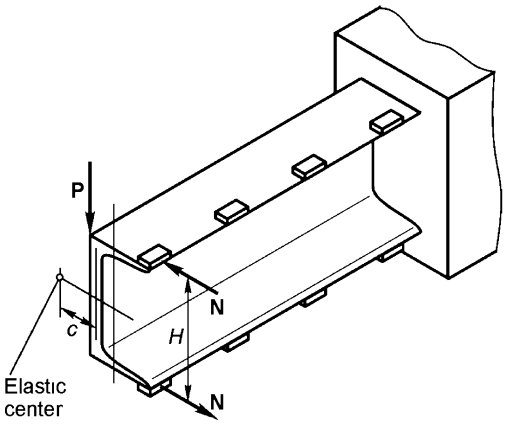

Fig. 278

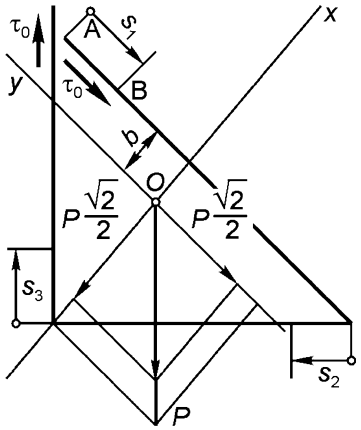

Fig. 279

As the force P is applied not in the elastic centre then this beam will be twisted simultaneously with bending. This twist will be excluded for all beam sections if in the sections where the first strips have been cut we apply the couple of forces N counterbalancing the moment of the force P with respect to the elastic centre, i.e. $N = Pc/H$.

Thus the first upper strip is compressed and the first lower strip is tensed by the forces N. All the other strips do not bear any forces under the system bending. Naturally this statement is valid only if the strips are considered as rigid. If they had considerable strains then arising forces should be derived in the same manner as forces in the rivets in problem 11.

67. Let us decompose the force P along the principal axes x and y (Fig. 279) and cut the cross-section at the corner point A. At the same time we introduce indeterminate shear stress flow τ_0. Then the shear stress at an arbitrary point B will be the sum of τ_0 and of the shear stresses expressed by Zhuravskiy formula due to the force P components

$$\tau = \tau_0 + \frac{P\sqrt{2}}{2\delta}\left(\frac{S_x^*}{J_x} + \frac{S_y^*}{J_y}\right).$$

After simple calculations we get

$$b = a\,\frac{\sqrt{2}}{2}\,\frac{1}{2+\sqrt{2}}\,, \quad J_x = \frac{a^3\delta}{6}\left(2+\sqrt{2}\right), \quad J_y = \frac{a^3\delta}{6}\,\frac{1+2\sqrt{2}}{2+\sqrt{2}}\,.$$

For each of the cross-section's three parts we obtain

$$\tau_1 = \tau_0 + \frac{3\sqrt{2}}{2}\,\frac{P}{a^3\delta}\left[\frac{s_1\,a\sqrt{2} - s_1^2}{2+\sqrt{2}} + \frac{s_1\,a\sqrt{2}}{1+2\sqrt{2}}\right], \tag{1}$$

$$\tau_2 = \tau_0 + \frac{3\sqrt{2}}{2}\,\frac{P}{a^3\delta}\left[\frac{\frac{\sqrt{2}}{2}\,s_2^2 - s_2\,a\sqrt{2}}{2+\sqrt{2}} + \frac{2a^2 + s_2\,a\sqrt{2} - \left(1+\sqrt{2}\right)s_2^2}{1+2\sqrt{2}}\right],$$

$$\tau_3 = \tau_0 + \frac{3\sqrt{2}}{2}\,\frac{P}{a^3\delta}\left[\frac{\sqrt{2}}{2}\,\frac{s_3^2 - a^2}{2+\sqrt{2}} + \frac{a^2 - a\left(2+\sqrt{2}\right)s_3 + \left(1+\sqrt{2}\right)s_3^2}{1+2\sqrt{2}}\right],$$

where s_1, s_2 and s_3 are coordinates measured along the contour from the corner points.

As no mutual displacements may occur in the cross-cut A, we must satisfy the condition

$$\int_s \gamma\,ds = 0\,,$$

or

$$\int_0^{a\sqrt{2}} \tau_1\,ds_1 + \int_0^a \tau_2\,ds_2 + \int_0^a \tau_3\,ds_3 = 0.$$

From this relation the magnitude of τ_0 is determined as

$$\tau_0 = \frac{3\sqrt{2}}{2}\,\frac{P}{a\delta}\left[\frac{\sqrt{2}}{3\left(2+\sqrt{2}\right)^2} - \frac{1}{1+2\sqrt{2}}\right].$$

Substituting τ_0 into relation (1) and preforming the necessary calculations we get

$$\tau_1 = \frac{P}{a\delta}\left(-0.47 + 1.66\,\zeta_1 - 0.62\,\zeta_1^2\right),$$
$$\tau_2 = \frac{P}{a\delta}\left(0.64 - 0.095\,\zeta_2 - 0.90\,\zeta_2^2\right),$$
$$\tau_3 = \frac{P}{a\delta}\left(-0.35 - 1.89\,\zeta_3 + 1.78\,\zeta_3^2\right),$$

where $\zeta_i = \dfrac{s_i}{a} \quad (i = 1, 2, 3)$.

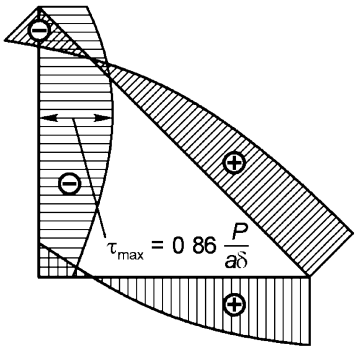

Fig. 280

Figure 280 represents the shear stress diagram from which it is clear that

$$\tau_{\max} = 0.86\frac{P}{a\delta}\,.$$

68. Let us separate the element of the beam of the length dx at the distance x from its free end (Fig. 281)

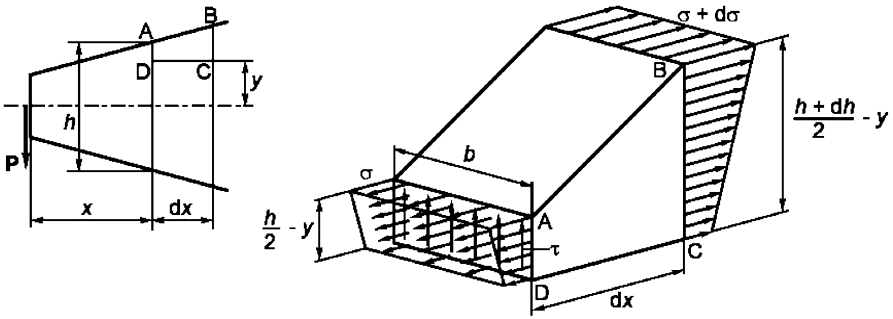

Fig. 281

This element in turn is divided into two parts by a horizontal plane at the distance y from the middle line of the beam. Now let us consider the equilibrium condition of the upper part $ABCD$. Obviously it looks like

$$\int_y^{(h+dh)/2} (\sigma + d\sigma)\, b\, dy - \int_y^{h/2} \sigma\, b\, dy = \tau\, b\, dx\,.$$

As $\sigma = \dfrac{12M}{bh^3}\,y$, then $\sigma + d\sigma = \dfrac{12\,y}{b}\left[\dfrac{M}{h^3} + d\left(\dfrac{M}{h^3}\right)\right]$.

Now we can rewrite the equilibrium condition as follows:

$$\frac{12}{b}\left[\frac{M}{h^3} + d\left(\frac{M}{h^3}\right)\right] \int_y^{(h+dh)/2} y\, dy - \frac{12M}{bh^3} \int_y^{h/2} y\, dy = \tau\, dx\,,$$

from which

$$\tau = 3\frac{M}{bh^2}\frac{dh}{dx} + \frac{6}{b}\left(\frac{h^2}{4} - y^2\right)\frac{d}{dx}\left(\frac{M}{h^3}\right).$$

If the law of h and M variation is linear, then, as the specified $h_1 = 2h_0$, we get

$$h = h_0\left(1 + \frac{x}{l}\right), \quad M = Px,$$

$$\tau = \frac{6P}{\left(1+\frac{x}{l}\right)^2 b h_0}\left[\frac{1}{2}\frac{x}{l} + \frac{1}{h_0^2}\left(\frac{h^2}{4} - y^2\right)\frac{1-2\frac{x}{l}}{\left(1+\frac{x}{l}\right)^2}\right].$$

The diagrams of τ for the five equidistant beam cross-sections are shown in Fig. 282.

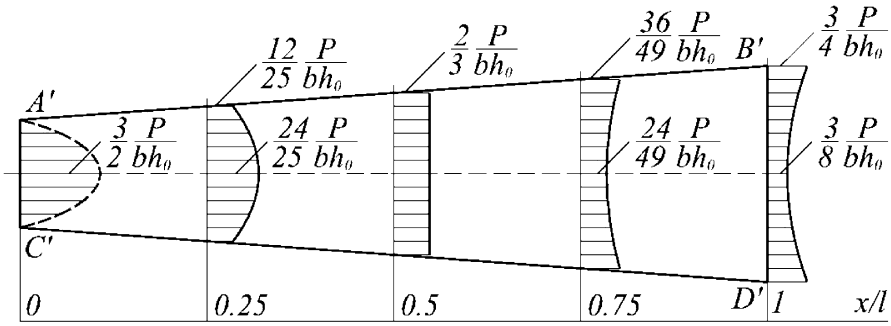

Fig. 282

Here, in contrast to any beam of the constant cross-section height, the shear stresses at the upper and the lower points of the cross-section do not vanish as the section plane is not perpendicular to the outer upper ($A'B'$) and lower ($C'D'$) surfaces. The diagram for the free end cross-section is plotted by dashed line because the law of stress distribution along this cross-section is completely determined by the manner of the external load P application.

If the beam thickness varies not too fast depending on x, i.e. the angle of the beam widening or narrowing is small enough, then the above solution is exactly the same as the solution for the wedge obtained by the elasticity theory methods.

69. As the specified beam is very long then if we cut it at the i-th support its right part can be considered as a very long beam similar to the specified beam but loaded now by the moment M_i and not by the moment M. The same can be said concerning the support number $i+1$, $i+2$ and so on. Therefore if the bending moment at the $i+1$-th support accounts some part of the i-th moment then the $i+2$-th moment accounts exactly for the same part of the $i+1$-th one, i.e.

$$M_{i+1} = x\,M_i, \qquad M_{i+2} = x\,M_{i+1} = x^2 M_i \quad \text{etc.}$$

Let us write the expression of the three moments theorem for the i-th and the $i+1$-th span. As any external loads within the spans are absent we get

$$M_i\,a + 2\,M_{i+1}\,(a+a) + M_{i+2}\,a = 0\,.$$

Substituting the relations for M_{i+1} and M_{i+2} we arrive at the equation

$$1 + 4x + x^2 = 0\,,$$

from which we find

$$x = -2 \pm \sqrt{3}\,.$$

As the absolute value of M_i must be decreasing with i then the absolute value of x must be less than 1 so we take the "plus" sign before the radical[2]. Then

$$x = -\left(2 - \sqrt{3}\right).$$

Let us note that as x is negative then the bending moments at the neighbouring supports will be of different signs. The bending moment at the i-th support is

$$M_i = M\,x^{i-1} = M\left(\sqrt{3} - 2\right)^{i-1}.$$

To derive the rotation angle of the cross-section at the i-th support we apply to the basic system the unit moment at this support and then multiply the obtained bending moments diagram occupying the i-th span only with the bending moments diagram caused by the external moment M at this span which is plotted in Fig. 283 assuming that the moments M_i and M_{i+1} are positive.

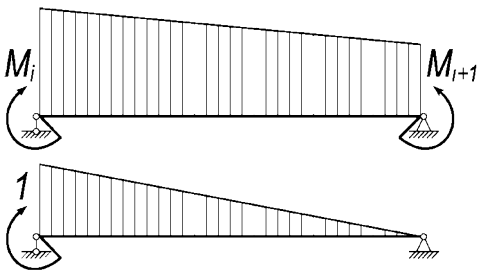

Fig. 283

The result is: $EJ\,\theta_i = \dfrac{M\,a}{6}\sqrt{3}\left(\sqrt{3} - 2\right)^{i-1}$.

70. Let us write the system of $n-2$ equations that are required for determination of the moments at the supports:

[2] The "minus" sign before the radical corresponds to the case when the moment is applied not at the left end but at the right end support. Then the absolute value of x will be greater than 1, so the absolute value of M_i will increase with i.

$$
\begin{aligned}
M + 4M_2 + M_3 &= 0\,,\\
M_2 + 4M_3 + 4M_4 &= 0\,,\\
&\dots\\
M_{n-2} + 4M_{n-1} &= 0\,.
\end{aligned}
$$

Assuming that $M_i = A\,x^{i-1}$ and substituting this value of M_i in all equations except the first and the last we arrive at

$$
\begin{aligned}
&1 + 4x + x^2 = 0\,,\\
&x = -2 \pm \sqrt{3}\,.
\end{aligned}
$$

Now it is easy to reveal that all equations except the first and the last are valid if we assume that

$$
\begin{aligned}
M_2 &= A\,x_1 + B\,x_2\,,\\
M_3 &= A\,x_1^2 + B\,x_2^2\,,\\
&\dots\dots\\
M_i &= A\,x_1^{i-1} + B\,x_2^{i-1},
\end{aligned}
$$

where

$$
x_1 = -2 + \sqrt{3}\,, \quad x_2 = -2 - \sqrt{3}\,,
$$

A and B are arbitrary constants that are chosen in order to satisfy the first and the last equations of the system

$$
\begin{aligned}
&M + 4\,(A\,x_1 + B\,x_2) + A\,x_1^2 + B\,x_2^2 = 0,\\
&Ax_1^{n-3} + B\,x_2^{n-3} + 4A\,x_1^{n-2} + 4\,B\,x_2^{n-2} = 0,
\end{aligned}
$$

from which we have

$$
A = M\,\frac{x_2^{n-2}}{x_1\left(x_2^{n-1} - x_1^{n-1}\right)}\,, \quad B = -M\,\frac{x_1^{n-2}}{x_2\left(x_2^{n-1} - x_1^{n-1}\right)}\,.
$$

Finally we get

$$
M_i = M\,\frac{\left(-2 - \sqrt{3}\right)^{n-i} - \left(-2 + \sqrt{3}\right)^{n-i}}{\left(-2 - \sqrt{3}\right)^{n-1} - \left(-2 + \sqrt{3}\right)^{n-1}}\,.
$$

If M_i is known then we need not work hard to determine the rotation angle of the cross-section at the i-th support. Multiplying the diagrams shown in Fig. 283 we arrive at

$$
EJ\,\theta_i = M_i\,\frac{a}{3} + M_{i+1}\,\frac{a}{6}\,.
$$

71. Let us denote the normal reaction of the right support as X_1. Then the friction force will be fX_1 (Fig. 284).

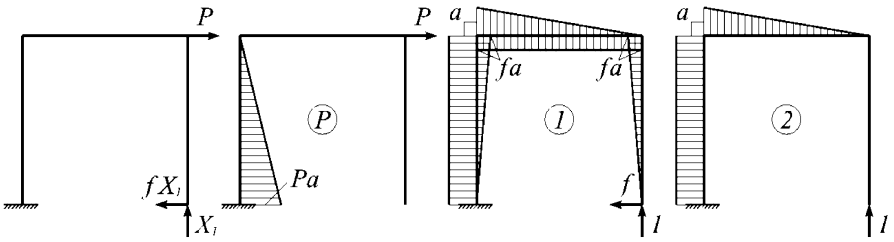

Fig. 284

If we solve the problem by the force method we have

$$\delta_{11}\, X_1 + \delta_{1P} = 0\,.$$

As $\delta_{11}X_1$ is the displacement in the direction of X_1, caused by the forces X_1 and fX_1, and δ_{1P} - the displacement in the same direction caused by the load P, then δ_{11} is calculated by multiplying the diagrams (1) and (2) and δ_{1P} - by multiplying the diagrams (P) and (2) as follows:

$$\delta_{11} = \frac{a^3}{EJ}\left(\frac{4}{3} - f\right), \quad \delta_{1P} = -\frac{Pa^3}{2EJ}\,.$$

Then the reaction is

$$X_1 = \frac{P}{2\left(\frac{4}{3} - f\right)} = \frac{3P}{8 - 6f}\,.$$

The diagram of resultant bending moments is shown in Fig. 285.

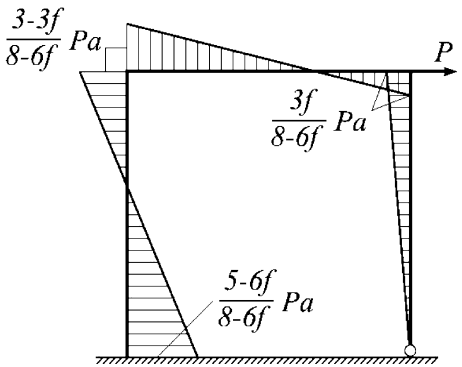

Fig. 285

72. Under the condition of applying loads at frame nodes a frame having rigid angles can be analyzed like a truss, i.e. in assumption that its rods undergo only compression or tension. To make sure of this let us consider

some frame which consists of several closed contours (Fig. 286) providing that the system remains geometrically unchanged if the rigid nodal joints are replaced with the pinned ones.

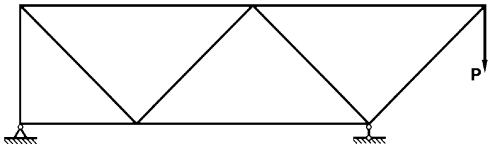

Fig. 286

Suppose that the frame is loaded by the forces applied only at nodes (the force P and the support reactions). Applying the forces method we disclose static indeterminacy of the frame by fitting pins at its nodes and introducing the nodal moments $X_1, X_2, X_3, ...$ as the reactions of the withdrawn elastic constraints (Fig. 287).

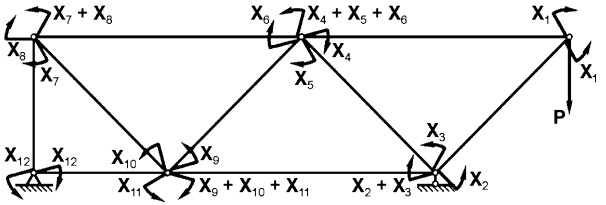

Fig. 287

Thus we obtain 12 equations of usual type for this system:

$$\begin{aligned}
\delta_{11}\,X_1 + \delta_{12}\,X_2 + ... + \delta_{1P} &= 0\,,\\
\delta_{21}\,X_1 + \delta_{22}\,X_2 + ... + \delta_{2P} &= 0\,,\\
&\dots\\
\delta_{12\,1}\,X_1 + \delta_{12\,2}\,X_2 + ... + \delta_{12\,P} &= 0\,,
\end{aligned}$$

where the coefficients δ_{11}, δ_{12},... are derived by multiplying the diagrams of the bending moments caused by the unit moments applied instead of the moments X_1, X_2,... Coefficients δ_{1P}, δ_{2P},... are derived by multiplying the same ones and the diagrams of the bending moments caused by the load P. But the load P and in general any forces applied at frame nodes do not produce any bending moments if the frame rods are connected by pins. Hence

$$\delta_{1P} = \delta_{2P} = ... = 0\,. \tag{2}$$

As equations (1) are independent, the determinant of the system is not equal to zero (see the next problem). For this case if condition (2) is valid we obviously obtain

$$X_1 = X_2 = ... = 0\,.$$

Therefore, under the specified conditions the system with the rigid nodes is equivalent to the system with the pinned rod joints.

But rigorously, the bending moments arise nevertheless in the system (Fig. 286) due to elongation or shortening of rods.

These bending moments can be derived from the same equations (1) if we take into account the displacements due to rod tension or compression while calculating coefficients $\delta_{11}, \delta_{12}, \ldots, \delta_{1P}, \delta_{2P}, \ldots$ But obviously the stresses that correspond to these moments will be sufficiently less than the stresses caused by normal forces.

In fact, displacements of any pinned bar are proportional to Ml^2 divided by EJ under bending by moment M and to Pl divided by EA under tension by force P. In the given case these magnitudes have the same order, i.e. $\frac{Ml^2}{EJ} \sim \frac{Pl}{EA}$. But $M = \sigma_b W$, $P = \sigma_t A$, therefore we have $\frac{\sigma_b}{\sigma_t} \sim \frac{J}{Wl}$, i.e. the ratio of σ_b to σ_t has the magnitude of order J divided by Wl. But J/W is equal to maximal distance of section point from the neutral axis that crosses the centroid. Therefore the right part of the above proportion is considerably small as the ratio of the section height part to the rod length. Correspondingly, σ_b has the magnitude of the same order in comparison with σ_t.

73. Let us consider the spring ring quarter (Fig. 288). The rotation of cross-section A with respect to cross-section B is absent but the deflection in the axial direction takes place.

The shear force $P/4$ and the torsion moment X_1 arise in section C.

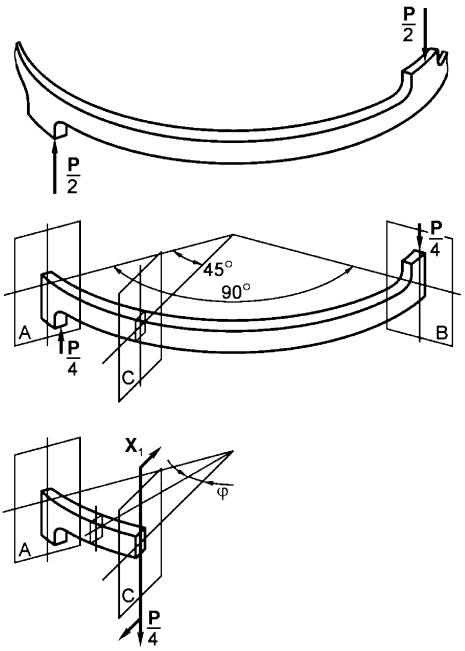

Fig. 288

Let us determine the unknown value X_1 by the method generally used for disclosing of frame static indeterminacy

$$\delta_{11} X_1 = 0\,,$$

$$\delta_{11} = \frac{1}{EJ}\int\limits_0^{\pi/4} M_{1b}^2\, R\; d\varphi + \frac{1}{C}\int\limits_0^{\pi/4} M_{1t}^2\, R\; d\varphi,$$

$$\delta_{1P} = \frac{1}{EJ}\int\limits_0^{\pi/4} M_{1b}\, M_{Pb}\, R\; d\varphi + \frac{1}{C}\int\limits_0^{\pi/4} M_{1t}\, M_{Pt}\, R\; d\varphi,$$

where

$$M_{1b} = \sin\varphi, \qquad M_{1t} = \cos\varphi,$$

$$M_{Pb} = -\frac{PR}{4}\sin\varphi, \quad M_{Pt} = \frac{PR}{4}\,(1-\cos\varphi)\,,$$

C is torsional rigidity. For the square cross-section $C = 0.141\,Ga^4$.

After integration we arrive at

$$\delta_{11} = \frac{R}{4EJ}\left(\frac{\pi}{2}-1\right) + \frac{R}{4C}\left(\frac{\pi}{2}+1\right),$$

$$\delta_{1P} = -\frac{PR^2}{16EJ}\left(\frac{\pi}{2}-1\right) + \frac{PR^2}{16C}\left(2\sqrt{2}-\frac{\pi}{2}-1\right),$$

$$X_1 = \frac{PR}{4}\,\frac{\dfrac{\pi}{2}-1-\dfrac{EJ}{C}\left(2\sqrt{2}-\dfrac{\pi}{2}-1\right)}{\dfrac{\pi}{2}-1+\dfrac{EJ}{C}\left(\dfrac{\pi}{2}+1\right)}\,.$$

For the square cross-section under $\mu = 0.3$ we have

$$\frac{EJ}{C} = \frac{E\,\dfrac{a^4}{12}}{0.141\,\dfrac{E}{2(1+\mu)}\,a^4} = \frac{1+\mu}{0.846} \approx 1.54\,;$$

then the sought torsional moment is

$$X_1 = 0.0375\,\frac{PR}{4}\,.$$

The resultant bending moment is

$$M_b = -\frac{PR}{4}\,0.962\,\sin\varphi.$$

The resultant torsion moment is

$$M_t = \frac{PR}{4}(1 - 0.962\,\cos\varphi).$$

The vertical displacement of section C with respect to section A is

$$\lambda_C = \frac{R}{EJ} \int_0^{\pi/4} M_b \, M_b' \, d\varphi + \frac{R}{C} \int_0^{\pi/4} M_t \, M_t' \, d\varphi,$$

where M_b and M_t are bending and torsional moments,

M_b' and M_t' the corresponding moments caused by unit vertical load applied at section C, i.e.

$$M_b' = -R \sin\varphi, \quad M_t' = R(1 - \cos\varphi).$$

Thus we obtain

$$\lambda_C = \frac{PR^3}{4EJ} 0.962 \int_0^{\pi/4} \sin^2\varphi \, d\varphi + \frac{PR^3}{4C} \int_0^{\pi/4} (1 - 0.962\cos\varphi)(1 - \cos\varphi) \, d\varphi$$

$$= \frac{PR^3}{16EJ} 0.962 \left(\frac{\pi}{2} - 1\right) + \frac{PR^3}{16C} \left[\pi - 2\sqrt{2} - 0.962\, 2\sqrt{2} + 0.962 \left(\frac{\pi}{2} + 1\right)\right];$$

or finally we arrive at

$$\lambda_C = \frac{PR^3}{EJ} 0.0405.$$

In order to determine the deflection of the spring completely λ_c should be multiplied by twice the number of working rings $2n$:

$$\lambda = 2n \frac{PR^3}{EJ} 0.0405\,, \quad \text{or} \quad \lambda = 0.972 \frac{PR^3}{Ea^4} n\,.$$

Comparing this value with the camber of the square section coil spring that has the same number of working coils n, i.e.

$$\lambda = \frac{PR^3 2\pi n}{0.141\, Ga^4} \approx 116 \frac{PR^3}{Ea^4} n\,,$$

we arrive at the conclusion that the slotted spring is about 120 times more stiff than the coil spring.

74. Let us consider some plane closed frame of constant rigidity EJ and suppose that the diagram of bending moments is constructed (Fig. 289). Let us cut the frame outline in some arbitrary point and derive the cross-sectional mutual rotation angle at the point of the cut. This angle vanishes from the continuity condition. In order to determine the mutual rotation angle we must calculate the integral [7]

$$\int_s \frac{M M_1}{EJ} ds$$

where M_1 is the bending moment caused by the unit moments applied at the point of the cut (Fig. 289), i.e. $M_1 = 1$.

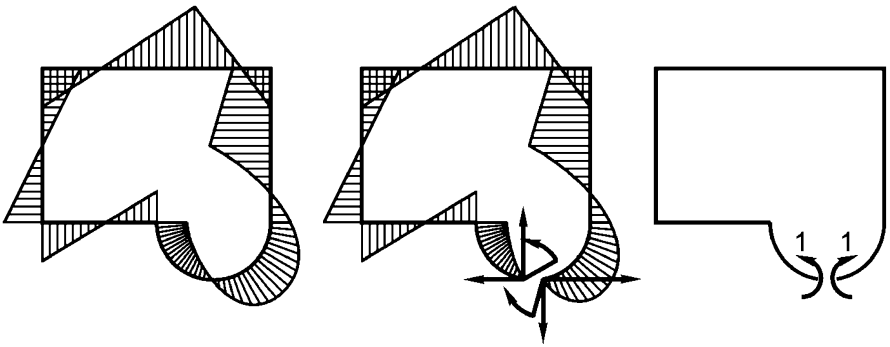

Fig. 289

Therefore in case of constant rigidity we arrive at

$$\int_s M\,ds = 0.$$

The proved statement is valid not only for closed frames but in general for any rod construction fixed in such a manner that its end cross-sections have the same angle of rotation. For example, under arbitrary load the bending moments diagram area vanishes for each of the constructions depicted in Fig. 290 in case of $EJ = const$.

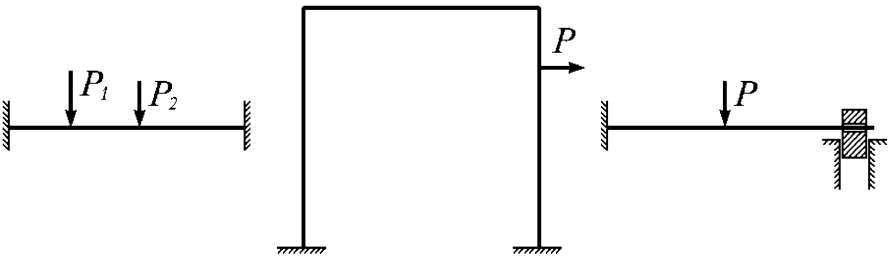

Fig. 290

75. Let us note preliminarily that the area ΔA that is swept by any beam under bending is determined as the integral

$$\Delta A = \int_s \frac{M M_{1q}}{EJ} ds,$$

where M is the bending moment due to external load, and M_{1q} is the bending moment caused by the distributed load of unit intensity ($q = 1$ N/m).

The easiest way to derive this relation is to apply the same method as for the usual linear and angular displacements.

In order to calculate the variation of the area restricted by closed frame we should preliminarily derive the expression for M_{1q}, by applying the unit distributed load $q = 1$ (Fig. 291).

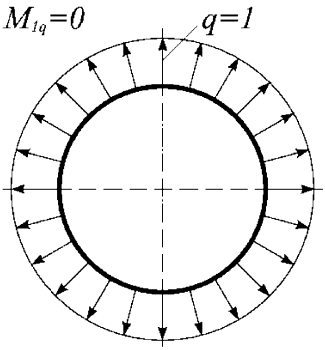

Fig. 291

But for the closed ring frame $M_{1q} = 0$, therefore $\Delta A = 0$. Thus the supposed statement is proved. It is absolutely clear that this statement is valid on the one hand only within the limits where the elongation of the ring contour can be reasonably neglected, and on the other hand under the condition that the displacements of the system are small enough. For the considerably slender ring under sufficient variation of its contour shape the area restricted by the contour will not remain unchanged.

76. Let us reduce the external load to the junction ends in the form of shear forces and bending moments (Fig. 292) [11].

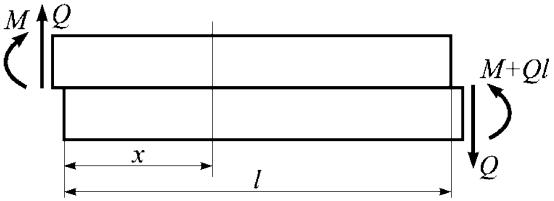

Fig. 292

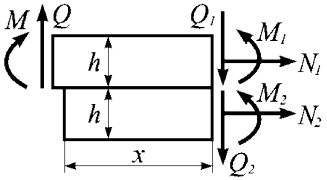

Fig. 293

The internal forces and moments relating to the upper sheet are denoted by the index "one" and the ones relating to the lower sheet by index "two". The equilibrium equations for the left junction part of length x (Fig. 293) give

$$\begin{aligned} N_1 &= -N_2 = N, \\ Q_1 + Q_2 &= Q, \\ .M_1 + M_2 &= M + Qx + Nh. \end{aligned} \tag{1}$$

The mutual displacement Δ along the x axis arising between the lower surface of the upper sheet and the upper surface of the lower one can be determined as the integral of the strain difference

$$\Delta = \int (\epsilon_1 - \epsilon_2) dx + C,$$

but

$$\epsilon_1 = \frac{N}{Ebh} + \frac{6M_1}{Ebh^2}, \quad \epsilon_2 = -\frac{N}{Ebh} - \frac{6M_2}{Ebh^2},$$

therefore

$$\Delta = \frac{1}{Ebh} \int \left[2N + \frac{6}{h} (M_1 + M_2) \right] dx + C, \tag{2}$$

The magnitude of Δ is expressed through the shear stresses τ_g in the glue layer by the obvious expression

$$G_g \frac{\Delta}{\delta} = \tau_g,$$

where G_g is the glue shear modulus and δ is the thickness of the glue layer.

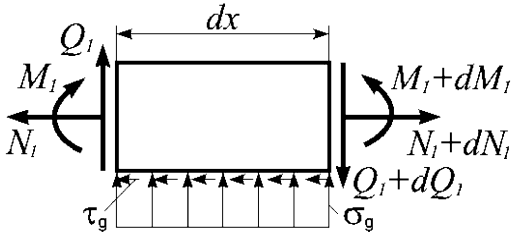

Fig. 294

It follows from the equilibrium condition of the upper sheet element of length dx (Fig. 294) that

$$b\tau_g = N', \tag{3}$$

therefore

$$G_g \frac{\Delta}{\delta} = \frac{N'}{b}.$$

Differentiating both parts of this equality with respect to x and substituting the expression for $M_1 + M_2$ from the relation (1) into relation (2) we arrive at the equation from which the value of N can be determined:

$$N'' - \frac{8G_g}{Eh\delta} N = \frac{6G_g}{Eh^2\delta} (M + Qx).$$

If we denote

$$\frac{8G_g}{Eh\delta} = \alpha^2, \tag{4}$$

then we get

$$N = A \sinh \alpha x + B \cosh \alpha x - \frac{3}{4h}(M + Qx).$$

The constants A and B are derived from the boundary conditions for the tensile force at the ends of the conglutination segment

$$N_{x=0} = N_{x=l} = 0.$$

Finally we obtain

$$N = \frac{3\sinh\alpha x}{4h\sinh\alpha l}\left[M\left(1-\cosh\alpha l\right)+Ql\right]+\frac{3M}{4h}\cosh\alpha x-\frac{3}{4h}\left(M+Qx\right) \quad (5)$$

and the shear stress τ_g in the glue layer in accordance with relation (3) will be

$$\tau_g = \frac{3\alpha\cosh\alpha x}{4bh\sinh\alpha l}\left[M\left(1-\cosh\alpha l\right)+Ql\right]+\frac{3\alpha M}{4bh}\sinh\alpha x-\frac{3}{4bh}Q\,. \quad (6)$$

The glue layer undergoes not only shear but also tension and compression in the direction perpendicular to the surface of glueing.

The normal stress in the glue layer is

$$\sigma_g = \frac{y_2-y_1}{\delta}E_g\,,$$

where y_1 and y_2 are vertical displacements of the upper and the lower sheets, E_g is the glue elasticity modulus.

Let us add also two more equilibrium equations for the element dx (Fig. 294):

$$\sigma_g b = Q_1'\,, \quad (7)$$

$$Q_1 = M_1' - \frac{h}{2}N'. \quad (8)$$

Substituting σ_g into relation (7) and then Q_1 into relation (8) we obtain:

$$\left(y_2-y_1\right)\frac{bE_g}{\delta} = M_1'' - \frac{h}{2}N''.$$

But as $EJy_1'' = M_1$, and $EJy_2'' = M_2$ we arrive at

$$\frac{M_2-M_1}{EJ}\,\frac{bE_g}{\delta} = \left(M_1-\frac{h}{2}N\right)^{(IV)}.$$

Finally we exclude the moment M_2 from this equation using relation (1). As a result we obtain the following equation:

$$\left(M_1-\frac{h}{2}N\right)^{(IV)} + \frac{2bE_g}{\delta EJ}\left(M_1-\frac{h}{2}N\right) = \frac{bE_g}{\delta EJ}\left(M+Qx\right).$$

If we denote

$$M_1-\frac{h}{2}N = Y, \quad \frac{2bE_g}{\delta EJ} = 4k^4;$$

then

$$Y^{(IV)} + 4k^4\,Y = 2k^4\left(M+Qx\right).$$

The homogeneous equation

$$Y^{(IV)} + 4k^4\,Y = 0$$

is satisfied by the functions $\sinh kx \sin kx$, $\cosh kx \cos kx$, $\sinh kx \cos kx$, $\cosh kx \sin kx$ and by any combination of these functions. Such combinations that are the most suitable for practical use were suggested by A.N. Krylov and named after him as Krylov functions. They are suitable as the derivative of any Krylov function gives some other of these functions. The relations of the Krylov functions are given in Table 1.

Table 1. Krylov functions

n	$Y_n(x)$	$Y_n'(x)$	$Y_n''(x)$	$Y_n'''(x)$	$Y_n^{(IV)}(x)$
1	$\cosh x \cos x$	$-4Y_4$	$-4Y_3$	$-4Y_2$	$-4Y_1$
2	$\frac{1}{2}(\cosh x \sin x + \sinh x \cos x)$	Y_1	$-4Y_4$	$-4Y_3$	$-4Y_2$
3	$\frac{1}{2}\sinh kx \sin kx$	Y_2	Y_1	$-4Y_4$	$-4Y_3$
4	$\frac{1}{4}(\cosh x \sin x - \sinh x \cos x)$	Y_3	Y_2	Y_1	$-4Y_4$

Thus we have

$$Y = C_1Y_1(kx) + C_2Y_2(kx) + C_3Y_3(kx) + C_4Y_4(kx) + \frac{1}{2}(M + Qx), \quad (9)$$

where the constants C_1, C_2, C_3 and C_4 are derived from the four conditions

$$Y_{x=0} = M_{1x=0} = M, \quad Q_{1x=0} = Y'_{x=0} = Q, \quad M_{1x=l} = 0, \quad Y'_{x=l} = 0.$$

As a result after some transformations and replacement of the Krylov functions by their expressions we arrive at

$$C_1 = \frac{M}{2}, \qquad C_2 = \frac{Q}{2k},$$

$$C_3 = -M\frac{\sinh(kl) + \sin(kl)}{\sinh(kl) - \sin(kl)} - \frac{Q}{k}\frac{\cosh(kl) + \cos(kl)}{\sinh(kl) + \sin(kl)} - 2Q\,l\frac{\sinh(kl)\sin(kl)}{\sinh^2(kl) - \sin^2(kl)},$$

$$C_4 = 2M\frac{\cosh(kl) + \cos(kl)}{\sinh(kl) - \sin(kl)} + \frac{Q}{k}\frac{\sinh(kl) + \sin(kl)}{\sinh(kl) + \sin(kl)} + 2Q\,l\frac{\cosh(kl)\sin(kl) + \sinh(kl)\cos(kl)}{\sinh^2(kl) - \sin^2(kl)}.$$

Now the bending moment M_1 is determined from the expression

$$M_1 = Y + \frac{h}{2}N,$$

where N is specified by the function (5).

The normal stress in the glue layer according to equations (7) and (8) will be

$$\sigma_g = \frac{1}{b} Y'',$$

$$\sigma_g = \frac{k^2}{b} \left[-4C_1 Y_3(kx) - 4C_2 Y_4(kx) + C_3 Y_1(kx) + 4C_4 Y_2(kx) \right]. \qquad (10)$$

The positive value of σ_g corresponds to the compression of the glue layer. Using relations (6) and (10) we can construct the plots of normal and shear stress variation in the glue layer, and using the relations (5) and (9) obtain the diagrams of normal forces and bending moment in the upper sheet.

The problem is significantly simplified in the case of a considerably long glued joint as the stress in the glued layer has local character. In this case we can separate the decaying part of the solution and assume that

$$N = A \exp(-kx) - \frac{3}{4h}(M + Qx),$$

$$Y = \exp(-kx)\,(C_1 \sin kx + C_2 \cos kx) + \frac{1}{2}(M + Qx).$$

The constants A, C_1 and C_2 are calculated from the boundary conditions at the left end, i.e. at $x = 0$, where $N = 0$, $Y = M$, and $Y' = Q$.

77. Let us separate the bimetallic sheet elementary segment (Fig. 295) having the length ds and the initial curvature of the junction surface $1/\rho_0$ (bimetallic elements are often produced as curvilinear).

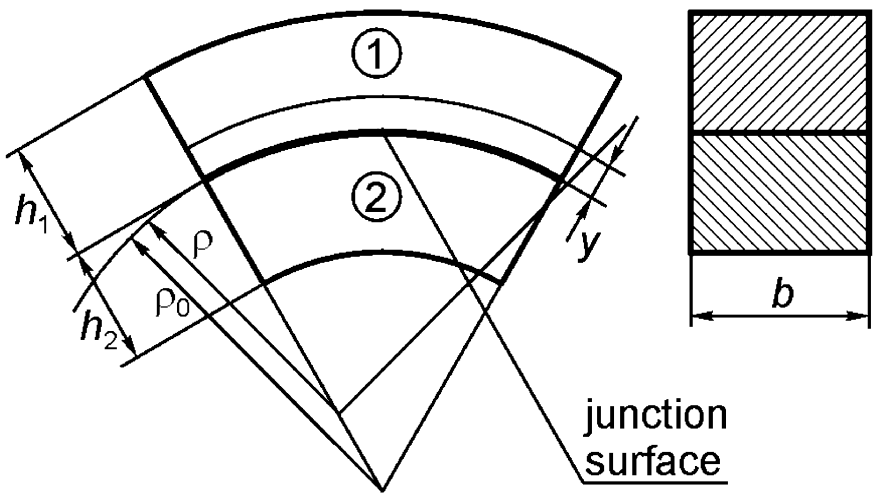

Fig. 295

The relative elongation of the fiber disposed at the distance y from the junction surface is combined of the two quantities: the elongation of the joint and the elongation due to sheet bending

$$y \left(\frac{1}{\rho} - \frac{1}{\rho_0} \right)$$

where $1/\rho$ is the curvature of the sheet after bending. Thus

$$\epsilon = \epsilon_0 + y\left(\frac{1}{\rho} - \frac{1}{\rho_0}\right).$$

Subtracting thermal elongation from this expression and multiplying the obtained difference by the elasticity modulus E we derive the stress acting in the fiber disposed at the distance y from the junction surface. For the first sheet we have

$$\sigma_1 = E_1\left[\epsilon_0 + y\left(\frac{1}{\rho} - \frac{1}{\rho_0}\right) - \alpha_1 t\right] \quad (0 \le y \le h_1),$$

and for the second one :

$$\sigma_2 = E_2\left[\epsilon_0 + y\left(\frac{1}{\rho} - \frac{1}{\rho_0}\right) - \alpha_2 t\right] \quad (-h_2 \le y \le 0);$$

where E_1 and E_2 are the elasticity moduli of the first and the second sheets.

The normal force and the bending moment in the bimetallic element cross-section are equal to zero. Hence

$$\int_0^{h_1} \sigma_1\, b\, dy + \int_{-h_2}^{0} \sigma_2\, b\, dy = 0, \quad \int_0^{h_1} \sigma_1\, b\, y\, dy + \int_{-h_2}^{0} \sigma_2\, b\, y\, dy = 0.$$

Substituting σ_1 and σ_2 and integrating we arrive at

$$\epsilon_0\left(E_1h_1 + E_2h_2\right) - t\left(\alpha_1E_1h_1 + \alpha_2E_2h_2\right) + \frac{1}{2}\left[\frac{1}{\rho} - \frac{1}{\rho_0}\right]\left(E_1h_1^2 - E_2h_2^2\right) = 0,$$

$$\frac{\epsilon_0}{2}\left(E_1h_1^2 - E_2h_2^2\right) - \frac{t}{2}\left(E_1\alpha_1h_1^2 - E_2\alpha_2h_2^2\right) + \frac{1}{3}\left[\frac{1}{\rho} - \frac{1}{\rho_0}\right]\left(E_1h_1^3 + E_2h_2^3\right) = 0.$$

Excluding ϵ_0 from these relations we derive the curvature variation as follows

$$\frac{1}{\rho} - \frac{1}{\rho_0} = \frac{6t\left(\alpha_1 - \alpha_2\right)}{\dfrac{\left(E_1\,h_1^2 - E_2\,h_2^2\right)^2}{E_1\,E_2\,h_1\,h_2\left(h_1 + h_2\right)} + 4\left(h_1 + h_2\right)}.$$

The curvature variation is proportional to the temperature change and to the difference of the thermal expansion factors. The maximal curvature variation value can be obtained as it is seen from the above relation when we select such thicknesses of the component sheets that

$$E_1h_1^2 = E_2h_2^2.$$

Then

$$\frac{1}{\rho} - \frac{1}{\rho_0} = \frac{3}{2}\,t\,\frac{\alpha_1 - \alpha_2}{h_1 + h_2}.$$

78. The problem set specifies the ring cross-section as undeformable. It is well known that any figure displacement in its plane can be presented as some figure point linear displacement having two axial projections and following rotation of the whole figure about this point.

Let us consider any point in the ring section, for example the point O (Fig. 296), disposed at the inner radius a of the rings junction surface. Now the ring section full displacement can be presented as the point O displacements along the symmetry axis, perpendicularly to it and the cross-section rotation by the angle φ about the point O, following each other.

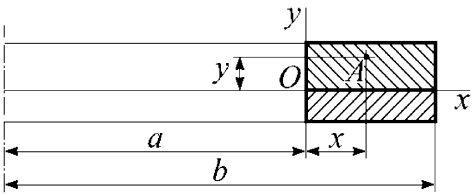

Fig. 296

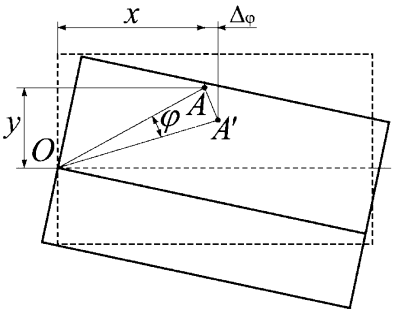

Fig. 297

The point O axial linear displacement corresponds to the ring movement as a solid body and causes no deformations. Therefore we disregard this displacement. The second (radial) component of the point O linear displacement we denote as Δ. Thus the point A radial displacement will be combined of the displacement Δ and the displacement caused by the section rotation about the point O. This second component denoted as Δ_φ is

$$\Delta_\varphi = y\,\varphi.$$

(see Fig. 297, assuming that the angle φ is small). So the point A radial displacement will be

$$\Delta + y\,\varphi,$$

and the circumferential relative elongation

$$\epsilon = \frac{\Delta + y\,\varphi}{a + x}.$$

The hoop stress in the first ring is equal to

$$\sigma_1 = E_1 \left(\frac{\Delta + y\,\varphi}{a + x} - \alpha_1\, t \right) \quad (0 \le y \le h_1),$$

and in the second ring

$$\sigma_2 = E_2 \left(\frac{\Delta + y\,\varphi}{a + x} - \alpha_2\, t \right) \quad (-h_2 \le y \le 0).$$

If we cut the ring by the axial diametrical plane and consider the equilibrium of its half we can easily make sure that the bending moment M and the tensile force N in the ring sections are equal to zero (Fig. 298).

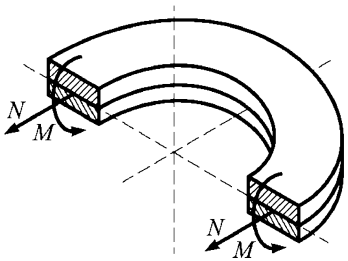

Fig. 298

Therefore

$$N = \int_0^{b-a}\int_0^{h_1} \sigma_1\, dx\, dy + \int_0^{b-a}\int_{-h_2}^{0} \sigma_2\, dx\, dy = 0\,,$$

$$M = \int_0^{b-a}\int_0^{h_1} \sigma_1\, y\, dx\, dy + \int_0^{b-a}\int_{-h_2}^{0} \sigma_2\, y\, dx\, dy = 0\,.$$

Substituting σ_1 and σ_2 in the relations we arrive at

$$E_1\left[\left(h_1\,\Delta + \frac{h_1^2\,\varphi}{2}\right)\ln\frac{b}{a} - \alpha_1\, t\,(b-a)\,h_1\right] + E_2\left[\left(h_2\,\Delta - \frac{h_2^2\,\varphi}{2}\right)\ln\frac{b}{a} - \alpha_2\, t\,(b-a)\,h_2\right] = 0\,,$$

$$E_1\left[\left(\frac{h_1^2}{2}\,\Delta + \frac{h_1^3\,\varphi}{3}\right)\ln\frac{b}{a} - \alpha_1\, t\,(b-a)\,\frac{h_1^2}{2}\right] + E_2\left[\left(-\frac{h_2^2}{2}\,\Delta - \frac{h_2^2\,\varphi}{2}\right)\ln\frac{b}{a} + \alpha_2\, t\,(b-a)\,\frac{h_2^2}{2}\right] = 0\,.$$

Excluding Δ from the above relations we get

$$\varphi = \frac{b-a}{\ln\dfrac{b}{a}}\,\frac{6t\,(\alpha_1-\alpha_2)}{\dfrac{\left(E_1\,h_1^2 - E_2\,h_2^2\right)^2}{E_1\,E_2\,h_1\,h_2\,(h_1+h_2)} + 4\,(h_1+h_2)}\,.$$

As in the previous problem the angle φ has its maximal value if

$$E_1\,h_1^2 = E_2\,h_2^2\,.$$

Then the sought angle is equal to

$$\varphi = \frac{3}{2}\,t\,\frac{b-a}{\ln\dfrac{b}{a}}\,\frac{\alpha_1-\alpha_2}{h_1+h_2}\,.$$

79. The sensor will be inoperative as the bimetallic plate clamped at its ends does not change its curvature under uniform heating.

Certainly, if the plate is simply supported then under uniform heating it would be bent by the circle arc. In the given case the plate is also affected by the moments applied at the ends that are clamped. Under their action the plate will be bent by the circle arc also but in the opposite direction (Fig. 299).

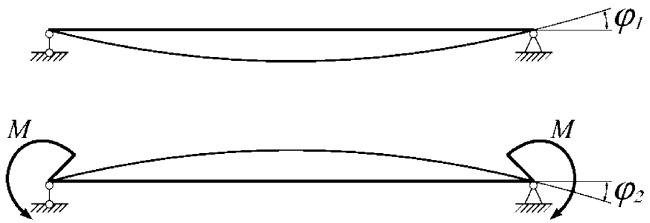

Fig. 299

Imposing the requirement of rotation angles φ_1 and φ_2 equality at the plate ends we inevitably must require the identity of both circle arc curvatures. It means that the resultant rotation angles and displacements of all plate points vanish under the condition $\varphi_1 = \varphi_2$. Therefore the bimetallic plate clamped at its ends will not be bent under uniform heating.

Hence, the system shown in Fig. 74 would correspond to its destination if, for example, the clamped fixation of its ends would be replaced by the pinned one.

80. Let us mentally cut the frame (Fig. 300) and apply the internal moment M_0 and the forces N and Q in the cross-section we have cut.

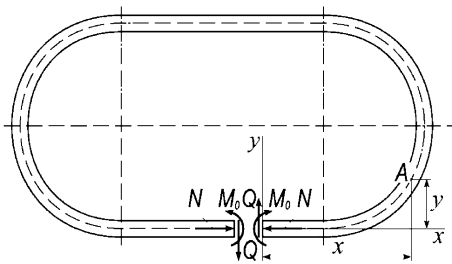

Fig. 300

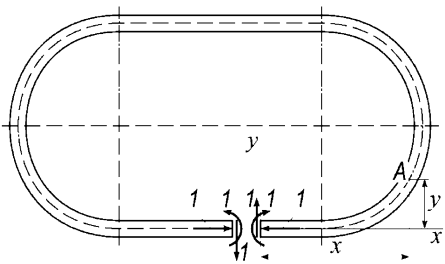

Fig. 301

The bending moment in the section A caused by these loads is

$$M_b = M_0 + Q\,x + N\,y\,.$$

If the frame is cut then its curvature will be changed under heating. As the temperature and cross-section shape do not vary then the curvature change remains constant at all points of the frame contour. But if this is so then the temperature action can be replaced by the action of some equivalent moment M_t applied in the section we have cut.

Now, let us require that the mutual linear and angular displacements of the cross-section caused by the moment M_0, and the forces N and Q would be equal to the same mutual displacements caused by the action of temperature equivalent moment M_t.

The bending moments caused by the unit loads applied along the directions of the sought angular, vertical and horizontal mutual displacements (Fig. 301) will be correspondingly $1\,,\quad x\,,\quad y\,.$
Then we get

$$\int_s (M_0 + Q\,x + N\,y)\;1\;ds = \int_s M_t\,1\;ds\,,$$

$$\int_s (M_0 + Q\,x + N\,y)\;x\;ds = \int_s M_t\,x\,ds\,,$$

$$\int_s (M_0 + Q\,x + N\,y)\;y\;ds = \int_s M_t\,y\,ds\,,$$

or

$$(M_0 - M_t)\int_s ds + Q\int_s x\,ds + N\int_s y\,ds = 0\,,$$

$$(M_0 - M_t)\int_s x\,ds + Q\int_s x^2\,ds + N\int_s x\,y\,ds = 0\,,$$

$$(M_0 - M_t)\int_s y\,ds + Q\int_s x\,y\,ds + N\int_s y^2\,ds = 0\,,$$

from which we find $Q = N = 0,\ M_0 = M_t$.

Therefore the moment M_0 is equal to the equivalent temperature moment M_t. It means that the curvature change caused by the moments M_0 will be identical to the curvature change caused by the temperature. Thus the curvature of the uniformly heated closed bimetallic frame remains unchanged.

81. The plane of the bending moment in the suggested problem coincides with the diagonal AB of the rectangular cross-section (Fig. 302).

We hope that our reader knows that in this case the second diagonal CD of the rectangular cross-section represents the neutral line where the stresses vanish. Of course it is valid for elastic strains only.

Let us pose the natural question, will the neutral line save its position further, i.e. if plastic strains appear? We can answer this question in the affirmative. The strains in a cross-section vary by linear law. They are proportional to the distance from the neutral line. So the strains and therefore the stresses remain unchanged along some strip KL that is parallel to the diagonal CD. But the diagonal AB intersects such a strip exactly at its middle, so the moment of the stresses with respect the axis AB is equal to zero.

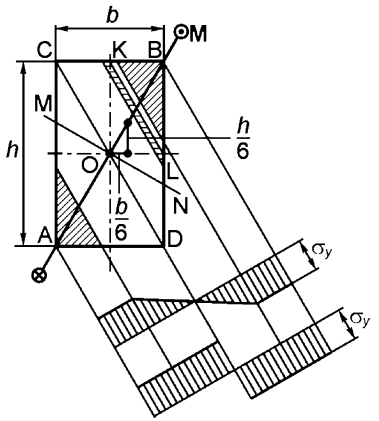

Fig. 302

Thus the assumption of the neutral line position invariance does not contradict the condition that the bending moment remains in the same plane.

Now it is very easy to derive the limit bending moment. The constant tensile stress that is equal to the yield limit in tension σ_y occurs in the limit state in the area of the triangle CBD. Exactly the same but compressive stress occurs in the area of the triangle ACD (Fig. 302).

The sought moment withstands the moment of external forces and should be calculated with respect to the axis MN that is perpendicular to the plane of the external moment action.

It is easy to establish that the moment is

$$M_{\text{lim}} = 2\sigma_y \frac{bh}{2} \sqrt{\left(\frac{h}{6}\right)^2 + \left(\frac{b}{6}\right)^2},$$

or

$$M_{\text{lim}} = \sigma_y \frac{bh}{6} \sqrt{h^2 + b^2}\,.$$

82. Let us denote the current vertical coordinate measured upwards from the cross-section's lower end as y (see Fig. 303). The bending moment is proportional to the section height H, and we shall consider that $M = KH$, where K is the coefficient depending on the cross-section position at the beam. In particular at the beam middle $K = \gamma\, b\, l^2/\,8$, where γ is the specific weight of concrete and l is the beam length.

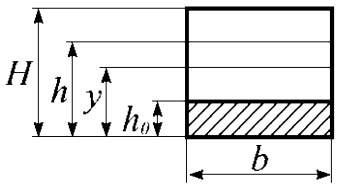

Fig. 303

Let us denote increasing section height as a variable h. When the next in its turn layer Δh is imposed on the beam surface, then the additional compressive stress (negative) caused by the enlarged beam weight arises in the layer disposed at the distance y from the lower end. It is equal to

$$\Delta\sigma = -\frac{12K\Delta h}{bh^3}\left(y - \frac{h}{2}\right),$$

and stress in the layer y under some thickness H of the whole section is determined by the following integral

$$\sigma = -\frac{12K}{b}\int\limits_{y}^{H}\left(\frac{y}{h^3} - \frac{1}{2h^2}\right)dh = -\frac{6K}{bH}\left(1 - \frac{y}{H}\right), \qquad (y > h_0).$$

This is valid for $y > h_0$. In case of $y < h_0$ we should integrate from h_0 to H and add initial stresses that the beam had before the concrete layer superposition, i.e.

$$\sigma = -\frac{12K}{b}\int\limits_{h_0}^{H}\left(\frac{y}{h^3} - \frac{1}{2h^2}\right)dh - \frac{12Kh_0}{bh_0^3}\left(y - \frac{h_0}{2}\right)$$

or

$$\sigma = -\frac{6K}{bH}\left(1 - \frac{y}{H}\right) - \frac{6K}{bh_0}\left(3\frac{y}{h_0} - 2\right), \qquad (y < h_0).$$

If we divide the obtained stresses by the maximal stress arising in the initial state (when section height is h_0), i.e. by $\dfrac{6K}{bh_0}$, then we get

$$\sigma^\star = -\frac{h_0}{H}\left(1 - \frac{y}{H}\right), \qquad (y > h_0),$$

$$\sigma^\star = -\frac{h_0}{H}\left(1 - \frac{y}{H}\right) - 3\frac{y}{h_0} + 2, \qquad (y < h_0).$$

The diagrams of the stresses $\sigma^\star$ along the section height $H = 4h_0$ are shown in Fig. 304.

Thus, the stresses due to the own weight of the beam reinforced in the described manner are greater than in the initial beam, though undoubtedly the increasing of section height improves the general strength.

The additional shrinkage stresses are easily determined independently of the previous problem solution.

As the additional stresses vary along the section height linearly (as the sections remain plane) we can write

$$\sigma = E(A + B\,y + \alpha), \qquad (y > h_0),$$

$$\sigma = E(A + B\,y), \qquad (y < h_0).$$

The coefficients A and B are determined from the conditions that the tensile force and the bending moment caused by the additional stresses are equal to zero, i.e.

$$\int_F \sigma\, b\, dy = 0, \quad \int_F \sigma\, b y\, dy = 0\,,$$

or

$$A\,H + B\,\frac{H^2}{2} = -\alpha\,(H - h_0)\,,$$

$$A\frac{H^2}{2} + B\frac{H^3}{3} = -\alpha\left(\frac{H^2}{2} - \frac{h_0^2}{2}\right),$$

from which we have

$$A = -\alpha\left(1 - \frac{h_0}{H}\right)\left(\frac{3h_0}{H} - 1\right), \quad B = -\frac{6\alpha}{H}\,\frac{h_0}{H}\left(1 - \frac{h_0}{H}\right).$$

The diagram of the additional shrinkage stresses in case of $H = 4\,h_0$ is shown in Fig. 305

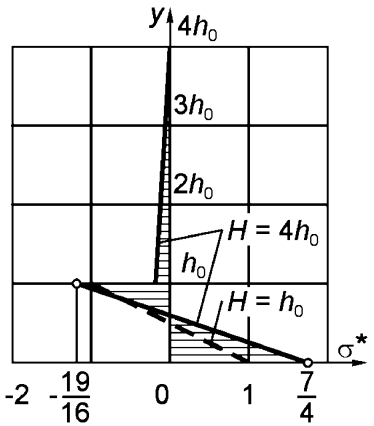

Fig. 304

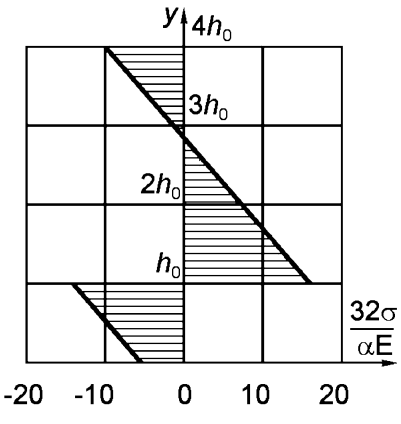

Fig. 305

3. Complex Stress State, Strength Criteria, Anisotropy

83. See the results in Table 2.

Table 2. The hollow cylinder internal cavity variation

Case	Pressure acting on	Diameter d_1	Volume V
Fig.78a	Faces	$\left(1+\frac{\mu}{E}\,p\right)d_1$	$\left(1-p\frac{1-2\mu}{E}\right)V$
Fig.78b	Cylindrical surfaces	$\left(1-\frac{1-\mu}{E}\,p\right)d_1$	$\left(1-2p\frac{1-2\mu}{E}\right)V$
Fig.78c	Whole surface	$\left(1-\frac{1-2\mu}{E}\,p\right)d_1$	$\left(1-3p\frac{1-2\mu}{E}\right)V$

So the internal cavity diameter increases only under the pressure acting on the cylinder faces and decreases in the two other cases. The internal cavity volume decreases in all the cases specified in the problem set.

84. Every plane containing one of the axes x, y or z and equally inclined to another two axes is principal.

Let's take the element represented in Fig. 79 and separate a new elementary parallelepiped as shown in Fig. 306.

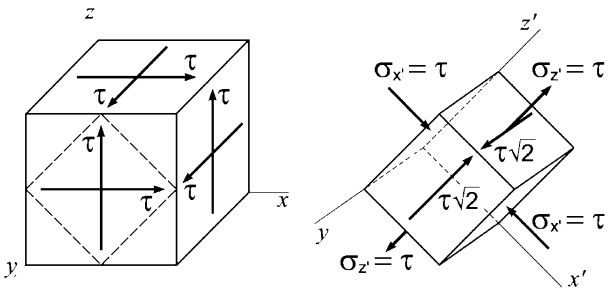

Fig. 306

Axis x' is principal ($\sigma_{x'} = -\tau$). The other two principal stresses can be found according to the relation:

$$\sigma_{pr} = \frac{\sigma_{z'}}{2} \pm \sqrt{\frac{\sigma_{z'}^2}{4} + \tau_{yz'}^2}$$

or

$$\sigma_{pr} = \frac{\tau}{2} \pm \sqrt{\frac{\tau^2}{4} + \left(\tau\sqrt{2}\right)^2}, \quad \sigma' = -\tau, \quad \sigma'' = +2\tau.$$

Thus we obtain

$$\sigma_1 = 2\tau, \quad \sigma_2 = -\tau, \quad \sigma_3 = -\tau.$$

This problem may also be solved by using the general method of principal stresses calculation known from the triaxial stress state theory. Let's write the following determinant:

$$\begin{vmatrix} \sigma_x - \sigma & \tau_{xy} & \tau_{xz} \\ \tau_{yx} & \sigma_y - \sigma & \tau_{yz} \\ \tau_{zx} & \tau_{zy} & \sigma_z - \sigma \end{vmatrix} = 0\,. \tag{1}$$

In our case

$$\sigma_x = \sigma_y = \sigma_z = 0\,, \quad \tau_{xy} = \tau_{xz} = \tau_{yz} = 0\,.$$

That is why

$$\begin{vmatrix} -\sigma & \tau & \tau \\ \tau & -\sigma & \tau \\ \tau & \tau & -\sigma \end{vmatrix} = 0\,,$$

or

$$\sigma^3 - 3\tau^2\sigma - 2\tau^3 = 0\,,$$

and the three roots of this equation are

$$\sigma_1 = 2\tau\,, \quad \sigma_2 = -\tau\,, \quad \sigma_3 = -\tau\,.$$

85. It is necessary to show that in the first case at least one and in the second — two of the principal stresses are equal to zero. For that let's rewrite equation (1) as follows:

$$\sigma^3 - J_1\sigma^2 + J_2\sigma - J_3 = 0\,,$$

where

$$J_1 = \sigma_x + \sigma_y + \sigma_z\,,$$
$$J_2 = \sigma_x\sigma_y + \sigma_y\sigma_z + \sigma_x\sigma_z - \tau_{xy}^2 - \tau_{xz}^2 - \tau_{yz}^2\,,$$
$$J_3 = \begin{vmatrix} \sigma_x & \tau_{xy} & \tau_{xz} \\ \tau_{yx} & \sigma_y & \tau_{yz} \\ \tau_{zx} & \tau_{zy} & \sigma_z \end{vmatrix}$$

are the invariants of a stress state.

In the first case according to the properties of the determinant

$$J_3 = \begin{vmatrix} \sigma_x & \tau_{xy} & \tau_{xz} \\ k\sigma_x & k\tau_{xy} & k\tau_{xz} \\ \tau_{zx} & \tau_{zy} & \sigma_z \end{vmatrix} = 0\,,$$

and one of the cubic equation roots vanishes. In the second case $J_3 = 0$ and $J_2 = 0$ and therefore already two roots of the cubic equation are equal to zero.

Using the above proved we can say at once, for example, that the stress state represented by the tensor

$$\begin{pmatrix} 800 & 200 & 400 \\ 200 & 50 & 100 \\ 400 & 100 & 200 \end{pmatrix}$$

is uniaxial.

86. These stress states are equally dangerous. Actually, the work done by the normal stresses in the first case is equal to the work done by the same stresses in the second case. The same is valid for the shear stresses. Consequently, the internal energy will also be identical for these two cases. Namely this fact is the condition of the two stress states equal danger (equivalence) for any energetic strength theory independently on the type of energy used as strength criterium (the shape distortion energy or the full energy).

87. Let us consider the stress state of the element (Fig. 307) taken from the cylinder at the depth x below the level of the liquid.

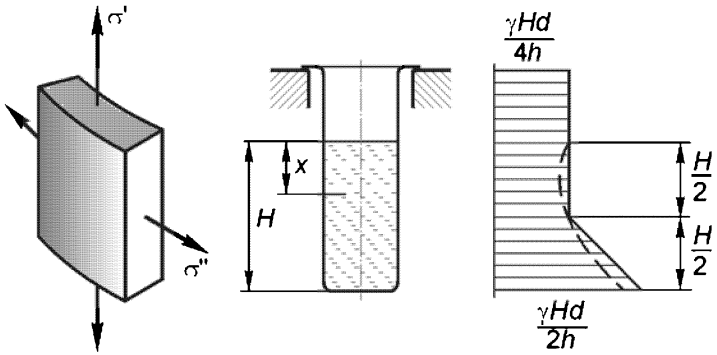

Fig. 307

The stress σ' is constant along the generatrix length and is equal to the liquid weight $\gamma \dfrac{\pi d^2}{4} H$ divided by the cylinder normal cross-section area $\pi D h$

$$\sigma' = \gamma \frac{Hd}{4H} .$$

The hoop stress above the liquid level is $\sigma'' = 0$ and below it equals to

$$\sigma'' = \frac{pd}{2h} = \frac{\gamma x d}{2h} .$$

The equivalent stress according to the strength criterium of maximal shear stresses $\sigma_{eq} = \sigma_1 - \sigma_3$. Consequently, if $\sigma' \geq \sigma''$ then we have $\sigma_{eq} = \sigma' - 0 = \sigma'$. And for $\sigma' \leq \sigma''$ we get $\sigma_{eq} = \sigma'' - 0 = \sigma''$. Thus, for $x \leq H/2$

$$\sigma_{eq} = \sigma' = \frac{\gamma H d}{4h},$$

and in case of $x \geq H/2$

$$\sigma_{eq} = \sigma'' = \frac{\gamma x d}{2h}.$$

The diagram of σ_{eq} is shown in Fig. 307. This diagram inflects at $x = H/2$ which is a consequence of the fact that in this point the planes corresponding to the principal stresses σ_1 and σ_2 change their places. The diagram of σ_{eq} obtained by the energetic theory of strength is shown in Fig. 307 by dashed line.

88. Let us consider the stress state of the cylinder points disposed near its upper (A) and lower (B) generatrices (Fig. 308), where σ'_p and σ''_p are the stresses caused by the pressure p, and σ'_M is the bending stress.

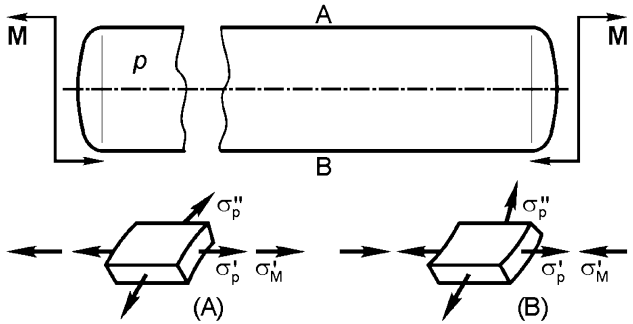

Fig. 308

It is easy to establish that

$$\sigma'_p = \frac{pd}{4h}, \quad \sigma''_p = \frac{pd}{2h}, \quad \sigma'_M = \frac{4M}{\pi d^2 h}, \tag{1}$$

and since $2\sigma'_p = \sigma''_p$ therefore if

$$|\sigma'_M| \leq \sigma'_p$$

then we have the following condition for both points A and B:

$$\sigma_{eq} = \sigma_1 - \sigma_3 = \sigma''_p - 0 = \sigma''_p$$

And if $|\sigma'_M| > \sigma'_p$ then at point A

$$\sigma_{eq} = \sigma_1 - \sigma_3 = \left(\sigma'_p + \sigma'_M\right) - 0 = \sigma'_p + \sigma'_M,$$

but at point B

$$\sigma_{eq} = \sigma_1 - \sigma_3 = \sigma''_p + \left(\sigma'_M - \sigma'_p\right) = \sigma'_p + \sigma'_M$$

Consequently, in all cases points A and B are equally dangerous. The diagrams of σ_{eq} and σ'_M are shown in Fig. 309.

Values of σ'_p, σ''_p and σ'_M are determined by expression (1). For $|\sigma'_M| < \sigma'_p$ the strength safety factor for the system does not depend upon the value of the applied moment M. This conclusion is the consequence of using the strength theory of maximum shear stresses which disregards the contribution of σ_2, i.e. of the intermediate principal stress. According to the energetic strength theory σ_{eq} depends upon the moment M. This dependence is shown in Fig. 309 as the diagram plotted by the dashed line.

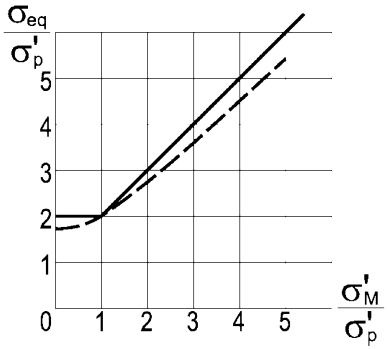

Fig. 309

89. The solution presented in the set of this problem is not correct because the stresses σ_1 and σ_2 are calculated there with the mistakes.

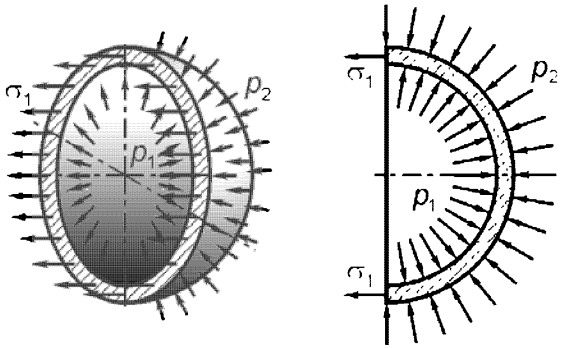

Fig. 310

Let's consider the equilibrium condition of the sphere part (Fig. 310):

$$p_1\,\pi\left(R-\frac{h}{2}\right)^2 - p_2\,\pi\left(R+\frac{h}{2}\right)^2 = \sigma_1\,2\pi Rh.$$

In ordinary conditions the quantity $h/2$ in brackets can be neglected in comparison with R. And here it cannot be done because the values of p_1 and p_2 are large but the difference between them is small. That is why

$$(p_1{-}p_2)\,R^2 - (p_1+p_2)\,Rh + (p_1-p_2)\,\frac{h^2}{4} = \sigma_1\,2Rh\,.$$

The third member in the left part of the equation can be neglected.

If p_1 and p_2 differed considerably then we could neglect the second member also but now it can't be done. Thus

$$\sigma_1 = \sigma_2 = \frac{(p_1 - p_2)\, R}{2h} - \frac{p_1 + p_2}{2}, \quad \sigma_3 = -p_1,$$

$$\sigma_{eq} = \frac{p_1 - p_2}{2h} R - \frac{p_1 + p_2}{2} + p_1 = 51 \text{ MPa},$$

$$n_y = \frac{\sigma_y}{\sigma_{eq}} = \frac{300}{51} = 5.88\,.$$

90. Let's denote the pressure acting on the cylinder and tube contact surface as p_1, and derive principal stresses for both details.

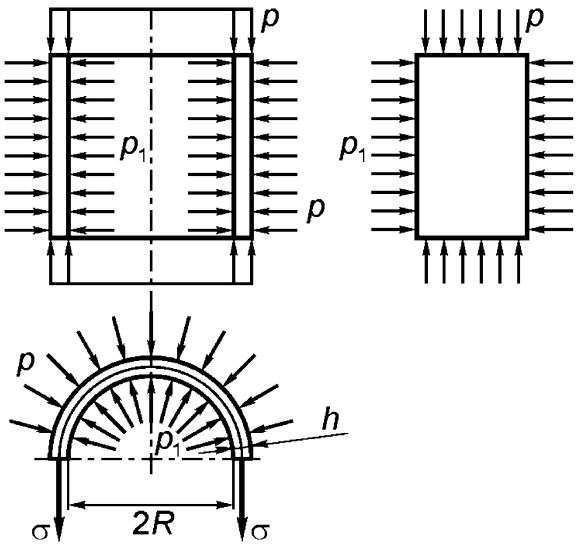

Fig. 311

From the equilibrium conditions for the tube (Fig. 311) we get

$$\sigma = p_1 \frac{R}{h} - p \frac{R + h}{h}.$$

Near the internal surface another two principal stresses will be $-p$ and $-p_1$, thus the hoop relative elongation of the tube will be

$$\varepsilon_t = \frac{1}{E_t} \left[\sigma - \mu_t \left(-p - p_1\right)\right],$$

where E_t is the elasticity modulus and μ_t is Poisson's ratio of the tube material. Substituting σ we arrive at

$$\varepsilon_t = \frac{1}{E_t}\left[\frac{p_1 R}{h} - \frac{p\,(R+h)}{h} + \mu_t\,(p+p_1)\right].$$

For the cylinder we have

$$\varepsilon_c = \frac{1}{E_c}\left[-p_1 - \mu_c\,(-p-p_1)\right].$$

But $\varepsilon_t = \varepsilon_c$; from this condition we derive p_1 :

$$p_1 = p\frac{\dfrac{1}{E_t}\left(\dfrac{R}{h}+1-\mu_t\right)+\dfrac{\mu_c}{E_c}}{\dfrac{1}{E_t}\left(\dfrac{R}{h}+\mu_t\right)+\dfrac{1-\mu_c}{E_c}}.$$

Excluding p_1 from the expression for σ we obtain

$$\sigma = p\frac{R}{h}\frac{\dfrac{1-2\mu_t}{E_t}-\dfrac{1-2\mu_c}{E_c}}{\dfrac{1}{E_t}\left(\dfrac{R}{h}+\mu_t\right)+\dfrac{1-\mu_c}{E_c}} - p\,.$$

Suppose that

$$\frac{1-2\mu_t}{E_t} > \frac{1-2\mu_c}{E_c}.$$

Then it is easy to show that $p_1 > p$ and $\sigma > -p$. Consequently,

$$\sigma_1 = \sigma\,,$$
$$\sigma_2 = -p\,, \quad \sigma_{eq} = \sigma_1 - \sigma_3 = \sigma + p_1\,,$$
$$\sigma_3 = -p_1\,,$$

from which

$$\sigma_{eq} = p\left(\frac{R}{h}+1\right)\frac{\dfrac{1-2\mu_t}{E_t}-\dfrac{1-2\mu_c}{E_c}}{\dfrac{1}{E_t}\left(\dfrac{R}{h}+\mu_t\right)+\dfrac{1-\mu_c}{E_c}}.$$

As R/h is significantly greater than unit, then

$$\sigma_{eq} = pE_t\left(\frac{1-2\mu_t}{E_t}-\frac{1-2\mu_c}{E_c}\right),$$

and we can write the following condition under which the plastic deformations appear in the tube

$$pE_t\left(\frac{1-2\mu_t}{E_t}-\frac{1-2\mu_c}{E_c}\right) = \sigma_y\,.$$

If $\dfrac{1-2\mu_t}{E_t} < \dfrac{1-2\mu_c}{E_c}$ then we shall have $p_1 < p$. In this case the contact between the tube and the cylinder will be absent and both bodies will be deformed independently.

Let's solve the numerical example in order to estimate the pressure p value. For the steel cylinder:

$$E_c = 200 \text{ GPa}, \quad \mu_c = 0.3\,.$$

For the organic glass tube we specify:

$$E_t = 3 \text{ GPa}, \quad \mu_t = 0.35\,, \quad \sigma_y = 75 \text{ MPa}.$$

The calculation gives

$$p = \frac{\sigma_y}{1 - 2\mu_t - \dfrac{E_t}{E_c}(1 - 2\mu_c)} = 255 \text{ MPa}.$$

This number is approximate (guiding) because the solution does not consider the changes in the organic glass properties under the pressure and the value of μ_t is given not exactly.

91. The ends of the curvilinear wire will be pushed out by the pressure and the wire will be straightening.

If the wire is held in its curvilinear state, then the buoyancy forces will be equal to the product of the pressure p and the non-compensated area A (see Fig. 312 where AA is the cross-section having maximal deflection from the axis of the holes). It is obvious that the area A cannot be greater than the wire cross-section area.

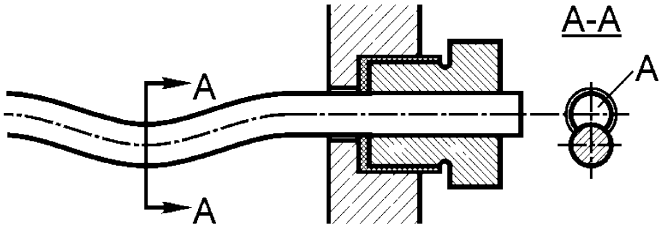

Fig. 312

If the wire is absolutely flexible then it will be straightened completely and the axial tension in it will vanish as $A = 0$. The stress state for this case is shown in Fig. 313.

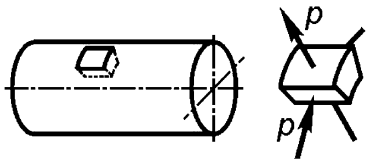

Fig. 313

If the wire has some bending rigidity then it will not be straightened completely and it will undergo some tension pA. The bending stresses will occur in the wire besides this tension.

92. The described experiment setting does not exclude the influence of volume variation. The relative variation of the vessel's internal cavity volume is equal to the relative variation of the vessel's material volume. That is why we need to add the vessel's material compressibility coefficient to the compressibility coefficient found by the specified method in order to define the proper value of the compressibility coefficient.

The relative volume variation measured by the mercury D meniscus is equal to

$$\Delta V = \Delta V_C - \Delta V_A\,,$$

where ΔV_c is the liquid C volume variation, and ΔV_A is the vessel's internal cavity volume variation. Thus:

$$\Delta V_C = \beta_C V p, \quad \Delta V_A = \beta_A V p,$$

$$\Delta V = pV\left(\beta_C - \beta_A\right), \quad \beta_C = \frac{\Delta V}{pV} + \beta_A\,,$$

β_C is the sought liquid compressibility coefficient, β_A is the vessel's material compressibility coefficient, and V is the vessel's internal cavity volume.

That is why the vessel's material volume variation can be neglected only in the case if $\beta_A \ll \beta_C$.

If the vessel for example is made of glass, then

$$\beta_A = 0.0255 \text{ GPa}^{-1}.$$

Compressibility coefficients for liquids vary within very wide limits and have the following values shown in Table 3.

Table 3. Compressibility coefficient for liquids

Liquid	Compressibility coefficient
Mercury	0.039 GPa^{-1}
Water	0.51 GPa^{-1}
Spirit	0.77 GPa^{-1}
Ether	1.45 GPa^{-1}

Hence the amendment β_A is of great importance for liquids having low compressibility.

93. The second rod can bear the greater load.

Really, the disruption in the first case will be preceded by the neck forming and the rupture will take place under the cross-section area significantly less than the original one. In the second case the neck will not or almost will not form because the thick main parts of the rod will prevent shear in the planes inclined to the rod's axis within the region weakened by the recess. The disruption will occur without narrowing of the cross-section.

If the specimen's material is not plastic but fragile then the first specimen would be not weaker than the second one and for some materials, most sensitive to local stresses, it would be even stronger.

94. The pure shear will be homogeneous, i.e. such that the stresses remain constant in all points of a body if we apply the following techniques:

1) The torsion of the straight thin tube (not necessarily circular) with constant thickness of walls (Fig. 314a).

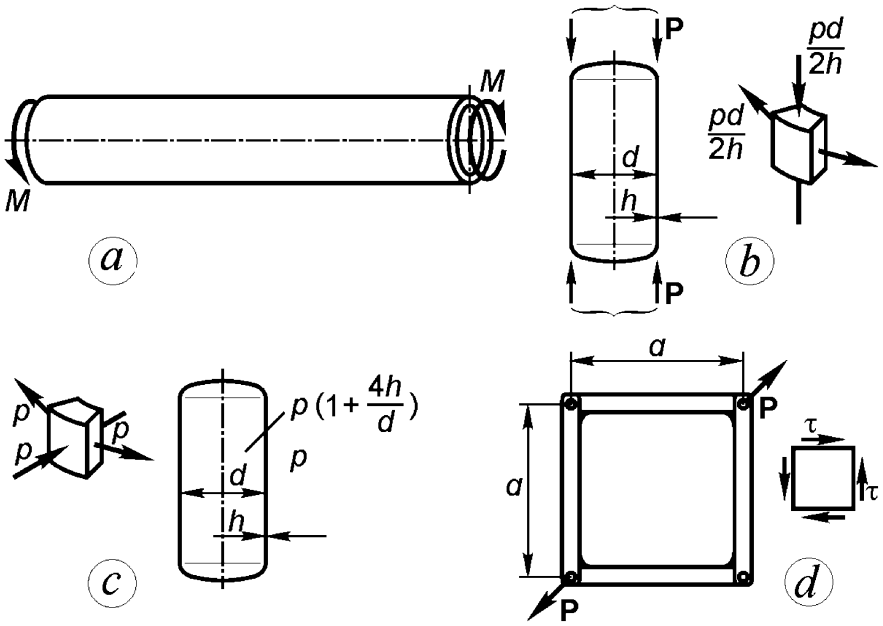

Fig. 314

2) The simultaneous loading of the thin-walled cylindrical vessel by the internal pressure p and the axial compressive force $P = 0.75\,p\pi d^2$. In this case the axial compressive stresses will be equal to the hoop tensile ones for all points sufficiently distant from the bottoms (Fig. 314b).

3) The simultaneous loading of the thin-walled cylindrical vessel by the external pressure p and internal pressure $p\left(1+\dfrac{4h}{d}\right)$ (Fig. 314c). Walls of this cylinder will be compressed in normal direction to the middle surface by stress p and with the same stress tensed in circular direction. In axial direction the cylinder is not tensed.

4) The stretching of the hinged rod rectangle with the plate fixed in it by the diagonal force P. If the rods of the rectangle are comparatively rigid then tangent stresses in horizontal and vertical plate cross-sections are

$$\tau_h = \frac{P_h}{ah} = \frac{P}{h\sqrt{a^2+b^2}} = \frac{P_V}{bh} = \tau_V = \tau\,; \quad \text{for the square } \tau = \frac{P}{a\,h\,\sqrt{2}}\,,$$

where P_h and P_V are the force P horizontal and vertical components, a and b are the rectangle base and height, h is the plate thickness (Fig. 314d).

The stress state in the boundary regions under real conditions will be slightly different from the pure shear in all the cases given above.

The pure shear will be nonhomogeneous, i.e. such that the values of stresses in all points of a body are not the same, for example, under torsion of the prismatic beam with arbitrary cross-section shape or when a sufficiently thick tube is loaded by the internal pressure p (Fig. 315).

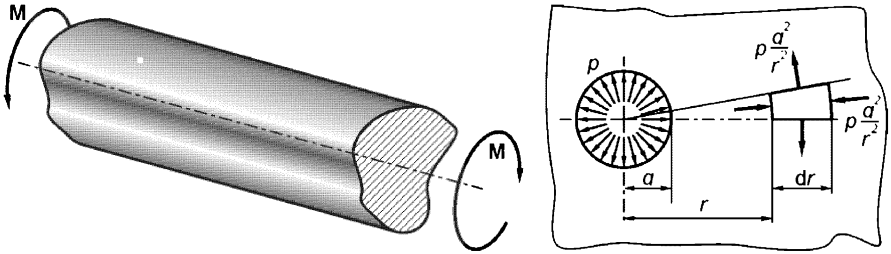

Fig. 315

95. The only one method of creating the all-round homogeneous tension known at the present time is the following:

The previously cooled solid homogeneous ball is quickly heated. The stress state indicated above will occur in the ball center. Unfortunately this method is not suitable for investigation of material properties under this stress state, for example, for determining the so-called rupture characteristic.

All-round (but not homogeneous) tension occurs in the central part of the cylindrical specimen with the ring recess under its tension (Fig. 316)[1].

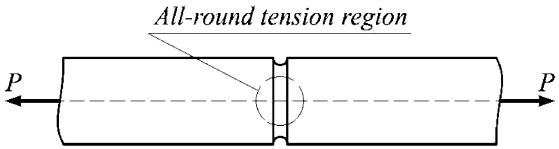

Fig. 316

96. The easiest way to explain this phenomenon is to use the strength theory.

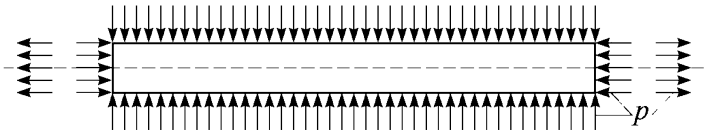

Fig. 317

Let's add and subtract axial forces pA (A is the specimen cross-section area) as shown in Fig. 317. Then the external load acting on the rod is

[1] The radius of the recess profile is supposed to be of the same order as the specimen diameter.

presented as a combination of all-round compression and axial tension. According to the theory of maximum shear stresses as well as to the energetic theory, the all-round pressure has no influence on plastic deformation onset. And the axial tension causes rupture with forming of the neck.

The phenomenon can be explained also from the positions of equilibrium state stability.

If some cause provokes local narrowing of the rod then the tensile force equal to the product of the pressure on the areas difference $A_1 - A_2$ appears in the cross-section of the least area. Here A_1 is the rod cross-section area in the zone sufficiently distant from local narrowing; A_2 is the least area of rod cross-section in the place of narrowing. The occurrence of this tensile force leads to further development of neck, growth of the tensile force and the following rupture.

97. The consideration stated in the problem set can not serve as foundation for doubts in the solution correctness.

The tension diagram shown in Fig. 91a was obtained for the uniaxial stress state. But in the zone of recess the stress state is triaxial, excluding the points laying on the surface. The hoop and the radial stresses here are tensile ones. That's why the axial stress here reaches values greater than σ_y.

98. It will be the points A and B (Fig. 318) near the hole contour.

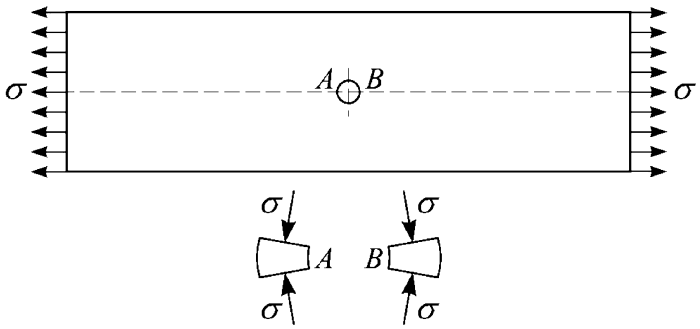

Fig. 318

99. Using the combination of the foregoing data for local stresses caused by the forces and the moments separately for solving the problem will not lead to positive result, and here we have to apply the following technique:

First of all let us consider the stress state of the cylinder points distant from the hole (rectangle $abdc$, Fig. 319a).

Obviously $\tau = \dfrac{2M}{\pi d^2 h}$, $\sigma = \dfrac{P}{\pi d h}$.

The principal stresses σ_1 and σ_3 can be found according to the formula

$$\sigma_{1,3} = \frac{\sigma}{2} \pm \frac{1}{2}\sqrt{\sigma^2 + 4\tau^2}$$

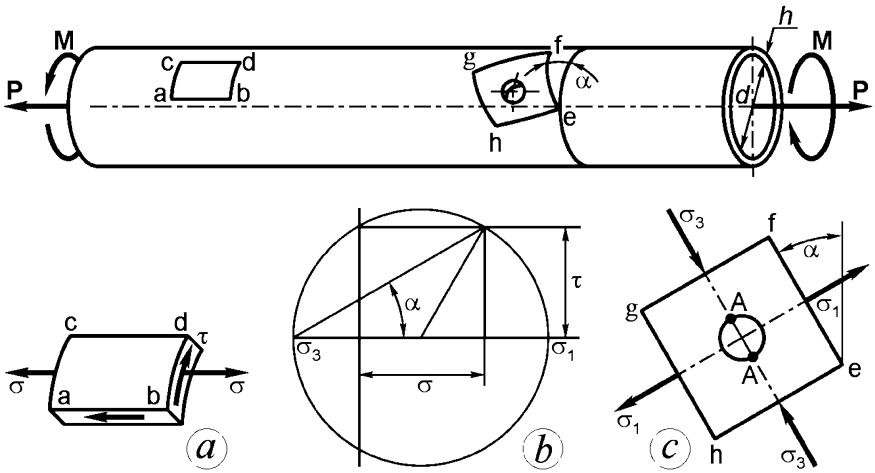

Fig. 319

The maximum stress σ_1 acts in the plane which is inclined to the normal circle arc at the angle α. According to the plane stress properties (see Fig. 319b) this angle can be found from the correlation $\tan 2\alpha = \dfrac{2\tau}{\sigma} = \dfrac{4M}{Pd}$.

Now let's isolate by the principal planes the tube element $efgh$ containing the considered hole and the local stresses zone subjacent to it (Fig. 319c). If the plate[1] with hole is loaded in such a manner then according to reference data we have $\sigma_{\max} = 3\sigma' - \sigma''$, where σ' is the largest and σ'' the smallest of the considered stresses. In the given case

$$\sigma' = \sigma_1, \quad \sigma'' = \sigma_3, \quad \sigma_{\max} = \sigma + 2\sqrt{\sigma^2 + 4\tau^2}$$

This stress occurs near the hole contour at the ends of the diameter orientated along the line of σ_3 action (points A , Fig. 319c).

100. This problem takes place among the simplest problems of the small plastic deformations theory. For its solution it is necessary first of all to reconstruct the diagram $\sigma = f(\varepsilon)$ into the diagram $\tau = \varphi(\gamma)$.

The plasticity theory ascertains that the stresses intensity

$$\sigma_i = \frac{1}{\sqrt{2}}\sqrt{(\sigma_2 - \sigma_3)^2 + (\sigma_3 - \sigma_1)^2 + (\sigma_1 - \sigma_2)^2}$$

and the deformations intensity

$$\varepsilon_i = \frac{\sqrt{2}}{3}\sqrt{(\varepsilon_2 - \varepsilon_3)^2 + (\varepsilon_3 - \varepsilon_1)^2 + (\varepsilon_1 - \varepsilon_2)^2}$$

for the given material are related through the definite functional dependence

[1] Cylindrical shell in the zone of hole can be referred as plate if $\rho^2/\sqrt{Rh} < 0.1$ where ρ is the hole radius, R is radius of the cylinder, and h – its thickness. See Lurie A.I. [15].

$$\sigma_i = \Phi(\varepsilon_i) \tag{1}$$

which is invariable for all stress states.

In the particular case of tension we have

$$\sigma_1 = \sigma, \quad \sigma_2 = \sigma_3 = 0, \quad \sigma_i = \sigma,$$

$$\varepsilon_1 = \varepsilon, \quad \varepsilon_2 = \varepsilon_3 = \mu\varepsilon, \quad \varepsilon_i = \frac{2}{3}(1+\mu)\varepsilon.$$

If we accept $\mu = 0.5$ then $\varepsilon_i = \varepsilon$.

For torsion

$$\sigma_1 = \tau, \quad \sigma_2 = 0, \quad \sigma_3 = -\tau, \quad \sigma_i = \sqrt{3}\tau,$$

$$\varepsilon_1 = \frac{\gamma}{2}, \quad \varepsilon_2 = 0, \quad \varepsilon_3 = -\frac{\gamma}{2}, \quad \varepsilon_i = \frac{\gamma}{\sqrt{3}},$$

But according to expression (1)

$$\sigma = \Phi(\varepsilon), \quad \tau\sqrt{3} = \Phi\left(\frac{\gamma}{\sqrt{3}}\right).$$

The first of these equations is the equation of the material tension diagram. Consequently, the diagram reconstruction is made by simple replacement of σ with $\tau\sqrt{3}$ and of ε with $\gamma/\sqrt{3}$.

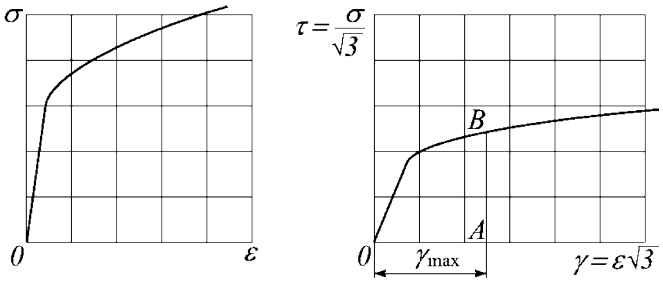

Fig. 320

An example of such a reconstruction is given in Fig. 320.

The shear angle γ at the distance ρ from the beam axis will be:

$$\gamma = \rho\theta, \quad \gamma_{\max} = \frac{d}{2}\theta, \tag{2}$$

where d is the cross-sectional diameter. The torsion moment is equal to

$$M = 2\pi \int_0^{d/2} \tau\rho^2 d\rho;$$

but as the distance $\rho = \dfrac{d}{2}\dfrac{\gamma}{\gamma_{\max}}$, then

$$M = \frac{\pi d^3}{4\gamma_{\max}^3} \int_0^{\gamma_{\max}} \tau\gamma^2 d\gamma. \tag{3}$$

The integral at the right side of this expression is the inertia moment of the curvilinear triangle OAB with respect to the ordinate axis (Fig. 320).

Thus we can determine the necessary dependence in the following way: Assigning the value of $\gamma_{\max}$ we calculate the inertia moment of the OAB triangle. Then according to the formulas (2) and (3) we determine θ and M. The sought dependence can be constructed by repeating this operation for the set of several $\gamma_{\max}$ values.

101. Let us consider the wooden cube (Fig. 321). The axis z is directed along the fibres, the axis x is normal to the annual growth layers and the axis y tangentially to them. The coordinate planes coincide with the planes of elastic symmetry.

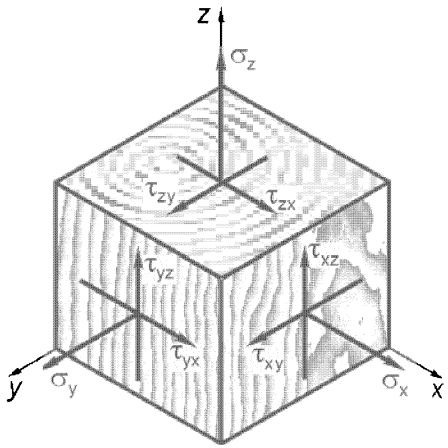

Fig. 321

Relative elongation in the axis z direction will depend linearly on the stresses σ_x, σ_y and σ_z, i.e.

$$\varepsilon_x = C_{11}\,\sigma_x + C_{12}\,\sigma_y + C_{13}\,\sigma_z\,,$$

where C_{11}, C_{12}, C_{13} are elastic constants.

Analogically we can write

$$\varepsilon_y = C_{21}\,\sigma_x + C_{22}\,\sigma_y + C_{23}\,\sigma_z\,,$$

$$\varepsilon_z = C_{31}\,\sigma_x + C_{32}\,\sigma_y + C_{33}\,\sigma_z\,.$$

The shear angles are proportional to the corresponding tangential stresses:

$$\gamma_{yz} = C_{44}\,\tau_{yz}\,, \quad \gamma_{zx} = C_{55}\,\tau_{zx}, \quad \gamma_{xy} = C_{66}\,\tau_{xy}\,.$$

It is easy to establish that according to the displacements reciprocity principle $C_{12} = C_{21}, C_{13} = C_{31}, C_{23} = C_{32}$. Thus we obtain nine elastic constants: C_{11}, C_{12}, C_{13}, C_{22}, C_{23}, C_{33}, C_{44}, C_{55}, C_{66}.

It can be shown that these constants are independent [1].

The medium that possesses anisotropic properties of such type is called *orthotropic*. Compliance coefficients C_{ij} seem unusual. That is the reason why in the mechanics of composites it is accepted to use ordinary notation for elastic constants E, μ, G, but supply them with the corresponding indices. These coefficients for the orthotropic medium given in matrix form are represented below:

$$\left\| \begin{array}{cccccc} \frac{1}{E_1} & -\frac{\mu_{21}}{E_2} & -\frac{\mu_{31}}{E_3} & 0 & 0 & 0 \\ -\frac{\mu_{12}}{E_1} & \frac{1}{E_2} & -\frac{\mu_{32}}{E_3} & 0 & 0 & 0 \\ -\frac{\mu_{13}}{E_1} & -\frac{\mu_{23}}{E_2} & \frac{1}{E_3} & 0 & 0 & 0 \\ 0 & 0 & 0 & \frac{1}{G_{23}} & 0 & 0 \\ 0 & 0 & 0 & 0 & \frac{1}{G_{31}} & 0 \\ 0 & 0 & 0 & 0 & 0 & \frac{1}{G_{12}} \end{array} \right\|$$

Here E_1, E_2, E_3 are the elasticity moduli corresponding to three the axes of anisotropy. Poisson coefficients μ are supplied with two indices. The first one corresponds to the axis along which the specimen is tensed by the force, and the second one to that axis along which the narrowing is measured. Indices of the shear modulus G correspond to the two axes laying in the plane of shear. The positions of these indexes can be assigned at random. The indices of μ cannot be treated in such a manner.

102. Using the matrix given in the previous problem solution let us write Hook's law relationships for the flat anisotropic specimen tensed along the axes 1 and 2 :

$$\varepsilon_1 = \frac{1}{E_1}\sigma_1 - \frac{\mu_{21}}{E_2}\sigma_2 \tag{1}$$

$$\varepsilon_2 = -\frac{\mu_{12}}{E_1}\sigma_1 + \frac{\sigma_2}{E_2}$$

Solving it with respect to stresses, we get:

$$\sigma_1 = \frac{E_1}{1 - \mu_{12}\,\mu_{21}}\left(\varepsilon_1 + \mu_{21}\varepsilon_2\right), \tag{2}$$

$$\sigma_2 = \frac{E_2}{1 - \mu_{12}\,\mu_{21}}\left(\varepsilon_2 + \mu_{12}\varepsilon_1\right).$$

If the strains ε_1 and ε_2 are simultaneously positive then the stresses must be positive also. Consequently

$$\mu_{12}\,\mu_{21} < 1\,.$$

According to the work reciprocity principle the matrix of the elastic coefficients must be symmetric and therefore

$$\mu_{21}/E_2 = \mu_{12}/E_1 .$$

If we exclude μ_{12} from the last formula then we obtain $\mu_{21} < \sqrt{E_2/E_1}$ and correspondingly we get $\mu_{12} < \sqrt{E_1/E_2}$.

As the experiments gave $E_2/E_1 = 1/16$ then Poisson coefficient μ_{21} has to be less than 0.25, but it occurred equal to 0.32. This fact substantiates the supposition about the error made during the experiment or during the following calculations.

103. The strip's deflection ratio for plywood $f_1/f_2 \neq E_{2t}/E_{1t}$ in the general case, because plywood bending rigidity depends not only upon thickness and orientation of layers, but also upon their distance from the middle plane.

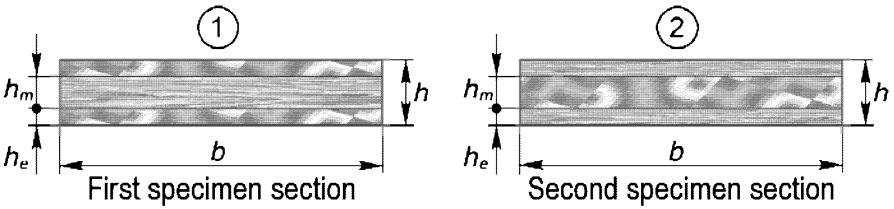

Fig. 322

Let us take the three-layer plywood as the simplest example (Fig. 322). Then we denote the thickness of the external layers as h_e, and the thickness of the middle layer as h_m. Elasticity moduli of wood across and along its fibers are denoted as E' and E'' correspondingly.

Now let's calculate E_{1t} and E_{2t}. For the first specimen under tension by force P we have

$$\sigma' b\, h_m + 2\sigma'' b\, h_e = P ,$$
$$\varepsilon b\,(E' h_m + 2E'' h_e) = P .$$

But as $\sigma = \varepsilon E_{1t} = \dfrac{P}{bh}$ then the first strip modulus

$$E_{1t} = \frac{E' h_m + 2E'' h_e}{h} . \tag{1}$$

By transposition of E' and E'' we obtain the second strip modulus

$$E_{2t} = \frac{E'' h_m + 2E' h_e}{h} . \tag{2}$$

Now let's find the reduced elasticity moduli under bending E_{1b} and E_{2b}. For the first specimen under its bending by a moment M we have

$$2b \int_0^{h_m/2} \sigma' z\, dz + 2b \int_{h_m/2}^{h_m/2+h_e} \sigma'' z\, dz = M ,$$

where z is the current distance from the neutral axis,

$$\sigma' = E' \frac{z}{\rho}, \quad \sigma'' = E'' \frac{z}{\rho}.$$

That is why

$$2b\frac{E'}{\rho} \int_0^{h_m/2} z^2 dz + 2b\frac{E''}{\rho} \int_{h_m/2}^{h_m/2+h_e} z^2 dz = M,$$

or after integration

$$\frac{2}{3}\frac{b}{\rho}\left\{E'\frac{h_m^3}{8} + E''\left[\left(\frac{h_m}{2}+h_e\right)^3 - \left(\frac{h_m}{2}\right)^3\right]\right\} = M.$$

But as it is known

$$E_{1b}\frac{bh^3}{12}\frac{1}{\rho} = M,$$

from which

$$E_{1b} = (E' - E'')\left(\frac{h_m}{h}\right)^3 + E''. \tag{3}$$

By transposition of E' and E'' we obtain

$$E_{2b} = (E'' - E')\left(\frac{h_m}{h}\right)^3 + E'. \tag{4}$$

It is easy to see from expressions (1)-(4) obtained above that in the general case

$$\frac{E_{1t}}{E_{2t}} \neq \frac{E_{1b}}{E_{2b}}.$$

If we accept for example that $h_m = \frac{h}{2}$, and $h_e = \frac{h}{4}$, then

$$\frac{E_{1t}}{E_{2t}} = 1, \quad \frac{E_{1b}}{E_{2b}} = \frac{E' + 7E''}{7E' + E''}.$$

104. Tension along the axes 1 and 2 causes no shear. That is why the deformations ε_1, ε_2 caused by the stresses σ_1 and σ_2 may be considered independently, and the shear γ caused by the stress τ may be treated separately.

Let's consider an elementary cell shown in Fig. 323. The forces P_1 and P_2 are expressed through the conditional stresses σ_1 and σ_2. Let us accept two diameters of wire $2d$ as the "thickness" of the net. The netting has such "thickness" at the lay location. Other values taken into calculation are the netting segment lengths along the axes 1 and 2 falling at one force, that is $\frac{b}{2}\cos\alpha$ and $\frac{a}{2} + \frac{b}{2}\sin\alpha$. As a result we have

$$P_1 = \sigma_1\, b\, d\cos\alpha, \quad P_2 = \sigma_2\,(a + b\sin\alpha)\, d.$$

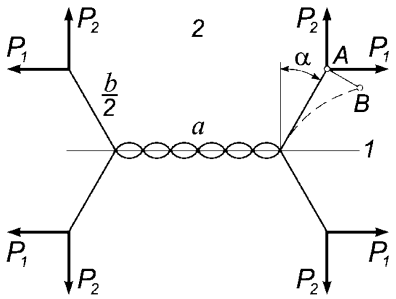

Fig. 323

Forces P_1 and P_2 at every element's "spur" end produce transverse force $Q = P_1 \cos\alpha - P_2 \sin\alpha$, which gives bending displacement AB (Fig. 323):

$$AB = \frac{1}{3}\frac{Q(b/2)^3}{EJ}.$$

This allows us to find the element's relative elongations along the axes 1 and 2 :

$$\varepsilon_1 = \frac{Qb^3}{12EJ}\,\frac{\cos\alpha}{a + b\sin\alpha}, \quad \varepsilon_2 = -\frac{Qb^3}{12EJ}\,\frac{\sin\alpha}{b\cos\alpha}.$$

At first we exclude Q and then express P_1 and P_2 through the conditional stresses σ_1 and σ_2 :

$$\varepsilon_1 = \sigma_1 \frac{b^3 d}{12EJ}\,\frac{b\cos^3\alpha}{a + b\sin\alpha} - \sigma_2 \frac{b^3 d}{12EJ}\sin\alpha\cos\alpha,$$

$$\varepsilon_2 = -\sigma_1 \frac{b^3 d}{12EJ}\sin\alpha\cos\alpha + \sigma_2 \frac{b^2 d}{12EJ}\,\frac{a + b\sin\alpha}{b}\,\frac{\sin^2\alpha}{\cos\alpha}$$

Comparing the structure of these relations with the expressions (1) of problem 102, it is easy to establish that

$$E_1 = \frac{12EJ}{b^3 d}\,\frac{\frac{a}{b} + \sin\alpha}{\cos^3\alpha}, \quad E_2 = \frac{12EJ}{b^3 d}\,\frac{\cos\alpha}{\left(\frac{a}{b} + \sin\alpha\right)\sin^2\alpha},$$

$$\mu_{21} = \frac{\cos^2\alpha}{\left(\frac{a}{b} + \sin\alpha\right)\sin\alpha}, \quad \mu_{12} = \frac{\sin\alpha}{\cos^2\alpha}\left(\frac{a}{b} + \sin\alpha\right).$$

There is something obscure in this answer, at first glance. The product $\mu_{12}\,\mu_{21}$ is equal to one. And if we return to the solution of problem 102, then we shall see from equation (2) that the stresses σ_1 and σ_2 become infinite under arbitrary relationships between ε_1 and ε_2. It is the consequence of the netting schematization incompleteness. The bending of the wire in a cell was taken into account but the displacements caused by wire tension were ignored. This is the reason of the arising discrepancy which is rather typical for the nettings. It can be eliminated, of course, if necessary. But now we shall not do these cumbersome calculations.

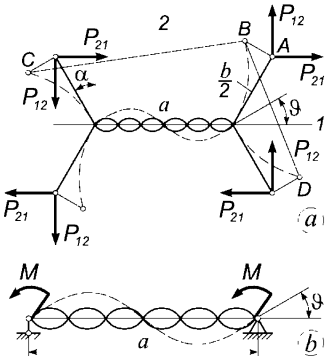

Fig 324

Let us turn to determining the reduced shear modulus, ignoring wire tension deformations as before. For that we shall again consider an elementary cell (Fig 324a). Now it is loaded by the forces P_{12} and P_{21} which we relate to the shear stress τ by the technique already used

$$P_{12} = \tau\, b\, d \cos\alpha\,, \quad P_{21} = \tau\, d\,(a + b\sin\alpha).$$

It is easy to check that these relations satisfy equilibrium conditions for the cell.

Now we must find the displacement AB (Fig. 324a). If the twisted crosspiece of length a is not deformed then the segment AB would be equal to $Q\,b^3/(24EJ)$ as before. And here this deflection must be greater by $\vartheta\, b/2$, where ϑ is the section slope angle at the end of the twisted segment (Fig. 324a). It can be obtained by the ordinary procedure for the simply supported beam (Fig. 324b) and is equal to $Ma/(12EJ)$. Let us remark that the wire at the segment of length a is twisted but not soldered. That is why its bending rigidity is taken as two times greater than for the other segments. The moment $M = Q\,b$. Thus the displacement AB will be

$$AB = \frac{Q\,b^3}{24EJ} + \frac{Q\,a\,b^2}{24EJ} = \frac{Q\,b^2}{24EJ}\,(a+b)\,,$$

where $Q = P_{12}\sin\alpha - P_{21}\cos\alpha = -\tau\, d\, a\cos\alpha\,.$

Now we need to find the shear angle of the deformed cell. It is equal to the difference of the segments' AC and AD rotation angles (Fig. 324a), i.e.

$$\gamma = \frac{2AB\sin\alpha}{a + b\sin\alpha} - \frac{2AB\cos\alpha}{b\cos\alpha}\,, \quad or \quad \gamma = -\frac{Q\,b^2}{12EJ}\,\frac{a\,(a+b)}{b(a+b\sin\alpha)}\,.$$

Substituting the expression for Q through stress τ we obtain

$$\gamma = \tau\,\frac{a^2 b\, d}{12EJ}\,\frac{(a+b)\cos\alpha}{a + b\sin\alpha}$$

from which we find the reduced shear modulus

$$G = \frac{2EJ}{a^2 b\, d}\,\frac{a + b\sin\alpha}{(a+b)\cos\alpha}.$$

105. Let's simplify the problem and find the reduced elasticity moduli supposing that Poisson ratios of fiber and matrix are the same and equal to μ [21].

Let σ_1 be the average stress under tension along the axis 1. But the stresses σ_{1f} and σ_{1m} for fibers and matrix differ in such measure as the moduli E_f and E_m differ. As fiber and matrix must have equal elongations then

$$\varepsilon_1 = \sigma_{1f}/E_f\,, \quad \varepsilon_1 = \sigma_{1m}/E_m\,,$$

and mean stress is determined as

$$\sigma_1 = \left(\sigma_{1f}A_f + \sigma_{1m}A_m\right)/\left(A_f + A_m\right)\,,$$

where A_f and A_m are cross-section areas of fibers and matrix strips. This expression can be written in the following conventional way [1,21]

$$\sigma_1 = \sigma_{1f}V_f + \sigma_{1m}V_m\,,$$

where V_f and V_m are fibers and matrix volume fractions in the composite.

Expressing σ_1 and σ_2 through ε_1 we obtain

$$\sigma_1 = \varepsilon_1(E_fV_f + E_mV_m)\,,$$

from which

$$E_1 = E_fV_f + E_mV_m\,. \tag{1}$$

If the flat specimen is tensed by the stress σ_2 applied along the axis 2 then its relative elongation along the axis 2 will be

$$\varepsilon_2 = \left(\sigma_2\frac{b_f}{E_f} + \sigma_2\frac{b_m}{E_m}\right)/\left(b_f + b_m\right)\,,$$

where b_f and b_m are fibers and matrix strip widths. As a result

$$\varepsilon_2 = \sigma_2\left(\frac{V_f}{E_f} + \frac{V_m}{E_m}\right),$$

and the reduced elasticity modulus

$$E_2 = \frac{1}{\dfrac{V_f}{E_f} + \dfrac{V_m}{E_m}}\,. \tag{2}$$

As regards Poisson ratio, it remains common: $\mu_{12} = \mu_{21} = \mu$.

Let us note that if we liken fiber and matrix to the springs of stiffnesses c_f and c_m then longitudinal and transverse tension of composite will be correspondingly similar to the parallel and sequential connection of these springs (Fig. 325).

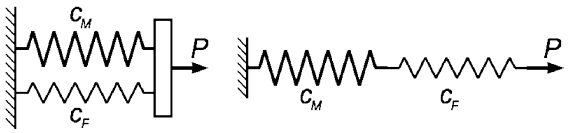

Fig. 325

The item we still need to determine is the composite shear modulus. If the specimen is loaded by tangential forces (Fig. 326) then the mutual shear of the strips takes place, and the average shear angle is

$$\gamma_{av} = \left(\frac{\tau b_f}{G_f} + \frac{\tau b_m}{G_m} \right) / \left(b_f + b_m \right),$$

or

$$\gamma_{av} = \tau \left(\frac{V_f}{G_f} + \frac{V_m}{G_m} \right),$$

from which we obtain the sought shear modulus

$$G = 1/ \left(\frac{V_f}{G_f} + \frac{V_m}{G_m} \right) \tag{3}$$

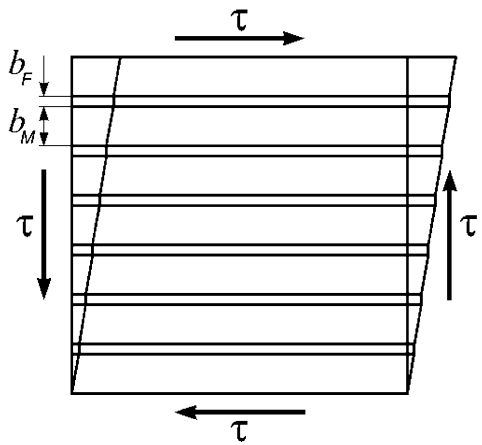

Fig. 326

The difference between Poisson ratios of fiber and matrix under longitudinal tension and under shear has no effect on composite rigidity. That is why expressions (1) and (3) can be used in this case, too. Poisson ratio μ_{21} can be found by averaging of the transverse contraction under longitudinal tension. But the matter stands in quite another way under the specimen's tension along the axis 2. Unequal shortening of fiber and matrix leads to force interaction between them which reveals itself as local tangent stresses near the edges of the specimen. These stresses either strain fiber and compress matrix or on the contrary compress fiber and strain matrix. The tangent

stresses are localized only in the narrow region having depths of about two-three times the diameters of the fiber. The peculiarities in distribution of the local tangent stresses and shear deformations are usually referred to as edge effect.

The region of the edge effect is excluded while calculating the modulus, and the following analysis clarifies that modulus E_2 due to the difference of fiber and matrix Poisson ratios μ_f and μ_m becomes slightly greater than the value given by expression (2).

106. Such simplification is inadequate. The shear restraint takes place under tension of the cross-ply laminate specimen. In other words, the layers mutually prevent the shear at an angle of φ along the fibers. Such restraint does not exist in a one-way reinforced specimen. And its elasticity modulus will be noticeably less than for cross-ply laminate. This difference is especially visible in the range of φ from 5 to 45 degrees.

107. Certainly no. For example, a $\pm 45^0$ cross-reinforced sheet has equal elasticity moduli along two diagonal axes but this material is anisotropic.

4. Stability

108. The length of the rod's upper free part is equal to

$$l - \lambda = l - \frac{P}{c}$$

The equilibrium state with curved axis for this segment will exist if

$$P > \frac{\pi^2 EJ}{4(l - P/c)^2},$$

and for the lower rod's part of length $\lambda = P/c$ in case of

$$P > \frac{4\pi^2 EJ}{(P/c)^2}.$$

Let's denote

$$\frac{\lambda}{l} = \frac{P}{cl} = p, \quad \frac{\pi^2 EJ}{l^3 c} = p_0.$$

Then the above written curvilinear equilibrium shapes' existence conditions take the form

$$p(1-p)^2 > \frac{1}{4}p_0, \quad p^3 > 4p_0. \tag{1}$$

As $\lambda \le l$ then $0 \le p \le 1$. On this interval of p we plot functions $p(1-p)^2$ and p^3 (Fig. 327) and see that their maximal values are correspondingly $\frac{4}{27}$ and 1.

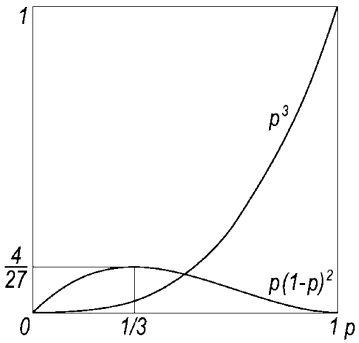

Fig. 327

Then from the relations (1) we find the conditions necessary to prevent the rod's buckling

$$\frac{1}{4}p_0 > \frac{4}{27} \text{ and } 4p_0 > 1,$$

from which

$$p_0 > \frac{16}{27};$$

but as we previously denoted

$$p_0 = \frac{\pi^2 EJ}{l^3 c};$$

therefore the spring's stiffness must be less than the following value

$$\frac{27}{16}\frac{\pi^2 EJ}{l^3}.$$

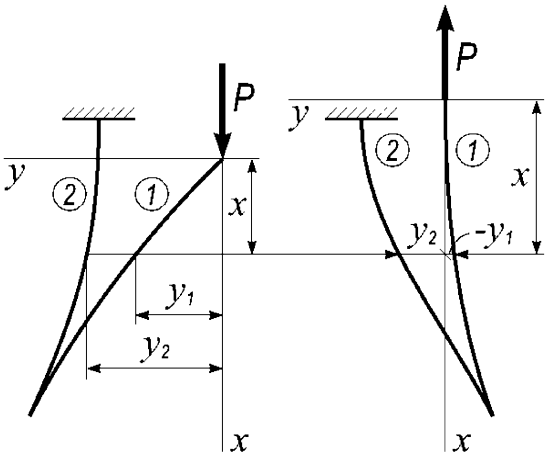

Fig. 328

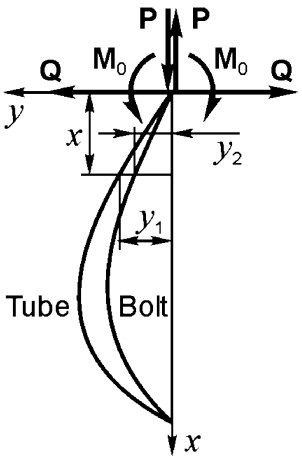

Fig. 329

109. Let's consider the contour of the bent plate (Fig. 328).

Deflection curve differential equations for the first and the second parts of the plate under the force P directed downwards will be as follows

$$EJy_1'' + Py_1 = 0,$$

$$EJy_2'' - Py_2 = 0.$$

Denoting $\dfrac{P}{EJ} = \alpha^2$ we get

$$y_1'' + \alpha^2 y_1 = 0, \quad y_2'' - \alpha^2 y_2 = 0,$$

from which

$$y_1 = A_1 \sin \alpha x + B_1 \cos \alpha x, \quad y_2 = A_2 \sinh \alpha x + B_2 \cosh \alpha x$$

The constants are determined from the conditions:

1) at $x = 0$ $y_1 = 0$,
2) at $x = l$ $y_1 = y_2$,
3) at $x = l$ $y_1' = y_2'$,
4) at $x = 0$ $y_2' = 0$.

From the first and the last conditions we get

$$B_1 = A_2 = 0,$$

from the second and the third one:

$$A_1 \sin \alpha l = B_2 \cosh \alpha l,$$

$$A_1 \cos \alpha l = B_2 \sinh \alpha l,$$

from which follows

$$\tan \alpha l \tanh \alpha l = 1 \tag{1}$$

or

$$\alpha l = 0.938, \quad P_{cr} = \frac{0.88EJ}{l^2}$$

If the force P is directed upwards, the sign of α^2 is changed by the opposite one and the transcendental equation (1) arrives at

$$\tan i\alpha l \tanh i\alpha l = 1.$$

But $\tan i\alpha l = -\dfrac{\tanh \alpha l}{i}$, and $\tanh i\alpha l = i \tan \alpha l$. Therefore

$$\tan \alpha l \tanh \alpha l = -1,$$

whence

$$\alpha l = 2.35, \quad P_{cr} = \frac{5.53EJ}{l^2}$$

110. Let's imagine to remove the nut from the bolt and consider the forces acting on the tube and the bolt. The deflection curves of the bolt and the tube after buckling and the internal forces and moments P, Q and M_0 also are shown in Fig. 329. Obviously we have for the tube

$$M_b = Py_1 - Qx - M_0,$$

for the bolt

$$M_b = -Py_2 + Qx + M_0.$$

Differential equations for deflection curves of tube and bolt are as follows:

$$E_1 J_1 y_1'' + Py_1 = Qx + M_0,$$
$$E_2 J_2 y_2'' - Py_2 = -Qx - M_0.$$

Let's denote

$$\frac{P}{E_1 J_1} = \alpha_1^2, \quad \frac{P}{E_2 J_2} = \alpha_2^2,$$

then we have

$$y_1'' + \alpha_1^2 y_1 = \frac{Q}{P}\alpha_1^2 x + \frac{M_0}{P}\alpha_1^2 x + \frac{M_0}{P}\alpha_1^2,$$

$$y_2'' - \alpha_2^2 y_2 = -\frac{Q}{P}\alpha_2^2 x - \frac{M_0}{P}\alpha_2^2.$$

Solving these equations we get

$$y_1 = A_1 \sin\alpha_1 x + B_1 \cos\alpha_1 x + \frac{Q}{P}x + \frac{M_0}{P},$$

$$y_2 = A_2 \sinh\alpha_2 x + B_2 \cosh\alpha_2 x + \frac{Q}{P}x + \frac{M_0}{P}.$$

The last two terms of both expressions are particular solutions of the equations. Constants A_1, B_1, A_2, B_2, Q, and M_0 are derived from the following conditions:

at $x = 0$

$$y_1 = 0, \quad y_2 = 0, \quad y_1' = y_2',$$

at $x = l$

$$y_1 = 0, \quad y_2 = 0, \quad y_1' = y_2'.$$

From the first three conditions we get

$$B_1 = B_2 = -\frac{M_0}{P}, \quad A_2 = A_1\frac{\alpha_1}{\alpha_2}. \tag{1}$$

The last three conditions give

$$A_1 \sin\alpha_1 l + B_1 \cos\alpha_1 l + \frac{Q}{P}l + \frac{M_0}{P} = 0,$$

$$A_2 \sinh\alpha_2 l + B_2 \cosh\alpha_2 l + \frac{Q}{P}l + \frac{M_0}{P} = 0,$$

$$A_1\alpha_1 \cos\alpha_1 l - B_1\alpha_1 \sin\alpha_1 l = A_2\alpha_2 \cosh\alpha_2 l + B_2\alpha_2 \sinh\alpha_2 l.$$

If we substitute B_1, B_2, and A_2 from (1) in these equations, then

$$A_1 \sin\alpha_1 l + \frac{Q}{P}l + \frac{M_0}{P}(1 - \cos\alpha_1 l) = 0,$$

$$A_1\frac{\alpha_1}{\alpha_2}\sinh\alpha_2 l + \frac{Q}{P}l + \frac{M_0}{P}(1 - \cosh\alpha_2 l) = 0,$$

$$A_1\alpha_1(\cos\alpha_1 l - \cosh\alpha_2 l) + \frac{M_0}{P}(\alpha_1 \sin\alpha_1 l + \alpha_2 \sinh\alpha_2 l) = 0.$$

Equating the determinant of the set of equations to zero we arrive at

$$\begin{vmatrix} \sin\alpha_1 l & l & 1-\cos\alpha_1 l \\ \dfrac{\alpha_1}{\alpha_2}\sinh\alpha_2 l & l & 1-\cosh\alpha_2 l \\ \alpha_1(\cos\alpha_1 l-\cosh\alpha_2 l) & 0 & \alpha_1\sin\alpha_1 l+\alpha_2\sinh\alpha_2 l \end{vmatrix} = 0,$$

from which

$$2z_1 z_2(\cosh z_2\cos z_1 - 1) = \left(z_2^2 - z_1^2\right)\sinh z_2 \sin z_1, \qquad (2)$$

where $z_1 = \alpha_1 l$, $z_2 = \alpha_2 l$. Under the prescribed rigidity relation we can express z_2 in z_1 and then by solving transcendental equation (2) find the critical force of tightening P.

Specifically, for $E_1J_1 = E_2J_2 = EJ$ we have $z_1 = z_2 = z$ and then $\cosh z\cos z = 1$, from which

$$z = 4.73, \quad P_{cr} = \frac{z^2 EJ}{l^2} = \frac{22.4EJ}{l^2}$$

111. Let's consider the bent state of the rod and remove the upper support (Fig. 330). We denote the vertical reaction of this support by P_1 and the horizontal one by Q.

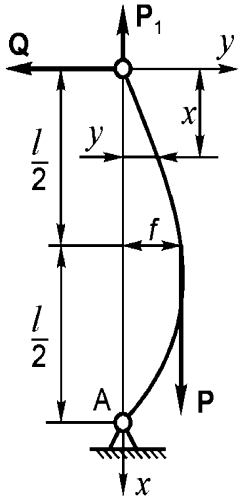

Fig. 330

The first question arising here is the one about the magnitude of these reactions. The force Q can be found from the zero sum of moments about the point A condition, that gives

$$Q = P\frac{f}{l}.$$

Before the beginning of buckling the force $P_1 = P/2$. As the deflection of the rod from its straight state can be assumed to be infinitely small, then under buckling the force P_1 can be also taken equal to $P/2$ (see the solution

of problem 112). Now let us write the differential equations of the deflection curve for two segments of the rod:

$$EJy_1'' = P_1 y_1 - Qx \qquad \left(0 \le x \le \frac{l}{2}\right),$$

$$EJy_2'' = P_1 y_2 - Qx - P(y_2 - f) \qquad \left(\frac{l}{2} \le x \le l\right),$$

or otherwise

$$y_1'' - \alpha^2 y_1 = -2\alpha^2 \frac{f}{l} x,$$

$$y_2'' + \alpha^2 y_2 = -2\alpha^2 \frac{f}{l} x + 2\alpha^2 f,$$

where

$$\alpha^2 = \frac{P}{2EJ}$$

Solving the equations we get

$$y_1 = A \sinh \alpha x + B \cosh \alpha x + \frac{2f}{l} x,$$

$$y_2 = C \sin \alpha x + D \cos \alpha x - \frac{2f}{l} x + 2f.$$

At $x = 0 \quad y_1 = 0,$
at $x = l/2 \quad y_1 = y_2 = f$ and $y_1' = y_2',$
at $x = l \quad y_2 = 0.$

Hence
1) $B = 0,$
2) $A \sinh \frac{\alpha l}{2} + B \cosh \frac{\alpha l}{2} + f = f,$
3) $C \sin \frac{\alpha l}{2} + D \cos \frac{\alpha l}{2} + f = f,$
4) $A\alpha \cosh \frac{\alpha l}{2} B\alpha \sinh \frac{\alpha l}{2} + \frac{2f}{l} = C\alpha \cos \frac{\alpha l}{2} - D\alpha \sin \frac{\alpha l}{2} - \frac{2f}{l},$
5) $C \sin \alpha l + D \cos \alpha l = 0.$

It follows from the second relation that $A = 0$ (i.e. the rod's upper part is the straight line). The last three relations arrive at :

$$C \sin \frac{\alpha l}{2} + D \cos \frac{\alpha l}{2} = 0,$$

$$C\alpha \cos \frac{\alpha l}{2} - D\alpha \sin \frac{\alpha l}{2} - \frac{4f}{l} = 0,$$

$$C \sin \alpha l + D \cos \alpha l = 0$$

In the case where the determinant of the equations' set is not equal to zero all constants C, D, f vanish. Then $y_1 = y_2 = 0$ and the rod remains

straight. The solution may be nontrivial if the determinant is equal to zero. That makes it possible to derive the critical force P :

$$\begin{vmatrix} \sin\frac{\alpha l}{2} & \cos\frac{\alpha l}{2} & 0 \\ \alpha\cos\frac{\alpha l}{2} & -\alpha\sin\frac{\alpha l}{2} & -\frac{4}{l} \\ \sin\alpha l & \cos\alpha l & 0 \end{vmatrix} = 0,$$

from which follows

$$\sin\frac{\alpha l}{2} = 0, \quad \frac{\alpha l}{2} = \pi, \quad P_{cr} = \frac{8\pi^2 EJ}{l^2}.$$

If the upper end of the rod were able to move in vertical direction, the critical force would be four times less, i.e. $18.7\dfrac{EJ}{l^2}$.

112. We can assert that the deflection curve configuration of the bent rod under the given compressive force will be just the same independent of the causes which give rise to this force.

If the rod's deviation from the straight form is given then the force that compresses the rod must be the same under any circumstances. Infinitely decreasing the rod's curvature we shall unavoidably come to the conclusion that the critical force for the observed rod will be the same both in the ordinary case of applying "dead" load and in the examined case of temperature loading.

We can also argue as follows: The bending moment in a rod is proportional to deflection y, and compressive force variation takes place at vertical displacement that is proportional to the second power of y'. Hence the value of y can always be chosen small enough to neglect variation of force.

113. The formal approach of approximating function selection can lead to the result that is extremely far from reality.

Thus, for example, let's assume that the shape of the simply supported compressed rod elastic curve (Fig. 331) is expressed by the following function

$$y = A\left(\sin\frac{\pi x}{l} + \frac{l}{m}\sin\frac{\pi m x}{l}\right). \tag{1}$$

While $m \to \infty$ this function comes extremely close to the exact solution for the elastic curve shape, i.e. $\lim y\,|_{m\to\infty} = A\sin\dfrac{\pi x}{l}$.

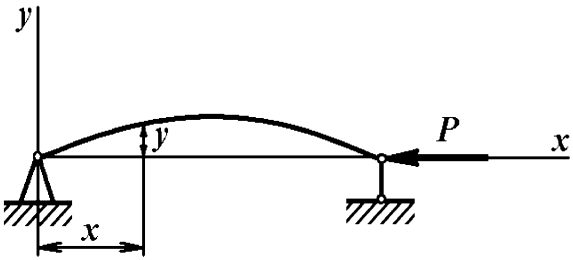

Fig. 331

But the critical force P determined by the energetic method after substitution of this function happens to be equal

$$P_{cr} = \frac{EJ\int_0^l y''^2 dx}{\int_0^l y'^2 dx} = \frac{1+m^2}{2}\frac{\pi^2 EJ}{l^2}$$

and as we see under $m \to \infty$ infinitely moves away from the exact solution.

The peculiarity of function (1) lies in the fact that it reflects the form of the primitive function y well, but abruptly diverges from it with respect to the second derivative, i.e. by the expression of curvature.

The example is very instructive because the general rule is visually underlined with the help of it. During selection of the approximating function we should also keep in mind the approximation degree of its derivatives including the highest of them entering the expression for energy.

114. At first let's analyze the auxiliary task.

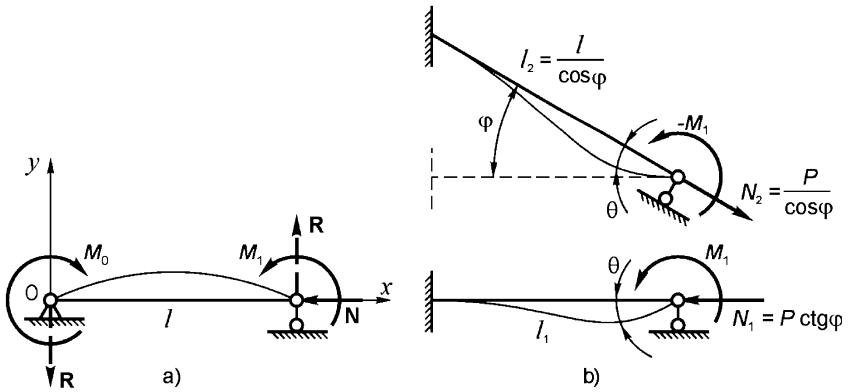

Fig. 332

Let's take a hinged rod of length l loaded by compressive force N and moments M_0 and M_1 (Fig. 332a). The differential equation of the rod deflection curve is

$$EJy'' = M_0 - Rx - Ny,$$

where R is the reaction of supports. Then we get

$$y = A\sin\alpha x + B\cos\alpha x + \frac{1}{EJ\alpha^2}(M_0 - Rx) \qquad (1)$$

where $\alpha^2 = \dfrac{N}{EJ}$.

Obviously at $x = 0$ and $x = l$ the displacement $y = 0$. Let's assume in addition that at $x = 0 \quad y' = 0$. Using these conditions and taking into account that

$$R = \frac{M_0 - M_1}{l}$$

we exclude the values of A, B, M_0, and R from relation (1). Then we get

$$y = \frac{M_1}{EJ\alpha^2} \frac{(1-\cos\alpha l)(\alpha l - \sin\alpha l)}{\alpha l \cos\alpha l - \sin\alpha l} \left[\frac{1-\cos\alpha x}{1-\cos\alpha l} + \frac{\alpha x - \sin\alpha x}{\alpha l - \sin\alpha l}\right]$$

The value of moment M_1 remains undetermined.

The slope angle of the rod at the right support is equal to

$$\theta = y'_{x=l} = \frac{M_1}{EJ\alpha} \frac{-2 + 2\cos\alpha l + \alpha l \sin\alpha l}{\alpha l \cos\alpha l - \sin\alpha l}. \tag{2}$$

If the force N is not compressive but tensile then the value of α must be changed by $i\alpha$, $\cos\alpha l$ by $\cosh\alpha l$ and $\sin\alpha l$ by $i\sinh\alpha l$. Then relation (2) will take form

$$\theta = -\frac{M_1}{EJ\alpha} \frac{-2 + 2\cosh\alpha l - \alpha l \sinh\alpha l}{\alpha l \cosh\alpha l - \sinh\alpha l} \tag{3}$$

Now let's return to the given system of rods (Fig. 332b). The lower horizontal rod is compressed by the force $N_1 = P\cot\varphi$ and the upper is tensed by the force $N_2 = P/\sin\varphi$.

At the point of the force P application the displacements of both rods are equal to zero accurate to the higher order infinitesimal value. Left ends of the rods are rigidly fixed. Therefore the scheme of the fixed-hinged rod (Fig. 332a) corresponds to the fastening and loading conditions for the rods belonging to the given frame. The only one thing remaining to be done is to satisfy the junction conditions. These conditions are reduced to the equality of angles θ and the equilibrium of moments in the common point.

Let's return to the relations (2) and (3). We replace αl by $\alpha_1 l_1$ in the first of the relations and by $\alpha_2 l_2$ in the second one. It is obvious that

$$\alpha_1 l_1 = l\sqrt{\frac{P\cot\varphi}{EJ}}, \quad \alpha_2 l_2 = \frac{l}{\cos\varphi}\sqrt{\frac{P}{EJ\sin\varphi}} \tag{4}$$

As moments in the junction point are directed towards each other then in one of the relations (2) or (3) the sign of M_1 is changed by the opposite one. Equating angles θ we arrive at the transcendental equation

$$\frac{1}{\alpha_1 l_1} \frac{-2 + 2\cos\alpha_1 l_1 + \alpha_1 l_1 \sin\alpha_1 l_1}{\alpha_1 l_1 \cos\alpha_1 l_1 - \sin\alpha_1 l_1} = \frac{1}{\alpha_2 l_2 \cos\varphi} \frac{-2 + 2\cosh\alpha_2 l_2 - \alpha_2 l_2 \sinh\alpha_2 l_2}{\alpha_2 l_2 \cosh\alpha_2 l_2 - \sinh\alpha_2 l_2}$$

The following relation should be added to the equation

$$\alpha_1 l_1 = \alpha_2 l_2 \cos^{3/2}\varphi.$$

Calculating the value of $\alpha_1 l_1 = \sqrt{\frac{Pl^2}{EJ}}\cot\varphi$ for several values of φ we obtain the results presented in Table 4.

Table 4. Critical values of dimensionless load

$\varphi\circ$	0	10	20	30	40	50	60	70	80	90
$P_{cr}l^2/EJ$	0	5.55	11.46	18.21	26.57	38.08	56.18	91.37	196.9	∞

115. Let's suppose that point A came out of the plane $BCDE$ and apply forces P_1 to the beams BD and CE in point A (Fig. 333) whereupon we shall consider the beams separately.

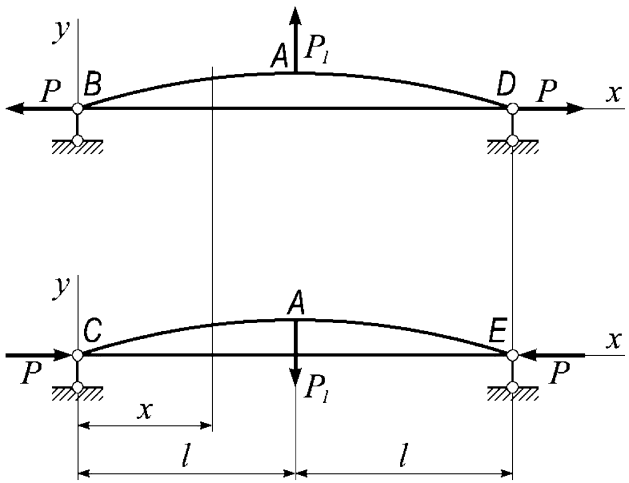

Fig. 333

The differential equation of beam BD bending is

$$EJy'' - Py = -\frac{1}{2}P_1 x.$$

For beam CE we have

$$EJy'' + Py = +\frac{1}{2}P_1 x.$$

The solution of these equations will be correspondingly:

$$y_1 = C_1 \sinh \alpha x + C_2 \cosh \alpha x + \frac{1}{2}\frac{P_1}{P}x,$$

$$y_2 = C_3 \sin \alpha x + C_4 \cos \alpha x + \frac{1}{2}\frac{P_1}{P}x,$$

where

$$\alpha^2 = \frac{P}{EJ}$$

At the point $x = 0$ the deflection y in both cases is equal to zero. That is why $C_2 = C_4$. For the symmetric modes of buckling at $x = l$ the slope $y' = 0$, therefore

$$C_1 = -\frac{P_1}{2P\alpha}\frac{1}{\cosh \alpha l},\ C_3 = -\frac{P_1}{2P\alpha}\frac{1}{\cos \alpha l}.$$

Finally from the condition of the beam deflections equality at point A we obtain

$$C_1 \sinh \alpha l = C_3 \sin \alpha l,$$

or taking into account the preceding relation

$$\tanh \alpha l = \tan \alpha l,$$

from which

$$\alpha l = 3.926, \quad P_{cr} = \frac{15.4EJ}{l^2}. \tag{1}$$

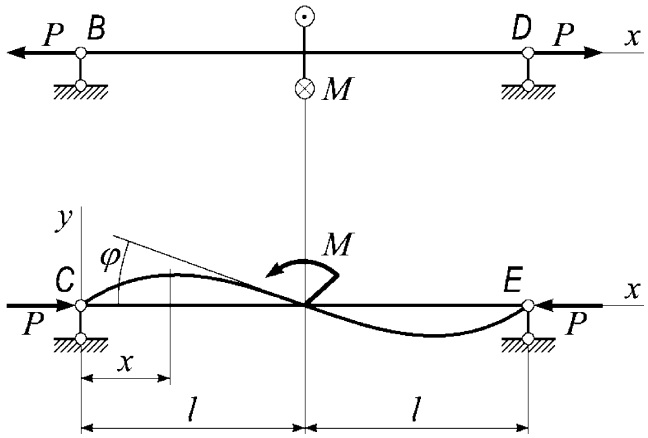

Fig. 334

Besides the above there is another possibility of buckling for the compressed rod CE. This rod can bend by two half-waves with point A being immovable. Under these conditions the rod BD will be twisted. Let's consider both rods separately (Fig. 334). The deflection curve differential equation for the rod CE is

$$EJy'' + Py = \frac{M}{2l}x,$$

from which

$$y = C_1 \sin \alpha x + C_2 \cos \alpha x + \frac{M}{2Pl}x.$$

The boundary conditions are

$$\begin{aligned} &\text{at} \quad x = 0 \quad y = 0 \\ &\text{at} \quad x = l \quad y = 0 \\ &\text{at} \quad x = l \quad y' = -\varphi \end{aligned} \tag{2}$$

where φ is the rotation angle of the rod BD middle section which is equal to

$$\varphi = \frac{M}{2}\frac{l}{c},$$

where c is the torsional stiffness of the tensed thin rod that according to the solution of problem 28 is

$$c = \frac{1}{3}Gbh^3 + \frac{Pb^2}{12}.$$

The boundary conditions (2) yield

$$\begin{aligned} C_2 &= 0, \\ C_1 \sin \alpha l + \frac{M}{2P} &= 0, \\ C_1 \alpha \cos \alpha l + \frac{M}{2Pl} &= -\frac{M}{2}\frac{1}{\frac{1}{3}Gbh^3 + \frac{Pb^2}{12}}. \end{aligned}$$

Transferring the free terms to the right side and dividing the second equation by the third one we obtain

$$\frac{1}{\alpha}\tan \alpha l = \frac{\frac{1}{P}}{\frac{1}{Pl} + \frac{l}{\frac{1}{3}Gbh^3 + \frac{Pb^2}{12}}}.$$

As

$$P = \alpha^2 EJ, \quad G = \frac{E}{2(1+\mu)}, \quad J = \frac{bh^3}{12},$$

where μ is Poisson's ratio, then

$$\tan \alpha l = \alpha l \frac{\frac{2}{1+\mu} + \frac{b^2}{12l^2}\alpha^2 l^2}{\frac{2}{1+\mu} + \alpha^2 l^2\left(\frac{b^2}{12l^2} + 1\right)}.$$

As b is significantly less than l and αl must have the magnitude of about 3 or 4 units, then it is clear that on the right-hand side of the equation the terms containing b^2 can be neglected. Then we arrive at

$$\tan \alpha l = \frac{2\alpha l}{2 + (1+\mu)\alpha^2 l^2}.$$

For $\mu = 0.3$

$$\alpha l = 3.51, \quad P_{cr} = \frac{12.3EJ}{l^2} \tag{3}$$

This value of P_{cr} is less than the one calculated before (1). Hence the stability loss of the rod CE will occur by two half-waves.

If the load P increases then the internal force in the compressed rod remains almost unchanged, and the greater part of the load will be perceived by the tensed diagonal BC.

The system considered in this problem is the analogue of the thin-walled panel $BCDE$ (Fig. 335) working under the conditions of the shear. Such elements are typical for aircraft and rocket constructions. Their buckling under the shear causes the formation of diagonal waves. Nevertheless, the panel that has lost its ability to bear the additional compressive load along the diagonal CE successfully perceives the tensile forces acting in perpendicular direction.

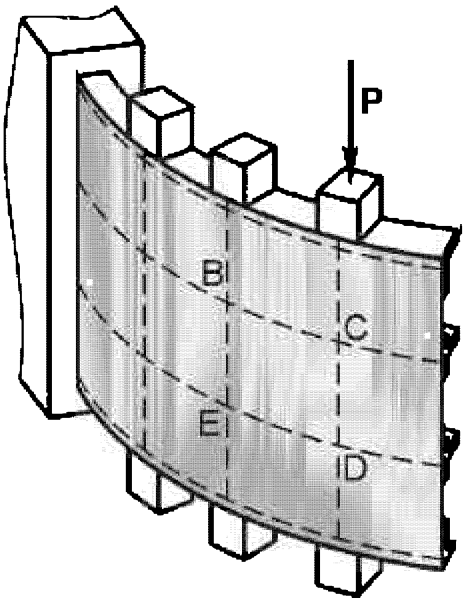

Fig. 335

116. Assuming that displacements are small let's derive the differential equation of the beam deflection curve.

Let's introduce the coordinate system x, y, z shown in Fig. 336. The bending moments caused by the force P and the torque M in the section x are

in plane xy : Py and Mz',

in plane xz : Pz and $-My'$.

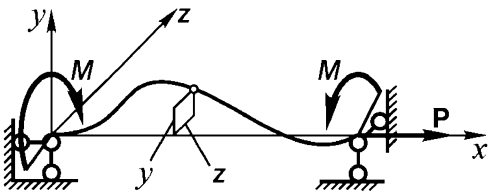

Fig. 336

The positive and negative sign in front of the moment term is taken as depending on the fact whether the moment is directed towards the increasing or the decreasing of the axial line positive curvature in the corresponding plane of bending.

If we accept that beam bending rigidities in the planes xy and xz are the same, then the equations of axial line bending can be written as follows

$$EJy'' = Py + Mz', \quad EJz'' = Pz - My'. \tag{1}$$

Let's find the solution in the form

$$y = A\cos\alpha_1 x + B\sin\alpha_1 x + C\cos\alpha_2 x + D\sin\alpha_2 x,$$
$$z = A\sin\alpha_1 x - B\cos\alpha_1 x + C\sin\alpha_2 x - D\cos\alpha_2 x,$$

where α_1 and α_2 are the roots of the quadratic equation

$$\alpha^2 + \frac{M}{EJ}\alpha + \frac{P}{EJ} = 0. \tag{2}$$

In case of the hinged rod we have the following boundary conditions

$$at \quad x = 0, \quad y = z = 0,$$
$$at \quad x = l, \quad y = z = 0.$$

Applying these relations we obtain four equations

$$A + C = 0,$$
$$B + D = 0;$$
$$A\cos\alpha_1 l + B\sin\alpha_1 l + C\cos\alpha_2 l + D\sin\alpha_2 l = 0,$$
$$A\sin\alpha_1 l - B\cos\alpha_1 l + C\sin\alpha_2 l - D\cos\alpha_2 l = 0.$$

Equating the determinant of the system to zero we arrive at

$$\cos(\alpha_2 - \alpha_1)l = 1,$$

or

$$(\alpha_2 - \alpha_1)l = 0, \quad 2\pi; \quad 4\pi; \ldots$$

But according to equation (2)

$$\alpha_2 - \alpha_1 = \pm 2\sqrt{\left(\frac{M}{2EJ}\right)^2 - \frac{P}{EJ}},$$

hence

$$M_{cr} = \pm 2\sqrt{EJ}\sqrt{P_e + P},$$

where P_e is Euler critical force

$$P_e = \frac{\pi^2 EJ}{l^2}$$

Thus if the tensile force P increases then the critical moment grows. If the force P is compressive then the moment M decreases. For the compressive force value $P = P_e$ the magnitude of M_{cr} vanishes as ought to be expected.

117. The rod cannot loose its stability. Assume that the rod was bent due to some cause (Fig. 337). In the ordinary case, i.e. under loading by longitudinal forces only, such deformation causes the rise of bending moment $M = Py$ tending to increase the rod curvature.

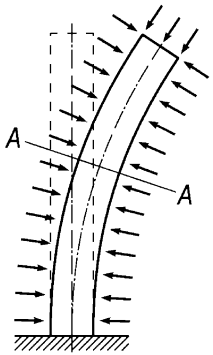

Fig. 337

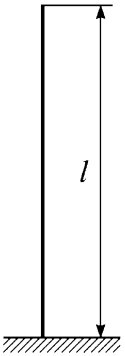

Fig. 338

Under sufficiently large force P the rod will not take its initial straight equilibrium form after bending causes removal. Then we say that the straight form of rod equilibrium is unstable.

The considered problem is absolutely different. External moments do not affect the rod in its bent configuration. Pressure acting on the rod surface disposed above the cross-section AA does not cause the internal bending moment in this section and is reduced only to the normal force equal pA where A is the cross-section area. That is why if the causes of bending are withdrawn then the rod freely returns to the initial straight form even under sufficiently great value of pressure p. Thus the straight form of equilibrium is always stable.

The confirmation of the aforesaid can be observed in everyday life. Indeed atmospheric pressure does not prevent the thin straw from keeping its straight form independently of its length and rigidity!

118. The rod will loose its stability under the same length as the vertically standing column (Fig. 338) having specific weight equal to the weight difference of liquid and wood.

119. The most convenient way to answer the given question is to apply energy relations. The complementary energy U_b that the column receives while bending is taken from the potential of external and internal forces. Usually we write the energy balance for a compressed bar as follows:

$$U_b = P\lambda \tag{1}$$

where λ is the displacement of the axial compressive force application point. If the point does not move, as for example during hinged rod heating (see problem 112), then all the same $P\lambda$ can be treated as the internal forces potential variation arising earlier as a result of the constrained heating. In the considered example the matter stands just the same. The force P arises as a consequence of pressure action on the column. The column is compressed. It accumulates the energy of compression. Under the column's bending this energy decreases by $P\lambda$ where λ is the difference between the bent rod length and its length before bending.

However, in our case relation (1) should be revised as it does not reflect the variation of the pressure forces potential. We must calculate the liquid's volume variation ΔV under the column's bending. If the volume increased then the potential of the pressure forces decreases and we must add the product $p\Delta V$ to $P\lambda$. If the volume decreases then we must subtract the product $p\Delta V$. It is obvious that the latter takes place in the given case. Hence instead of (1) we must write

$$U_b = P\lambda - p\Delta V$$

Obviously $\Delta V = A\lambda$ where A is the rod's cross-section area, and the force P is derived from the condition that relative longitudinal elongation ε is equal to zero:

$$\varepsilon = \frac{P}{EA} - \frac{2\mu p}{E} = 0.$$

Then $P = 2\mu pA$ and finally we get

$$U_b = p\lambda(2\mu - 1).$$

The left part of the relation is positive and the right part is negative... And they cannot be equal. That is why the rod does not loose its stability.

120. A liquid-filled tube will behave exactly the same as a freely standing column loaded by its own weight. That is why the tube will loose its stability if the total weight of tube and liquid contained in it is greater than the critical weight of the rod having the same length and rigidity.

121. The system looses its stability in the same manner as in the case when the load is applied directly to the tube. In the given case $P_{cr} = \pi^2 EJ/l^2$

Sometimes we can hear that in the considered case the tube can not loose its stability under any conditions. Such an opinion is based on a false position that the presence of the internal compressive forces is of great importance while the stability analysis by Euler. In reality the latter is not the case.

In order to obtain the correct solution of the given problem it is sufficient to consider the deflected configuration of the tube (Fig. 339). The differential equation of deflected tube axial line is the same as for the compressed column

$$y'' + \frac{P}{EJ}y = 0.$$

From which follows the mentioned above magnitude of the critical force for the hinged tube.

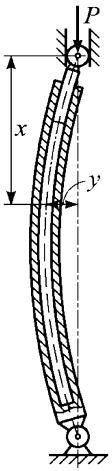

Fig. 339

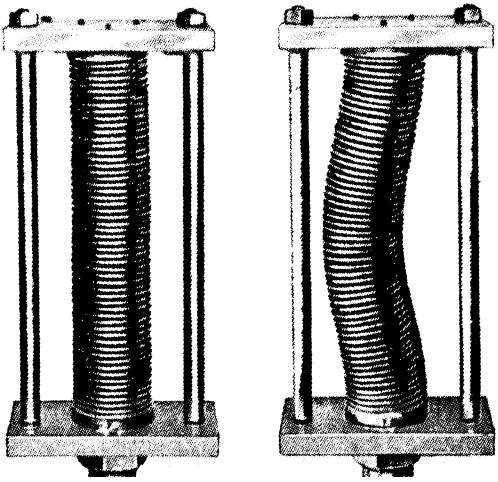

Fig. 340

122. After analysis of the previous problem we can say at once that the tube will loose its stability when

$$pA = \frac{4\pi^2 EJ}{l^2}$$

where A is the area of tube cross-section.

The critical pressure existence for the given system can be easily detected if we consider the balance of system energy. The volume of the tube's internal cavity in the bent state grows by $A\lambda$ because the tube under bending rises out from the upper plug by a value λ, where

$$\lambda = \frac{1}{2}\int_0^l y'^2 dx.$$

The critical force is derived from the condition

$$p_{cr} A\lambda = U_b,$$

In case of ordinary compression of the rod we have

$$P_{cr}\lambda = U_b,$$

from which we obtain the same

$$p_{cr} A = P_{cr} = \frac{4\pi^2 EJ}{l^2}$$

The considered case of buckling is obviously displayed under loading of a thin-walled sylphon by the internal pressure (Fig. 340). The magnitude of critical pressure for this case is obtained by the same way as for a rod. But

instead of rigidity EJ we must take some equivalent bending rigidity of the sylphon, and instead of A the area of the sylphon cross-section calculated by mean diameter should be taken.

123. Let's suppose that the tube is slightly bent for some reason. The tube's bent part is shown in Fig. 341 where its curvature is taken as positive. The mass of the liquid inside the tube's segment dx at a given moment is

$$dm = \frac{\gamma}{g} A dx, \tag{1}$$

where A is the area of the tube's orifice.

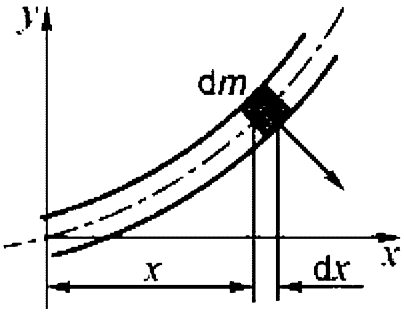

Fig. 341

While the curvature of the channel is $1/\rho = d^2y/dx$ the flowing liquid at section dx gives the inertial force

$$dm\frac{v^2}{\rho} = \frac{y}{g} A\, dx\, v^2 \frac{d^2y}{dx^2},$$

directed out of the center of curvature. The intensity of the inertial force, i.e. force falling at unit length of arc, will be

$$q = -\frac{\gamma}{g} A v^2 \frac{d^2y}{dx^2}$$

The negative sign is taken because the force q for positive curvature is directed opposite to the displacement y. But it is known that

$$EJ\frac{d^4y}{dx^4} = q.$$

Hence

$$EJ\frac{d^4y}{dx^4} + \frac{\gamma}{g} A v^2 \frac{d^2y}{dx^2} = 0.$$

Let's denote

$$\frac{\gamma}{g}\frac{Av^2}{EJ} = \alpha^2.$$

Then we get

$$\frac{d^4y}{dx^4} + \alpha^2 \frac{d^2y}{dx^2} = 0,$$

from which

$$y = A_1 \sin \alpha x + B \cos \alpha x + Cx + D.$$

At $x = 0$ and $x = l$ we have $d^2y/dx^2 = 0$ and $y = 0$. It follows from these conditions that

$$B = 0, \quad C = 0, \quad D = 0, \quad A_1 \sin \alpha l = 0,$$

$$\alpha l = \pi, \quad v_{cr} = \frac{\pi}{l} \sqrt{\frac{g}{\gamma} \frac{EJ}{A}} \tag{2}$$

It is very surprising that the mode of stability loss obeys sinus law, i.e. is the same as for axial compression. Moreover, buckling occurs under the speed for which the reaction of stream is equal to Euler's critical force. In fact, the reaction of stream, i.e. jet force of stream, as is well known is equal to:

$$P = \frac{dm}{dt} v,$$

where dm/dt is mass consumption per second, and v velocity of stream. (Curiously, the thrust of a rocket engine is defined by this formula). According to (1)

$$P = \frac{\gamma}{g} A v^2.$$

Substituting here v from (2) we get that the force of the stream reaction is equal to Euler's critical force $P = \pi^2 EJ/l^2$. But one should not consider that the tube is compressed by the force of a stream response. The tube looses its stability without external compressive force as it takes place in the case considered in problem 121.

124. Let's consider the well-known statement: "let's take the least non-zero root of an equation...". The expression became commonplace due to its evidence, and nobody usually thinks over its substance. Certainly "the least"- because we are interested in the first minimal value of the critical force. "Non-zero"- because under zero root we have an unbent initial mode of equilibrium. This solution is not relevant.

If we analyze the considered system for the case $R/l \leq 0.5$ we should take exactly zero value of αl. The system represents a mechanism where friction forces are absent. The rod looses its stability as a solid body under the action of infinitely small force P. For $R/l = 0.5$ both end faces are restricted by arcs of circumference the center of which is at the middle of the rod (Fig. 342a). It is the limit value of parameter R/l , as with further increase the bending modes of buckling appear. Thus, disregarding friction forces, critical states are characterized by the curve OAB in Fig. 343.

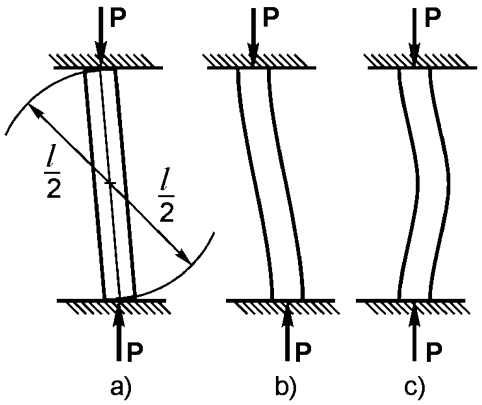

Fig. 342

As radius R increases the column buckling appears with more and more curvature of the rod under presence of transverse sliding of end faces or free transverse displacement of plates. In extreme case for $R = \infty$ the mode of column instability is shown in Fig. 342b, i.e. for this case $\alpha l = \pi$ and, hence, $P_{cr} = \pi^2 EJ/l^2$.

If plates can not freely move in transverse direction, and friction forces are sufficient to avoid the sliding, then the critical states of column depending on R/l are described by curve C (Fig. 343). For $R/l = \infty$ the mode of column buckling is presented in Fig. 342c. In this case $P_{cr}/P = 4$ and hence

$$P_{cr} = \frac{4\pi^2 EJ}{l^2} .$$

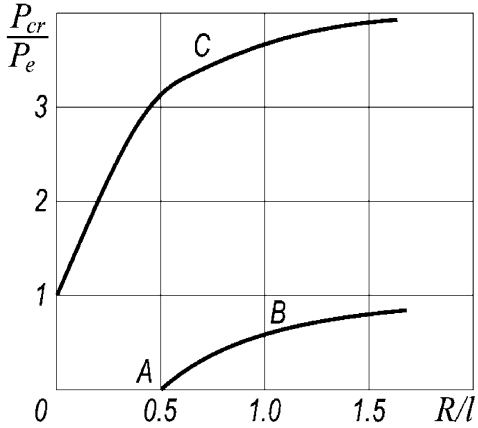

Fig. 343

125. The rod looses its stability under action of force $P = \pi^2 EJ/l^2$ and then by its middle part touches the tube walls.

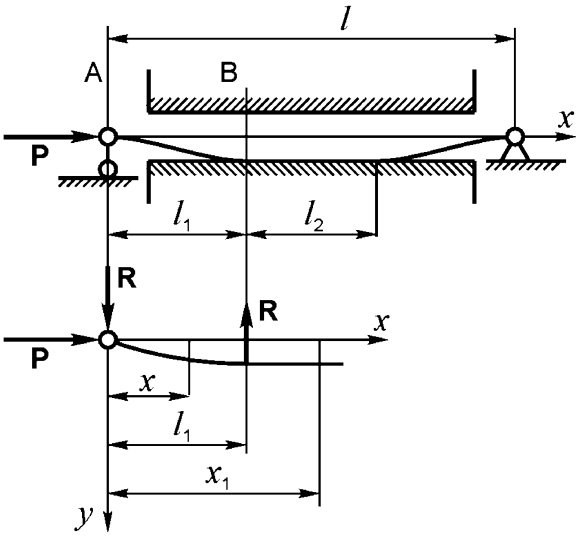

Fig. 344

Let's accept that for $P > \pi^2 EJ/l^2$ there exists a zone l_2 of the rod's tight contact with the tube walls (Fig. 344) and derive the equation of the deflection curve of the rod at the section $0 \le x \le l_1$

$$EJy'' + Py = Rx\,,$$

$$y = A\sin\alpha x + B\cos\alpha x + \frac{R}{P}x \qquad \left(\alpha^2 = \frac{P}{EJ}\right);$$

with boundary conditions: at $x = 0$ $y = 0$, at $x = l_1$ $y = \Delta$, at $x = l_1$ $y' = 0$, whence $B = 0$,

$$A\sin\alpha l_1 + \frac{R}{P}l_1 = \Delta\,, \quad A\alpha\cos\alpha l_1 + \frac{R}{P} = 0\,. \tag{1}$$

The rod remains straight at the section l_2. Hence at this section $M_b = 0$. That's why according to Fig. 344

$$P\Delta - Rx_1 + R\,(x_1 - l_1) = 0\,,$$

whence

$$R = P\frac{\Delta}{l_1}\,.$$

We derive from equation (1)

$$A = \frac{\Delta}{\pi}\,,$$

$$l_1 = \frac{\pi}{\alpha}, \qquad P = \frac{\pi^2 EJ}{l_1^2}\,, \tag{2}$$

$$y = \frac{\Delta}{\pi}(\sin \alpha x + \alpha x); \tag{3}$$

it follows from relation (2), that for $l_1 = l/2$

$$P = \frac{4\pi^2 EJ}{l^2}. \tag{4}$$

It means, that in case

$$\frac{\pi^2 EJ}{l^2} < P < \frac{4\pi^2 EJ}{l^2}$$

the rod touches the wall only in one point, and only for

$$P > \frac{4\pi^2 EJ}{l^2}$$

the rod is adjacent to the wall along the segment.

If the middle straight segment becomes long enough, then it may buckle too. Let's determine the length l_1 under which it happens. The critical force for the middle segment will be

$$P = \frac{4\pi^2 EJ}{l_2^2}, \qquad (l_2 = l - 2l_1).$$

But on the other hand $P = \pi^2 EJ/l_1^2$. Equating these forces we find

$$l_1 = \frac{l}{4}, \quad P = \frac{16\pi^2 EJ}{l^2}.$$

When the middle segment is bent, l_1 changes its value stepwise and becomes equal to $l/6$. Considering now each one-third of the rod as the new independent rod, we can keep the above-derived equations by substituting l for $l/3$. From equation (4) we arrive at

$$l_1 = \frac{l}{6}, \quad P = \frac{36\pi^2 EJ}{l^2}.$$

It means that for

$$P > \frac{36\pi^2 EJ}{l^2}$$

adjacency to the walls along the segment begins again.

For

$$\frac{16\pi^2 EJ}{l^2} < P < \frac{36\pi^2 EJ}{l^2}$$

the rod touches the walls at three points.

During unloading the rod will move away from the upper wall not under the force value $P = 16\pi^2 EJ/l^2$, but, obviously, under $P = 9\pi^2 EJ/l^2$.

The rod's main equilibrium modes are shown in Fig. 345 where the intervals of force variation under loading and unloading are given also.

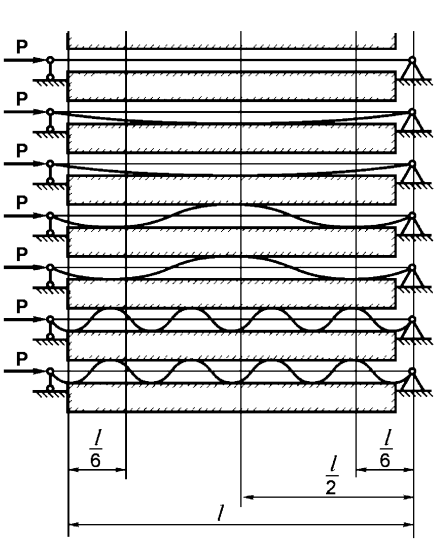

Loading	Unloading
$P \leqslant \frac{\pi^2 EJ}{l^2}$	$P \leqslant \frac{\pi^2 EJ}{l^2}$
$\frac{\pi^2 EJ}{l^2} \leqslant P \leqslant \frac{4\pi^2 EJ}{l^2}$	$\frac{\pi^2 EJ}{l^2} \leqslant P \leqslant \frac{4\pi^2 EJ}{l^2}$
$\frac{4\pi^2 EJ}{l^2} \leqslant P \leqslant \frac{16\pi^2 EJ}{l^2}$	$\frac{4\pi^2 EJ}{l^2} \leqslant P \leqslant \frac{9\pi^2 EJ}{l^2}$
$\frac{16\pi^2 EJ}{l^2} \leqslant P \leqslant \frac{36\pi^2 EJ}{l^2}$	$\frac{9\pi^2 EJ}{l^2} \leqslant P \leqslant \frac{36\pi^2 EJ}{l^2}$
$\frac{36\pi^2 EJ}{l^2} \leqslant P \leqslant \frac{144\pi^2 EJ}{l^2}$	$\frac{36\pi^2 EJ}{l^2} \leqslant P \leqslant \frac{81\pi^2 EJ}{l^2}$
$\frac{144\pi^2 EJ}{l^2} \leqslant P \leqslant \frac{324\pi^2 EJ}{l^2}$	$\frac{81\pi^2 EJ}{l^2} \leqslant P \leqslant \frac{324\pi^2 EJ}{l^2}$
$\frac{324\pi^2 EJ}{l^2} \leqslant P \leqslant \frac{1296\pi^2 EJ}{l^2}$	$\frac{324\pi^2 EJ}{l^2} \leqslant P \leqslant \frac{729\pi^2 EJ}{l^2}$

Fig. 345

For any values of force P the bent segments of the rod between the inflection point and the neighbour point of adjoining to the wall have the length l_1 and are described by expression (3), derived for the left end segment. The bending moment

$$EJy'' = -EJ\frac{\Delta\pi}{l_1^2}\sin\alpha x$$

has maximal value $M_{\max} = EJ\Delta\pi/l_1^2$.

The maximum stress is equal to

$$\sigma_{\max} = \frac{P}{A} + \frac{EJ\Delta\,\pi}{l_1^2 W}$$

where W is the section modulus.

If the rod has circular cross-section then

$$\sigma_{\max} = \frac{4P}{\pi d^2} + \Delta\frac{\pi}{2}\frac{Ed}{l_1^2}. \tag{5}$$

Let's consider two examples:

1) Suppose that compressive force P is equal to

$$\frac{30\pi^2 EJ}{l^2}.$$

It is seen from the plots (Fig. 345) that under the condition

$$\frac{16\pi^2 EJ}{l^2} \leq P \leq \frac{36\pi^2 EJ}{l^2} \qquad l_1 = const = \frac{l}{6}.$$

It follows from relation (5) that

$$\sigma_{\max} = \frac{3\pi dE}{8l^2}(5\pi d + 48\Delta).$$

2) Let's suppose that the force is $P = 49\pi^2 EJ/l^2$. For the interval

$$\frac{36\pi^2 EJ}{l^2} \le P \le \frac{144\pi^2 EJ}{l^2}$$

l_1 depends upon P. Hence according to expression (2)

$$l_1 = \frac{\pi}{\sqrt{\frac{P}{EJ}}} = \frac{l}{7}.$$

Then it follows from relation (5) that

$$\sigma_{\max} = \frac{49\,\pi dE}{16l^2}(\pi d + 8\Delta).$$

126. The problem concerns the spatial bending of rods and is essentially more difficult than the previous one. Moreover, it is one of the most complicated problems presented in this book.

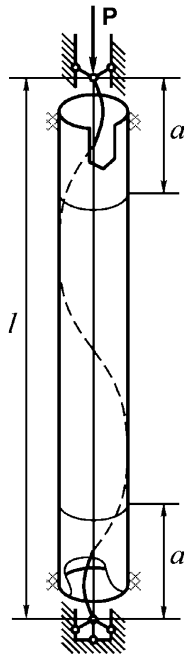

Fig. 346

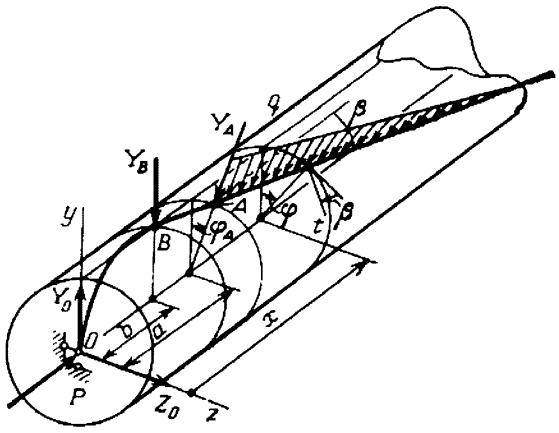

Fig. 347

Under Euler force P_e the rod, as it should be, bends by the sinusoidal half-wave and is pressed to the tube at the mid-point of the rod span. As the compressive force increases, the deflection curve obtains bicurvature and the spiral line (as shown in Fig. 346) begins to form in the middle part and later

develops more. If the compressive force increases, the length of the end spans a decreases and the number of coils in the middle part increases. The shape of the deflection curve is uniquely determined by the force P, and it can be considered to be the same as for loading and unloading of the rod if friction is small.

The main difficulty of this problem solving consists in revealing the mechanism of the rod's adjacency to the tube: how many contact points exist, where are they situated and in what order do they change each other.

It is not convenient to trace this sequence in the process of the force gradual growth, but quite the contrary. Let's suppose that the rod is compressed by the force that considerably exceeds Euler force and then this force gradually decreases.

The solutions of the previously discussed problems 59, 60, 64 lead to the idea that the uniformly distributed contact load of intensity q arises along the formed spiral line, i.e. at the middle part of the rod (Fig. 347). At the ends of this segment (point A) the concentrated force Y_a probably arises as in problems 59 and 64. Then it is necessary to draw the deflection curve from the point A to the hinge support O. And this was found to be correct. But as a result of attempts to derive the desired equations we find that one more contact point, namely point B, must exist between points A and O. The reaction at this point is Y_B .

Let the point O be the coordinates' origin. The y-axis is drawn parallel to the force Y_B, and the reaction of the hinged support is resolved along the axes y and z into components Y_O and Z_O. The unknowns in this scheme are forces Y_O, Y_A, Y_B, Z_0, the distributed load q, lengths of the spans a and b, and also the angles: φ_A and the angle of the spiral line β. The load P and the clearance between rod and tube Δ are considered to be given.

The bending moment in the cross-section $x > a$ is derived as the sum of the moments produced by the forces with respect to the axis t that is perpendicular to the rod's axial line (Fig. 347).

$$\begin{aligned} M = {} & Y_0(x\cos\varphi\cos\beta + \Delta\sin\varphi\sin\beta) \\ & - Y_B(x-b)\cos\varphi\cos\beta - Y_B\Delta\sin\varphi\sin\beta \\ & - Y_A(x-a)\cos(\varphi-\varphi_A)\cos\beta - Y_A\Delta\sin(\varphi-\varphi_A)\sin\beta \\ & + Z_O x\sin\varphi\cos\beta - Z_o\Delta\cos\varphi\sin\beta - P\Delta\cos\varphi - M_q \end{aligned} \tag{1}$$

The last summand in the equation is the moment of load q, distributed along the segment AC, and can be found by integration of the elementary moment:

$$dM_q = q\,ds\,(x-\zeta)\cos(\varphi-\psi)\cos\beta + q\,ds\,\Delta\sin(\varphi-\psi)\sin\beta,$$

where the element of the helical line arc is $ds = d\zeta/\cos\beta$.

The expression for the moment can be written as follows:

$$M_q = \frac{q}{\cos\beta}\int_a^x [(x-\zeta)\cos(\varphi-\psi)\cos\beta + \Delta\sin(\varphi-\psi)\sin\beta]\,d\zeta.$$

As $\Delta\, d\psi = d\zeta \tan\beta$, then

$$M_q = \frac{q\Delta}{\sin\beta} \int_{\varphi_A}^{\varphi} [(x-\zeta)\cos(\varphi-\psi)\cos\beta + \Delta\sin(\varphi-\psi)\sin\beta]\, d\psi.$$

Integrating by parts we obtain

$$M_q = q\Delta\left\{(x-a)\sin(\varphi-\varphi_A)\cot\beta + \Delta\,[1-\cos(\varphi-\varphi_A)]\,(1-\cot^2\beta)\right\} \quad (2)$$

As the curvature of the helical line is constant, the bending moment M defined by (1) must be constant along the length, too. But there are four types of variables in its expression: $x\cos\varphi$, $x\sin\varphi$, $\cos\varphi$, $\sin\varphi$. They ought to be grouped, and the coefficients near each of them must be equated to zero. Thus we arrive at the following four equations:

$$Y_O - Y_B - Y_A\cos\varphi_A + \frac{q\Delta}{\sin\beta}\sin\varphi_A = 0,$$

$$Y_A\sin\varphi_A - Z_O + \frac{q\Delta}{\sin\beta}\cos\varphi_A = 0,$$

$$Y_B b + Y_A a\cos\varphi_A + Y_A\Delta\sin\varphi_A\tan\beta - Z_O\Delta\tan\beta - \frac{q\Delta}{\cos\beta}\left[a\sin\varphi_A\cot\beta - \Delta\left(1-\cot^2\beta\right)\cos\varphi_A\right] = 0,$$

$$Y_O - Y_B + Y_A\left(\frac{a}{\Delta}\sin\varphi_A\cot\beta - \cos\varphi_A\right) + \frac{q\Delta}{\sin\beta}\left[\frac{a}{\Delta}\cos\varphi_A\cot\beta + \left(1-\cot^2\beta\right)\sin\varphi_A\right] = 0.$$

By solving the equations jointly we have

$$\begin{aligned}
Y_O &= \frac{q\Delta}{\sin\beta}\frac{1}{\sin\varphi_A}\left(\frac{a}{b} - 1 + \frac{\Delta}{a}\sin\varphi_A\cos\varphi_A\cot\beta\right),\\
Y_B &= \frac{q\Delta}{\sin\beta}\frac{a}{b}\frac{1}{\sin\varphi_A},\\
Y_A &= \frac{q\Delta}{\sin\beta}\left(\frac{\Delta}{a}\cot\beta - \cot\varphi_A\right), \qquad (3)\\
Z_O &= \frac{q\Delta}{\sin\beta}\frac{\Delta}{a}\sin\varphi_A\cot\beta.
\end{aligned}$$

If these conditions are fulfilled the bending moment M (1) is independent of the coordinate s along the helical line and is equal to

$$M = -q\Delta^2(1-\cot^2\beta) - P\Delta\cos\beta.$$

It's value is related to the curvature of the helical line $\sin^2\beta/\Delta$ by the obvious expression

$$M = -EJ\frac{1}{\Delta}\sin^2\beta.$$

Assuming β to be small, we obtain

$$q\Delta = P\beta^2 - EJ\beta^4/\Delta^2 . \tag{4}$$

Let's exclude q in equations (3). Then we have

$$\begin{aligned}
\frac{Y_0}{k^2EJ} &= (1-\frac{\beta^2}{k^2\Delta^2})\frac{1}{\sin\varphi_A}\left[\left(\frac{a}{b}-1\right)\beta+\frac{\Delta}{a}\sin\varphi_A\cos\varphi_A\right],\\
\frac{Y_B}{k^2EJ} &= \frac{a\beta}{b\sin\varphi_A}\left(1-\frac{\beta^2}{k^2\Delta^2}\right), \qquad (5)\\
\frac{Y_A}{k^2EJ} &= \left(1-\frac{\beta^2}{k^2\Delta^2}\right)\left(\frac{\Delta}{a}-\beta\cot\varphi_A\right),\\
\frac{Z_0}{k^2EJ} &= \frac{\Delta}{a}\left(1-\frac{\beta^2}{k^2\Delta^2}\right)\sin\varphi_A ,
\end{aligned}$$

where

$$k^2 = P/(EJ) . \tag{6}$$

Now we should only smoothly "draw" the helical line from point A through point B to the support O.

Differential equations of the deflection curve at the segment OB are:

$$\begin{aligned}
EJy_1'' &= -Py_1 + Y_0x ,\\
EJz_1'' &= -Pz_1 + Z_0x .
\end{aligned}$$

Solving them, we obtain

$$\begin{aligned}
y_1 &= C_1\sin kx + C_2\cos kx + \frac{Y_0}{k^2EJ}x ,\\
z_1 &= C_3\sin kx + C_4\cos kx + \frac{Z_0}{k^2EJ}x .
\end{aligned}$$

The functions are the same but the boundary conditions are different:

$$\begin{aligned}
&at \quad x=0: \qquad y_1 = 0 ,\ z_1 = 0 ,\\
&at \quad x=b: \qquad y_1 = \Delta ,\ y_1' = 0, z_1 = 0 .
\end{aligned}$$

From these five conditions we can derive not only four constants but force Y_0, also. As a result we have

$$y_1 = \Delta\frac{kx\cos kb - \sin kx}{kb\cos kb - \sin kb} , \qquad z_1 = \frac{Z_0\,b}{k^2EJ}\left(\frac{x}{b}-\frac{\sin kx}{\sin kb}\right), \tag{7}$$

$$\frac{Y_o}{k^2EJ} = \Delta\frac{k\cos kb}{kb\cos kb - \sin kb} . \tag{8}$$

Function z_1 without changing is valid at section AB, and function y for this section (now y_2) is determined from the solution of the new equation

$$EJy_2'' = -Py_2 + Y_0x - Y_B(x-b) ,$$

whence

$$y_2 = C_5 \sin kx + C_6 \cos kx + \frac{Y_0}{k^2 EJ}\, x - \frac{Y_B}{k^2 EJ}\,(x-b)\,.$$

Now function y_2, as y_1 also, should be equal to Δ at the point $x = b$, and its derivative must vanish. It may be rewritten as function y_1 but adding the component corresponding to the force Y_B:

$$y_2 = \Delta \frac{kx\cos kb - \sin kx}{kb\cos kb - \sin kb} - \frac{Y_B}{k^2 EJ}\left[(x-b) - \frac{1}{k}\sin k(x-b)\right]. \qquad (9)$$

We only have to satisfy the deflection curve junction conditions at the cross-section A. Here at $x = a$:

$$y_2 \cos\varphi_A + z_1 \sin\varphi_A = \Delta\,, \quad y_2' = -\beta \sin\varphi_A\,, \quad z_1' = \beta\cos\varphi_A\,,$$

and in addition we equate the relations (3) and (8) for Y_0 .

Eliminating by equations (3) the forces Z_o and Y_B after simple transformation we obtain four equations

$$\frac{ka\cos kb - \sin ka}{kb\cos kb - \sin kb} \times \cos\varphi_A + \beta_0(1-\beta_0^2)\frac{ka}{kb}\left[\sin k\,(a-b) - k\,(a-b)\right]$$
$$\times \cot\varphi_A + \left(1-\beta_0^2\right)\left(\frac{kb}{ka}\frac{\sin ka}{\sin kb} - 1\right)\sin^2\varphi_A - 1 = 0\,,$$

$$\frac{\cos kb - \cos ka}{kb\cos kb - \sin kb} + \beta_0\left(1-\beta_0^2\right)\frac{ka}{kb}\left[\cos k\,(a-b) - 1\right]$$
$$\times \frac{1}{\sin\varphi_A} + \beta_0 \sin\varphi_A = 0\,,$$

$$\frac{kb}{ka}\left(1-\beta_0^2\right)\left(\frac{\cos ka}{\sin ka} - \frac{1}{kb}\right)\sin\varphi_A = \beta_0\cos\varphi_A\,, \qquad (10)$$

$$\frac{\cos kb}{kb\cos kb - \sin kb} - \left(1-\beta_0^2\right)\left(\frac{ka}{kb} - 1\right)\frac{\beta_0}{\sin\varphi_A} + \frac{1}{ka}\cos\varphi_A = 0\,,$$

where

$$\beta_0 = \beta/(k\Delta)\,. \qquad (11)$$

We have to find the four unknowns: φ_A, ka, kb, and β_0 from these four transcendental equations.

Only one simplification is possible: to evaluate $\tan\varphi_A$ from the third equation and exclude $\sin\varphi_A$ and $\cos\varphi_A$. Nevertheless we must solve three transcendental equations simultaneously. But at the same time there is one favorable circumstance. Equations should be solved only once. They do not include freely varying parameters. The prescribed force P and clearance Δ enter into ka, kb, and β_0 and their influence becomes clear after the system is solved.

Numerical solution of the equations can be fulfilled by various methods, but in all the cases it is necessary to know roughly the domain of unknowns.

The guide we can use in the search is the approximate solution of the same problem. It can be found from the minimum condition of the system's potential energy:

$$U = \frac{1}{2}\int EJy''^2 dx - P\frac{1}{2}\int y'^2 dx\,.$$

Let's assume that not only the middle part of the rod is the helical line, but the segment AB also. The transition curve equation at the segment OB can be written as:

$$y = \Delta\left(\frac{1}{\pi}\sin\frac{\pi x}{b} + \frac{x}{b}\right).$$

The first and the second derivatives of the function can be substituted in the potential energy expression. For the helical line segment

$$y' = \beta, \quad y'' = -\beta^2/\Delta\,.$$

Integrating we obtain the functional U that has its minimum at values $kb \approx 2.29$ and $\beta_o = \sqrt{2}/2$. Such initial approximation has become very useful and sufficiently accurate. Solving numerically the system of equations (10) we get

$ak = 4.8098\,, \quad bk = 2.5824\,, \quad \beta_0 = 0.71146\,,$
$\tan\varphi_A = 13.154\,, \quad \varphi_A = 1.4949 = 85.65^o.$

If we return to the expressions (5),(6), and (11) we obtain

$$a = 4.8098\sqrt{\frac{EJ}{P}}, \quad b = 2.5824\sqrt{\frac{EJ}{P}}, \quad \beta = 0.71146\sqrt{\frac{P\Delta^2}{EJ}},$$

$$Y_0 = 0.31170P\sqrt{\frac{P\Delta^2}{EJ}}, \quad Y_B = 0.65626P\sqrt{\frac{P\Delta^2}{EJ}},$$

$$Y_A = 0.075696P\sqrt{\frac{P\Delta^2}{EJ}},$$

$$Z_O = 0.10237\sqrt{\frac{P\Delta^2}{EJ}}, \quad q = 0.24996\,\frac{P^2\Delta}{EJ}.$$

As it is seen from the above relations the magnitudes of the sought parameters do not depend upon the length of the rod. Naturally the forces arising near one end of the rod do not depend upon the things happening at the other end. The segment of full adjoining separates the end spans by an insuperable obstacle.

However, the obtained solution validity limits depend upon the rod length. If it is small or the force P is not great enough, then the segment of full adjoining degenerates into the point and $a = l/2$. It means that the obtained solution remains correct if

$$a = 4.8098\sqrt{\frac{EJ}{P}} < \frac{l}{2} \tag{12}$$

or

$$P > 9.376\, P_e\,.$$

If the load is smaller, then the problem must be solved again. Let's discuss the main peculiarities of this solution.

The scheme given in Fig. 347 is the same, but $a = l/2$, so the axis coinciding with the direction of the force Y_A is the axis of skew symmetry for the deflection curve. Hence the moment of the forces Y_o, Y_B, and Z_o with respect to this axis is equal to zero, reflecting the condition of equilibrium:

$$\left[Y_o - Y_B\left(1 - \frac{2b}{l}\right)\right]\sin\varphi_A - Z_o\cos\varphi_A = 0\,.$$

The force Y_A is also found from the equilibrium

$$Y_A = 2\,(Y_o - Y_B)\cos\varphi_A + 2Z_o\sin\varphi_A\,.$$

At $x = l/2$ we have

$$y_1 = \Delta\cos\varphi_A\,, \quad z_1 = \Delta\sin\varphi_A\,, \quad y_1'\cos\varphi_A + z_1'\sin\varphi_A = 0\,. \tag{13}$$

Now we need only to substitute the functions y_1 and z_1 and to transform the obtained equations in order to "hide" the given parameters P and Δ into the dimensionless parameters. It can be done only with the clearance Δ. As regards the given force P, it is kept into the independent parameter

$$k_0 = \sqrt{\frac{Pl^2}{EJ}}.$$

It forces us further to solve the system of transcendental equations many times for the specified values of k_o.

Let's introduce the nondimensional unknown $b_0 = b/l$ and reduce all the forces to the new dimensionless form:

$$\frac{Y_0\,l}{P\Delta} = Y_O^o\,, \quad \frac{Y_b\,l}{P\Delta} = Y_B^o\,, \quad \frac{Y_A\,l}{P\Delta} = Y_A^o\,, \quad \frac{Z_O\,l}{P\Delta} = Z_O^o\,.$$

Applying relations (13), we arrive at:

$$\frac{\frac{1}{2}k_0\cos k_0b_0 - \sin\frac{k_0}{2}}{k_0b_0\cos k_0b_0 - \sin k_0b_o} + Y_B^o\left[\frac{1}{k_o}\sin\left(\frac{1}{2}k_0 - k_0b_0\right) - \frac{1}{2} + b_0\right] = \cos\varphi_A, \tag{14}$$

$$Z_O^o\left(\frac{1}{2} - b_0\frac{\sin\,(k_0/2)}{\sin k_0b_0}\right) = \sin\varphi_A; \tag{15}$$

$$F_1 = k_0\frac{\cos k_0b_0 - \cos\frac{k_0}{2}}{k_0b_0\cos k_0b_0 - \sin k_0b_0}\cos\varphi_A + Y_B^o\left[\cos k_0\left(\frac{1}{2} - b_0\right) - 1\right] \times \cos\varphi_A + Z_O^o\left(1 - k_0b_0\frac{\cos\,(k_0/2)}{\sin k_0b_0}\right)\sin\varphi_A = 0\,; \tag{16}$$

$$F_2 = [Y_O^o - Y_B^o\,(1 - 2b_0)]\sin\varphi_A - Z_O^o\cos\varphi_A = 0\,; \tag{17}$$

$$Y_O^o = \frac{k_0\cos k_0 b_0}{k_0 b_0\cos k_0 b_0 - \sin k_0 b_0}\,; \tag{18}$$

$$Y_A^o = (Y_O^o - Y_B^o)\cos\varphi_A + Z_O^o\sin\varphi_A\,. \tag{19}$$

Here Y_A^o means half of the total force Y_A^o.

The procedure of numerical solution is obvious enough. We specify the value of k_0. It must be slightly less than 9.6 as seen from (12). Let's accept $k_0 = 9.5$. The expected values of the unknowns b_0 and φ_A will be close to 0.25 and 1.43 respectively. This follows from the junction condition of the sought solution with that obtained above.

Then the calculations can proceed. By using Eqs. (14), (15), and (18) we calculate Y_B^o, Y_O^o and Z_O^o, and then the left parts F_1 and F_2 of the equations (16) and (17). Naturally, they do not vanish under accepted values of b_0 and φ_A. That is why the calculation of F_1 and F_2 is carried out two times more. The first one for the shifted b_0 and the second one for the shifted φ_A. When these three values of F_1 and three values of F_2 in the vicinity of the unknown solution are determined the following linear approximation can be written:

$$F_1 = A_{11}b_0 + A_{12}\varphi_A - B_1 = 0,$$
$$F_2 = A_{21}b_0 + A_{22}\varphi_A - B_2 = 0,$$

that is, we determine the coefficients of the linear approximation A_{ij} and B_i of two functions F_1 and F_2. These two relations can be considered as two equations in two unknowns, and the improved values of b_0 and φ_A can be determined from the system. Additionally, the equations (10) have been solved by the same method but with three unknowns.

If the initial approximation was chosen successfully, as is the case, and as we have the neighbour solution then the procedure quickly converges and b_0 and φ_A are calculated with the prescribed accuracy. Further Y_A^o is calculated by (19) and we make a step towards k_0 decreasing. This process continues until the value of Y_A^o changes its sign from plus to minus. It means that the rod looses its contact at the middle point, and we need to derive one more new system of equations for determining conditions of contact at the points B. But before doing this let's quote the results of our calculations. The force Y_A^o becomes equal to zero under $k_0 = 8.807$. It means that when

$$\sqrt{\frac{Pl^2}{EJ}} < 8.807 \quad \text{or} \quad P < 7.859\,P_e,$$

the rod at the middle point A has no contact with the tube.

Let's analyze now the solution for the new stage of loading, or more correctly for unloading, because our analysis proceeds towards the load P decreasing. At this new stage the contact of the rod with the tube takes place at point B, and at the middle point A the contact is absent.

The Eqs. (16), (17), and (18) remain unchanged, in relation (19) the force Y_A^o is supposed to be equal to zero, and Eqs. (14) and (15) are replaced with the new equation, expressing the fact that point A of the rod axis permanently lies at the former force Y_A^o action line, i.e. at the normal to the point of the former contact:

$$y_1 \sin\varphi_A = z_1 \cos\varphi_A \qquad (x = l/2).$$

As a result we obtain

$$Y_O^o = \frac{k_0 \cos k_0 b_0}{k_0 b_0 \cos k_0 b_0 - \sin k_0 b_0}, \quad Z_O^o = Y_O^o \frac{b_0 \sin 2\varphi_A}{1 - 2b_0 \sin^2 \varphi_A},$$

$$Y_B^o = Y_O^o + Z_O^o \tan\varphi_A,$$

$$F_1 = \left\{ k_0 \frac{\cos k_0 b_0 - \cos\dfrac{k_0}{2}}{k_0 b_0 \cos k_0 b_0 - \sin k_0 b_0} + Y_B^o \left[\cos k_0 \left(\frac{1}{2} - b_0 \right) - 1 \right] \right\}$$
$$\times \cos\varphi_A \sin k_0 b_0 + Z_O^o \left(\sin k_0 b_0 - k_0 b_0 \cos\frac{k_0}{2} \right) \sin\varphi_A = 0,$$

$$F_2 = \left\{ \frac{\dfrac{k_0}{2} \cos k_0 b_0 - \sin\dfrac{k_0}{2}}{k_0 b_0 \cos k_0 b_0 - \sin k_0 b_0} + Y_B^o \left[\frac{1}{k_o} \sin k_0 \left(\frac{1}{2} - b_0 \right) - \frac{1}{2} + b_0 \right] \right\}$$
$$\times \sin\varphi_A \sin k_0 b_0 - Z_O^o \left(\frac{1}{2} \sin k_0 b_0 - b_0 \sin\frac{k_0}{2} \right) \cos\varphi_A = 0.$$

The equations' solution shows, that while the load P decreases to the value $4P_e$, the two contact points B merge in one, lying at the middle of the span.

Let's analyze the result considering the process of the rod's natural loading. The beginning is obvious. Until $P < P_e$ the rod keeps its straight form. Under $P = P_e$ the rod bends and contacts the tube at the only one point disposed in the middle of the rod span.

Under $P = 4P_e$ the deflection curve obtains a spatial form. The rod buckles sideways, and the contact point splits into two which move away from each other as force increases. The rod's middle point leaves the channel surface, at first moves off it, and later approaches it again, and once more contacts the tube under the load $P = 7.859P_e$. Further the three-point contact scheme is kept until $P = 9.376P_e$, and then the helical line with the segment of full adjacency to the tube's surface near the middle point of contact is initiated.

Now it is not very difficult to determine the bending stresses in the rod. The rod has maximal curvature at the helical segment. Hence

$$\sigma_b = E \frac{d}{2\rho} = E \frac{d\beta^2}{2\Delta},$$

where d is the diameter of the rod's cross-section.

The angle β is known. It is equal to $0.71146\sqrt{\frac{P\Delta^2}{EJ}}$. Hence $\sigma_b = 5.16\frac{P\Delta}{d^3}$

127. The points of inflexion of the rod deflection curve (Fig. 348) separate it into sections having rigidities $EJ_1$and EJ_2. The length of segment l_1 is derived from the condition of critical force equality for both segments. Obviously,

$$P_{cr} = \frac{\pi^2 EJ_1}{4l_1^2} = \frac{\pi^2 EJ_2}{(l-2l_1)^2}\,, \tag{1}$$

whence

$$l_1 = \frac{l}{2}\frac{\sqrt{k}}{\sqrt{k}+1}\,,$$

where

$$k = \frac{EJ_1}{EJ_2}\,.$$

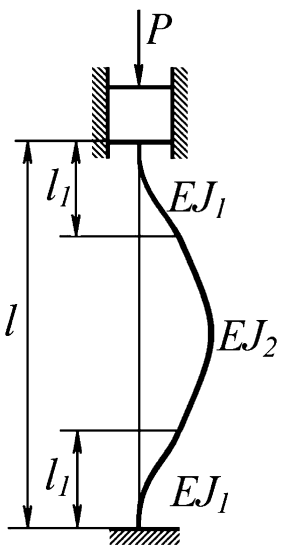

Fig. 348

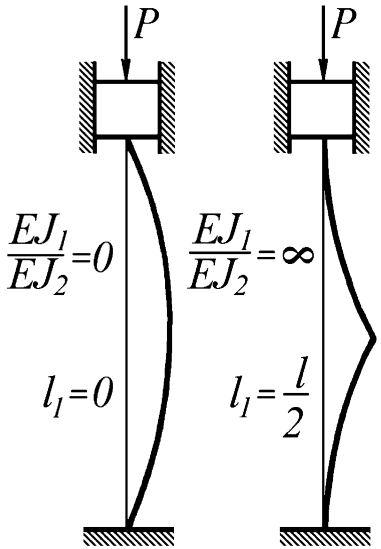

Fig. 349

If $k = 1$ then, as it should be expected, $l_1 = l/4$. For $k = 0$ we have $l_1 = 0$, and for $k = \infty$ we obtain $l_1 = l/2$. The bent rod deflection curve modes for these particular cases are shown in Fig. 349. The critical force is derived from expression (1) by eliminating l_1:

$$P_{cr} = \frac{\pi^2 EJ_1}{l^2}\frac{\left(1+\sqrt{k}\right)^2}{k} \tag{2}$$

If the rod under buckling bulges in the opposite direction, i.e. not rightward but to the left, then we have to interchange the rigidities EJ_1 and EJ_2 in the obtained expressions. The magnitude of l_1 changes also, but the critical force remains the same. Actually, if the rod bulges to the left the interchange of EJ_1 on EJ_2 gives

$$P_{cr} = \frac{\pi^2 EJ_2}{l^2} \frac{\left(1 + \sqrt{1/k}\right)^2}{1/k}$$

which leads to expression (2).

A subtlety is hidden in the problem. If the rod really has opening slots in its construction, as it is shown in the problem set as a possible variant, then an ordinary stability problem can become a special one. While opening of the slots the central axis of the cross-section moves stepwise to a new position, and at the point of the supposed inflection the small but finite jump of bending moment arises under arbitrarily small rod flexure. This special question is analyzed further by easier examples, such as problem 141 and some others.

128. It is seen from Fig. 350 that the position of weight does not change if the rod deflects from vertical. Force P does not produce work. The stability of the straight equilibrium state is maintained under any P.

129. Here the rod naturally looses its stability under $P = \pi^2 EJ/(4l^2)$, differently to the previous case.

Until the rope has not lied on the wall of the tube, i.e. until the deflection f has not exceeded Δ, the relation between P and f is expressed by the straight-line segment (Fig. 352)

$$P = \frac{\pi^2 EJ}{4l^2} = const\,.$$

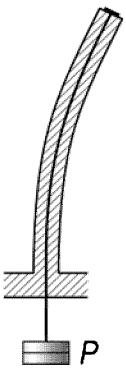

Fig. 350

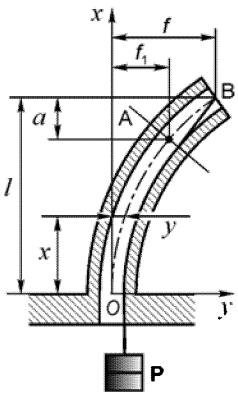

Fig. 351

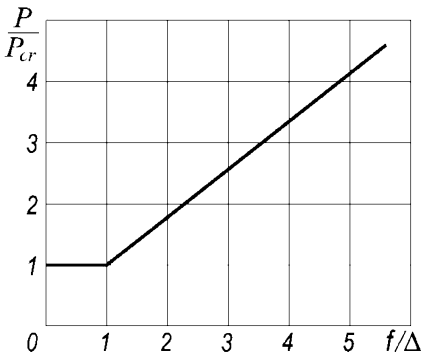

Fig. 352

The bending deflection is unknown. Deflections from the straight line can be found only by the theory considering large displacements. A curious

peculiarity of the problem consists in the fact that under growing deflections further displacement f is determined on the base of ordinary linear theory.

After the section of the rope has lied on the bent wall of the tube we have two segments: OA and AB (Fig. 351).

The bending moment at the segment OA is equal to $P\Delta$, and the tube bends by the second-order curve

$$y = \frac{P\Delta}{2EJ}x^2.$$

The deflection of point A will be

$$f_1 = \frac{P\Delta}{2EJ}(l-a)^2.$$

If the rod at the segment AB does not bend, then the displacement of point B would be as follows:

$$\frac{P\Delta}{2EJ}(l-a)^2 + y'_{x=l-a}a = \frac{P\Delta}{2EJ}(l-a)^2 + \frac{P\Delta}{EJ}(l-a)a.$$

But the second segment is bent exactly as much as necessary for point B to deflect from the tangent AB by Δ. Hence,

$$f = \frac{P\Delta}{2EJ}(l-a)^2 + \frac{P\Delta}{EJ}(l-a)a + \Delta,$$

or

$$f = \frac{P\Delta}{2EJ}\left(l^2 - a^2\right) + \Delta.$$

The magnitude of a is the length of the rod clamped by one end, which buckles under force P, i.e.

$$P = \frac{\pi^2 EJ}{4a^2}$$

Hence,

$$a^2 = \frac{\pi^2 EJ}{4P}$$

and then

$$f = \Delta\left(\frac{Pl^2}{2EJ} - \frac{\pi^2}{8} + 1\right)$$

or

$$\frac{f}{\Delta} = \frac{\pi^2}{8}\left(\frac{P}{P_e} - 1\right) + 1,$$

where $P_e = \frac{\pi^2 EJ}{4l^2.}$. The deflection f dependence upon force P is shown in Fig. 352.

130. In the second case critical force will be four times greater than in the first one. It is enough to consider the bent column for both cases (Fig. 353) to ascertain this result.

For the first case

$$P_{cr} = \frac{\pi^2 EJ}{4l^2}.$$

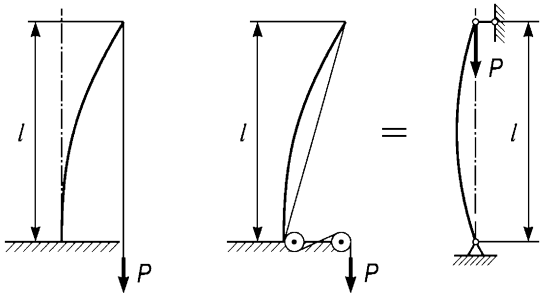

Fig. 353

The force direction in the second case crosses the lower beam's end (follows it) during bending. As a result, the bending moment at the clamped end is permanently equal to zero. Therefore, the second case of column loading has no difference with the case of the rod hinged at both ends (Fig. 353). That is the reason why here $P_{cr} = \pi^2 EJ/l^2$.

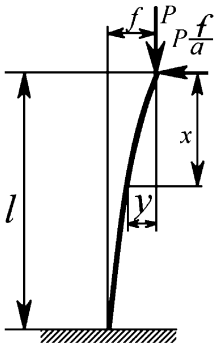

Fig. 354

131. Let's decompose force P into vertical and horizontal components (Fig. 354) :

$$P_v \approx P\,, \quad P_h \approx P\,\frac{f}{a}$$

and write the equation of the beam deflection curve as:

$$EJy'' = -Py + P\,\frac{f}{a}\,x.$$

Let's denote $\dfrac{P}{EJ} = \alpha^2$. Then the equation and its solution will be

$$y'' + \alpha^2 = \alpha^2 \frac{f}{a}\, x\,,$$

$$y = A \sin \alpha x + B \cos \alpha x + \frac{f}{a}\, x\,.$$

In order to derive A, B and f we have the next boundary conditions

$$\text{at} \quad x = 0 \quad y = 0\,, \quad \text{at} \quad x = l \quad y = f\,, \quad y' = 0\,,$$

whence

$$B = 0\,, \quad A \sin \alpha l + \frac{f}{a}\, l = f\,, \quad A\alpha \cos \alpha l + \frac{f}{a} = 0\,.$$

The critical value of force P is found from the following transcendental equation:

$$\tan \alpha l = \alpha l \left(1 - \frac{a}{l}\right). \tag{1}$$

If $a = \infty$ (the first case of the previous problem),

$$\alpha l = \frac{\pi}{2}, \quad P_{cr} = \frac{\pi^2 EJ}{4l^2}.$$

If $a = l$ (the second case of the previous problem),

$$\alpha l = \pi\,, \quad P_{cr} = \frac{\pi^2 EJ}{l^2}.$$

For $a = 0$ the force action line permanently crosses the initial vertical at point $x = 0$. It is possible only for the case when the rod's upper end does not move (Fig. 355). Thus

$$\tan \alpha l = \alpha l\,, \quad \alpha l = 4.49\,, \quad P_{cr} = 20.19 \frac{EJ}{l^2}.$$

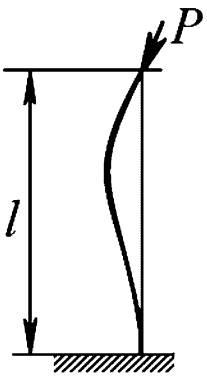

Fig. 355

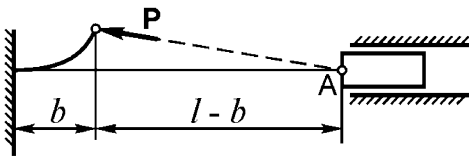

Fig. 356

132. After analysis of the previous two problems the correct solution of the given problem does not cause any difficulties.

The left rod of length b is under action of rotating compressive force (Fig. 356), the action line of which permanently passes through point A. That is the reason why the critical force for the left rod will not be $\pi^2 EJ/(4b^2)$ as it seems at first glance. It must be found from the transcendental equation (1) solution of the previous problem if we replace in it l with b, and a with $-(l-b)$, i.e. $\tan \alpha b = \alpha l$, where $\alpha = \sqrt{P/(EJ)}$.

The critical force for the right rod is

$$P_{cr} = \frac{\pi^2 EJ}{(l-b)^2}$$

The stability safety factor of the rods will be the same if critical forces are equal. Therefore

$$\alpha = \sqrt{\frac{P_{cr}}{EJ}} = \frac{\pi}{l-b}, \quad \tan\frac{\pi b}{l-b} = \frac{\pi l}{l-b}.$$

From this relation we derive the sought ratio b/l :

$$\tan\frac{\pi b/l}{1-b/l} = \frac{\pi}{1-b/l}, \quad \frac{b}{l} = 0.301.$$

133. It is not necessary to consider the contact pressure between rod and rope for critical force determination.

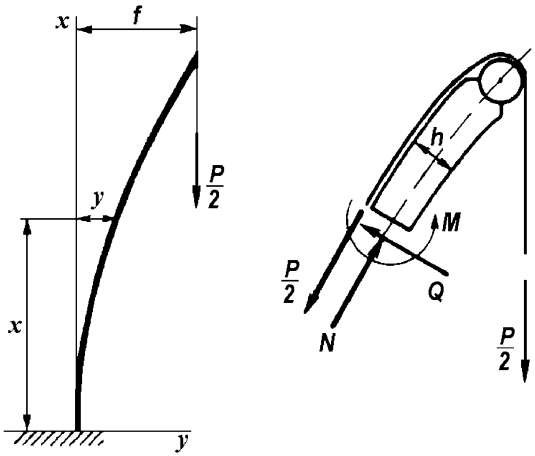

Fig. 357

We cut the part of the rod (Fig. 357) and determine the bending moment

$$M = \frac{P}{2}\left(f - y + \frac{h}{2}\right) - \frac{P}{2}\frac{h}{2},$$

where $h/2$ is half of the rod thickness. Hence

$$EJy'' = \frac{P}{2}(f - y)\,.$$

Thus we have the ordinary case of a clamped rod loaded by force $P/2$:

$$\left(\frac{P}{2}\right)_{cr} = \frac{\pi^2 EJ}{4l^2}\,.$$

134. Let's consider the equilibrium condition for the ring's bent element of length ds (Fig. 358).

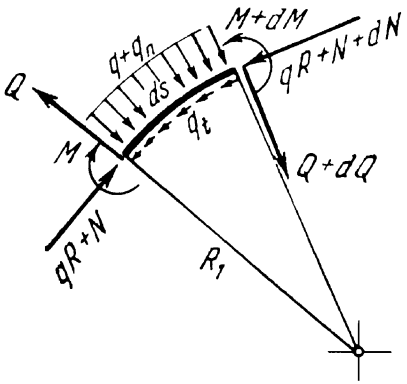

Fig. 358

Bending moment M, shear force Q, and normal force arise in the ring's cross-section. Normal force is presented as a sum of undercritical force qR and its small increment N. One or another peculiarity of external load q behavior is taken into consideration by introduction of normal q_n and tangential q_t components. In detail, if a ring is loaded by forces of gas or liquid pressure: $q_n = q_t = 0$. The new local curvature radius of the element is denoted as R_1

$$\frac{1}{R_1} = \frac{1}{R} - \varkappa \tag{1}$$

where $\varkappa$ is the variation of the ring arc curvature.

The element's equilibrium equations are:

$$Q = \frac{dM}{ds}, \quad \frac{dN}{ds} + q_t + \frac{Q}{R_1} = 0\,, \quad q + q_n + \frac{dQ}{ds} - \frac{N + qR}{R_1} = 0\,.$$

Eliminating $1/R_1$ and taking into consideration that $\varkappa$, Q and N are small quantities, we hold only their first orders. Then

$$Q = \frac{dM}{ds}, \quad \frac{dN}{ds} + q_t + \frac{Q}{R} = 0\,, \quad qR\varkappa + q_n + \frac{dQ}{ds} - \frac{N}{R} = 0\,.$$

As $M = EJ\varkappa$, then excluding further N and Q, we obtain

$$EJ\frac{d^3\varkappa}{ds^3}+\left(qR+\frac{EJ}{R^2}\right)\frac{d\varkappa}{ds}+\frac{dq_n}{ds}+\frac{1}{R}q_t=0\,. \qquad (2)$$

Let's assume that the ring is loaded by the pressure, following the surface normal. Then, as mentioned before, $q_n=q_t=0$ and

$$EJ\frac{d^3\varkappa}{ds^3}+\left(qR+\frac{EJ}{R^2}\right)\frac{d\varkappa}{ds}=0\,.$$

If we assume that $\varkappa=A\sin\dfrac{ns}{R}$, we arrive at

$$-EJ\frac{n^3}{R^3}+\left(qR+\frac{EJ}{R^2}\right)\frac{n}{R}=0\,,$$

whence

$$q_{cr}=\frac{(n^2-1)EJ}{R^2}.$$

The quantity q_{cr} has the least nonzero value when $n=2$. As a result we obtain

$$q_{cr}=\frac{3EJ}{R^3}.$$

Now let's discuss the load q application in a different way. Assume that the ring is loaded by radial forces created by the great amount of rubber threads collected in a bundle at the ring center (Fig. 125b). The load q in this case is directed to the center of the ring (follows it). Under the arc's ds rotation the load tangent component q_t arises

$$q_t=q\frac{dw}{ds},$$

where w is radial displacement of the ring points.

If threads are compliant enough or if each thread is pulled independently, then radial displacement w causes no change in the normal component of external forces and, hence, $q_n=0$.

The variation of curvature $\varkappa$ is related to w as follows:

$$\varkappa=\frac{d^2w}{ds^2}+\frac{w}{R^2},$$

and equation (2) takes the form

$$EJ\frac{d^3}{ds^3}\left(\frac{d^2w}{ds^2}+\frac{w}{R^2}\right)+\left(qR+\frac{EJ}{R^2}\right)\frac{d}{ds}\left(\frac{d^2w}{ds^2}+\frac{w}{R^2}\right)+\frac{q}{R}\frac{dw}{ds}=0. \qquad (3)$$

Assuming $w=A\sin\dfrac{ns}{R}$, we get

$$q_{cr}=\frac{\left(n^2-1\right)^2EJ}{(n^2-2)R^3}$$

If $n = 2$

$$q_{cr} = \frac{9EJ}{2R^3},$$

i.e. the critical load turns out to be 1.5 times greater than for the case of hydrostatic loading.

If threads having some stiffness are pulled by one common force (weight), then the redistribution of loads occurs under ring bending. In the regions where threads are additionally tensed the displacement w is positive, and are shortened in those regions where w is negative. When the normal component q_n varies, then we obtain the additional component $q_n = Kw$ in equation (3), where K is the stiffness coefficient of threads. As a result

$$q_{cr} = \frac{EJ}{R^3}\frac{\left(n^2-1\right)^2 + \dfrac{KR^4}{EJ}}{n^2-2}.$$

The increasing of thread stiffness K leads to a rise of critical load; this is obvious. The occurring additional forces are directed in such a way, that they restore the ring's circular form. The lowest critical value of q_{cr} is reached, in general, not when $n = 2$, but under some other integer-valued n, depending upon the magnitude of K.

135. Let's consider the system in the deflected position (Fig. 359)

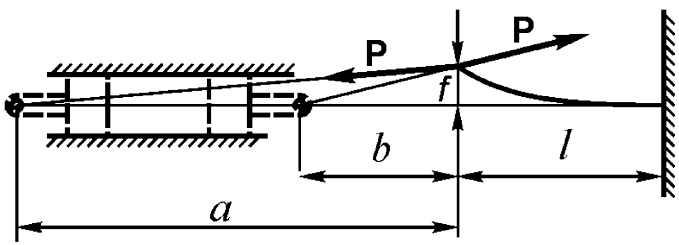

Fig. 359

The length of the connecting rods a is more than the length of con-rod b. That's why the up-directed component of force arises. It is equal to

$$P_1 = P\left(\frac{f}{b} - \frac{f}{a}\right).$$

The deflection f under action of this force will be

$$f = \frac{P_1 l^3}{3EJ}.$$

Excluding P_1 we find the magnitude of the critical force:

$$P_{cr} = \frac{3EJ}{l^3\left(\dfrac{1}{b} - \dfrac{1}{a}\right)}.$$

136. The proposed problem has the same topic as the previous one. Initially the moments are mutually balanced, and the rod is not stressed. However, the moments behave in different ways under system deflection. Under bending in plane xz (Fig. 360) the plane of the moment M_2 rotates in conjunction with the end cross-section. The plane of moment M_1 does not change. Under bending in plane xy the plane of the moment M_2 does not change, but the plane of action of moment M_1 rotates.

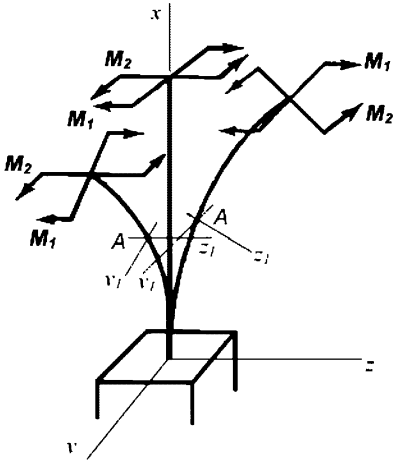

Fig. 360

For simplicity let's accept that the rod bending rigidities in two planes are the same and lengths of ropes by which loads P are transferred are sufficiently great. It allows to consider that rotation of moment M_1 in one plane and M_2 in another plane completely coincides with the rotation of the end section. Let's denote angles of rotation of the cross-section relative to axis y and z correspondingly by φ_y and φ_z. Then the moments in the current cross-section A with respect to the moving coordinates y_1 and y_2 will be

$$M_{y_1} = M_1(\varphi_z - y') + M_2 y',$$
$$M_{z_1} = M_1 z' + M_2(\varphi_y - z').$$

As a result we obtain two equations:

$$EJ_y z'' = M_1(\varphi_z - y') + M_2 y',$$
$$EJ_z y'' = M_1 z' + M_2(\varphi_y - z'). \qquad (1)$$

As $J_y = J_z = J$, and $M_1 = M_2$, then

$$EJz'' = M\varphi_z, \quad EJy'' = M\varphi_y,$$

Whence

$$z = \frac{M}{EJ}\left(\varphi_z \frac{x^2}{2} + A_1 x + B_1\right), \quad y = \frac{M}{EJ}\left(\varphi_y \frac{x^2}{2} + A_2 x + B_2\right).$$

At $x = 0$, $z = 0$ $z' = 0$ $y = 0$ $y' = 0$, therefore $A_1 = A_2 = 0$; $B_1 = B_2 = 0$. At $x = l$, $y' = \varphi_z$ and $z' = \varphi_y$; then

$$\varphi_y = \frac{Ml}{EJ}\varphi_z; \quad \varphi_z = \frac{Ml}{EJ}\varphi_y.$$

It is obvious that φ_y and φ_z are not equal to zero only in the case, if

$$\frac{Ml}{EJ} = \pm 1,$$

that gives the magnitude of the critical moment.

137. Consider equation (1) of the previous problem. Taking $M_1 = M$, and $M_2 = 0$ we arrive at

$$EJ_y z'' = M(\varphi_z - y')$$

$$EJ_z y'' = Mz'.$$

It follows that

$$y = A\sin\alpha x + b\cos\alpha + \varphi_z x + C$$

$$z = \frac{EJ_z}{M}(A\alpha\cos\alpha x - B\alpha\sin\alpha x + \varphi_z + D),$$

where

$$\alpha^2 = \frac{M^2}{EJ_y EJ_z}.$$

At $x = 0$ we have $y = z = 0$, and also $y' = z' = 0$. Then

$$B + C = 0, \quad A\alpha + \varphi_z = 0,$$

$$A\alpha + \varphi_z + D = 0, \quad B\alpha^2 = 0.$$

from which

$$B = C = D = 0.$$

At $x = l$ angle $y' = \varphi_z$. This yields $A\cos\alpha l = 0$. Hence, the critical state takes place when

$$\alpha l = \frac{\pi}{2} \quad \text{or} \quad \frac{Ml}{\sqrt{EJ_y EJ_z}} = \frac{\pi}{2}.$$

The interchange of J_y and J_z does not change the value of the critical moment. Therefore the cases of loading in Fig. 128a and 128b are equivalent.

138. The differential equation of the rod deflection curve (Fig. 361) will be

$$EJy'' = P(f + R\varphi - y),$$

whence

$$y = A\sin\alpha x + B\cos\alpha x + f + R\varphi,$$

where, as usual, $\alpha^2 = \dfrac{P}{EJ}$.

At $x = 0$, $y = 0$ and $y' = 0$.

At $x = l$, $y = f$ and $y' = \varphi$. This yields

$$B + f + R\varphi = 0, \quad A = 0,$$

$$A\sin\alpha l + B\cos\alpha l + R\varphi = 0,$$

$$A\alpha\cos\alpha l - B\alpha\sin\alpha l = \varphi.$$

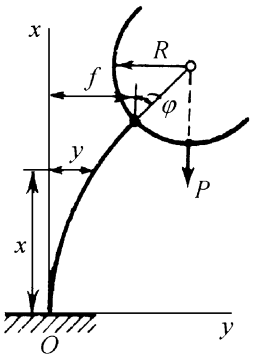

Fig. 361

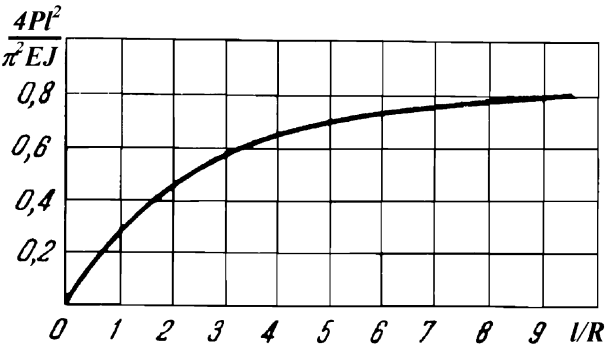

Fig. 362

If we construct the determinant for the system of three equations in unknowns B, f and φ and equate this to zero we arrive at the transcendental equation

$$\frac{l}{R} = \alpha l\tan\alpha l.$$

The dependence of critical force upon l/R is shown in Fig. 362.

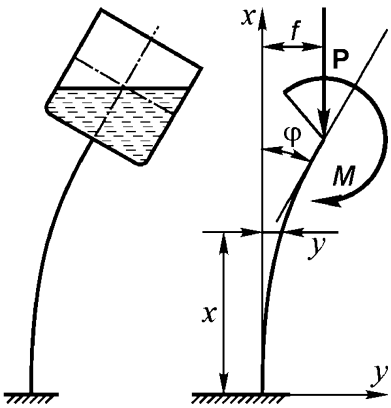

Fig. 363

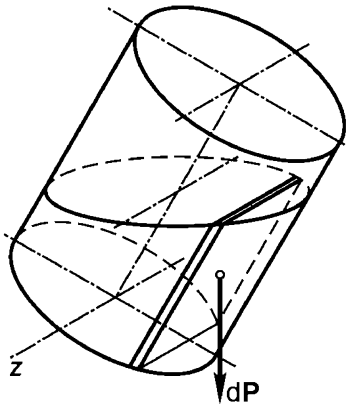

Fig. 364

139. The differential equation of the rod deflection curve (Fig. 363) will be as follows

$$EJy'' = P(f - y) + M. \tag{1}$$

The force P is obviously equal to the weight of the liquid $P = \gamma\pi R^2 h$, where γ is specific weight of liquid.

Moment M is determined by summation of moments of elementary forces dP (Fig. 364) with respect to the axis z. The angle φ of tank rotation is assumed to be small. After integrating we obtain

$$M = \frac{\gamma\pi R^2}{4}\left(2h^2 + R^2\right)\varphi. \tag{2}$$

The solution of equation (1) is

$$y = A\sin\alpha x + B\cos\alpha x + f + \frac{\left(2h^2 + R^2\right)}{4h}\varphi = 0.$$

At $x = 0$, $y = 0$ and $y' = 0$.
At $x = l$, $y = f$ and $y' = \varphi$
The conditions yield

$$B + f + \frac{\left(2h^2 + R^2\right)}{4h}\varphi = 0, \quad A = 0,$$

$$A\sin\alpha l + B\cos\alpha l + \frac{\left(2h^2 + R^2\right)}{4h}\varphi = 0,$$

$$A\alpha\cos\alpha l - B\alpha\sin\alpha l = \varphi.$$

From the last two equations we get

$$\frac{\alpha l\tan\alpha l}{4\dfrac{h}{l}}\left(2\frac{h^2}{l^2} + \frac{R^2}{l^2}\right) = 1.$$

Substituting the value P, we obtain

$$\alpha l = \sqrt{\frac{P}{EJ}}\,l = \sqrt{\frac{\gamma\pi R^2 l^3}{EJ}}\sqrt{\frac{h}{l}}.$$

Then the sought value h/l is determined from the transcendental equation

$$\frac{a}{4}\frac{\tan a\sqrt{\frac{h}{l}}}{\sqrt{\frac{h}{l}}}\left(2\frac{h^2}{l^2} + b^2\right) = 1 \tag{3}$$

and depends on two parameters

$$a = \sqrt{\frac{\gamma\pi R^2 l^3}{EJ}} \quad \text{and} \quad b = \frac{R}{l}.$$

The level of liquid under which the rod buckles can be found for any specific case and depends upon the parameters.

If the contents of the tank did not possess liquidity property, for example if the tank had been filled with sand, the moment M would be smaller than (2), namely:

$$M = \gamma\pi R^2 \frac{h^2}{2}\varphi.$$

This would cause a considerable growth of critical load. The greater the diameter of the tank the greater the difference in critical forces will be as more as . The contents mobility adds to the fact that for the scheme shown in Fig. 365 stability loss is also possible. The critical level of filling h/l is determined from the same transcendental equation (3) by replacing circular tangent (tan) with hyperbolic tangent (tanh).

140. As the bending rigidity in plane xz is large we can consider that in the undercritical state the rod remains straight. Under transition to the adjacent state of equilibrium, bending in plane xy is accompanied by torsion of the rod.

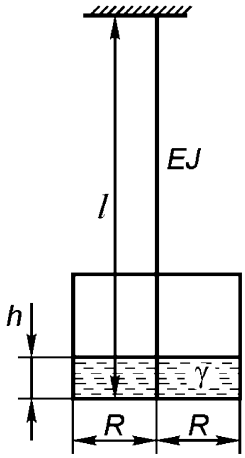

Fig. 365

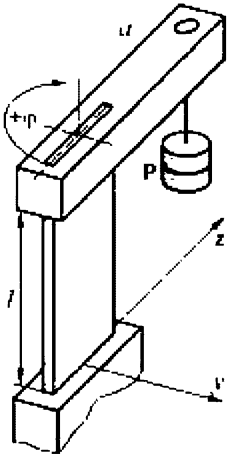

Fig. 366

Let's represent the system given in the problem set in a more general view (Fig. 366) and write the main relations:

$$EJ\,y'' = M_b\,; \quad GJ_t\,\varphi' = M_t\,. \tag{1}$$

The positive direction of angle φ is shown in Fig. 366.

The torsional rigidity GJ_t for the narrow strip, as known, is equal to $Gbh^3/3$. But in the given case, because the rod is compressed, the torsional rigidity decreases, while the compressive force increases (see problem 28). Therefore in the given case

$$GJ_t = Gbh^3/3 - Pb^2/12\,. \tag{2}$$

If we expand the right sides of equations (1), we arrive at the following simple system of differential equations:

$$EJ\,y'' + P\,y = P\,y_l + Pa\,(\varphi_l - \varphi),$$
$$GJ_t\,\varphi' = Pa\,y', \tag{3}$$

where y_l and φ_l are displacement and angle of rotation of the rod's end, i.e. at $x = l$.

Eliminating φ from the first equation, we obtain

$$EJy''' + \left(P + \frac{P^2a^2}{GJ_t}\right) y' = 0,\ y''' + k^2y' = 0,$$

where

$$k^2 = \frac{1}{EJ}\left(P + \frac{P^2a^2}{GJ_t}\right). \tag{4}$$

Thus,

$$y = A\sin kx + B\cos kx + C.$$

For $x = 0$ the displacement y and its derivative y' vanish. Hence,

$$y = C\,(1 - \cos kx)\,,\ \varphi = C\frac{Pa}{GJ_t}\,(1 - \cos kx)\,.$$

Substituting y and φ in equation (3) we prove that the first of them is satisfied either if $C = 0$ either under the condition $\cos kl = 0$, from which $kl = \pi/2$; so from condition (4) we get

$$\frac{l^2}{EJ}\left[P + \frac{P^2a^2}{G\dfrac{bh^3}{3} - \dfrac{Pb^2}{12}}\right] = \frac{\pi^2}{4}.$$

If $a = 0$, then $P_{cr} = \pi^2EJ/(4l^2)$, as expected.

Let's denote:

$$X = \frac{P_{cr}4l^2}{\pi^2EJ}\,,\ A = \frac{8}{\pi^2\,(1+\mu)}\frac{l^2}{b^2}\,,\ \alpha^2 = \frac{a^2}{b^2}\,.$$

Here X is understood as the measure of critical force decrease in comparison with the case of rod central loading.

Now we arrive at

$$X^2(\alpha^2 - \frac{1}{12}) + X(A + \frac{1}{12}) - A = 0\,, \tag{5}$$

or

$$X = \frac{1}{2(\alpha^2 - 1/12)}\left[\sqrt{\left(A - \frac{1}{12}\right)^2 + 4\alpha^2} - A - \frac{1}{12}\right].$$

In the special case of $\alpha^2 = 1/12$, the dimensionless critical force is determined from equation (5) as

$$X = \frac{12A}{12A+1}.$$

141. The given problem touches fundamentally new questions of stability and it can not be solved by ordinary means.

Actually, reducing the compressive forces, shown in Fig. 132c, to the axis of the rod, we obtain the following scheme of loading (Fig. 367).

The rod is compressed by forces P and simultaneously is bent by moments $M = Pe$ acting in the direction opposite to the rotation of the rod ends. The equation of the deflection curve will be

$$EJy'' = -Py + Pe,$$

or

$$y'' + \alpha^2 y = \alpha^2 e, \ (\alpha^2 = \frac{P}{EJ}),$$

whence

$$y = A\sin\alpha x + B\cos\alpha x + e,$$

at $x = 0$ deflection $y = 0$, and for $x = 2l$, too; hence,

$$A = e\frac{\cos 2\alpha l - 1}{\sin 2\alpha l}, \quad B = -e,$$

$$y = e\left[\frac{\cos 2\alpha l - 1}{\sin 2\alpha l}\sin\alpha x - \cos\alpha x + 1\right].$$

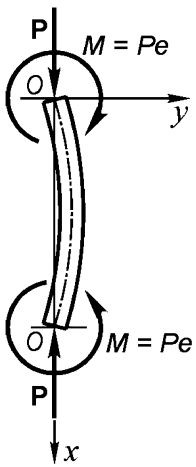

Fig. 367

Thus we determine certain magnitudes of deflections that the rod would have if from the very beginning of loading by the moments Pe a gradual increase with growth of load P would have been applied. So the above calculations do not catch the critical transfer from the rod's straight equilibrium to a curvilinear state, and we obtain in pure form the case of longitudinal-transverse bending.

Let's consider main postulates of stability analysis. An elastic system is called stable if for any infinitely small (emphasize: infinitely small) deviation from the equilibrium state the system itself returns to its initial state.

Such approach, however, does not answer the question, whether the system would return to its initial state if we deflected it "slightly stronger", i.e. apply to the system a small, but finite deflection (not infinitely small) that is greater than some value specified in advance (even if it is a very small value). May it happen that a system under any infinitely small deflection will return to its initial state, and under some small but greater than prescribed magnitude of deflection will not return?

Actually, it may. For example, a ball laying on the top of a sphere in a small hollow (Fig. 368) can serve as a mechanical analogue of the above mentioned. If a small deflection is applied to the ball, it will return to its initial state but if we impart sufficiently great deflection, it will not return to its initial state. If the hollow was absent the state of equilibrium would simply be unstable.

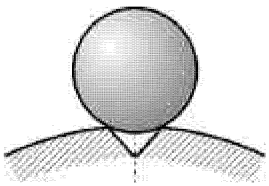

Fig. 368

In such a way we come to the new stability criterion, based on imparting on the system not an infinitely small disturbance, but small ones that are greater than the value prescribed before. Such an evaluation of stability is called the stability criterion "in large quantities". The ordinary criterion of stability, based on imparting to a system an infinitely small displacement, is called a criterion "in small quantities".

This terminology is applied to the stability of elastic systems from the general theory of motion stability and now has become generally accepted.

The rod in the considered example is stable "in small quantities", but not always stable "in large quantities". Actually, if we impart a very small deflection from the straight equilibrium state to the rod then the restoring moment Pe will be greater than the deflecting moment Py (as y can be infinitely small), and after removal of reasons causing the small deflection, the rod will return to its straight equilibrium state. It will take place under

any value of P not exceeding $4\pi^2 EJ/\left(2l^2\right)$, and the rod loses its stability "in small quantities" by the deflection mode, shown in Fig. 132b.

External disturbances (distortion of rod, eccentricity of force application, random impacts) under real conditions always have finite value, and depending on these conditions the rod transfers to a new equilibrium state under action of bigger or smaller force. In the theory of motion stability such a phenomenon is called bifurcation point. Therefore the conception of stability and instability "in large quantities" is inevitably connected with absence or existence of appropriate external excitations.

Stability in large quantities is the extension of the classic scheme that brings it closer to our intuitive-everyday understanding of stability. It is a complex of system properties and disturbances, acting on the system. Therefore the analysis of possible equilibrium states is only part of the stability investigation and does not solve the problem completely. This will be seen by the example of some of the following problem solutions.

Let's return to the given scheme of the compressed column and derive the equations of the deflection curve under large displacements. As these equations are required in further analysis we shall derive them in a more general form than necessary for solution of the considered problem. The derivation is taken from [18].

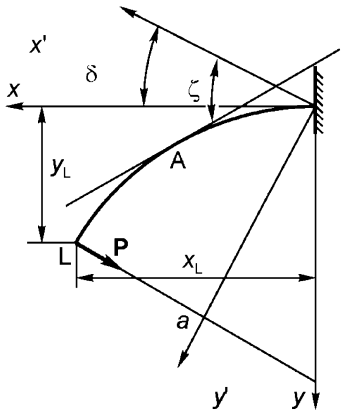

Fig. 369

The segment of the rod strongly bent by force P is shown in Fig. 369. Let's introduce two coordinate systems: the system xy oriented by the tangent and normal to the deflection curve at the rod's clamped end, and the system $x'y'$ oriented by force P.

Let's denote the angle between the direction of force and axis x as δ (in our case $\delta = 0$); and the current angle between the tangent to the arc of the deflection curve and axis x' as ζ.

The curvature of the beam in any arbitrary point will be obviously expressed through the angle ζ as follows:

$$\frac{1}{\rho} = \frac{d\zeta}{ds},$$

where ds is the element of the beam arc. The bending moment in point A is equal to

$$M_b = P(y'_L - y'),$$

where y'_L is the coordinate of point L. Now it is obvious that

$$\frac{d\zeta}{ds} = \frac{P}{EJ}(y'_L - y').$$

Differentiating this equation by s we arrive at:

$$\frac{d^2\zeta}{ds^2} = -\frac{P}{EJ}\frac{dy'}{ds};$$

but $dy'/ds = \sin\zeta$, therefore

$$\frac{d^2\zeta}{ds^2} = -\frac{P}{EJ}\sin\zeta.$$

Let's denote

$$\frac{P}{EJ} = \frac{\beta^2}{l^2}. \tag{1}$$

Then

$$l^2\frac{d^2\zeta}{ds^2} = -\beta^2\sin\zeta,$$

or

$$l^2 d\left(\frac{d\zeta}{ds}\right) = -2\beta^2\sin\frac{\zeta}{2}\cos\frac{\zeta}{2}\,ds.$$

Multiplying two parts of the equality by $\frac{d\zeta}{ds}$ after integrating we get:

$$\left(l\frac{d\zeta}{ds}\right)^2 = 4\beta^2\left(C_1 - \sin^2\frac{\zeta}{2}\right). \tag{2}$$

Let's denote the constant C_1 by k^2 and $\sin(\zeta/2)$ by $k\sin\psi$, i.e.

$$\sin\frac{\zeta}{2} = k\sin\psi. \tag{3}$$

Then equation (2) will arrive at

$$l\frac{d\zeta}{ds} = 2\beta k\cos\psi. \tag{4}$$

But from (3)

$$\frac{d\zeta}{ds} = 2k\frac{\cos\psi}{\sqrt{1 - k^2\sin^2\psi}}\frac{d\psi}{ds},$$

therefore

$$l\frac{d\psi}{ds} = \beta\sqrt{1-k^2\sin^2\psi}\,, \quad \beta\frac{ds}{l} = \frac{d\psi}{\sqrt{1-k^2\sin^2\psi}}\,.$$

By integration of the relation we obtain

$$\beta\frac{s}{l} = F(\psi) - F(\psi_0)\,. \tag{5}$$

Here by $F(\psi)$ is denoted the elliptical integral of the first order

$$F(\psi) = \int_0^{\psi} \frac{d\psi}{\sqrt{1-k^2\sin^2\psi}}\,.$$

Values of the integral are given by tables in handbooks depending on k and ψ.

Now let's derive the equation of deflection curve $x'(s)$ and $y'(s)$:

$$dx' = \cos\zeta\, ds, \quad dy' = \sin\zeta\, ds\,,$$

or

$$dx' = \left(1 - 2\sin^2\frac{\zeta}{2}\right) ds\,, \quad dy' = 2\sin\frac{\zeta}{2}\cos\frac{\zeta}{2} ds\,.$$

If we substitute here $\sin(\zeta/2) = k\sin\psi$, we arrive at

$$\frac{dx'}{l} = \frac{2}{\beta}\sqrt{1-k^2\sin^2\psi}\, d\psi - \frac{ds}{l}, \quad \frac{dy'}{l} = \frac{2}{\beta}k\sin\psi\, d\psi\,.$$

Let's integrate the equations from zero to s:

$$\frac{x'}{l} = \frac{2}{\beta}\left[E(\psi) - E(\psi_0)\right] - \frac{s}{l}\,,$$
$$\frac{y'}{l} = \frac{2}{\beta}k\left[\cos\psi_0 - \cos\psi\right], \tag{6}$$

where $E(\psi)$ denotes the elliptical integral of the second order

$$E(\psi) = \int_0^{\psi} \sqrt{1-k^2\sin^2\psi}\, d\psi\,.$$

This function is also given by tables in handbooks.

Transformation to the coordinate system xy gives

$$\frac{x}{l} = \frac{x'}{l}\cos\delta + \frac{y'}{l}\sin\delta\,,$$
$$\frac{y}{l} = \frac{y'}{l}\cos\delta - \frac{x'}{l}\sin\delta\,. \tag{7}$$

Now let's consider the boundary conditions for the rod. At $s = l$ we have:

$$M_b = Pe\cos\zeta_L.$$

Hence

$$\frac{d\zeta}{ds} = -\frac{Pe\cos\zeta_L}{EJ},$$

or according to (1)

$$\frac{d\zeta}{ds}\, l = -\beta^2 \frac{e}{l}\cos\zeta_L .$$

On the basis of the relation (4) we have

$$2k\cos\psi_L = -\beta\frac{e}{l}\cos\zeta_L ,$$

but as

$$\cos\zeta_L = 1 - 2\sin^2\frac{\zeta_L}{2},$$

then from (3) we obtain

$$\cos\zeta_L = 1 - 2k^2\sin^2\psi_L .$$

Thus we have the first boundary condition in the following final form:

$$\text{at } s = l \qquad 2k\cos\psi_L = -\beta\frac{e}{l}\left(1 - 2k^2\cos^2\psi_L\right). \tag{8}$$

The second boundary condition is:

$\zeta = 0$ at $s = 0$, or in accordance with (3) $\psi_0 = 0$.

The relation (5) for $s = l$ takes the form

$$F(\psi_L) = \beta . \tag{9}$$

From (6) we find

$$\frac{x_L}{l} = \frac{x'_L}{l} = \frac{2}{\beta}E(\psi_L) - 1 .$$

The mutual displacement of rod ends λ will be

$$\lambda = 2l - 2x'_L ,$$
$$\frac{\lambda}{l} = 4\left[1 - \frac{1}{\beta}E(\psi_L)\right].$$

Maximal deflection is equal to

$$f = y'_L = \frac{2l}{\beta}k\,(1 - \cos\psi_L) . \tag{10}$$

Now let's derive the relation between force P and maximal deflection f for some prescribed ratio $e/(2l)$. The calculation sequence will be as follows. Divide equation (8) by (9) term by term:

$$k\frac{\cos\psi_L}{F(\psi_L)} = -\frac{e}{2l}\,(1 - 2k^2\sin^2\psi_L). \tag{11}$$

For given $e/(2l)$ we specify k, and then in accordance with tables we find ψ_L in such a way that equation (11) will be satisfied. Then from (9) we find β, and then

$$\frac{P}{P_e} = \frac{P(2l^2)}{\pi^2 EJ} = \frac{4\beta^2}{\pi^2}\,.$$

From equation (10) we find $f/(2l)$. Thus we get a point of the relation

$$\frac{P}{P_A} = \varphi\left(\frac{f}{2l}\right).$$

Let's take, for example, $e/(2l) = 0.02$ and compose Table 5, specifying $k = \sin 5^o, \sin 10^o, \ldots$

Table 5. Numerical results

k	ψ_L	β	P/P_e	$f/(2l)$
0.08716	118°	2.06	1.72	0.0620
0.1736	101°	1.778	1.28	0.118
0.259	97°	1.725	1.21	0.168
0.342	94°	1.694	1.156	0.216
0.707	90°	1.854	1.39	0.381

In accordance with the table we draw the curve shown in Fig. 370. Two additional curves are also drawn in the figure. The first corresponds to the case $e = 0$; the second one starting at the point $P/P_e = 4$ corresponds to the rod bending by the mode shown in Fig. 132b.

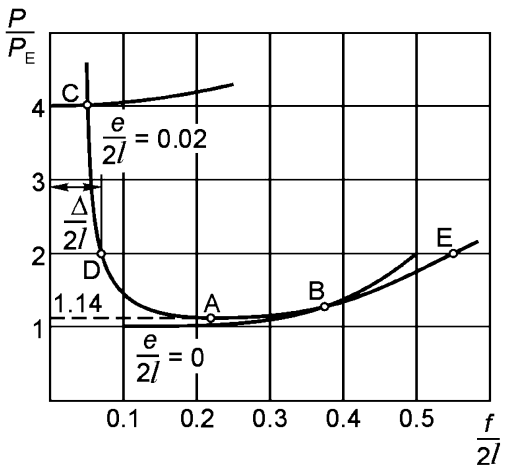

Fig. 370

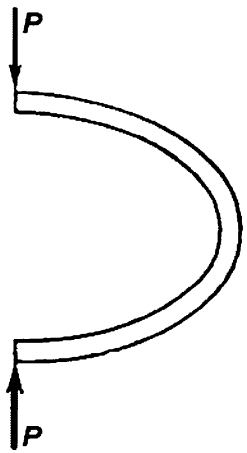

Fig. 371

Let's discuss the obtained result. The curve $e/(2l) = 0.02$ decreases at small deflections and then grows starting from the point $P/P_e = 1.14$. At point B it crosses the curve $e/(2l) = 0$. This point is common for all curves independently of $e/(2l)$. Here $k = 1/\sqrt{2}$ and from equation (11) it follows

that for any $e/(2l)$ we have $\cos\psi_L = 0$. This means that the moment at the rod end vanishes and the rotation angle at the end is 90^o (Fig. 371).

The curve $e/(2l) = 0.02$ does not intersect the coordinate axes. In its left part it asymptotically converges to a straight line $f/2l = 0.04$. Therefore the column is always stable in small quantities if the buckling only in the mode shown in Fig. 132c is considered. But under the force $P = 4\pi^2 EJ/(2l^2)$ at any $e/(2l)$ the rod loses its stability in the mode shown in Fig. 132b.

Let's now suppose that for $e/(2l) = 0.02$ the rod is loaded, for example, by the force

$$P = \frac{2\pi^2 EJ}{(2l)^2}, \quad \left(\frac{P}{P_e} = 2\right).$$

Under these conditions the rod keeps its straight form. Let's try to deviate it from the vertical line specifying a certain curvature of its axis. If this deviation is small then the rod itself will return to its initial state. If the deviation is sufficiently large (greater than the value $\Delta/(2l)$, Fig. 370) the rod will assume a new curvilinear equilibrium state, corresponding to point E (Fig. 370).

Depending on the value of the imparted deviation the system may return to its initial position, or may not. But it will occur under magnitude of force P which is greater than a certain value. In the case of $e/(2l) = 0.02$ it takes place under $P > 1.14P_e$ (point A Fig. 370) and $P < 4P_e$, where the stability loss happens independently of the imparted deviation magnitude. Thus we arrive at a new concept of a possible critical load interval, in which the transfer to a new equilibrium state is possible: $1.14P_e \le P < 4P_e$.

The column buckling will happen at the specified interval earlier or later depending on the precision of rod manufacturing and on the fact how strictly the load P obeys the condition of its central application. But somehow, the critical loads in such systems are determined in the indicated interval as probable ones.

For $P \ge 4P_e$ the transfer to a new equilibrium state is inevitable.

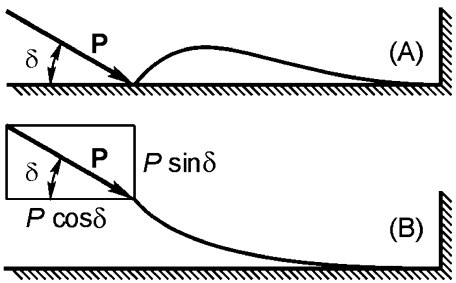

Fig. 372

142. While solving the problem it is necessary to consider separately the equilibrium configuration (A) (Fig. 372) under which the end of the beam

remains pressed to the plane. The transfer from the straight configuration to this equilibrium state will occur, as is well known, under the longitudinal force value

$$P_{cr}\cos\delta = \frac{20.2\,EJ}{l^2}.$$

Now let's consider the equilibrium state of type (B) (Fig. 372). It is clear that transfer to such an equilibrium state can not be realized by small (infinitely small) deviation of the system from its initial state. Actually, if we want the beam do not return to its initial straight state and used the configuration of type (B) then we would need to impart to the beam's end the deflection which is great enough for the moment caused by force $P\cos\delta$ and leading the beam away from its initial state which would be greater than the restoring moment produced by the force $P\sin\delta$. In other words, we should impart a displacement greater than some prescribed value. The system itself after that will not return to its initial state.

Now let's consider the conditions under which the equilibrium configurations of type (B) are possible. In our case the deflection curve can exist only in such a form when all points of the bent beam are above the horizontal plane. Two cases are possible here: the whole beam is bent (B_1) (Fig. 373a) and only a part of the beam is bent (B_2) (Fig. 373b).

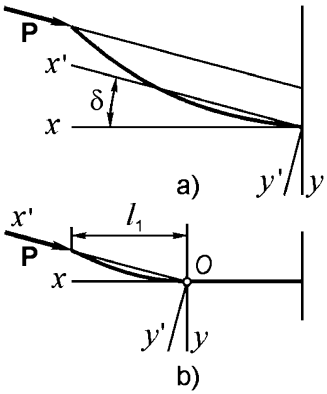

Fig. 373

Consider the first case (Fig. 373a). At the beam's end, i.e. at $s = l$ the curvature vanishes $(d\zeta/ds = 0)$. Therefore from relation (4) of the previous problem it follows that $\psi_L = \pi/2$. At $s = 0$ we have $\zeta = -\delta$. Using the relation (3) of the previous problem we obtain

$$-\sin\frac{\delta}{2} = k\sin\psi_0\,, \tag{1}$$

and from (1) and (5) of problem 141

$$\beta^2 = \frac{Pl^2}{EJ}\left[F\left(\frac{\pi}{2}\right) - F\left(\psi_0\right)\right]^2. \tag{2}$$

Coordinates of beam ends in the system $x'y'$ according to (6) of problem 141 are

$$\frac{x'_L}{l} = 2\frac{E\left(\frac{\pi}{2}\right) - E(\psi_0)}{F\left(\frac{\pi}{2}\right) - F(\psi_0)} - 1\,,$$
$$\frac{y'_L}{l} = \frac{2k\cos\psi_0}{F\left(\frac{\pi}{2}\right) - F(\psi_0)}\,. \tag{3}$$

The horizontal displacement of the point of force application is derived from the first relation (7) of problem 141:

$$\frac{\lambda}{l} = 1 - \frac{x'_L}{l}\cos\delta - \frac{y'_L}{l}\sin\delta\,. \tag{4}$$

Now we can draw the $Pl^2/(EJ)$ dependence on λ/l for equilibrium modes of type (B_1) shown in Fig. 373a for some values of δ $(10°, 20°, 30°)$. Specifying values of k we determine ψ_0 from (1). From relation (2) applying the tables of elliptical integrals we find $Pl^2/(EJ)$, and from (3) and (4) the magnitude of λ/l.

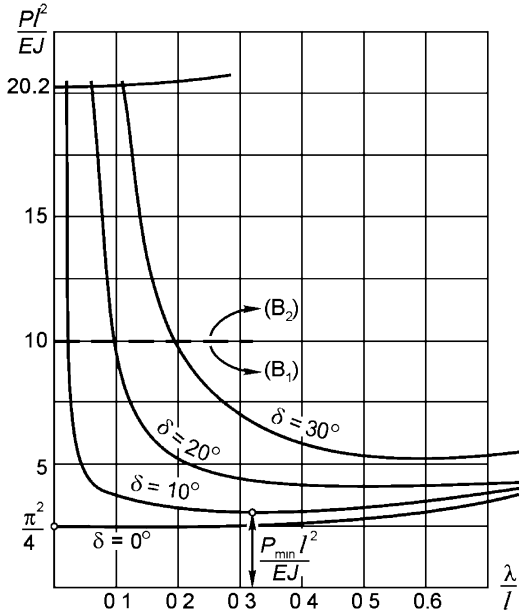

Fig. 374

Three curves are shown in Fig. 374. In plotting the curve we take into account that for equilibrium mode of type (B_1) (Fig. 373a) the action line of the force P crosses the y axis above the coordinate origin and ψ_0 remains greater than $-\pi/2$. The dashed line in Fig. 374 is the upper boundary for

these curves. For greater values of $Pl^2/(EJ)$ the sought relation should be determined corresponding to the equilibrium mode of type (B_2) (Fig. 373b). In this case $\psi_0 = -\pi/2$ at point O (Fig. 373) and instead of (1) we have

$$k = \sin\frac{\delta}{2}\,. \tag{1'}$$

Instead of (2) we obtain

$$\frac{Pl^2}{EJ}\,\frac{l_1^2}{l^2} = \left[F\left(\frac{\pi}{2}\right) - F\left(\psi_0\right)\right]^2. \tag{2'}$$

Instead of (3) and (4) we get

$$\frac{x_L'}{l}\,\frac{l}{l_1} = 2\frac{E\left(\frac{\pi}{2}\right) - E\left(\psi_0\right)}{F\left(\frac{\pi}{2}\right) - F\left(\psi_0\right)} - 1\,, \tag{3'}$$

$$\frac{y_L}{l_1} = 0\,,$$

$$\frac{\lambda}{l}\,\frac{l}{l_1} = 1 - \frac{x_L'}{l}\,\frac{l}{l_1}\cos\delta\,. \tag{4'}$$

Thus, here we find k from (1'). For some arbitrary $Pl^2/(EJ)$ from (2') we determine l_1/l, and from (3') and (4') we find λ/l. The results of the calculations are shown by the curves (Fig. 374) drawn above the dashed line.

Let's discuss the obtained results. If $\delta = 0$ then buckling by Euler exists for

$$\frac{Pl^2}{EJ} = \frac{\pi^2}{4} \approx 2.46\,.$$

For $\delta \neq 0$ under $Pl^2/(EJ) < 20.2/\cos\delta$ the instability occurs only "in large". The deflection magnitude that is necessarily imparted in order to transfer the beam into a new equilibrium state, decreases with increasing of load P. At the same time beam buckling (depending on δ) can not occur under forces smaller than a particular value. Thus for

$$\delta = 10^\circ \qquad \frac{P_{\min}l^2}{EJ} \approx 3.25\,,$$

$$\delta = 20^\circ \qquad \frac{P_{\min}l^2}{EJ} \approx 4.25\,,$$

$$\delta = 30^\circ \qquad \frac{P_{\min}l^2}{EJ} \approx 5.25\,.$$

In any case P_{cr} is determined as probable at the interval

$$P_{\min} < P_{cr} < \frac{20.2EJ}{l^2\cos\delta}$$

where $P_{\min} = f(\delta)$.

143. Before buckling the ring is under action of external uniformly distributed load $q = P/R$. Under ordinary conditions, if q remains unchanged during bending of the ring, the loss of stability will occur under

$$q = \frac{3EJ}{R^3}.$$

After buckling the ring takes a close to elliptical form.

However, in the present problem the ring is always stable "in small". Actually, if the ring bends for some reasons taking the form of an ellipse, the distributed load $q = P/R$ will increase where the curvature increases and decreases where the curvature lessens. The load q will increase near the ends of the ellipse's longer axis and will decrease near the ends of the shorter axis (Fig. 375). The difference of loads will restore the circular form of the ring.

To prevent the circular shape of the ring from being restored it is necessary to impart the ring with a sufficiently big curvature of such magnitude that at some segment the ring would loose contact with the thread. The configuration of the ring deflection curve is easily revealed by a simple experiment which consists in sticking a paper strip in a ring shape and tightening it by the ordinary thin thread.

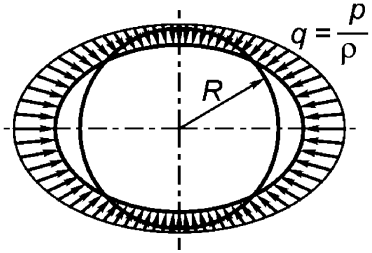

Fig. 375

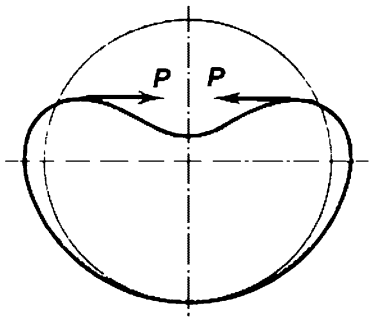

Fig. 376

The configuration of the ring after buckling is shown in Fig. 376.

Let's consider the right half of the ring and cut it at the point where the thread leaves the contact with the ring (Fig. 377, point 1). The bending moment M_1 and normal compressive force N arise in the ring section. Transverse force obviously vanishes, as otherwise the equilibrium conditions for the ring segment $O1$ are not satisfied.

To analyze the equilibrium conditions for the shown elastic ring shape we apply the relations derived earlier in solving problem 141. These equations were derived for a straight elastic rod. Here we have a ring of constant curvature $1/R$. But a ring of constant curvature is obtained from a straight rod by applying to its ends the moment $M = EJ/R$. Hence the problem (and not only the one under consideration) of bending for an elastic beam with constant initial curvature is reduced to a bending problem of a straight beam of the same length and rigidity by addition of moments $M = EJ/R$ applied at the rod's ends to a given load.

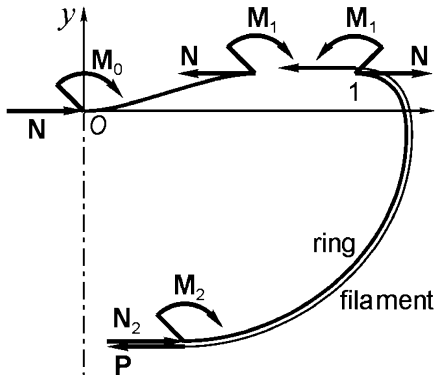

Fig. 377

The length of the segment $O1$ is denoted by l_1. The arc s we shall count from 0 to 1. The relation (1) of problem 141 for the first segment of the ring will be as follows

$$\beta = l_1 \sqrt{\frac{N}{EJ}}\,. \tag{1}$$

At $s = 0$ and $s = l_1$ $\zeta_0 = \zeta_1 = 0$ and according to (3) of problem 141 we obtain

$$\sin\psi_0 = 0\,,\ \ \sin\psi_1 = 0\,.$$

As the angle ψ increases along arc s, passing at the inflexion point the magnitude $\pi/2$ (see problem 141), then assuming $\psi_0 = 0$, we get $\psi_1 = \pi$.

The curvature of the beam at point 1 in accordance with (4) of problem 141 will be

$$\left(\frac{d\zeta}{ds}\right)_1 = 2\,\frac{\beta}{l_1}\,k_1 \cos\psi_1\,,$$

or

$$\left(\frac{d\zeta}{ds}\right)_1 = -2k_1\sqrt{\frac{N}{EJ}}\,. \tag{2}$$

The expression (5) of problem 141 at $s = l_1$ arrives at

$$l_1\sqrt{\frac{N}{EJ}} = F_1(\pi) = 2F_1\left(\frac{\pi}{2}\right), \tag{3}$$

where $F_1(\pi/2)$ is the full elliptical integral of first kind under modulus k_1 (for the second segment modulus is k_2). We take into account that

$$F\left(n\frac{\pi}{2}\right) = nF\left(\frac{\pi}{2}\right).$$

Coordinates of point 1 according to expression (6) of problem 141 will be

$$x_1 = \frac{2}{\sqrt{\frac{N}{EJ}}} 2E_1\left(\frac{\pi}{2}\right) - l_1\,, \tag{4}$$

$$y_1 = \frac{4k_1}{\sqrt{\frac{N}{EJ}}}\,. \tag{5}$$

Now let's consider the second segment of the ring, i.e. segment $1-2$. Here the ring is under action of a distributed load of magnitude proportional to the ring curvature. It is known that in the case of uniformly distributed load the problem of a rod's large displacement is solved not by elliptical tabulated integrals, but by ultra-elliptical nontabulated integrals. However, in the given case we have a considerably easier problem. As a thread is absolutely flexible we can consider the thread and the ring together as a whole ring with the same rigidity EJ and suppose that at point 1 of the second segment the ring is under action of the compressive force $N-P$ and moment M_1. And for such load a problem of large displacements can easily be solved by elliptical integrals.

Under such an approach to the problem the load q acting outside the ring becomes the internal force acting on both ring and fibre. Also, we can conclude from the above that under distributed load proportional to the deformed beam curvature the problem of big displacements is solved by elliptical integrals. The conclusion is rather general but not well known.

As at the second ring segment the inflexion points are absent and, hence, $d\zeta/ds$ does not vanish anywhere at the segment, then value C_1 in the relation (2) of problem 141 must be greater than unity. If, as in problem 141, we denote C_1 as k^2 and $\sin(\zeta/2)$ as $k\sin\psi$ then we arrive at elliptical integrals with modulus greater than unity. There are no tables for such integrals. That is why the expressions (3)-(6) of problem 141 should be rearranged.

Let's denote for the second segment

$$C_1 = \frac{1}{k_2^2},\quad \sin\frac{\zeta}{2} = \sin\psi, \tag{6}$$

then equation (2) of problem 141 will be as follows

$$l_2\frac{d\zeta}{ds} = \pm\frac{2\beta}{k_2}\sqrt{1-k_2^2\sin^2\psi}\,,$$

where l_2 is the length of the second segment. As the curvature of the second segment is negative we take the minus sign:

$$\frac{d\zeta}{ds} = -\frac{2}{k_2}\sqrt{\frac{N-P}{EJ}}\sqrt{1-k_2^2\sin^2\psi}\,. \tag{7}$$

Substituting here instead of $d\zeta/ds$ the expression

$$\frac{2\cos\psi}{\sin(\zeta/2)}\,\frac{d\psi}{ds}\,,$$

obtained from (6) we get

$$ds = \frac{k_2}{\sqrt{\dfrac{N-P}{EJ}}} \frac{d\psi}{\sqrt{1-k_2^2 \sin^2 \psi}}, \tag{8}$$

whence

$$s = \frac{k_2}{\sqrt{\dfrac{N-P}{EJ}}} \left[F_2(\psi) - F_2(\psi_0)\right]. \tag{9}$$

Further as in problem 141

$$dx = dx' = \left(1 - 2\sin^2 \frac{\zeta}{2}\right) ds,$$

$$dy = dy' = 2 \sin \frac{\zeta}{2} \cos \frac{\zeta}{2}\, ds.$$

If we substitute here $\sin(\zeta/2)$ from (6) and ds from (8) we arrive at

$$dx = \frac{2}{k_2 \sqrt{\dfrac{N-P}{EJ}}} \sqrt{1-k_2^2 \sin^2 \psi}\, d\psi - \left(\frac{2}{k_2^2} - 1\right) ds,$$

$$dy = \frac{2}{k_2 \sqrt{\dfrac{N-P}{EJ}}} \frac{k_2^2 \sin 2\psi}{\sqrt{1-k_2^2 \sin^2 \psi}}\, d\psi.$$

After integration we find

$$x - x_0 = \frac{2}{k_2 \sqrt{\dfrac{N-P}{EJ}}} \left[E_2(\psi) - E_2(\psi_0)\right] - \left(\frac{2}{k_2^2} - 1\right) s, \tag{10}$$

$$y - y_0 = \frac{2}{k_2 \sqrt{\dfrac{N-P}{EJ}}} \left[\sqrt{1-k_2^2 \sin^2 \psi_0} - \sqrt{1-k_2^2 \sin^2 \psi}\right]. \tag{11}$$

Now let's consider boundary conditions for the second segment.

At point 1, i.e. at the beginning of the second segment, $\zeta_1 = 0$, and at the end (point 2) $\zeta_2 = -180°$. According to (6)

$$\sin \psi_1 = 0, \quad \sin \psi_2 = -1.$$

Let's accept $\psi_1 = 180°, \psi_2 = 270°$.

As $F(n\pi/2) = nF(\pi/2)$, then from (9) for the end of the second segment we obtain

$$l_2 = \frac{k_2 F_2\left(\dfrac{\pi}{2}\right)}{\sqrt{\dfrac{N-P}{EJ}}}. \tag{12}$$

If we substitute $\psi = 180^\circ$ into equation (7) we derive the ring curvature at point 1 of the second segment

$$\frac{d\zeta}{ds} = -\frac{2}{k_2}\sqrt{\frac{N-P}{EJ}}\,.$$

The curvature has no discontinuity at point 1. Therefore we equate the obtained curvature to the value that was found at point 1 of the first segment (2), i.e.

$$k_1\sqrt{\frac{N}{EJ}} = \frac{1}{k_2}\sqrt{\frac{N-P}{EJ}}. \tag{13}$$

Coordinate x of the end of the second segment is equal to zero, and the coordinate of the second segment origin must coincide with the coordinate of the first segment end x_1 (4). Therefore from (10) at $s = l_2$, $x = 0$ and $x_0 = x_1$ (4) we obtain

$$-\frac{4}{\sqrt{\frac{N}{EJ}}}E_1\left(\frac{\pi}{2}\right) + l_1 = \frac{2}{k_2\sqrt{\frac{N-P}{EJ}}}E_2\left(\frac{\pi}{2}\right) - \left(\frac{2}{k_2^2} - 1\right)l_2\,. \tag{14}$$

By analogy we find y to be the distance between points 0 and 2

$$y = \frac{4k_1}{\sqrt{\frac{N}{EJ}}} + \frac{2}{k_2\sqrt{\frac{N-P}{EJ}}}\left(1 - \sqrt{1-k_2^2}\right). \tag{15}$$

Now from equations (3),(12),(13) and (14) we eliminate $\sqrt{N/(EJ)}$ and $\sqrt{(N-P)/(EJ)}$. Then we arrive at

$$\frac{2}{k_2^2}E_2\left(\frac{\pi}{2}\right) - \left(\frac{2}{k_2^2} - 1\right)F_2\left(\frac{\pi}{2}\right) = 2k_1\left[F_1\left(\frac{\pi}{2}\right) - 2E_1\left(\frac{\pi}{2}\right)\right], \tag{16}$$

$$\frac{l_1}{l_2} = \frac{2k_1F_1(\pi/2)}{F_2(\pi/2)}\,. \tag{17}$$

But the sum of lengths l_1 and l_2 is equal to half of the ring arc

$$l_1 + l_2 = \pi/R\,,$$

whence

$$\frac{l_1}{\pi R} = \frac{l_1/l_2}{1 + l_1/l_2}\,. \tag{18}$$

From (3) and (13) we find

$$\sqrt{\frac{NR^2}{EJ}} = \frac{2F_1(\pi/2)}{\pi l_1/(\pi R)}, \tag{19}$$

$$\frac{PR^2}{EJ} = \frac{NR^2}{EJ}(1 - k_1^2k_2^2)\,. \tag{20}$$

Thus the sequence of calculations will be as follows.

Specifying k_1 (or value of modular angle $\alpha_1 = \arcsin k_1$) and using tables of full elliptical integrals, we select k_2 satisfying equation (16). Practically it can be done by drawing plots of right- and left-hand parts of the equation dependence versus k_1 and k_2.

From (17) and (18) we find $l_1/\pi R$, and from (19) and (20) the magnitude of load P. The deflection w (decreasing of vertical diameter) corresponding to force P will be (15)

$$w = 2R - y\,,$$

$$\frac{w}{R} = 2 - \frac{1}{\sqrt{\dfrac{NR^2}{EJ}}}\left[\frac{2}{k_1 k_2^2}(1 - \sqrt{1 - k_2^2}) - 4k_1\right]. \tag{21}$$

Thus we derive one point of the dependence

$$\frac{PR^2}{EJ} = f\left(\frac{w}{R}\right).$$

The results of calculation are shown in Fig. 378 as a curved line, similar to the ones obtained in the three previous problems. The minimum value of critical force is equal to

$$P_{\min} = 2.1\frac{EJ}{R^2}\,.$$

However, this value is only formally lower, because the displacement w/R is equal to 2.65, i.e. the decreasing of ring diameter is greater than the diameter itself. The ring contour takes the form of the curved line shown in Fig. 379.

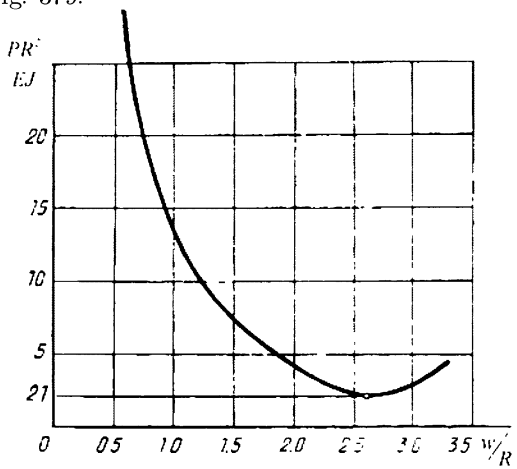

Fig. 378

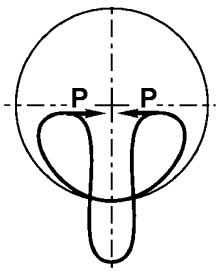

Fig. 379

It is clear that under real conditions the initial ring shape deviations from the circular one are insignificant, i.e. w/R remains essentially less than unity.

For small values of w/R calculation gives much higher values of $PR^2/(EJ)$, which can not be placed in the scale of the plot (Fig. 378). It is convenient to rearrange the obtained formulas in this case, taking into account that k_1 and k_2 are small values. For this case

$$F_1\left(\frac{\pi}{2}\right) \approx \frac{\pi}{2}\left(1+\frac{k_1^2}{4}+\ldots\right),$$

$$F_2\left(\frac{\pi}{2}\right) \approx \frac{\pi}{2}\left(1+\frac{k_2^2}{4}+\ldots\right).$$

According to (17), (18), (19) and (20)

$$\frac{l_1}{l_2} \approx 2k_1,\ \frac{l_1}{2\pi} \approx \frac{2k_1}{1+2k_1},\ \sqrt{\frac{NR^2}{EJ}} \approx \frac{1+2k_1}{2k_1},\ \frac{PR^2}{EJ} \approx \frac{1+4k_1}{4k_1^2}. \quad (22)$$

At last

$$\frac{w}{R} = 2 - \frac{2k_1}{1+2k_1}\left[\frac{2}{k_1k_2^2}\left(1-1+\frac{k_2^2}{2}\right)-4k_1\right],$$

$$\frac{w}{R} \approx 4k_1. \quad (23)$$

Thus for small w/R, eliminating k_1 from (22) and (23), we obtain

$$\frac{PR^2}{EJ} \approx 4\,\frac{1+w/R}{(w/R)^2} \approx \frac{4}{(w/R)^2}\,.$$

Returning to the conception of stability in large quantities, described in problem 140, we see that a final solution for the current problem has not been obtained. Only equilibrium modes are found, and it follows from the analysis that the ring "is very stable". In order to predetermine system stability we must take into account the set of reasonably limited real existing disturbances and such types of initial ring imperfections as ring deflection and inhomogeneity of material. None of the problems had been analyzed in such a way up to the present time.

The considered problem is no exception in this sense. The stability theory of elastic systems can not yet give a satisfactory solution of very important practical problems, such as stability of spherical shells under external pressure and cylindrical shells under axial compression.**144.** For the first time this problem in a similar form was analyzed in [13].

It is impossible to give a unique answer to the given question. Let's consider the process of rod motion. An ordinary equation of stability

$$M = EJy'' = -Py$$

will become complicated owing to the introduced transverse inertial forces of intensity q, i.e. it will take the form

$$EJy^{iv} = -Py'' + q\,.$$

But

$$q = -\frac{\gamma A}{g}\frac{\partial^2 y}{\partial t^2},$$

where γ is weight density of the rod material, and A is the cross-sectional area. We obtain the differential equation

$$\frac{\gamma A}{g}\frac{\partial^2 y}{\partial t^2} + EJ\frac{\partial^4 y}{\partial x^4} + P\frac{\partial^2 y}{\partial x^2} = 0. \tag{1}$$

Assume that

$$y = \sum T_m \sin\frac{m\pi x}{l},$$

where T_m is an unknown function of time t.

Let us substitute the expression into equation (1). Then we arrive at

$$\frac{\gamma A}{g}\frac{d^2 T_m}{dt^2} + \frac{\pi^4 EJ}{l^4}m^2(m^2-\eta^2)T_m = 0, \tag{2}$$

where

$$\eta^2 = \frac{Pl^2}{\pi^2 EJ}.$$

In our case $\eta^2 = 10$.

If $m^2 > \eta^2$, equation (2) is solved in trigonometric functions, that corresponds to periodic vibrations of the rod.

If $m^2 < \eta^2$, equation (2) is solved in exponential functions

$$T_m = A_m \exp(k_m t) + B_m \exp(-k_m t),$$

where

$$k_m = \sqrt{\frac{\pi^4 EJg}{\gamma A l^4}m^2(\eta^2 - m^2)},$$

and magnitude m takes three integer values $1, 2, 3$.

Certainly, we are interested only in components having unlimited increase in time. Thus we can write

$$y = A_1 \exp(k_1 t)\sin\frac{\pi x}{l} + A_2 \exp(k_2 t)\sin\frac{2\pi x}{l} + A_3 \exp(k_3 t)\sin\frac{3\pi x}{l}.$$

The index of exponent k_m, characterizes velocity of either mode increase and depends upon the value of m. For $m = 1, 2, 3$ and $\eta^2 = 10$ the magnitude of $m^2(\eta^2 - m^2)$, entering the radical expression for k_m, takes the values 9, 24 and 9 respectively. Thus, velocity of deflection growth for two half-wave bending modes is found to be greater than for one or three half-wave modes. Perhaps it is the only thing that we can reliably be assert in connection with the given question.

The fact is that we know nothing about magnitudes of A_1, A_2, and A_3 characterizing the initial deflection of the rod. Even if we consider these

parameters as statistically equivalent then the obtained solution of the linear problem says nothing about the behaviour of the rod in the range of big displacements. If we go further in our investigation and try to analyze the behaviour of the rod under big displacements then we find that the initial data is not enough for a full solution of the problem.

Really, what does the question mean: "What mode will the rod bend?" Obviously at first we should come to agreement where the process of motion ends, what bounds vertical displacement of the rod's upper end or what is the duration of force action. But all these questions would take us too far.

145. The proposed problem again touches upon a principal question of elastic system stability analysis, and its solution results in the necessity to give a new formulation of the stability criterion.

Let's imagine that the rod deflects slightly from the initial equilibrium position (Fig. 380).

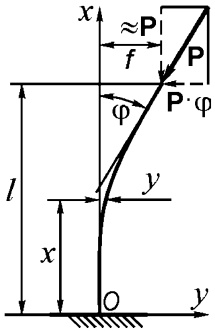

Fig. 380

The equation of the deflection curve is

$$EJy'' = P(f - y) - P\varphi(l - x)\,,$$

from which

$$y = A\sin\alpha x + B\cos\alpha x + f - \varphi(l - x),$$

where $\alpha^2 = \dfrac{P}{EJ}$.

At $x = 0$ $y = 0$ and $y' = 0$.

At $x = l$ $y = f$ and $y' = \varphi$.

The implementation of these conditions results in four equations:

$$\begin{aligned} B + f - \varphi l &= 0,\\ A\alpha + \varphi &= 0,\\ A\sin\alpha l + B\cos\alpha l &= 0,\\ A\cos\alpha l - B\sin\alpha l &= 0. \end{aligned}$$

Considering the last two equations it is easy to establish that independently of selecting αl the constants A and B are equal to zero because the determinant

$$\begin{vmatrix} \sin \alpha l & \cos \alpha l \\ \cos \alpha l & -\sin \alpha l \end{vmatrix}$$

is not equal to zero. But if $A = B = 0$, the only equilibrium mode of the rod is an initial straight mode.

In all the problems considered before two concepts were permanently identified: "loss of stability" and "existence of another equilibrium state except the initial". Therefore in the given case we should decide between the two variants: either to refuse the usual and deeply-rooted identification of the given concepts or to accept that the system keeps its stability under any value of force P.

The first is correct. The initial equilibrium state is stable only up to a certain value of force P. Under forces exceeding this value, which we shall call critical as earlier, the transition occurs not to a new equilibrium state, but to some form of motion with increasing deflection from the initial equilibrium state. The criterion of instability is the condition of specified form of motion arising and is called the dynamic criterion of stability.

Let's discuss the following mechanical model shown in Fig. 381. Two homogenous rods having masses m_1 and m_2 are connected by a spring of stiffness c. The same spring connects the lower rod with the hinge support. Line of force P action permanently coincides with the direction of the upper rod axis.

Assume the angles of the rod's rotation φ_1 and φ_2 as generalized coordinates. Then the displacements of the mass center of each rod will be

$$y_1 = l\varphi_1\,, \qquad y2 = l\varphi_2 + 2l\varphi_1\,,$$

where $2l$ is length of each rod.

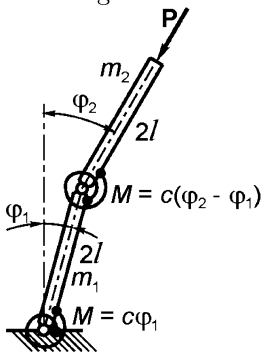

Fig. 381

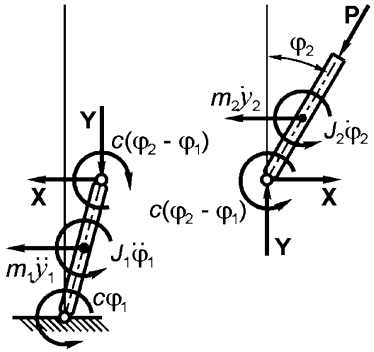

Fig. 382

Moments of inertia of each rod with respect to the central transverse axis are equal to

$$J_1 = \frac{m_1 l^2}{3} \quad \text{and} \quad J_2 = \frac{m_2 l^2}{3}\,.$$

If we introduce the interaction forces in the hinge (Fig. 382) the equations of motion can be derived.

For the upper rod

$$Y = P\,, \quad X = P\varphi_2 + m_2\, y_2\,, \tag{1}$$

$$J_2\, \varphi_2 + m_2\, y_2\, l + c\,(\varphi_2 - \varphi_1)\,.$$

For the lower rod

$$c\,\varphi_1 + J_1\, \varphi_1 - c\,(\varphi_2 - \varphi_1) + X2l + m_1\, y_1\, l - Y2l\,\varphi_1 = 0\,. \tag{2}$$

Eliminating y_1, y_2, X, and Y and expressing moments of inertia in terms of masses we obtain two linear differential equations in unknowns φ_1 and φ_2:

$$\frac{4}{3}\, m_2 l^2\, \varphi_2 + 2\, m_2 l^2\, \varphi_1 + c\,(\varphi_2 - \varphi_1) = 0\,,$$

$$(4m_2 l^2 + \frac{4}{3} m_1 l^2)\, \varphi_1 + 2m_2 l^2\, \varphi_2 + (2c - 2Pl)\varphi_1 + (2Pl - c)\varphi_2 = 0\,. \tag{3}$$

As usual we assume

$$\varphi_1 = A_1 e^{kt}, \quad \varphi_2 = A_2 e^{kt}. \tag{4}$$

After substitution we arrive at two equations in unknowns A_1 and A_2 :

$$A_1\left(2\, m_2 l^2 k^2 - c\right) + A_2\left(\frac{4}{3}\, m_2 l^2 k^2 + c\right) = 0\,,$$

$$A_1\left(4m_2 l^2 k^2 + \frac{4}{3} m_1 l^2 k^2 + 2c - 2Pl\right) + A_2\left(2m_2 l^2 k^2 + 2Pl - c\right) = 0\,.$$

In order to derive the conditions of non-trivial solution existence the determinant must equal zero. It gives a quadratic equation relative to k^2 :

$$\left(\frac{m_2 k^2 l^2}{c}\right)^2 (3 + 4\mu) + \frac{m_2 k^2 l^2}{c}\, 3\,(8 + \mu - 5\frac{Pl}{c}) + \frac{9}{4} = 0, \tag{5}$$

where $\mu = m_1 / m_2$.

The free term of equation (5) does not depend on force P. Hence, we can not determine such P that k will vanish, and therefore if we return to the expressions (4) we shall see that angles φ_1 and φ_2 can not be constant. The system has no equilibrium state except the initial one. The considered model has the same property as the clamped rod loaded by follower force.

It is easy to establish from equation (5) that value k^2 under any force P remains negative. This means that k does not have real values and conditions of aperiodic motion are absent. Let's assume that

$$kl\sqrt{\frac{m_2}{c}} = \varepsilon + i\omega\,,$$

and find the condition under which ε may have a positive value. This corresponds to the appearance of oscillatory motion with increasing amplitude.

Separating real and imaginary parts in equation (5) we arrive at

$$\left[\left(\varepsilon^2-\omega^2\right)^2-4\varepsilon^2\omega^2\right](3+4\mu)+3\left(\varepsilon^2-\omega^2\right)\left(8+\mu-5\frac{Pl}{c}\right)+\frac{9}{4}=0\,,$$

$$4\varepsilon\omega\left(\varepsilon^2-\omega^2\right)(3+4\mu)+6\varepsilon\omega\left(8+\mu-5\frac{Pl}{c}\right)=0\,.$$

By excluding ω, we get

$$\varepsilon^4 4\,(3+4\mu)+\varepsilon^2 6\left(8+\mu-5\frac{Pl}{c}\right)+\frac{9}{4}\frac{\left(8+\mu-5\frac{Pl}{c}\right)^2}{3+4\mu}-\frac{9}{4}=0\,,$$

from which

$$\varepsilon^2=\frac{3}{4}\,\frac{5\dfrac{Pl}{c}-8-\mu\pm\sqrt{3+4\mu}}{3+4\mu}\,.$$

The least value of P under which ε^2 (and hence one of the roots ε) takes a positive value is

$$P_{cr}=\frac{c}{5l}\left(8+\mu-\sqrt{3+4\mu}\right).$$

The magnitude of critical force depends on the mass distribution between rods. If $m_1=m_2$ then $\mu=1$. And

$$P_{cr}=\frac{c}{5l}\,(9-\sqrt{7})\,.$$

If the mass of the first rod is small in comparison with the second mass $\mu=0$ and

$$P_{cr}=\frac{c}{5l}(8-\sqrt{3}).$$

The value of μ infinitely increases as the mass of the upper rod decreases in comparison with the mass of the lower one. Thus P_{cr} infinitely increases, also, and it is clear. In the case of the absence of transverse inertial forces the upper rod will always lay on the same straight line with the lower one.

For systems allowing stability estimation on the basis of equilibrium state analysis, i.e. for ordinary systems, the dynamic criterion gives the same results as the static criterion. Let's consider, for example, the same rod system under action of load retaining its direction (Fig. 383). Such load is called "dead" force. In this case instead of equations (1) we have

$$Y=P,\qquad X=m_2\,y_2,$$

$$J_2\,\varphi_2+m_2\,y_2\,l+c\,(\varphi_2-\varphi_1)-P2l\varphi_2\,.$$

Equation (2) remains unchanged. Instead of equation (3) we get

$$\frac{4}{3}m_2l^2\ \varphi_2 + 2m_2l^2\ \varphi_1 + c(\varphi_2 - \varphi_1) - 2Pl\varphi_2 = 0,$$

$$(4m_2l^2 + \frac{4}{3}m_1l^2)\ \varphi_1 + 2m_2l^2\ \varphi_2 + (2c - 2Pl)\varphi_1 - c\varphi_2 = 0\,,$$

and instead of (5) we arrive at

$$\left(\frac{m_2k^2l^2}{c}\right)^2 (3+4\mu) + \frac{m_2k^2l^2}{c}\,3\left[8+\mu-\frac{Pl}{c}(8+2\mu)\right]$$

$$+\frac{9}{4}\left[1-\frac{6Pl}{c}+4\left(\frac{Pl}{c}\right)^2\right] = 0\,. \tag{6}$$

Now the free term of the equation depends on force P and for

$$P = \frac{c}{4l}\,(3 \pm \sqrt{5})$$

is equal to zero. Hence zero values are possible for k, and the solution exists for which φ_1 and φ_2 (4) are independent of time, i.e. exists for the equilibrium state at

$$P_{cr} = \frac{c}{4l}\,(3 - \sqrt{5})\,.$$

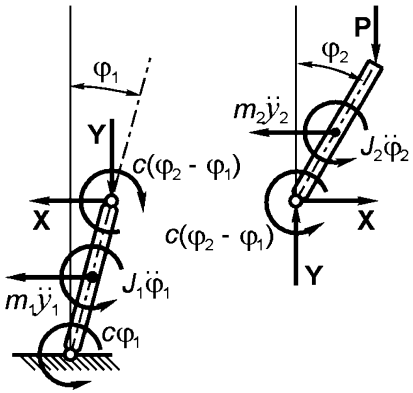

Fig. 383

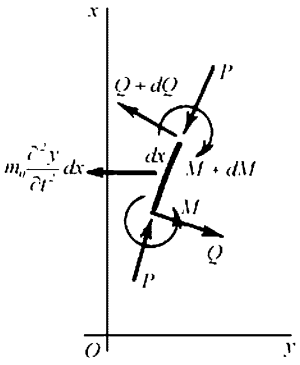

Fig. 384

Here the magnitude of critical force does not depend on mass distribution, as the parameter μ does not enter into the free term of equation (5) and (6) and can not enter into it.

Let's return to the elastic rod and derive the equation of motion. The element of length dx is loaded by forces and moments applied in its cross-sections (Fig. 384) and by distributed inertial forces of intensity $m_0\partial^2 y/\partial t^2$ are also applied, where m_0 is mass per unit length of rod material.

By projecting forces on the normal to the deflection curve we obtain

$$dQ + P\,\frac{\partial^2 y}{\partial x^2}\,dx + m_0\,\frac{\partial^2 y}{\partial t^2}\,dx = 0.$$

As

$$Q = EJ\frac{\partial^3 y}{\partial x^3},$$

then

$$EJ\frac{\partial^4 y}{\partial x^4} + P\frac{\partial^2 y}{\partial x^2} + m_0\frac{\partial^2 y}{\partial t^2} = 0;$$

m_0 shall be considered as a constant value.

Let us assume

$$y = Ye^{i\ \ t},$$

where Y depends only on coordinate x. For real values of the motion has the character of harmonic vibrations. If is complex

$$= a \pm bi,$$

then

$$y = Ye^{(\mp b+ia)t} = Ye^{\mp bt}(\cos at + i\sin at). \tag{7}$$

Hence the motion will occur either with decreasing or with increasing amplitude and depends on the sign of b.

Substituting y in the equation of motion and introducing dimensionless parameters

$$\beta^2 = \frac{Pl^2}{EJ}, \quad \omega = \ \ l^2\sqrt{\frac{m_0}{EJ}}, \quad \zeta = \frac{x}{l};$$

we obtain

$$\frac{d^4Y}{d\zeta^4} + \beta^2\frac{d^2Y}{d\zeta^2} - \omega^2 Y = 0. \tag{8}$$

The solution of the equation is

$$Y = C_1\sin\alpha_1\zeta + C_2\cos\alpha_1\zeta + C_3\sinh\alpha_2\zeta + C_4\cosh\alpha_2\zeta, \tag{9}$$

where

$$\alpha_1^2 = \frac{\beta^2}{2} + \sqrt{\frac{\beta^4}{4} + \omega^2},$$

$$\alpha_2^2 = -\frac{\beta^2}{2} + \sqrt{\frac{\beta^4}{4} + \omega^2}.$$

At the clamped beam end independent of conditions of loading we have $Y = 0$ and $dY/d\zeta = 0$. Hence

$$C_2 + C_4 = 0, \quad \alpha_1 C_1 + \alpha_2 C_3 = 0.$$

At the free end of the rod the bending moment is equal to zero, and in the case of follower force the transverse force vanishes too. Therefore at $x = l$ (or at $\xi = 1$)

$$\frac{d^2Y}{d\zeta^2} = 0 \quad \text{and} \quad \frac{d^3Y}{d\zeta^3} = 0\,,$$

that gives two additional equations:

$$-C_1\alpha_1^2 \sin\alpha_1 - C_2\alpha_1^2 \cos\alpha_1 + C_3\alpha_2^2 \sinh\alpha_2 + C_4\alpha_2^2 \cosh\alpha_2 = 0;$$
$$-C_1\alpha_1^3 \cos\alpha_1 + C_2\alpha_1^3 \sin\alpha_1 + C_3\alpha_2^3 \cosh\alpha_2 + C_4\alpha_2^3 \sinh\alpha_2 = 0\,.$$

In the case of "dead" force P the last condition would have another form. Here transverse force is not equal to zero but it is equal to $-Py'_{x=l}$.

Let's equate the determinant of the four obtained equations to zero. Then

$$\alpha_1^4 + \alpha_2^4 + \alpha_1\alpha_2(\alpha_1^2 - \alpha_2^2)\sin\alpha_1 \sinh\alpha_2 + 2\alpha_1^2\alpha_2^2 \cos\alpha_1 \cosh\alpha_2 = 0\,,$$

or

$$\beta^4 + 2\omega^2 + \beta^2\omega \sin\alpha_1 \sinh\alpha_2 + 2\omega^2 \cos\alpha_1 \cosh\alpha_2 = 0\,. \tag{10}$$

In case of "dead" force, instead of expression (10) we get

$$2\omega^2 - \beta^2\omega \sin\alpha_1 \sinh\alpha_2 + (\beta^4 + 2\omega^2)\cos\alpha_1 \cosh\alpha_2 = 0\,. \tag{11}$$

The relation (10) allows to draw the dependence of eigenfrequencies ω of rod vibrations on the dimensionless force β^2 (Fig. 385). By dashed line the frequency variation for the case of "dead" force is shown in this plot.

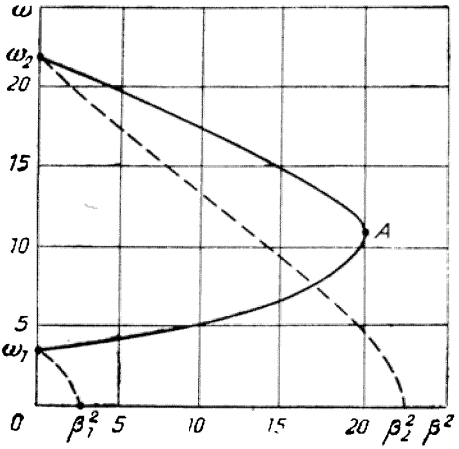

Fig. 385

For $\beta = 0$ we have first ω_1 and second ω_2 eigenfrequencies of clamped rod vibrations. As "dead" force increases the frequencies (and all higher frequencies too) decrease and vanish under forces taking critical values, i.e.

$$\text{for } \beta^2 = \beta_1^2 = \frac{\pi}{4} \quad \text{or for} \quad P = \frac{\pi^2 EJ}{4l^2}\,,$$

and in general for

$$P = \frac{n^2\pi^2 EJ}{4l^2} \quad (n = 1, 3, 5, ...).$$

In the case of follower force lower frequency increases while increasing of P and at point A the curve lines of the first and second tones merge. If we expand the plot to areas of higher frequencies then we can see that such merging of curves exists as well for the third and fourth frequencies, the fifth and sixth and so on.

For determination of the critical value of force P in this case we should find the minimal value of P under which the multiplicity of roots ω of equation (10) takes place. It means that for a further increase of β the roots become complex-conjugate and the root with negative imaginary part, i.e. $= a - b\,i$ exists. According to relation (7) it corresponds to the occurrence of mode of vibrations with increasing amplitude. It is seen from Fig. 385 that multiplicity of roots takes place at point A.

Carrying out the numerical calculation we find

$$\beta^2 = 20.05 \quad (\omega = 11.016),$$

hence

$$P_{cr} = 20.05\,\frac{EJ}{l^2}.$$

The obtained result is correct only for rod mass uniformly distributed along its length. For another distribution of mass the critical force will be different. This is very important to note as sometimes we encounter attempts to determine critical force in such problems by applying the different tricks which do not satisfy the dynamics laws. Such approach presets the neglect of mass distribution and leads to principal incorrectness of the solution.

146. The loading case a became well known in literature under the name Reut problem [19].

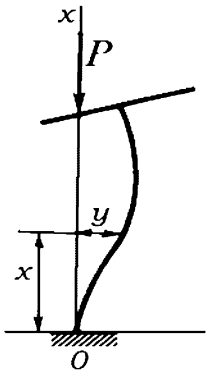

Fig. 386

The rod has no equilibrium state except the initial straight. Actually (Fig. 386)

$$EJy'' = -Py;$$

and further

$$y = A\sin\alpha x + B\cos\alpha x\,;$$

at $x = 0$ $y = 0$ and $y' = 0$, hence

$$B = 0 \text{ and } A = 0\,.$$

Let's analyze the modes of motion. Assume that mass of the flat disk at the end of the rod is small. Function Y in relation (9) derived during solution of the previous problem is valid. The two first boundary conditions are valid also:

$$Y = 0 \text{ and } \frac{dY}{d\zeta} = 0 \quad \text{at } \zeta = 0\,,$$

that is

$$C_2 + C_4 = 0,\ \alpha_1 C_1 + \alpha_2 C_2 = 0.$$

At $x = l$ $(\zeta = 1)$ we have

$$EJy'' = -Py\,, \quad EJy''' = -Py',$$

or

$$Y'' + \beta^2 Y = 0\,, \quad Y''' + \beta^2 Y' = 0\,.$$

Returning to the solution (9) of the previous problem we obtain

$$C_1(-\alpha_1^2 + \beta^2)\sin\alpha_1 + C_2(-\alpha_1^2 + \beta^2)\cos\alpha_1$$
$$+ C_3(\alpha_2^2 + \beta^2)\sinh\alpha_2 + C_4(\alpha_2^2 + \beta^2)\cosh\alpha_2 = 0\,,$$
$$C_1(-\alpha_1^3 + \beta^2\alpha_1)\cos\alpha_1 + C_2(\alpha_1^3 - \beta^2\alpha_1)\sin\alpha_1$$
$$+ C_3(\alpha_2^3 + \beta^2\alpha_2)\cosh\alpha_2 + C_4(\alpha_2^3 + \beta^2\alpha_2)\sinh\alpha_2 = 0\,.$$

Equating the determinant to zero we arrive at the transcendental equation

$$\beta^4 + 2\omega^2 + \beta^2\omega\sin\alpha_1\sinh\alpha_2 + 2\omega^2\cos\alpha_1\cosh\alpha_2 = 0\,.$$

which completely coincides with equation (10) of problem 145. Thus, the critical force will be the same as in the previous problem

$$P_{cr} = 20.05\,\frac{EJ}{l^2}\,.$$

One could guess about the coincidence of results in advance. Forces at the end of rods in both cases are identical. The difference is only in the coordinate frame for y and x (Fig. 387).

In the case of loading b (Fig. 388) the problem can be solved on the basis of ordinary analysis of equilibrium modes. The equation is the following

$$EJy'' = -Py - p\varphi(l-x)\,,$$

or

$$y'' + \alpha^2 y = -\alpha^2\varphi(l-x), \qquad \left(\alpha^2 = \frac{P}{EJ}\right),$$

whence

$$y = A\sin\alpha x + B\cos\alpha x - \varphi(l-x)\,.$$

At $x = 0 \quad y = 0$ and $y' = 0$, and at $x = l \quad y' = \varphi$. Then we obtain the next three equations:

$$B - \varphi l = 0\,, \qquad A\alpha + \varphi = 0\,, \qquad A\cos\alpha l - B\sin\alpha l = 0\,.$$

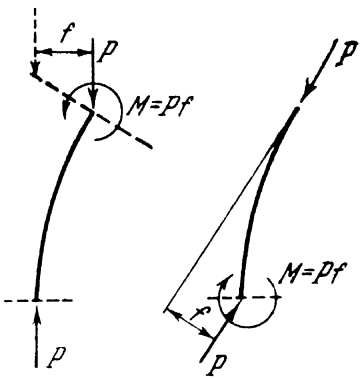

Fig. 387

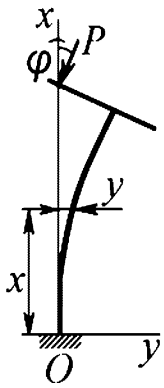

Fig.388

By equating the determinant of the system to zero we obtain

$$\tan\alpha l = -\alpha l\,.$$

The least nontrivial root of the equation is

$$\alpha l = 2.029\,,$$

whence

$$P_{cr} = 4.115\,\frac{EJ}{l^2}.$$

147. The system is similar to the one considered in problem 145. Here, is necessary to derive equations of motion for stability analysis.

Let's consider the rod element (Fig. 389) of length dx. If we balance all force projections onto the y axis we arrive at

$$\frac{\partial Q}{\partial x}\,dx + m_0\frac{\partial^2 y}{\partial t^2}\,dx + P\frac{l-x-dx}{l}\left(\frac{\partial y}{\partial x} + \frac{\partial^2 y}{\partial x^2}\,dx\right) - P\frac{l-x}{l}\frac{\partial y}{\partial x} = 0,$$

or

$$\frac{\partial Q}{\partial x} + m_0 \frac{\partial^2 y}{\partial t^2} + \frac{\partial}{\partial x}\left[P\,\frac{l-x}{l}\,\frac{\partial y}{\partial x}\right] = 0\,.$$

But as

$$\frac{\partial Q}{\partial x} = EJ\,\frac{\partial^4 y}{\partial x^4}\,,$$

then

$$EJ\frac{\partial^4 y}{\partial x^4} + \frac{\partial}{\partial x}\left[P\frac{l-x}{l}\frac{\partial y}{\partial x}\right] + m_0\frac{\partial^2 y}{\partial t^2} = 0\,. \tag{1}$$

Here m_0 is mass per unit length of rod material. These values (as well as EJ) do not depend upon x.

Equation (1) of problem 145 has a structure that presumes computer calculation. But there is hope that for a homogeneous rod it is possible to reduce the equation solution in tabulated Bessel functions or related to them. However, even in this case the problem is solved more quickly by computing. Let's suppose

$$y = Ye^{i\ \ t}$$

and go to the dimensionless form

$$\frac{d^4Y}{d\zeta^4} + \beta^2\frac{d}{d\zeta}\left[(1-\zeta)\frac{dY}{d\zeta}\right] - \omega^2 Y = 0\,,$$

where

$$\beta^2 = \frac{Pl^2}{EJ}\,, \qquad \omega^2 = \frac{m_0 l^4}{EJ}\quad{}^2, \qquad \zeta = \frac{x}{l}\,.$$

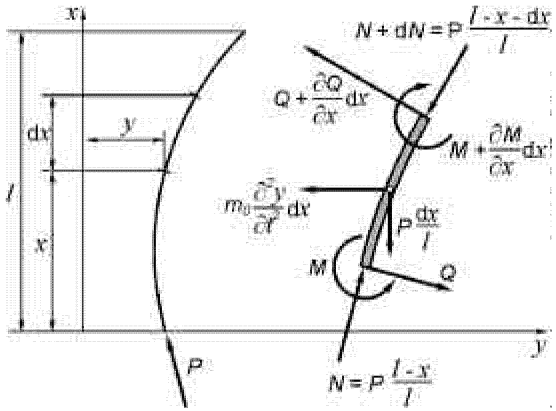

Fig. 389

Boundary conditions are

$$\text{at } \zeta = 0 \qquad \frac{d^2Y}{d\zeta^2} = 0, \ \frac{d^3Y}{d\zeta^3} = 0,$$

$$\text{at } \zeta = 1 \qquad \frac{d^2Y}{d\zeta^2} = 0, \ \frac{d^3Y}{d\zeta^3} = 0.$$

The solution we find in expanded form is as follows

$$Y = \sum_{n=0,1,2,} A_n \zeta^n.$$

According to the boundary conditions at the rod's ends $A_2 = A_3 = 0$,

$$\sum A_n n(n-1) = 0\,, \qquad \sum A_n n(n-1)(n-2) = 0\,. \tag{2}$$

We have the recurrent formula for the term of series determination

$$A_n = \frac{1}{n(n-1)(n-2)(n-3)} \{\omega^2 A_{n-4} + \beta^2 \left[A_{n-3}\,(n-3)^2 - A_{n-2}\,(n-2)\,(n-3)\right]\}.$$

Constants A_0 and A_1 remain indeterminate. They must be selected in such a way that the two last boundary conditions are satisfied. As in expressions (2) A_0 and A_1 are linearly dependent and we can write

$$\sum A_n n(n-1) = K_0 A_0 + K_1 A_1 = 0\,,$$

$$\sum A_n n(n-1)(n-2) = L_0 A_0 + L_1 A_1 = 0\,.$$

The existence condition for the nontrivial solution is following:

$$K_0 L_1 + K_1 L_0 = 0\,. \tag{3}$$

The calculation algorithm is described below.

1) Specify β and ω.

2) If we assume that $A_0 = 0$ and $A_1 = 0$ we derive terms of the series by the recurrent formula. For the given problem it is enough to take 20 or 30 terms. Then calculate $\sum A_n n(n-1) = K_0$ and $\sum A_n n(n-1)(n-2) = L_0$.

3) Repeat the calculation setting $A_0 = 1$ and $A_1 = 0$: then the obtained sums are equal to K_1 and L_1 respectively. Then the magnitude of D (3) is calculated.

4) Change ω and calculate D again. Compare it with the previous one. If the sign of D does not change then proceed the calculation further. If the sign changes it means that the sought value for the given force has been passed. By interpolation we find ω. As a result, we plot the dependence of ω on β^2, which is shown in Fig. 390.

As in the case of problem 145 the frequencies of the first and second modes merge under critical force P :

$$\beta^2_{cr} = 109.69 \qquad (\omega = 23.02).$$

The critical force is

$$P_{cr} = 109.69\,\frac{EJ}{l^2}.$$

The rod vibration modes for several values of P are shown in Fig. 390. Moreover the cases of compressive and tensile force P also are considered. It is interesting that for some values of P the nodal points become imaginary.

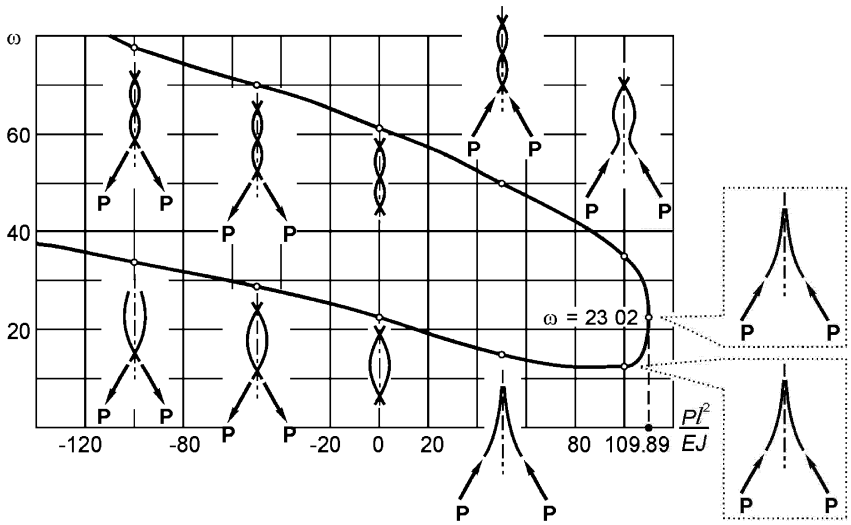

Fig. 390

148. Obviously here problem 145 is repeated though under different boundary conditions. Relation (9) of problem 145 is valid, only the boundary conditions are changed. Now we have

$$\frac{d^2Y}{d\zeta^2} = 0 \quad \text{and} \quad \frac{d^3Y}{d\zeta^3} = 0 \quad \text{at } \zeta = 0$$

$$\frac{d^2Y}{d\zeta^2} = 0 \quad \text{and} \quad \frac{d^3Y}{d\zeta^3} = 0 \quad \text{at } \zeta = 1 \tag{1}$$

Then we obtain four equations:

$$\begin{aligned}
-\alpha_1^2 C_2 + \alpha_2^2 C_4 &= 0\,,\\
-\alpha_1^3 C_1 + \alpha_2^3 C_3 &= 0\,,\\
-\alpha_1^2 C_1 \sin\alpha_1 - \alpha_1^2 C_2 \cos\alpha_1 + \alpha_2^2 C_3 \sinh\alpha_2 + \alpha_2^2 C_4 \cosh\alpha_2 &= 0\,,\\
-\alpha_1^3 C_1 \cos\alpha_1 + \alpha_1^3 C_2 \sin\alpha_1 + \alpha_2^3 C_3 \cosh\alpha_2 + \alpha_2^3 C_4 \sinh\alpha_2 &= 0\,,
\end{aligned}$$

By equating the determinant to zero we obtain the transcendental equation

$$2\omega(\cos\alpha_1 \cosh\alpha_2 - 1) + \beta^2 \sin\alpha_1 \sinh\alpha_2 = 0\,, \tag{2}$$

which is analyzed.

The question about rod behaviour is solved depending on the character of function $\omega = f(\beta)$. If for some value of dimensionless force β^2 the frequency ω becomes equal to zero then the rod has equilibrium forms different from the straight one. If there are no zero points for ω, then it is necessary to derive the conditions of frequency multiplicity, corresponding to the conditions of motion with increasing amplitude.

Another solution given by L.I. Balabukh is also extremely effective.

Let's return to equation (8) of problem 145. By differentiating it twice with respect to ζ and denoting $d^2Y/d\zeta^2 = Y_0$ we obtain the same equation:

$$\frac{d^4Y_0}{d\zeta^4} + \beta^2\frac{d^2Y_0}{d\zeta^2} - \omega^2 Y_0 = 0\,,$$

but boundary conditions will be different

$$Y_0 = 0 \quad \text{and} \quad \frac{dY_0}{d\zeta} = 0 \quad \text{at } \zeta = 0,$$

$$Y_0 = 0 \quad \text{and} \quad \frac{dY_0}{d\zeta} = 0 \quad \text{at } \zeta = 1. \tag{3}$$

Hence the solution will be the same as for the compressed rod clamped by its ends (Fig. 391). But here we know that the rod does not have oscillatory modes of buckling. A new equilibrium mode appears under $P_{cr} = 4\pi^2 EJ/l^2$.

We can also ascertain this by analyzing equation (2) which is just the same for the boundary conditions (1) as well as for the conditions of (3).

Fig. 391

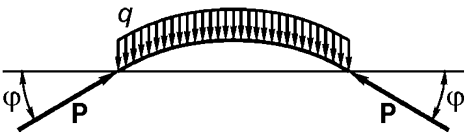

Fig. 392

It is clear that the equilibrium mode of the rod shown in Fig. 391 is relative as it should be considered in the coordinate frame attached to the rod that is under an accelerated motion in space (Fig. 392). Here two components $P\varphi$ are balanced by D'Alembert's forces of inertia $q = 2P\varphi/l$.

It is clear that the described operation of the equation's double differentiation leads to the specified conclusions only for the case of the homogeneous rod. For the case of nonuniform mass distribution or for variable rigidity the result will be different.

As an analogue we can consider two rigid rods connected to each other by a spring of stiffness c (Fig. 393). The system moves with acceleration if the angle of rotation φ rises. If we introduce the balancing inertial forces at the center of mass we obtain the condition of stability as follows

$$2c\varphi = P\varphi a\,, \quad \text{or} \quad P_{cr} = \frac{2c}{a}\,,$$

where a is the distance between hinge and the center of mass.

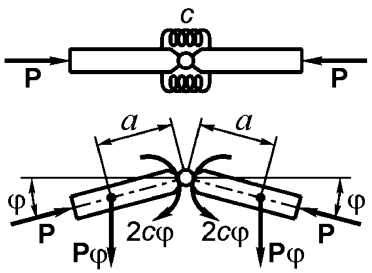

Fig. 393

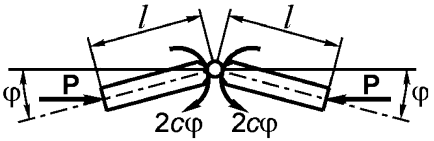

Fig. 394

For loading by forces P keeping their direction (Fig. 394) it is natural that the distribution of mass would have no significance. In this case

$$P_{cr} = \frac{2c}{l},$$

where l is the length of each rod.

149. The given problem seems to be easy but contains the same difficulties as we met in the previous problems.

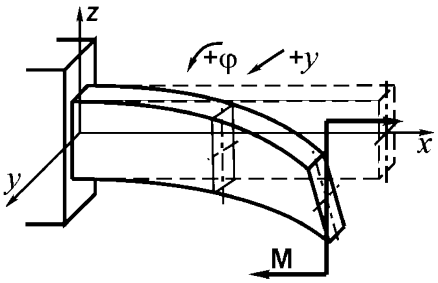

Fig. 395

Let's try to find existence conditions for equilibrium modes different from the initial and assume that the beam buckled and came out of the plane of initial bending (Fig. 395). Also, let's denote lateral displacement of the beam axis as y, and the angle of cross-section rotation with respect to the x axis as φ. The directions shown in Fig. 395 for y and φ shall be taken as positive.

If beam deflects from its initial state then the bending moment in the plane of minimum rigidity arises in its cross-sections. The moment is equal to $M\varphi$ and is directed towards the increase of beam curvature. The torsional moment occurring in the cross-section of the deflected beam is equal to My' and is directed in such a way that it tries to decrease angle φ. Hence

$$M_b = +M\varphi\,, \qquad M_t = -My'.$$

On the other hand

$$M_b = EJ\,y'', \qquad M_t = GJ_t\,\varphi',$$

where

$$J = \frac{bh^3}{12}\,, \qquad J_t = \frac{bh^3}{3}.$$

Now we obtain the equations

$$EJ\,y'' = M\varphi\,, \qquad GJ_t\,\varphi' = -My'. \tag{1}$$

Their solutions will be as follows:

$$\varphi = A\sin\alpha x + B\cos\alpha x, \qquad y = -\frac{GJ_t}{M}\,(A\sin\alpha x + B\cos\alpha x) + C,$$

where

$$\alpha^2 = \frac{M^2}{EJ\,GJ_t}\,,$$

A, B, and C are arbitrary constants which are found from the following boundary conditions:

at $x = 0$ we have $\varphi = 0,\ y = 0,\ y' = 0$. Then we arrive at

$$B = 0\,, \quad -\frac{GJ_t}{M}B + C = 0\,, \quad A = 0\,.$$

As $A = B = C = 0$, it follows that for all finite values of moment M there are no forms of equilibrium different from the plane bending form. We only have to investigate modes of motion and try to find the conditions under which beam motion with deflection increasing in time is possible.

Before we proceed to this analysis let us remark that in the case of the moment following to the end section (Fig. 396) the beam also has no equilibrium modes different than the initial form of plane bending. Only in the case of "semi-follower" moment shown in the same Fig. 396 by dashed line the existence of a new equilibrium mode is possible for

$$M = \frac{\pi}{2l}\sqrt{EJGJ_t}\,.$$

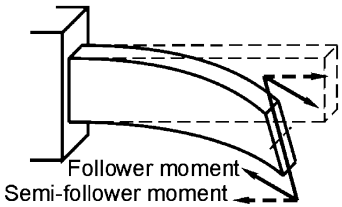

Fig. 396

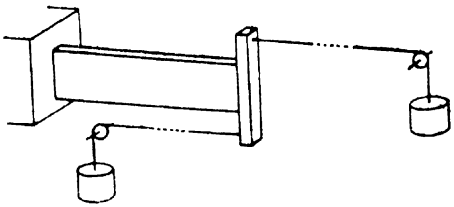

Fig. 397

The "semi-follower" moment can be realized by means of two weights (Fig. 397). It is interesting to note that the possibility of applying the specified forces or moments by means of gravity loads is for the present time a guaranty for the fact that stability of the system can be analyzed by looking for neighbouring forms of equilibrium in all known cases of loading. Till now it was not necessary to find modes of motion under loading by gravity forces.

Let's derive the equations of rod motion. For this it is necessary to consider the distributed inertial force

$$q_{in} = -\rho A \frac{\partial^2 y}{\partial t^2}$$

and distributed inertial moment due to the rotation of masses about the rod's axis

$$m_{in} = \rho J_p \frac{\partial^2 \varphi}{\partial t^2},$$

where ρ is density of the material, and J_p is cross-section polar moment of inertia.

As it is known

$$q = \frac{\partial^2 M_b}{\partial x^2}, \; m = \frac{\partial M_t}{\partial x},$$

therefore differentiating the first equation of (1) by x twice, and the second equation once and adding to the right-hand member q_{in} and m_{in} respectively we arrive at

$$\begin{aligned} EJ \frac{\partial^4 y}{\partial x^4} &= M \frac{\partial^2 \varphi}{\partial x^2} - \rho A \frac{\partial^2 y}{\partial t^2}, \\ GJ_t \frac{\partial^2 \varphi}{\partial x^2} &= -M \frac{\partial^2 y}{\partial x^2} + \rho J_p \frac{\partial^2 \varphi}{\partial t^2}. \end{aligned} \tag{2}$$

Let's assume

$$y = Yl \exp\left(i\omega \sqrt{\frac{EJ}{\rho A l^4}}\, t\right), \; \varphi = \Phi \sqrt{\frac{EJ}{GJ_t}} \exp\left(i\omega \sqrt{\frac{EJ}{\rho A l^4}}\, t\right),$$

where Y and Φ are dimensionless values, depending on the dimensionless coordinate $\zeta = x/l$ and ω is a dimensionless frequency.

Equation (2) arrives at

$$\frac{\partial^4 Y}{\partial \zeta^4} - M_0 \frac{\partial^2 \Phi}{\partial \zeta^2} - \omega^2 Y = 0\,,$$
$$\frac{\partial^2 \Phi}{\partial \zeta^2} + M_0 \frac{\partial^2 Y}{\partial \zeta^2} + k^2 \omega^2 \Phi = 0\,, \tag{3}$$

where M_0 is the dimensionless moment, and k geometric characteristics:

$$M_0 = \frac{Ml}{\sqrt{EJ\,GJ_t}}\,,\ k^2 = \frac{EJ}{GJ_t}\,\frac{J_p}{Al^2}\,. \tag{4}$$

The solution of the system (3) by means of functional analysis yields cumbersome transformations. That is why here it is more convenient to use a computer. Let's find functions Y and Φ in the form of power series

$$Y = \sum_{n=0,1,2,} A_n \zeta^n,\ \Phi = \sum_{n=0,1,2,} B_n \zeta^n.$$

Substituting Y and Φ in equations (3) we arrive at recurrence formulas

$$A_n = \frac{1}{n(n-1)(n-2)(n-3)} \left[\omega^2 A_{n-4} + M_0 B_{n-2}(n-2)(n-3)\right],$$
$$B_{n-2} = -M_0\, A_{n-2} - \frac{k^2\omega^2}{(n-2)(n-3)} B_{n-4}. \tag{5}$$

We can restrict calculations to 20-30 terms per series.

At the clamped end for $x = 0$ ($\zeta = 0$) we have $y = 0, \partial y/\partial x = 0$ and $\varphi = 0$, hence, $A_0 = A_1 = B_0 = 0$.

At the end of the rod (for $\zeta = 1$) we have

$$EJ \frac{\partial^2 y}{\partial x^2} = M\varphi\,;\ GJ_t \frac{\partial \varphi}{\partial x} = -M \frac{\partial y}{\partial x}\,;\ EJ \frac{\partial^3 y}{\partial x^3} = M \frac{\partial \varphi}{\partial x}\,.$$

The last boundary condition expresses the equality of shear force to zero at the rod's end. Actually shear force is obtained from the equilibrium condition of the element (Fig. 398). Equating to zero the sum of moments of forces with respect to the z_1 axis we get

$$Q = \frac{\partial M_b}{\partial x} - M \frac{\partial \varphi}{\partial x}, \quad \text{or} \quad Q = EJ \frac{\partial^3 y}{\partial x^3} - M \frac{\partial \varphi}{\partial x}\,.$$

In dimensionless form we obtain

$$\frac{d^2 Y}{d\zeta^2} - M_0\, \Phi = 0\,, \quad \frac{d\Phi}{d\zeta} + M_0 \frac{dY}{d\zeta} = 0\,, \quad \frac{d^3 Y}{d\zeta^3} - M_0 \frac{d\Phi}{d\zeta} = 0\,,$$

or substituting $\zeta = 1$,

$$\sum A_n n(n-1) - M_0 \sum B_n = 0,$$
$$\sum B_n n + M_0 \sum A_n n = 0, \tag{6}$$
$$\sum A_n n(n-1)(n-2) - M_0 \sum B_n n = 0.$$

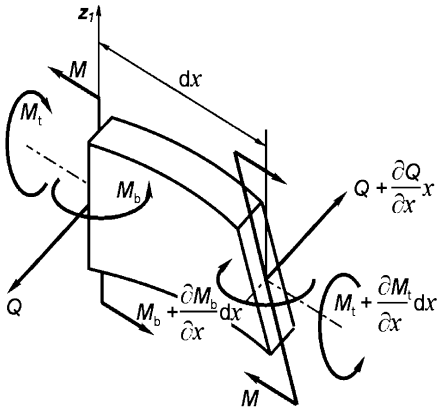

Fig. 398

In calculating the coefficients A_n and B_n the first three remain undetermined. We must choose them so that the conditions (6) are satisfied. But equations (6) are homogeneous with respect to A_2, A_3 and B_1. That is why we can write them in the form

$$a_{11}A_2 + a_{12}A_3 + a_{13}B_1 = 0\,,$$
$$a_{21}A_2 + a_{22}A_3 + a_{23}B_1 = 0\,,$$
$$a_{31}A_2 + a_{32}A_3 + a_{33}B_1 = 0\,.$$

In order to obtain a nontrivial solution it is necessary to satisfy the condition

$$D = \begin{vmatrix} a_{11} & a_{12} & a_{13} \\ a_{21} & a_{22} & a_{23} \\ a_{31} & a_{32} & a_{33} \end{vmatrix} = 0\,.$$

The calculation order will be as follows.

First, prescribe the parameter

$$k^2 = \frac{EJ}{GJ_t}\frac{J_p}{Al^2} = \frac{1+\mu}{24}\frac{b^2}{l^2}\,.$$

Then, settle M_0 and ω.

Next, suppose that $A_2 = 1$, $A_3 = B_1 = 0$ and using recurrence formulas (5) determine the coefficients A_n and B_n, and then the left parts of equations (6). They are equal respectively to a_{11}, a_{21} and a_{31}. Then assume that $A_2 = 0$, $A_3 = 1$, $B_1 = 0$. Now the left parts of equations (6) give magnitudes of a_{12}, a_{22} and a_{32}. Finally if we assume $A_2 = A_3 = 0$ and $B_1 = 1$ we find a_{13}, a_{23} and a_{33}. Calculating the determinant we prove that it is not equal to zero. Then changing the value of ω we seek $D = 0$ and we find the frequencies of the natural vibrations for the given moment M_0.

Changing M_0 we watch the behaviour of frequencies and as it was done in the previous examples we find the conditions of their multiplicity.

For $M_0 = 0$ we have frequencies of bending (ω_b) and torsional (ω_t) natural vibrations. As M_0 increases, frequencies come close and for critical value of moment M_0 frequencies become multiple (points A in Fig. 399).

The dependence of M_{0cr} on parameter k is shown in Fig. 400. M_{0cr} vanishes for $k = 0.445$. This is the case when the frequency of the first bending mode ω_b coincides with the frequency ω_t of the first mode of torsional vibrations.

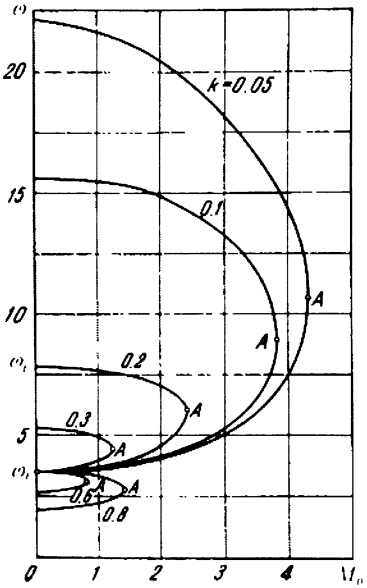

Fig. 399

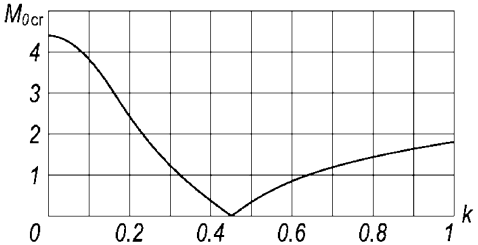

Fig. 400

It should be noted that the first least frequency always merges with the second one independently of the fact whether it is interpreted as bending or torsional mode. For example, if $k = 0.05$ the first torsional frequency $\omega_{1t} = 31.4$ while the bending frequencies are $\omega_{1b} = 3.5$ and $\omega_{2b} = 22$. As the moment increases bending frequencies merge. While parameter k increases, the first torsional frequency decreases and when it becomes less than the second bending frequency the first bending one merges with it under increase of M_0. This is seen from plots shown in Fig. 399.

In the case of follower moment, i.e. when the moment plane rotates together with the end section, the boundary conditions change and instead of (6) we have

$$\begin{aligned} \sum A_n n(n-1) &= 0\,, \\ \sum B_n n &= 0\,, \\ \sum A_n n(n-1)(n-2) &= 0\,. \end{aligned} \tag{7}$$

The critical values of moment for conditions (7) are the same as for conditions (6). The coincidence of results is not accidental. It follows from the mutual conversion of rod loading conditions at the left and right ends just as it was done for systems considered in problems 145 and 146.

150. The problem entered the literature as the E.L. Nikolai's problem [6]. The solution of this problem in 1927 revealed for the first time the existence of such systems where stability analysis can not be performed on the basis of searching equilibrium states according to Euler's approach. Actually for the easiest case when column rigidities in two principal planes are equal we have the following equations of equilibrium:

$$EJy'' = -Py + Mz',$$
$$EJz'' = -Pz - My'. \tag{1}$$

They are obtained from equations (1) of problem 116 if we replace the sign of P with the opposite one.

The solution remains unchanged:

$$y = A\cos\alpha_1 x + B\sin\alpha_1 x + C\cos\alpha_2 x + D\sin\alpha_2 x\,,$$
$$y = A\sin\alpha_1 x - B\cos\alpha_1 x + C\sin\alpha_2 x - D\cos\alpha_2 x\,,$$

where $\alpha_1$and α_2 are the roots of the quadric equation

$$\alpha^2 + \frac{M}{EJ}\alpha - \frac{P}{EJ} = 0\,. \tag{2}$$

While deriving equations (1) we assume that displacements y and z refer to the line of action of force P. Therefore as the origin of x, y and z is at the point of force P application (Fig. 401) we obtain the boundary conditions:

at $x = 0$ $\quad y = z = 0\,,$
at $x = l$ $\quad y' = z' = 0\,.$

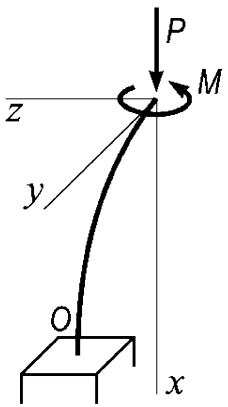

Fig. 401

This gives

$$A + C = 0, \quad B + D = 0\,,$$

$$-A\alpha_1 \sin\alpha_1 l + B\alpha_1 \cos\alpha_1 l - C\alpha_2 \sin\alpha_2 l + D\alpha_2 \cos\alpha_2 l = 0\,,$$
$$A\alpha_1 \cos\alpha_1 l + B\alpha_1 \sin\alpha_1 l + C\alpha_2 \cos\alpha_2 l + D\alpha_2 \sin\alpha_2 l = 0\,.$$

Equating the determinant of the system to zero we get

$$\alpha_1^2 + \alpha_2^2 = 2\alpha_1\alpha_2 \cos[(\alpha_1 - \alpha_2)l]\,. \tag{3}$$

But according to equation (2)

$$\alpha_1\alpha_2 = -\frac{P}{EJ}\,, \quad \alpha_1^2 + \alpha_2^2 = \left(\frac{M}{EJ}\right)^2 + \frac{2P}{EJ}\,,$$

$$\alpha_1 - \alpha_2 = 2\sqrt{\left(\frac{M}{EJ}\right)^2 + \frac{2P}{EJ}}\,,$$

whence equation (3) yields

$$\cos\sqrt{\left(\frac{Ml}{EJ}\right)^2 + \frac{4Pl^2}{EJ}} = -\left(1 + \frac{M^2}{2PEJ}\right).$$

For nontrivial values of moment M the equation can not be satisfied, since the absolute value of the right side is more than unity. Only in the case $M = 0$

$$\cos\sqrt{\frac{4Pl^2}{EJ}} = -1,$$

and then we obtain an ordinary value for the critical force

$$P_{cr} = \frac{\pi^2 EJ}{4l^2}.$$

So for arbitrarily small but non-zero value of M and arbitrarily large force P the rod does not have equilibrium states different from the straight one. Exactly the same result is obtained in the case where the plane of torque M rotates together with the rod end section while bending. In case of a "semi-follower" moment, produced by two weights, the system has equilibrium states that are different from the initial. We have seen the same in the solution of problem 137. Thus, we reveal an analogy with the behaviour of the system considered in the previous problem. However, there we only had one external load factor: moment M. In the given problem we have two loads: force P and torque M. If only force P is applied then while it increases the transfer to a new equilibrium state occurs. But for torque (excluding "semi-follower") the transfer to new forms of motion is characteristic. That is why it is interesting to look for the behaviour of the system in the area of action of both loads and find out where the type of motion occurs earlier, and where the static form of equilibrium.

By differentiating equations (1) twice by x and adding terms corresponding to inertial forces, we obtain

$$EJ_1\frac{\partial^4 y}{\partial x^4} - M\frac{\partial^3 z}{\partial x^3} + P\frac{\partial^2 y}{\partial x^2} + \rho A\frac{\partial^2 y}{\partial t^2} = 0\,,$$
$$EJ_2\frac{\partial^4 z}{\partial x^4} + M\frac{\partial^3 y}{\partial x^3} + P\frac{\partial^2 z}{\partial x^2} + \rho A\frac{\partial^2 z}{\partial t^2} = 0\,. \qquad (4)$$

As we shall see further the behaviour of the system substantially depends on the ratio of principal bending rigidities. That is why in equations (4) instead of single rigidity we introduce two: EJ_1 and EJ_2.

Now it is more convenient to have the origin of coordinates at the clamped end (Fig. 402). Regardless of loading conditions at $x = 0$ we have $y = z = 0$ and $\partial y/\partial x = \partial z/\partial x = 0$.

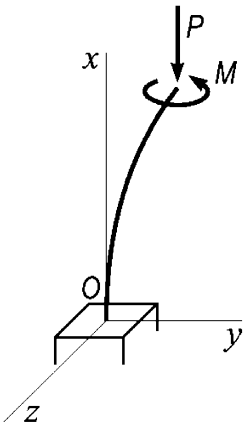

Fig. 402

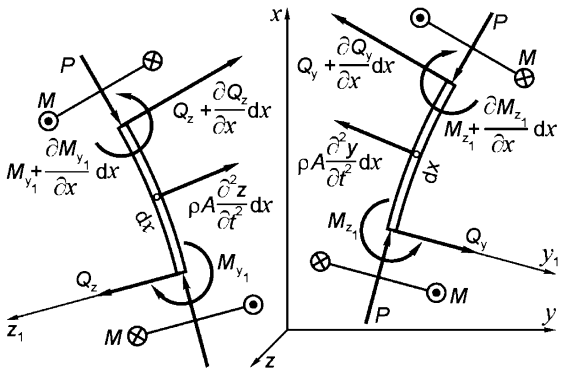

Fig. 403

The shear forces Q_y and Q_x expressions for the bent rod become more complicated by insertion of a term containing torque, i.e.

$$Q_y = \frac{\partial M_{z_1}}{\partial x} - M\frac{\partial^2 z}{\partial x^2}\,, \qquad Q_z = \frac{\partial M_{y_1}}{\partial x} + M\frac{\partial^2 y}{\partial x^2}\,,$$

where M_{z_1} and M_{y_1} are bending moments with respect to the movable axes y_1, z_1. It is easy to derive the required relations if we balance the sum of moments produced by forces acting on element dx with respect axes y_1 and z_1 (see Fig. 403, where projections of this element on planes xy and xz are shown). At the end of the rod

$$Q_y = -P\frac{\partial y}{\partial x}\,, \qquad Q_z = -P\frac{\partial z}{\partial x}\,,$$

therefore at $x = l$ we have two boundary conditions invariant with moment M behaviour:

$$\left| EJ_1 \frac{\partial^3 y}{\partial x^3} + P\frac{\partial y}{\partial x} - M\frac{\partial^2 z}{\partial x^2} \right|_{x=l} = 0\,,$$
$$\left| EJ_2 \frac{\partial^3 z}{\partial x^3} + P\frac{\partial z}{\partial x} + M\frac{\partial^2 y}{\partial x^2} \right|_{x=l} = 0\,, \tag{5}$$

If the plane of torque M action rotates together with the rod's end section under bending then $M_{y_1} = M_{z_1} = 0$ at $x = l$, and then we have two additional conditions:

$$\left| \frac{\partial^2 y}{\partial x^2} \right|_{x=l} = 0 \quad \text{and} \quad \left| \frac{\partial^2 z}{\partial x^2} \right|_{x=l} = 0\,. \tag{6}$$

If the plane of torque M action does not rotate under bending of the rod, then at $x = l$ we have $M_{y_1} = M\partial z/\partial x$ and $M_{z_1} = -M\partial y/\partial x$ and then

$$\left| EJ_1 \frac{\partial^2 y}{\partial x^2} - M\frac{\partial z}{\partial x} \right|_{x=l} = 0\,,$$
$$\left| EJ_2 \frac{\partial^2 z}{\partial x^2} + M\frac{\partial y}{\partial x} \right|_{x=l} = 0\,. \tag{7}$$

Finally, in case of "semi-follower" torque we get

$$\left| EJ_1 \frac{\partial^2 y}{\partial x^2} - M\frac{\partial z}{\partial x} \right|_{x=l} = 0\,,$$
$$\left| \frac{\partial^2 z}{\partial x^2} \right|_{x=l} = 0\,. \tag{8}$$

Let's apply the dimensionless parameters. For this let's suppose that

$$y = Yle^{i\omega at},\ z = \sqrt{\frac{EJ_2}{EJ_1}}\,Zle^{i\omega at},$$

where Y and Z are dimensionless sought functions which depend on x only, ω is dimensionless frequency and

$$a = \sqrt{\frac{EJ_1}{\rho Al^4}}\,.$$

As independent variable instead of x we shall take $\zeta = x/l$. After substituting x, y and z in equation (4) we obtain the system of ordinary differential equations

$$\frac{d^4Y}{d\zeta^4} - M_0\frac{d^3Z}{d\zeta^3} + \beta^2\frac{d^2Y}{d\zeta^2} - \omega^2 Y = 0\,,$$
$$\frac{d^4Z}{d\zeta^4} + M_0\frac{d^3Y}{d\zeta^3} + \frac{\beta^2}{k^2}\frac{d^2Z}{d\zeta^2} - \frac{\omega^2}{k^2}Z = 0\,, \tag{9}$$

where M_0 and β^2 are dimensionless torque and force:

$$M_0 = \frac{Ml}{\sqrt{EJ_1\,EJ_2}}\,, \qquad \beta^2 = \frac{Pl^2}{EJ_1}\,.$$

Coefficient k characterizes the ratio of rigidities

$$k = \sqrt{\frac{EJ_2}{EJ_1}}\,.$$

It is supposed that EJ_1 is minimal rigidity, therefore $k \geq 1$.

By using dimensionless parameters let's rearrange the boundary conditions also.

At $\zeta = 0$ we have $Y = Z = 0\,,\ \dfrac{dY}{d\zeta} = \dfrac{dZ}{d\zeta} = 0.$

For the rod end, i.e. for $\zeta = 1$ in case of loading by torque, where the plane rotates together with the end section, we obtain

$$\left|\frac{d^3Y}{d\zeta^3} + \beta^2\frac{dY}{d\zeta} - M_0\frac{d^2Z}{d\zeta^2}\right|_{\zeta=1} = 0\,,$$

$$\left|\frac{d^3Z}{d\zeta^3} + \frac{\beta^2}{k^2}\frac{dZ}{d\zeta} + M_0\frac{d^2Y}{d\zeta^2}\right|_{\zeta=1} = 0\,, \tag{10}$$

$$\left|\frac{d^2Y}{d\zeta^2}\right|_{\zeta=1} = 0\,, \quad \left|\frac{d^2Z}{d\zeta^2}\right|_{\zeta=1} = 0\,, \tag{11}$$

If the torque's plane of action does not rotate during the rod's bending, then the first two conditions are valid but the last two take the form

$$\left|\frac{d^2Y}{d\zeta^2} - M_0\frac{dZ}{d\zeta}\right|_{\zeta=1} = 0\,, \quad \left|\frac{d^2Z}{d\zeta^2} + M_0\frac{dY}{d\zeta}\right|_{\zeta=1} = 0\,, \tag{12}$$

For the case of "semi-follower" torque again the conditions (10) are valid and instead of relations (11) we get

$$\left|\frac{d^2Y}{d\zeta^2} - M_0\frac{dZ}{d\zeta}\right|_{\zeta=1} = 0\,, \quad \left|\frac{d^2Z}{d\zeta^2}\right|_{\zeta=1} = 0\,, \tag{13}$$

Only computer analysis is appropriate for solving the problem. The algorithm was given while solving the previous problems.

Let's assume that

$$Y = \sum A_n\zeta^n, \qquad Z = \sum B_n\zeta^n,$$

and substitute Y and Z in equations (9). After that we arrive at the recurrence formulas:

$$\begin{aligned} A_n = {} & \frac{1}{n(n-1)(n-2)(n-3)}\,[M_0B_{n-1}(n-1)(n-2)(n-3) \\ & -\beta^2A_{n-2}(n-2)(n-3) + \omega^2A_{n-4}], \\ B_n = {} & \frac{1}{n(n-1)(n-2)(n-3)}\,[M_0A_{n-1}(n-1)(n-2)(n-3) \\ & -\frac{\beta^2}{k^2}B_{n-2}(n-2)(n-3) + \frac{\omega^2}{k^2}B_{n-4}]. \end{aligned} \tag{14}$$

As at the clamped end $Y = Z = 0$, $\dfrac{dY}{d\zeta} = \dfrac{dZ}{d\zeta} = 0$ then obviously

$$A_0 = A_1 = B_0 = B_1 = 0\,.$$

Another four coefficients A_2, A_3, B_2 and B_3 must be chosen in such a way that they satisfy the boundary conditions at the column end, i.e. at $\zeta = 1$. For this consider relations (10) and also relations (11), or (12), or (13) in accordance with the conditions of loading.

As coefficients A_2, A_3, B_2 and B_3 enter in all given equations linearly, the following four equations in the unknown coefficients can be written as

$$\begin{aligned}
a_{11}A_2 + a_{12}A_3 + a_{13}B_2 + a_{14}B_3 &= 0\,,\\
a_{21}A_2 + a_{22}A_3 + a_{23}B_2 + a_{24}B_3 &= 0\,,\\
a_{31}A_2 + a_{32}A_3 + a_{33}B_2 + a_{34}B_3 &= 0\,,\\
a_{41}A_2 + a_{42}A_3 + a_{43}B_2 + a_{44}B_3 &= 0\,.
\end{aligned} \tag{15}$$

The two first equations are obtained from relations (10), and the bottom two either from (11), (12), or (13) in accordance with the type of torque M.

If for the prescribed magnitudes of parameters M_0, β, k and ω specify $A_2 = 1$, and $A_3 = B_2 = B_3 = 0$, then according to the recurrence formulas (14) we can determine $A_4, B_4, A_5, B_5, \ldots$ Then by summing for certain n (for example $n = 30$) we determine values of derivatives of functions Y and Z at $\zeta = 1$, i.e.

$$\left|\frac{dY}{d\zeta}\right|_{\zeta=1} = \sum A_n n, \quad \left|\frac{dZ}{d\zeta}\right|_{\zeta=1} = \sum B_n n, \quad \left|\frac{d^2Y}{d\zeta^2}\right|_{\zeta=1} = \sum A_n n(n-1), \ldots$$

The calculated sums are substituted into the relations (10) and (11), (12) or (13) and we obtain coefficients a_{11}, a_{21}, a_{31}, a_{41} of system (15). If we repeat all calculations assuming that $A_3 = 1$, and $A_2 = B_2 = B_3 = 0$, then obviously we find coefficients a_{12}, a_{22}, a_{32}, a_{42}. Then we should specify $B_2 = 1$ and at last $B_3 = 1$. Thus by fourfold repeating of calculations we find all the coefficients of system (15).

The condition of nontrivial solution existence for Y and Z is the equality to zero of the determinant

$$\begin{vmatrix}
a_{11} & a_{12} & a_{13} & a_{14}\\
a_{21} & a_{22} & a_{23} & a_{24}\\
a_{31} & a_{32} & a_{33} & a_{34}\\
a_{41} & a_{42} & a_{43} & a_{44}
\end{vmatrix} = D = 0\,. \tag{16}$$

Thus, the analysis of stability is reduced to elaboration of the relations between M_0, β, k, and ω, for which the condition (16) is valid. For practical purposes first of all we should fix the parameter k, then β and finally M_0. Specifying different ω we find such a value for which the determinant D is equal to zero. Then we change M_0 and again ω is determined. Thus we establish the relation of ω and M_0 for specified β and k. Such a dependence is shown in Fig. 404 for $k = 2$.

Obviously we do not need to plot all the relations or print a lot of calculated data. It is easy to program the algorithm by adding the criteria of estimating the behaviour of frequency in dependence of M_0 and β. If frequency vanishes it means that we find a new equilibrium state. If frequencies of the first two modes merge then we find the kind of motion. Naturally the ratio of rigidities k^2 must remain unchanged during calculations.

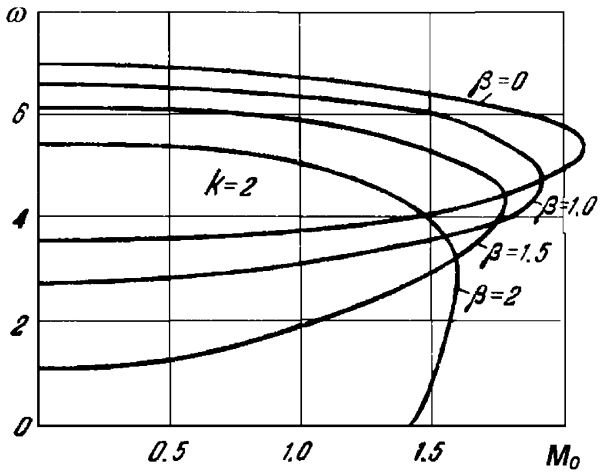

Fig. 404

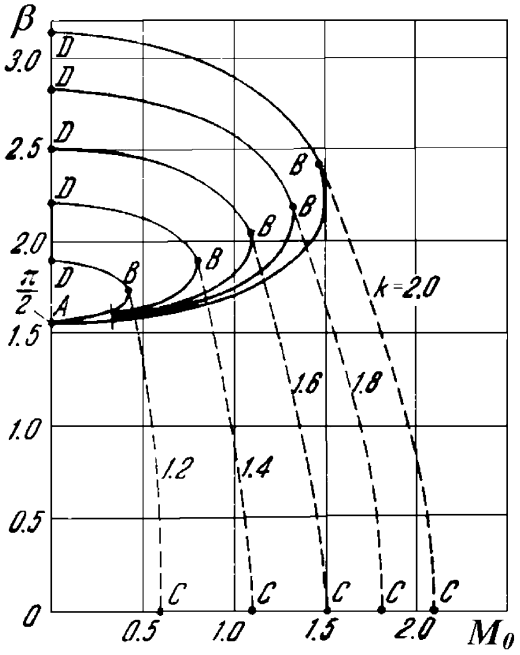

Fig. 405

Results of searching the critical values of parameters M_0 and β are shown in Fig. 405. For boundary conditions (11) and (12) they turn out to be absolutely equal. In other words, there is no difference between loading by follower and non-follower torque. For each fixed $k = \sqrt{EJ_2/EJ_1}$ the stability domain (Fig. 405) is bounded by the curvilinear quadrangle $OABC$. The point A is common for all curves. Here $\beta = \dfrac{\pi}{2} = \sqrt{Pl^2/(EJ_1)}$, which corresponds to critical force

$$P_{cr} = \frac{\pi^2 EJ_1}{4l^2}\,.$$

Curves AB define the conditions of transfer to a new equilibrium state and correspond to bending in the plane of minimal rigidity EJ_1. It is interesting that while torque increases the critical force increases too. This happens because the applied torque forces the rod to deviate from the plane of minimal rigidity during bending.

The upper segments of curves ABD, shown in Fig. 405, correspond to the equilibrium state associated with bending in the plane of maximal rigidity. The magnitude of parameter β at points D is k times greater than at point A.

From the right side the stability domain is bounded by the condition of transition to the oscillatory mode of motion. The transition boundaries are shown in Fig. 405 by dashed lines BC.

If $k \to 1$ the stability domain collapses in a straight-line segment OA. Point D merges with A, and C with O.

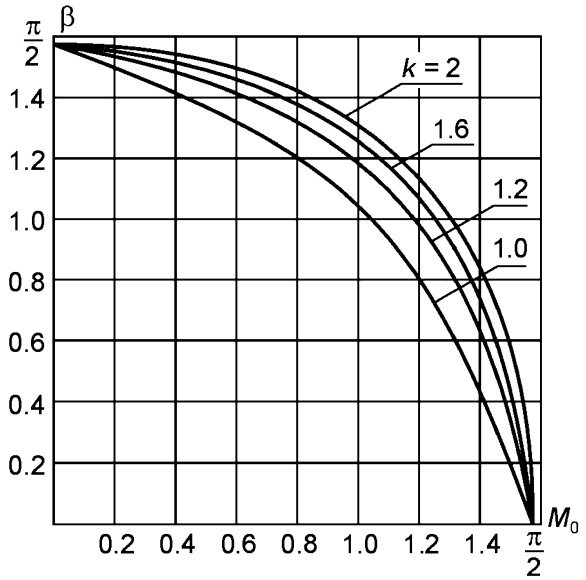

Fig. 406

For "semi-follower" torque the modes of motion with increasing amplitude are not found. Only new equilibrium states ($\omega = 0$) appear for certain values of M and P.

The determination of critical states here can be produced analytically, but there is no need of doing this as there is an according program and it is easier to compute these calculations by the algorithm already used.

The curves bounding the stability region are shown in Fig. 406 and do not require explanation.

151. Let's assume that cross-sections of the strip do not distort. Then axial strain can be presented as a linear function in y (Fig. 407)

$$\varepsilon_x = \varepsilon_0 + \varkappa y\,,$$

where $\varkappa$ is variation of strip curvature in plane xy. Axial stress will be as follows

$$\sigma_x = E(\varepsilon_0 + \varkappa y - \alpha t)\,,$$

where αt is thermal strain.

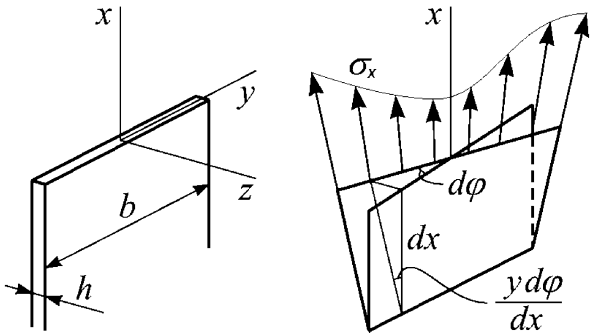

Fig. 407

As normal force in a cross-section and bending moment M_z are equal to zero then

$$\int_A \sigma_x dA = 0\,, \qquad \int_A \sigma_x y dA = 0\,,$$

whence

$$\varepsilon_0 = \frac{1}{b}\int_{-b/2}^{+b/2} \alpha t\, dy\,, \quad \varkappa = \frac{12}{b^3}\int_{-b/2}^{+b/2} \alpha t\, y\, dy\,.$$

If twisting appears stresses σ_x produce the resultant moment with respect to the x axis (Fig. 407) which is equal to

$$M_x = \int y\frac{d\varphi}{dx}\sigma_x\, y\, dA, \quad \text{or} \quad M_x = \frac{d\varphi}{dx}\int \sigma_x\, y^2 dA\,.$$

Moreover, the moment of shear stresses occurs in the strip under twisting. As is well known, it is equal to

$$M_\tau = \frac{1}{3} b h^3 G \frac{d\varphi}{dx} .$$

The sum of these moments is equal to zero, therefore

$$\frac{1}{3} b h^3 G + \int_A \sigma_x y^2 dA = 0 .$$

Substituting here σ_x we find

$$-\int_{-b/2}^{+b/2} (\varepsilon_0 + \varkappa y - \alpha t)\, y^2 dy = \frac{b h^2}{6(1+\mu)} ,$$

where μ is the Poisson coefficient. By excluding ε_0, we obtain

$$\int_{-b/2}^{+b/2} \alpha t \,(y^2 - \frac{b^2}{12})\, dy = \frac{b h^2}{6(1+\mu)} . \qquad (1)$$

This is the condition of transition to a new equilibrium state.

It should be noted that for the linear law of temperature distribution along axis y, i.e. for

$$\alpha t = A + B y ,$$

the left side of the expression (1) vanishes for any values of A and B. Hence, for linear distribution of temperature a new form of equilibrium does not exist.

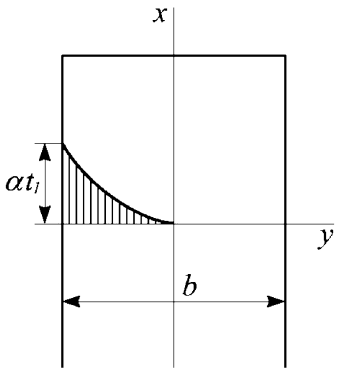

Fig. 408

Let's suppose that the thermal strains in the left half of the strip are distributed by quadratic law (Fig. 408)

$$\alpha t = \frac{4 \alpha t_1}{b^2} y^2 .$$

Then the expression (1) takes the form

$$\int_{-b/2}^{0} \frac{4\,\alpha\,t_1}{b^2}\,y^2\left(y^2-\frac{b^2}{12}\right)dy=\frac{bh^2}{6(1+\mu)}\,,$$

or

$$\alpha\,t_{1\,cr}=\frac{15}{1+\mu}\,\frac{h^2}{b^2}\,.$$

It should be noted that for a relatively thinner sheet the temperature of stability loss (buckling) is lower.

152. Let's return to the solution of problem 123. It is easy to make sure that the pipeline, clamped by one end, does not have equilibrium states except the initial straight configuration. Actually, let's use from the solution of problem 123 that

$$y=A\sin\alpha x+B\cos\alpha x+Cx+D,$$

but for the different boundary conditions, namely:

$$\begin{aligned}&\text{at } x=0 \quad y=0 \quad \text{and} \quad y'=0\,,\\ &\text{at } x=l \quad y''=0 \quad \text{and} \quad y'''=0\,,\end{aligned}$$

whence

$$\begin{aligned}B+D&=0\,,\\ A\alpha+C&=0\,,\\ A\sin\alpha l+B\cos\alpha l&=0\,,\\ A\cos\alpha l-B\sin\alpha l&=0\,.\end{aligned}$$

It follows from the last two relations that nonzero solutions for A and B exist if

$$\sin^2\alpha l+\cos^2\alpha l=0,$$

which is impossible. Hence, $A=B=C=D=0$, and the rod does not have equilibrium states different than the initial straight one.

It is necessary to look for the modes of motion [16]. It should be noted that existence of these modes is easily revealed, if the compressed air is applied through the elastic rubber hose. Just the same oscillatory motion can be observed in the process of water delivery through a hose lying, for example, on wet slippery ice during the skating-rink flooding.

Let mass of pipe per unit length be m_T, and mass of liquid per unit length be m_L. The masses of segment dx (Fig. 409) are $m_T\,dx$ and $m_L\,dx$ respectively. The inertial force arising at the segment dx during the pipeline's transverse motion is equal to

$$-\frac{\partial^2 y}{\partial t^2}\,(m_T+m_L)\,dx.$$

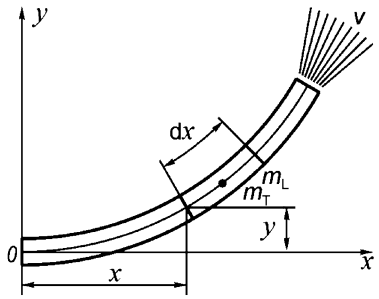

Fig. 409

As the particle flow rotates with angular velocity $\partial^2 y/\partial x \partial t$ the Coriolis acceleration appears. The corresponding inertial force will be:

$$-2\,\frac{\partial^2 y}{\partial x \partial t}\,v\,m_L\,dx.$$

With the same sign we write the expression for force, caused by the curvature of flow (or by normal acceleration):

$$-\frac{\partial^2 y}{\partial x^2}\,v^2 m_L\,dx\,.$$

The resultant of these forces divided by dx gives the intensity of the transverse "external" load. Hence,

$$EJ\frac{\partial^4 y}{\partial x^4} = -\frac{\partial^2 y}{\partial t^2}\,(m_T + m_L) - 2\,\frac{\partial^2 y}{\partial x \partial t}\,v\,m_L - \frac{\partial^2 y}{\partial x^2}\,v^2 m_L.$$

Let's rearrange the equation to the dimensionless form. Assume, that

$$y = Y l \exp\left[(\varepsilon + i\omega)a_0 t\right], \qquad a_0 = \sqrt{\frac{EJ}{(m_T + m_L)l^4}}\,, \quad x = l\zeta\,. \tag{1}$$

Then we arrive at

$$\frac{d^4 Y}{d\zeta^4} + \beta^2\,\frac{d^2 Y}{d\zeta^2} + 2\,\beta\,\varkappa\,(\varepsilon + i\omega)\frac{dY}{d\zeta} + (\varepsilon + i\omega)^2\,Y = 0\,, \tag{2}$$

where

$$\beta = v\sqrt{\frac{m_L l^2}{EJ}}\,, \quad \varkappa = \sqrt{\frac{m_L}{m_T + m_L}}\,, \tag{3}$$

The first parameter characterizes the flow rate of the liquid through the pipeline, the second parameter the ratio between the mass of the liquid and mass of the tube.

At the clamped end $Y = 0$ and $dY/d\zeta = 0$ for $\zeta = 0$. At the free end of the rod for $\zeta = 1$ we have

$$\frac{d^2 Y}{d\zeta^2} = 0 \quad \text{and} \quad \frac{d^3 Y}{d\zeta^3} = 0\,.$$

Now the problem is reduced to determination of this domain of parameters β and $\varkappa$ variation, where the real part of exponent index $\varepsilon + i\omega$ (1) takes positive values.

Taking into account that we can commit the determination procedure to a computer we set

$$Y = \sum C_n \zeta^n.$$

It follows from the first two boundary conditions that $C_0 = C_1 = 0$. Two other conditions take the form

$$\sum C_n n(n-1) = 0, \qquad \sum C_n n(n-1)(n-2) = 0\,. \tag{4}$$

Assuming the coefficients C_2 and C_3 as unknowns let's write the equation (4) as follows:

$$a\,C_2 + b\,C_3 = 0\,, \qquad c\,C_2 + d\,C_3 = 0. \tag{5}$$

The condition of nontrivial solutions existence is obvious:

$$\begin{vmatrix} a & b \\ c & d \end{vmatrix} = ad - bc = 0. \tag{6}$$

Now let's transform the complex form of the equation to the real-valued one. Suppose that

$$Y = Y_1 + iY_2$$

and respectively

$$C_n = A_n + iB_n, \quad Y_1 = \sum A_n \zeta^n, \quad Y_2 = \sum B_n \zeta^n.$$

By substituting Y in equation (2) and separating it on real and imaginary parts, we obtain recurrence formulas for A_n and B_n determination:

$$\begin{aligned} A_n = {} & \frac{1}{n(n-1)(n-2)(n-3)}\,[-\beta^2 A_{n-2}(n-2)(n-3) \\ & -2\,\beta\,\varkappa\,\varepsilon\,A_{n-3}(n-3) + (\omega^2 - \varepsilon^2)A_{n-4} \\ & +2\,\beta\,\varkappa\,\omega B_{n-3}(n-3) - 2\,\omega\,\varepsilon B_{n-4}]\,, \\ B_n = {} & \frac{1}{n(n-1)(n-2)(n-3)}\,[-\beta^2 B_{n-2}(n-2)(n-3) \\ & -2\,\beta\,\varkappa\,\varepsilon\,B_{n-3}(n-3) + (\omega^2 - \varepsilon^2)B_{n-4} \\ & -2\,\beta\,\varkappa\,\omega A_{n-3}(n-3) - 2\,\omega\,\varepsilon A_{n-4}]\,. \end{aligned} \tag{7}$$

Equation (6) can also be split into real and imaginary parts, supposing

$$a = a_1 + i\,a_2\,, \quad b = b_1 + i\,b_2\,, \quad c = c_1 + i\,c_2\,, \quad d = d_1 + i\,d_2\,.$$

Then we obtain two equations:

$$\begin{aligned} D_1 &= a_1 d_1 - a_2 d_2 - b_1 c_1 + b_2 c_2 = 0\,, \\ D_2 &= a_1 d_2 + a_2 d_1 - b_1 c_2 - b_2 c_1 = 0\,. \end{aligned} \tag{8}$$

Specifying $C_2 = 1$ ($A_2 = 1, B_2 = 0$) , and $C_3 = 0$ ($A_3 = B_3 = 0$), and comparing equations (4) and (5) we can see that the first sum (4) is equal to a, and the second is equal to c. Hence for $A_2 = 1$ and $B_2 = A_3 = B_3 = 0$ we have

$$a_1 = \sum A_n n(n-1)\,,$$
$$a_2 = \sum B_n n(n-1)\,,$$
$$c_1 = \sum A_n n(n-1)(n-2)\,,$$
$$c_2 = \sum B_n n(n-1)(n-2)\,.$$

If we specify that $C_2 = 0$, and $C_3 = 1$, i.e. accept $B_2 = A_2 = B_3 = 0$, $A_3 = 1$ and calculate coefficients A_n and B_n by the recurrence formulas (7), then we obtain

$$b_1 = \sum A_n n(n-1)\,,$$
$$b_2 = \sum B_n n(n-1)\,,$$
$$d_1 = \sum A_n n(n-1)(n-2)\,,$$
$$d_2 = \sum B_n n(n-1)(n-2)\,.$$

This is the procedure for calculating the values entering equation (8). Thus the algorithm for computer calculations is defined.

At first we must construct a subprogram for calculation of values D_1 and D_2 (8) for the fixed parameters $\varkappa$, β, ω and ε. Power series converge quickly and values A_n and B_n for $n > 30$, as a rule, have magnitudes less than machine zero.

Then for fixed $\varkappa$ and β we determine such ε and ω that satisfy the system (8). The search is accomplished by means of simplest linear interpolation. Specifying three points in plane ε, ω, we determine three values of D_1 and D_2 (8) for these points. Using three values of D_1 and D_2 we draw two planes in space:

$$D_1 = D_1(\varepsilon, \omega) \text{ and } D_2 = D_2(\varepsilon, \omega).$$

The line of their intersection crosses the plane ε, ω at the point with coordinates corresponding to the roots of equations (8). Then we determine the next approximation until the prescribed accuracy is satisfied. If we produce calculations while changing the parameter β, then we can observe the variation of frequency ω and damping parameter ε in dependence on flow velocity for given $\varkappa$, i.e. for given ratio between masses of media and tube.

Several such curves are shown in Fig. 410. It is significant that in the problem under consideration we do not observe frequency mergence that we encountered earlier. It can be explained by the fact that flow velocity is not only exciting but at the same time the damping factor is appearing in

presence of Coriolis forces. Damping exists even for very small velocity v, and the roots of the characteristic equation will not be imaginary but complex.

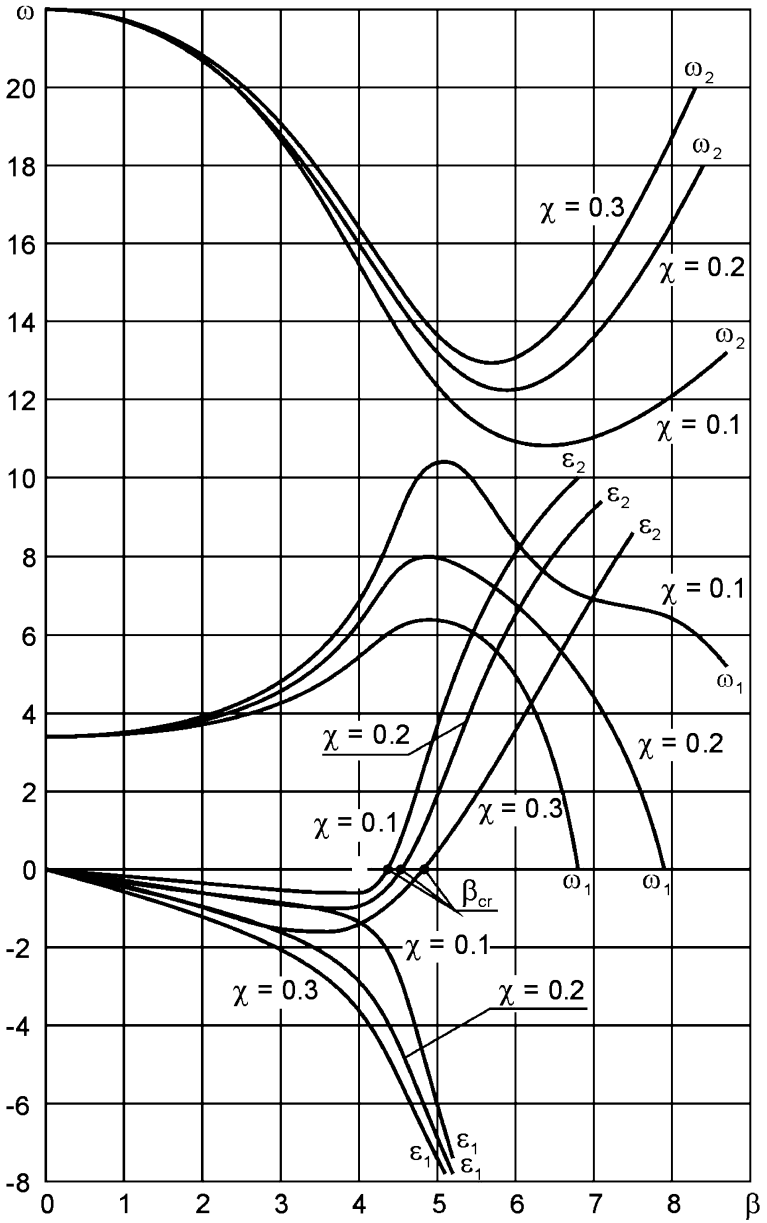

Fig. 410

If flow velocity grows then the first frequency ω (for small $\varkappa$) increases and then decreases and vanishes, but value ε in all the cases remains negative.

It means that the increasing deviations of the first mode type do not occur, but oscillatory or aperiodic damped motion takes place.

The first transition of ε to a positive half-plane occurs for frequencies corresponding to the second mode. The corresponding curves in the plot (Fig. 410) are noted by index $(\varepsilon_2,\ \omega_2)$.

Dependence of oscillation frequencies ω and critical flow velocity β on the parameter

$$\varkappa = \sqrt{\frac{m_L}{m_T + m_L}}$$

appears intricate (Fig. 411). For $\varkappa < 0.545$ vibrations of second mode are excited. For greater $\varkappa$ vibrations by third mode occur, revealed by a sharp frequency increase. Then for greater relative mass of the liquid the vibrations occur by fourth mode and frequencies increase. In a limiting case where tube mass is small in comparison with mass of the liquid the frequency and critical velocity unrestrictedly increase. If rod mass is equal to zero ($\varkappa = 0$) then the system is stable for any flow velocity.

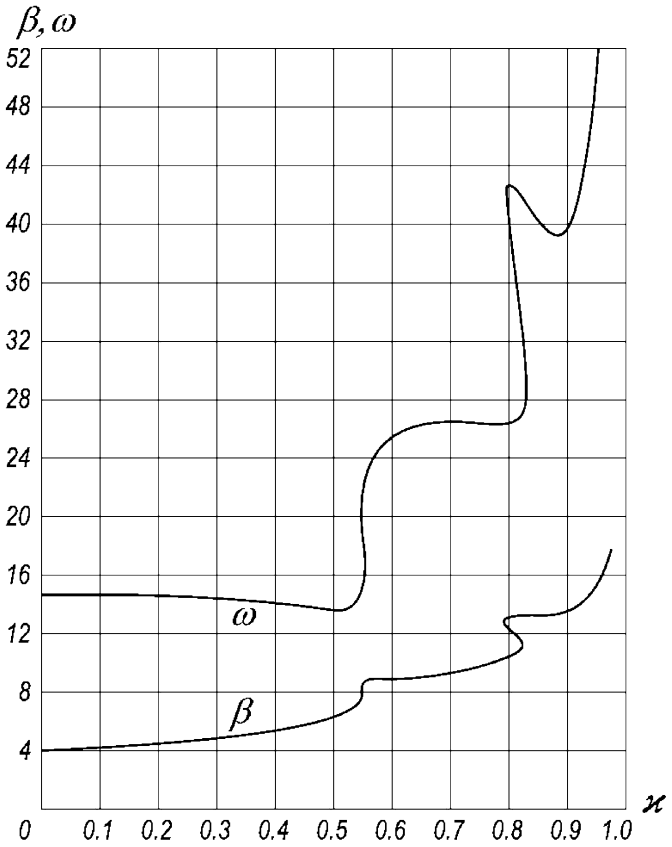

Fig. 411

153. In this case the rod also can loose its stability of plane bending mode, but it will happen under large displacements of the considerably bent rod. That excludes the application of ordinary theory of plane bending mode stability.

When we talk about lateral buckling of the strip then the word "narrow" is added not to show that in the opposite case it will not buckle, as it may seem at first sight, but in order to underline that the beam practically is not bent in the plane of bending at the moment of stability loss.

The tangling of the device thread (hairspring) is an example illustrating the fact that the loss of plane bending mode stability may occur also for the strip being bent in the plane of minimal rigidity.

Everybody knows the plane spiral spring which is installed at the balance axis of pocket and wrist watches (Fig. 412). A hairspring is also installed at the measuring cursor axis of many measuring devices: manometers, barometers, airplane speedometers, altimeters, voltmeters, amperemeters among others.

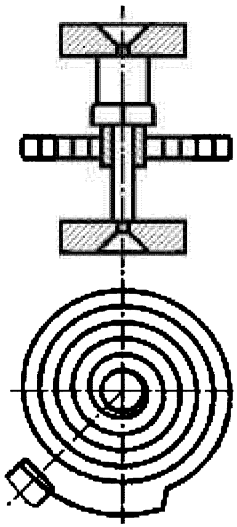

Fig. 412

The strip of a hairspring installed in a device is bent in the plane of minimal rigidity. For a certain angle of axis rotation, which is called the angle of tangling, the hairspring looses its stability of plane bending, it tangles. That is why the operating angle of rotation is set always lower than the angle of tangling.

154. The proposed problem provides a rather wide scope of research. On the one hand, we can restrict ourselves only to stability analysis with respect to axisymmetric turnover. Such a solution is rather simple. On the other hand, it is interesting to consider the existence of nonsymmetrical equilibrium states

and establish the conditions of ring exit from its plane of curvature accompanied by torsion. Here it is necessary to derive preliminarily the equilibrium equations of more general type than are used for stability analysis of the plane bending mode.

At first let's consider the stability of the ring with respect to axisymmetric turnover.

As a result of preliminarily turning inside out the initial hoop (circumference) strain $\varepsilon = 2x/R$ arises at the point A with coordinates x, y (Fig. 413). Let's impart small axisymmetric angular deflection ϑ to the ring. Point A moves to A', and additional elongation arises. The increment of hoop strain is equal to the ratio of projection of segment AA' onto the x axis to the radius R:

$$\Delta\varepsilon = \frac{OA}{R}[\cos(\alpha - \vartheta) - \cos\alpha].$$

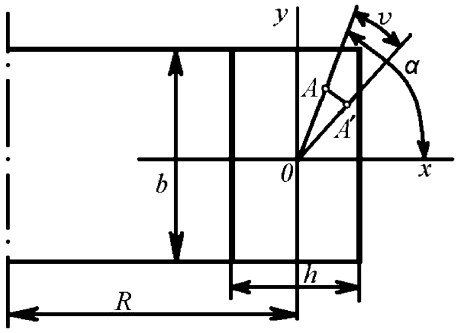

Fig. 413

As angle θ is small let's replace $\sin\vartheta$ with ϑ and $\cos\vartheta$ with $1 - \vartheta^2/2$ and then

$$\varepsilon + \Delta\varepsilon = \frac{2x}{R} + \frac{1}{R}\left(y\vartheta - x\frac{\vartheta^2}{2}\right).$$

The elastic strain energy will be

$$U = \frac{1}{2}\int_s\int_A (\varepsilon + \Delta\varepsilon)^2 dA\, ds\,,$$

where integration is produced along the circular arc s and by cross-sectional area A.

As strain is axisymmetric then $\varepsilon + \Delta\varepsilon$ does not depend upon s, and then

$$U = \frac{\pi E}{R}\int_A \left(2x - x\frac{\vartheta^2}{2} + y\vartheta\right)^2 dA\,,$$

or

$$U = \frac{\pi E}{R}\left[J_y\left(2 - \frac{\vartheta^2}{2}\right)^2 + J_x\vartheta^2\right],$$

where J_x and J_y are the area second moments with respect to the principal axes x and y.

The derivative of U by ϑ is as follows:

$$\frac{\partial U}{\partial \vartheta} = \frac{\pi E}{R}\left[-2(2 - \frac{\vartheta^2}{2})\vartheta J_y + 2J_x\vartheta\right].$$

The derivative vanishes at $\vartheta = 0$. Hence the ring turned inside-out is in equilibrium state. In order to establish whether this state is stable or unstable, let's take the second derivative.

$$\left(\frac{\partial^2 U}{\partial \vartheta^2}\right)_{\vartheta=0} = \frac{\pi E}{R}(-4J_y + 2J_x).$$

If $\left(\frac{\partial^2 U}{\partial \vartheta^2}\right)_{\vartheta=0} > 0$ the equilibrium state is stable, if $\left(\frac{\partial^2 U}{\partial \vartheta^2}\right)_{\vartheta=0} < 0$ is unstable. Hence the condition of stability of the inside-out ring under the axisymmetric disturbances is as follows:

$$J_x > 2J_y\,, \quad \text{or} \quad b > h\sqrt{2}\,.$$

Now we pass to a more general analysis of the problem.

Let's derive the equilibrium equations of the rod bent in its principal plane in the presence of small disturbances connected with torsion and bending in the second plane. Let's do this in a more general form than required for the given problem in order to apply the obtained equations further.

So let's consider an element of the beam with small curvature of length ds (Fig. 414). Six internal force factors occur in a rod cross-section. At the invisible opposite side the reciprocal force factors having corresponding increments occur. In order to simplify them they are not shown in the figure.

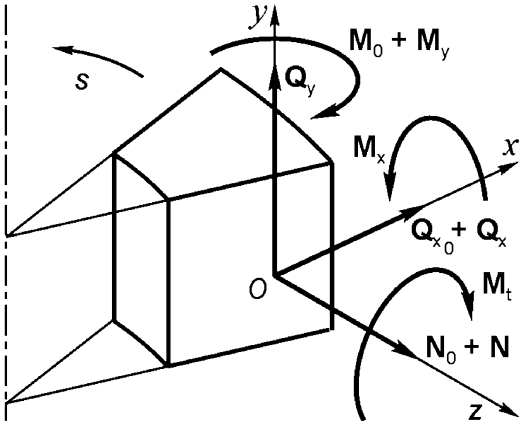

Fig. 414

At undercritical state only the force factors lying in the plane of curvature M_0, Q_{x0} and N_0 are nonzero. After additional bending and torsion of the beam the additional force factors: Q_x, Q_y, N, M_x, M_y, and M_t arise. We assume that they are small.

Let's denote small increments of curvature in planes yz and xz as p and q, and twist, as r, and derive the linear equations of the deformed element equilibrium. The principle of linearization is ordinary. Force factors of the undercritical state are introduced in equilibrium equations with account of element shape variation, and small additional force factors – disregarding the shape change, i.e. by the configuration of the undercritical state.

In order to make this procedure more clear let's derive the first equation of the equilibrium in greater detail.

The balance of all force projections onto the x axis yields

$$\begin{aligned}&Q_{x0} + Q_x - (Q_{x0} + Q_x + dQ_{x0} + dQ_x)\\ &-(N_0 + N + dN_0 + dN)\\ &\times \left(\frac{1}{R} + q\right) ds - (Q_y + dQ_y)\, r ds = 0.\end{aligned}$$

If we neglect values of higher infinitesimal order and products of Q_x by q and of Q_y by r we obtain

$$-Q'_{x\,0} - Q'_x - \frac{N_0}{R} + N_0\, q + \frac{N}{R} = 0\,.$$

At undercritical state $Q_x = N = 0$, $q = 0$, and therefore

$$Q'_{x0} + \frac{N_0}{R} = 0\,. \tag{1}$$

By summation of the first and second equation we arrive at

$$Q'_{x0} + N_0\, q + \frac{N}{R} = 0\,.$$

Similarly, if we balance the sum of force projections onto the axes y and z and resultant moments with respect to three axes we obtain five additional equations. Let's write out the system completely:

$$Q'_{x0} + N_0\, q + \frac{N}{R} = 0\,, \tag{2}$$

$$Q'_y + r Q_{x0} - p\, N_0 = 0\,, \tag{3}$$

$$N' - Q_{x0}\, q - \frac{Q_x}{R} = 0\,, \tag{4}$$

$$M'_x + \frac{M_t}{R} - Q_y - M_0\, r = 0\,, \tag{5}$$

$$M'_y + Q_x = 0\,, \tag{6}$$

$$M_t' - \frac{M_x}{R} + M_0\, p = 0\,. \tag{7}$$

In addition to equation (1) we obtain two further equilibrium equations for the undercritical state. Totally we now have three equations:

$$Q_{x0}' + \frac{N_0}{R} = 0\,, \tag{8}$$

$$N_0' - \frac{Q_{x0}}{R} = 0\,, \tag{9}$$

$$M_0' + Q_x = 0\,. \tag{10}$$

In all the above equations under $1/R$ we mean the curvature of the beam in the undercritical state which is dependent on the value of moment M_0.

The increments of curvature p and q and twist r are proportional to moments M_x, M_y and M_t :

$$M_x = EJ_x\, p\,, \qquad M_y = EJ_y\, q, \qquad M_t = GJ_t\, r.$$

Now from the general equation let's return to the considered problem. For the inside-out ring the equations (2)-(7) are simplified, as $N_0 = Q_0 = 0$, and M_0 and $1/R$ are constant. Thus we have

$$Q_x' + \frac{N}{R} = 0\,, \tag{11}$$

$$Q_y' = 0\,, \tag{12}$$

$$N' - \frac{Q_x}{R} = 0\,, \tag{13}$$

$$M_x' + \frac{M_t}{R} - Q_y - M_0\, r = 0\,, \tag{14}$$

$$M_y' + Q_x = 0\,, \tag{15}$$

$$M_t' - \frac{M_x}{R} + M_0\, p = 0\,. \tag{16}$$

If we differentiate equation (14) by s, taking into account that $Q_y' = 0$ we obtain

$$M_x'' + \frac{1}{R}\, M_k' - M_0\, r' = 0\,,$$

or

$$EJ_x\, p'' + (\frac{1}{R}\, GJ_t - M_0)\, r' = 0\,.$$

Equation (14) will take the form:

$$GJ_t\, r' = (\frac{1}{R}\, EJ_x - M_0)\, p\,. \tag{17}$$

Eliminating r we arrive at

$$p'' + \frac{k^2}{R^2}\, p = 0\,,$$

where

$$k^2 = \frac{R^2}{EJ_x\, GJ_t}\left(\frac{1}{R}GJ_t - M_0\right)\left(\frac{1}{R}EJ_x - M_0\right). \tag{18}$$

Therefore we obtain

$$p = A\sin\frac{ks}{R} + B\cos\frac{ks}{R}\,,$$

$$r = \frac{1}{GJ_t}\left(\frac{1}{R}EJ_x - M_0\right)\frac{R}{k}\left(-A\cos\frac{ks}{R} + B\sin\frac{ks}{R}\right) + C.$$

As the ring is closed, functions p and r must be periodical, i.e. return to the same values under variation of s by $2\pi R$. Hence k must be an integer.

In the case of the inside-out ring

$$M_0 = \frac{2}{R}EJ_y\,,$$

and from expression (18) we get

$$k^2 = n^2 = \left(1 - 2\frac{EJ_y}{GJ_t}\right)\left(1 - 2\frac{EJ_y}{EJ_x}\right), \tag{19}$$

where n is any integer number.

If $EJ_x = 2EJ_y$, then $n = 0$, and we arrive at the case of axisymmetric overturn of the ring. Now let's suppose that $EJ_x > 2EJ_y$. Then the second multiplier on the right-hand side of expression (19) will be positive. Let's determine the sign of the first multiplier

$$1 - 2\frac{EJ_y}{GJ_t} = 1 - 2\frac{E\dfrac{bh3}{12}}{\dfrac{E}{2(1+\mu)}\,\beta bh^3} = 1 - \frac{1+\mu}{3\beta}.$$

The coefficient of torsion rigidity β for a beam of rectangular cross-section is less than 0.333. Hence, the written expression is negative, and therefore $n^2 < 0$.

Thus, if $EJ_x > 2EJ_y$ or if $b > h\sqrt{2}$ then $n^2 < 0$ and nonsymmetrical equilibrium states do not exist. It means that the condition for stability of the inside-out ring

$$b > h\sqrt{2}$$

is correct for nonsymmetrical modes of buckling as well as for symmetric ones[1].

[1] The problems that are close to the considered one and connected with questions of ring overturn under action of distributed and concentrated moments are considered in detail in [5].

155. The solution is completely described by the equations obtained for the previous problem.

If heat is supplied through the internal surface then $t_1 > t_2$, and the constant moment arises in the ring

$$M_0 = EJ_y\,\alpha\,\frac{t_1 - t_2}{h}\,,$$

where α is the coefficient of thermal expansion.

Value k^2 (18) must be an integer

$$n^2 = \frac{R^2}{EJ_x\,GJ_t}\left(\frac{GJ_t}{R} - M_0\right)\left(\frac{EJ_x}{R} - M_0\right),$$

whence

$$M_0 = \frac{1}{2R}\left[EJ_x + GJ_t \pm \sqrt{(EJ_x + GJ_t)^2 + 4\,EJ_x\,GJ_t\,(n^2 - 1)}\right].$$

The least positive value of moment M_0 will be for $n = 0$

$$M_{0t} = \frac{EJ_x}{R}\,.$$

(The case of $n = 0$ and $M_0 = GJ_t/R$ does not satisfy the condition of displacement continuity.)

If heat is supplied through the external surface and $t_2 > t_1$, then we ought to find the least by a negative value of the modulus for moment M_0. This will be the case for $n = 2$

$$|M_{0t}| = \frac{1}{2R}\left[\sqrt{(EJ_x + GJ_t)^2 + 12EJ_xGJ_t} - EJ_x - GJ_t\right].$$

Thus under internal heating the stability loss occurs by symmetric mode, and for external heating by nonsymmetrical mode with twisting.

156. The equations obtained in solving problem 154 also give the answer for the specified question.

As $1/R = 0$ the equations (12), (14) and (16) will arrive at

$$Q_y' = 0\,, \qquad M_x' - Q_y - M_0\,r = 0\,, \qquad M_t' + M_0\,p = 0\,,$$

where the axes position corresponds to that shown in Fig. 415.

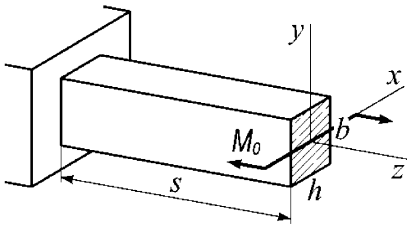

Fig. 415

Substituting $M_x = EJ_x\, p$ and $M_t = GJ_t\, r$ and excluding r we get

$$p'' + \frac{M_0^2}{GJ_t\, EJ_x}\, p = 0\,.$$

But $M_0 = EJ_y/R$. It should be noted that R is understood here as the initial radius of the uncut ring but not a radius of curvature at an undercritical state.

Let's denote

$$\frac{(EJ_y)^2}{GJ_t\, EJ_x} = k^2.$$

Then

$$p = A\sin\frac{ks}{R} + B\cos\frac{ks}{R}\,.$$

The angle of cross-section rotation with respect to the x axis is determined by integration of p by s :

$$\vartheta_x = A\frac{R}{k}\left(1 - \cos\frac{ks}{R}\right) + B\frac{R}{k}\sin\frac{ks}{R}.$$

Here the arbitrary constant of integration is already chosen in such a way that at $s = 0$ the angle ϑ_x vanishes.

In order to obtain the transverse displacement in axis y direction we should integrate the last expression by s once more:

$$y = A\frac{R}{k}\left(s - \frac{R}{k}\sin\frac{ks}{R}\right) + B\frac{R^2}{k^2}\left(1 - \cos\frac{ks}{R}\right)\,.$$

Here the constant of integration is again chosen from the condition that the displacement at the origin of coordinates is equal to zero. As for $s = 2\pi R$ values of ϑ_x and y are equal to zero and we arrive at the two equations

$$A(1 - \cos 2\pi k) + B\sin 2\pi k = 0\,,$$
$$A(2\pi R - \frac{R}{k}\sin 2\pi k) + B\frac{R}{k}(1 - \cos 2\pi k) = 0\,.$$

Equating the determinant to zero we find the least root $2\pi k = 2\pi$. Hence, $k = 1$, and then

$$\frac{EJ_y}{\sqrt{GJ_t\, EJ_x}} = 1\,.$$

But

$$EJ_x = E\,\frac{b^3 h}{12}\,, \qquad EJ_y = E\,\frac{bh^3}{12}\,, \qquad GJ_t = \frac{E}{2(1+\mu)}\beta h^3 b\,,$$

from which it follows that

$$\frac{b^2}{h^2} = \frac{1+\mu}{6\beta}. \tag{1}$$

Let's assume that $\mu = 0.3$. As regards the coefficient of torsion rigidity β it has a complicated dependence on ratio b/h.

The tabulated data of coefficient β are given in textbooks on strength of materials, but they are not suitable for the solution of this transcendental equation. This is why we use the relation taken from [3]

$$\beta = \frac{1}{3}\left[1 - \frac{192}{\pi^5}\frac{h}{b}\sum_{i=1,3,} \frac{1}{i^5}\tanh\frac{i\pi b}{2h}\right].$$

After several trial calculations we find the solution of equation (1):

$$\frac{b}{h} = 1.16\,.$$

The straight equilibrium state is stable for

$$b > 1.16\,h\,.$$

157. In the problem we consider only three geometrical discrepancies (in plane). While mounting, the discrepancies out of plane will naturally appear too. But now we refer them to the category of disturbances which for an unstable equilibrium state guarantee spontaneous growth of displacements out of plane and the following transformation of the ring axis line to the space curve.

At first we have to determine forces arising while the construction is assembled. For this purpose we apply the canonical equation of force method (Fig. 416)

$$\begin{aligned}
&\delta_{11}X_1 + \delta_{12}X_2 + \delta_{13}X_3 = \Delta_1,\\
&\delta_{21}X_1 + \delta_{22}X_2 + \delta_{23}X_3 = \Delta_2,\\
&\delta_{31}X_1 + \delta_{32}X_2 + \delta_{33}X_3 = \vartheta,
\end{aligned} \tag{1}$$

where X_1 and X_2 are the sought forces, and X_3 is the sought moment, δ_{ik} are the displacements caused by unit forces [7].

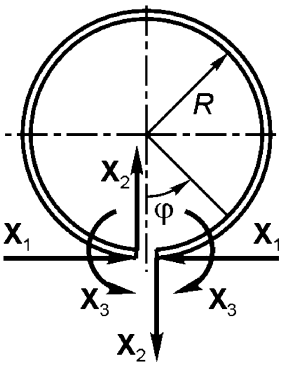

Fig. 416

The unit moments will be

$$M_1 = R(1-\cos\psi)\,; \quad M_2 = -R\sin\psi\,; \quad M_3 = 1\,,$$

and coefficients

$$\delta_{ik} = \int_0^{2\pi} \frac{M_i M_k}{EJ_y} R\,d\psi \qquad (i,k = 1,2,3),$$

whence

$$\delta_{11} = \frac{3\pi R^3}{EJ_y}\,, \quad \delta_{12} = \delta_{21} = \delta_{23} = \delta_{32} = 0\,,$$

$$\delta_{13} = \delta_{31} = \frac{2\pi R^2}{EJ_y}\,, \quad \delta_{22} = \frac{\pi R^3}{EJ_y}\,, \quad \delta_{33} = \frac{2\pi R}{EJ_y}\,.$$

Axes x and y in a cross-section are shown in Fig. 417.

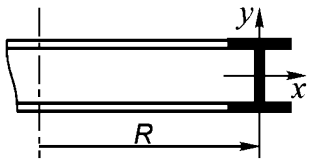

Fig. 417

Substituting the determined values δ_{ik} in equations (1) and solving them, we derive

$$X_1 = \frac{EJ_y}{\pi R^3}(\Delta_1 - \vartheta R), \quad X_2 = \frac{EJ_y}{\pi R^3}\Delta_2, \quad X_3 = \frac{EJ_y}{\pi R^2}\left(\frac{3}{2}\vartheta R - \Delta_1\right).$$

The bending moment in ring cross-sections is determined as follows:

$$\begin{aligned} M &= X_1 M_1 + X_2 M_2 + X_3 M_3 \\ &= \frac{EJ_y}{\pi R^2}\left[\frac{1}{2}\vartheta R + (\vartheta R - \Delta_1\cos\psi - \Delta_2\sin\psi\right]. \end{aligned}$$

Let's denote:

$$\theta_0 = \frac{\vartheta}{\pi}\frac{EJ_y}{EJ_x}\,, \qquad \delta_1 = \frac{\Delta_1}{\pi R}\frac{EJ_y}{EJ_x}\,, \qquad \delta_2 = \frac{\Delta_2}{\pi R}\frac{EJ_y}{EJ_x}\,;$$

then

$$M = \frac{EJ_x}{R}\left[\frac{1}{2}\theta_0 - \delta_2\sin\psi + (\theta_0 - \delta_1)\cos\psi\right].$$

Let's replace the origin of angle ψ to another point and assume that:

$$\frac{\delta_2}{\sqrt{\delta_2^2 + (\theta_0 - \delta_1)^2}} = \sin\psi_0, \quad \frac{\theta_0 - \delta_1}{\sqrt{\delta_2^2 + (\theta_0 - \delta_1)^2}} = \cos\psi_0, \quad \psi + \psi_0 = \varphi.$$

Now bending moment $M_o = M$ of the undercritical state arrives at

$$M_0 = \frac{EJ_x}{R}\left(\frac{1}{2}\theta_0 + \Delta\cos\varphi\right),$$

where

$$\Delta = \sqrt{\delta_2^2 + (\theta_0 - \delta_1)^2}\,.$$

Thus instead of three independent parameters Δ_1, Δ_2 and ϑ we obtain only two. That substantially simplifies the following interpretation of calculations.

The following equations we take from the solution of problem 154. It follows from the equations (10) and (8) of problem 154 that

$$Q_{x0} = -\frac{dM_0}{ds} = \frac{EJ_x}{R^2}\,\Delta\sin\varphi\,,$$

$$M_0 = -\frac{dQ_0}{ds} = -\frac{EJ_x}{R^2}\,\Delta\cos\varphi\,.$$

Further we analyze the conditions of small out-of-plane bending of the ring. We use the equations (3),(5) and (7) of the same problem

$$\frac{dQ_y}{ds} + r\,Q_{x0} - p\,N_0 = 0\,,$$

$$\frac{dM_x}{ds} + \frac{M_t}{R} - Q_y - M_0\,r = 0\,,$$

$$\frac{dM_t}{ds} - \frac{M_x}{R} + M_0\,p = 0\,;$$

here

$$p = M_x/(EJ_x),\ \ r = M_t/(GJ_t),$$

p is curvature variation out of plane, and M_x is the corresponding bending moment, r is twist, M_t is torsional moment, and Q_y is out-of-plane shear force.

In the three above equations we should only replace Q_{x0}, N_0, and M_0 by functions derived earlier, and then transfer the equations to dimensionless form. After transformations we arrive at

$$\overline{Q_y}' = -\Delta[(rR)\sin\varphi + (pR)\cos\varphi]\,,$$

$$(pR)' = -g(rR) + \overline{Q_y} + (\frac{1}{2}\theta_0 + \Delta\cos\varphi)(rR)\,,$$

$$(rR)' = \frac{1}{g}(1 - \frac{1}{2}\theta_0 - \Delta\cos\varphi)(pR)\,.$$

On the left-hand side of the equations the derivatives of three sought functions are taken with respect to φ. Here $\overline{Q_y} = Q_y R^2/(EJ_x)$ is the dimensionless shear force, (pR) is the dimensionless increment of curvature and (rR) is twist. The ratio of rigidities $GJ_t/(EJ_x)$ is designated as g.

The equations allow to draw the stability region of the ring plane equilibrium state in plane Δ, θ_0 for fixed parameter g.

In general, the determination of the region bounds is performed as follows. First, specify magnitudes of Δ and θ_0. The integration of equations can be started from any value $\varphi = \varphi_0$, specifying any value of $\overline{Q_y^0}$, $(pR)^0$ and $(rR)^0$. When φ arrives at the value $\varphi_0 + 2\pi$ we get three finite values of the sought functions $\overline{Q_y^{2\pi}}$, $(pR)^{2\pi}$ and $(rR)^{2\pi}$. Each of them is linear in specified initial values, i.e.

$$\begin{aligned}
\overline{Q_y^{2\pi}} &= a_{11}\,\overline{Q_y^0} + a_{12}\,(pR)^0 + a_{13}\,(rR)^0\,,\\
(pR)^{2\pi} &= a_{21}\,\overline{Q_y^0} + a_{22}\,(pR)^0 + a_{23}\,(rR)^0\,,\\
(rR)^{2\pi} &= a_{31}\,\overline{Q_y^0} + a_{32}\,(pR)^0 + a_{33}\,(rR)^0\,.
\end{aligned}$$

But as $\overline{Q_y^{2\pi}} = \overline{Q_y^0}$, $(pR)^{2\pi} = (pR)^0$, $(rR)^{2\pi} = (rR)^0$ then

$$\begin{aligned}
(a_{11} - 1)\,\overline{Q_y^0} + a_{12}\,(pR)^0 + a_{13}\,(rR)^0 &= 0\,,\\
a_{21}\,\overline{Q_y^0} + (a_{22} - 1)\,(pR)^0 + a_{23}\,(rR)^0 &= 0\,,\\
a_{31}\,\overline{Q_y^0} + a_{32}\,(pR)^0 + (a_{33} - 1)\,(rR)^0 &= 0\,.
\end{aligned}$$

The condition of nontrivial solution existence that means an exit of the ring deflection curve out of plane is the equality to zero of the determinant:

$$\begin{vmatrix}
a_{11} - 1 & a_{12} & a_{13}\\
a_{21} & a_{22} - 1 & a_{23}\\
a_{31} & a_{32} & a_{33} - 1
\end{vmatrix} = D = 0\,.$$

The determinant terms a_{ik} are calculated by ordinary method, i.e. by thrice-repeated integration of differential equations with the initial conditions $\overline{Q_y^0} = 1$, $(pR)^0 = (rR)^0 = 0$, then $\overline{Q_y^0} = 0$, $(pR)^0 = 1$, $(rR)^0 = 0$ and finally $\overline{Q_y^0} = (pR)^0 = 0, (rR)^0 = 1$. The method is well known as the method of initial parameters.

It seems that an algorithm can be realized very easily. But during calculations we meet the unforeseen obstacle – a sharp loss of accuracy while calculating the determinant. We loose at least six to seven significant digits. And as the terms of determinant D are obtained as a result of numeric integration, it should be performed with unjustified high accuracy. While the probable results can be nevertheless obtained, the sense of the dissatisfaction remains.

That is why it is more preferable to expand functions in trigonometric series:

$$(pR) = A_0 + \sum_{i=1}^{\infty} A_i \cos i\varphi,\ (rR) = \sum_{i=1}^{\infty} B_i \sin i\varphi.$$

After substitution into equations and collecting terms we obtain the existence condition of adjacent space equilibrium states in the form of equality to zero of the determinant of banded matrix being five terms wide:

$$\begin{vmatrix} a_{11} & a_{12} & 0 & 0 & 0 & 0 & 0 & \dots \\ a_{21} & a_{22} & a_{23} & 0 & 0 & 0 & 0 & \dots \\ 0 & a_{32} & a_{33} & a_{34} & a_{35} & 0 & 0 & \dots \\ 0 & a_{42} & a_{42} & a_{44} & a_{45} & a_{46} & 0 & \dots \\ \dots & \dots & \dots & \dots & \dots & \dots & \dots & \dots \\ \dots & 0 & a_{i,i-2} & a_{i,i-1} & a_{ii} & a_{i,i+1} & a_{i,i+2} & 0 \\ \dots & \dots & \dots & \dots & \dots & \dots & \dots & \dots \end{vmatrix} = 0,$$

where

$$a_{11} = 1 - \theta_0/2\ ,\ a_{12} = -\Delta/2,\ a_{21} = \Delta,$$

$$a_{22} = -g - 1 + \theta_0/2,\ a_{23} = \Delta/2,\ a_{32} = -\Delta(3g + \theta_0/2)/2,$$

$$a_{33} = 4g + (1 - \theta_0/2)(-g + \theta_0/2) - \Delta^2/12,\ a_{34} = \Delta(1 - 2\theta_0)/6,$$

$$a_{35} = -\frac{\Delta^2}{12},\ a_{i,i-2} = -\frac{\Delta^2}{4}\frac{i}{i-2},\ a_{i,i-1} = \frac{\Delta}{2}\frac{i - \theta_0(i-1)}{i-2},$$

$$a_{i,i} = g(i-1)^2 + \frac{\Delta^2}{2}\frac{(i-1)^2 + 1}{(i-1)^2 - 1} + (1 - \frac{1}{2}\theta_0)(-g + \frac{\theta_0}{2}),$$

$$a_{i,i+1} = \frac{\Delta}{2}\frac{i - 2 - \theta_0(i-1)}{i},\ a_{i,i+2} = -\frac{\Delta^2}{4}\frac{i-2}{i}.$$

The calculations were performed with the determinant 10×10 and in fact they did not demand excessive computer time. The stability regions for several values of $g = GJ_t/(EJ_x)$ are shown in Fig. 418.

The parameters θ_0 and Δ are calculated beforehand by means of specified Δ_1, Δ_2, ϑ. If the point with coordinates θ_0, Δ appears in the given diagram to be lower than the corresponding curve the plane equilibrium state of the ring is stable.

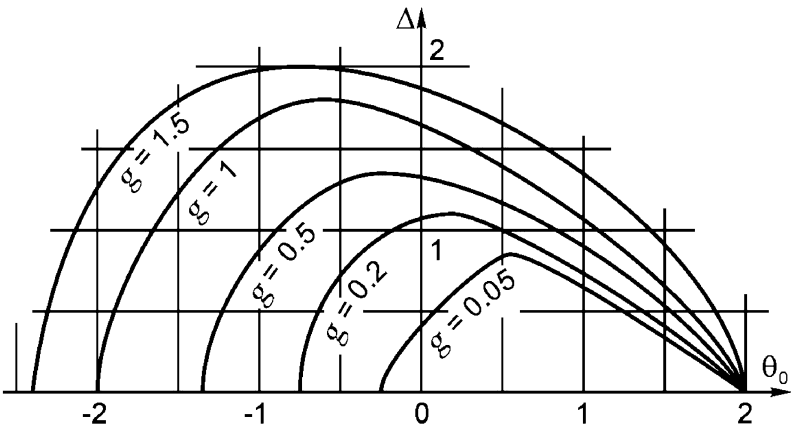

Fig. 418

The antisymmetric modes of equilibrium were also considered:

$$(pR) = \sum_{i=1}^{\infty} A_i \sin i\varphi\,, \qquad (rR) = B_0 + \sum_{i=1}^{\infty} B_i \cos i\varphi\,.$$

but they gave the greater values of critical parameters θ_0 and Δ.

158. The probability of rod buckling to one or another side is determined by its initial deflection, random imperfections of material and deviations of force P action line from the rod's axis.

The extent of random factor influence depends on rigidity of the rod. The most probable is, obviously, bending in plane of minimal rigidity, i.e. in our case with respect to the axis z (Fig. 419). We only have to verify whether bending rigidity changes under variation of moment sign. In the case where rigidity remains invariant the rod buckling to the right side or to the left will be equiprobable. If rigidity is different then the most probable will be bending to the side of minimal rigidity.

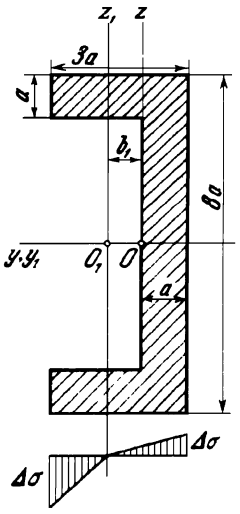

Fig. 419

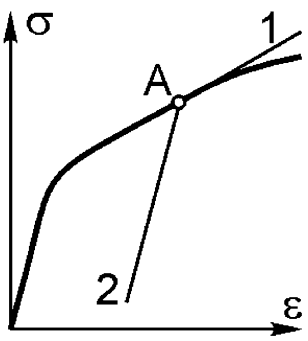

Fig. 420

Suppose that the stress-strain diagram of material compression is given (Fig. 420). The stress σ arising in the rod's cross-sections exceeds the yield limit (point A in diagram) according to the problem set. Under column bending the layers disposed at the concave side are loaded additionally and stresses increase in accordance with the straight line 1. Layers at the convex side are unloaded and the relation between σ and ε is plotted by the straight line 2. The tangent of the straight line 1 inclination angle we denote as D, and of straight line 2, as E. It is obvious that E is the modulus of elasticity. As a result, the diagram of additional bending stress distribution takes the form of a piece-wise line (Fig. 419). The position of the neutral line z_1 is derived from the condition

$$\int_A \Delta\sigma \, dA = 0, \tag{1}$$

as normal force in the cross-section does not change and is permanently equal to P.

In case of column buckling to the left, the axis $z_1$deflects from the central axis z to the left also. If the column buckles to the right side, the neutral axis will move to the right.

Let's consider the first case. The axis z_1 is displaced to the left. At the convex side of column we have

$$\Delta\sigma = E\frac{y_1}{\rho} \qquad (y_1 \geq 0),$$

and at the concave side

$$\Delta\sigma = D\frac{y_1}{\rho} \qquad (y_1 \leq 0).$$

According to expression (1) we have

$$E \int\limits_{left} y_1 \, dA = D \int\limits_{right} y_1 \, dA,$$

where the first integral is taken by the area disposed at the left side of the axis z_1, and the second, at the right side of the axis z_1 (Fig. 419). Determining the first moment of the mentioned areas with respect to the axis z_1, we find

$$b_1 = \frac{2a}{1-d}\left(1 + 2d - \sqrt{6d + 3d^2}\right),$$

where $d = D/E$.

If the rod buckles to the right side then the axis z_1 displaces rightward by the value

$$b_2 = \frac{a}{2(1-d)}\left(2 + d - \sqrt{12 - 3d^2}\right).$$

Now let's determine the moment of stresses $\Delta\sigma$ with respect to the transverse axis z_1. It should be noted that the axis can be taken arbitrarily as the normal force due to stresses $\Delta\sigma$ vanishing for specified $b_1$and b_2.

While buckling of the column to the left

$$M_1 = \frac{1}{\rho_1}\left[\int\limits_{left} y_1^2 \, dA = D \int\limits_{right} y_1^2 \, dA\right].$$

The expression can be rewritten as

$$M_1 = \frac{EJ_1}{\rho_1},$$

where

$$J_1 = \frac{2}{3}a(2a - b_1)^3 + \frac{d}{3}\left[8a(a + b_1)^3 - 6ab_1^3\right].$$

Eliminating b_1, we obtain

$$J_1 = \frac{8a^4 d}{(1-d)^2}\left[7 + 22\,d + 7\,d^2 - 4(2+d)\sqrt{6\,d + 3\,d^2}\right].$$

While buckling of the column to the right side we similarly obtain:

$$J_2 = \frac{2a^4 d}{(1-d)^2}\left[10 - 2\,d + d^2 - (4-d)\sqrt{12\,d - 3\,d^2}\right].$$

In the variation range of d from zero to one, we obtain

$$J_2 \le J_1\,.$$

Hence the probability rightward deflection of the column is greater than leftward. The column buckling is more probable in the case when it bends in such a way that the opened side of the shape is at the concave side of the beam.

159. Loss of stability is possible for tension springs with preliminary tightened coils.

The coils of such springs are tightly compressed. The contact pressure between coils decreases while increasing the tensile force. Elongation of the spring occurs only for force which is greater than the force of preliminary tightening P_0 (Fig. 421).

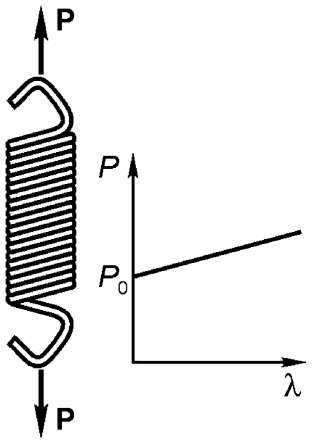

Fig. 421

Loss of stability takes place with skewness and bending of coils (Fig. 422). It turns out that each coil "does not await" the moment, when it can move away from the neighbouring one, but slides along the surface of contact, bending in its plane. Work done by force P during its axial displacement transfers to the energy of coil bending

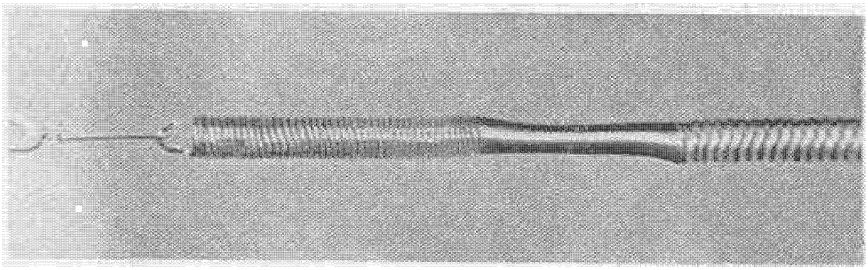

Fig. 422

The schematic model for critical force derivation is shown in Fig. 423.

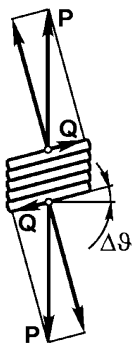

Fig. 423

According to formula (3) (see the solution of problem 53) we have

$$\Delta\vartheta = \frac{Q}{C_{sh}}.$$

But $Q = P\Delta\vartheta$. Excluding Q we obtain

$$P_{cr} = C_{sh}.$$

So from relation (4) of the same problem

$$P_{cr} = \frac{Ed^4 l}{8D^3 n}.$$

As in the given case we have $l/n = d$, then

$$P_{cr} = \frac{Ed^5}{8D^3}.$$

160. Let's consider the system in a configuration deflected from the vertical state configuration.

Equations of equilibrium for the node (Fig. 424a) will be as follows:

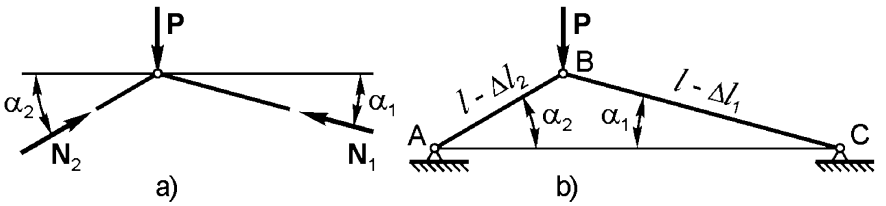

Fig. 424

$$P = N_1 \sin\alpha_1 + N_2 \sin\alpha_2\,, \quad N_1 \cos\alpha_1 = N_2 \cos\alpha_2\,. \tag{1}$$

From the triangle ABC (Fig. 424b) we have

$$\begin{aligned}(l - \Delta l_1)\cos\alpha_1 + (l - \Delta l_2)\cos\alpha_2 &= 2l\cos\alpha_0\,,\\ (l - \Delta l_1)\sin\alpha_1 &= (l - \Delta l_2)\sin\alpha_2\,.\end{aligned} \tag{2}$$

Let's assume that deflections from the vertical line are small and deflections in vertical direction are arbitrarily large. Let's denote as

$$\alpha_2 = \alpha + \beta\,, \quad \alpha_1 = \alpha - \beta\,,$$

where angle α characterizes the displacement of the node downward, and small angle β the displacement in horizontal direction. In analogy

$$N_1 = N - \Delta N\,, \quad N_2 = N + \Delta N\,.$$

Let's denote by c the rod stiffness on compression, then

$$\Delta l_1 = \frac{N - \Delta N}{c}\,, \quad \Delta l_2 = \frac{N + \Delta N}{c}\,.$$

Further we substitute α_1, α_2, N_1, N_2, Δl_1 and Δl_2 in equations (1) and (2) and linearize them by neglecting small products $\beta\,\Delta N$. Only the first powers of these values are held. As a result instead of (1) and (2) we obtain

$$P = 2N\sin\alpha\,, \quad N\beta\sin\alpha - \Delta N\cos\alpha = 0\,,$$

$$\left(l - \frac{N}{c}\right)\cos\alpha = l\cos\alpha_0, \quad \left(l - \frac{N}{c}\right)\beta\cos\alpha - \frac{\Delta N}{c}\sin\alpha = 0\,.$$

The first and the third of the equations allow to determine angle α versus force P for the symmetric equilibrium state

$$\frac{P}{2cl} = \sin\alpha\left(1 - \frac{\cos\alpha_0}{\cos\alpha}\right). \tag{3}$$

The second and the forth equations are homogeneous in unknown values β and ΔN, characterizing the lateral deflection. Let's equate the determinant of this system to zero

$$\begin{vmatrix} N\sin\alpha & -\cos\alpha \\ \left(l - \dfrac{N}{c}\right)\cos\alpha & -\dfrac{1}{c}\sin\alpha \end{vmatrix} = 0\,,$$

whence we have

$$\frac{N}{c} - l\cos^2\alpha = 0\,.$$

Expressing N through P, we arrive at

$$\frac{P}{2cl} - \sin\alpha\cos^2\alpha = 0\,,$$

or according to relation (3)

$$\cos\alpha_0 = \cos\alpha - \cos^3\alpha\,.$$

The dependence of $\cos\alpha_0$ upon $\cos\alpha$ is plotted in Fig. 425. The plot must be interpreted in the following way. The angle α_0 is specified. The system is not loaded. Here $\alpha = \alpha_0$ (point A in Fig. 425). While loading the angle α decreases and $\cos\alpha$ grows. Point B characterizes transfer to a nonsymmetric shape. The corresponding value of force P can be determined from relation (3). When angle α becomes small enough, the symmetric equilibrium state becomes stable again (point C). Existence of nonsymmetric states is possible only for $\cos\alpha_0 < 2\sqrt{3}/9$ or for $\alpha_0 > 67^0 25'$.

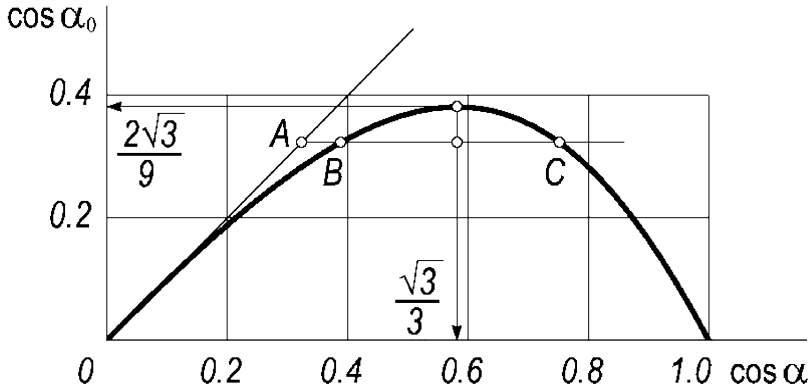

Fig. 425

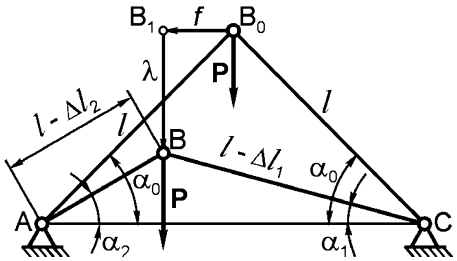

Fig. 426

The behaviour of the system in the postcritical state can be analyzed if we refuse the assumption that the angle α is small. However, here it is easier to

solve the problem by an energetic approach. If we introduce the displacements λ and f (Fig. 426) then it is easy to derive the following relations from the analysis of the tetragons CBB_1B_0 and ABB_1B_0:

$$l\cos\alpha_0 + f = (l - \Delta l_1)\cos\alpha_1\,,$$
$$l\sin\alpha_0 - \lambda = (l - \Delta l_1)\sin\alpha_1\,,$$
$$l\cos\alpha_0 - f = (l - \Delta l_2)\cos\alpha_1\,,$$
$$l\sin\alpha_0 - \lambda = (l - \Delta l_1)\sin\alpha_2\,.$$

Eliminating α_1 and α_2, we obtain

$$\Delta l_1 = l - \sqrt{(l\sin\alpha_0 - \lambda)^2 + (l\cos\alpha_0 + f)^2}\,,$$
$$\Delta l_2 = l - \sqrt{(l\sin\alpha_0 - \lambda)^2 + (l\cos\alpha_0 - f)^2}\,.$$

The total potential energy of the system will be

$$U = \frac{1}{2}c(\Delta l_1)^2 + \frac{1}{2}c(\Delta l_2)^2 - P\lambda\,.$$

The first derivatives of U by λ and f are equal to zero in the equilibrium state, and stability or instability of the equilibrium state is defined by the sign of the second derivatives.

We leave to readers the opportunity to perform this analysis themselves.

161. The problem falls into a category of the most difficult, and the obstacles begin already while determining internal forces.

We assume that the rod's mass per unit length is m. Let's determine interaction forces of segments of length dx (Fig. 427) and other rod elements. The segments AB and AC generate forces from the left and the right sides of section dx which are balanced. The remaining $CD = l - 2x$ pulls segment dx rightward and the force is derived by integration of the interaction forces of segments dx and dx_1.

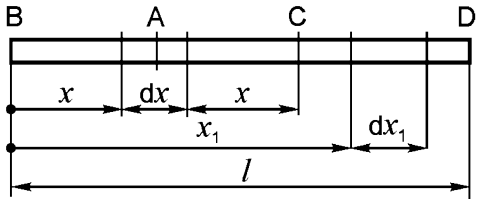

Fig. 427

According to Newton's law the elementary interaction force is

$$f\frac{dm\,dm_1}{(x_1 - x)^2}\,,$$

where f is gravitational constant, ρ is material density, and A is area of cross-section. If we divide this force by dx, then we obtain the intensity of external

longitudinal force q in a point A, which is caused by gravitation of the dx_1 segment's mass

$$dq = \frac{f\rho^2 A^2 dx_1}{(x_1 - x)^2}\,. \tag{1}$$

We integrate by x_1 from $2x$ to l_1 :

$$q = f\rho^2 A^2 \int_{2x}^{l} \frac{dx_1}{(x_1 - x)^2}\,,$$

or

$$q = f\rho^2 A^2 \left(\frac{1}{x} - \frac{1}{l - x}\right). \tag{2}$$

The intensity q at the rod ends becomes infinite which seems to be strange by itself. But that is not at all the case.

Normal compressive force N at the ends of a rod cross-section must vanish, however we have

$$N = \int_0^x q dx = f\rho^2 A^2 \ln x(l - x)\,|_0^x\,. \tag{3}$$

And this means that normal force becomes infinite at the rod's ends as well as intensity q.

The paradox consists in the fact that we consider a one-dimensional rod, while it has a transverse measure and determination of forces ought to be produced with regard to this fact. This, however, is met by technical difficulties.

Let's restrict ourselves only by the case of rectangular cross-section $a \times b$ and consider two elements dx and dx_1 (Fig. 428).

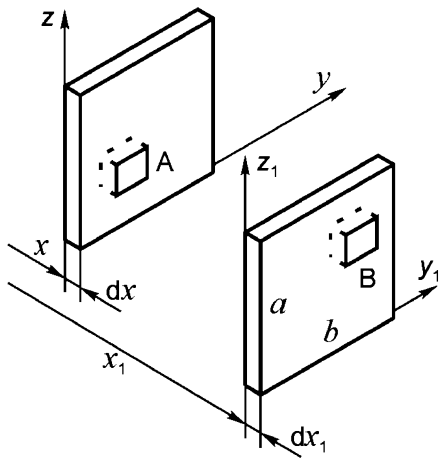

Fig. 428

Mass $\rho\,dx\,dy\,dz$ (point A) is attracted by mass $\rho\,dx_1\,dy_1\,dz_1$ (point B) by force

$$f\frac{\rho^2}{r^2}\,dx\,dy\,dz\,dx_1\,dy_1\,dz_1,$$

where r is the distance between points A and B :

$$r^2=(x_1-x)^2+(y_1-y)^2+(z_1-z)^2.$$

In order to obtain a projection on axis x, the derived force should be multiplied by the cosine of the angle between segment AB and axis x, i.e. by $(x_1-x)/r$. Thus, in order to obtain the correct value dq (1) we have to preliminarily integrate by y_1 and y (from zero to a) and by z_1 and z (from zero to b) the following expression:

$$\frac{f\rho^2(x_1-x)\,dx_1\,dy_1\,dz_1\,dz}{[(x_1-x)^2+(y_1-y)^2+(z_1-z)^2]^{3/2}}\,.$$

This integration is cumbersome enough but can be produced in elementary functions. Omitting computation we present the final result as follows

$$\begin{aligned}dq=2f\rho^2(x_1-x)\{&a\ln\frac{\sqrt{(x_1-x)^2+a^2+b^2}-a}{\sqrt{(x_1-x)^2+a^2+b^2}+a}\\&-a\ln\frac{\sqrt{(x_1-x)^2+a^2}-a}{\sqrt{(x_1-x)^2+a^2}+a}+b\ln\frac{\sqrt{(x_1-x)^2+a^2+b^2}-b}{\sqrt{(x_1-x)^2+a^2+b^2}+b}\\&-b\ln\frac{\sqrt{(x_1-x)^2+b^2}-b}{\sqrt{(x_1-x)^2+b^2}+b}-2\sqrt{(x_1-x)^2+b^2}\\&+2\sqrt{(x_1-x)^2+a^2+b^2}+2(x_1-x)-2\sqrt{(x_1-x)^2+a^2}\\&+2\frac{ab}{x_1-x}\arctan\left[\frac{x_1-x}{ab}\sqrt{(x_1-x)^2+a^2+b^2}\right]-\frac{ab\pi}{x_1-x}\}dx_1\end{aligned}\tag{4}$$

In order to find the distributed load $q(x)$, the obtained expression should be integrated by x_1 from $x_1=2x$ to $x_1=l$. But we restrict ourselves by the analysis of the obtained function in the vicinity of the left end of the rod only as the transverse measure of the rod (a and b) is significant only at relatively small distances x_1-x. Let's introduce the variable $(x_1-x)/a=\zeta$ which varies from zero to some current value ζ. In order to simplify calculations let's also accept $b=a$, i.e. we will consider a square section. Then:

$$\begin{aligned}q=f\rho^2a^3\,2\{&(\zeta^2-1)\ln\frac{\sqrt{\zeta^2+2}-1}{\sqrt{\zeta^2+2}+1}-\zeta^2\ln\frac{\sqrt{\zeta^2+1}-1}{\sqrt{\zeta^2+1}+1}\\&-2\sqrt{\zeta^2+2}+2\sqrt{\zeta^2+1}-\frac{4}{3}(\zeta^2+1)^{3/2}+\frac{2}{3}(\zeta^2+2)^{3/2}+\frac{2}{3}\zeta^3\\&+2\zeta\arctan\left(\zeta\sqrt{\zeta^2+2}\right)-\pi\zeta\}.\end{aligned}\tag{5}$$

Relation (2) derived earlier correspondingly yields in the vicinity of the rod's left end:

$$q = f\rho^2 \frac{a^3}{\zeta}, \tag{6}$$

and the assumption arises that q by relation (6) and q by (5) will be practically equal when the distance from the rod end is sufficiently large. In fact let's calculate and draw a table:

Table 6. The results obtained by relation (5) and(6)

$\zeta = x/a$	0	1	2	3	4	5
$q(6)/(f\rho^2 a^3)$	∞	1.0000	0.5	0.3333	0.25	0.2
$q(5)/(f\rho^2 a^3)$	2.9732	0.878	0.4811	0.3274	0.2475	0.1988

Thus, we see that accuracy of distributed load q determined by the simple relation (6) is adequate if the distance from the left rod end is greater than $5a$. Just the same effect takes place near the other end of the rod but q has the opposite sign.

The length of the rod can be correspondingly separated into three segments: the main one where expression (2) can be used ($\Delta < x < l - \Delta$) and two end sections of length $\Delta \approx 5a$. This means that all the end peculiarities can be considered within the limits of one integration step when further we shall have to integrate the rod deflection curve using a constant integration step. The two to three hundred steps are enough in case of equal apportionment of length l. Probably the rod length l will exceed the cross-section measure a by dozen or hundred thousands of times. But this question will be discussed later.

Now we can also address the question about compressive force N in the rod cross-sections. According to equation (3) we obtain for two segments:

$$N = \int_0^x q\,dx \quad (x < \Delta),$$

$$N = \int_0^{\Delta} q\,dx + f\rho^2 a^4 \ln\left(\frac{x}{\Delta}\frac{l-x}{l-\Delta}\right) \quad (x > \Delta). \tag{7}$$

At $l > x > l - \Delta$ the equations written above must be symmetrically rearranged from the left to the right end.

Laws of q and N variation along the rod's length are shown by draft plots in Fig. 429.

The integral of q by (5) for the left segment can be taken in elementary functions, but combination of logarithms and arctangents occurs to be so cumbersome, that it is preferable to use digital integration. For the middle (main) part of the rod it is easier to use the analytic equations (2) and (3).

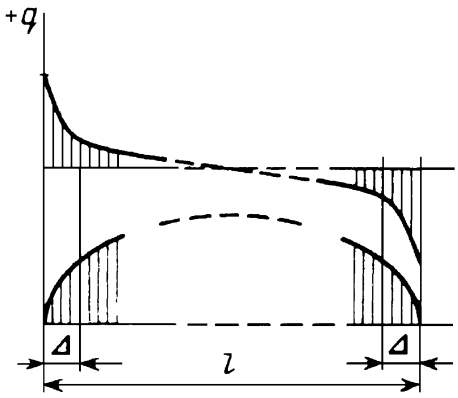

Fig. 429

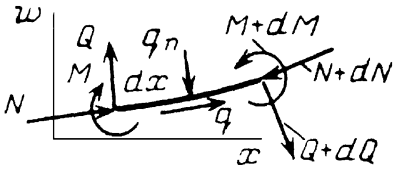

Fig. 430

Let's turn to the stability analysis and consider rod segment dx in a bent state (Fig. 430).

Let's introduce shear force Q, bending moment M, normal force N and external force of intensity q_n normal to the deflection curve. This arises as a result of distributed forces q rotation.

It follows from the equilibrium that

$$\frac{dN}{dx} = q\,, \quad \frac{dM}{dx} = Q\,, \quad \frac{dQ}{dx} + N\frac{d^2w}{dx^2} + q_n = 0\,.$$

Whence we arrive at the ordinary differential equation of the compressed and slightly bent rod deflection curve

$$EJ\frac{d^4w}{dx^4} + N\frac{d^2w}{dx^2} + q_n = 0, \tag{8}$$

where w is transverse deflection.

Now it is necessary to establish dependence q_n upon the shape of deflection curve, and this question makes the considered problem essentially differ from all problems of compressed rod stability which we have encountered so far.

At undercritical state, forces of mutual attraction of the two rod elements dx and dx_1 were directed along the rod axis (along axis x). Under rod bending they rotate as it is shown in Fig. 431.

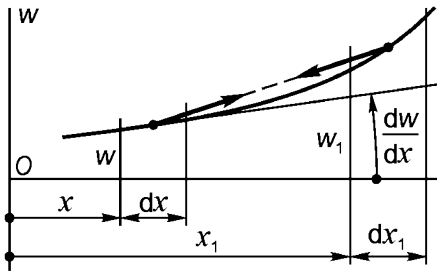

Fig. 431

The force

$$p = f\,\frac{dm\,dm_1}{(x_1 - x)^2}\,, \tag{9}$$

produced by the action of mass dm_1 at segment dx rotates by the slope angle $(w_1 - w)/(x_1 - x)$ during rod bending, and its normal component at segment dx (only of mass dm_1) will be

$$-p\left[\frac{w_1 - w}{x_1 - x} - \frac{dw}{dx}\right].$$

The "minus" sign is written because the component is directed to the centre of curvature of the deflection curve, but it was directed to the same side as the outer normal in deriving equation (8).

If we divide p by dx and integrate by x_1 assuming x invariable (as parameter) we obtain q_n for given x as follows

$$q_n(x) = -\int_l \frac{f\rho^2 A^2}{(x_1 - x)^2}\left[\frac{w_1 - w}{x_1 - x} - \frac{dw}{dx}\right] dx_1 \tag{10}$$

Apparently the deflection w as a function of x remains under the definite integral sign, and equation (8) occurs to be the integro-differential. We have not met such a fact neither in problems of rod stability nor in other problems of elastic system stability.

Let's transform the equation to dimensionless form. We specify $X = x/l$ and $X_1 = x_1/l$ as independent variables. The deflection w is replaced with product $l\eta$ and derivative $d(\ )/dx$ is denoted as $(\ )'$. Then equation (8) arrives at

$$\eta^{(IV)} + GN_x\eta'' - G\int_0^1 (\frac{\eta_1 - \eta}{X_1 - X} - \eta')\frac{dX_1}{(X_1 - X)^2} = 0, \tag{11}$$

where G is a parameter characterizing stability

$$G = f\rho^2 A^2 l^2/(EJ), \quad N_x = N/(f\rho^2 A^2). \tag{12}$$

Let's denote the step of integration by ΔX and ΔX_1. It must be small enough in order to produce integration with acceptable accuracy, and at the same time it must be large enough in order to consider the peculiarities of the end effect within the limits of segment ΔX near the ends of the rod that in turn depends on the ratio l/a. It should be interpreted in the following way. For example, if we specify $\Delta X = 0.01$, then at least $(5a)$ must keep within the limits of $0.01l$, which follows from the above given table. It means that the ratio l/a should exceed 500. The condition is obviously fulfilled.

According to expression (7), function N_x will be

$$N_x = \Delta N_x + \ln\left(\frac{X}{\Delta X}\frac{1 - X}{1 - \Delta X}\right), \tag{13}$$

where ΔN_x is the dimensionless force at the end of the first section ΔX obtained by integration of q by (5) and then transformed to dimensionless form, i.e.

$$\Delta N = \frac{f\rho^2 A^2}{a}\int_0^{\Delta X} 2\,\{\}\,dX = \frac{f\rho^2 A^2}{l}\int_0^{\Delta X} 2\,\{\}\,d\zeta;$$

$$\Delta N_x = \int_0^{\Delta X} 2\,\{\}\,d\zeta.$$

Here figure brackets contain just the same expression as in equation (5). The integral can be taken numerically until $\zeta = 10$, for example, and then in dependence on the specified number of steps (or of ΔX value) is supplemented to the end of section ΔX by an analytical expression.

For the square cross-section the part of ΔN_x, which is determined numerically up to $\zeta = 10$ ($X = 10a$), is equal to 3.87784. For another shape of cross-section it will have another value. It does not depend on rod length. The second part of ΔN_x depends upon the number of steps (i.e. on ΔX) and upon the ratio l/a.

According to (2) near the left rod end we have

$$q = \frac{f\rho^2 A^2}{l}\,\frac{1}{X}\,, \tag{14}$$

and in dimensionless form it will be $q_x = 1/X$.

For example, let's divide the length l into 500 segments, then $\Delta X = 0.002$. And let's assume the ratio l/a as equal to 10^4, then $10a$ is equal exactly to half of the segment ΔX and the second part of ΔN_x will be defined by the integral

$$\int_{\Delta X/2}^{\Delta X} \frac{1}{X}\,dX = \ln 2.$$

Finally for such separation we have

$$\Delta N_x = 3.8778 + \ln 2 = 4.571\,.$$

So one more dimensionless parameter l/a appears as we see. It can be explained by the fact that the edge peculiarity, which does not depend on length l, has a different degree of influence on rod stability in dependence upon the rod length. But, by all probabilities, this influence is not essential.

The question arises, what needs to be done with equation (11). And we shall apply the following algorithm.

Let's expand η_1 in series by powers of $X_2 = X_1 - X$ rightward and leftward from the point of coordinate X.

At first, rightward:

$$\eta_1 = \eta + \eta' X_2 + \frac{1}{2}\eta'' X_2^2 + \frac{1}{6}\eta''' X_2^3 + \frac{1}{24}\eta^{IV} X_2^4 + \frac{1}{120}\eta^{V} X_2^5 + \frac{1}{720}\eta^{VI} X_2^6 + \ldots$$

Let's restrict our approximation by the sixth derivative. Then the last term of equation (11) will take the form

$$-G\int_0^{1-X}[\frac{1}{2}\eta''X_2\frac{1}{X_2^2}+\frac{1}{6}\eta'''+\frac{1}{24}\eta^{IV}X_2+\frac{1}{120}\eta^{V}X_2^2$$
$$+\frac{1}{720}\eta^{VI}X_2^3]dX_2. \qquad (15)$$

Here again singularity occurs at $X_2=0$. Let's analyze the first component by taking the integral of this component along two intervals: the first interval from $X_2=0$ to $X_2=\Delta X$ and the second from $X_2=\Delta X$ to $X_2=1-X$

$$\int_0^{1-X}X_2\frac{1}{X_2^2}dX_2=\int_0^{\Delta X}X_2\frac{1}{X_2^2}\,dX_2+\int_{\Delta X}^{1-X}\frac{dX_2}{X_2}\,.$$

The first integral needs to take into account the shape of the rod cross-section. For this we use the earlier obtained equation (4), which in dimensionless form gives:

$$\frac{1}{X_2^2}=-\frac{dq_x}{dX_2},$$

and then the integral can be taken by parts

$$\int_0^{\Delta X}X_2\frac{1}{X_2^2}dX_2=-\int_0^{\Delta X}X_2\frac{dq_x}{dX_2}\,dX_2=-X_2\,q_x\,|_0^{\Delta X}+\int_0^{\Delta X}q_xdX_2$$

But in accordance with (14) $q_2=1/\Delta X$ at $X_2=\Delta X$ and for $X_2=0$ it has a peak but finite value. As a result

$$\int_0^{\Delta X}X_2\frac{1}{X_2^2}dX_2=-1+\Delta N_x\,,$$

and the integral is equal to

$$\int_{\Delta X}^{1-X}\frac{1}{X_2}\,dX_2=\ln\frac{1-X}{\Delta X}.$$

Therefore expression (15) arrives at

$$-G[\frac{1}{2}\eta''(-1+\Delta N_x+\ln\frac{1-X}{\Delta X})+\frac{1}{6}\eta'''(1-X)$$
$$+\frac{1}{48}\eta^{(IV)}(1-X)^2+\frac{1}{360}\eta^{(V)}(1-X)^3+\frac{1}{2880}\eta^{(VI)}(1-X)^4].$$

If $X=1$, then we must assume zero value for the multiplier near η'' enclosed in round brackets as the length of the rod's right part is equal to zero.

For the left part of the rod (leftward from the point of coordinate X) we obtain an analogous expression, where we should write X instead of $1-X$ and the signs of η''' and $\eta^{(V)}$ must be reversed, i.e.

$$-G[\frac{1}{2}\eta''(-1+\Delta N_x+\ln\frac{X}{\Delta X})-\frac{1}{6}\eta'''X$$
$$+\frac{1}{48}\eta^{(IV)}X^2-\frac{1}{360}\eta^{(V)}X^3+\frac{1}{2880}\eta^{(VI)}X^4]$$

Here at $X=0$ the term in round brackets ought to be equal to zero also as the left part is absent.

The integral part of equation (11) is replaced with the sum of the last two expressions. Let's preliminarily introduce the notation $Y=\eta''$. Then:

$$-\frac{G}{2880}[(1-X)^4+X^4]Y^{(IV)}-\frac{G}{360}[(1-X)^3-X^3]Y'''$$
$$+\{1-\frac{G}{48}[(1-X)^2+X^2]\}Y''-\frac{G}{6}(1-2X)Y'$$
$$+GT_xY=0$$

where the coefficient T_x is formed from three parts: the expression N_x and two components, obtained for the right and left part of the rod:

$$T_x=N_x-\frac{1}{2}(-1+\Delta N_x+\ln\frac{1-X}{\Delta X})-\frac{1}{2}(-1+\Delta N_x+\ln\frac{X}{\Delta X}).$$

At $X=0$ the third component is equal to zero, and at $X=1$ the second component vanishes. For the remaining values of X, laying within the interval from $X=\Delta X$ to $X=1-\Delta X$, we obtain after easy transformations

$$T_x=1+\ln\frac{\sqrt{X(1-X)}}{1-\Delta X}.$$

We only have to rewrite the equation in a traditional form:

$$Y^{(IV)}+f_3Y'''+f_2Y''+f_1Y'+f_0Y=0,$$

where

$$f_3=8\frac{(1-X)^3-X^3}{(1-X)^4+X^4},\quad f_2=\frac{60}{G}\frac{G[(1-X)^2+X^2]-48}{(1-X)^4+X^4},$$
$$f_1=480\frac{1-2X}{(1-X)^4+X^4},\quad f_0=-T_x\frac{2880}{(1-X)^4+X^4}.$$

At the ends of the rod we have $Y=Y'=0$. Further, as usual in such problems we integrate the equation twice specifying at $X=0$ in turn $Y'''=1$ and $Y''=0$ and then vice versa $Y'''=0$ and $Y''=1$. Then, varying G by steps we find such value of it when the determinant of the two following equations vanishes:

$$Y(1)=a_{11}Y''(0)+a_{12}Y'''(0)=0,$$
$$Y'(1)=a_{21}Y''(0)+a_{22}Y'''(0)=0.$$

As a result of the search we obtain the critical value of the parameter:

$$G_{cr}=43.85\,.$$

First of all, in such a problem it is interesting to know the actual length of a rod which can keep straight under the conditions of self-gravitation. Let's calculate for a steel rod of square cross-section:

$$l_{cr}^2 = \frac{G_{cr}EJ}{f\rho^2 A^2} = \frac{G_{cr}E}{12f\rho^2};$$

with gravitation constant $f = 6.672 \cdot 10^{-11}\,\mathrm{Nm^2/kg^2}$, modulus of elasticity $E = 19.6 \cdot 10^{10}\,\mathrm{N/m^2}$, and density $\rho = 7800\,\mathrm{kg/m^3}$.

The calculation gives us $l_{cr} = 13,300\,\mathrm{km}$. The result is really astronomic. But that was expected.

In conclusion, it must be admitted that the energy method provides more facilities in determination of the critical parameter. And this can be used here as the system is conservative. This analysis was carried out simultaneously with the above considered as an alternative but not without creative gambling [2].

The rod mass is divided into n parts. The variation of external force potential under rod bending by the specified mode can be determined by pair consideration of mutual displacements of n masses. The energy of bending can be derived if the deflection curve shape is given. Particularly, if we roughly suppose that the rod bends taking the form of a quadratic parabola arc then the value of the critical parameter is determined even without computer calculations and is $G_{cr} = 72$. Such an approximation explicitly is not sufficient. We can determine the energy of bending by finite-difference method, specifying the deflections w of elementary masses, and then choose the deflections from the condition that the total potential energy has minimal value. The accuracy of calculations as well as their awkwardness is defined by number n. But the result is reached rather quickly. For $n = 32$ and for $n = 80$ the values of G_{cr} coincide to the third significant digit. The critical parameter occurs equal to 49.7.

It seems that this value is probably more trustworthy than the above obtained. Because after all we solved the integro-differential equation approximately and it should be remembered that transformations were complicated enough. In such cases even under the highest extent of check-up, nobody is insured against possible mistakes.

162. The result obtained in the previous problem indicates that the interest in such problems is not in the area of their practical application, but exclusively in peculiarities which are connected with the integral behaviour of external forces under small disturbances of a system.

Let's consider the self-gravitating ring (Fig. 432a). Obviously, the forces of the particles' mutual attraction due to their complete symmetry can be reduced to a uniformly distributed load of intensity q. It seems that the load can be easily determined, in any case without those "adventures", which accompanied us during the solution of the previous problem. The ring is not a straight rod and the end effects should not appear.

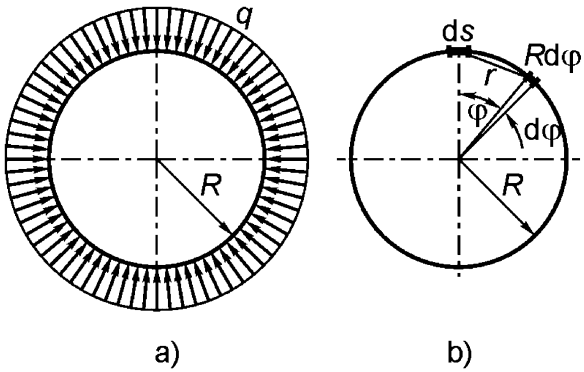

Fig. 432

Let's denote ring mass per unit of arc length as m. The gravity force of element $R\,d\varphi$ mass (Fig. 432b) attraction to the mass of element ds, according to Newton's law is:

$$f\frac{m\,ds\,m\,R\,d\varphi}{r^2}\,.$$

Multiplying this expression by $\sin(\varphi/2)$ we derive the radial component of the force. If we divide the expression by ds then we shall find the intensity of the force. And at last eliminating $r = 2R\sin(\varphi/2)$, we obtain

$$q = \frac{fm^2}{4R}\int_0^{2\pi}\frac{d\varphi}{\sin(\varphi/2)} = \frac{fm^2}{2R}\ln\left(\tan\frac{\varphi}{4}\right)\Big|_0^{2\pi}\,. \tag{1}$$

So the one-dimensional scheme of gravity force determination is not suitable for the ring by the same reason as for the rod. We obtain infinity. It is necessary to integrate with respect to the cross-sectional area, as it was shown in Fig. 428 for the straight rod.

But we want to hold it off for now and shall not jump yet into the ocean of computations. The expected result is obvious enough. As equation (1) prompts

$$q = \frac{fm^2}{R}K, \tag{2}$$

where K is an unknown dimensionless coefficient which depends upon the shape of the ring's cross-section.

Now let's consider small deflections of the ring from its plane circular state. They are defined by the displacements u and w (Fig. 433), and the angle of rotation of the arc element is

$$\vartheta = \frac{dw}{Rd\varphi} - \frac{u}{R}\,.$$

Under small disturbances, load q varies and obtains small additional components: normal q_n and tangential q_t, respectively. It is necessary to calculate these.

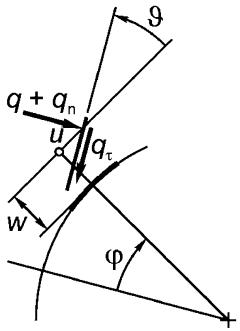

Fig. 433

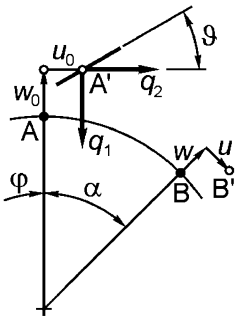

Fig. 434

Let's fix an arbitrarily chosen point A with the angular coordinate φ and denote its deflections as u_0 and w_0 (Fig. 434). The deflections of some point B will be u and w.

The distance between points A and B is r and the distance between points A' and B' is equal to $r + \Delta r$. It is easy to ascertain that

$$\Delta r = (w + w_0)\sin\frac{\alpha}{2} + (u - u_0)\cos\frac{\alpha}{2}\,.$$

The vertical and horizontal components of gravity force per unit length of mass A' by mass B' are as follows

$$dq_1 = \frac{fm^2R\,d\alpha}{(r+\Delta r)^3}\left[R + w_0 - (R+w)\cos\alpha + u\sin\alpha\right],$$

$$dq_2 = \frac{fm^2R\,d\alpha}{(r+\Delta r)^3}\left[(R+w)\sin\alpha - u\cos\alpha + u_0\right].$$

If we project the forces onto the normal and tangent direction to the arc element at point A', we obtain

$$d(q+q_n) =$$

$$= \frac{fm^2R\,d\alpha}{(r+\Delta r)^3}\left[(R+w_0) - (R+w)\cos\alpha + u\sin\alpha - \left(\frac{dw_0}{d\varphi} - u_0\right)\sin\alpha\right],$$

$$dq_t =$$

$$= \frac{fm^2R\,d\alpha}{(r+\Delta r)^3}\left[\left(\frac{dw_0}{d\varphi} - u_0\right)(1-\cos\alpha) - (R+w)\sin\alpha - u\cos\alpha + u_0\right]$$

As

$$(r+\Delta r)^{-3} = r^{-3}(1 - 3\frac{\Delta r}{r})\,,$$

then

$$d(q+q_n) = \frac{fm^2d\alpha}{8R^2\sin^3(\alpha/2)}[R(1-\cos\alpha) + w_0 - w\cos\alpha$$

$$+u\sin\alpha-\left(\frac{dw_0}{d\varphi}-u_0\right)\sin\alpha$$

$$-\frac{3}{2}(w+w_0)(1-\cos\alpha)-\frac{3}{2}(u-u_0)\sin\alpha]\,;$$

$$dq_t=\frac{fm^2\,d\alpha}{8R^2\sin^3(\alpha/2)}[-R\sin\alpha+\left(\frac{dw_0}{d\varphi}-u_0\right)(1-\cos\alpha)$$

$$-w\sin\alpha-u\cos\alpha+u_0$$

$$+\frac{3}{2}(w+w_0)\sin\alpha+\frac{3}{2}(u-u_0)(1+\cos\alpha)]\,.$$

Now it is necessary to integrate these equations with respect to α from zero to 2π for fixed u_0 and w_0, but for variable u and w.

As it is usually done, it is natural to assume that the deflections u and w obey the periodicity condition, which provides that the ring deflection curve is non-stretched while bending:

$$w_0=A\cos n\varphi,\qquad w=A\cos n(\varphi+\alpha)\,,$$
$$u_0=-\frac{A}{n}\sin n\varphi,\qquad u=-\frac{A}{n}\sin n(\varphi+\alpha)\,.$$

Further, in order to simplify calculations, we preset $n=2$. However, it can not be excluded that the number of waves n may differ but such probability is small.

Since we analyze stability according to a one-dimensional scheme we inevitably meet with the already known improper integral (1). That is why we use expression (2) written above. If we compare it with equation (1) then it is easy to conclude that the transfer to a three-dimensional scheme reduces this integral into the quantity $4K$.

After rather cumbersome integration with respect to α we obtain

$$q_n=\frac{fm^2}{8R^2}A(24K-\frac{104}{3})\cos 2\varphi\,,$$
$$q_t=-\frac{fm^2}{8R^2}A\frac{32}{3}\sin 2\varphi.$$

We only have to derive the equations of equilibrium for the bent ring. But this work has been done in solving problem 134.

Let's rewrite equation (2) of problem 134:

$$\frac{EJ}{R^3}\frac{d^3\varkappa}{d\varphi^3}+(qR+\frac{EJ}{R^2})\frac{1}{R}\frac{d\varkappa}{d\varphi}+\frac{1}{R}\frac{dq_n}{d\varphi}+\frac{1}{R}q_t=0\,,\qquad(3)$$

where $\varkappa$ is the curvature variation

$$\varkappa=\frac{1}{R^2}(\frac{d^2w}{d\varphi^2}+w)=-\frac{3A}{R}\cos 2\varphi\,.$$

Now we only have to substitute $\varkappa$, q_n and q_t into equation (3) and find the condition of critical state. If we write it in traditional form, then we shall obtain

$$q_{cr} = \frac{26K}{11}\frac{EJ}{R^3},$$

and if we substitute q from (2), then we arrive at

$$\left(\frac{fm^2R^2}{EJ}\right)_{cr} = \frac{26}{11}.$$

The result is extremely comforting. The unknown was cancelled and there is no need to carry out a complicated integration in order to find it.

For square cross-section we get

$$\left(\frac{f\rho^2R^2}{E}\right)_{cr} = \frac{13}{66}.$$

Finally let's calculate the critical radius of the steel ring of square cross-section. The required data are given in the previous problem.

The result is the following: $R_{cr} = 3083\,\text{km}$.

163. Let's imagine that balls BB have turned by a certain small angle φ with respect to the axis OA (Fig. 435). After that the inertial forces of the balls will not remain parallel to the axis OA and the pair of forces creates the moment

$$M = m\omega^2 l\alpha\, 2a,$$

which will twist the rod OA. But as we have $\alpha = \varphi a/l$, then

$$M = 2m\omega^2 a^2\varphi.$$

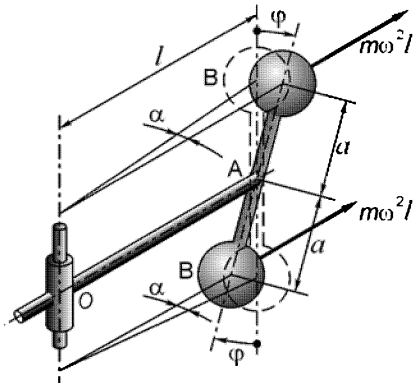

Fig. 435

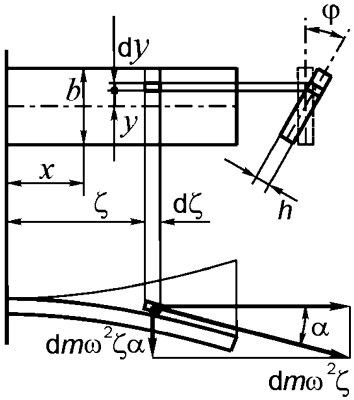

Fig. 436

On the other hand, for the twisted rod we have

$$M = \frac{GJ_p}{l}\varphi,$$

where GJ_p is torsional rigidity of the rod; therefore it yields

$$\omega = \sqrt{\frac{GJ_p}{2mla^2}}\,.$$

This is the critical angular velocity for the given system. If velocity exceeds this value then the rod OA is twisted.

164. Let's assume that some section disposed at a distance ζ from the axis has turned by angle φ under rod torsion (Fig. 436). Let's separate the rod's element $d\zeta\, dy\, h$ located at a distance y from the rod axis. If the section rotates by angle φ then elementary inertial force $dm\,\omega^2\zeta$ gives the transverse component $dm\,\omega^2\zeta\alpha$.

The elementary torsional moment of this force will be

$$dM = dm\,\omega^2\zeta\alpha y\,.$$

But we know that

$$dm = \frac{\gamma}{g}h d\zeta dy,\ \alpha = \varphi\frac{y}{\zeta}\,,$$

where γ is the specific weight of the rod material. Then the torsional moment in the cross-section x is determined as follows:

$$M = \int_{-b/2}^{+b/2}\int_0^l \frac{\gamma}{g}h\omega^2\varphi y^2 dy\, d\zeta = \frac{\gamma}{g}\frac{b^3h}{12}\omega^2\int_0^l \varphi\, d\zeta\,.$$

The normal force in the same cross-section is obtained by integration of the expression

$$\omega^2\zeta\, dm = \frac{\gamma}{g}h\omega^2\zeta\, d\zeta\, dy\,,$$

that yields

$$N = \int_{-b/2}^{+b/2}\int_x^l \frac{\gamma}{g}h\omega^2\zeta\, d\zeta\, dy = \frac{\gamma}{g}\frac{\omega^2 bh}{2}(l^2 - x^2).$$

From the condition of rod torsion we have

$$\frac{d\varphi}{dx} = \frac{M_t}{C},$$

where C is torsional rigidity. In the given case the magnitude of C depends on force N (see problem 28):

$$C = \frac{1}{3}bh^3G + \frac{Nb^2}{12}, \quad C = \frac{1}{3}bh^3G + \frac{\gamma}{g}\frac{b^3h}{24}\omega^2(l^2 - x^2).$$

In the previous problem the rods' OA had circular section and their rigidity did not depend on tensile force. Now we obtain

$$\frac{d\varphi}{dx}C = \frac{\gamma}{g}\frac{b^3h}{12}\omega^2\int_x^l \varphi\, d\zeta.$$

Let's differentiate both parts of the equation with respect to x :

$$\frac{d}{dx}\left(C\frac{d\varphi}{dx}\right) = -\frac{\gamma}{g}\frac{b^3h}{12}\omega^2\varphi\,.$$

But it follows from the relation for C that

$$\frac{\gamma}{g}\frac{b^3h}{12}\omega^2 = \frac{1}{x}\frac{dC}{dx}\,,$$

that is why

$$x\frac{d}{dx}\left(C\frac{d\varphi}{dx}\right) = \frac{dC}{dx}\varphi\,.$$

Independent of the type of function C the solution of the equation will be

$$\varphi = x\left[A\int\frac{dx}{x^2C} + B\right],$$

where A and B are arbitrary constants.

Let's evaluate an integral

$$\int\frac{dx}{x^2C} = \int\frac{dx}{\left[\frac{1}{3}bh^3G + \frac{\gamma}{g}\frac{b^3h}{24}\omega^2(l^2-x^2)\right]x^2} = \frac{1}{p}\left[-\frac{1}{x} + \frac{k}{2}\ln\frac{1+kx}{1-kx}\right],$$

where it is denoted

$$p = \frac{1}{3}bh^3G + \frac{\gamma}{g}\frac{b^3h}{24}\omega^2l^2, \qquad k^2 = \frac{1}{p}\frac{\gamma}{g}\frac{b^3h}{24}\omega^2.$$

Thus we arrive at

$$\varphi = \frac{A}{p}(-1 + \frac{k}{2}x\ln\frac{1+kx}{1-kx}) + Bx.$$

For $x = 0$ we have $\varphi = 0$, from which $A = 0$. Then for $x = l$ we have $M_t = 0$ $(d\varphi/dx = 0)$, and then $B = 0$.

Hence for any angular velocity ω, the rod remains straight.[2]

165. A thin homogeneous disk rotating about the axis perpendicular to its plane can loose its stability. For disks of ordinary thickness the critical speed ω_{cr} is higher than its value under which the disk is ruptured. If we consider a very thin metallic or, even better rubber, disk, then by experiment we can obtain the buckling mode shape presented in Fig. 437.

We can explain the occurrence of such an equilibrium state by the following. Assume that the disk is perfectly balanced and suppose that some external disturbance caused some deflection of the disk in its plane in such a

[2] While the author was preparing the first edition of this monograph L.I. Balabuch proved that a prismatic rod of arbitrary cross-section shape does not have a critical angular velocity at all.

way that disk balance was upset. If the center of disk gravity has been displaced rightward as shown in Fig. 437, then the compressive radial stresses arise to the left of the immovable axis. That is why for sufficiently large angular speed of disk the buckling can appear at this region; as a result the disbalance will increase more yet. If this process does not cause the failure of the disk then its mode shape after stability loss will be something like the one shown in Fig. 437.

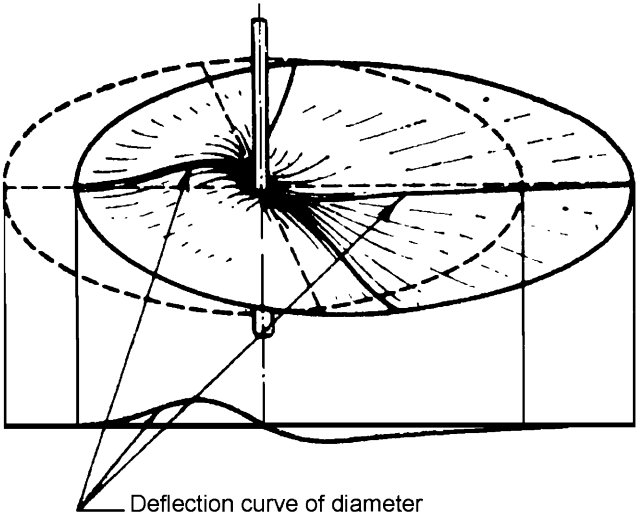

Fig. 437

166. Let's determine force P which we need to apply in order to deflect the ring from its axis by some small value w (Fig. 438). Obviously

$$P = \sum_{1}^{n} N_i \cos(i\frac{2\pi}{n} - \varphi_0),$$

where i is the number of spokes, and N_i is normal force in spoke cross-sections.

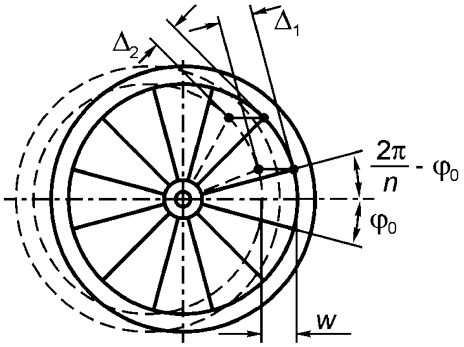

Fig. 438

If we denote elongation of i's spoke as Δ_i then

$$N_i = \frac{EA\Delta_i}{l}.$$

But

$$\Delta_i = w\cos(i\frac{2\pi}{n} - \varphi_0),$$

thus we get

$$P = w\frac{EA}{l}\sum_1^n \cos^2(i\frac{2\pi}{n} - \varphi_0).$$

It can be shown that

$$\sum_1^n \cos^2(i\frac{2\pi}{n} - \varphi_0) = \frac{n}{2},$$

and then

$$P = w\frac{EAn}{2l}.$$

The critical angular speed is determined by the condition [10]

$$P = m\omega_{cr}^2 w = w\frac{EAn}{2l},$$

from which we have

$$\omega_{cr} = \sqrt{\frac{EAn}{2ml}}.$$

167. Under certain pressure (in the area of appreciable elongations) the spherical equilibrium state becomes unstable. If local contraction of the sphere wall arises due to some cause then it continues to progress. Wall thickness becomes non-uniform and the sphere slightly elongates (Fig. 439a). The phenomenon is analogous to the process of necking of a tensed specimen. The same can be observed during blowing up of a volleyball bladder. A similar phenomenon is observed while blowing up a bicycle inner tube (Fig. 439b).

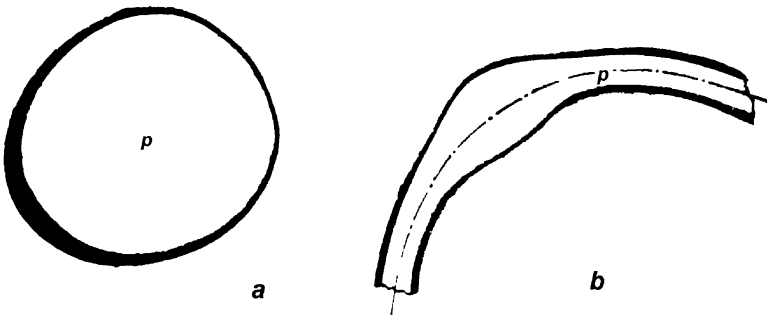

Fig. 439

168. If some external reason causes the local necking of the specimen the cylindrical shape can be restored by a small tensile force after the reason that caused the necking is removed. Thus up to certain value of tensile force the cylindrical form of the specimen is stable.

For sufficiently large tensile force even infinitely small local necking will cause in the vicinity of necking stress growth of such magnitude that the rod will not be able to restore its cylindrical form even if the reason that caused the necking is removed. The contraction will progress and the neck will be generated at the specimen. The cylindrical equilibrium state becomes unstable.

169. The presented shape of the tested specimen does not leave doubts that its failure is preceded by local loss of stability. In reality it is not necessarily realized in pure form. Particular conditions are required for that. But the average statistical regularity of the wooden structure predetermines the regularity of wave formation as well.

Wood has layer structure. Soft relatively thick layers alternate with thin and rigid ones. Maximal stress arises in rigid layers. Local deflection of the layer causes deflection of neighbouring ones too. The shape of local bending is the same for all rigid layers, but it is shifted in phase. As a result, the inclined strip of the "fault" or "shear" (it is difficult to find a name) occurs. The cracks are generated in this region later. The angle of strip inclination as well as critical stress are defined by the ratio of layer thickness and by the ratio of their modulus of elasticity [14]. Naturally, this kind of failure can be realized not only in the case of wood testing but under certain conditions in case of laminar composite testing, too.

5. Various Questions and Problems

170. This is an often posed question and seems to be old-fashioned. The unexpressed tonality of a passive perception of the environment reverberates in it. Let's see, they say, how nature is rich and what it gives to us? But in our time side by side with the question "*what is it made from*" the question "*how is it made*" is of great significance. For example, sprayed liquid aluminium at cooling speed at about 10^5 degrees per second does not have enough time to crystallize. Clinkering in inert medium under high pressure of the amorphous metal obtained by such method makes possible to manufacture aluminium details of strength at least one and a half times higher than the ones produced by traditional methods. This is expensive but in aviation and space-rocket production we cannot do without it.

Nowadays we should look for the highest strengths in the domain of thin fibres, which provide a basis for composite materials. Thin glass fibre, carbon fibre, and boric fibre have an ultimate stress of up to 3500 MPa. But we ought to remember that high ultimate stress is not the sole benefit. In many cases it gives way to other merits, for example specific weight. Just due to this reason, steel fibre which frequently is just as strong is moved to the second position in comparison with glass and carbon fibres. Artificially grown filamentary crystals of metals and their chemical compounds that are widely spread in nature and are generally considered as substances of mineral origin have extremely high ultimate stress. Among them we can find such ones that in common perception are considered as precious stones – sapphire (Al_2O_3) and garnet ($Al_5Y_3O_{12}$).

But we should warn the reader against the conceptions "strength of specimen" and "strength of construction".

Specimen strength under test conditions is actually determined by the ultimate stress value. Let's consider a detail produced of the same material as the tested specimen. The detail's strength under work conditions is determined not only by the ultimate stress value but by another characteristics too. As for the strength of detail produced of the same material then it is determined not only by the ultimate stress value under work conditions, but by another characteristics too. The elongation at rupture is the most essential among them. Some other characteristics are important too, for example the sensitivity to local stresses, the impact toughness etc., but they cannot be

obtained so unambiguously as the first one. Therefore the detail produced of materials with higher ultimate stress frequently turns out to be less durable under working conditions than just the same one but produced of materials with lower ultimate stress.

The ultimate stress of some steels can be raised to up to 2800 MPa by heat treatment methods in combination with, for example, intermediate mechanical hardening. But the significance of the obtained result cannot be estimated by this criterion alone.

171. Wood bears greater load under tension along the fibres. For example, dry fir-tree wood has an ultimate stress in compression of $\sigma_{uc} \approx 55$ MPa, and in tension $\sigma_{ut} \approx 72$ MPa, for beech it is $\sigma_{uc} \approx 67$ MPa, and $\sigma_{ut} \approx 82$ MPa.

This property of wood follows from its anisotropy. Rigid layers interchange with soft ones. Under longitudinal compression the rigid layers bear the main load. Under sufficiently high forces in these layers local buckling appears, which cause quick rupture of the specimen. Textolite and some other types of composite materials have the same property.

172. It is well known that the modulus of elasticity of steel is equal to 200 GPa, but only few people are aware of materials with higher modulus of elasticity. The according reference data in ascending order of elasticity modulus are given in Table 7:

Table 7. Elasticity modulus of some materials

Cobalt and nickel	210 GPa
Rhodium	290 GPa
Beryllium	290 GPa
Wolfram and molybdenum	350 GPa
Whiskers (filamentary crystals):	
Sapphire	500 GPa
Graphite	690 GPa

Diamond takes priority over the non-constructional materials: $E = 1050$ GPa.

173. The elasticity modulus for some rubber types reaches values of $0.4 - 0.5$ MPa. The least modulus of elasticity among the metals is found for lead ($E = 18$ GPa) and calcium ($E = 21$ GPa).

174. The answer to this question depends upon the magnitude of considered strains. Usually we assume that rubber does not obey Hook's law. This may be the case for strains of about 100% and more.

For the case of strains of less than $10 - 20\%$ we can assume with accuracy sufficient for practical purposes that all types of rubber, as a rule, follow Hook's law. No other materials have such large strains up to proportional limit.

175. Small cracks as well as larger cracks and structural defects exist in a glass medium just as in any material. Glass is very sensitive to defects. Under loading they easily grow and cause quick failure. The behaviour of window glass and glass dishes under loading, especially under impact, clearly indicates that. Thus, glass has the worst reputation as a constructional material. However, forces of molecular cohesion of glass allow its ultimate stress to reach that of steel and even exceed it. Tests of thin fibers undoubtedly confirms this.

Thin glass fibre can not develop large cracks. This is an inherent characteristic of fiber. If there is a large crack, fiber does not exist. But also if fiber exists, then there is no large crack, and we have high strength. We do not know what is the cause and what the effect. But though fiber is strong it is sensitive to microdefects.

The boundary of two media is obviously an obstacle for crack propagation. If fibers are combined in a bundle by compound material the growing crack may only be able to progress through the cross-section of one fiber but not any further. It will be blocked by the compound material. That is the cause of the significant difference in strength, for example, of a fiberglass plastic fishing-rod and a glass tube of the same diameter.

176. The reduced elasticity modulus of the rope is lower than the elasticity modulus of its component threads because elongation of the rope in tension occurs not only due to the elongation of threads, but also due to their partial bending and twisting. The reduced modulus of elasticity of the rope while stretching does not remain constant, i.e. a diagram of rope elongation is not linear even for elastic strains. During the initial stage of stretching the threads are packed and clearances between them gradually decrease. Local deformations gain a more noticeable role during further stretching. They occur in zones of mutual contact of threads.

177. According to the set of the problem, displacements of the beam are proportional to the acting loads. Hence, we can use the reciprocity principle for displacements.

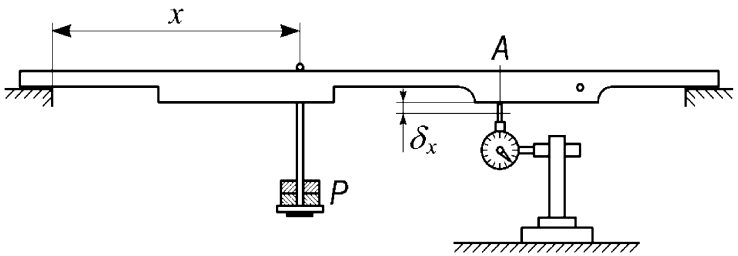

Fig. 440

The displacement of the cross-section with coordinate x can be measured placing an indicator under point A and loading the beam at x cross-section

(Fig. 440). Moving the weight, we measure δ_x at point A for different values of x. The obtained relation $\delta_x = f(x)$ represents the deflection curve of the beam.

If the weight P is so big that it is difficult to move it then we can decrease it. Afterwards, according to the specified condition we can determine the deflection curve for a given value of force P by proportionally increasing the measured deflections.

178. Fibres composing a thread are shorter than the thread itself. That is why the strength of a thread depends not only upon the strength of the individual fibres but upon their mutual cohesion as well. The latter is defined by forces of friction between fibres. For a twisted thread each fibre is whipped and tightened by neighbouring ones, and cohesion forces of fibres are much higher than for untwisted thread.

Cohesion forces strongly depend on the length of fibres. That is why a long-stapled cotton costs more than short-stapled cotton.

It is interesting that threads twisted of artificial fibre have lower rupture strengths than untwisted ones. Artificial fibre has greater length, being equal to the thread length. Therefore, fibres need no interconnection, and twisting yields to rising of additional stresses only, which results in quicker rupture.

The problem under consideration has something in common with the item we encountered in solving problems 17 and 175. A twisted or plaited rope represents a special kind of composite that was intuitially found by humans in ancient times. Air is a cohesive medium that ideally prevents crack growth. The only trouble is that despite this "cohesive medium" fiber length is inefficient. Twisting and plaiting provide friction between neighbouring fibres and decrease length.

179. The student has hopefully now mastered the concepts of strength and rigidity. Though alloyed steel has higher strength, its modulus of elasticity E is approximately the same as for other types of steel, i.e. about 200 GPa. That is why the exchange of ordinary steel by alloyed steel causes no improvement in our case.

180. Let's consider two states of an elastic body (not necessarily a cylinder) laying on a rigid plane.

The first state: the body is under action of its weight. The second state: the body is under action of a certain pressure p, uniformly distributed along its surface. According to the reciprocity theorem the work done by the first system of forces at the displacements caused by the second system of forces is equal to the work done by the second system of forces at the displacement of the first system.

For the first specified state of the elastic body the work done by weight forces at displacements caused by the pressure is

$$\int_V \gamma\, dV\, w_p\,,$$

where γ is specific weight, $\gamma\, dV$ is the weight of elementary volume, and w_p is vertical displacement of some point of an elastic body under action of uniform pressure p. Naturally, this displacement is measured with respect to the rigid plane. But elastic elongations for all points of the body under uniform pressure will be constant and equal to

$$\varepsilon = -\frac{p}{E}(1-2\mu)\,.$$

Hence, vertical displacement w_p is proportional to the distance from the rigid plane. Then

$$\int_V \gamma\, w_p\, dV = \gamma \int_V w_p\, dV = \gamma V w_p^*\,,$$

where w_p^* is the displacement of the elastic body centroid.

If the centroid of the elastic body is at a distance H from the foundation, then

$$w_p^* = H\frac{p}{E}(1-2\mu)\,.$$

Thus,

$$\int_V \gamma\, w_p\, dV = \gamma V \frac{Hp}{E}(1-2\mu)\,.$$

On the other side, according to the reciprocity theorem this quantity is equal to the work done by pressure p at the sought volume variation ΔV, caused by forces of its weight, i.e.

$$\gamma V \frac{Hp}{E}(1-2\mu) = p\Delta V,$$

which yields

$$\Delta V = \gamma V H \frac{1-2\mu}{E}\,.$$

If we rotate the body in such a manner that the center of gravity will occur at different height, then ΔV will change respectively.

Naturally, the obtained solution is valid for any body independent upon its shape. Obviously, for the given cylinder during transfer from state I to state II (Fig. 157) its volume will increase by

$$P\left(\frac{H}{2} - R\right)\frac{1-2\mu}{E}\,.$$

181. The problem solution is similar to the previous one

$$p\,\Delta V_P = P\,\Delta\,(AB)_p\,,$$

where ΔV_P is the sought volume variation caused by forces P, and $\Delta(AB)_p$ is the variation of distance between points A and B caused by pressure p. Obviously, we have

$$\Delta(AB)_p = -p\frac{1-2\mu}{E}(AB)\,,$$

where AB is the distance between points of force application. Hence, the sought volume variation is equal to

$$\Delta V_P = -P\,AB\,\frac{1-2\mu}{E}\,.$$

182. The explanation is faulty. According to the cited considerations the tube, independent of its cross-section shape, must always decrease its curvature under action of internal pressure, i.e. straighten itself up. However, experience shows that a tube of circular cross-section does not react to internal pressure at all, and a tube having cross-section with reversal arrangement of longer and shorter axes under action of internal pressure does not decrease its curvature but increases it.

The author of the above given explanation did not take into consideration that besides forces P_1 and P_2 acting upon surfaces S_1 and S_2 there exists one more force acting at the tube bottom. The moment of this force is exactly equal to the difference of moments of forces P_1 and P_2, thus the bending moment in any cross-section of the tube vanishes. Therefore we do not need to calculate magnitudes of these forces in order to check the above mentioned. The surface of the tube to the right from an arbitrary cross-section AA (Fig. 441) represents a closed surface, and pressure will give only tensile force in the cross-section which is equal to the product of pressure and section area "in clearance".

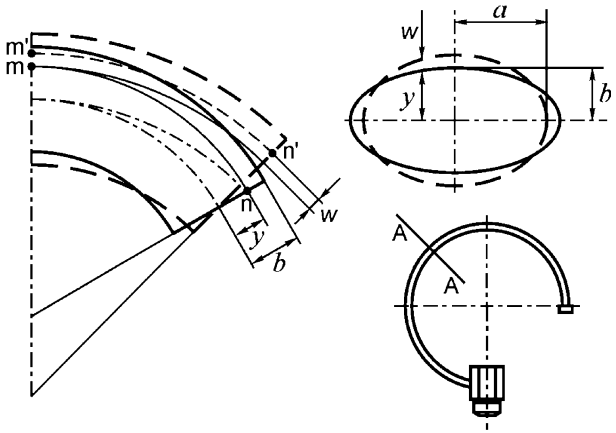

Fig. 441

The forces of pressure will not produce the bending moment at all for any tube shape. The distortion of the cross-sectional contour is the necessary condition of tube operation. Under action of internal excessive pressure the contour of the tube's cross-section tends to have circular shape independently of its initial configuration. Here the shorter axis of section will slightly increase and the longer one will decrease, and the whole contour will take such form as is roughly shown by the dashed line in Fig. 441. Due to that fact each longitudinal fibre of the tube will have a certain displacement parallel to the shorter axis of the cross-section. In Fig. 441 this displacement for fibre mn is denoted as w.

When the fibre mn moves by value w it will transfer to the arc of the larger radius and tensile stresses will arise in it. In fibres lying below the neutral axis compressive stresses will occur. Thus the tube will straighten itself.

The above said explains why a tube of circular cross-section does not react to internal pressure. In this case the contour of the cross-section is only tensed and the value of w will be infinitesimally small. That is why the curvature change of the tube of circular cross-section is insignificant and is not observed during ordinary experiments.

If the larger axis of the cross-section is in the plane of tube symmetry, then the value of w will have an opposite sign and tube curvature under internal pressure will not decrease but increase.

183. In the proposed problem the calculations are produced correctly. There is no reason to search for any algebraic mistake. We deal with the surprise, which the "momentless" theory of shells may present to unsophisticated researcher while deriving displacements.

Here we can use two ways in order to find displacements.

The first method: Assuming that the principle of initial dimensions invariability is valid we consider also bending moments and shear forces in addition to tensile forces. In other words we depart from the "momentless" condition.

The second method: Remaining within the frames of the "momentless" shell theory we construct the equilibrium equations for the deformed shell the shape of which is distorted by arising displacements. This method is often used while deriving displacements of so-called "soft" shells – shells that weakly resist bending.

184. Let's consider one section of the shaped cylinder (Fig. 442). Let's denote the internal pressure as p and admissible stress by σ_{adm}.

The thickness of the cylindrical part of the section is determined by admissible stress as follows:

$$\delta = \frac{pr}{\sigma_{adm}}$$

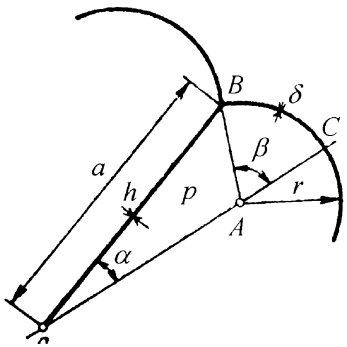

Fig. 442

The supporting internal wall works in tension and is under action of forces transmitted to it from two adjacent circular cylinders. The force pr is acting per unit height of cylinder. The tensile force in a wall is

$$2pr\sin(\beta-\alpha).$$

The admissible stress for the wall is supposed to be the same as for the circular cylinder. That is why thickness of the wall is

$$h=\frac{2pr\sin(\beta-\alpha)}{\sigma_{adm}}.$$

Now let's find construction weight per unit length of the shaped cylinder

$$P=\gamma n(2\beta r\delta+ah),$$

where γ is specific weight of the material and n is the number of sections.

After substitution of δ and h we obtain

$$P=2\gamma n\frac{pr}{\sigma_{adm}}[\beta r+\sin(\beta-\alpha)]. \tag{1}$$

Let's determine the volume of the internal chamber per unit of height.

The volume of sector ABC is equal to $\frac{1}{2}\beta r^2$, and for triangle OAB we have $\frac{1}{2}ar\sin(\beta-\alpha)$, therefore

$$V=2n\left[\frac{1}{2}\beta r^2+\frac{1}{2}ar\sin(\beta-\alpha)\right],$$

or

$$V=nr[\beta r+a\sin(\beta-\alpha)].$$

Returning to relation (1) we arrive at

$$P=2\frac{\gamma p}{\sigma_{adm}}V.$$

This means that for a given volume of compressed gas the construction weight can not be changed by varying of quantities α, β, a, and n. The ordinary smooth cylinder has the same weight for the same volume of the chamber but is easier in production. Thus the proposed construction does not meet our expectations.

An objection is expected. The conclusion that the construction shows no promise is made on the basis of the assumption that the stress state is uniaxial. But the shaped cylinder is tensed in axial direction, too...

This is quite true. Therefore the condition of strength should be written in the following form

$$\sigma_{eq} = \sigma_1 - \sigma_3 \leq \sigma_{adm};$$

where σ_1 is maximal principal stress. It is positive and can be either circumferential or axial stress depending on the fact which of them is greater. σ_3 is the least of three principal stresses and is equal to zero.

Now let's imagine that for some ratio of parameters the axial stress occurs to be greater than circumferential, and that we made a mistake considering the lesser one, the circumferential stress. But if construction is unpromising for the less stress condition then it will be even more unpromising for the greater one.

185. The question set in the problem does not specify how the load P was applied to the spring. Was it applied gradually or suddenly? If load was applied gradually, by increment portions, so that in any moment of loading the system was in equilibrium state, then expression (1) is not valid. The position energy lost by weight will not be P^2/c, but $P^2/(2c)$ and balance of energies will be retained.

If load was applied suddenly, then the weight will have the kinetic energy too, which is equal to difference of energies (1) and (2). Further weight will have oscillatory motion about its equilibrium state until its kinetic energy is dissipated.

186. In the best case we obtain the following answer on the question set in the problem.

The rotation angle of the coil in the axial plane is determined by twisting of the spring arc segment of length AB, if cross-section B is assumed as conditionally immovable, i.e.

$$\psi = \frac{M_t\, l_{AB}}{GJ_p} = \frac{PR\, l_{AB}}{GJ_p} \qquad (l_{AB} = 2\pi R\, n_{AB})\,.$$

However, this answer is wrong. Coils of the spring do not rotate in the axial plane at all ($\psi = 0$).

"But we can not agree with this" an inquisitive reader might say. If we consider an infinitesimal coil segment of length ds (Fig. 443), then, obviously, one cross-section rotates in the axial plane with respect to another. Therefore,

if we assume that some cross-section is immovable then another one will surely rotate in the axial plane. This means, the statement that angle ψ is equal to zero at any cross-section is incorrect.

However, we should not forget that the considered element of the coil rotates also in plane $y_1 z_1$ by angle ϑ (angle of the coils' inclination variation). Thus if the cross section (2) is twisted in the axial plane by the angle

$$d\varphi = \frac{M_t\, ds}{G J_p}\,,$$

then simultaneously it rotates backward in the same plane by the angle $\vartheta \dfrac{ds}{R}$ (see Fig. 443).

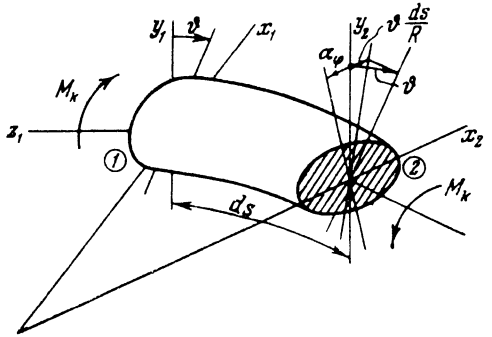

Fig. 443

The angle of cross-section (2) rotation in the axial plane is obviously

$$d\psi = d\varphi - \vartheta \frac{ds}{R}\,,$$

but it is known that

$$\vartheta = \frac{PR^2}{G J_p}\,,$$

and as $M_t = PR$, then, evidently, $d\psi = 0$.

We can make sure that this conclusion is valid applying different but more simple arguments.

Let's consider an arbitrary cross-section of the coil. If it really rotates in the axial plane of the spring by the supposed angle ψ, then it would "fulfil" that depending upon the fact whether the lower or upper spring end is immovable or not. But the cross-section "knows nothing" about these details, and it has no choice but to keep its place.

187. Let's consider the spring as a space beam. Torque $M_t = PR\cos\alpha$ and bending moment $M_b = PR\sin\alpha$ arise in each coil cross-section of the tensed spring (Fig. 444).

Let's preliminarily derive the increase of spring height ΔH :

$$\Delta H = \int_l \frac{M_b M_{1b}\, ds}{EJ} + \int_l \frac{M_t M_{1t}\, ds}{GJ_p}\,,$$

where M_{1b} and M_{1t} are bending moment and torque caused by unit forces applied instead of forces P, which accordingly are equal to

$$M_{1b} = R\sin\alpha\,, \quad M_{1t} = R\cos\alpha\,;$$

hence

$$\Delta H = \frac{PR^2 l}{EJ}\sin^2\alpha + \frac{PR^2 l}{GJ_p}\cos^2\alpha\,, \tag{1}$$

where l is the length of spring coils.

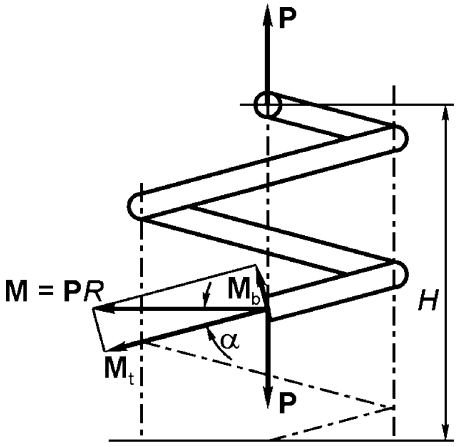

Fig. 444

Let's find the angle of the spring's upper end rotation in the horizontal plane with respect to its lower end. If we apply unit moments to the spring ends (Fig. 445a), we arrive at

$$M_{1b} = -\cos\alpha\,, \quad M_{1t} = \sin\alpha\,,$$
$$\Delta\varphi = \int_l \frac{M_b M_{1b}\, ds}{EJ} + \int_l \frac{M_t M_{1t}\, ds}{GJ_p}\,, \tag{2}$$
$$\Delta\varphi = PRl\left(\frac{1}{GJ_p} - \frac{1}{EJ}\right)\sin\alpha\cos\alpha\,.$$

Let's consider the spring involute (Fig. 445b). Obviously we have

$$R^2\varphi^2 + H^2 = l^2.$$

As l is constant then

$$2R\varphi^2\Delta R + R^2 2\varphi\Delta\varphi + 2H\Delta H = 0\,,$$

where Δ denotes the increment of the corresponding variable.

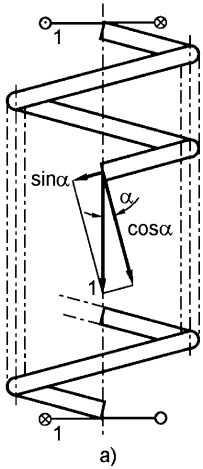

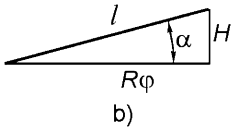

Fig. 445

From this expression we obtain

$$\Delta R = -\frac{R}{\varphi}\Delta\varphi - \frac{H}{R\varphi^2}\Delta H\,.$$

Substituting here $\Delta\varphi$ and ΔH we get:

$$\Delta R = -\frac{PR^2 l}{\varphi}\left(\frac{1}{GJ_p} - \frac{1}{EJ}\right)\cos\alpha\sin\alpha - \frac{PHRl}{\varphi^2}\left(\frac{\sin^2\alpha}{EJ} + \frac{\cos^2\alpha}{GJ_p}\right). \quad (3)$$

It follows from the triangle shown in Fig. 445b that

$$l = \frac{\varphi R}{\cos\alpha} \quad \text{and} \quad H = \varphi R\tan\alpha.$$

Besides it we obviously have

$$\varphi = 2\pi n\,, \quad \Delta\varphi = 2\pi\,\Delta n\,,$$

where n is the number of coils. If we eliminate l, H, and φ from (1), (2), and (3) we get:

$$\Delta H = 2\pi n\frac{PR^3}{\cos\alpha}\left(\frac{\sin^2\alpha}{EJ} + \frac{\cos^2\alpha}{GJ_p}\right),$$

$$\Delta n = PR^2 n\left(\frac{1}{GJ_p} - \frac{1}{EJ}\right)\sin\alpha\,,$$

$$\Delta R = -\frac{2PR^3\sin\alpha}{GJ_p} + \frac{PR^3}{EJ}\sin\alpha(1-\tan^2\alpha)\,.$$

If the spring is coiled with round wire having the diameter d then

$$GJ_p = G\frac{\pi d^4}{32}\,, \quad EJ = G(1+\mu)\frac{\pi d^4}{32}\,,$$

and then we arrive at

$$\Delta H = + \frac{64PR^3n}{Gd^4} \frac{1+\mu\cos^2\alpha}{(1+\mu)\cos\alpha},$$

$$\Delta n = + \frac{32PR^2n}{G\pi d^4} \frac{\mu\sin\alpha}{(1+\mu)},$$

$$\Delta R = - \frac{32PR^3}{G\pi d^4} \frac{\sin\alpha}{1+\mu} \frac{1+2\mu\cos^2\alpha}{\cos^2\alpha}.$$

The signs of the right part of the obtained relations indicate that under spring tension its length increases ($\Delta H > 0$), the number of coils increases ($\Delta n > 0$) and the radius decreases ($\Delta R < 0$). If angle α is small then we get

$$\Delta H = \frac{64PR^3n}{Gd^4},$$

$$\Delta n = \frac{32PR^2n}{G\pi d^4} \frac{\mu\alpha}{1+\mu},$$

$$\Delta R = - \frac{32PR^3}{G\pi d^4} \frac{1+2\mu}{1+\mu}\alpha.$$

188. In order to obtain the characteristics with decreasing stiffness for the shaped spring we should provide its preliminary compression, for example, by means of the second spring (Fig. 446). The number of operating coils will increase under loading of such a system.

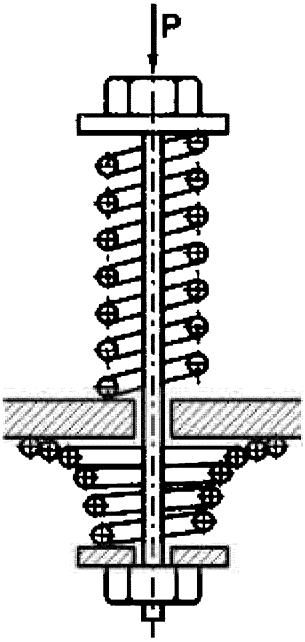

Fig. 446

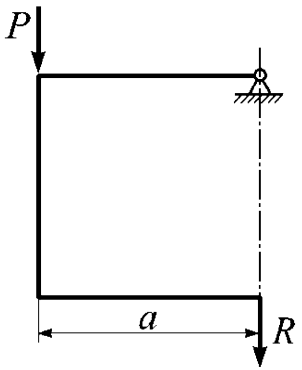

Fig. 447

189. The given configuration of the system is not the equilibrium state. If we try to determine the reaction of the lower support disregarding deformation of the system we would obtain a result of no practical sense:

$$R = \pm\infty.$$

Actually, by equating to zero the sum of all force moments about the upper hinge (Fig. 447), we obtain:

$$R \times 0 + Pa = 0\,,$$

from which we find the above value of reaction R.

Hence, it is necessary to consider the displacement of the lower roller in order to determine the reaction. Let's assume that the system equilibrium occurs under angular displacement φ of the lower support (Fig. 448).

Obviously, from the equilibrium condition we have $P = R\varphi$. The line segment AB has increased as a result of frame deformation by

$$a(1 - \cos\varphi) \approx \frac{a\varphi^2}{2}.$$

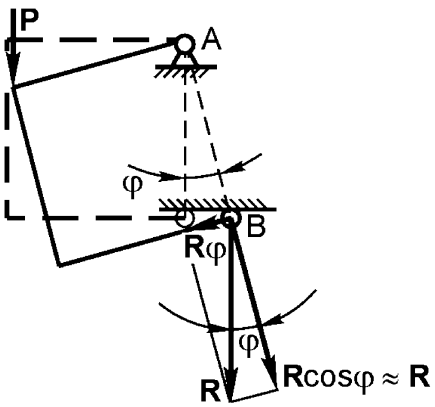

Fig. 448

On the other hand, the same value can be obtained by multiplying moment diagrams of specified forces by moment diagrams of unit forces (Fig. 449). Thus we get

$$\frac{Ra^3}{EJ}\frac{5}{3}(1 + \frac{\varphi}{2}) = \frac{a\varphi^2}{2}.$$

As displacements of the frame are small, the quantity of $\varphi/2$ in brackets is negligibly small in comparison with unity and we can neglect it. Further substituting P/R instead of φ on the right-hand side of the equation we arrive at

$$R = \sqrt[3]{\frac{3P^2EJ}{10a^2}}.$$

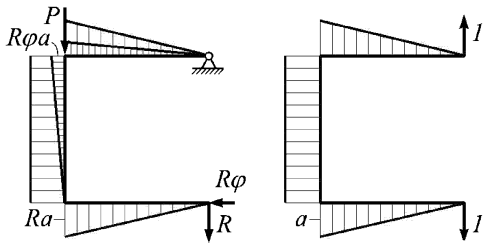

Fig. 449

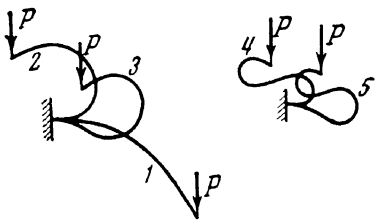

Fig. 450

190. A system, similar to the one shown in Fig. 169, can have new equilibrium shape modes under large displacements.

Particularly, if stress in the rod does not exceed the proportional limit, then under $P > 3.2EJ/l^2$ the beam has two additional equilibrium states (2 and 3) (Fig. 450) besides the main initial one. State 2 is stable, and state 3 is unstable. If $P > 7.1EJ/l^2$ the unstable equilibrium states 4 and 5 (Fig. 450) are possible etc. Naturally, if we gradually increase force P the state 1 can not transform into state 2 or any other one. However, if we preliminarily bend the beam in such a way that its free end occurs at the left of the clamped end, and afterwards load it by force $P > 3.2EJ/l^2$, then the beam will take equilibrium state 2.

191. Let's take two arbitrarily oriented systems of coordinates where one of them XYZ has its origin at point A and the second one, xyz its origin at point B (Fig. 451).

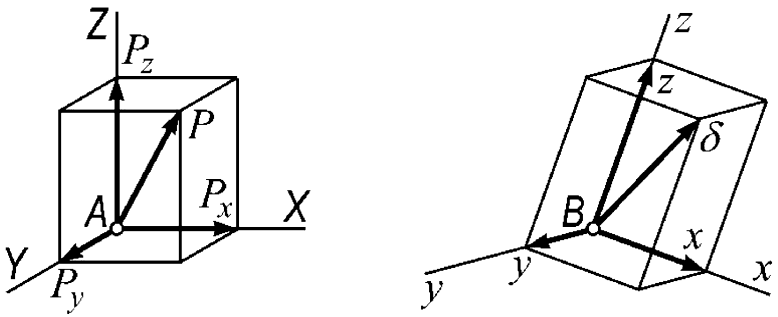

Fig. 451

The force P components along the axes XYZ are denoted as P_x, P_y, P_z, so that

$$P_x = Pl\,, \quad P_y = Pm\,, \quad P_z = Pn\,,$$

where l, m, n are the directional cosines of force P in the basis XYZ.

The components of point B displacement in the basis xyz are denoted as x, y, z. The displacement components will relate with force components by the linear equations:

$$P_x = Pl = c_{xx}x + c_{xy}y + c_{xz}z\,,$$
$$P_y = Pm = c_{yx}x + c_{yy}y + c_{yz}z\,, \qquad (1)$$
$$P_z = Pn = c_{zx}x + c_{zy}y + c_{zz}z\,,$$

where $c_{xx}, c_{xy}, \ldots$ are certain constant coefficients characterizing corresponding stiffnesses. For example, c_{xy} is a force which we must apply at point A along the x direction, in order to obtain displacement of point B along y direction as equal to unity.

Taking the square of both parts for each equation (1) and summarizing them we obtain

$$\begin{aligned} P^2 = {} & (c_{xx}^2 + c_{xy}^2 + c_{zx}^2)x^2 + (c_{xy}^2 + c_{yy}^2 + c_{zy}^2)y^2 \\ & + (c_{xz}^2 + c_{yz}^2 + c_{zz}^2)z^2 + 2(c_{xx}c_{xy} + c_{yx}c_{yy} + c_{zx}c_{zy})xy \\ & + 2(c_{xx}c_{xz} + c_{yx}c_{yz} + c_{zx}c_{zz})xz + 2(c_{xy}c_{xz} + c_{yy}c_{yz} + c_{zy}c_{zz})yz. \end{aligned}$$

Thus we see that the displacement vector at point B will describe a surface of second order with the center at the same point. It can be a single-napped or double-napped hyperboloid or ellipsoid. According to the physical nature of the problem the surface should not have infinitely distant points; hence it will be ellipsoid or those surfaces in the ellipsoid will be degenerate.

It is clear that the considered above does not serve as exact proof, but only is a simple guess. The rigorous proof, that is not given here due to necessary cumbersome calculations, consists in the following. By rotation of coordinate systems XYZ and xyz the equations (1) are transformed in such a way that the six coefficients $c_{xy}, c_{yx}, c_{xz}, c_{zx}, c_{yz}$, and c_{zy} vanish. For this purpose three angles of rotation of the first system and three angle of rotation of the second one are chosen in a proper way. Then

$$Pl = c_{xx}x, \quad Pm = c_{yy}y, \quad Pn = c_{zz}z,$$

from which we obtain the equation of the ellipsoid eliminating l, m, n

$$\frac{x^2}{(\frac{P}{c_{xx}})^2} + \frac{y^2}{(\frac{P}{c_{yy}})^2} + \frac{z^2}{(\frac{P}{c_{zz}})^2} = 1.$$

192. If the cross-section of the ring rotates in the axial plane by angle φ then circumferential elongation $\varepsilon = \Delta/a$ occurs at point A with coordinates ρ, α (Fig. 452). But according to Fig. 452 we have

$$\Delta = \rho[\sin(\alpha + \varphi) - \sin\alpha], \quad a = R + \rho\sin\varphi.$$

As ρ is considerably less than R we assume that $a \approx R$. Therefore, we arrive at

$$\varepsilon = \frac{\rho}{R}\,[\sin(\alpha + \varphi) - \sin\alpha]\,,$$
$$\sigma = E\,\frac{\rho}{R}\,[\sin(\alpha + \varphi) - \sin\alpha]\,. \qquad (1)$$

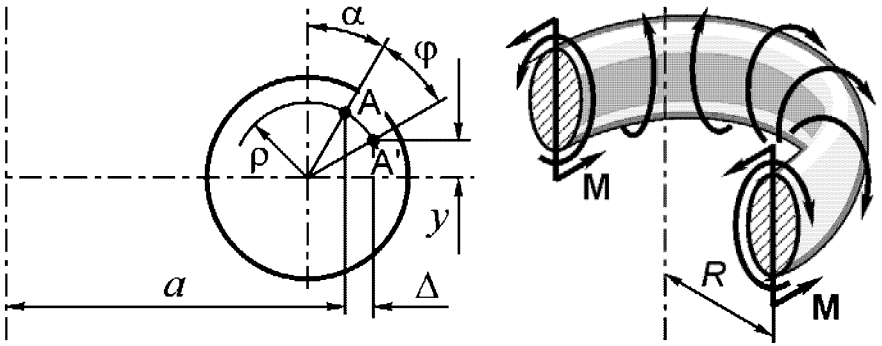

Fig. 452

Stresses σ produce bending moments in a ring cross-section with respect to the horizontal diameter, and this reads

$$M = \int\limits_F \sigma y \, dA,$$

where dA and y are equal to

$$dA = \rho \, d\alpha \, d\rho, \qquad y = \rho \cos(\alpha + \varphi).$$

Then we obtain

$$M = \frac{E}{R} \int\limits_0^r \int\limits_0^{2\pi} \rho^3 [\sin(\alpha + \varphi) - \sin\alpha] \cos(\alpha + \varphi) \, d\rho \, d\alpha \tag{2}$$

or

$$M = \frac{Er^4}{4R} \pi \sin\varphi.$$

On the other hand, $M = mR$ as follows from the one-half of the ring equilibrium condition (Fig. 452). Hence,

$$\sin\varphi = \frac{4mR^2}{E\pi r^4}.$$

For $0 \le \varphi \le \pi/2$ the moment m increases, attaining under $\varphi = \pi/2$ its maximum value

$$m_{\max} = \frac{E\pi r^4}{4R^2}.$$

Further growth of angle φ requires a lower moment. For $\varphi = \pi$, i.e. when the ring has turned inside-out, $m = 0$. In this case the ring is in unstable equilibrium state, and under infinitely small deflection returns to its initial state.

At $\varphi > \pi$ the moment $m < 0$. This means that in order to keep a ring in the given state it is necessary to apply the moment of reversed sign.

We can consider the magnitude of moment $m_{\max}$ obtained above as a critical value of moment under which the so-called "overturn" of the ring will occur.

193. The relation (1) of the previous problem obtained for stresses σ

$$\sigma = E\,\frac{\rho}{R}\,[\sin(\alpha+\varphi) - \sin\alpha]$$

changes by introduction of the additional term

$$E\,\frac{x}{R} = E\,\frac{\rho\sin\alpha}{R},$$

which represents the preliminary bending stresses. Now we have

$$\sigma = E\frac{\rho}{R}\sin(\alpha+\varphi).$$

Instead of the relation (2) we get

$$M = \frac{E}{R}\int\limits_0^r\int\limits_0^{2\pi}\rho^3\sin(\alpha+\varphi)\cos(\alpha+\varphi)\,d\rho\,d\varphi = 0\,.$$

It means that the ring having specified preliminary stresses will turn inside-out in the axial plane without applying external forces. Such a ring can be regarded as an elastic mechanism. The reader can easily testify the above said by experiment.

There are proposals to use the described phenomenon for measuring the so-called internal damping arising in materials under deformation.

194. The given problem can be solved in frames of a static approach.

Let's derive the law of balancing moment variation at the cable shaft end disregarding the dynamic effect, caused by nonuniform rotation of the shaft. The moment at the shaft entrance is constant. Let's simplify the problem assuming that axes of shaft and braid represent a single plane curve of variable curvature $1/\rho$ along its length. Neglecting the friction forces we derive the equilibrium equation of the shaft element of length ds (Fig. 453). Reactions of the braid acting on the element are normal to the surface of the shaft and do not produce a moment with respect to the x axis. That is why by equating to zero the sum of moments with respect to the axis x we obtain

$$\frac{dM_x}{ds} = \frac{M_y}{\rho}. \tag{1}$$

Hence, if friction forces are absent then the moment M_x changes along s only so far as the moment M_y exists, i.e. a bending moment in the plane perpendicular to the plane of the shaft curvature. Let's consider a point A with polar coordinates r and ψ in the shaft's cross-section (Fig. 454). Normal stress at this point can be presented in the form of two summands. The first

one is the stress which occurs in the shaft due to its distortion by the shape of the braid, i.e.

$$\sigma' = Er \sin\psi \left(\frac{1}{\rho} - \frac{1}{\rho_0}\right),$$

where $1/\rho_0$ is curvature of the shaft before it was placed into a braid.

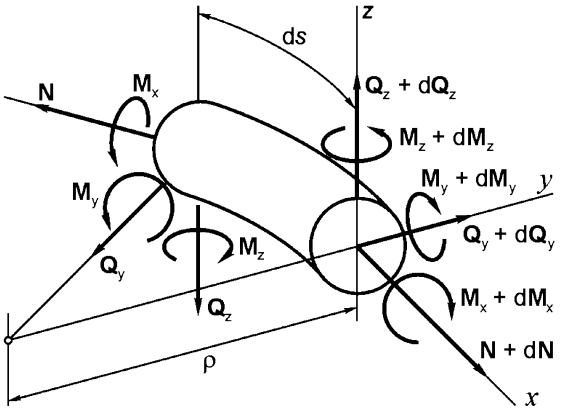

Fig. 453

The second term represents the stresses which occurs at point A after shaft rotation in the braid by angle φ.

At first we find the displacement of point A along the y axis (Fig. 454):

$$r\sin(\psi + \varphi) - r\sin\psi.$$

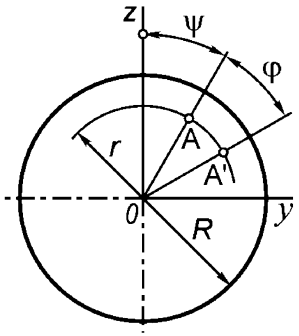

Fig. 454

Relative elongation along axis x will be

$$\frac{r}{\rho}\left[\sin(\psi + \varphi) - \sin\psi\right],$$

and stress

$$\sigma'' = E\,\frac{r}{\rho}\left[\sin(\psi + \varphi) - \sin\psi\right].$$

Total stress is

$$\sigma_x = \sigma' + \sigma'' = Er\left[\frac{1}{\rho}\sin(\psi+\varphi) - \frac{1}{\rho_0}\sin\psi\right].$$

Now let's find the bending moment M_y :

$$M_y = \int\limits_A \sigma z\, dA,$$

or

$$M_y = \int\limits_0^R \int\limits_0^{2\pi} Er\left[\frac{1}{\rho}\sin(\psi+\varphi) - \frac{1}{\rho_0}\sin\psi\right] r\cos(\psi+\varphi) r\, d\psi\, dr,$$

whence

$$M_y = \frac{EJ}{\rho_0}\sin\varphi.$$

Equation (1) will take the form

$$\frac{dM_x}{ds} = \frac{EJ}{\rho\rho_0}\sin\varphi.$$

We integrate the equation by s, assuming that all cross-sections have turned by the same angle φ

$$M_x = EJ\sin\varphi \int\limits_0^s \frac{ds}{\rho\rho_0} + C.$$

If at one shaft end (for $s = 0$) moment M_1 is applied, then the balancing moment M_2 at $s = l$ will be as follows:

$$M_2 = M_1 + EJ\sin\varphi \int\limits_0^l \frac{ds}{\rho\rho_0}.$$

Thus we see that the balancing moment at the shaft end has an additional component varying proportionally to the sine of the shaft's rotation angle. If we specify equal values of moments M_1 and M_2 then under shaft rotation the equilibrium conditions will not be fulfilled and rotation at exit will not be uniform.

Moment M_2 will not depend on angle φ if

$$\int\limits_0^l \frac{ds}{\rho\rho_0} = 0.$$

The sufficient condition for normal operation of the speedometer shaft is $1/\rho_0 = 0$, i.e. as long as the cable shaft is straight before placing it into a braid.

195. Under rod tension all fibres are stressed equally. Let's denote the tensile force in each of them as N. Let's multiply N by the number of fibres n in the monolayer, by $\sin\varphi$, and by the average radius r of $(+\varphi)$ monolayer. Then we obtain the moment of forces N about the axis of the rod: $Nnr\sin\varphi$. The monolayer $(-\varphi)$ produces a moment of reverse sign: $Nn(r-h)\sin\varphi$, where h is thickness of the monolayer. We see that the moments are not balanced. And the same happens with every pair of $(\pm\varphi)$ monolayers. A torque arises and it causes rod twisting. In order to avoid this we should either decrease the number of fibres in strands during winding of $(+\varphi)$ monolayers into a simple proportion

$$n_{(+\varphi)} = n_{(-\varphi)}\frac{r_{(+\varphi)} - h}{r_{(+\varphi)}},$$

or include additionally the last a $(-\varphi)$ monolayer with the number of fibres chosen for compensation of the moments produced by all pairs of $(\pm\varphi)$ monolayers.

196. Under tube bending the volume of the internal chamber does not change. This means that the energy of compressed gas also does not change. Hence the delivered gas has no way to influence the frequency of vibration other than of by its own mass. But it is negligibly small.

Thus the frequency of rod vibration does not depend upon pressure.

197. It is convenient to consider mass M movement in principal coordinates x, y (Fig. 455). They possess the property that force applied along axis x causes deflection only along axis x and force applied along axis y causes displacement along axis y only. In our case axes x and y are rotated by angle 22.5^0 with respect to the vertical and horizontal axes (see problem 41).

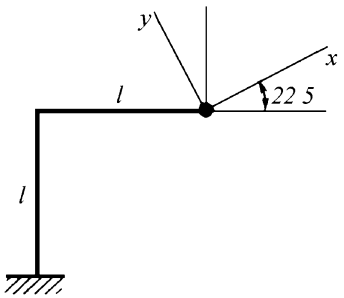

Fig. 455

It is easy to derive that force P_x directed by axis x causes the displacement of mass

$$\delta_x = \frac{P_x}{6EJ}(5 - 3\sqrt{2}),$$

and force P_y causes the displacement

$$\delta_y = \frac{P_y l^3}{6EJ}(5 + 3\sqrt{2}).$$

Now we write the equations of motion as follows

$$M\,x + \frac{6EJ}{l^3}\frac{1}{5 - 3\sqrt{2}}x + X = 0,$$
$$M\,y + \frac{6EJ}{l^3}\frac{1}{5 + 3\sqrt{2}}y + Y = 0. \qquad (1)$$

Forces X and Y are the components of total friction force T. If mass M is moving, the resultant force T is directed along the tangent to the mass trajectory and then

$$X = T\frac{x}{\sqrt{x^2 + y^2}}, \qquad Y = T\frac{y}{\sqrt{x^2 + y^2}}.$$

If $x = y = 0$, then we have two possibilities. The first: in case of small deflection the friction force can keep the mass in a certain range of immobility, and then

$$X = X_1 = -\frac{6EJ}{l^3}\frac{1}{5 - 3\sqrt{2}}x\,, \qquad Y = Y_1 = -\frac{6EJ}{l^3}\frac{1}{5 + 3\sqrt{2}}y\,. \qquad (2)$$

But the resultant of these forces cannot be greater than T. Therefore, the relations (2) are correct only under the condition

$$\sqrt{X_1^2 + Y_1^2} < T,$$

which corresponds to the mass stop, i.e. the final point of the trajectory.

If this condition is not satisfied then force T must be decomposed by axes x and y in the components

$$X = -T\frac{X_1}{\sqrt{X_1^2 + Y_1^2}}, \qquad Y = -T\frac{Y_1}{\sqrt{X_1^2 + Y_1^2}}.$$

Let's transform the equations (1) to dimensionless form by denoting

$$x = l\zeta, \qquad y = l\eta, \qquad t = \varkappa t,$$

where τ is dimensionless time.

We assume that

$$\varkappa^2 = \frac{Ml^3}{6EJ}(5 + 3\sqrt{2}),$$

then equation (1) can be rearranged in the following form

$$\frac{d^2\zeta}{d\tau^2} + 12.2\,\zeta + X_0 = 0\,,$$
$$\frac{d^2\eta}{d\tau^2} + \eta + Y_0 = 0\,. \qquad (3)$$

In case of motion, i.e. for $d\zeta/d\tau \neq 0$ or $d\eta/d\tau \neq 0$, the dimensionless components of friction force X_0 and Y_0 are defined by the relations

$$X_0 = T_0 \frac{\dfrac{d\zeta}{d\tau}}{\sqrt{(\dfrac{d\zeta}{d\tau})^2 + (\dfrac{d\eta}{d\tau})^2}}, \qquad Y_0 = T_0 \frac{\dfrac{d\eta}{d\tau}}{\sqrt{(\dfrac{d\zeta}{d\tau})^2 + (\dfrac{d\eta}{d\tau})^2}},$$

where $T_0 = T\varkappa^2/(Ml)$.

In case $\dfrac{d\eta}{d\tau} = \dfrac{d\zeta}{d\tau} = 0$ for $\sqrt{12.2^2\zeta^2 + \eta^2} < T_0$ the integration is stopped. If

$$\sqrt{12.2^2\zeta^2 + \eta^2} > T_0$$

then

$$X_0 = -T_0 \frac{12.2\zeta}{\sqrt{12.2^2\zeta^2 + \eta^2}}, \qquad Y_0 = -T_0 \frac{\eta}{\sqrt{12.2^2\zeta^2 + \eta^2}}.$$

The system of equations (3) is integrated by τ numerically. The step of integration must be chosen as much less than the least period of free vibrations. Obviously, from the first of the equations (3) $\omega^2 = 12.2$ and the corresponding dimensionless period of free vibrations will be $2\pi/\omega = 1.8$. The step $\Delta\tau$ is chosen as equal to 0.01. The initial deflections ζ_0 and η_0 of mass M must be chosen in such a way that $\sqrt{12.2^2\zeta_0^2 + \eta_0^2} > T_0$, otherwise the system in the initial state will be self-inhibiting. In other words mass M must be moved off the ellipse of self-braking. The equation for the ellipse follows from the condition $\sqrt{12.2^2\zeta_0^2 + \eta_0^2} = T_0$, or

$$\frac{\zeta_0^2}{(T_0/12.2)^2} + \frac{\eta_0^2}{T_0^2} = 1.$$

Let's specify $T_0 = 0.01$; $\zeta_0 = \eta_0 = 0.01$.

The ellipse of immobility for given T_0 and the trajectory of mass movement for the specified initial deflection are shown in Fig. 456.

198. The problem does not pose general difficulties. Naturally, the beam obtained by the described method will oscillate near its equilibrium state as an ordinary beam clamped at both ends, and the deflection h has no influence on its frequency.

Let's write the equation of movement of the elastic beam (Fig. 457)

$$EJy^{(IV)} = -\frac{q}{g}\frac{\partial^2 y}{\partial t^2},$$

where y is the deflection with respect to the equilibrium state.

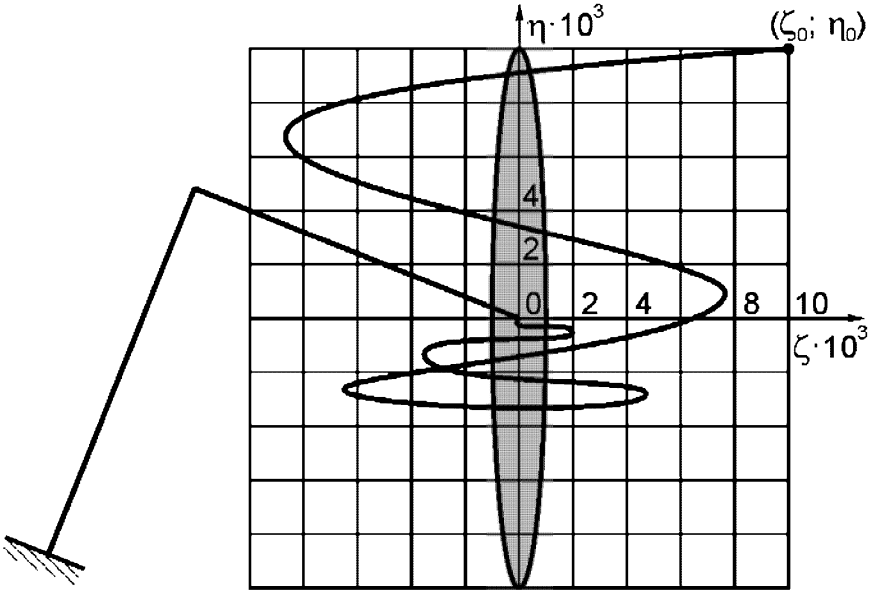

Fig. 456

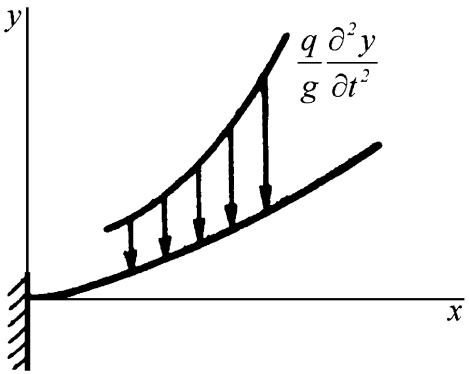

Fig. 457

Assuming $y = Y \sin \omega t$, we obtain

$$Y^{(IV)} - a^4 Y = 0 \ (a^4 = \frac{q\omega^2}{gEJ}),$$

whence

$$Y = A \sin ax + B \cos ax + C \sinh ax + D \cosh ax.$$

This function must satisfy the following boundary conditions:

at $x = 0$ $Y = 0$ and $Y' = 0$,

at $x = l$ $Y = 0$ and $Y' = 0$.

Equating to zero the determinant of the obtained homogeneous system we arrive at the following transcendental equation:

$$\cos al \cosh al = 1.$$

From which $al = 4.73$ or $\omega = 4.73^2\sqrt{\dfrac{gEJ}{ql^4}}$.

Up to this point everything was done as usual. But in this problem the length l itself depends on q.

The shape of the beam deflection curve in its initial equilibrium state reads as a curve of the fourth order

$$y_0 = \frac{q}{EJ}(\frac{x^4}{24} + C_3x^3 + C_2x^2 + C_1x + C_0).$$

As y_0 and y_0' vanish at $x = 0$, then $C_0 = C_1 = 0$. At $x = l$ we have $y_0' = 0$ and $y_0'' = 0$. It yields

$$y_0 = \frac{q}{EJ}(\frac{x^4}{24} - \frac{lx^3}{9} + \frac{l^2x^2}{12}).$$

But at $x = l$ the deflection is equal to h. From which the length l is determined as:

$$l^4 = \frac{72EJh}{q}.$$

Now let's return to the relation for frequency in which we exclude l^4 :

$$\omega = \frac{4.73^2}{\sqrt{72}}\sqrt{\frac{g}{h}} = 2.63\sqrt{\frac{g}{h}}\,.$$

The vibration eigenfrequency of the beam constructed in such a way occurred to be neither dependent on mass of the beam nor on its rigidity, and is defined only by h.

These fact seems to be of great interest.

If we paraphrasing Gardner's sophism about interesting numbers [9] we can say that there are no uninteresting problems, since, otherwise, all known problems should be separated into two classes - interesting and uninteresting. But one can find among the uninteresting problems at least one most uninteresting, and it would force us to treat it with interest and transfer it into the class of interesting. Acting further by such a way we should come to the conclusion that there are no uninteresting problems among those known to us.

199. The described phenomenon is well known and in the last years was named "negativism". However, it would be useless to search for examples of such kind among conservative systems.

Recall that we call systems "conservative" if work done by forces is determined only by the initial and final system states and does not depend upon the way of transition from one state to another. Such systems loaded by gravitational forces are obvious examples of this type.

A system is nonconservative if the work done by forces depends on the type of transition from one state to another. Forward and backward transition in such systems can be chosen in such a way that in case of a closed cycle (deflection and returning to initial state) useful work will be done. In any case the energy conservation principle is not broken here. It is clear that the energy is taken from the sources which are related to the external forces. For example, if forces arise due to hydro- or aerodynamic flow, then the kinetic energy of flow partially transforms into work done during the cycle of system deflection and returning to its initial state.

Let's consider the simplest model illustrating the difference between conservative and nonconservative systems.

Two rigid rods are joined by a hinge (Fig. 458a). Elastic springs holding the rods in vertical position are installed on hinges.

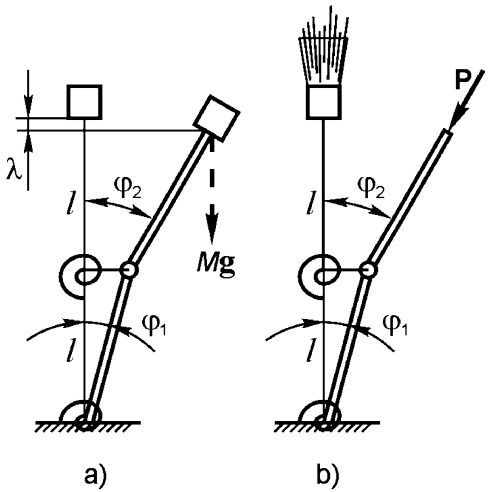

Fig. 458

If at the free end of the upper rod a weight of mass M is applied, then by deviation of the system from its vertical state the force Mg produces work:

$$Mg\lambda = Mgl(2 - \cos\varphi_1 - \cos\varphi_2).$$

The main idea is that work is determined only by magnitudes of angles φ_1 and φ_2 and does not depend on the consequences of their changing.

Now let us consider a nonconservative system. We change the method of loading. Let's suppose that force P is produced by jet thrust of a rocket engine, installed at the end of the rod (Fig. 458b). During rotation of the upper rod the force is always directed along its axis.

It is not possible to determine the work done by force P under the deflection of rods by the specified angles φ_1 and φ_2. Besides the quantities of angles φ_1 and φ_2 we must know in what way they have been changed until they have reached their final values.

Suppose, for example, that we turned both rods from their initial state by the same angle φ_1. Force P will turn but will not produce any work. Then let's turn the upper rod further to the magnitude of angle φ_2. The force P will turn but again it will not produce work. Thus, by the specified order of angular displacement the work done by force P is equal to zero.

Let's consider another consequence of loading. Let's turn only the lower rod by the angle φ_1, and leave the upper rod vertical. The force P will produce work through the distance $l(1-\cos\varphi_1)$. Now let's turn the upper rod by angle φ_2. The force will turn but again it will not produce any work. Thus total work is equal to $Pl(1-\cos\varphi_1)$.

By combining the order of angle change for the transition to the specified state φ_1, φ_2 we can obtain the work done by force P, not only the positive but the negative as well. For this purpose it is sufficient, for example, to turn the upper rod by angle $\varphi_2 - \varphi_1$, and then turn both rods by the angle φ_1.

Now let's consider the example of negativism.

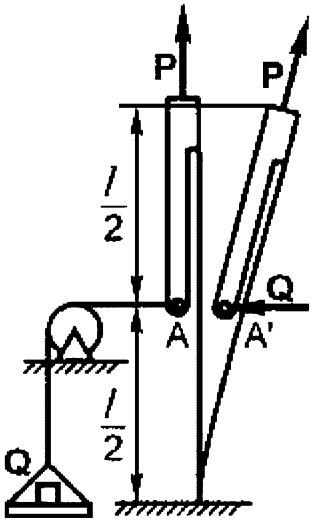

Fig. 459

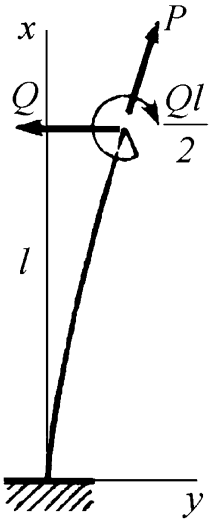

Fig. 460

The elastic rod is stretched (stretched !) by the follower force P (Fig. 459). A rigid lever of length $l/2$ is attached to the rod's end. The end of the lever can be loaded by force Q. We apply the weight Q at the bowl and under its action point A moves to the state A', and weight, contrary to expectations, does not move down but moves up. But that is possible only under certain conditions. Let's determine these.

At first, the differential equation of the rod deflection curve needs to be written. Beforehand, the force Q and its moment are brought to the end of the rod (Fig. 460)

$$EJy'' = Py + M(x),$$

where $M(x)$ means the bending moment due to force Q and horizontal component of force P. As $M(x)$ is linear along x, it is more convenient to rewrite the equation as follows

$$y^{(IV)} - k^2 y'' = 0 \qquad (k^2 = P/(EJ)).$$

Its solution will be

$$y = A \sinh kx + B \cosh kx + Cx + D.$$

For $x = 0$ function $y = 0$ and $y' = 0$. Then

$$y = A(\sinh kx - kx) + B(\cosh kx - 1).$$

Now we should satisfy the boundary conditions at the rod's end. For $x = l$

$$EJy'' = Ql/2, \quad EJy'' = Q.$$

Now we can determine constants A and B

$$A = \frac{Q}{kP}(\cosh kl - \frac{kl}{2}\sinh kl), \quad B = \frac{Q}{kP}(\frac{kl}{2}\cosh kl - \sinh kl).$$

Let's derive the deflection

$$AA' = y_{x=l} - \frac{l}{2} y'_{x=l}.$$

After easy transformations we get

$$AA' = \frac{Ql}{P}\left[\left(\frac{1}{kl} + \frac{kl}{4}\right)\sinh kl - \cosh kl\right].$$

The condition of negativism is $AA' > 0$ or

$$(\frac{1}{kl} + \frac{kl}{4})\tanh kl > 1.$$

It is satisfied for $kl > 2.4$ or $P > 5.76EJ/l^2$.

It would not be out of place to give one more example of negativism [17] (Fig. 461).

The compressive follower force P and moment M are applied to the free end of the clamped rod. If force $P < \pi^2 EJ/l^2$, the system behaves "naturally": the end cross-section rotates towards the direction of moment action. But under $P > \pi^2 EJ/l^2$, negativism occurs and the end cross-section rotates against the moment.

200. Assume that the cylinder turned inside-out has its original shape, i.e. the shape of a cylinder of radius R. Let's analyze stresses which will appear in it under this condition.

The relative elongation in circumferential direction for layers that are at a distance z from the median surface (Fig. 462) will be determined by change of the cylinder curvature from $1/R$ to $-1/R$.

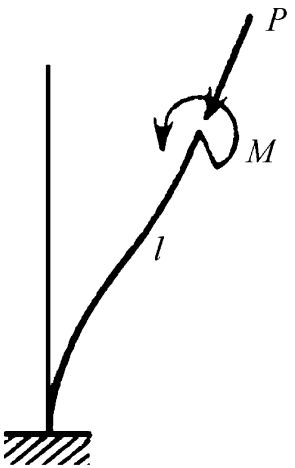

Fig. 461

If the length of the fibre in element $d\varphi$ before deformation (Fig. 462) was

$$(R+z)d\varphi,$$

then for the cylinder turned inside-out it will be

$$(R-z)d\varphi.$$

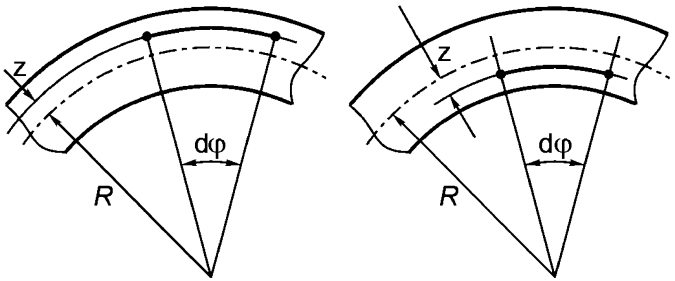

Fig. 462

The relative elongation in circumferential direction will be

$$\varepsilon_t = \frac{(R-z)d\varphi - (R+z)d\varphi}{(R+z)d\varphi} \approx -z\frac{2}{R}.$$

The relative elongation in axial direction ε_x is equal to zero. Hence, we obtain

$$\sigma_t = \frac{E}{1-\mu^2}(\varepsilon_t + \mu\varepsilon_x) = -\frac{zE}{1-\mu^2}\frac{2}{R},$$

$$\sigma_x = \frac{E}{1-\mu^2}(\varepsilon_x + \mu\varepsilon_t) = -\mu\frac{zE}{1-\mu^2}\frac{2}{R}.$$

Thus, we come to the conclusion, that in order to preserve its cylindrical shape for the inside-out cylinder, it is necessary to apply at its ends the stresses σ_x, shown in Fig. 463.

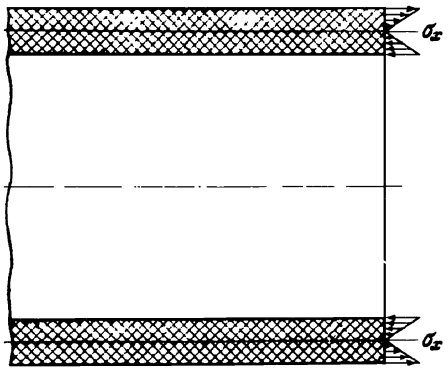

Fig. 463

Obviously, the actual shape of the inside-out cylinder will be just the same as the cylinder would have being loaded at its ends by the reverse system of forces (Fig. 464). The resultant moment M of stresses σ_x at unit arc length of the section contour will be as follows

$$M = -\int_{-h/2}^{h/2} \sigma_x z\, dz = \mu \frac{Eh^3}{12(1-\mu^2)} \frac{2}{R}.$$

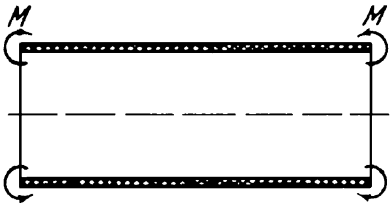

Fig. 464

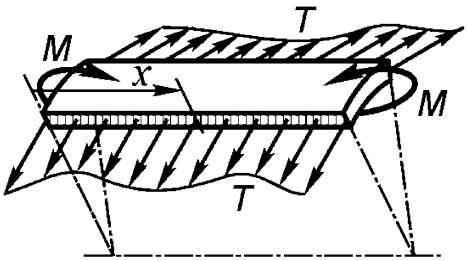

Fig. 465

Let's separate a strip of unit width from the cylinder by two axial sections, as it is shown in Fig. 465. We can consider the strip as a beam on elastic foundation, because the radial component of forces T, acting upon the strip from neighbouring parts of the shell, is proportional to the deflection of the strip w.

Force T per unit length becomes

$$T = \frac{w}{R} Eh,$$

and its radial component is

$$q = -\frac{T}{R} = -\frac{w}{R^2} Eh.$$

The negative sign of q is taken because the load is directed opposite to the deflection. But

$$\frac{EJ}{1-\mu^2}\,w^{(IV)} = q = -\frac{w}{R^2}Eh,$$

where

$$\frac{EJ}{1-\mu^2} = \frac{Eh^3}{12(1-\mu^2)}$$

is the strip rigidity under the constrained bending. Then we have

$$w^{(IV)} + 4k^4 w = 0, \qquad 4k^4 = \frac{12(1-\mu^2)}{R^2h^2}.$$

Solving the equation, we get

$$w = (A\sin kx + B\cos kx)\exp(-kx) + (C\sin kx + D\cos kx)\exp(+kx).$$

As the cylinder is long enough, we can restrict ourselves to analyzing the deflections in the region of a single contour. Discarding the increasing part of the solution, i.e. assuming $C = D = 0$, we obtain

$$w = (A\sin kx + B\cos kx)\exp(-kx).$$

Constants A and B are determined from the conditions:

$$\text{at } x = 0 \qquad M_b = \frac{EJ}{1-\mu^2}\,w'' = M,$$

$$\text{at } x = 0 \qquad Q = M_b' = 0 \qquad (w''' = 0),$$

or

$$\frac{Eh^3}{12(1-\mu^2)}2k^2A = \mu\frac{Eh^3}{12(1-\mu^2)}\frac{2}{R}, \quad A + B = 0,$$

whence

$$A = -B = -\frac{\mu}{k^2R},$$

$$w = \frac{\mu}{k^2R}\exp(-kx)(\cos kx - \sin kx), \qquad w_{\max} = w\,|_{x=0} = \frac{\mu}{k^2R}.$$

But as

$$k^2 = \frac{\sqrt{3(1-\mu^2)}}{Rh},$$

then

$$w_{\max} = \frac{\mu h}{\sqrt{3(1-\mu^2)}}.$$

For $\mu = 1/2$

$$w_{\max} = h/3.$$

The exaggerated shape of the inside-out cylinder is shown in Fig. 466.

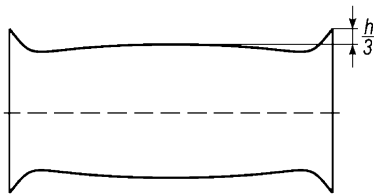

Fig. 466

201. Let's find the roots of the characteristic equation

$$\alpha^4 - \frac{h\sigma_x}{D}\alpha^2 + 4k^4 = 0.$$

Solving it we get

$$\alpha^2 = \frac{h\sigma_x}{2D} \pm \sqrt{\left(\frac{h\sigma_x}{2D}\right)^2 - 4k^4}.$$

The summand specified in the problem set can be neglected in case

$$\frac{h\sigma_x}{2D} << 2k^2,$$

which after substitution of values D and k arrives at the condition

$$\sigma_x << \frac{E}{\sqrt{3(1-\mu^2)}}\frac{h}{R}.$$

It is easy to establish that this condition is not always valid in many practical problems. That is why we should not forget this circumstance while analyzing the boundary effect.

In case of extremely small thickness, i.e. for shells with negligibly small bending rigidity (soft shells), the boundary effect can be studied only if we consider the component containing the second derivative of w. In this equation (1) (see the problem set) limit transfer is possible. Multiplying all members of the equation by D and equating it to zero, we arrive at

$$w'' - \beta^2 w = -\frac{p}{h\sigma_x} + \frac{\mu}{R},$$

where $\beta^2 = \dfrac{E}{R^2\sigma_x}$.

This yields

$$w = A\exp(-\beta x) + B\exp(+\beta x) + \frac{1}{\beta^2}\left(\frac{p}{h\sigma_x} - \frac{\mu}{R}\right).$$

If we discard the increasing part of w and determine A in such a way that at $x = 0$ the variable w vanishes, we obtain

$$w = R\left(\frac{pR}{Eh} - \mu\frac{\sigma_x}{E}\right)(1 - \exp(-\beta x)).$$

The damping rate is defined by the value β.

202. Let's consider the problem by suggesting that no forces are applied to the exit (closure) loop (Fig. 180, on the right). It is natural to assume that at distance l the angle of twisting β remains constant, and uniformly distributed load of intensity q appears between strands at the same segment. A similar situation was encountered for problem 126. The line of contact is straight, and the axial line of each strand is a helical curve having a radius that is equal to the radius of the strand cross-section.

Thus, the twist represents two equally inscribed helical curves within each other. Naturally, they can coincide only within certain geometric limits. In other words, each rod bent by a helical curve must reserve free space for another one.

At an arbitrarily chosen contact point A (Fig. 467) the surface of each rod bent in helical fashion has a negative Gaussian curvature. The first principal line of curvature S_1 represents the circle of radius R. The radius of the second principal line of curvature S_2 is defined by the difference:

$$\rho(S_2) = R/\sin^2\beta - R,$$

where the first component at the right-hand side is the radius of the curvature of the rod's central helical curve. Thus, $\rho(S_2) = R/\tan^2\beta$.

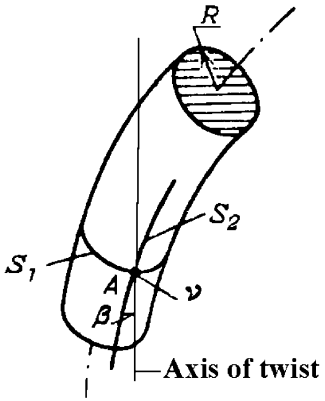

Fig. 467

The normal ν at point A is simultaneously the surface normal of the second spiral rod, and the sequence of contact points A forms the axis of the twist. This is the vertical straight line, shown in Fig. 467.

It is not difficult to understand that the second rod will fit in the aperture formed by the first one only in case that the curvature of curve S_1 is greater than the curvature of S_2, i.e. if $\beta < 45^0$. This is the existence condition of the contact between the rods along the common straight line – the axis of twist.

The above can also be interpreted slightly differently. Let's imagine that we have cut the twist by the plane perpendicular to its axis. In the section we obtain neighbour cross-sections of two twisted rods. These will be two contacting circles if $\beta = 0$ (Fig. 468a).

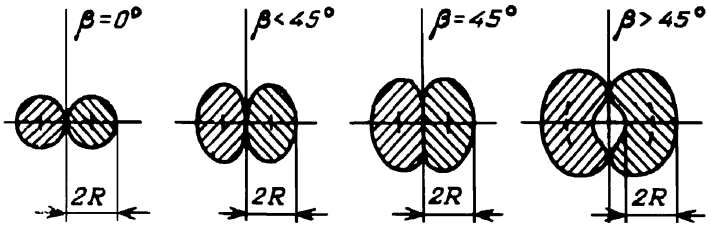

Fig. 468

As twist angle increases the two osculating circles are transformed into two sections that appear like ellipses (Fig. 468b). For $\beta = 45^0$ their curvature in the point of contact (Fig. 468c) vanishes, and for $\beta > 45^0$ the two-thread spring of compact coiling is formed by the twin, and its cross-section is shown in Fig. 468d.

Let's assume that $\beta < 45^0$ and cut the twin by the cross-section common for the two strands. The internal forces in this common section are self-balanced, and their resultant is reduced to moments M_1 and M_2 and force Q_1 (Fig. 469).

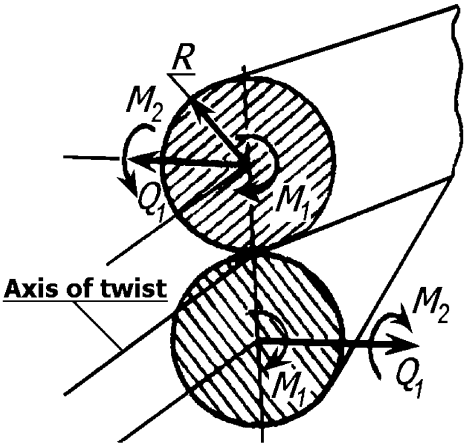

Fig. 469

The moments M_1 and M_2 are neither torque nor bending. They arise in sections that are not perpendicular to the strands' axis.

It follows from the equilibrium condition that

$$Q_1 R = M_1. \tag{1}$$

Let's plot the imaginary cylindric surface of radius R with the axis coinciding with the axis of the twin (Fig. 470). The deflection curve of each of the two strands will occur on the cylinder surface as a helical line. At the initial reference point of x the moments M_1 and M_2 are applied, their vectors are shown in Fig. 470 together with force Q_1. Moreover, the contact load of intensity q appears in radial direction of the built cylinder.

Now it is necessary to select such values of M_1, M_2, Q_1 and q so that at an arbitrarily chosen point B (Fig. 470) moments M_1, M_2 and force Q_1 are the same as at point O, independent of x and φ.

Let's choose x_1, y_1, z_1 as a moving coordinate system with origin at point B. The component of forces in x_1 axis direction is equal to zero, because Q_1 and q are perpendicular to the axis x_1. The components in axes y_1 and z_1 direction are as follows

$$Y_{1B} = -Q_1 \cos\varphi - \int_0^x q \sin(\varphi - \psi) d\zeta,$$

$$Z_{1B} = -Q_1 \sin\varphi + \int_0^x q \cos(\varphi - \psi) d\zeta;$$

ψ and ζ are connected by the obvious relation:

$$\zeta = R\psi \cot\beta, \quad d\zeta = R \cot\beta \, d\psi.$$

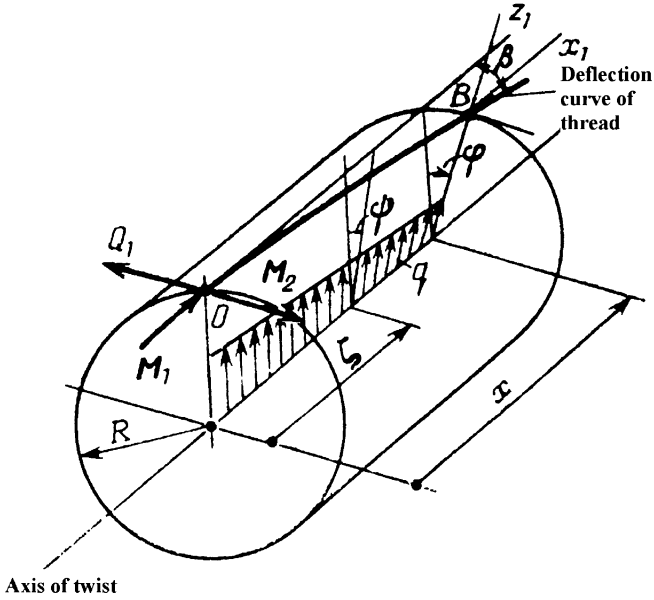

Fig. 470

If we eliminate $d\zeta$ after integration we obtain

$$Y_{1B} = -Q_1 \cos\varphi - qR \cot\beta (1 - \cos\varphi),$$

$$Z_{1B} = -Q_1 \sin\varphi + qR \cot\beta \sin\varphi.$$

The component along the y_1 axis must equal $-Q_1$, and the component along the z_1 axis vanishes. Both conditions are valid if

$$Q_1 = qR \cot\beta. \tag{2}$$

Now let's find the components of moment by axes x_1, y_1, and z_1

$$M_{Bx_1} = M_1 - Q_1 R(1-\cos\varphi) + \int_0^x qR\sin(\varphi-\psi)d\zeta,$$

$$M_{By_1} = M_2\cos\varphi + Q_1 x\sin\varphi - \int_0^x q(x-\zeta)\cos(\varphi-\psi)d\zeta,$$

$$M_{Bz_1} = M_2\sin\varphi - Q_1 x\cos\varphi - \int_0^x q(x-\zeta)\sin(\varphi-\psi)d\zeta.$$

Expressing ζ through ψ and by integration we arrive at

$$M_{Bx_1} = M_1 - Q_1 R(1-\cos\varphi) + qR^2\cot\beta(1-\cos\varphi),$$

$$M_{By_1} = M_2\cos\varphi + Q_1 x\sin\varphi - qR\cot\beta[x\sin\varphi - R(1-\cos\varphi)\cot\beta],$$

$$M_{Bz_1} = M_2\sin\varphi - Q_1 x\cos\varphi - qR\cot\beta(-x\cos\varphi + R\sin\varphi\cot\beta).$$

But M_{Bx_1} must be equal to M_1; $M_{By_1} = M_2$, and M_{Bz_1} must be equal to zero independent of x and φ. It is easy to establish that these requirements are fulfilled if in addition to condition (2) one more will be ensured:

$$M_2 = qR^2\cot^2\beta. \tag{3}$$

Now, after analyzing the section normal to the twin axis let's consider the sections normal to the strands' axes and determine the bending moment M_b and torque M_t (Fig. 471), and also tensile N and shear Q forces.

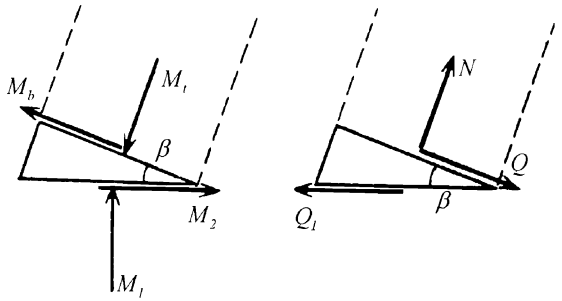

Fig. 471

It is obvious from the equilibrium conditions that

$$M_b = M_2\cos\beta - M_1\sin\beta;$$

$$M_t = M_1\cos\beta + M_2\sin\beta,$$

$$Q = Q_1\cos\beta, \qquad N = Q_1\sin\beta.$$

Using the relations (1)-(3) we obtain

$$\begin{aligned} M_b &= q_0 R^2(\cot^2\beta - 1), \\ M_t &= 2q_0 R^2 \cot\beta, \\ Q &= q_0 R \cot\beta, \\ N &= q_0 R, \end{aligned} \tag{4}$$

where q_0 is contact load, brought to the axial line of the strand:

$$q_0 = q\cos\beta.$$

On the other hand, the bending moment is related with the curvature variation, and torque is related with the twist of the rod. Then we have

$$M_b = EJ\frac{\sin^2\beta}{R}, \qquad M_t = GJ_p\frac{\sin\beta\cos\beta}{R}. \tag{5}$$

Here EJ is bending rigidity, GJ_p is torsional rigidity, $\sin^2\beta/R$ is the curvature of the helical line and $\sin\beta\cos\beta/R$ its twist.

Let's substitute here M_b and M_t from (4) and after eliminating q_0, we obtain

$$\tan\beta = \frac{1}{\sqrt{2e+1}}, \tag{6}$$

where $e = EJ/(GJ_p)$. For tubular or solid circular sections $e = 1+\mu$ (μ is Poisson's ratio). If $\mu = 0.5$, then $\beta \approx 26.6^0$.

Substituting β from (6) into the relations (5) and (4), we derive[1]

$$\begin{aligned} M_b &= \frac{EJ}{2R}\frac{1}{e+1}, \quad M_t = \frac{GJ_p}{2R}\frac{\sqrt{2e+1}}{e+1}, \\ q_0 &= \frac{GJ_p}{4R^3}\frac{1}{e+1}, \quad N = \frac{GJ_p}{4R^2}\frac{1}{e+1}, \\ Q &= \frac{GJ_p}{4R^2}\frac{\sqrt{2e+1}}{e+1}. \end{aligned}$$

203. It follows from the equilibrium conditions that

$$m\omega^2(l+u) = P = f(u).$$

We solve the equation in u graphically (Fig. 472). The points of straight line $m\omega^2(l+u)$ intersection with curve $P = f(u)$ are the roots of the equation. Drawing several straight lines we determine the dependence of $m\omega^2 l$ in u (Fig. 472).

For $m\omega^2 l = 1.0$ the ball changes its position stepwise by moving from the point that is characterized by the displacement magnitude $u = 1.8$ to the point $u = 7$. The reverse change occurs under $m\omega^2 l = 0.8$.

It is clear that the direct jump can occur also at $m\omega^2 l < 1.0$ (but greater than 0.8), if only a sufficiently large deviation is applied to the ball.

[1] See also [8].

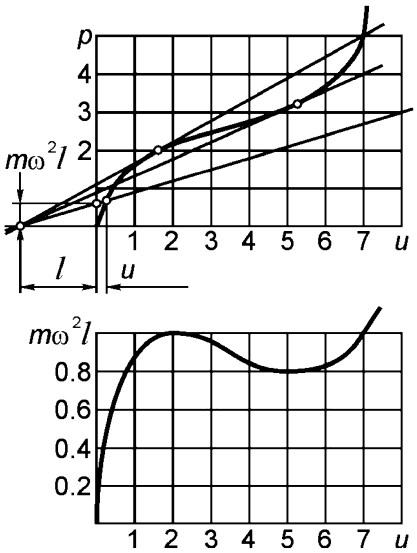

Fig. 472

204. The height of point O location of the deformed system above the horizontal plane will be $H - w$. Then the slope angle of rods with respect to the horizon will be

$$\alpha = \frac{H - w}{l}.$$

We denote compressive force as in rods N, then from the equilibrium conditions obviously follows

$$P = 3N\alpha = 3N\frac{H - w}{l}.$$

On the other hand, force N is defined by the value of each rod shortening

$$N = \frac{EA\Delta l}{l}.$$

From the purely geometric considerations (Fig. 473) we express Δl through w as

$$\Delta l = l - l\,\frac{\cos\alpha_0}{\cos\alpha}.$$

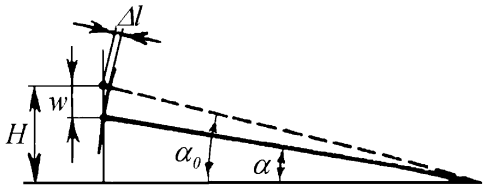

Fig. 473

As angles α_0 and α are small we arrive at

$$\Delta l \approx l \left[\frac{1 - \frac{\alpha_0^2}{2}}{1 - \frac{\alpha^2}{2}} \right] = \frac{l}{2}(\alpha_0^2 - \alpha^2).$$

Substituting α_0 and α we obtain

$$\Delta l = \frac{w}{l}(H - \frac{w}{2}).$$

Then force N will be

$$N = \frac{EA}{l^2} w(H - \frac{w}{2}).$$

Finally force P will be expressed as follows

$$P = \frac{3EA}{l^3} w(H - w)(H - \frac{w}{2}).$$

The obtained relation can be rewritten in dimensionless form

$$\frac{Pl^3}{3EAH^3} = \frac{w}{H}(1 - \frac{w}{H})(1 - \frac{1}{2}\frac{w}{H})$$

and plotted as the curve presented in Fig. 474.

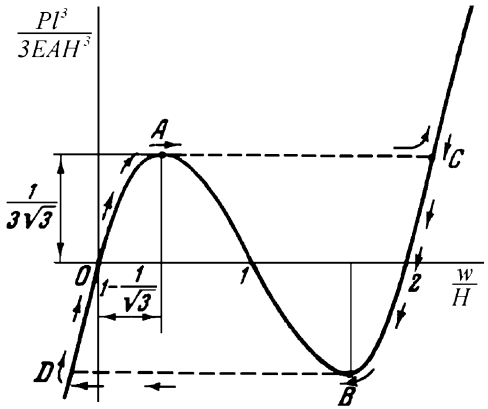

Fig. 474

The curve has two extremal points A and B. In the first segment OA the deflection increases simultaneously with the load growth. When force P reaches the magnitude corresponding to the first extremum, the deflection changes stepwise (AC as it is shown by arrows). Under further increase of load the deflection w continues to increase. If we now unload the system then rods will take their free state under the deflection $w/H = 2$, i.e. the nodal point of rods will occur below the immovable horizontal plane by value H. Applying a load of opposite sign we may cause the reverse jump of the system BD and return it to its initial state.

The segment AB of the curve corresponds to unstable equilibrium states. Thus, for values of force P laying between two extrema (Fig. 474)

$$-\frac{1}{\sqrt{3}}\frac{EAH^3}{l^3} < P < +\frac{1}{\sqrt{3}}\frac{EAH^3}{l^3},$$

the system has three equilibrium states: two of them are stable and the third one, intermediate, is unstable.

Particularly, at $P = 0$ this unstable state corresponds to the position of rods in a horizontal plane ($w/H = 1$). Under the slightest deviation of rods with respect to this disposition the system will take either the upper or lower position.

205. Let's suppose that under the load action the rectangular cross-section is not deformed and rotates by angle φ about some point O, disposed at distance c from the axis of rotation (Fig. 475).

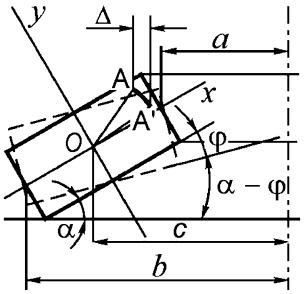

Fig. 475

Let's consider point A with coordinates x and y in a section of the spring. After cross-section rotation the point will take a new position A' that is closer to the axis of symmetry by

$$\Delta = [x\cos(\alpha-\varphi) - y\sin(\alpha-\varphi)] - [x\cos\alpha - y\sin\alpha].$$

As angles α and β are small we can write:

$$\cos\alpha \approx 1 - \frac{1}{2}\alpha^2, \qquad \sin\alpha \approx \alpha;$$

$$\cos(\alpha-\varphi) \approx 1 - \frac{1}{2}(\alpha-\varphi)^2, \qquad \sin(\alpha-\varphi) \approx (\alpha-\varphi),$$

and then we obtain

$$\Delta = x\varphi(\alpha - \frac{\varphi}{2}) + y\varphi.$$

The circumferential relative elongation corresponding to the displacement Δ will be

$$\varepsilon_t = \frac{\Delta}{c - x\cos\alpha + y\sin\alpha} \approx \frac{\Delta}{c-x},$$

$$\varepsilon_t = \frac{x\varphi\,(\alpha - \varphi/2) + y\varphi}{c - x}.$$

Stress σ_t is equal to $\sigma_t = E\varepsilon_t$.

Now let's determine normal force in the axial section of the spring

$$N = \int\limits_{c-b}^{c-a}\int\limits_{-h/2}^{+h/2} \sigma_t\, dx\, dy.$$

Substituting the expression for σ_t obtained above we have

$$N = E\int\limits_{c-b}^{c-a}\int\limits_{-h/2}^{+h/2} \frac{x\varphi(\alpha - \frac{\varphi}{2}) + y\varphi}{c - x}\, dx\, dy$$

$$= Eh\varphi(\alpha - \frac{\varphi}{2})(a - b + c\ln\frac{b}{a}).$$

But considering the equilibrium conditions for one-half of the ring (Fig. 476) we make sure that $N = 0$. From this condition we find

$$c = \frac{b - a}{\ln(b/a)}.$$

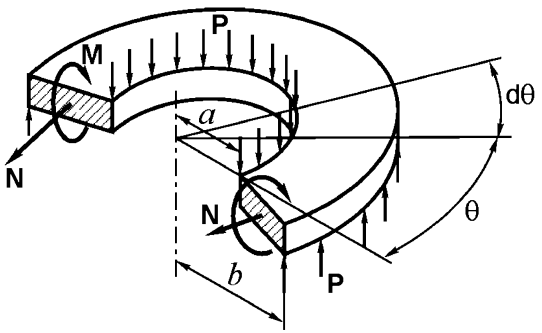

Fig. 476

Now let's find moment M

$$M = \int\limits_{c-b}^{c-a}\int\limits_{-h/2}^{+h/2} \sigma_t\,[x\sin(\alpha - \varphi) + y\cos(\alpha - \varphi)]\, dx\, dy,$$

$$M = E\int\limits_{c-b}^{c-a}\int\limits_{-h/2}^{+h/2} \frac{x\varphi(\alpha - \varphi/2) + y\varphi}{c - x}\,[x(\alpha - \varphi) + y]\, dx\, dy,$$

$$M = Eh\left[\varphi(\alpha - \frac{\varphi}{2})(\alpha - \varphi)\left(\frac{b^2}{2} - \frac{a^2}{2} + 2ca - 2cb + c^2\ln\frac{b}{a}\right) + h^2\varphi\ln\frac{b}{a}\right].$$

On the other hand, it follows from the equilibrium condition for the one–half ring (Fig. 476), that

$$2M = \int_0^{\pi} \frac{P}{2\pi b} b^2 \sin\theta d\theta - \int_0^{\pi} \frac{P}{2\pi a} a^2 \sin\theta d\theta, \quad M = \frac{P}{2\pi}(b-a).$$

Thus we arrive at

$$\frac{P}{2\pi}(b-a) = Eh\varphi[\left(\alpha - \frac{\varphi}{2}\right)(\alpha-\varphi) \times \left(\frac{b^2}{2} - \frac{a^2}{2} + 2ca - 2cb + c^2 \ln\frac{b}{a}\right) + \frac{h^2}{12}\varphi \ln\frac{b}{a}]$$

If we eliminate c from the relation and substitute $H/(b-a)$ and $w/(b-a)$, where w is the spring deflection, instead of α and φ correspondingly we get

$$P = \frac{2\pi Eh}{(b-a)^2} w \left[(H - \frac{w}{2})(H-w)(\frac{1}{2}\frac{b+a}{b-a} - \frac{1}{\ln\frac{b}{a}}) + \frac{h^2}{12}\ln\frac{b}{a}\right].$$

By direct numeric calculation it is possible to establish that for $1 < b/a < 4$ the following relation is valid

$$\frac{1}{2}\frac{b+a}{b-a} - \frac{1}{\ln\frac{b}{a}} \approx \frac{1}{12}\ln\frac{b}{a}.$$

Therefore

$$P = \frac{\pi Eh}{6(b-a)^2} w \ln\frac{b}{a}\left[\left(H - \frac{w}{2}\right)(H-w) + h^2\right].$$

The obtained relationship between force P and spring deflection w is nonlinear and depending on the ratio H/h can have different character.

Some curves of the dependence of P_0 on w/h

$$P_0 = P\frac{6(b-a)^2}{\pi Eh^4 \ln(b/a)}$$

are shown in Fig. 477 for different H/h, i.e.

$$P_0 = \frac{w}{h}\left[\left(\frac{H}{h} - \frac{1}{2}\frac{w}{h}\right)\left(\frac{H}{h} - \frac{w}{h}\right) + 1\right].$$

Let's analyze how the form of the spring characteristic $P_0 = f(w/h)$ changes depending on H/h. The curve corresponding to $H/h = 0$ represents a characteristic of the plane disk spring. The increase of height H causes first of all the increase of initial spring rigidity and then the disruption of curve monotonicity.

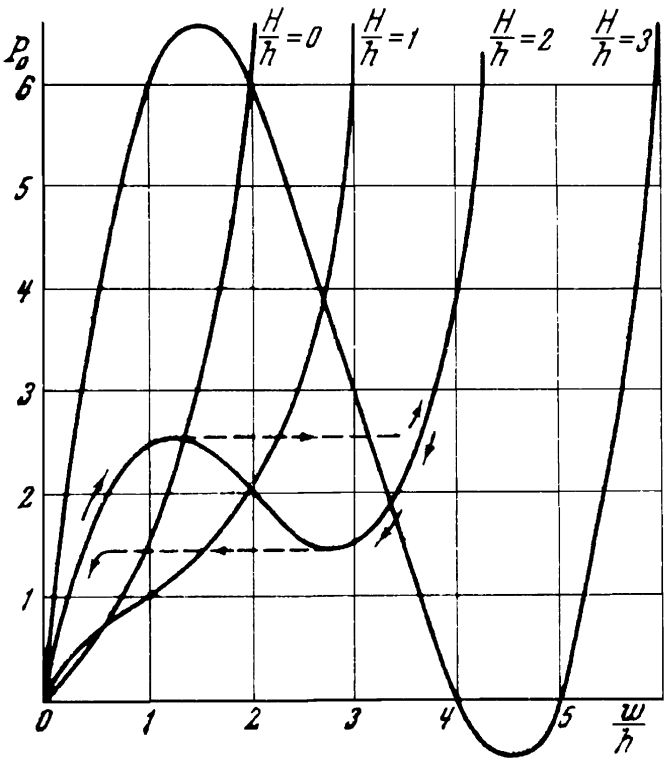

Fig. 477

For the value $H/h = \sqrt{2}$ (it is easy to determine from the analysis of the obtained relation) the segment with negative derivative between two extreme points appears in the characteristic of the spring. This segment may be called a segment of negative stiffness, because the increase of deflection in the given case occurs during the decrease of the load. Such a regime of spring operation is unstable, and forces corresponding to points of extrema will be critical for the given spring. Since the force reaches its first extremum, the spring will stepwise change its deflection omitting the unstable region. Further operation will follow the right stable increasing part of the characteristic. Unloading of the spring will cause the reverse jump of the deflection, corresponding to the second critical force.

Further increase of spring height H gives, as shown in Fig. 477, even greater distortion of the characteristic and for $H/h > 2\sqrt{2}$ the last one begins to intersect the abscissa axis. Hence, under the force $P = 0$ the spring has three forms of equilibrium, two of which are stable and the third one – intermediate – being unstable. Such a spring after clicking out and unloading does not return to its initial state and keeps the residual deflection, corresponding to the point of curve intersection with the abscissa axis.

Compare the solutions of this problem with those of problem 204.

206. Let's consider the equilibrium condition of the tube in the deviated state (Fig. 478).

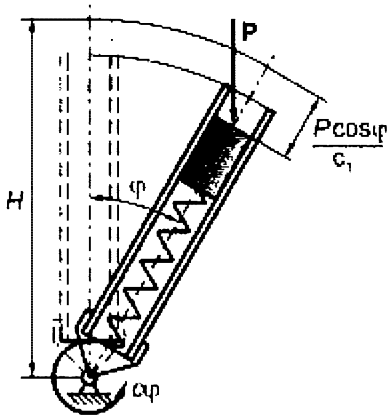

Fig. 478

If we denote the distance from the upper edge of the piston to the hinge at the beginning of loading as H, then, obviously, we have

$$P(H - \frac{P\cos\varphi}{c_1})\sin\varphi = c\varphi, \tag{1}$$

from which we obtain

$$\frac{P}{Hc_1} = \frac{1}{2\cos\varphi}\left[1 \pm \sqrt{1 - \frac{4c}{c_1H^2}\varphi\cot\varphi}\right].$$

Let's denote:

$$\frac{P}{Hc_1} = p, \qquad \frac{4c}{c_1H^2} = \lambda. \tag{2}$$

Then we arrive at

$$p = \frac{1}{2\cos\varphi}\left[1 \pm \sqrt{1 - \lambda\varphi\cot\varphi}\right].$$

Under various λ the dependence p on φ has different character. This dependence is shown in Fig. 479 for values $\lambda = 0.5, 1.0$, and 1.2 under $0 \le \varphi \le \pi$. The obtained curves correspond to the equilibrium states, representing the deflected configuration with respect to vertical line. In addition, the vertical equilibrium state exists also (equation (1) is always satisfied at $\varphi = 0$). In Fig. 479 this equilibrium state is represented by points on the axis of ordinates. In case of $\lambda = 0.5$ and, in general, for all values of interval $0 < \lambda < 1$ the curves $p = p(\varphi)$ intersect the axis of ordinates at two points, the lower of which corresponds to the first critical value of parameter p. For $\lambda = 0.5$ $P_{cr} = 0.147$. In general,

$$P_{cr} = \frac{1}{2}(1 - \sqrt{1-\lambda}), \text{ or } P_{cr} = \frac{Hc_1}{2}\left[1 - \sqrt{1 - \frac{4c}{c_1H^2}}\right].$$

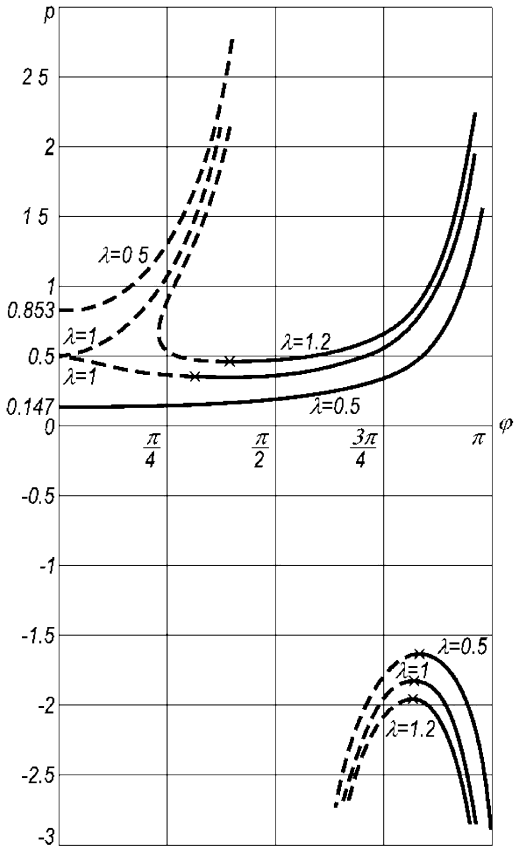

Fig. 479

Now we must analyze the stability of the specified equilibrium states. The criterion of equilibrium state stability is the condition of total potential energy minimum

$$U = \frac{c\varphi^2}{2} + \frac{c_1\Delta^2}{2} + P(H - \Delta)\cos\varphi.$$

The first two components of the relation are the strain energy, and the last one is the variation of external force P potential. As $\Delta = (P\cos\varphi)/c_1$, we obtain

$$U = \frac{c\varphi^2}{2} + PH\cos\varphi - \frac{P^2\cos^2\varphi}{2c_1}.$$

The condition $dU/d\varphi = 0$ is the equilibrium condition (condition of energy extremum), and as it should be expected, it is the same as obtained earlier in equation (1). The condition of energy minimum can be written as

$$\frac{d^2U}{d\varphi^2} > 0,$$

or

$$c - PH\cos\varphi + \frac{P^2}{c_1}\cos 2\varphi > 0.$$

According to the relations (2) we have

$$\frac{\lambda}{4} - p\cos\varphi + p^2\cos^2 2\varphi > 0.$$

Analyzing the obtained curves we notice that some segments of these curves satisfy the stability condition and some of them not. In Fig. 479 the segments corresponding to unstable equilibrium are drawn by dashed lines. The stability condition for the axis of ordinates yields

$$\frac{\lambda}{4} - p + p^2 > 0,$$

whence we obtain

$$p < \frac{1}{2}(1 - \sqrt{1-\lambda}) \text{ and } p > \frac{1}{2}(1 + \sqrt{1-\lambda}).$$

For example, at $\lambda = 0.5$ the vertical state of the tube is unstable under the condition

$$0.853 > p > 0.147.$$

In Fig. 479 the increase of angle φ as a function of force P in case of $\lambda = 0.5$ is shown by arrows. At the beginning, the angle φ remains equal to zero. Under $p = 0.147$ the tube deflects from the vertical and further, as force P increases, the angle φ asymptotically verges towards the value $\varphi = \pi$. Under that for $\varphi > \pi/2$ the piston will be pulled from the tube by force P. In the real system the displacement of the piston and, therefore, the increase of force P also are restricted by tube length.

The plotted curves show that angle φ can also asymptotically verge towards the value $\pi/2$, for example, for case $\lambda = 0.5$ when $p > 0.853$. It means that for sufficiently large force the shortening of the spring, being in the tube, increases so much, and at the same time the arm of force P decreases so quickly, that the force is not able to turn the tube below the horizontal. For the limit at $\varphi = \pi/2$ the shortening of spring $(P\cos\varphi)/c_1$ is equal to H, which is easy to establish. However, these equilibrium states are unstable.

In case of $\lambda > 1$, i.e. for sufficiently great stiffness of the helical spring, or for sufficiently small height or stiffness of the second spring c_1, the vertical state of the tube remains stable under any value of load P, though deflected forms of tube equilibrium exist also. The tube will take such equilibrium state if certain external load imparts sufficiently great lateral deflection to it.

The branches of curves $p = p(\varphi)$ for negative values of p are plotted in Fig. 479 also. These curves show that for $\pi/2 \leq \varphi < \pi$ the tube can have an equilibrium state under force of another sign. It is easy to imagine this type of equilibrium if we consider that theoretically the piston can move in the

tube by values greater than H. For $\Delta > H$ force P having another sign will hold the tube in the specified state of equilibrium.

Thus we have considered the equilibrium states for $0 \le \varphi < \pi$. However, the whole variety of possible states is not exhausted by that. Analysis of this question could be continued by extending the area of angle φ variation beyond the limits of π to the right and beyond the limit of zero to the left.

The considered problem is an example of the simplest nonlinearity, where we can easily get full solution and visually show its multiple-valuedness. And in the general case, the solution of nonlinear problems is one of the most difficult and actual problems of contemporary mathematics and mechanics.

207. By reduced flexural rigidity here and in other similar cases we mean the coefficient of proportionality in the moment-curvature equation for bending:

$$\frac{1}{\rho} = \frac{M}{(EJ)_r}.$$

The most convenient way to determine it for the given example is the energy method.

Let's consider a structural cell of the rod by length $2a$ (Fig. 480). Forces of preliminary tightening in sections I and II are not shown.

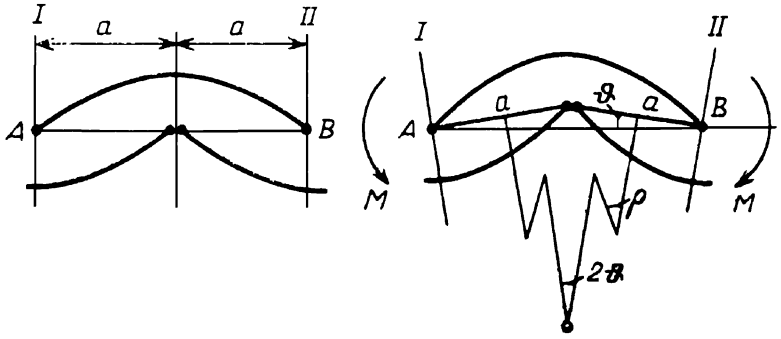

Fig. 480

If bending moment M is applied to the section, then the initially straight thread will take the form of a broken line, which is one of a series of regular polygon sides. Points A and B will come closer by value $2a\vartheta^2/2$, and the potential energy of the upper bent rod will increase by $Sa\vartheta^2$. Two halves of the lower rod will obtain the same increment of energy. Thus

$$2Sa\vartheta^2 = M\frac{2\vartheta}{2},$$

where the right side of the equation represents the work of moments M done at the reciprocal angular displacement of sections I and II .

As radius ρ of thread curvature we, naturally, take the apothem formed by the thread polygon: $\rho = \dfrac{a}{2\vartheta}$. Excluding ϑ we find

$$\frac{1}{\rho} = \frac{M}{Sa^2}, \qquad (EJ)_r = Sa^2.$$

208. If we consider the spokes as a continuous elastic medium, then for any point of the rim the force acting from the side of the spokes will be proportional to radial displacement w of the corresponding point of the rim. Thus we have a problem of the ring based on elastic foundation analysis. The $n/(2\pi R)$ spokes fall per unit of rim length. The force $\dfrac{EA}{l}w$ acts from the direction of each spoke on the rim, where l is the length of spoke ($l \approx R$), and A is area of spoke cross-section.

Thus, the force acting on unit of rim length is equal

$$\frac{EAN}{2\pi R^2}w = kw,$$

from which

$$k = \frac{EAn}{2\pi R^2}. \tag{1}$$

Now let's derive a differential equation of the ring deflection curve. The angle φ referred to the top of the ring we choose as an independent variable (Fig. 481).

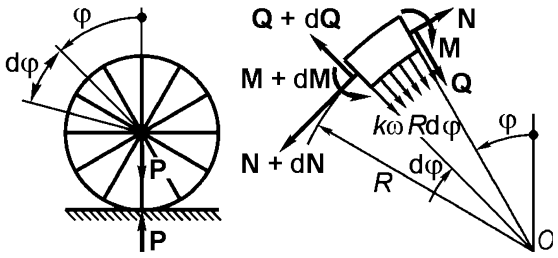

Fig. 481

Let's separate from the ring an elementary segment of length $R\,d\varphi$ and apply the internal forces N, Q and M to its cross-sections. The force $kwR\,d\varphi$ will act from the side of the spokes on this segment. Consider the equilibrium of the elementary segment. If we balance all forces in the radial direction we obtain

$$\frac{dQ}{d\varphi} = N + kRw.$$

It follows from the condition of equality to zero of all force projections onto the axis tangent to the circle arc that

$$\frac{dN}{d\varphi} + Q = 0.$$

Let's equate to zero the sum of moments of forces with respect to point O

$$R\frac{dN}{d\varphi} + \frac{dM}{d\varphi} = 0,$$

and eliminate Q and N from these equations. Then we arrive at

$$kR^2\frac{dw}{d\varphi} = \frac{dM}{d\varphi} + \frac{d^3M}{d\varphi^3}.$$

The curvature variation $\Delta(1/\rho)$ is related to the bending moment M by the following equation

$$M = EJ\Delta(\frac{1}{\rho}),$$

but we know that

$$\Delta\left(\frac{1}{\rho}\right) = -(\frac{w}{R^2} + \frac{1}{R^2}\frac{d^2w}{d\varphi^2}).$$

As for positive deflection w directed out of the circle center the curvature of the ring decreases, then at the right side of the relation we place a minus sign. The curvature variation in the relation consists of two terms. The first component w/R^2 corresponds to the curvature variation due to simple extension of the ring. The second component $\dfrac{1}{R^2}\dfrac{d^2w}{d\varphi^2}$ that is equal to d^2w/ds^2 represents an ordinary curvature variation the same as we had in straight beam bending.

Now after substitution of M the differential equation arrives at its final form

$$\frac{d^5w}{d\varphi^5} + 2\frac{d^3w}{d\varphi^3} + a^2\frac{dw}{d\varphi} = 0,$$

where

$$a^2 = \frac{R^4k}{EJ} + 1. \tag{2}$$

The solution of the equation is

$$w = C_0 + C_1\cosh\alpha\varphi\cos\beta\varphi + C_2\sinh\alpha\varphi\sin\beta\varphi + C_3\cosh\alpha\varphi\sin\beta\varphi + C_4\sinh\alpha\varphi\cos\beta\varphi,$$

where

$$\alpha = \sqrt{\frac{a-1}{2}}, \qquad \beta = \sqrt{\frac{a+1}{2}}. \tag{3}$$

Since the ring deforms symmetrically with respect to the vertical axis, the function w must be even, i.e. if we change the sign of φ from plus to minus

it must remain unchanged. That is why the arbitrary constants C_3 and C_4, staying near odd functions, are supposed to be equal to zero. The remaining constants are determined from the conditions:

$$a) \quad \text{at } \varphi = \pi, \qquad \frac{dw}{d\varphi} = 0,$$

$$b) \quad \text{at } \varphi = \pi, \qquad Q = -\frac{P}{2},$$

$$c) \quad \int_0^{\pi} w\, d\varphi = 0.$$

The latter condition means that under wheel loading the upper and the lower points remain in vertical line. Really, if we consider an element of the wheel rim before and after deformation (Fig. 482), then it is easy to establish that the condition of its inextensibility will be written as follows

$$dv + w\, d\varphi = 0,$$

where v is the displacement at a tangent to the arc of contour, or

$$v = -\int w d\varphi.$$

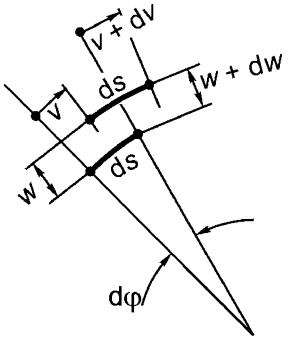

Fig. 482

As the displacement in tangent direction at points $\varphi = 0$ and $\varphi = \pi$ vanishes, then it yields the condition c).

If $C_3 = C_4 = 0$ the expression for bending moment yields

$$M = -\frac{EJ}{R^2}\left(w + \frac{d^2w}{d\varphi^2}\right)$$

and shear force

$$Q = \frac{1}{R}\frac{dM}{d\varphi}.$$

Thus we arrive at

$$M = -\frac{EJ}{R^2}(C_0 - 2\alpha\beta C_1 \sinh\alpha\varphi \sin\beta\varphi + 2\alpha\beta C_2 \cosh\alpha\varphi \cos\beta\varphi),$$

$$Q = 2\alpha\beta\frac{EJ}{R^2}[(\alpha C_1 + \beta C_2)\cosh\alpha\varphi \sin\beta\varphi + (\beta C_1 - \alpha C_2)\sinh\alpha\varphi \cos\beta\varphi].$$

Now if we expand the boundary conditions *a*), *b*), and *c*) we obtain

a) $C_1(\alpha \sinh\alpha\pi \cos\beta\pi - \beta\cosh\alpha\pi \sin\beta\pi)$

$+C_2(\beta\sinh\alpha\pi \cos\beta\pi + \alpha\cosh\alpha\pi \sin\beta\pi) = 0;$

b) $C_1(\alpha\cosh\alpha\pi \sin\beta\pi + \beta\sinh\alpha\pi \cos\beta\pi)$

$$-C_2(\alpha \sinh\alpha\pi \cos\beta\pi - \beta\cosh\alpha\pi \sin\beta\pi) = -\frac{P}{4EJ}\frac{R^3}{\alpha\beta},$$

c) $C_0\pi + \dfrac{C_1}{\alpha^2+\beta^2}(\alpha\sinh\alpha\pi \cos\beta\pi + \beta\cosh\alpha\pi \sin\beta\pi)$

$$+\frac{C_2}{\alpha^2+\beta^2}(\alpha\cosh\alpha\pi \sin\beta\pi - \beta\sinh\alpha\pi \cos\beta\pi) = 0.$$

After solution of these equations:

$$C_0 = \frac{PR^3}{2\pi a^2 EJ},$$

$$C_1 = -\frac{P}{4EJ}\frac{R^3}{\alpha\beta}\frac{\alpha\cosh\alpha\pi \sin\beta\pi + \beta\sinh\alpha\pi \cos\beta\pi}{a(\sinh^2\alpha\pi + \sin^2\beta\pi)},$$

$$C_2 = \frac{P}{4EJ}\frac{R^3}{\alpha\beta}\frac{\alpha\sinh\alpha\pi \cos\beta\pi - \beta\cosh\alpha\pi \sin\beta\pi}{a(\sinh^2\alpha\pi + \sin^2\beta\pi)}.$$

Finally the relations for w and M take the form

$$w = \frac{PR^3}{4\alpha\beta EJ}\left(\frac{2\alpha\beta}{\pi a^2} - A_1\cosh\alpha\varphi\cos\beta\varphi + B_1\sinh\alpha\varphi\sin\beta\varphi\right), \tag{4}$$

$$M = -\frac{PR}{2}\left(\frac{1}{\pi a^2} + A_1\sinh\alpha\varphi\sin\beta\varphi + B_1\cosh\alpha\varphi\cos\beta\varphi\right), \tag{5}$$

where for the sake of abbreviation we denote:

$$A_1 = \frac{\alpha\cosh\alpha\pi \sin\beta\pi + \beta\sinh\alpha\pi \cos\beta\pi}{a(\sinh^2\alpha\pi + \sin^2\beta\pi)},$$

$$B_1 = \frac{\alpha\sinh\alpha\pi \cos\beta\pi - \beta\cosh\alpha\pi \sin\beta\pi}{a(\sinh^2\alpha\pi + \sin^2\beta\pi)}. \tag{6}$$

The force, falling at one spoke, obviously, will be equal to

$$P_s = \frac{EA}{R}w. \tag{7}$$

Let's produce numerical calculations. From the relations (1) and (2) assuming that the moduli of elasticity of rim and spokes are equal, we obtain

$$a^2 = \frac{R^2 An}{2\pi J} + 1 = \frac{(\pi \cdot 0.2^2/4) \cdot 36 \cdot 31^2}{2\pi \cdot 0.3} + 1 = 577.7\,, \qquad a = 24.04\,.$$

Further according to (3) we calculate

$$\alpha = \sqrt{\frac{24.04 - 1}{2}} = 3.395\,, \qquad \beta = \sqrt{\frac{24.04 + 1}{2}} = 3.539\,.$$

Now we find

$$\sinh \alpha\pi \approx \cosh \alpha\pi \approx \frac{1}{2} \exp 10.66\,,$$

$$\sin \beta\pi = -0.992\,, \quad \cos \beta\pi = +0.1223\,.$$

According to (6), we have

$$A_1 = -0.245 \exp(-10.66)\,, \qquad B_1 = +0.326 \exp(-10.66)\,.$$

The relations (5) and (7) can be rewritten as follows

$$M = P[-0.00855 + 3.80 \exp(-10.66) \sinh \alpha\varphi \sin \beta\varphi$$
$$-5.05 \exp(-10.66) \cosh \alpha\varphi \cos \beta\varphi] \quad \text{N cm}\,,$$

$$P_s = P[0.0278 + 0.514 \exp(-10.66) \cosh \alpha\varphi \cos \beta\varphi$$
$$+ 0.683 \exp(-10.66) \sinh \alpha\varphi \sin \beta\varphi] \quad \text{N}\,.$$

From the above we see that for small values of φ the second and the third components in square brackets are too small, and M and P_s practically do not change. Applying these expressions we draw the diagram of bending moment M and force in spokes P_s (Fig. 483).

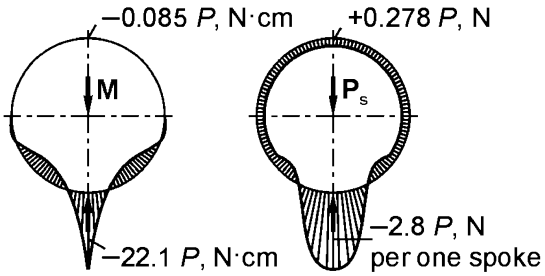

Fig. 483

Under the load $P = 400\,\text{N}$ we obtain $M_{\max} = 880\,\text{N·cm}$; maximal force in the spoke is $P_{s\max} = 112$ N. It is clear that the obtained result does not take into account the preliminary stretching of spokes, which is applied while assembling. Naturally, this preliminary stretching must exceed $P_{s\max}$ by absolute value.

The analyzed problem was for the first time solved by N.E. Zhukovsky.

209. Analyzing the problem of arrow speed dependence upon bow-string deflection w (Fig. 484) we use the results of problem 141, which are typical for large deflections of elastic rod analysis. The elastic beam shown in Fig. 369 can be considered similar to half of a bow arc.

At $s = l$ the equation (5) of problem 141 solution takes the form

$$\beta = F(\psi_L) - F(\psi_0). \tag{1}$$

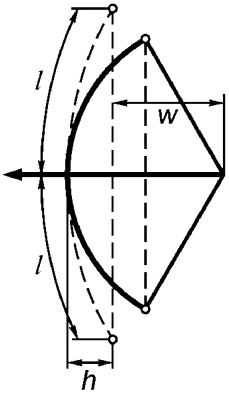

Fig. 484

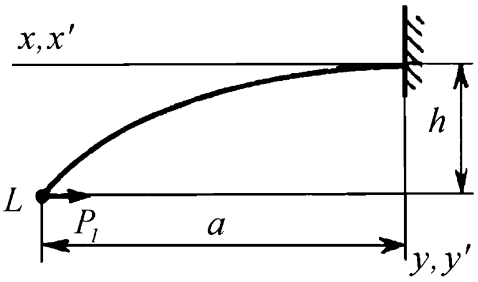

Fig. 485

The curvature of the beam is equal to zero ($d\zeta/ds = 0$) at $s = l$. Therefore from relation (4) of problem 141 it follows that

$$k\cos\psi_L = 0, \quad \text{i.e. } \psi_L = \frac{\pi}{2}. \tag{2}$$

At $s = 0$ $\zeta = \delta$. From this condition using relation (3) of problem 141 we obtain

$$\sin\frac{\delta}{2} = k\sin\psi_0. \tag{3}$$

At first let's consider the first stage of beam bending – tension of the bow-string (see Fig. 485). In this case, as it is seen from Fig. 369, $\delta = 0$. Therefore it follows from (3'), that $\psi_0 = 0$.

And for this case we also have

$$x_L = a, \quad y_L = h.$$

The relations (5) and (7) of problem 141 give

$$\beta = l\sqrt{\frac{P_1}{EJ}} = F(\frac{\pi}{2}),$$

$$\frac{a}{l} = \frac{2}{\beta}E\left(\frac{\pi}{2}\right) - 1, \quad \frac{h}{l} = \frac{2k}{\beta}.$$

Let's specify several values of k. Then, using tables of elliptical integrals, we determine β, a/l, and h/l from the corresponding equations. The results are presented in Table 8.

Table 8. Results of numeric calculations

$\arcsin k$	0	5^0	10^0	15^0
β	1.571	1.574	1.583	1.598
a/l	1	0.990	0.967	0.931
h/l	0	0.111	0.219	0.324

Interpolating the obtained data for given quantity $h/l = 0.3$ we find the following quantities:

$$\beta = l\sqrt{\frac{P_1}{EJ}} = 1.59\,, \qquad \frac{a}{l} = 0.945\,.$$

Thus we obtain the force P_1 in the stretched bow-string and the length of bow-string a, which remains unchanged under further system deformation.

Now let's consider the second stage of beam bending. Here the value ψ_0 is not equal to zero and remains unknown. We shall determine this value in the following way. Let's specify values of k and ψ_0. From equation (3') we find δ using the condition $k\sin\psi_0 = \sin\dfrac{\delta}{2}$. Then from (1') we determine

$$\beta = F(\frac{\pi}{2}) - F(\psi_0).$$

The equations (6) of problem 141 yield

$$\frac{x'_L}{l} = \frac{2}{\beta}[E(\frac{\pi}{2}) - E(\psi_0)] - 1\,, \qquad \frac{y'_L}{l} = \frac{2}{\beta}k\cos\psi_0\,,$$

and it follows from the equations (7) of problem 141 that

$$\frac{x_L}{l} = \frac{x'_L}{l}\cos\delta + \frac{y'_L}{l}\sin\delta\,,$$
$$\frac{y_L}{l} = \frac{y'_L}{l}\cos\delta - \frac{x'_L}{l}\sin\delta\,.$$

Finally we determine the length of the bow-string (Fig. 486)

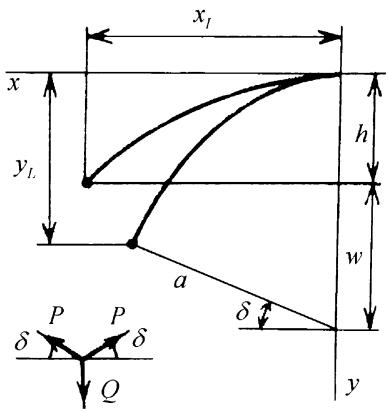

Fig. 486

$$a = \frac{x_L}{\cos\delta},$$

whence

$$\frac{a}{l} = \frac{x_L/l}{\cos\delta}.$$

This ratio must be equal to 0.945. Under a constant k we specify several values of ψ and repeat calculations until the value a/l becomes equal to 0.945. The same calculations we produce for several values of k. The results are compiled in Table 9.

Table 9. Results of numeric calculations

$\arcsin k$	15^0	20^0	25^0	30^0	35^0
ψ_0	6^0	15^0	20^0	21^0	23^0
x/l	0.943	0.932	0.906	0.883	0.850
y/l	0.294	0.325	0.366	0.425	0.472
β	1.493	1.358	1.299	1.317	1.326

Then we calculate the deflection w (Fig. 486)

$$\frac{w}{l} = \frac{a}{l}\sin\delta + \frac{y_L}{l} - \frac{h}{l},$$

and from the equilibrium condition for forces (Fig. 486) we get the force Q :

$$Q = 2P\sin\delta, \qquad \frac{Ql^2}{EJ} = 2\beta^2\sin\delta.$$

For the same values of k and ψ_0 we obtain the results given in Table 10.

Table 10. Results of numeric calculations

w/l	$Ql^2/(EJ)$
0.045	0.24
0.192	0.651
0.337	0.967
0.459	0.22
0.585	0.54

The curve for the dependence of dimensionless load $Ql^2/(EJ)$ upon dimensionless displacement w/l is plotted in Fig. 487. The area bounded by this curve at the interval $0 - w/l$ gives the amount of elastic strain energy transmitted to the arrow while shooting. The integral energy curve is shown in Fig. 487 also. This curve is obtained by simple planimetry of the first plot.

Now let's proceed to numerical calculations. At the prescribed value $w/l = 0.6$ (see Fig. 487)

$$\frac{Ul}{EJ} = 0.53,$$

$$U = 0.53\frac{EJ}{l} = 0.53\frac{10^6\cdot\pi\cdot 2^4}{64\cdot 60} = 6950 \text{ N cm}$$

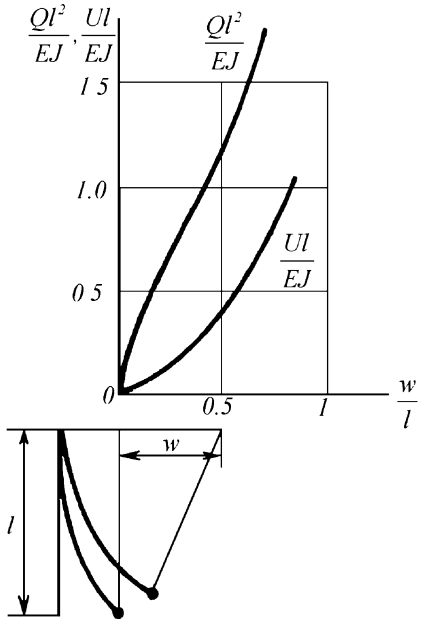

Fig. 487

Let's equate this energy to the kinetic energy of the arrow:

$$U = \frac{mv^2}{2}, \qquad v = \sqrt{\frac{2U}{m}},$$

$$v = \sqrt{\frac{2 \cdot 6950 \cdot 981}{0.40}} = 5800 \text{ cm/s} = 58 \text{ m/s}.$$

In reality the speed v will be less because some part of energy transfers to the kinetic energy of the bow-string and arc of the bow. The force Q which should be applied in order to impart the calculated speed to the arrow will be also obtained by the curve plotted in Fig. 487:

$$\frac{Ql^2}{EJ}\Big|_{\frac{w}{l}=0\,6} = 1.6, \qquad Q = 1.6\frac{10^6 \cdot \pi \cdot 2^4}{64 \cdot 60^2} = 350 \text{ N}.$$

References

1. Alfutov NA, Zinoviev PA, Popov BG (1984) Multilayer Composite Plates and Shells Analysis. Mashinostroenie, Moscow
2. Alfutov NA, Popov BG (1988) Self-gravitating Rod Stability Analysis. Mechanics of Solid Body 5: 177–180
3. Arutyunyan NH, Abramyan BL (1963) Torsion of Elastic Bodies. Physmatgis, Moscow
4. Balabukh LI, Vulfson MN, Mukoseev BV, Panovko YG (1970) On Work Done by Reaction Forces of Moving Supports. In: Research on Theory of Constructions 18, Moscow
5. Biezeno CB,Grammel R (1950) Technical Dynamics. Gostehizdat, Moscow
6. Bolotin VV (1961) Nonconservative Problems in the Theory of Elastic Stability. Fizmatgiz, Moscow
7. Feodosiev VI (1988) Strength of Materials. Vyshaya Shkola, Moscow
8. Fotinich ED (1989) Twisted Configuration as Extreme Equilibrium Mode of Bent-Twisted Rod. Mechanics of Solid Body 3: 192–195
9. Gardner M (1971) Mathematical Puzzles and Amusements. Mir, Moscow
10. Korobov AP (1935-1936) Design of Wheels with Great Number of Spokes. In: Proceedings of Novocherkassk Industrial Institute. Structural part. Vol. 4, #18
11. Korotkova SE (1968) Analysis of Beeing Bent Overlapping Glued Joint. In: Strength of Materials and Theory of Constructions VII. Kiev
12. Lave A (1935) Mathematical Theory of Elasticity. ONTI, Moscow
13. Lavrentyev MA, Ishlinskiy AY (1949) Stability of Rod Subjected to Supercritical Load. In: Reports of USSR Academy of Science. Vol.65,#6
14. Lokteva IV, Feodosiev VI (1987) Local Stability Loss of Layered Structure under Compression. Mechanics of Solid Body 5: 189–192
15. Lurye AI (1947) Statics of thin elastic shells. Gostekhizdat, Moscow
16. Mukhin ON (1965) Dynamic Stability Criteria of Pipe Containing Fluid. In: Reports of USSR Academy of Science. Mechanics #3
17. Panovko YG, Gubanova II (1979) Stability and Vibrations of Elastic Systems. Nauka, Moscow
18. Popov EP (1948) Nonlinear problems of Thin Rod Statics. Gostekhizdat, Moscow
19. Reut VI (1939) On Theory of Elastic Stability. In: Proceedings of Odessa Institute of Civil and Municipal Construction. Constructions Analysis Considering Plastic Properties of Materials. Stroyvoenmorizdat, Moscow #1
20. Uzhik GV (1948) Stress Strain State of Bar with Recess. In: Reports of USSR Academy of Science. Department of Technical Science #10
21. Vasiliev VV (1988) Mechanics of Composite Made Structures. Mashinostroenie, Moscow

Index